University of South Florida

DIGITAL COMMONS
@ UNIVERSITY OF SOUTH FLORIDA

Digital Commons @ University of South Florida

USF Tampa Graduate Theses and Dissertations

USF Graduate Theses and Dissertations

March 2018

Application of Modern Foraminiferal Assemblages to Paleoenvironmental Reconstruction: Case Studies from Coastal and Shelf Environments

Christian Haller
University of South Florida, challer@mail.usf.edu

Follow this and additional works at: https://digitalcommons.usf.edu/etd

 Part of the Geology Commons

Scholar Commons Citation

Haller, Christian, "Application of Modern Foraminiferal Assemblages to Paleoenvironmental Reconstruction: Case Studies from Coastal and Shelf Environments" (2018). *USF Tampa Graduate Theses and Dissertations.*
https://digitalcommons.usf.edu/etd/7627

This Dissertation is brought to you for free and open access by the USF Graduate Theses and Dissertations at Digital Commons @ University of South Florida. It has been accepted for inclusion in USF Tampa Graduate Theses and Dissertations by an authorized administrator of Digital Commons @ University of South Florida. For more information, please contact digitalcommons@usf.edu.

Application of Modern Foraminiferal Assemblages to Paleoenvironmental Reconstruction: Case Studies from Coastal and Shelf Environments

by

Christian Haller

A dissertation submitted in partial fulfillment
of the requirements for the degree of
Doctor of Philosophy
with a concentration in Geological Oceanography
College of Marine Science
University of South Florida

Co-Major Professor: Pamela Hallock Muller, Ph.D.
Co-Major Professor: Albert C. Hine, Ph.D.
Christopher G. Smith, Ph.D.
Ping Wang, Ph.D.
David J. Mallinson, Ph.D.

Date of Approval:
April 05, 2018

Keywords: Leeuwin Current, Pliocene, Australia, sea level, Holocene, Gulf of Mexico

Copyright © 2018, Christian Haller

Acknowledgments

I am grateful for the continuous support and encouragement provided by my dissertation advisors Dr. Pamela Hallock Muller and Dr. Al Hine. I am in debt with my co-advisor at the U.S. Geological Survey: Dr. Chris Smith, your patience and support has made this dissertation possible. I thank Dr. Ping Wang, and Dr. David Mallinson, members of my dissertation committee, for helping to vet my work in contributions to the field of sedimentology and micropaleontology. Likewise, I thank the scientists and technicians at the U.S. Geological Survey, and the IODP in College Station, TX for their work that benefited my research in the past years. I wish to thank specifically Marci Marot, Terry McCloskey, C. Scott Adams, Alisha Ellis, and Cathryn Wheaton for help with work in the field, Nick Zaremba and Nancy DeWitt for assistance with GPS analysis. I appreciate the help of the Grand Bay National Estuarine Research Reserve staff who permitted the field activities in their reserve. At USF I honor the work of Tony Greco, the Electron Microscopy Lab manager, to reserve time on the scanning electron microscope for my work. I want to extend my thanks to Elizabeth A. Brown and Benjamin Ross for sample preparation and assisting with the peculiarities of the lab's SEM device. Thanks also goes to Jorijntje Henderiks, Jeroen Groeneveld, Soma Baranwal, Briony Mamo, and Resti Jatiningrum who were excellent paleontologists on Expedition 356 and contributed significantly to the shipboard data that were used in this work.

This research would have been impossible without the academic and financial support from the U.S. Science Support Program, the U.S. Geological Survey in St. Petersburg, Florida, USF Graduate Endowed Fellowship, and several graduate student grants provided by SEPM, GSA, the Cushman Foundation, and AAPG.

Table of Contents

List of Tables

List of Figures and Plates

Abstract

The aim of paleoenvironmental studies is to reconstruct characteristics of the past environment from fossil assemblages preserved in sedimentary strata. Thus, studies of modern surface assemblages, quantitatively correlated to the environmental parameters, are required before reliable interpretations can be made. For this dissertation, two different techniques were applied in two case studies: a reconstruction making use of a benthic foraminiferal transfer function from the intertidal marshes in the eastern Mississippi Sound, Alabama/Mississippi, and a qualitative reconstruction of ocean current activity on the Western Australian shelf.

Modern salt-marsh foraminifera were collected from Grand Bay, Pascagoula, Fowl River, and Dauphin Island across several elevation transects and different salinity regimes. Cluster analysis yielded nine dead biofacies and five live assemblages from Open Estuarine to Upland Transition. Canonical correspondence analysis indicated a strong relationship between distributions of dead biofacies and elevation. Both dissolution of calcareous species in the organic marsh sediment and the long-term accumulative nature of the dead assemblage favored the use of non-estuarine dead assemblages. A Weighted Average-Partial Least Squared transfer function was applied to the surface data and yielded a Root Mean Squared Error of Prediction (RMSEP) of 0.14 m, which represents 33% Mean Range of Tide at Grand Bay and 39% at Dauphin Island. The transfer function was applied to two sedimentary cores from Grand Bay and two from Dauphin Island, which revealed disparate developments between the regions during the last 1,900 years. While both Dauphin Island cores indicated relative sea-level trends aligned with other Gulf of Mexico studies, Grand Bay was likely impacted by a river avulsion event disconnecting Grand Bay from fluvial sediment influx, and by the erosion of a protective headland, Grand

Batture Island. Sediments spanning the last ~100 years contained increased abundances of low marsh foraminifera likely associated with coastline erosion, which was most prominently displayed by a lithology shift towards grey silt in the Dauphin Island cores.

Surface carbonate sediments from Western Australia's Northwestern Shelf and Carnarvon Ramp were collected from 127–264 m water depth. Foraminiferal assemblages changed between 127 m and 145–264 m due to rapidly decreasing water temperature in the thermocline, and loss of sufficient light for support of "larger" benthic foraminifera. Latitudinal differences were likely caused by three factors: (1) limited influence of the warm Leeuwin Current to support tropical taxa at the sampled depths, (2) reduced habitat diversity on the narrow Carnarvon Ramp compared to surrounding shelves, and (3) differing water-mass characteristics. The gathered information was used to interpret the assemblages from a Carnarvon Ramp core (total depth 300 m), providing insight into the activity of the warm, surficial Leeuwin Current for the last 3.54 My (Pliocene). Abundant infaunal taxa were inferred to indicate low oxygenation, increased supply of organic matter, and high sea-surface productivity during the absence of the Leeuwin Current above the coring site. Dominance of epifaunal species signified higher oxygenation at the sediment-water interface when upwelling of nutrient-rich waters was effectively suppressed by the Leeuwin Current. Around 1.14 Ma, waning of hypoxic conditions was initiated until a more substantial change was marked at 0.91 Ma. Suspension-feeding sponges became common sediment constituents during a Leeuwin Current flow optimum at ~0.6 Ma. The epifaunal taxa dominance persisted on the modern shelf, yet short episodes of infaunal peaks were likely caused by lateral shifts and fluctuating influence of the Leeuwin Current during more intense glacial cycles.

Chapter 1.

Introduction

Rationale

Reconstruction of past conditions of climate, oceanographic water masses, and sea level continues to be an important topic among geoscientists, physicists, and oceanographers (e.g., Das et al., 2013; Groeneveld et al., 2017; Müller-Navarra et al., 2017). Length of reconstructions vary and require different sampling resolutions, however all studies have in common that they extend the knowledge of a parameter beyond historic recordings. Some studies attempt to deliver a baseline for modeling future developments (e.g., climate change, Masson-Delmonte et al., 2013), others seek to understand conditions during glacials and interglacials (Kennett, 1977; Mudelsee et al., 2014; Gulick et al., 2017)

Common proxies for environmental conditions are planktonic and benthic foraminifera, which react to temperature, nutrient availability, oxygenation, bathymetric depth, salinity, pollution, sea-level, and other environmental parameters (Scott, 1975; Coccioni, 2000; Gooday, 2003; Hallock et al., 2003; Osterman, 2003; Murray, 2006). Either the species abundance or the geochemical signal in the calcium carbonate of the foraminiferal test can be applied as proxies. The preservation of foraminiferal tests in sedimentary strata provides a fossil record for researchers to analyze at a defined point in time. However, the reconstruction process requires the knowledge of modern data to compare to, often called a training set. The stratigraphic data can then be qualitatively or quantitatively (numerical modelling techniques) compared to infer past environmental conditions (Juggins and Birks, 2012).

This dissertation reconstructs paleoenvironments in two different geological settings, on different reconstruction time scales, and explores the use of two different reconstruction techniques based on foraminifera (Fig. 1.1):

a) The eastern Mississippi Sound salt marshes in the northern Gulf of Mexico are geological environments in the tidal zone. Sedimentary records are relatively short (few decimeters to meters) and were initiated after the decrease in rate of the Holocene sea-level rise (<8,000 years ago). Modern benthic foraminifera were used to inform a quantitative, predictive transfer function which then was applied for reconstruction of the paleo-marsh elevation and sea level. Results were integrated in the interpretation of the regional geological history (Fig. 1.1, left side).
b) The Western Australian shelf is a tropical to temperate carbonate depositional system influenced by the Leeuwin Current and Western Australian Current, both of which influence benthic communities. A detailed study of modern surface samples with excellent preservation laid the foundation for a paleo reconstruction. Samples recovered down to 300 m below sea floor (~3.54 Ma) are indicative of food availability or oxygenation status and are used to infer intensity of the Leeuwin Current (Fig. 1.1, center)

Overview of Dissertation

In addition to this Introduction, this dissertation is composed of four chapters with a central theme of analyses of distributions of foraminifera and the application of this information to fossil assemblages to help interpret paleoenvironmental conditions and variability. The final chapter showcases the overall conclusions and possible future directions.

- Chapter 2 describes the surface distributions of live and dead foraminiferal assemblages in the tidal marshes of the barrier island and estuarine complex of the eastern Mississippi

Sound. Several living and dead biofacies are described and related to their elevation in the tidal zone. This work has been submitted for publication in the *Journal of Foraminiferal Research* and is currently in peer-review.

- Chapter 3 assesses downcore foraminiferal abundances and sedimentological parameters of two eastern Mississisippi Sound locations (Grand Bay: fringing marshes; Dauphin Island: back-barrier marshes). In a transfer function, the regional dataset presented in chapter 2 is applied to reconstruct paleo-marsh elevation and sea level in a chronologic framework. The relative sea-level trends are compared between the sampling sites and set into perspective with other Gulf of Mexico studies. Difficulties and pitfalls of foraminiferal training datasets are discussed. This work has been submitted for publication in the Elsevier journal *Marine Geology*.
- Chapter 4 examines benthic foraminifera from mudlines recovered during International Ocean Discovery Program (IODP) Expedition 356 "Indonesian Throughflow" at four drill-sites on Carnarvon Ramp and Northwest Shelf. The species diversity is displayed on six micrograph plates. Bathymetric and latitudinal trends in assemblages are detailed and related to water mass characteristics. This chapter has been peer reviewed and resubmitted with revisions for publication in SEPM Special Publication "*Geologic Problem Solving with Microfossil IV*" associated with the 2017 NAMS-SEPM Microfossils IV conference in Houston, Texas (USA).
- Chapter 5 reports foraminiferal abundances and lithology of fossil benthic foraminifera from IODP drill-site U1460, located on the Carnarvon Ramp, offshore Western Australia. High abundance of infaunal taxa is associated with upwelling, while a gradual increase of epifaunal taxa requiring more oxygen is interpreted as indicating the initiation of the Leeuwin Current. This chapter has been submitted for publication in the Elsevier journal *Marine Micropaleontology*.
- Chapter 6 offers a summary of the work completed for this dissertation and discusses possible future research avenues for the two major sections.

References

Coccioni, R., 2000. Benthic Foraminifera as Bioindicators of Heavy Metal Pollution, in: Martin, R.E. (Ed.), Environmental Micropaleontology: The Application of Microfossils to Environmental Geology. Springer US, Boston, MA, pp. 71–103.

Das, O., Wang, Y., Donoghue, J., Xu, X., Coor, J., Elsner, J., Xu, Y.J., 2013. Reconstruction of paleostorms and paleoenvironment using geochemical proxies archived in the sediments of two coastal lakes in northwest Florida. Quaternary Science Reviews 68, 142–153. 10.1016/j.quascirev.2013.02.014

Gooday, A.J., 2003. Benthic foraminifera (Protista) as tools in deep-water palaeoceanography: Environmental influences on faunal characteristics. Advances in Marine Biology 46, 1–90. 10.1016/S0065-2881(03)46002-1

Groeneveld, J., Henderiks, J., Renema, W., McHugh, C.M., De Vleeschouwer, D., Christensen, B.A., Fulthorpe, C.S., Reuning, L., Gallagher, S.J., Bogus, K., Auer, G., Ishiwa, T., Expedition, S., 2017. Australian shelf sediments reveal shifts in Miocene Southern Hemisphere westerlies. Science Advances 3, e1602567. 10.1126/sciadv.1602567

Gulick, S.P.S., Shevenell, A., Montelli, A., Fernandez, R., Smith, C., Warny, S., Bohaty, S.M., Sjunneskog, C., Leventer, A., Frederick, B., Blankenship, D., 2017. Initiation and long-term instability of the East Antarctic Ice Sheet. Nature 552, 225–229. 10.1038/nature25026

Hallock, P., Lidz, B.H., Cockey-Burkhard, E.M., Donnelly, K.B., 2003. Foraminifera as Bioindicators in Coral Reef Assessment and Monitoring: The FORAM Index. Environmental Monitoring and Assessment 81, 221–238. 10.1023/A:1021337310386

Juggins, S., Birks, H.J.B., 2012. Quantitative environmental reconstructions from biological data, in: Birks, H.J.B., Lotter, A.F., Juggins, S., Smol, J.P. (Eds.), Tracking Environmental Change Using Lake Sediments: Data Handling and Numerical Techniques. Springer Netherlands, Dordrecht, pp. 431–494.

Kennett, J.P., 1977. Cenozoic evolution of Antarctic glaciation, the circum-Antarctic Ocean, and their impact on global paleoceanography. Journal of Geophysical Research 82, 3843–3860. 10.1029/JC082i027p03843

Masson-Delmonte, V., Schulz, M., Abe-Ouchi, A., Beer, J., Ganopolski, A., Rouco, J.F., Jansen, E., Lambeck, K., Luterbacher, J., Naish, T., Osborn, T., Otto-Bliesner, B., Quinn, T., Ramesh, R., Maisa Rojas, M., Shao, X., Timmermann, A., 2013. Information from Paleoclimate Archives, in: Stocker, T.F., Qin, D., Plattner, G.-K., Tignor, M., Allen, S.K., Boschung, J., Nauels, A., Xia, Y., Bex , V., Midgley, P.M. (Eds.), Climate Change 2013: The Physical Science Basis. Contribution of Working Group I to the Fifth Assessment Report of the Intergovernmental Panel on Climate Change. Cambridge University Press, Cambridge, United Kingdom and New York, NY, USA, pp. 383–464.

Mudelsee, M., Bickert, B., Lear, C.H., Lohmann, G., 2014. Cenozoic climate changes: A review based on time series analysis of marine benthic δ18O records. Reviews of Geophysics 52, 333–374. 10.1002/2013RG000440

Müller-Navarra, K., Milker, Y., Schmiedl, G., 2017. Applicability of transfer functions for relative sea-level reconstructions in the southern North Sea coastal region based on salt-marsh foraminifera. Marine Micropaleontology 135, 15–31. 10.1016/j.marmicro.2017.06.003

Murray, J.W., 2006. Ecology and Applications of Benthic Foraminifera. Cambridge University Press, 426 pp.

Osterman, L.E., 2003. Benthic foraminifers from the continental shelf and slope of the Gulf of Mexico: an indicator of shelf hypoxia. Estuarine, Coastal and Shelf Science 58, 17–35. 10.1016/S0272-7714(02)00352-9

Scott, D.B., 1975. Quantitative studies of marsh foraminiferal patterns in southern California and their application to Holocene stratigraphic problems. Maritime Sediments Special Publication 1, 153-170.

Figures

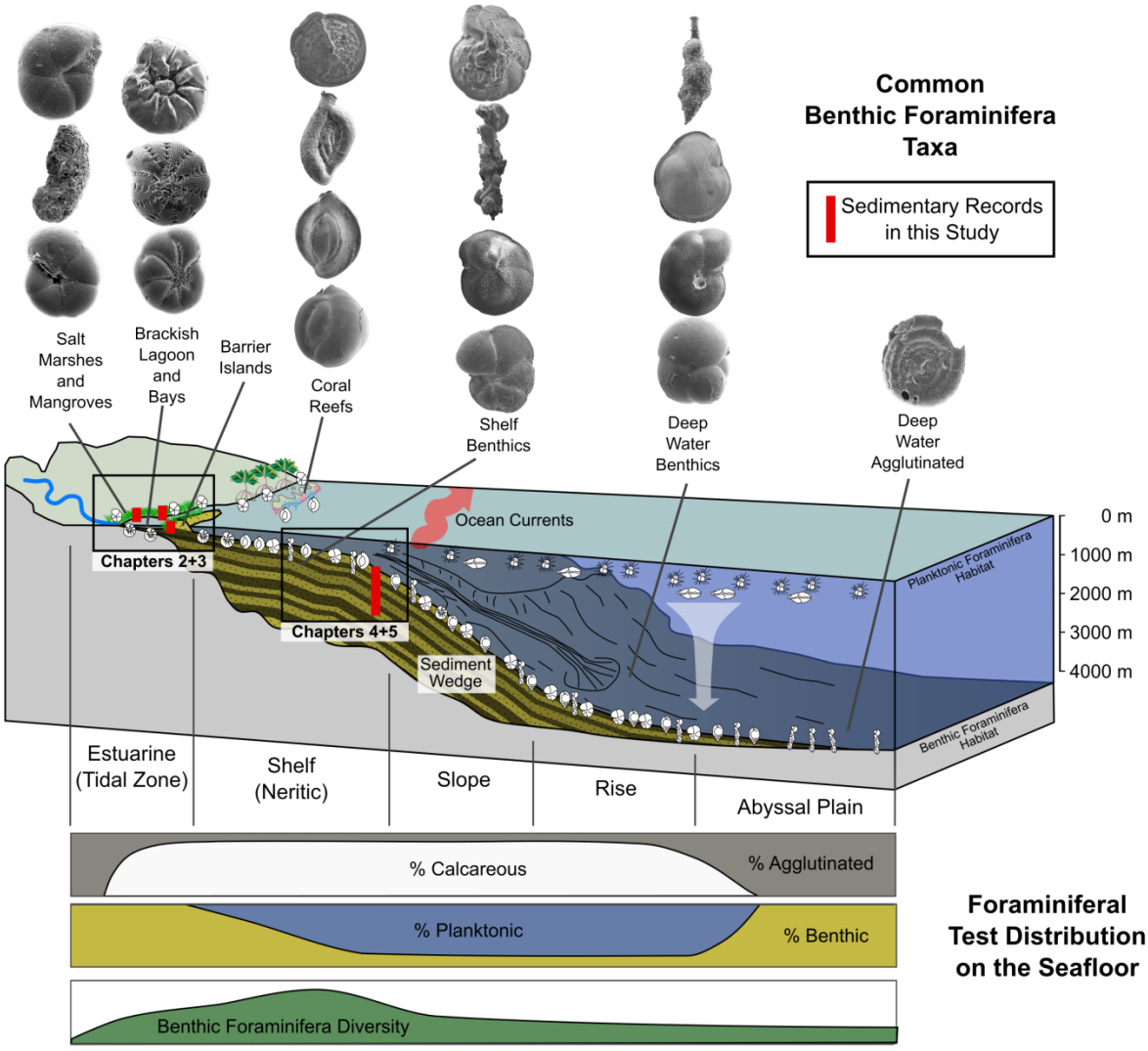

Figure 1.1. Location of study areas in the tidal zone (left) and on the outer shelf (center). The sediments of the salt marshes and brackish estuaries are dominated by low-diversity assemblages of agglutinated taxa and stress tolerant calcareous taxa respectively. Near the upland, only few species can survive prolonged exposure to air, fresh-water intrusion, and desiccation stress. The continental shelves are the bathymetric depths of highest benthic diversity and are characterized calcareous benthic taxa. Planktonic foraminifera require water depths sufficient for their life mode and increase in abundance in sea floor sediments in correlation with water depth. The deepest parts of the oceans lie below the Calcite Compensation Depth and receive only little food and sediment input. These abyssal plains are dominated by agglutinated taxa.

Chapter 2.

Distribution of Modern Salt-Marsh Foraminifera from the Eastern Mississippi Sound, U.S.A.

Abstract

This study documented surface distributions of live and dead foraminiferal assemblages in the tidal marshes of the barrier island and estuarine complex of eastern Mississippi Sound (Grand Bay, Pascagoula River, Fowl River, Dauphin Island). A total of 71,833 specimens and 38 species were identified from a gradient of different elevation zones across the study area. We identified five assemblages for the live and nine biofacies for the dead assemblage from estuarine, low marsh, middle marsh, high marsh, and upland transition environments. Although dissolution of calcareous tests was observed in the dead assemblages, characteristic species and abundance patterns dependent on elevation in the intertidal zone were similar between living assemblages and dead biofacies. The eastern Mississippi Sound estuaries are dominated by *Ammonia tepida, Cribroelphidium poeyanum, Cribroelphidium excavatum,* and *Paratrochammina simplissima*. The low marshes are dominated by *Ammotium salsum, Ammobaculites exiguus,* and *Miliammina fusca*. The dominant species in the middle marshes is *Arenoparrella mexicana*. The most abundant species in the high marshes is *Entzia macrescens*. The upland–marsh transition zones are dominated by *Trochamminita irregularis* and *Pseudothurammina limnetis*. Canonical correspondence analysis was applied to further study the relationship between *a priori* defined biofacies and measured environmental data (elevation, grain size, organic matter, and salinity) to test the hypothesis that distribution of foraminiferal assemblages is driven by elevation and hence flooding frequency. Salinity was the second most important explanatory variable of dead assemblages.

Riverine freshwater from the Pascagoula River markedly influences the live and dead assemblage in the Pascagoula River Marsh, which is expressed by low diversity and densities, and dominance by *Ammoastuta inepta*. The relationship between the measured environmental system variables and assemblage distributions can be used in future Gulf-wide paleo-environmental studies.

Introduction

Benthic foraminifera are abundant in estuaries and tidal marshes. Species abundances and distributions vary depending on environmental parameters such as food availability, oxygenation, temperature, salinity, pH, and sediment texture (Phleger, 1970; Martin, 2000; Calvo-Marcilese et al., 2013; Bolliet et al., 2014; Ellis et al., 2014; Schwing et al., 2015; Abu-Zied et al., 2016). Assemblage compositions narrowly defined by environmental parameters are crucial for the use of salt-marsh foraminifera as tools in paleo-sea level and paleo-environmental reconstructions during the Holocene (Edwards and Wright, 2015). For example salinity fluctuations due to rainfall, tidal inundation, and evaporation are key factors controlling marsh assemblages on local (De Rijk, 1995; Horton and Murray, 2007), regional (Kemp et al., 2009), and global scales (Murray, 2006). Their characteristic occurrence and abundance in association with specific environments and elevations in the tidal zone permits application as sea-level proxies for quantification of former sea levels (e.g., Barnett et al., 2016).

Foraminifera assemblages typically observed in tidal marsh sediments have low diversity (Murray, 2006) with only a small number of taxa in both the tropical and temperate regions of the world (Phleger, 1970; Sen Gupta, 1999). However, documentation of the distribution of modern tidal marsh foraminifera in a new study area is essential to reconstruct paleo-sea level or paleo-environments related to locally specific tidal zones and species occurrences (e.g., Phleger and Walton, 1950; Scott and Medioli, 1978; Horton and Edwards, 2006; Kemp et al., 2009; Edwards and Wright, 2015; Hayward et al., 2015; Milker et al., 2015; Müller-Navarra et al., 2017).

Previous studies of foraminifera in the Mississippi Sound and contiguous tidal marshes found qualitative differences between high and low marsh (e.g., Phleger, 1954). Further works treated the northeastern Gulf of Mexico in low resolution (Phleger, 1960), focused on the continental shelf (e.g., Phleger, 1951; Phleger and Parker, 1951; Parker, 1954), delta-plain environments (e.g., Scott et al., 1991) and large bays (e.g., Osterman and Smith, 2012). Comparing the datasets generated by Phleger (1954) and Anderson (1968), Lamb (1972) demonstrated a long-term change of dominant estuarine species in the Mississippi Sound from "lagoonal" to "open gulf": *Ammobaculites* and *Miliammina* taxa were replaced by *Ammonia* and *Elphidium* taxa. Lamb (1972) attributed the species succession to the construction of Dauphin Island Bridge, which restricted freshwater inflow from Mobile Bay into Mississippi Sound and increased the sound salinity by 10. Other possibilities presented are strengthened erosion increasing tidal inlet dimensions.

We continued work in the Mississippi Sound salt-marshes by documenting the distribution of foraminifera from four geographically adjacent sampling regions representing a diversity of tidal marsh environments of the eastern Mississippi Sound (Fig. 2.1). A total of 88 stations from Fowl River, Grand Bay, Pascagoula, and Dauphin Island contributed to the dataset of 168 estuarine and marsh sediment samples. We identified elevation-dependent biofacies at each of these sites and described the spatial distribution of the principal tidal marsh foraminiferal assemblages found within the Mississippi Sound tidal marshes. We considered the implications of these inter- and intra-site variations for future environmental reconstructions in the Mississippi Sound area.

Regional Setting

The Mississippi Sound area is a well-mixed lagoon or estuary of ~6 m water depth with a diurnal microtidal (<0.5 m) regime (Cipriani and Stone, 2001). The marsh and estuarine characteristics are differentiated by hydrogeomorphic variability related to a mix of fluvial systems and mainland or barrier island marsh environments. Where river inputs are substantial, salinity tends to be nearly zero in vicinity

of creek and river mouths and reaches 20–25 in open areas of the sound (Priddy et al., 1955). Away from major river mouths, salinity is more uniform and marsh platforms fringe the mainland or occur behind the barrier islands. Sedimentary facies in the sound are typically muddy with interspersed event beds (winter storm and hurricane reworking) with physical, wave-driven disturbance down to 5 cm, and bioturbation down to 10–12 cm, eliminating most stratification (Velardo, 2005). The sound is fringed in the intertidal zone by brackish to salt marshes, both on the mainland coastal plains and the back-side of the barrier island chain.

Three hydrogeomorphic areas between Mobile Bay (Alabama) to the east and the town of Pascagoula (Mississippi) to the west have been sampled for this study: An oligohaline to brackish river marsh (Pascagoula Marsh, PG, Fig. 2.1A); two mainland fringing marshes (Grand Bay Marsh, GB, Fig. 2.1B, and the Fowl River Marsh, FR, Fig. 2.1C); and a back-barrier fringing marsh (Dauphin Island Marsh, DA, Fig. 2.1D).

Mean range of tide in the area is ~40 cm (microtidal; Table 2.1). The mainland marshes at Pascagoula, Grand Bay, and Fowl River are particularly wide, with low relief and microtopography. Marsh zones are traditionally assigned based upon dominant vegetation (e.g., Redfield, 1972; Brinson, 1993). The frequently flooded low marsh zone along the channel margin is populated by a thin band of *Spartina alterniflora* (salt-marsh cordgrass; see Appendix A1). The *Spartina* quickly grades into the middle marsh vegetation zone of *Juncus roemerianus* (black needle rush), which dominates the Mississippi Sound marshes in vast expanses (Appendix A1). The higher middle marsh to upland frequently contains salt pans with very sparse and stunted vascular plants. The upland is vegetated by *Pinus elliottii* (maritime slash pine).

Methods

Sampling Strategy

The top 1 cm of sediment at 87 different stations (66 marsh and 21 estuary) were sampled between April 2013 and May 2016 across two spatial scales (Appendix A1). Samples were collected from

marsh and aquatic environments along kilometer-scale transects along the Pascaguola River (10 km) and Grand Bay fringing marsh (2.5–5 km) extending offshore in Mississippi Sound. Additional sampling was conducted along small-scale transects (tens to hundreds of meters) from upland transition to marsh edge in Fowl River, Grand Bay, and Dauphin Island (Fig. 2.1).

Surface-sediment volumes up to 70 cm^3 were carefully collected with a spoon and stored in centrifuge tubes. At most stations a second sample (B sample) was taken to assess small-scale variability (patchiness) in foraminiferal assemblages within a maximum distance of 1 m from the first sample, as suggested by Buzas et al. (2015). At all stations, surface elevations were determined and, at most stations, further sediment was acquired for organic-content assessment and grain-size analysis.

At each marsh site, salinity was measured using a YSI handheld multi-parameter field meter (YSI ProPlus, ©) if sufficient pore water was encountered (Appendix A2). Values were read after a minimum of 15 minutes for equilibration. Ground elevation was surveyed with a differential GPS setup consisting of a kinematic rover and base station positioned at the closest National Geodetic Survey benchmark (Appendix A1). Two Asthech Z-Extreme SMG-ZX-3 receivers, one at the benchmark site with a choke-ring antenna and another as a roving-geodetic antenna, delivered a horizontal precision of <0.056 m and vertical precision of <0.047 m (Appendix A1). All measurements were referenced to the North American Vertical Datum of 1988 (NAVD88). At estuarine locations, the YSI multi-parameter field meter probe was submerged ca. 50 cm below water level. Horizontal error was not determined at estuarine sites. Water depths were recorded at an accuracy of 0.1 m with the Garmin echoMap 50s sounder system mounted on the boat. Given the astronomical mean tidal range of 0.417 m measured at the Grand Bay NERR tide gauge (NOAA Tides and Currents), a nominal error of 0.43 m can be assumed (Appendix A1).

Sediment Analysis

The grain-size distribution of the top centimeter of sediment was determined with a Beckman Coulter LS 200 size analyzer (Appendix A2). Prior to analysis, samples were treated with hydrogen peroxide overnight and heated on a hotplate to digest particulate organic matter. Before transferring the

aliquot into the analyzer, all sediment >1 mm was removed by sieving. Grain-size interpretations were based on the Folk and Ward (1957) method measured in micrometers and are reported as differential volume (percent of total sample) calculated with the software package Gradistat (modified after Blott and Pye, 2001; Bernier et al., 2014).

Standard mass-loss techniques were used to measure organic matter content as mass (g) of dry organic matter per mass of dry sediment (see Marot et al., 2014). A subsample of wet sediment was weighed and then dried at 60°C for two days to remove interstitial water; the dry mass was recorded. Dry sediment was powdered and homogenized using a porcelain mortar and pestle. Approximately 5 g of dry, homogenized, powdered sediment was placed in pre-weighed crucibles. The vessels were then placed in a muffle furnace, dried at 110°C, reweighed, and ashed at 550°C. The pre-ash weight from the second drying at 110°C and the post-ash weight were used to quantify mass of organic matter. Percent carbon content (%LOI OC) was estimated as 40% of the organic matter mass fraction (Dean, 1974; Santisteban et al., 2004; Appendix A2).

Foraminiferal Analyses

Foraminiferal surface samples were stained with 2 g rose Bengal powder per liter of 90% ethanol on the day of collection, as described by Walton (1952), Bernhard (2000), and Murray (2000). Staining periods of two weeks or more were used with daily agitation as recommended by Schönfeld et al. (2012). Various workers (e.g., Bernhard, 1988; Hannah and Rogerson, 1997) have noted that dead foraminiferal cytoplasm will react with rose Bengal weeks to months after a foraminifer's death (Hannah and Rogerson, 1997). As suggested by Schönfeld et al. (2012), only tests having all chambers stained bright red were considered living at the time of collection. Agglutinated foraminifera with opaque tests were opened with a needle, if necessary. Following staining, sediment volume of each sample was determined to the nearest 1 ml. Sediment was stirred on an orbital shaker with 2 ml of 4% Calgon solution (sodium hexametaphosphate) for 60 min to promote clay disaggregation. Foraminiferal samples were then wet-sieved through 850 μm and 63 μm sieves. Both fractions were dried at 50°C and the 63–850 μm fraction

dry-sieved through 125 μm and 150 μm hand-sieves. A microsplitter was used to split the 125–850 um size-fraction for time-efficiency and to ensure a representative population (total specimens >300; Fatela and Taborda, 2002).

Foraminiferal census counts can be found in Appendix A3 and the most abundant taxa are illustrated in Figure 2.2. Foraminiferal specimens were identified following the taxonomy of Vance et al. (2006) and Kemp et al. (2009); see Appendix A4. Specimens of the species *Ammobaculites exiguus* and *Ammotium salsum* were combined into a single group because these two species show the same coarse-grained surface texture and were commonly broken, making them difficult to ascribe them to the species or even genus level. Foraminiferal density data were standardized to 10 cm^3 for intercomparison. For avoiding confusion of abbreviated genera of the same first letter we modified the common abbreviation scheme to three letters (Appendix A4).

Statistical Analysis

A cutoff value of a minimum of 57 specimens per sample was used for inclusion into statistical analyses. Taxa of any sample representing at least 2% of the assemblage in one sample were included, since abundances below this value approach the confidence limit, convey little meaning, and are not reliable indicators of foraminiferal patterns (Koch, 1987; Buzas, 1990). The arcsine transformation $\text{asin}(p^{1/2})$, which was intended for nominal data ranging from 0 to 1, was used on proportional data.

We applied a hierarchical clustering (Mello and Buzas, 1968) with the Unweighted Pair Group Method with Arithmetic Mean (UPGMA) algorithm and Bray-Curtis similarity index using transformed proportional data to classify dead and live foraminiferal assemblages into biofacies. The Bray-Curtis similarity is a common similarity measure for abundance data and dampens large contrasts in abundance; it delivers well-defined clusters at similarity values of 0.5 or higher (Stalder et al., 2015).

A Non-Metric Multidimensional Scaling (NMDS) analysis with Bray-Curtis similarity index was performed to determine a meaningful lower similarity limit for cluster analyses that mostly retained the estuarine/marsh separation but did not over compartmentalize.

The resulting foraminiferal assemblage clusters were analyzed by values of "Biofacies Fidelity" (BF), "Constancy" (C) and "Occurrence" (O), (BFCO analysis), to determine which species dominated within each cluster/biofacies (Hazel, 1977; Abbene et al., 2006; Culver et al., 2008). The value Occurrence is defined as the number of times a species occurred in a cluster. The value Constancy is the percentage of samples in which a species occurred in a biofacies. Biofacies Fidelity is a measure of species concentration in a biofacies and was calculated by the following equation (*A*):

(*A*) $$BF_{ji} = \frac{P_i}{\sum_{j=1}^{P} P_i}$$

where *j* is the species (*j* = a, b, c, n) and P_i is the percentage of occurrences of a species in a cluster (*I* = 1, 2, 3, p). A minimum value of 5 or higher for BF and C was considered to be characteristic of a biofacies. Furthermore, if a species scored 10 for either BF or C, but lower on the second variable, it was still considered essential.

Relationships between dead assemblages and environmental parameters were evaluated using Canonical Correspondence Analysis (CCA; ter Braak and Verdonschot, 1995). Environmental parameters included were salinity, elevation, sediment organic content, and sediment grain-size distribution.

Diversity in live and dead assemblages was assessed with Fisher's α, which is calculated with the equation (*B*):

(*B*) $$S = \alpha * ln\left(1 + \frac{N}{\alpha}\right)$$

where *S* is number of taxa in a sample, *N* is number of individuals and α is the Fisher's α.

To assess assemblage patchiness (Buzas et al., 2015), we used the non-parametric two-sample paired Wilcoxon tests between the two replicate samples at each station by using relative abundances. This is a test designed to compare two related samples. The significance level $\alpha = 0.05$ to test H_0 "no median shift (no difference)" was adopted, H_0 rejected if $p < 0.05$ and accepted if $p > 0.05$. The permutation p(exact) value was reported if $n < 26$.

The Cluster Analysis and CCA were calculating using PAST 3.16, a free software package for scientific data analysis (Hammer et al., 2001). PRIMER 7 (Primer-E) was used for NMDS analysis.

Results

Environmental Variables

Quantitatively, marsh sediments were finer grained and have higher organic carbon content than estuarine sediments for all locations. Marsh sediments from Pascagoula (PG), Grand Bay (GB), and Dauphin Island (DI) were mostly dominated by silt (averages 63%, *n* = 12; 62% *n* = 26; and 51% *n* = 14 respectively; Appendix A2). Estuarine samples from Pascagoula and Grand Bay contained higher percentages of sand (30%, *n* = 5; and 51%, *n* = 13 respectively; Appendix A2) than the two estuarine stations near Dauphin Island (sand = 15%), which were mostly silt (64%; Appendix A2).

On average, marsh sediment (8.4%, *n* = 60) had a higher organic carbon (OC) content than estuarine sediment (2.4%, *n* = 21; Appendix A2). With respect to the absolute range of OC for all sites, Grand Bay marsh had the highest (OC_{GB49S} = 18.6%) and the lowest (OC_{GB38S} = 0.65%) organic carbon content (Appendix A2). Similarly, Grand Bay estuarine samples also had the highest range, from 0.64% (GB67G) to 13.2% (GB35G), compared with Pascaguola (1.1–3.7%) and Dauphin Island (4.2–4.5%).

Measured pore-water salinity averages were higher in estuarine (25, *n* = 21; Appendix A2) than in marsh water (20, *n* = 32). However, variability was lower in estuarine waters (16–24) than in the marsh pore water (0.9–73).

Foraminiferal Census

The live (stained) and dead assemblages had similar numbers of species (*S* = 32 and 38, respectively); however, specimen counts for dead assemblages (N = 56,577) were nearly four times the living (N = 15,256; Appendix A3). Normalized dead and living densities both varied by four orders of magnitude (1–5,541 and 0–1,288 specimens cm^{-3}, respectively; Appendix A3). The living assemblages are dominated (in descending order) by *Miliammina fusca*, combined *Ammotium salsum*/*Ammobaculites exiguus* group, *Arenoparrella mexicana*, *Ammonia tepida*, *Ammoastuta inepta*, and *Trochammina inflata*. We also observed *Tiphotrocha comprimata*, *Paratrochammina simplissima*, *Haynesina germanica* and

Cribroelphidium excavatum in low numbers. Living calcareous taxa were most abundant in estuarine samples, with rare occurrences in marsh samples. Dominant dead taxa were similar to living with slight reordering: combined *Amt. salsum/Amb. exiguus* group, *Mlm. fusca*, *Are. mexicana, Amn. tepida*, *Tph. comprimata*, and *Tro. inflata*.

Cluster Analysis, Biofacies Fidelity and Constancy of live Foraminifera

Following the species abundance and sample density restrictions, a sufficient number of samples remained for the live assemblages (n = 80; S = 25) to apply Q-mode cluster analysis. The NMDS analysis yielded a similarity level of 0.45 to describe the dataset in a following cluster analysis (Fig. A5.1). The resulting dendrogram (Cophenetic Correlation Coefficient = 0.77) produced the following five distinct assemblages (Fig. 2.3; Fig. A5.2). Table 2.2 shows a summary of average species abundances in the live assemblages and the most important species highlighted by BFCO in grey boxes (full BFCO dataset see Appendix A6).

(L1) The Estuarine Assemblage (n = 16) is dominated by five calcareous and one agglutinated species, *Amn. tepida* (average abundance = 49%), *Par. simplissima* (14%), *Hay. germanica* (6%), *Cel. excavatum* (5%), *Ammonia parkinsoniana* (3%), and *Cribroelphidium poeyanum* (1%). All samples assigned are exclusively from estuarine environments.

(L2) Low Marsh Assemblage (n = 9) are from sites in both marsh and estuarine environments. The only characteristic species is *Hay. germanica* (3%).

(L3) The characteristic species of the Low Salinity Assemblage (n = 5) is *Ams. inepta* (91%). The samples of this biofacies are all located in the Pascagoula study area.

(L4) The Middle Marsh Assemblage (n = 49) contains a wide variety of taxa with three characteristic species: *Are. mexicana* (26%), *Tro. inflata* (10%), and *Tph. comprimata*.

(L5) In the Upland Transition Assemblage (n = 1), three species were found to be characteristic by BFCO: *Haplophragmoides wilberti* (73%), *Pseudothurammina limnetis* (22%), and *Siphotrochammina lobata* (3%).

An abundance trend from calcareous species in the Estuarine Assemblage, both test types in the Low Marsh Assemblage, and agglutinated species in the Middle Marsh and Upland Transition was observed. The *Amt. salsum*/*Amb. exiguus* group and *Mlm. fusca* were abundant across the Estuarine to the Middle Marsh Assemblage, with a peak in the Low Marsh Assemblage.

The dead assemblage dataset was only minimally reduced for statistical analysis (*n* = 156; S = 30). A similarity level of 0.48 was suggested by NMDS to yield detailed, but not strongly overlapping grouping (Fig. A5.3). Cluster analysis applied at the suggested similarity level indicated nine biofacies (Fig. A5.4; Cophenetic Correlation Coefficient = 0.77). Table 2.3 shows a summary of average species abundances and the most important species in the nine dead biofacies highlighted by BFCO scores in grey boxes (full BFCO dataset see Appendix A6).

(D1) The three sites comprising the Open Estuary Biofacies (n = 6) were characterized by three calcareous taxa: *Cel. excavatum* (average in biofacies = 20%), *Amn. parkinsoniana* (7%), and *Hay. germanica* (0.9%). The sites are located near Dauphin Island and the Mobile Bay Tidal Inlet, and in Pascagoula most distal from the river mouth (Fig. 2.5).

(D2) The Restricted Estuary/Marsh Channel Biofacies (n = 27) was characterized by a combination of agglutinated and calcareous species: *Par. simplissima* (10%), *Cel. excavatum* (3%), *Cel. poeyanum* (2%), and *Miliolinella subrotunda* (2%). This biofacies was generally found nearshore and in the tidal channels of Pascagoula and Grand Bay (Fig. 2.5).

(D3) The Low Marsh Biofacies (n = 29) was dominated by *Mlm. fusca* (41%) and *Amt. salsum*/*Amb. exiguus* group (41%). BFCO did not detect any characteristic species (C and BF values >5; Table 2.3). This assemblage was found in both estuarine and marsh samples (Fig. 2.5).

(D4) The characteristic species in the Low Salinity Biofacies (n = 6) was *Ams. inepta* (47%). The Low Salinity Biofacies was exclusively found in Pascagoula marsh stations.

(D5) For the Middle Marsh Biofacies A (n = 64) the BFCO analysis only highlighted *Trochammina* sp. A (2%). Abundant species were *Mlm. fusca* (28%), *Tph. comprimata* (17%), *Are. mexicana* (16%), and *Amt. salsum*/*Amb. exiguus* group (13%).

(D6) In Middle Marsh Biofacies B (n = 20) no taxon exceeds the minimum criteria for BFCO, although *Are. mexicana* (36%), *H. wilbeti* (22%), and *Tro. inflata* (13%) occurred in most samples (Table 2.3).

(D7) The High Marsh Biofacies (n = 2) was identified from a single site in the northeastern Grand Bay marsh environment (Fig. 2.5). The biofacies is characterized by *Miliammina petila* (3%), which occurred in low abundances. *Entzia macrescens* was abundant in both samples (81%).

(D8) Upland Transition Biofacies A (n = 2) was encountered in the northeastern Grand Bay marsh environment near the tree-line (Fig. 2.5). The BFCO analysis revealed *Haplophragmoides manilaensis* (14%), *Trochamminita irregularis* Cushman & Brönnimann, 1948 (39%), *Ent. macrescens* (14%), and Other agglutinated species (2%) as characteristic. Furthermore, *Ent. macrescens* (25%), *Hap. wilberti* (3%), and *Pst. limnetis* (16%) occurred in both samples.

(D9) The Upland Transition Biofacies B (n = 2) was located at one site in the Fowl River study area at the highest elevation of the FR sampling transect (Fig. 2.5). *Trochamminita irregularis* (4%) was the most characteristic species, with other high abundances of *Pst. limnetis* (79%) and *Hap. wilberti* (5%).

In general, the dead assemblage mirrored the trends presented by the live assemblage, however with higher species diversity.

Species Diversity

The Fisher's α diversity index is based on the number of species (S) and number of specimens (N) per sample (Murray, 2006; see Figs. 2.6B and 2.7B for plots of diversity).Values for α of the live assemblage in the Estuarine Biofacies ranged from 0.6 (PG89G A) at the most marine station in Pascagoula to 1.9 (PG85G A; Appendix A7). In the Low Marsh Biofacies, α ranged from 0.65 (PG82G A, an estuarine sample near the Pascagoula River mouth), to 2.09 (FR26S B). Lowest diversity was recorded in the Low Salinity Biofacies (0.5 to 1.14). Highest maximum diversities were encountered in the Middle Marsh Biofacies B, where α ranged from 0.75 (PG74S A) to 4.35 (GB284S B). The Upland Transition Biofacies diversity (0.81) was very low (FR17-6S A).

Dead assemblage diversity values were higher: Fisher's α of the Open Estuary Biofacies ranged from 0.93 (PG89G B) to 2.06 (DA189G A). In the Restricted Estuary/Marsh Channel Biofacies the diversity was slightly higher with α = 1.21 (GB62G B) to 3.12 (GB59G B) (Appendix A7). Low Marsh Biofacies A had a similar range of 0.68 (DA031S B) to 2.87 (PG80S A) and Low Marsh Biofacies B from 1.06 (DA035S A) to 2.02 (PG71S A). The middle marsh was most diverse with Middle Marsh Biofacies A at 1.29 (GB49S A) to 3.91 (GB18-4S A) and Middle Marsh Biofacies B at 1.23 (GB38S B) to 4.8 (GB18-3S A). The High Marsh Biofacies species diversity ranged from 1.4 (GB282S A) to 2.57 (GB282S B). The two Upland Transition Biofacies represent the lowest maximum diversities encountered, at 1.05 (GB280S B) to 1.91 (GB280S A), and 1.51 (FR17-6S A) to 1.82 (FR17-6S B) respectively.

Patchiness of Live and Dead Foraminiferal Assemblages

The Wilcoxon paired sample test (H_0 = same mean) as a measure of variability was calculated for live and dead assemblages between replicates (Appendix A7). Neither live nor dead assemblages showed a statistically significant difference between the two replicate samples at each station at the 95% confidence level (Figs. 2.6C and 2.7C). Live assemblages are least patchy in Low Marsh B (p = 0.81), and most variable in the Middle Marsh Biofacies (0.23), which correlates with a Fisher's α peak (Fig. 2.6B–C). In the dead assemblage we found the least between-replicate variability in the Open Estuary Biofacies (p = 0.69) and most in the Middle Marsh Biofacies A (p = 0.25), where Fisher's α biodiversity was highest (Fig. 2.7C). However, when patchiness was compared with intertidal elevation or Fisher's α diversity, no significant correlations were observed (Figs. A8.1–2).

Environmental Parameters of Live and Dead Foraminiferal Assemblages

Environmental variables co-varied with the living assemblage (Fig. 2.6D–F) produced a similar pattern as the dead assemblage (Fig. 2.7D–F). Organic content and salinity increased with biofacies elevation in both live and dead assemblages. The Estuarine Biofacies sustained salinities typical for brackish environments (average L1 = 24, D1 = 26, D2 = 26), with low organic content (averages: L1 =

1% LOI OC, D1 = 1%, D2 = 4%), reflecting the absence of vegetation. Low Marsh Biofacies were more brackish (average L2 = 19, D3 = 19), with low organic component (average L2 = 2% LOI OC, D3 = 6%). In both live and dead Low Salinity Biofacies, the freshest salinity was measured (average L3 = 13, D4 = 4). Middle Marsh Biofacies live and dead showed the widest range in both organics and salinity (Fig. 2.6D–F, Fig. 2.7D–F). High Marsh Biofacies organics were 5% LOI OC. At the station of the Upland Transition Biofacies, no salinity measurement was acquired due to lack of pore water.

Canonical Correspondence Analysis of Dead Assemblage

The cluster analysis of the dead foraminiferal assemblage distinguished nine biofacies, which were subsequently used in a Canonical Correspondence Analysis to test the hypothesis that these nine biofacies (*a priori* groups) are correlated to a set of six environmental variables measured simultaneously with foraminiferal sample collection. Environmental variables are elevation (Appendix A1), grain size (%Sand, %Silt, %Clay; Appendix A2), percent organic carbon (%LOI OC; Appendix A2), and salinity (Appendix A2). The first two axes explained 83% of the variance between the nine groups. Axis 1, Eigenvalue 0.52, explaining 70% of variance was totally dominant. Axis 2, Eigenvalue 0.096, captured 13% of the variance (Table 2.4).

The CCA confirmed that there were gradients within the dataset and that the biofacies determined by the Cluster Analysis were reasonable (Fig. 2.8A). However, three biofacies were not unequivocally distinguished as D3 Low Marsh Biofacies overlaps both D5 Middle Marsh Biofacies A, and D6 Middle Marsh Biofacies B. The lengths of the constraining variable arrows define their relative weight in explaining the variance in the foraminiferal dataset, and the arrow direction represents the approximate correlation to the ordination axes and other variable arrows. Distribution was primarily (70%) influenced by elevation, %LOI OC, and %Silt, with negative correlation to %Sand. The weakest vector, %Clay, correlated with axis 2 (13% of variance). The salinity vector is correlated with axis 1 and 2, pointing towards D6 Middle Marsh Biofacies B and the two estuarine biofacies D1 and D2.

The Species-Environment biplot (Fig. 2.8B) correlates species, which were defined previously with the BFCO method (Table 2.3), with the measured environmental variables. Calcareous species such as *Cel. excavatum*, *Cel. poeyanum, Amn. parkinsoniana* plot to the right (low elevation, low %LOI OC, low %Silt, high %Sand and salinity), agglutinated species characteristic of high marsh and upland transition, such as *Tta. irregularis, Sph. lobata*, *Hap. manilaensis*, and *Mlm. petila* were found on the left (high elevation, high %LOI OC, high %Silt, low %Sand and lower salinity). Taxa defining the middle marsh plot in the center. However, a strong preference for salinity can be observed; higher salinity taxa include: *Hap. wilberti*, *Tro. inflata*, *Are. mexicana* high salinity; low salinity: *Mlm. fusca*, *Trochammina* sp. A, *Ams. inepta*.

Discussion

Comparisons Live and Dead Assemblages

Foraminiferal diversity in marshes has been reported to be very low from many regions in the world (Fisher's α 0.5–3.5; Murray and Alve, 2000; Murray, 2006). Moreover, the recruitment rates of live foraminiferal populations are variable (e.g., Buzas et al., 2002), and the proportions, diversity and concentration of dead foraminiferal assemblages can be altered by taphonomic loss (Pilarczyk et al., 2014; Hayward et al., 2015). The concept of within-habitat "pulsating patches", introduced for foraminifera by Buzas et al. (2002), explains ecologic density variations based on food availability, oxygen, etc., which can lead to non-cyclical recruitment and thus temporal (e.g., daily, weekly, monthly, seasonally, and yearly) and spatial density variation. Furthermore, considerable variability in living foraminiferal density from one year to the next has been observed by Murray and Alve (2000). Taphonomic degradation differs among marsh zones, from minor to severe (Berkeley et al., 2009).

Cluster analyses delineated five live assemblages and nine dead biofacies. Within these, Fisher α diversity was correlated with number of samples (Figs. 2.6B and 2.7B). As observed in other studies (Horton and Edwards, 2003), species richness and abundance were higher in the dead assemblages than

the living, leading to an increase in the number of discernible biofacies. Nevertheless, the living assemblages and dead biofacies in our study reflect similar environmental zones. Out of 87 stations, the live assemblages assigned differed from the dead biofacies at only six stations (GB43G, GB45G, PG76S, PG77S, FR26S, and DA13S) and then only by one environmental zone higher or lower. Within the dead assemblage, one replicate pair was assigned different biofacies reflecting slightly different salinity conditions (DA035S A: D4 Low Salinity Biofacies; DA035S B: D3 Low Marsh Biofacies). Another single station replicate sample pair was assigned to different elevational zones (GB49S A, D5 Middle Marsh Biofacies A; GB49S B, D3 Low Marsh Biofacies). Thus, while the dead assemblage biofacies proved to be more consistent, the living and dead assemblages overwhelmingly recorded similar environments.

The specimen densities of the five live assemblages reflected the foraminiferal response to environmental factors. Since the samples stem from four sampling months between 2013 and 2016, the living densities might reflect different stages of foraminiferal bloom cycles. In the L1 Estuarine Assemblage and L4 Middle Marsh Assemblage, on average the highest densities (per 10 cm^3 volume) of live specimens were found (average of 299 and 250 specimens; Fig. 2.6A). In L2 Low Marsh Assemblage, densities averaged 192 specimens per 10 cm^3. L3 Low Salinity Assemblage and L5 Upland Transition Assemblage showed the lowest living densities (average of 34 and 88 specimens). The low numbers of live specimens in the L3 Low Marsh (all in Pascagoula study area) suggest a strong influence of freshwater input from the Pascagoula River floating above the saltwater wedge. The L5 Upland Transition Assemblage is infrequently inundated by seawater, which makes it prone to stress factors such as freshwater, desiccation, and heat.

In the nine biofacies of dead foraminifera test densities rapidly decreased from subtidal to intertidal environments. Highest test densities occurred in the D1 Open Estuary and D2 Restricted Estuary (average of 2,342 and 1,147 specimens per 10 cm^3; Fig. 2.7A). Intermediate densities were found in the following biofacies: D3 Low Marsh (394), D5 Middle Marsh A and D6 Middle Marsh B (404 and 371), D7 High Marsh (455), D8 Upland A and D9 Upland B (360 and 430). The lowest test densities (average

of 41) were found in the D4 Low Marsh Biofacies samples, which are found at three stations in the Pascagoula marshes and one Dauphin Island station.

Taphonomy

Calcareous specimens were primarily found at the submerged stations, but not exclusively. We observed a maximum relative abundance of live calcareous specimens of 64% (179 specimens per 10 cm^3 sediment) in the L1 Estuarine Biofacies compared to maximum relative abundances of dead calcareous tests in D1 Open Estuary and D2 Restricted Estuary Biofacies (95% and 31%; 2,221 and 410 specimens per 10 cm^3 sediment respectively; see Figs. 2.6A and 2.7A). The remaining subaerial biofacies contain a maximum of 12% calcareous specimens in the living and 1% in dead the assemblage, which is in accordance with the literature and shows that abundance of calcareous taxa is not necessarily indicative of low marsh or tidal channel environments (Horton and Edwards, 2006). The relatively few calcareous tests in the surface-sediment dead assemblage of our study area may be attributable to the low pH of intertidal salt marshes.

This dichotomy of calcareous test abundance in dead and living assemblages suggests that many calcareous tests were dissolved after the individual died, which is a common taphonomic alteration effect. The pH of typical coastal waters is within a range from 7.4 to 9.6 (Marion et al., 2011), but conditions may be more acidic associated with salt-marsh sediments (Scott and Medioli, 1980b). Alve and Nagy (1986) reported inner organic linings that remained after dissolution of tests under a pH range of 6.5 to 7.2. Murray (2006) found evidence of etching as early stage of dissolution of the calcareous test where the pH of the environment was below 7.8. Calcareous tests of foraminifera are frequently not preserved in salt marshes after burial of the individual due to acidity in interstitial water (Parker and Athearn, 1959; Berkeley et al., 2008). The biplots of percentage of calcareous specimen versus organics (Fig. A8.3) show that estuarine samples contain up to 5% LOI OC and still contain significant amounts calcareous tests (up to 100% live or dead). Increase in carbonic acid (e.g., from plant respiration at night as well as microbial respiration) and production of bicarbonate and/or increases in hydrogen sulfide from the degradation of

organic matter promotes more acidic conditions in marsh environments (Koretsky et al., 2003). Intertidal marsh samples however, contained up to 25% dead and 88% live calcareous specimens, with the majority having less than 5% and 10% respectively (Fig. A8.3). On average, the calcareous test percentage decreased from live to dead assemblages in the Restricted Estuary Biofacies from 64% to 29%, in the Low Marsh from 14% to 1%, and in Middle Marsh from 9% to 1% (Fig. 2.6A, Fig. 2.7A).

Post-depositional dissolution of calcareous tests has been reported from estuarine intertidal environments along the U.S. coastlines including Mobile Bay (Osterman and Smith, 2012), Nueces Bay (Buzas-Stephens and Buzas, 2005), Delmarva Peninsula (Culver et al., 1996), St. Catherines Island, Georgia (Goldstein and Watkins, 1999), Folly Island, South Carolina (Hippensteel, 2011), North Inlet, South Carolina (Tobin et al., 2005), and Albemale Estuarine System (Vance et al., 2006). Taphonomic alteration led many authors to conclude that if downcore (buried) assemblages experience similar effects to those affecting surface dead assemblages, then dead assemblages provide better proxies for environmental reconstruction than total assemblages (i.e., sum of live and dead; Murray, 2000; Horton and Murray, 2007). Our findings support the use of the dead assemblage in marsh surveys due to the taphonomic loss of calcareous taxa.

Patchiness of Modern Foraminifera

A number of studies have reported both spatial and temporal variability in density or assemblage composition (Buzas, 1969; Scott and Medioli, 1980a; Hippensteel et al., 2002; Buzas et al., 2015). Thus spatial and seasonal replicates are recommended with three or more replicates suggested in the literature (Schönfeld et al., 2012; Buzas et al., 2015; Milker et al., 2015). The Wilcoxon paired test that we applied to our two replicate sample set indicated that small-scale variability, also known as patchiness, was not statistically significant in either live or dead assemblages. Patchiness did not correlate with elevation in the tidal zone or with diversity (Figs. A8.1–2). Despite this insignificance, we observed higher dissimilarities particularly in the live middle marsh assemblage (Fig. 2.6C) and in the dead assemblage in the low and middle marsh biofacies (Fig. 2.7C). Kemp et al. (2011) assessed the patchiness and

distribution of six key marsh species (*Mlm. fusca*, *Tro. inflata*, *Are. mexicana*, *Tph. comprimata*, *Hap. wilberti*, and *Ent. macrescens*) of dead assemblages at Oregon Inlet marsh (North Carolina) and attributed their higher variability in the middle marsh to inconstant environmental conditions. Similar results or increased dissimilarity in the middle marsh were noted by Milker et al. (2015) at Tom's Creek Marsh, Oregon. De Rijk (1995) suggests that inundation frequency within the middle marsh is the most important influence on the spatial distribution of benthic foraminifera. In the Eastern Mississippi Sound marshes, the %LOI OC and salinity show wider variability in the low and middle marsh than elsewhere in the study area (Fig. 2.7D–E), which may contribute to the higher variability in abundance.

Biofacies Distribution

We observed significant differences in foraminiferal assemblages found in the Mississippi Sound marshes. Both live assemblages and dead biofacies showed a clear vertical zonation (Fig. 2.8A). The dead assemblage yielded a more detailed picture. The difference is a consequence of the larger number of species and higher densities (Figs. 2.6A and 2.7A). Based upon the improved detail of the dead assemblages as modern analogs for paleo-environmental reconstruction, the following discussion of vertical zonation is based only upon the dead assemblage.

The dead assemblage of foraminifera from the four study areas in the Mississippi Sound can be divided into elevation-dependent biofacies that are comparable to the characteristic pattern of vertical zonation observed in other temperate regions of the world (Kemp et al., 2009; Hawkes et al., 2010; Hayward et al., 2010; 2015; Milker et al., 2015). Overall, assemblages we identified showed regional coherency across most sampled locations.

The Eastern Mississippi Sound is relatively uniform (similar width, depth, surface water input and tidal regime) between Mobile Bay and Pascagoula, unlike some U.S. Atlantic coast marshes in the Albermale/Pamlico Sound (Kemp et al., 2009). This leads to the spatial dominance of a widespread middle marsh as compared to the narrow nature of low marsh, high marsh, and upland transition, which is demonstrated by the relatively uniform assemblage found throughout Grand Bay at a km-scale sampling

transect while the smaller m-scale transect at the northern end of Grand Bay highlights the elevational gradient. However, some regional differences in faunal compositions were noted. The variability among previous studies mirrors the range of parameters that influence the distributions of modern foraminifera (e.g., Phleger, 1970; De Rijk, 1995; Murray, 2006; Kemp et al., 2009).

The Open Estuary Biofacies was found at depths from -2.2 to -3.9 m and salinities from 23 to 28 at sites near Dauphin Island and one site in the Pascagoula River study area most offshore. Phleger (1954) and Lamb (1972) noted that high abundances of *Ammonia* and *Cribroelphidium* (combined >90%) are indicative of open gulf environment and increased salinity. *Ammonia tepida* reached up to 91% abundance, which is exemplary for medium-salinity estuarine settings (Buzas-Stephens et al., 2002; Haller, 2012; Poag, 2015; Romano et al., 2016).

The Restricted Estuary/Marsh Channel Biofacies was rich in calcareous taxa, mixed with typical species such as *Mlm. fusca*, the *Amt. salsum*/*Amb. exiguus group*, and *Par. simplissima* at subtidal stations proximal to the marsh edge (depth -2.3 to -0.7 m, salinity 18–25; Figs. 2.5 and 2.6A). The Low Marsh Biofacies is very similar to the Restricted Estuary Biofacies, as the presence of a low marsh assemblage at two estuarine stations in Pascagoula indicates (Fig. 2.5). Alternatively, this resemblance might be explained by sediment slumping or marsh-fringe erosion. The Low Marsh Biofacies was dominated by *Mlm. fusca*, the *Amt. salsum/Amb. exiguus* group, a species association that has often been reported from this environment from tidal flats and low marshes of the world (Kemp et al., 2009; Hawkes et al., 2010; Kemp et al., 2012, 2013; Milker et al., 2015). *Miliammina fusca* is often considered as indicator species of low marsh environments (Engelhart et al., 2013) and sometimes muddy substrates (Müller-Navarra et al., 2017).

The Low Salinity Biofacies was found at oligohaline stations such as the Pascagoula River salt marshes (salinity: 0.93–8). *Ammoastuta inepta* plays a dominant role at low salinities (Fig. 2.4, Table 2.4), as previously reported by Kemp et al. (2013) and Scott et al. (2001) from other North American marshes.

In the Middle Marsh the the *Amt. salsum*/*Amb. exiguus* group and *Mlm. fusca* decrease in proportion as *Tro. inflata*, *Sph. lobata*, and *Ent. macrescens* appear in low numbers, and *Are. mexicana* becomes dominant (up to 53%; Fig. 2.4). We recognized two sub-biofacies, which are found at similar elevations. Middle Marsh Biofacies A (-0.01–0.68 m) is characterized by medium abundances of *Are. mexicana*, low *Hap. wilberti* and occurrences of *Trochammina* sp. A (Table 2.3). In Middle Marsh Biofacies B (0.10–0.68 m), the abundance of *Hap. wilberti* and *Are. mexicana* increased while the *Amt. salsum/Amb. exiguus* group and *Mlm. fusca* further decreased (Fig. 2.5). The canonical correspondence analysis (Fig. 2.8) indicates influence of increased salinity in Middle Marsh Biofacies B. *Haplophragmoides wilberti* has been reported to be more abundant in higher salinity environments (De Rijk, 1995; Kemp et al., 2009), which suggests that Middle Marsh B experiences stronger evaporation.

The High Marsh Biofacies was foremost dominated by *Ent. macrescens* (76–86%), with co-occurrence of *Mlm. petila*. *Entzia macrescens* has commonly been reported from high marsh environments of the Gulf Coast (Phleger, 1965), Nova Scotia (Scott and Medioli, 1980b), St. Catherines Island (Goldstein and Watkins, 1998), Oregon (Milker et al., 2016), and England (Horton and Murray, 2007). *Entzia macrescens* has been observed in areas where the tides drain the salt marsh regularly (Gehrels and van de Plassche, 1999), but also higher elevations relative to the tidal frame and raised salinity (de Rijk and Troelstra, 1999; Horton et al., 1999; Shaw et al., 2016; Kemp et al., 2017). Similarly, *Mlm. petila* has been observed in the middle and high marshes of Siletz Bay, Oregon (Engelhart et al., 2013) and high marsh and upland transition zone of Coos Bay, Oregon (Milker et al., 2015).

The Upland Transition Biofacies was recognized from Fowl River and Grand Bay at 0.72 and 0.9 m respectively. This biofacies is dominated by *Tta. irregularis* with lower percentages of *Ent. macrescens*, *Hap. manilaensis*, and *Pst. limnetis* in Grand Bay, and *Hap. wilberti*, *Tro. inflata*, and *Pst. limnetis* in Fowl River (Table 2.3). Fowl River also contained larger proportions of unidentifiable, misshaped and broken specimens, which might be due to the high desiccation stress and most likely low salinity (no pore water was encountered). *Trochamminita irregularis* has been reported from the upland

transition of marshes in the northwestern Pacific region of the U.S.A. (Hawkes et al., 2010; Engelhart et al., 2013; Milker et al., 2015).

Conclusions

We documented the distribution of salt-marsh foraminifera from four study areas in the Mississippi Sound, which represent a wide variety of physiographic conditions. We used Cluster Analysis and Canonical Correspondence Analysis to identify elevation and salinity dependent biofacies, which are comparable to the vertical zonation reported from salt marshes in other regions of North America and around the world. Overall, assemblages showed a good coherency across sampled regions most likely because the Eastern Mississippi Sound is relatively uniform, dominated by a widespread middle marsh. True elevational gradients from tidal creek to upland can occur over short horizontal distances (m-scale) and are found far inland.

Both the live and dead assemblages in the eastern Mississippi Sound study areas showed a non-significant patchiness. The variability between two replicates placed apart 1 m increased in the low marsh and showed highest variability in the middle marsh. This may be explained by increased variability in salinity and organic content, but also more intense evaporation and variable microtopography. However, we suggest that future studies in the Gulf of Mexico marshes might increase the number of replicates to improve statistical validity.

Cluster Analysis performed on live and dead assemblages showed a general agreement with respect to species distribution, though subdivisions were not detected in the live assemblage due to lower densities of specimens. Both live and dead assemblages in the Eastern Mississippi Sound marshes show an elevation-dependent distribution with gradual abundance shifts. The dead biofacies is comparable to previously reported distributions for other intertidal sites in North America, but with noteworthy regional differences.

Subtidal estuarine environments were typically defined by abundant calcareous taxa such as *Amn. tepida*, and *Cel. excavatum*. Tidal channels and restricted estuarine environments were populated by a mix of coarsely agglutinated low-marsh taxa (e.g., the *Amt. salsum*/*Amb. exiguus* group, *Mlm. fusca*) and calcareous taxa including *C. exavatum, Amn. tepida*, and *Hay. germanica*. Low marsh environments were defined by abundant *Amt. salsum*/*Amb. exiguus* group, and agglutinated miliolids such as *Mlm. fusca*. In low salinity regimes, foraminiferal density decreased considerably and *Ams. inepta* greatly gained in proportion. With increasing elevation, *Amt. salsum*, *Amb. exiguus*, and *Mlm. fusca* were gradually replaced by *Are. mexicana, Trochammina* sp. A, *Tph. comprimata, Sph. lobata*, and *Tro. inflata*. In high marsh and upland transition environments, *Ent. macrescens, Pst. limnetis* and *Tta. irregularis* were the most common taxa.

For paleo-environmental reconstructions, the nine biofacies of the dead assemblages are recommended since they represent a fuller spectrum of the fauna present. The Canonical Correspondence Analysis performed on the regional dataset of 156 samples revealed the environmental influences on the foraminifera in the study area and corroborated the elevational dependence of the biofacies. A strong correlation with elevation was %LOI OC. The most important secondary influence is salinity, which is the environmental factor for distinguishing open estuarine from restricted estuarine, high freshwater input areas (Pascagoula River) from brackish salinities, and evaporation and desiccation influence in middle marshes. Any use of trade names is for descriptive purposes only and does not imply endorsement by the U.S. Government.

Acknowledgments

We thank the Grand Bay National Estuarine Research Reserve (NERR) in Moss Point, MS for permission to work in the Grand Bay Marsh. Marci Marot, Alisha Ellis and C. Scott Adams provided logistical support and helped sampling during our field activities. We thank Cathryn Wheaton for grain-size measurements, and Nancy DeWitt and Nicolas Zaremba for assistance with the GPS data processing.

Furthermore, Elizabeth A. Brown, Benjamin Ross, and Tony Greco assisted with the electron microscopy at the University of South Florida, College of Marine Science. This project was mainly carried out at the St. Petersburg Coastal and Marine Science Center, United States Geological Survey. Moreover, we thank internal USGS reviewer Stanley Locker for his comments. The foraminiferal census of this study is also available as USGS Data Release https://doi.org/10.5066/F7MC8X5F. Any use of trade names is for descriptive purposes only and does not imply endorsement by the U.S. Government.

References

Abbene, I.J., Culver, S.J., Corbett, D.R., Buzas, M.A., Tully, L.S., 2006. Distribution of foraminifera in Pamlico Sound, North Carolina, over the past century. Journal of Foraminiferal Research 36, 135–151. 10.2113/36.2.135

Abu-Zied, R.H., Al-Dubai, T.A.M., Bantan, R.A., 2016. Environmental conditions of shallow waters alongside the Southern Corniche of Jeddah based on benthic foraminifera, physico-chemical parameters and heavy metals. Journal of Foraminiferal Research 46, 149–170. 10.2113/gsjfr.46.2.149

Alve, E., Nagy, J., 1986. Estuarine foraminiferal distribution in Sandebukta, a branch of the Oslo Fjord. Journal of Foraminiferal Research 16, 261–284. 10.2113/gsjfr.16.4.261

Anderson, J.B., 1968. Ecology of foraminifera from Mississippi Sound and surrounding waters. Journal of Alabama Academy of Science 39, 261–269.

Barnett, R.L., Garneau, M., Bernatchez, P., 2016. Salt-marsh sea-level indicators and transfer function development for the Magdalen Islands in the Gulf of St. Lawrence, Canada. Marine Micropaleontology 122, 13–26. 10.1016/j.marmicro.2015.11.003

Berkeley, A., Perry, C.T., Smithers, S.G., Horton, B.P., 2008. The spatial and vertical distribution of living (stained) benthic foraminifera from a tropical, intertidal environment, north Queensland, Australia. Marine Micropaleontology 69, 240–261. 10.1016/j.marmicro.2008.08.002

Berkeley, A., Perry, C.T., Smithers, S.G., Horton, B.P., Cundy, A.B., 2009. Foraminiferal biofacies across mangrove-mudflat environments at Cocoa Creek, north Queensland, Australia. Marine Geology 263, 64–86. 10.1016/j.margeo.2009.03.019

Bernhard, J.M., 1988. Postmortem vital staining in benthic foraminifera; duration and importance in population and distributional studies. Journal of Foraminiferal Research 18, 143–146. 10.2113/gsjfr.18.2.143

Bernhard, J.M., 2000. Distinguishing live from dead foraminifera: Methods review and proper applications. Micropaleontology 46, 38–46. 10.2307/1486179

Bernier, J.C., Kelso, K.W., Buster, N.A., Flocks, J.G., Miselis, J.L., DeWitt, N.T., 2014. Sediment data collected in 2012 from the northern Chandeleur Islands, Louisiana, Data Series, Reston, VA.

Blott, S.J., Pye, K., 2001. GRADISTAT: A grain size distribution and statistics package for the analysis of unconsolidated sediments. Earth Surface Processes and Landforms 26, 1237-1248. Doi 10.1002/Esp.261

Bolliet, T., Jorissen, F.J., Schmidt, S., Howa, H., 2014. Benthic foraminifera from Capbreton Canyon revisited; faunal evolution after repetitive sediment disturbance. Deep Sea Research Part II: Topical Studies in Oceanography 104, 319–334. 10.1016/j.dsr2.2013.09.009

Brinson, M.M., 1993. A hydrogeomorphic classification for wetlands. U.S. Army Corps of Engineers, Waterways Experiment Station, Washington DC, p. 79.

Buzas-Stephens, P., Buzas, M.A., 2005. Population dynamics and dissolution of foraminifera in Nueces Bay, Texas. Journal of Foraminiferal Research 35, 248–258. 10.2113/35.3.248

Buzas-Stephens, P., Pessagno, E.A., Jr., Bowen, C.J., 2002. A review of species names for *Ammonia* and *Elphidium*, common foraminifera along the Texas Gulf Coast. Texas Journal of Science 54, 3–16.

Buzas, M.A., 1969. Foraminiferal species densities and environmental variables in an estuary. Limnology and Oceanography 14, 411–422. 10.4319/lo.1969.14.3.0411

Buzas, M.A., 1990. Another look at confidence limits for species proportions. Journal of Paleontology 64, 842–843.

Buzas, M.A., Hayek, L.-A.C., Jett, J.A., Reed, S.A., 2015. Pulsating patches: History and analyses of spatial, seasonal, and yearly distribution of living benthic foraminifera. Smithsonian Institution Scholarly Press, 91 pp.

Buzas, M.A., Hayek, L.-A.C., Reed, S.A., Jett, J.A., 2002. Foraminiferal densities over five years in the Indian River Lagoon, Florida: A model of pulsating patches. Journal of Foraminiferal Research 32, 68–92. 10.2113/0320068

Calvo-Marcilese, L., Pérez Panera, J.P., Cusminsky, G., Gómez, E.A., 2013. Micropaleontological record of Holocene estuarine stages in the Bahía Blanca estuary, Argentina. Journal of South American Earth Sciences 45, 147–159. 10.1016/j.jsames.2013.03.005

Cipriani, L.E., Stone, G.W., 2001. Net longshore sediment transport and textural changes in beach sediments along the southwest Alabama and Mississippi barrier islands, U.S.A. Journal of Coastal Research 17, 443–458.

Culver, S.J., Farrell, K.M., Mallinson, D.J., Horton, B.P., Willard, D.A., Thieler, E.R., Riggs, S.R., Snyder, S.W., Wehmiller, J.F., Bernhardt, C.E., Hillier, C., 2008. Micropaleontologic record of late Pliocene and Quaternary paleoenvironments in the northern Albemarle Embayment, North Carolina, U.S.A. Palaeogeography, Palaeoclimatology, Palaeoecology 264, 54–77. 10.1016/j.palaeo.2008.03.012

Culver, S.J., Woo, H.J., Oertel, G.F., Buzas, M.A., 1996. Foraminifera of coastal depositional environments, Virginia, U.S.A.; distribution and taphonomy. Palaios 11, 459–486. 10.2307/3515213

Cushman, A.J., Brönnimann, P., 1948. Some new genera and species of foraminifera from brackish water of Trinidad. Contributions from the Cushman Laboratory for Foraminiferal Research 24, 15–21.

De Rijk, S., 1995. Salinity control on the distribution of salt marsh foraminifera (Great Marshes, Massachusetts). Journal of Foraminiferal Research 25, 156–166. 10.2113/gsjfr.25.2.156

de Rijk, S., Troelstra, S., 1999. The application of a foraminiferal actuo-facies model to salt-marsh cores. Palaeogeography, Palaeoclimatology, Palaeoecology 149, 59–66. 10.1016/S0031-0182(98)00192-8

Dean, W.E., 1974. Determination of carbonate and organic matter in calcareous sediments and sedimentary rocks by loss on ignition; comparison with other methods. Journal of Sedimentary Research 44, 242–248. 10.1306/74d729d2-2b21-11d7-8648000102c1865d

Edwards, R., Wright, A.J., 2015. Foraminifera, Handbook of Sea-Level Research. John Wiley & Sons, Ltd, pp. 191–217.

Ellis, A.M., Culver, S.J., Mallinson, D.J., Corbett, D.R., Leorri, E., Buzas, M.A., Shazili, N.A.M., 2014. The influence of aquaculture on modern foraminifera and sediments in the Setiu estuary and lagoon, Terengganu, Malaysia: A spatial investigation. Journal of Foraminiferal Research 44, 390–415. 10.2113/gsjfr.44.4.390

Engelhart, S.E., Horton, B.P., Vane, C.H., Nelson, A.R., Witter, R.C., Brody, S.R., Hawkes, A.D., 2013. Modern foraminifera, $\delta^{13}C$, and bulk geochemistry of central Oregon tidal marshes and their application in paleoseismology. Palaeogeography, Palaeoclimatology, Palaeoecology 377, 13–27. 10.1016/j.palaeo.2013.02.032

Fatela, F., Taborda, R., 2002. Confidence limits of species proportions in microfossil assemblages. Marine Micropaleontology 45, 169–174. 10.1016/S0377-8398(02)00021-X

Folk, R.L., Ward, W.C., 1957. Brazos River bar [Texas]; a study in the significance of grain size parameters. Journal of Sedimentary Research 27, 3–26.

Gehrels, W.R., van de Plassche, O., 1999. The use of *Jadammina macrescens* (Brady) and *Balticammina pseudomacrescens* Brönnimann, Lutze and Whittaker (Protozoa: Foraminiferida) as sea-level indicators. Palaeogeography, Palaeoclimatology, Palaeoecology 149, 89–101. 10.1016/S0031-0182(98)00194-1

Goldstein, S.T., Watkins, G.T., 1998. Elevation and the distribution of salt-marsh foraminifera, St. Catherines Island, Georgia: A taphonomic approach. Palaios 13, 570–580. 10.2307/3515348

Goldstein, S.T., Watkins, G.T., 1999. Taphonomy of salt marsh foraminifera: an example from coastal Georgia. Palaeogeography, Palaeoclimatology, Palaeoecology 149, 103–114. 10.1016/S0031-0182(98)00195-3

Haller, C., 2012. Foraminifera as bio-indicators of anthropogenic impact in the Bay of Seine, France, in: Dauvin, J.-C., Brind'Amour, A., Dancié, C., Desroy, N., Le Hir, P., Lesourd, S., Morin, J. (Eds.), Rapport Seine-Aval COLMATAGE. GIP Seine-Aval, Rouen, p. 209.

Hammer, Ø., Harper, D.A.T., Ryan, P.D., 2001. PAST: Paleontological statistics software package for education and data analysis. Palaeontologia Electronica 4, 9. http://palaeo-electronica.org/2001_1/past/issue1_01.htm

Hannah, F., Rogerson, A., 1997. The temporal and spatial distribution of foraminiferans in marine benthic sediments of the Clyde Sea area, Scotland. Estuarine, Coastal and Shelf Science 44, 377–383. 10.1006/ecss.1996.0136

Hawkes, A.D., Horton, B.P., Nelson, A.R., Hill, D.F., 2010. The application of intertidal foraminifera to reconstruct coastal subsidence during the giant Cascadia earthquake of AD 1700 in Oregon, USA. Quaternary International 221, 116–140. 10.1016/j.quaint.2009.09.019

Hayward, B.W., Clark, K.J., Sabaa, A.T., Cochran, U., 2015. Taphonomically- and infaunally-adjusted salt marsh foraminiferal record of Late Holocene Earthquake displacemtns and a tsunami sand, New Zealand. Journal of Foraminiferal Research 45, 354–368. 10.2113/gsjfr.45.4.354

Hayward, B.W., Grenfell, H.R., Sabaa, A.T., Kay, J., 2010. Using foraminiferal faunas as proxies for low tide level in the estimation of Holocene tectonic subsidence, New Zealand. Marine Micropaleontology 76, 23–36. 10.1016/j.marmicro.2010.04.002

Hazel, J.E., 1977. Use of certain multivariate and other techniques in assemblage zonal biostratigraphy: examples utilizing Camrian, Cretaceous and Teriary benthic invertebrates, in: Kauffman, E.G., Hazel, J.E. (Eds.), Concepts and methods of biostratigraphy. Dowden, Hutchinson & Ross, Stroudsburg, Pa, pp. 187–212.

Hippensteel, S.P., 2011. Spatio-lateral continuity of hurricane deposits in back-barrier marshes. Geological Society of America Bulletin 123, 2277–2294. Doi 10.1130/B30261.1

Hippensteel, S.P., Martin, R.E., Nikitina, D., Pizzuto, J.E., 2002. Interannual variation of marsh foraminiferal assemblages (Bombay Hook National Wildlife Refuge, Smyrna, DE): Do foraminiferal assemblages have a memory? Journal of Foraminiferal Research 32, 97–109. 10.2113/0320097

Horton, B.P., Edwards, R.J., 2003. Seasonal distributions of foraminifera and their implications for sea-level studies, Cowpen Marsh, U.K., in: Leckie, R.M., Olson, H.C. (Eds.), SEPM Specieal Publication, pp. 21–30.

Horton, B.P., Edwards, R.J., 2006. Quantifying Holocene sea level change using intertidal foraminifera: Lessons from the British Isles. Cushman Foundation for Foraminiferal Research, Special Publication 40, p. 97.

Horton, B.P., Edwards, R.J., Lloyd, J.M., 1999. UK intertidal foraminiferal distributions: implications for sea-level studies. Marine Micropaleontology 36, 205-223. 10.1016/S0377-8398(99)00003-1

Horton, B.P., Murray, J.W., 2007. The roles of elevation and salinity as primary controls on living foraminiferal distributions: Cowpen Marsh, Tees Estuary, UK. Marine Micropaleontology 63, 169–186. 10.1016/j.marmicro.2006.11.006

Kemp, A.C., Buzas, M.A., Horton, B.P., Culver, S.J., 2011. Influence of patchiness on modern salt-marsh foraminifera used in sea-level studies (North Carolina, USA). Journal of Foraminiferal Research 41, 114–123. 10.2113/gsjfr.41.2.114

Kemp, A.C., Horton, B.P., Culver, S.J., 2009. Distribution of modern salt-marsh foraminifera in the Albemarle-Pamlico estuarine system of North Carolina, USA: Implications for sea-level research. Marine Micropaleontology 72, 222–238. 10.1016/J.Marmicro.2009.06.002

Kemp, A.C., Horton, B.P., Vann, D.R., Engelhart, S.E., Pre, C.A.G., Vane, C.H., Nikitina, D., Anisfeld, S.C., 2012. Quantitative vertical zonation of salt-marsh foraminifera for reconstructing former sea level, an example from New Jersey, USA. Quaternary Science Reviews 54, 26–39. 10.1016/J.Quascirev.2011.09.014

Kemp, A.C., Telford, R.J., Horton, B.P., Anisfeld, S.C., Sommerfield, C.K., 2013. Reconstructing Holocene sea level using salt-marsh foraminifera and transfer functions: lessons from New Jersey, USA. Journal of Quaternary Science 28, 617–629. 10.1002/jqs.2657

Kemp, A.C., Wright, A.J., Barnett, R.L., Hawkes, A.D., Charman, D.J., Sameshima, C., King, A.N., Mooney, H.C., Edwards, R.J., Horton, B.P., van de Plassche, O., 2017. Utility of salt-marsh foraminifera, testate amoebae and bulk-sediment δ13C values as sea-level indicators in Newfoundland, Canada. Marine Micropaleontology 130, 43–59. 10.1016/j.marmicro.2016.12.003

Koch, C.F., 1987. Prediction of sample size effects on the measured temporal and geographic distribution patterns of species. Paleobiology 13, 100–107.

Koretsky, C.M., Moore, C.M., Lowe, K.L., Meile, C., Dichristina, T.J., Van Cappellen, P., 2003. Seasonal oscillation of microbial iron and sulfate reduction in saltmarsh sediments (Sapelo Island, GA, USA). Biogeochemistry 64, 179–203. 10.1023/A:1024940132078

Lamb, G.M., 1972. Distribution of Holocene foraminifera in Mobile Bay and the effect of salinity changes, in: Scarbrough, W.L. (Ed.), Recent sedimentation along the Alabama coast. Alabama Geological Society, pp. 8–26.

Marion, G.M., Millero, F.J., Camões, M.F., Spitzer, P., Feistel, R., Chen, C.T.A., 2011. pH of seawater. Marine Chemistry 126, 89–96. 10.1016/j.marchem.2011.04.002

Marot, M.E., Adams, C.S., Richwine, K.A., Smith, C.G., Osterman, L.E., Bernier, J.C., 2014. Temporal changes in lithology and radiochemistry from the back-barrier environments along the Chandeleur Islands, Louisiana: March 2012-July 2013, Open-File Report, Reston, VA.

Martin, R.E., 2000. Environmental micropaleontology-The application of microfossils to environmental geology. Springer Science+Business Media, New York, 481 pp.

Mello, J.F., Buzas, M.A., 1968. An application of cluster analysis as a method of determining biofacies. Journal of Paleontology 42, 747–758. 10.2307/1302372

Milker, Y., Horton, B.P., Nelson, A.R., Engelhart, S.E., Witter, R.C., 2015. Variability of intertidal foraminiferal assemblages in a salt marsh, Oregon, USA. Marine Micropaleontology 118, 1–16. 10.1016/j.marmicro.2015.04.004

Milker, Y., Nelson, A.R., Horton, B.P., Engelhart, S.E., Bradley, L.-A., Witter, R.C., 2016. Differences in coastal subsidence in southern Oregon (USA) during at least six prehistoric megathrust earthquakes. Quaternary Science Reviews 142, 143–163. 10.1016/j.quascirev.2016.04.017

Müller-Navarra, K., Milker, Y., Schmiedl, G., 2017. Applicability of transfer functions for relative sea-level reconstructions in the southern North Sea coastal region based on salt-marsh foraminifera. Marine Micropaleontology 135, 15–31. 10.1016/j.marmicro.2017.06.003

Murray, J.W., 2000. The enigma of the continued use of total assemblages in ecological studies of benthic foraminifera. Journal of Foraminiferal Research 30, 244–245. 10.2113/0300244

Murray, J.W., 2006. Ecology and Applications of Benthic Foraminifera. Cambridge University Press, 426 pp.

Murray, J.W., Alve, E., 2000. Major aspects of foraminiferal variability (standing crop and biomass) on a monthly scale in an intertidal zone. Journal of Foraminiferal Research 30, 177–191. 10.2113/0300177

Osterman, L.E., Smith, C.G., 2012. Over 100 years of environmental change recorded by foraminifers and sediments in Mobile Bay, Alabama, Gulf of Mexico, USA. Estuarine Coastal and Shelf Science 115, 345–358. 10.1016/J.Ecss.2012.10.001

Parker, F.L., 1954. Distribution of the foraminifera in the northeastern Gulf of Mexico. Bulletin of The Museum of Comparative Zoology at Harvard College 110, 451–588.

Parker, F.L., Athearn, W.D., 1959. Ecology of marsh foraminifera in Poponesset Bay, Massachusetts. Journal of Paleontology 33, 333.

Phleger, F.B., 1951. Part I. Foraminifera distribution. Geological Society of America Memoirs 46, 1–84. 10.1130/MEM46-p1-0001

Phleger, F.B., 1954. Ecology of foraminifera and associated microorganisms from Mississippi Sound and environs. AAPG Bulletin 38, 584–646.

Phleger, F.B., 1960. Sedimentary patterns of microfaunas in Northern Gulf of Mexico, in: Shepard, F.P., Phleger, F.B., van Andel, T.H. (Eds.), Recent Sediments, Northwest Gulf of Mexico. AAPG Special Publication 21, pp. 267–301.

Phleger, F.B., 1965. Patterns of marsh foraminifera, Galveston Bay, Texas. Limnology and Oceanography 10, R169–R184. 10.4319/lo.1965.10.suppl2.r169

Phleger, F.B., 1970. Foraminiferal populations and marine marsh processes. Limnology and Oceanography 15, 522–534. 10.4319/lo.1970.15.4.0522

Phleger, F.B., Parker, F.L., 1951. Part II. Foraminifera species. Geological Society of America Memoirs 46, 1–80. 10.1130/MEM46-p2-0001

Phleger, F.B., Walton, W.R., 1950. Ecology of marsh and bay foraminifera, Barnstable, Massachusetts. American Journal of Science 248, 274–294. 10.2475/ajs.248.4.274

Pilarczyk, J.E., Dura, T., Horton, B.P., Engelhart, S.E., Kemp, A.C., Sawai, Y., 2014. Microfossils from coastal environments as indicators of paleo-earthquakes, tsunamis and storms. Palaeogeography, Palaeoclimatology, Palaeoecology 413, 144–157. 10.1016/j.palaeo.2014.06.033

Poag, C.W., 2015. Benthic foraminifera of the Gulf of Mexico - distribution, ecology, paleoecology. Texas A&M Univesity Press, College Station, 255 pp.

Priddy, R.R., Crisler, R.M., Sebren, C.P., Powell, J.D., Burford, H., 1955. Sediments of Mississippi Sound and inshore waters: a cumulative report of summer investigations, 1952, 1953, 1954, Mississippi State Geological Survey Bulletin 82, University, Mississippi, p. 54.

Redfield, A.C., 1972. Development of a New England salt marsh. Ecological Monographs 42, 201–237. 10.2307/1942263

Romano, E., Bergamin, L., Ausili, A., Magno, M.C., Gabellini, M., 2016. Evolution of the anthropogenic impact in the Augusta Harbor (Eastern Sicily, Italy) in the last decades: Benthic foraminifera as indicators of environmental status. Environmental Science and Pollution Research 23, 10514–10528. 10.1007/s11356-015-5783-x

Santisteban, J.I., Mediavilla, R., López-Pamo, E., Dabrio, C.J., Ruiz Zapata, M.B., Gil García, M.J., Castaño, S., Martínez-Alfaro, P.E., 2004. Loss on ignition: A qualitative or quantitative method for organic matter and carbonate mineral content in sediments? Journal of Paleolimnology 32, 287–299. 10.1023/B:JOPL.0000042999.30131.5b

Saunders, J.B., 1958. Recent foraminifera of mangrove swamps and river estuaries and their fossil counterparts in Trinidad. Micropaleontology 4, 79–92. 10.2307/1484254

Schönfeld, J., Alve, E., Geslin, E., Jorissen, F., Korsun, S., Spezzaferri, S., Fobimo-Group, 2012. The FOBIMO (FOraminiferal BIo-MOnitoring) initiative-Towards a standardised protocol for soft-bottom benthic foraminiferal monitoring studies. Marine Micropaleontology 94-95, 1–13. Doi 10.1016/J.Marmicro.2012.06.001

Schwing, P.T., Romero, I.C., Brooks, G.R., Hastings, D.W., Larson, R.A., Hollander, D.J., 2015. A decline in benthic foraminifera following the Deepwater Horizon event in the Northeastern Gulf of Mexico. Plos One 10, e0120565. 10.1371/journal.pone.0120565

Scott, D.B., Medioli, F.S., 1980a. Living vs. total foraminiferal populations: Their relative usefulness in paleoecology. Journal of Paleontology 54, 814–831. 10.2307/1304312

Scott, D.B., Medioli, F.S., 1980b. Quantitative studies of marsh foraminiferal distributions in Nova Scotia: implications for sea level studies. Cushman Foundation for Foraminiferal Research, Special Publication 17, p. 58.

Scott, D.B., Medioli, F.S., Schafer, C.T., 2001. Monitoring in coastal environments using foraminifera and thecamoebian indicators. Cambridge University Press, 177 pp.

Scott, D.B., Suter, J.R., Kosters, E.C., 1991. Marsh foraminifera and arcellaceans of the Lower Mississippi Delta: Controls on spatial distributions. Micropaleontology 37, 373–392. 10.2307/1485911

Scott, D.S., Medioli, F.S., 1978. Vertical zonations of marsh foraminifera as accurate indicators of former sea-levels. Nature 272, 528–531. 10.1038/272528a0

Sen Gupta, B.K., 1999. Modern foraminifera. Springer Netherlands, 371 pp.

Shaw, T.A., Kirby, J.R., Holgate, S., Tutman, P., Plater, A.J., 2016. Contemporary salt-marsh foraminiferal distribution from the Adriatic Coast of Croatia and its potential for sea-level studies. Journal of Foraminiferal Research 46, 314-332. 10.2113/gsjfr.46.3.314

Stalder, C., Vertino, A., Rosso, A., Rüggeberg, A., Pirkenseer, C., Spangenberg, J.E., Spezzaferri, S., Camozzi, O., Rappo, S., Hajdas, I., 2015. Microfossils, a key to unravel cold-water carbonate mound evolution through time: evidence from the eastern Alboran Sea. Plos One 10, e0140223. 10.1371/journal.pone.0140223

ter Braak, C.J.F., Verdonschot, P.F.M., 1995. Canonical correspondence analysis and related multivariate methods in aquatic ecology. Aquatic Sciences 57, 255–289. 10.1007/BF00877430

Tobin, R., Scott, D.B., Collins, E.S., Medioli, F.S., 2005. Infaunal benthic foraminifera in some North American marshes and their influence on fossil assemblages. Journal of Foraminiferal Research 35, 130–147. 10.2113/35.2.130

Vance, D.J., Culver, S.J., Corbett, D.R., Buzas, M.A., 2006. Foraminifera in the Albemarle Estuarine System, North Carolina: Distribution and recent environmental change. Journal of Foraminiferal Research 36, 15–33.

Velardo, B., 2005. Detailed geochronology of the Mississippi Sound during the Late Holocene, Department of Oceanography and Coastal Sciences. Louisiana State University, p. 95.

Walton, W.R., 1952. Techniques for recognition of living foraminifera. Contributions from the Cushman Foundation for Foraminiferal Research 3, 56–60.

Tables

Table 2.1. Tide gauge data from active NOAA tide gauges in the study areas. Abbreviations: MN = Mean Range of Tide, MHHW = Mean Higher-High Water, MTL = Mean Tide Level, MLLW = Mean Lower-Low Water.

Name	NOAA ID	MN (m)	MHHW (m NAVD88)	MTL (m NAVD88)	MLLW (m NAVD88)
Grand Bay NERR, MS	8740166	0.417	0.302	0.065	-0.183
West Fowl River Bridge, AL	8738043	0.404	0.306	0.058	-0.184
Dauphin Island, AL	8735180	0.358	0.213	0.028	-0.154

Table 2.2. Average percentage of specimens by species identified in live assemblages. Grey cells mark species identified by BFCO method as characterizing the respective assemblage. For full BFCO dataset see Appendix A6.

	Live Foraminifera	**L1** Estuarine Assemblage (%)	**L2** Low Marsh Assemblage (%)	**L3** Low Salinity Assemblage (%)	**L4** Middle Marsh Assemblage (%)	**L5** Upland Transition Assemblage (%)
calcareous	*Affinetrina alcidi*	0.1				
	Ammonia parkinsoniana	**3**	0.1		0.1	
	Ammonia tepida	**49**	7		7	
	Cribroelphidium excavatum	**5**	3		1	
	Cribroelphidium poeyanum	**1**	0.2			
	Haynesina germanica	**6**	**3**		0.6	
	Helenina anderseni				0.8	
	Miliolinella subrotunda	0.2				
	Other/indeterminate calcareous				0.1	
agglutinated	*Ammodiscus tenuis*				0.3	
	Ammoastuta inepta		2	**91**	8	
	Ammotium cassis	0.2	0.1		0.9	
	A. salsum/A. exiguus group	18	53	3	13	
	Arenoparella mexicana		0.2	4	**26**	
	Entzia macrescens				0.3	
	Haplophragmoides bonplandi			0.8		
	Haplophragmoides wilberti				3	**73**
	Haplophragmoides manilaensis				0.1	
	Leptohalysis scotti	0.1			0.1	
	Miliammina fusca	4	28	0.8	21	
	Other agglutinated				0.1	
	Paratrochammina simplissima	**14**	2		0.4	
	Pseudothurammina limnetis		0.1		0.1	**22**
	Siphotrochammina lobata				0.4	**3**
	Textularia earlandi				0.1	
	Tiphotrocha comprimata		0.1	0.3	**5**	
	Trochammina inflata				**10**	
	Trochammina sp. A				3	
	Trochamminita irregularis					2

Table 2.3. Average percentage of specimens by species identified in dead biofacies. Grey cells mark species identified by BFCO method as characterizing the biofacies. Full BFCO data in Appendix A6.

	Dead Biofacies	**D1** Open Estuary Biofacies (%)	**D2** Restricted Estuary/ Marsh Channel BF (%)	**D3** Low Marsh Biofacies (%)	**D4** Low Salinity Biofacies (%)	**D5** Middle Marsh Biofacies A (%)	**D6** Middle Marsh Biofacies B (%)	**D7** High Marsh Biofacies (%)	**D8** Upland Transition BF A (%)	**D9** Upland Transition BF B (%)
calcareous	*Affinitrina alcidi*						0.1			
	Ammonia parkinsoniana	**7**	2	0.1		0.1				
	Ammonia tepida	64	17	0.4	0.2	0.4	1			
	Cribroelphidium excavatum	**20**	**3**	0.2		0.2				
	Cribroelphidium poeyanum	0.4	**2**							
	Elphidium gunteri		0.2							
	Elphidium mexicanum	0.7								
	Haynesina germanica	**0.9**	1	0.1		0.1				
	Helenina anderseni					0.1				
	Miliolinella subrotunda	2	**2**	0.1						
	Pyrgo nasutus		0.1							
	Quinqueloculina jugosa		0.3							
	Other calcareous	0.1			0.2	0.1				
	Indeterminate planktonic				0.2	0.1				
agglutinated	*Ammodiscus tenuis*				0.1	0.4	0.1			
	Ammoastuta inepta		0.1	4	**47**	4	1			0.2
	A. salsum/A. exiguus group	3	52	41	4	13	6			
	Ammobaculites cf. *A. foliaceus*			1			0.1			
	Ammobaculites crassus				0.5	0.1				
	Ammotium cassis		0.2	0.5		1	0.5			
	Arenoparrella mexicana		0.5	2	2	16	36			0.3
	Entzia macrescens			2		2	0.8	81	25	1
	Haplophragmodes bonplandi			2	12	0.4	1			4
	Haplophragmoides manilaensis			0.1	0.1	0.1	1	1	**14**	
	Haplophragmoides wilberti		0.1	1		2	22	1	3	5
	Leptohalysis scotti		0.1	0.3		0.2	0.6			
	Miliammina fusca	0.4	9	41	27	28	9	0.8		
	Miliammina petila			0.1				**3**	0.3	
	Other agglutinated					0.1	0.2		**2**	0.5
	Paratrochammina simplissima	2	**10**	0.5		0.1	1			
	Pseudothurammina limnetis			0.6	4	3	0.4	2	16	79
	Siphotrochammina lobata		0.1	0.1		0.7	2	7		2
	Textularia earlandi					0.1	0.1			
	Tiphotrocha comprimata			2	2	17	3	4	0.4	
	Trochammina inflata		0.1	0.5		10	13			4
	Trochammina sp. A		0.1	1	0.2	**2**	0.7			
	Trochamminita irregularis					0.1	0.1		**39**	**4**

Table 2.4. Dead assemblage Canonical Correspondence Analysis scores for axes.

Axis	Eigenvalue	p	%	% cumulative
1	0.5154	0.001	70.29	70.29
2	0.0958	0.001	13.06	83.35
3	0.0567	0.001	7.73	91.08
4	0.0385	0.001	5.25	96.33
5	0.0269	0.001	3.67	100
6	3.90E-09	1.22E-01	5.32E-07	100

Figures

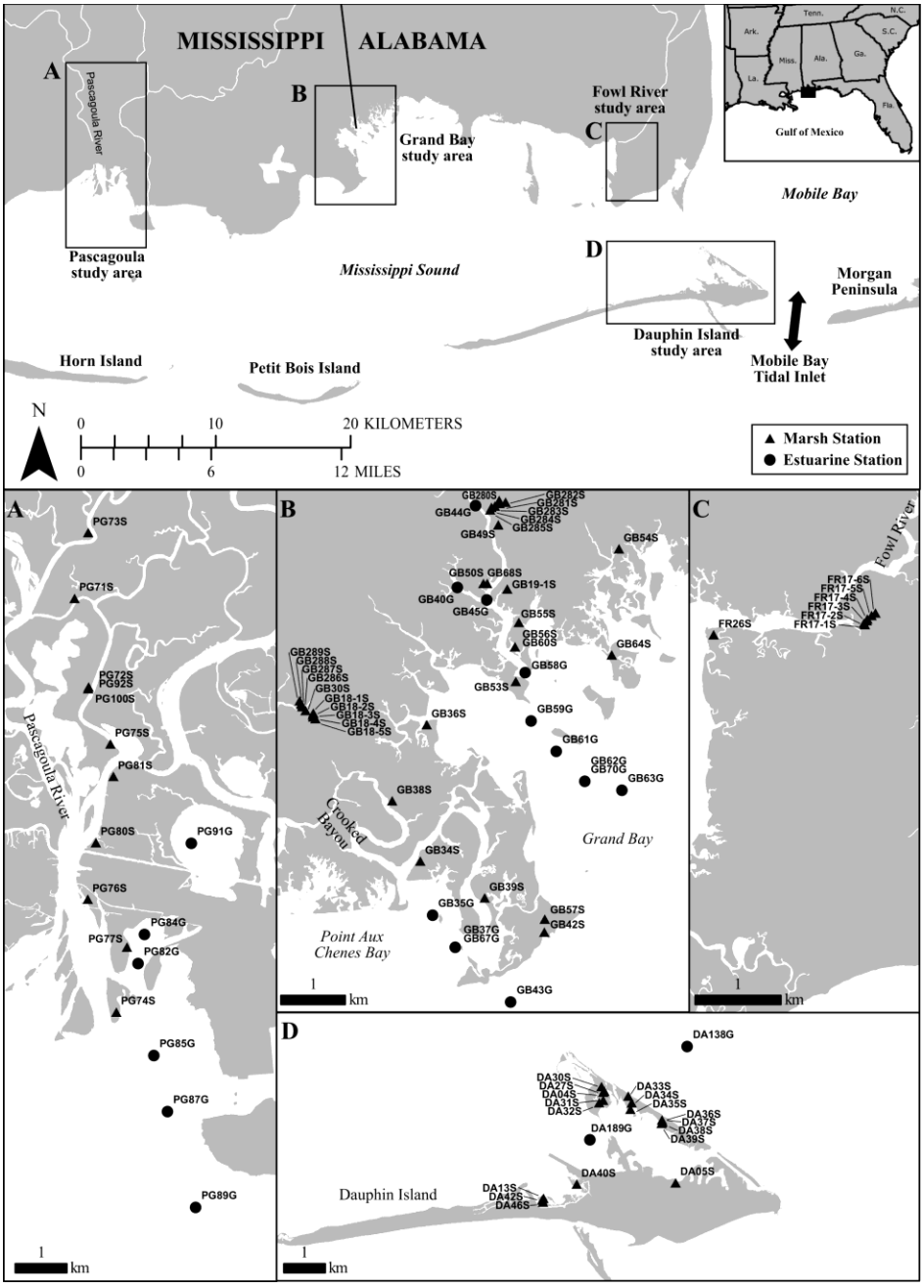

Figure 2.1. Location of study areas and sample sites, Mississippi Sound. (A) Pascagoula study area, (B) Grand Bay study area, (C) Fowl River study area, and (D) Dauphin Island study area. Filled circles represent estuarine stations sampled with a Ponar grab. Filled triangles represent marsh stations. Inset shows location in North America.

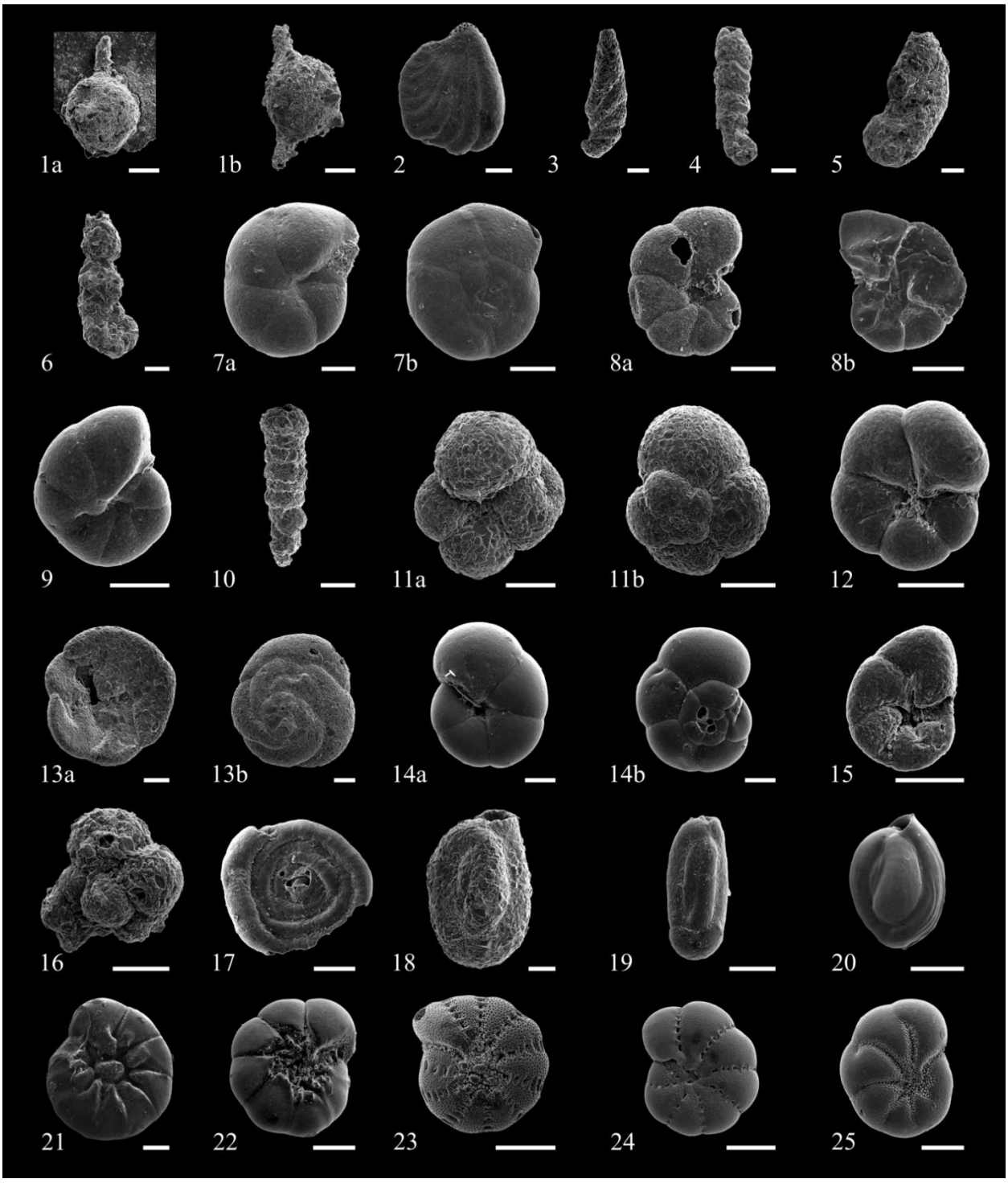
1a
1b
2
3
4
5
6
7a
7b
8a
8b
9
10
11a
11b
12
13a
13b
14a
14b
15
16
17
18
19
20
21
22
23
24
25

Figure 2.2. (previous page) Electron micrographs of taxa from the Eastern Mississippi Sound area. 1 *Pseudothurammina limnetis*, 1a attached to plant detritus, GB55S A; 1b loose specimen, GB50S A; 2 *Ammoastuta inepta*, side view, GB50S A; 3 *Ammotium cassis*, GB36S A; 4 *Ammotium salsum*, GB36G A; 5 *Ammobaculites exiguus*, GB43G A; 6 *Ammobaculites crassus*, GB40G A; 7 *Arenoparrella mexicana*, 7a umbilical side, GB36S A, 7b spiral side GB30SA; 8 *Entzia macrescens*, 8a umbilical side, GB30S A, 8b deflated, GB30S B; 9 *Haplophragmoides wilberti*, GB40G B; 10 *Leptohalysis scotti*, GB42S A; 11 *Paratrochammina simplissima*, 11a umbilical side, GB36G A, 11b, spiral side, GB36G A; 12 *Siphotrochammina lobata*, GB40G B; 13 *Tiphotrocha comprimata*, 13a umbilical side, GB36S A, 13b, spiral side, GB30S B; 14 *Trochammina inflata*, 14a umbilical side, GB30S A, 14b spiral side, GB30SB; 15 *Trochammina* sp. A, umbilical side, GB30SB; 16 *Trochamminita irregularis*, side view, GB280S A; 17 *Ammodiscus tenuis*, side view, GB56S A; 18 *Miliammina fusca*, side view, GB40G B; 19 *Miliammina petila*, side view, GB282S A; 20 *Quinqueloculina jugosa*, side view, GB63G B; 21 *Ammonia parkinsoniana*, umbilical view, GB34G B; 22 *Ammonia tepida*, umbilical view, GB63G B; 23 *Cribroelphidium excavatum*, side view, GB43G A; 24 *Cribroelphidium poeyanum*, side view, GB59G A; 25 *Haynesina germanica*, side view, GB40G B. Scale bars = 100 μm.

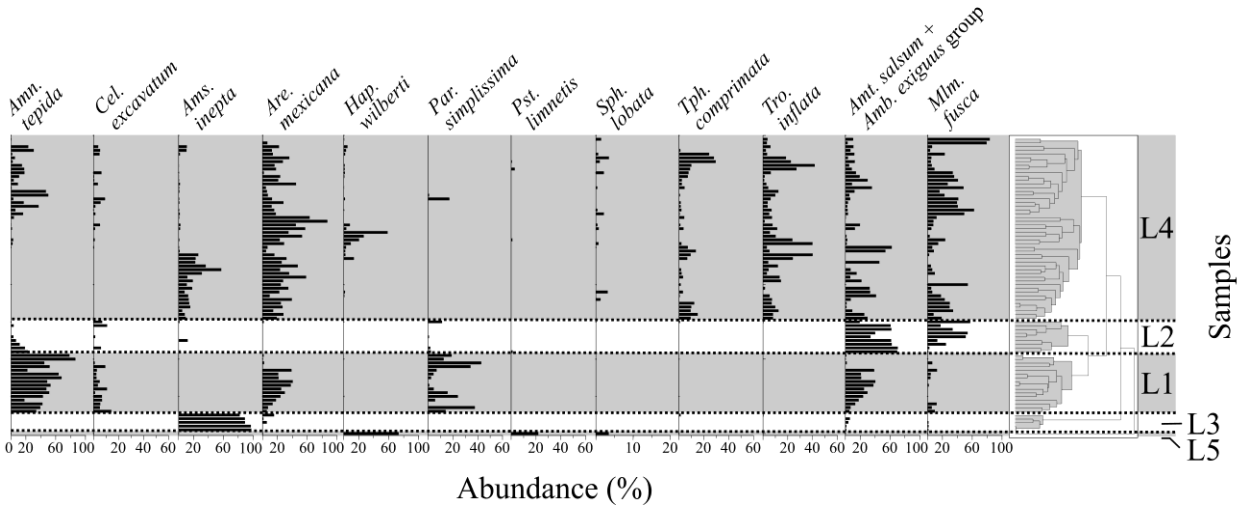

Figure 2.3. Species abundances of selected live foraminifera in salt-marshes of the Mississippi Sound. Abbreviations: L1 = Estuarine Assemblage, L2 = Low Marsh Assemblage, L3 = Low Salinity Assemblage, L4 = Middle Marsh Assemblage, L5 = Upland Transition Assemblage.

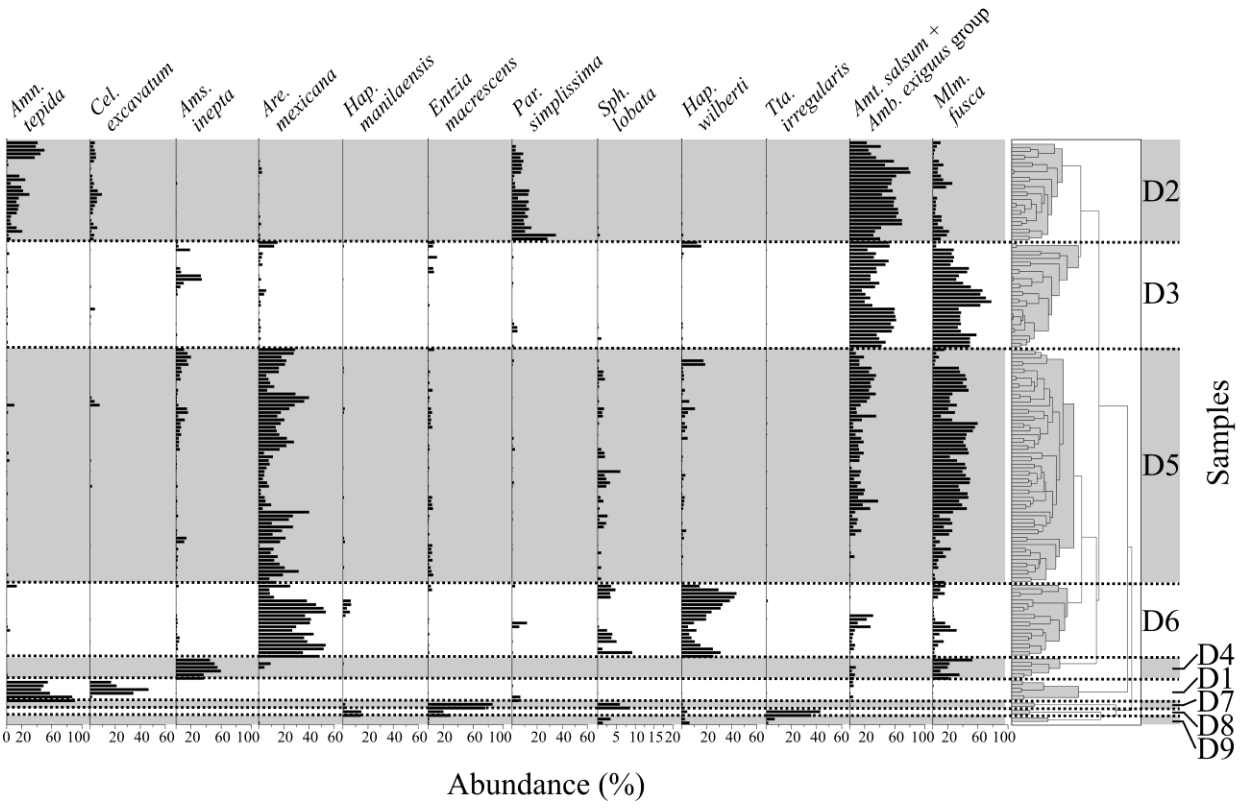

Figure 2.4. Species abundances of selected species in the dead assemblage biofacies. Abbreviations: D1 = Open Estuary Biofacies, D2=Restricted Estuary/Marsh Channel Biofacies, D3 = Low Marsh Biofacies, D4 = Low Salinity Biofacies, D5 = Middle Marsh Biofacies A, D6 = Middle Marsh Biofacies B, D7 = High Marsh Biofacies, D8 = Upland Transition Biofacies A, D9 = Upland Transition Biofacies B.

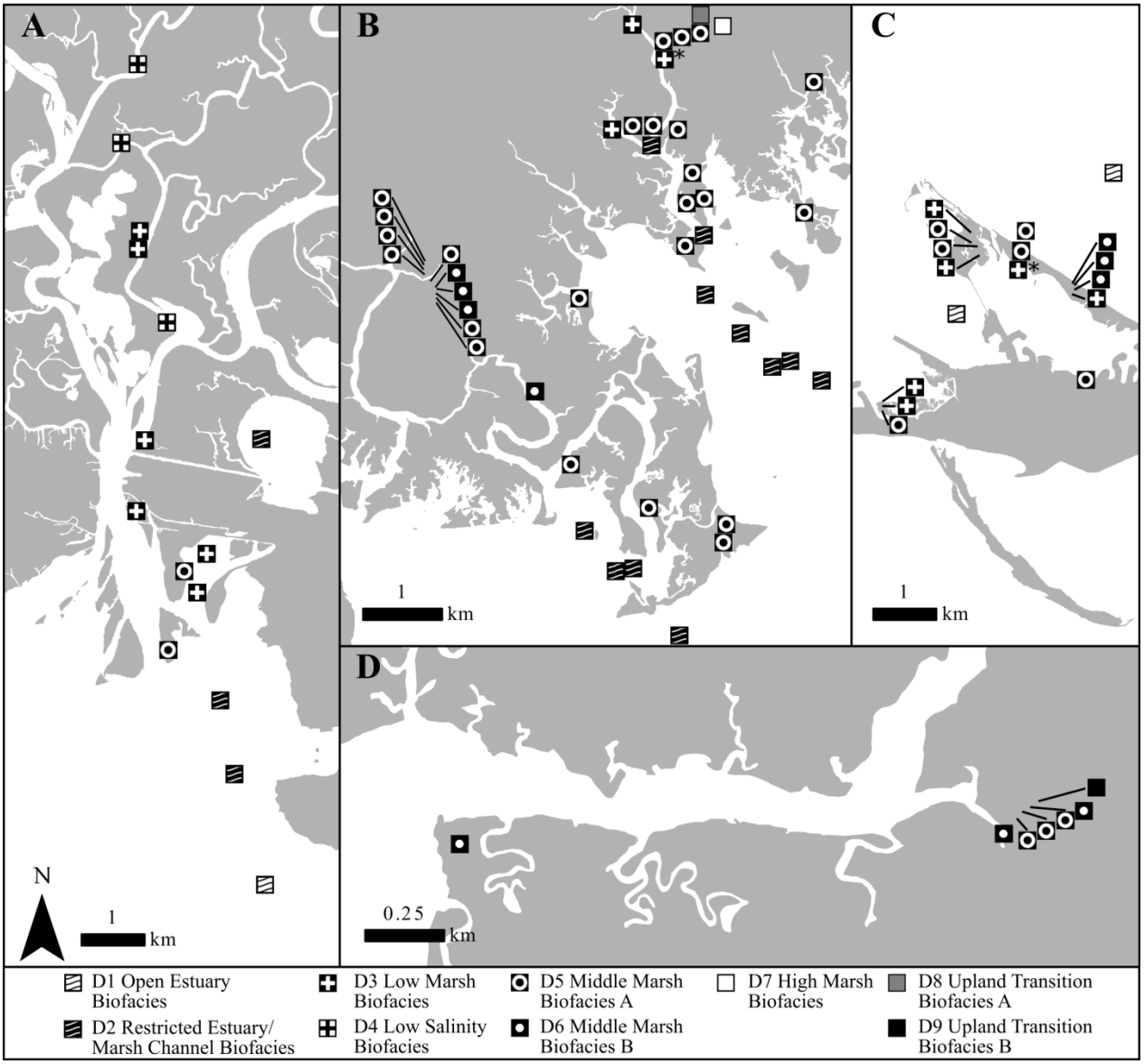

Figure 2.5. Spatial distribution of nine dead assemblage biofacies in Mississippi Sound sampling areas resulting from the Cluster Analysis. Asterisks denote stations at which replicates have been assigned different biofacies.

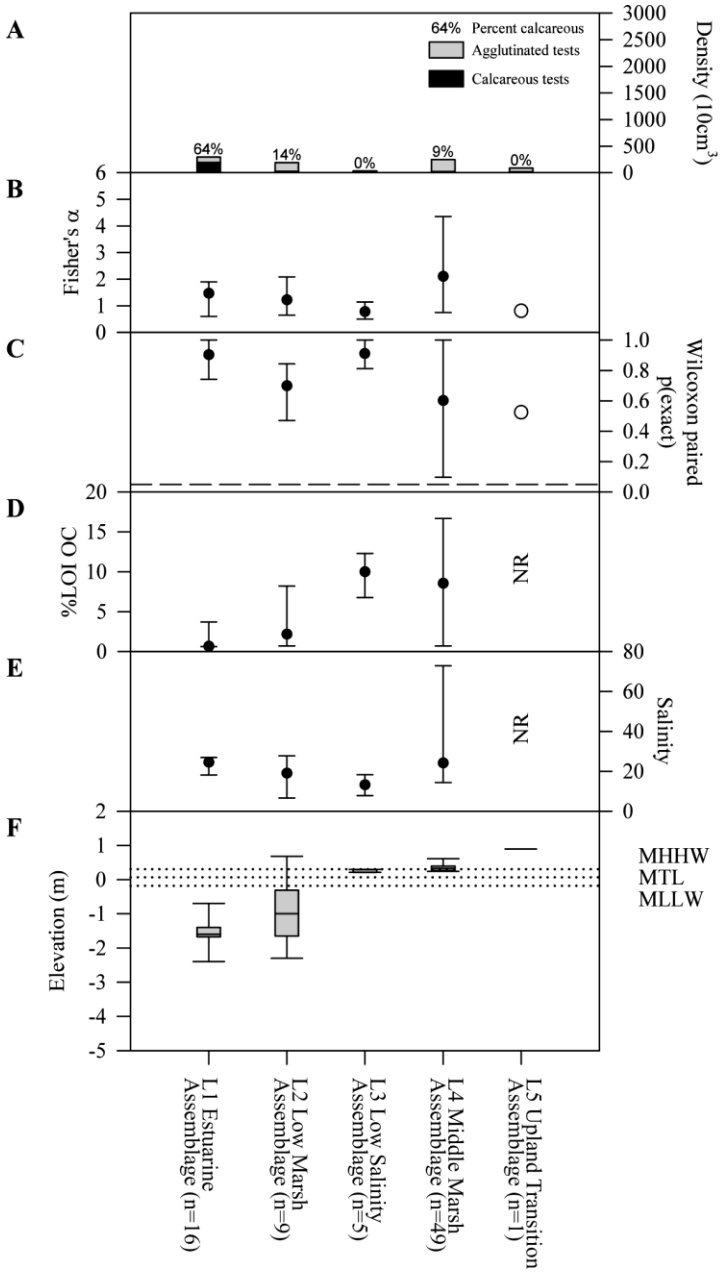

Figure 2.6. Foraminiferal and environmental data of the five live assemblage biofacies: (A) Average density of live foraminifera, (B) Fisher's α diversity, (C) Wilcoxon paired-test replicate similarity, dashed line indicates the significance level $\alpha = 0.05$ where $p < \alpha$ the sample means are considered different, (D) organic carbon estimate, (E) salinity, (F) elevation box plot of all stations of live assemblages. Number in brackets after biofacies name indicates number of samples (*n*). Note: Tidal datums (dotted lines) indicated are from Grand Bay NERR tide gauge.

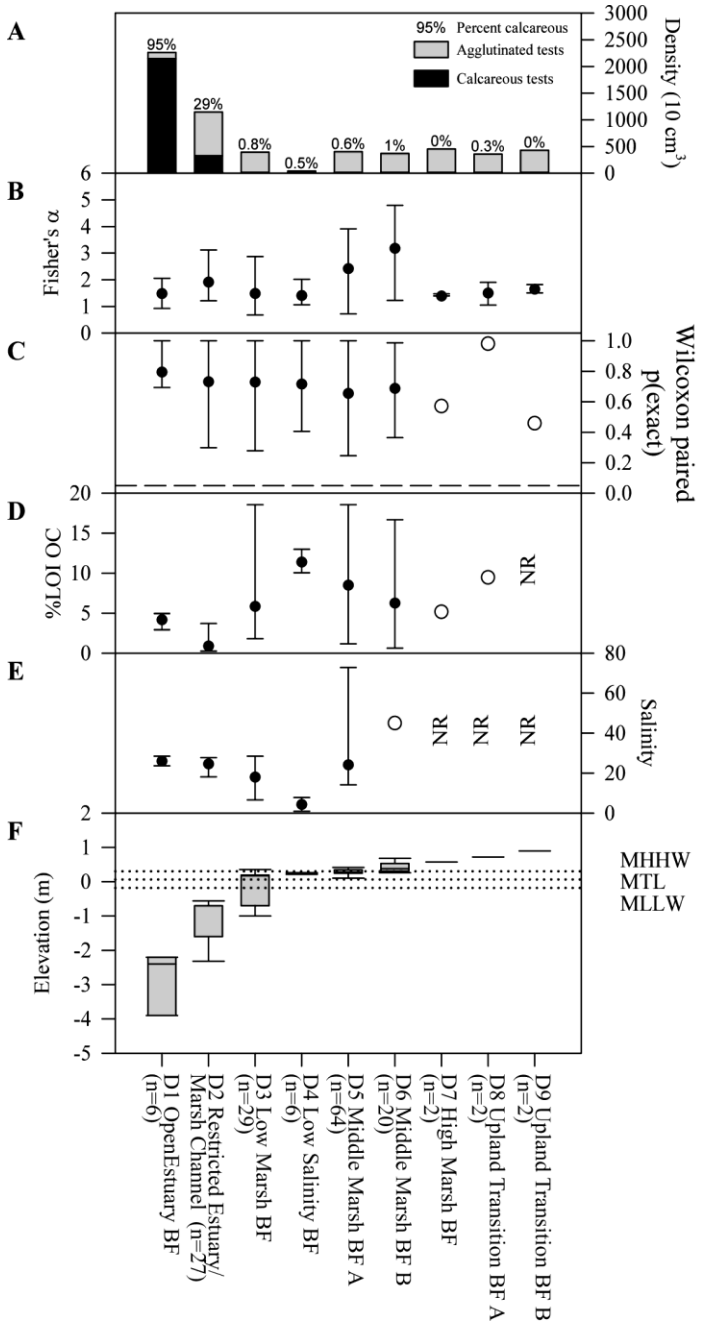

Figure 2.7. Foraminiferal and environmental data of the nine dead assemblage biofacies: (A) Average density of live foraminifera, (B) Fisher's α diversity, (C) Wilcoxon paired-test replicate similarity, dashed line indicates the significance level $\alpha = 0.05$ where $p < \alpha$ the sample means are considered different, (D) organic carbon estimate, (E) salinity, (F) elevation box plot of all stations of dead biofacies across all study areas. Number in brackets after biofacies name indicates number of samples (*n*). Note: Tidal datums (dotted lines) indicated are from Grand Bay NERR tide gauge

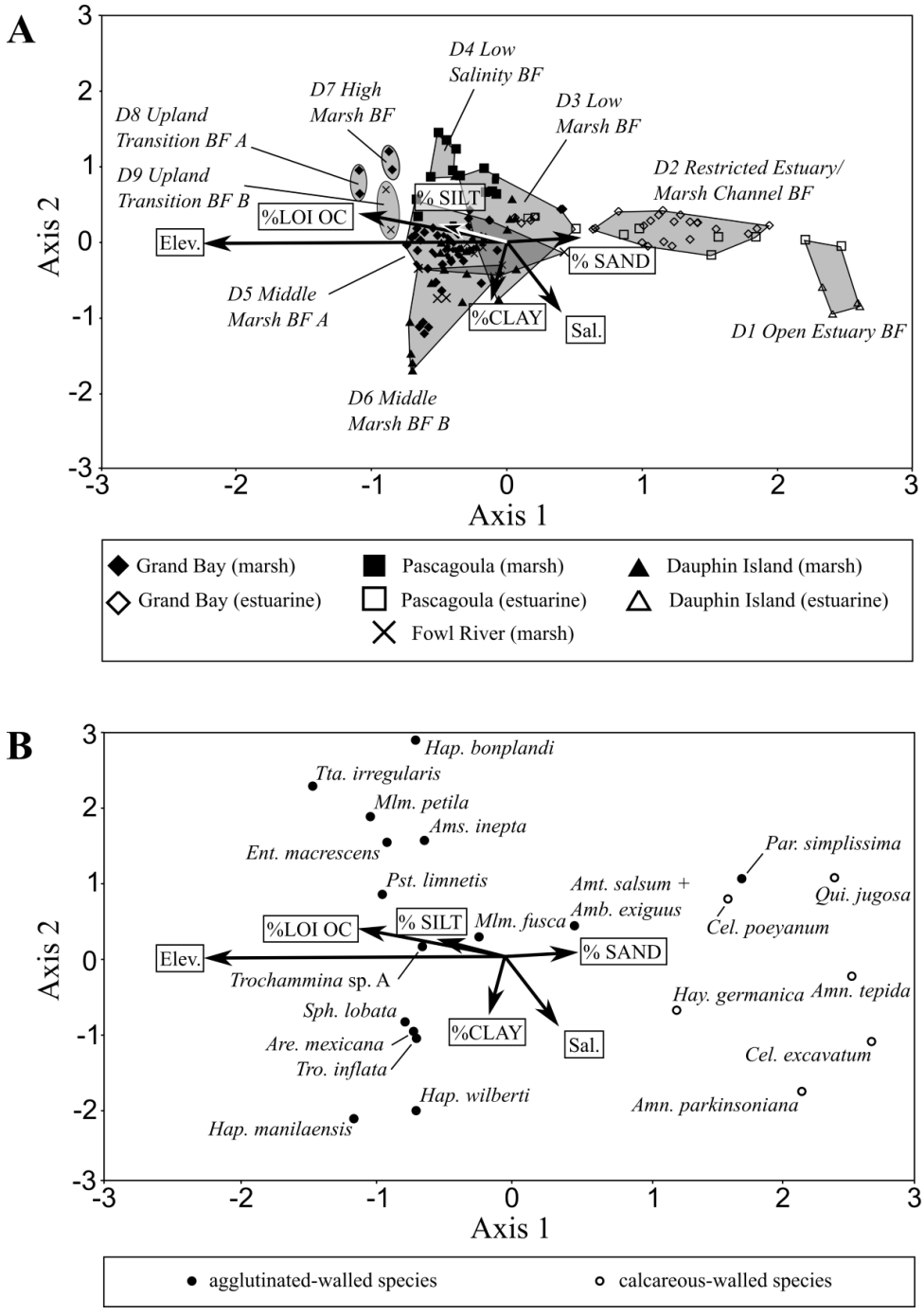

Figure 2.8. Canonical correspondence analysis plots of (A) sample-environment and (B) species-environment. The dataset comprises dead assemblage samples with counts greater than 57 individuals and species that reach 2% per sample. Biofacies envelopes (convex hulls) have no statistical meaning. Axis 1 explained variance = 70%, Axis 2 explained variance = 13% (Table 2.4). Abbreviations: %LOI OC = % Loss On Ignition Organic Carbon; Elev. = elevation in tidal zone in m NAVD88; Sal. = salinity.

Chapter 3.

Foraminifera as Proxies of Environmental Change and Relative Sea Level in Eastern Mississippi Sound Salt Marshes During the Last 1,000 Years

Abstract

Fossil foraminiferal assemblages and sediment obtained from two coastal (brackish-to-saline) marshes fringing eastern Mississippi Sound (U.S.A.) record the local to regional estuarine response to rising sea level and storms. Such coastal marshes provide numerous ecosystem services (e.g., biodiversity, nutrients/harmful materials retention, recreational/ commercial fisheries) as well as buffer human infrastructure from energetic physical processes (high riverine stage and discharge, coastal wave attack, and tidal and/or storm inundation). The stratigraphic framework of marshes is built from the long-term system response to ecological and physical processes; however, it also underpins and influences the short-term trajectories of the modern marsh. In the eastern Mississippi Sound, salt-marsh sediments are predominantly organic-rich silt, 50 to 100 cm thick, that overlay organic-poor silt and sand. Foraminifera in the marsh deposits are predominantly agglutinated species typical of salt marsh environments. Chronologic framework for the region was obtained using ^{137}Cs, ^{210}Pb and ^{14}C to establish sediment accumulation rates. Within-region comparison of cores revealed selective breakdown of indicator species resulting in incomplete foraminiferal surface training sets, which are common factors that may hamper reliable Paleo-Marsh Elevation (PME) and Relative Sea Level (RSL) reconstructions. Despite that, within-region paleo-environmental developments were reproduced. Differential centennial-scale RSL trends between Grand Bay and Dauphin Island from 200 to 1900 CE indicate that additional local-scale

processes drove sediment accumulation. Between-region differences on centennial timescales cannot be adequately explained without taking into account regional geomorphologic change. We suggest that the Grand Bay coring sites historically received enhanced sediment influx from the now-cut-off Escatawpa River system, and were sheltered by the now-submerged Grand Batture headland. Protection from storms and wave erosion expanded the marsh record at Grand Bay and led to apparently high RSL rise rates. Therefore, the Grand Bay and Dauphin Island regional records should be considered as independent of one another.

Additionally, we compared our proxy reconstruction with a Gulf of Mexico compound tide-gauge record spanning 1913–2016 CE, which indicated that in the 20th century marshes experienced a higher RSL rise than in instrumental records. During this time, abundances of Low Marsh foraminifera started spreading and, in Dauphin Island marshes, deposition shifted from peat to grey silt, which was likely initiated by fast encroaching shorelines and increased tidal inundation frequency. We suggest that not only small-scale process have to be taken into account during site selection (e.g. distance to avulsion channels, length of record), but also larger morphodynamic processes in the past.

Introduction

Salt marshes represent the tidally influenced transition zone between marine and terrestrial systems and are ecosystems with characteristic flora and fauna. They provide numerous ecosystem services (e.g., biodiversity, nutrients/harmful materials retention, recreational/commercial fisheries) and are a natural armoring against coastal hazards such as storm surges and impinging waves. This gives salt marshes a key role in extreme event and sea-level rise mitigation (Fagherazzi, 2014). In this context, the history of vertical and horizontal development of salt marshes in relation to late Holocene Relative Sea Level (RSL) changes needs to be better understood (Turner, 1991; Kearney and Turner, 2016; Kirwan et al., 2016; Plant et al., 2016).

The first recognition of the elevation-dependency of salt-marsh foraminifera was made in Louisiana and the New England region (U.S.A.) by Phleger and Walton (1950) and Phleger (1954), who also noted that foraminiferal assemblages can potentially be used to reconstruct paleo-environments. Scott and Medioli (1978) first used vertical zonation and species optima as proxies to reconstruct late Holocene tide levels in Nova Scotia (Canada). In the past 15–20 years, investigators have assessed RSL changes using the transfer-function techniques (Imbrie and Kipp, 1971) applied to records of foraminifera and other microfossils preserved in salt-marsh sediments (e.g., Gehrels and van de Plassche, 1999; Horton et al., 1999).

Surface distributions of benthic marsh foraminifera are driven by elevation relative to tidal levels, which is a substitute for frequency and duration of sea-water inundation (Scott and Medioli, 1978; Edwards and Horton, 2000). The relationship of salt-marsh foraminifera to elevation is set up empirically from a surface-sample dataset (i.e., training set) with a transfer function. Consistent with the geologic principle of uniformitarianism, it is assumed that relationships between organisms and environment did not change in time so that fossil abundances in a sediment core are analogous to modern surface distributions. Therefore, the fossil foraminiferal assemblage in a downcore sample can reveal the Paleo-Marsh Elevation (PME) at the time of deposition.

The Weighted Averages-Partial Least Squares (WA-PLS) method was introduced by ter Braak and Juggins (1993), which is a combination of unimodal (WA) and linear partial least-squares (PLS) methods to improve the performance of previously available transfer functions. These new statistical tools were subsequently tested and refined in numerous studies across Europe (Gehrels and van de Plassche, 1999; Leorri et al., 2008a; Leorri et al., 2008b; Müller-Navarra et al., 2017) and North America (Gehrels, 2000; Kemp et al., 2009b; Kemp et al., 2013b; Kemp et al., 2017a; Kemp et al., 2017b), confirming the applicability of intertidal foraminifera for RSL reconstructions. Modern applications in combination with fossils such as diatoms (Kemp et al., 2009b) and geochemical data (Engelhart et al., 2013) yield continuous time series with relatively small vertical and temporal uncertainties.

Previous studies of foraminifera in the Mississippi Sound have been qualitative (Phleger, 1954) or focused on submerged estuarine-lagoonal areas (Priddy et al., 1955; Lamb, 1972; Osterman and Smith, 2012) and continental shelf (Phleger, 1960; Osterman, 2003). Haller et al. (in review; see Chapter 2) sampled the sediments of the mainland and backbarrier marshes of Grand Bay, Pascagoula, Fowl River, and Dauphin Island considering the applicability of foraminifera for sea-level research. They concluded that the distribution of modern salt-marsh foraminifera in this region was strongly controlled by elevation, which is a prerequisite that has to be met for a successful sea-level reconstruction.

We expand upon the work by Haller et al. (in review; Chapter 2) by developing a regional transfer function for the Mississippi Sound salt marshes and applying it to reconstruct past regional RSL trends. For this we documented the historical (downcore) distribution of foraminifera in four cores from two environmentally distinctive salt marshes: Grand Bay (GB53R, GB60R) and Dauphin Island (DA40R, DA42R), representing an opportunity for comparison of different development between mainland and barrier island. We created age-depth models in combination with foraminiferal-derived Paleo-Marsh Elevation (PME) to calculate RSL histories for the two regions. We consider the implications of inter- and intra-site variations of RSL trends and address possible factors influencing the records. We further compare the RSL histories to two other recent U.S. Gulf Coast RSL reconstructions and to regional tide gauge records.

Study Area

The Mississippi Sound, located in the Northern Gulf of Mexico (Alabama/Mississippi) is an estuary-lagoon between Mobile Bay to the east and the Mississippi Delta to the west (Fig. 3.1A). The modern tidal setting of this region of the Gulf of Mexico is diurnal microtidal (Passeri et al., 2015; Table 3.1). The Sound encompasses an area ca. 2100 km^2 with water depths typically ranging from 2–5 m, and as much as 25 m in channels. The lagoon is fringed by a barrier-island chain (i.e., Cat Island, Ship Island, Horn Island, Petit Bois Island and Dauphin Island). During the Last Glacial Maximum, large paleo-

valleys were carved out on the coastal plain and slowly filled in during the Holocene transgression (Kindinger et al., 1994; Greene et al.; Blum et al., 2013). Following the slowdown of the Holocene transgression, a widespread dark greenish-gray to gray clay and silt, sandy mud (tidal flat) and basal peat (incipient marsh) was laid down over exposed Pleistocene sands (Rodriguez et al., 2008). This Pleistocene transgressive unconformity occurs at relatively shallow depth in the mainland marsh (~3–4 m; Kramer, 1990; Bregy et al., in press) and somewhat deeper (5–15 m) in the lagoon, Mobile Bay, and barrier islands (Rodriguez et al., 2008; Rose, 2010).

Grand Bay is a small bay (sub-bay) of the larger Mississippi Sound system. The bay's is interlinked with the Escatawpa River, which his currently a branch of the Pascagoula River system. Previous studies have suggested that the Escatawpa River flowed south–southeast into Grand Bay, creating a river delta that encompassed the entire Grand Bay estuary and was protected by the barrier island and headland Grand Batture Island (Fig. 3.1B; Otvos, 1985b; Eleuterius and Criss, 1991). While Grand Batture Island existed, erosion was limited due to attenuated tide and wave impacts within the Sound, and was buffered by sediment fed by the Escatawpa River. However, prior to 1848 when the first geographic map of the region was created, the river had diverted its course and had become a tributary of the Pascagoula River further west. The avulsion of the Escatawpa River terminated the fluvial sediment supply to Grand Bay (Eleuterius and Criss, 1991). Flank erosion of several subdeltas to marshy headlands with sand spits led to the formation of Grand Batture Island, which isolated Grand Bay from the Mississippi Sound. The sediment starvation of Grand Batture Island shrank the extent of the long and thin beaches. The modern Grand Bay salt-marsh platform reaches up to 5 km width and sustains almost mono-specific stands of the marsh grass *Juncus roemerianus* Scheele, which is the main constituent of peats formed between Mean Tide Level and Mean Higher High Water. At the nearby Grand Bay NERR tide gauge (NOAA ID 8740166), the reported semi-diurnal tidal regime has a Mean Range of Tide (MN) of 0.417 m (Table 3.1).

South of Grand Bay across Mississippi Sound, Dauphin Island is located approximately 3–20 km offshore and trends east to west (Fig. 3.1A). As mode of emergence, Dauphin Island is considered a

"composite platform" (Otvos, 1985a). The eastern third of the island is a pre-Holocene high, engulfed during Holocene sea-level rise, that prograded in response to complex alongshore and cross-shore processes. The remaining two thirds reflects lateral progradation derived from sediments bypassing the Mobile Pass ebb-tidal delta as well as erosion of the eastern portion of the island. Eastern Dauphin Island is located on a broad and low (ca. 2 m) Pleistocene core around which beach sands and fine lagoonal silts are draped (Fig. 3.1C; Otvos, 1985a). On the lagoonal side of the island's core, various pockets of backbarrier marshes receive sediment influx from storm-event overwash fans (Feagin and Williams, 2008). The tide gauge on the eastern end of Dauphin Island (NOAA ID 8735180) reported a tidal regime that is somewhat less pronounced with an MN of 0.358 m (Table 3.1).

Seven tide-gauge measurements from several northern Gulf of Mexico locations were used, which provided the longest 20th century instrumental records of sea level: (1) Key West (NOAA ID 8724580), (2) St. Petersburg (NOAA ID 8726520), (3) Cedar Key (NOAA ID 8727520), (4) Apalachicola (NOAA ID 8728690), (5) Pensacola (NOAA ID 8729840), (6) Dauphin Island (NOAA ID 8735180), and (7) Galveston Pier 21 (NOAA ID 8771450). We downloaded annual-average data from earliest available to 2016 CE for these stations from the Permanent Service for Mean Sea Level (PSMSL) at the National Oceanography Centre in Liverpool, United Kingdom (Holgate et al., 2012).

Methods

Surface Data

Foraminiferal Surface Training Set

The foraminiferal transfer function developed and employed in this paper is based on the data presented in Haller et al. (in review; Chapter 2). Using these surface distribution data we developed a regional-scale training set of 168 samples from four salt-marshes in the eastern Mississippi Sound area: Grand Bay (several long and short transects), Pascagoula (one shore-perpendicular transect), Fowl River (one short channel to upland transect), and Dauphin Island (four backbarrier transects).

Sampling locations and transect design are described in greater detail in Haller et al. (in review; Chapter 2). The surface samples (0–1cm) captured the ecological and geomorphological range of the salt marshes in the eastern Mississippi Sound, which includes low salinity to high salinity, and submerged (estuarine) to subaerial (marsh and upland). Foraminiferal test densities were measured and the sediment stained with rose Bengal to separate live and dead assemblages (Walton, 1952; Murray and Bowser, 2000). Replicates at most sites were taken to quantify assemblage variability (i.e., patchiness). Census under the stereo microscope utilized the size fraction 125–850 μm.

Transfer Function

We determined the length of the modern training set's environmental gradient using Detrended Correspondence Analysis (DCA), executed in the Canoco 5 © statistical package (Ter Braak and Šmilauer, 2012; Šmilauer and Lepš, 2014). The purpose of the DCA was to determine ecological response of foraminiferal assemblages to environmental parameters, which can be unimodal (Gaussian-like) or linear. Such environmental responses, determines appropriateness of a transfer function method. Within the linear and the unimodal transfer function methods, different approaches result from how model parameters are estimated (Birks, 1995; Juggins and Birks, 2012). Based on our axis 1 gradient length 4.1 SD>> 2SD, we developed a transfer function using the unimodal method Weighted Averaging-Partial Least Squares (WA-PLS; ter Braak and Juggins, 1993) in the software package C2 © (Juggins, 2016). The WA-PLS technique is considered superior to pure Weighted Averaging (WA) since it adds additional components, which improve the fit between measured and estimated correlation (see review in Birks, 2010). From the surface training set all subaerial samples were used and none trimmed, however none of the estuarine samples were included. For cross validation and performance assessment, we chose 10,000 bootstrapping cycles, which are expressed in the performance indicator correlation coefficient (R^2_{boot}) and Root Mean Squared Error of Prediction (RMSEP). In choosing among the number of components we sought to

balance model performance (low component number) against the possibility of overfitting the data through statistical complexity (high component number) as laid out by Barlow et al. (2013; Chapter 3.5).

Furthermore, in assuming unimodal taxa responses to the gradient of elevation, it is possible to calculate vertical species optima and tolerances using the WA regression. A species optimum is the elevation at which a species is (or is supposed to be) most abundant for the specific region and provides a reasonable representation of the surface data.

Downcore Data

Reconstruction Coring

We recorded stratigraphy at four sites, two in the Grand Bay National Estuarine Research Reserve (NERR; GB53R and GB60R), and two in the northwestern backbarrier marshes of Dauphin Island (DA40R and DA42R). Spatial distance to meandering channels and a continuous accumulation of the salt-marsh grass *Juncus roemerianus* were pre-requisites for site-selection. At each site we took a half-barrel core with a hand-operated Russian peat auger, which avoids compaction. Core lengths were 121 cm (GB53R), 101 cm (GB60R), 121 cm (DA40R), and 137 cm (DA42R) respectively. The half-barrel peat augers were stored in lengthwise split PVC halves, wrapped in plastic to decelerate oxidation and desiccation, and stored refrigerated. Stratigraphy was described visually using the un-oxidized cores.

Additionally, four acrylic push cores of 10.2 cm diameter were taken in the close vicinity of the peat auger sites to provide sufficient material for radiometric dating. The push cores were inserted by hand to a depth at which lithology was impenetrable, sealed with an expandable rubber plug, and extracted from the ground by hand. Core lengths were 67 cm (GB53M), 62 cm (GB60M), 65.5 cm (DA40M), and 72 cm (DA42M) with vertical compaction between 19.5 and 28 cm in all cores. Cores were stored upright and cooled until they were extruded and cut into contiguous 1 cm slices at a US

Geological Survey laboratory in St. Petersburg, Florida. Using the compaction information, all sample positions of the push cores were de-compacted linearly.

Fossil Foraminifera/Assemblages

The peat auger cores from the four sampling locations were sub-sampled in 1 cm slices for fossil foraminifera: four samples between 0 and 10 cm, every 5 cm between 10 and 50 cm, and below this every 20 cm. The outside of each slice was removed to limit contamination from smearing, and sediment volume was recorded using a graded syringe. The total assemblage of each sample was established for the size fraction 125–850 μm using the same laboratory processing and microscopy techniques employed for the surface training set (see Chapter 2). The commonly chipped and fragmented species *Ammotium salsum* and *Ammobaculites exiguus* were combined into one group. More detailed methods are presented in Chapter 2. The raw dataset of downcore census was published as a 2018 USGS Data Release.

Live Infaunal Foraminifera

Since it is necessary to know if it is valid to compare the dead assemblage of the training set to the total assemblage from the core samples, the influence of living foraminifera on the fossil total assemblage was assessed. Infaunal marsh foraminifera have been reported live from various locations along the U.S. coast (e.g., Goldstein and Harben, 1993; Goldstein et al., 1995; Hippensteel et al., 2000; Culver and Horton, 2005). By sampling the surface sediment (0–1 cm) for the foraminiferal training set, it was assumed that intertidal foraminifera were predominantly epifaunal and did not influence fossil abundances below (Scott and Medioli, 1980a, b; Edwards et al., 2004; Horton and Edwards, 2006). To test this hypothesis, we collected several short Russian peat auger cores from the Dauphin Island backbarrier marsh (Fig. 3.1C; DA33R, DA34R, and DA35R). At the time of sample collection (August, 2015), the salinity of Mississippi Sound at the Dauphin Island backbarrier sites

was 25. The cores were sub-sampled in 1-cm slices between 0 and 9 cm depth and smearing contamination removed. On the same day of sampling, the sediment was stored in buffered alcohol containing the protein-specific stain rose Bengal. After staining for a minimum of two weeks, laboratory processing and census followed the methods of Haller et al. (in review; Chapter 2).

Elevation Measurement

Elevation, as a surrogate for intertidal subaerial exposure, was measured with the differential GPS (dGPS) system described in Haller et al. (in review; Chapter 2) and referenced to NOAA benchmarks BH1755 (East Dauphin Island) and DO5986 (Grand Bay NEER). Since local tidal frames govern distribution of foraminiferal assemblages, absolute elevation measurements had to be normalized between the sampled regions in the training set as well as the core locations. The dGPS measured scale (North American Vertical Datum of 1988; NAVD88) was referenced to local tidal elevation datum Mean High Water (MHW) using the closest tide gauge with NAVD88 tie-in. For the tide gauges at Grand Bay, Fowl River, and Dauphin Island, the MHW datum was provided by NOAA's tide gauge website https://tidesandcurrents.noaa.gov (Table 3.1). However, the Pascagoula tide gauges used proprietary scaling and had to be referenced to the MHW datum of the Grand Bay NERR tide gauge, assuming little difference.

Age-Depth Model Development

The sediment accumulation history at the four sites was determined by radiometric dating of ^{210}Pb, ^{137}Cs, and ^{14}C.

Cores sediment from Grand Bay (GB53M and GB60M), were analyzed by gamma-ray spectrometry (Canberra, Inc.) to measure total ^{210}Pb (photopeak 46.5 keV), ^{226}Ra via (grand)daughter isotopes ^{214}Pb (photopeaks 295.7, 352.5 keV) and ^{214}Bi (609.3 keV), and ^{137}Cs (photopeak 661.6 keV) activities were measured using a planar-style high-purity, low-energy, germanium gamma-ray spectrometer (Canberra, Inc.) at the USGS St. Petersburg Coastal and Marine Science Center

Radioisotope Lab. All samples were corrected for self-absorption using a ^{238}U sealed-source procedure following procedure of Cutshall et al. (1983). Excess ^{210}Pb for each sample was determined as the difference between measured ^{210}Pb and measured ^{226}Ra. Resulting profiles, excess ^{210}Pb were used to develop chronologies using two different chronologic models – Constant Flux Constant Sedimentation (CFCS) and Constant Rate of Supply (CRS; Appleby, 2001; Smith et al., 2013). Profiles of ^{137}Cs were used as independent chronometers with the assumption that peak subsurface ^{137}Cs activities are an indicator for the atmospheric nuclear bomb testing period during the 1950s and 1960s, which reached its height circa in 1963.

In the two push cores from Dauphin Island (DA40M and DA42M), ^{210}Pb was measured by isotope dilution alpha spectrometry dating of ^{210}Po. This procedure assumes secular equilibrium between parent and (grand)daughter isotopes (Flynn, 1968; El-Daoushy et al., 1991). Supported ^{210}Pb was estimated by using asymptotic ^{210}Po concentrations at depth in the profile. The extrapolated supported ^{210}Pb values were compared with ^{226}Ra measurements on select core samples analyzed by gamma-ray spectrometry. Using the excess ^{210}Pb activities and the known half-life of ^{210}Pb, we estimated ages with the Constant Rate of Supply (CRS) model (Appleby and Oldfield, 1978; Binford, 1990). For detailed ^{210}Po dating methods at the USGS St. Petersburg, see Martin and Rice (1981).

For radiocarbon dating, 1 cm bulk sediment slices were collected from the basal peat of the auger cores and rinsed with de-ionized water over a 63 μm sieve. Horizontally growing *Juncus roemerianus* rhizome macrofossils were separated under a stereo microscope, removing ingrown rootlets. *Juncus roemerianus* rhizomes are preferred dating material due to shallow growth close to the paleo-marsh surface and short lifespan (Kemp et al., 2013a). Wood pieces and seeds were avoided due to uncertain amount of pre-aging prior to deposition. The samples were analyzed at the National Ocean Sciences Accelerator Mass Spectrometry facility (NOSAMS), where they first underwent standard treatment and then the percent modern ^{14}C was measured during sample combustion. All ^{14}C samples were age calibrated in the R package Bchron (Haslett and Parnell, 2008; Parnell et al., 2008) and the IntCal13 database (Reimer et al., 2013) for terrestrial radiocarbon samples.

Furthermore, the Bchron package for R was used to create age-depth models with Bayesian error estimates, combining the ^{210}Pb, ^{137}Cs, and ^{14}C ages into a continuous deposition history (Parnell et al., 2011). Bchron combines age estimates arising from different models and can treat different error types accordingly, as for example the probability spectra generated by radiocarbon calibration. The advantage of Bchron is the absence of user-required determinations of sections with different accumulation rates, model step length, and outlier likelihood (Parnell et al., 2011). The model determines outlier likelihood for each age estimate and cancels model calculation if model-inherent boundary conditions are not met by the data. In Bayesian modeling, the credible interval expands between two age estimates the farther they are apart, but delivers narrower intervals than older techniques such as linear interpolation. Following the development of age models, Bchron was used to calculate sediment accumulation rates and extract age predictions for downcore fossil samples with 2σ confidence intervals.

Relative Sea Level Reconstruction

After census of foraminifera in cores used for sea-level reconstruction, we applied the WA-PLS transfer function for PME estimates with sample-specific, boot-strapped, standard errors of prediction (Juggins and Birks, 2012). Barlow et al. (2013) suggested that the number of components should remain low (e.g., two to three) to avoid overfitting of during PLS regression as well as minimize unnecessary statistical complexity. Collectively, these allow for a more direct correlation of the ecological data and the environmental parameter of interest (ter Braak and Juggins, 1993; Barlow et al., 2013). Credibility of PME analogs was tested with the MinDC parameter calculated by the Modern Analogue Technique (MAT) transfer function. The MAT quantifies the similarity between fossil samples and the surface training set using a squared-chord distance-dissimilarity measure (Birks, 1995; Barlow et al., 2013). This is expressed as a Minimum Dissimilarity Coefficient (MinDC) for each fossil sample, meaning that higher values indicate larger distance while zero indicates an exact similarity with the closest modern sample (Jackson and Williams, 2004). As cut-off criterion in the reconstruction, we chose to reject

estimates that exceeded the tenth percentile of dissimilarity of pairings of reconstructed samples with the training set samples. We reconstructed RSL with the following equation:

(1) $RSL_i = \text{Sample altitude}_i - PME_i$

Where the altitude of downcore sample *i* was measured directly (depth below core top of known elevation) and Paleo-Marsh Elevation (PME_i) was estimated using the fossil foraminiferal abundances, both values given in meters relative to the MHW datum. Errors for RSL_i were adopted from the bootstrapped error of PME_i, since it was assumed that no additional compaction and measurement errors were incorporated in Sample altitude_i. Next, all RSL_i values were paired with age estimates from the corresponding Bchron age model. Relative sea-level trends were quantified by linear interpolation, while retaining sample-specific age and vertical uncertainties.

Results

Distribution of Modern Foraminifera

The regional-scale foraminiferal dataset provided by Haller et al. (in review; see Chapter 2) contains 168 samples taken from marsh (n = 127) and estuary (n = 41) environments in Grand Bay, Pascagoula, Fowl River, and Dauphin Island. In the dead assemblage, 38 species were identified, which were distributed across the elevation range. Sample elevations reached a maximal depth of -3.9 m in the estuarine samples, and ranged from -0.263 to 0.661 m MHW, with the majority of samples located between -0.2 and 0.2 m MHW (Fig. 3.2), which was spatially the most expansive area in the sampled mainland marshes. Cluster analysis found nine biofacies, which encompassed Open Estuary, Restricted Estuary, Low Marsh and Low Salinity Marsh, two Middle Marsh, High Marsh, and two Upland Transition biofacies (Table 3.2). The biofacies strongly overlapped and were characterized by gradual transitions of species abundances (Fig. 3.3). This is symbolized by species optima being only slightly higher in the Middle Marsh than the Low Marsh, with largely overlapping tolerances.

The Pascagoula low marshes with riverine freshwater input (Low Salinity Biofacies) were dominated by *Ammoastuta inepta* (Cushman & McCulloch, 1939). Other Low Marsh areas had high abundances of *Trochammina* sp. A sensu Culver et al. (1996), *Ammotium salsum* (Cushman & Brönnimann, 1948), *Ammobaculites exiguus* Cushman & Brönnimann, 1948, and *Miliammina fusca* (Brady, 1870). The Middle Marsh Biofacies was characterized by *Tiphotrocha comprimata* (Cushman & Brönnimann, 1948), *Trochammina inflata* (Montagu, 1808), and *Arenoparrella mexicana* (Kornfeld, 1931). The High Marsh and Upland Transition Biofacies were characterized by *E. macrescens* (Brady, 1870), *Haplophragmoides wilberti* Andersen, 1953, and *Trochamminita irregularis* Cushman & Brönnimann, 1948, which had relative abundances between 40 and 80%. A Canonical Correspondence Analysis with grain sizes, organic fraction (loss-on-ignition organic carbon) and measured vertical elevation as environmental variables indicated that elevation was the most influential in explaining variance of the foraminiferal abundances.

However, in this study we only utilized the marsh samples, since estuarine grab samples were mainly affected by marsh-edge sediment slumping into the channels, and high abundances of calcareous species that were less likely to be preserved in organic-rich sediment (Haller et al., in review; Chapter 2).

Reconstruction Core Stratigraphy

The two Grand Bay cores (GB53R and GB60R) had silts at the base overlain by peat deposits (Fig. 3.4). Core GB53R constitutes the full pattern of emerging salt marsh: coring penetrated inorganic bluish silt (120–105 cm), which graded into a light-grey silt with sparse vegetation macrofossils (105–90 cm depth). Salt-marsh roots appear first in patches above 90 cm and become denser near the core top (~20 cm depth to top). The neighboring core GB60R had a thicker peat sequence and bottomed out in the organic-rich grey silts. Salt-marsh peat with few macrofossils was present from 95 cm to 60 cm; from 60 to 0 cm a unit with abundant macrofossil roots followed. The modern *J. roemerianus* root layer extended from 20 cm depth to core top.

The stratigraphy between the cores from Dauphin Island was remarkably consistent (Fig. 3.5). Both DA40R and DA42R were characterized by an incompressible basal unit of blue silt grading into 10–15 cm layer of grey organic silt, followed by a 60–70 cm sequence of salt-marsh peat of increasing density. The upper 20 cm of both cores encompassed water-saturated grey silt, in which roots of the modern marsh vegetation were established. The sedimentary successions of all four cores indicated that the salt marshes emerged from tidal flat silts, which were thereafter colonized by intertidal salt-marsh grass (e.g., Redfield, 1972; Rodriguez et al., 2008).

Fossil Assemblages in Cores

The Grand Bay cores were mainly dominated by varying degrees of Low Marsh and Middle Marsh species (Fig. 3.4, Appendix B1). The base of core GB53R was a silt unit barren of foraminifera. With transition from silt to salt-marsh peat, foraminiferal densities increased to 1000 specimens/10 cm^3, and decreased to a minimum of 250 specimens/10 cm^3 between 20 and 15 cm. Maximum densities of 2000 specimens/10 cm^3) were counted at the core top. From 80–20 cm, *H. wilberti* and *A. mexicana* were the most abundant species. Between 20 cm and surface, Low Marsh foraminifera such as *M. fusca*, *A. inepta*, and the *Ammotium salsum* + *Ammobaculites* group increased, Middle Marsh species such as of *H. wilberti* waned. However, *A. mexicana* remained abundant above 20 cm depth.

The core GB60R was largely dominated by Middle Marsh species without strong compositional shifts. A pronounced density increase occurred as the lithology switched to denser salt-marsh peat at 60 cm depth. In the upper section (10 cm to top), *H. wilberti* increased markedly in abundance from <10% to >50%, whereas Middle Marsh species remained stable.

The two Dauphin Island cores exhibited relatively similar trends in foraminiferal assemblages (Fig. 3.5). Foraminiferal density increased rapidly when salt-marsh macrofossils started occurring (80–90 cm) and a foraminiferal assemblage dominated by *A. mexicana* was established. A species shift occurred at depths that marked the stratigraphic switch from dense salt-marsh peat to organic silt (20–25 cm):

Abundances of *A. mexicana* strongly decreased, as *M. fusca* and the *Ammotium salsum* + *Ammobaculites exiguus* group increased (up to 80% of specimens when combined).

Live Foraminifera in Cores

The three stained short cores from Dauphin Island were sampled between surface and 9 cm depth (Fig. 3.6). Coring station elevations ranged between -0.11 and 0.04 m MHW, between which typically Low Marsh and Middle Marsh Biofacies were prevalent. Common species found both living and dead were agglutinated forms such as *Ammotium*, *Haplophragmoides*, *T. comprimata*, *Affinetrina alcidi* Levy, Mathieu, Poignant, Rosset-Moulinier, Takayanagi & Saito, 1992, and *Pseudothurammina limnetis* (Scott & Medioli, 1980) (see Appendix B1). Dead foraminiferal test densities were within the range 200–350 specimens/10 cm^3, except for DA35R, which yielded only 50–160 specimens/10 cm^3, indicating a setting where recent test inputs are rapidly destroyed (Hippensteel et al., 2002). Dead assemblages and living specimens had infaunal maxima between 1 and 4 cm depth. However, DA34R had its peak in live tests at the surface. Proportion of living specimens generally decreased with depth from ~15% down to 4%.

Chronology of Cores

The five radiocarbon dates from basal salt-marsh macrofossils (Table 3.3) reveal that Dauphin Island cores contain the oldest and most compacted marshes with inception around 420 CE. Additional radiometric dates from nearby pushcores were used to complete chronologies near the surface, and ^{137}Cs activity peaks were applied to confirm ^{210}Pb CRS models (Appendix B2). Bchron developed integrated age-depth models combining the ^{210}Pb dates and ^{14}C dates, providing ages with 95% credible intervals (Appendix B3; Haslett and Parnell, 2008). From the age models, Bchron extracted age estimates for all foraminiferal sample depths so that each interpretation based on foraminiferal assemblages could be assigned an age.

Generally, the Grand Bay cores indicated significantly higher sediment accumulation rates than the Dauphin Island counterparts (Appendix B3). However, in the basal clay unit of all cores, few Low

Marsh specimens occurred contemporaneously with elevated sediment accumulation rates. When assemblages shifted to a Middle Marsh Biofacies, the sediment accumulation rates decreased. Since about 1900 CE the sediment accumulation rates increased sharply in all cores. This increase was accompanied by a shift to Low Marsh species in GB53R, DA40R, and DA42R. Furthermore, in the two Dauphin Island cores, the deposition of grey organic silt began.

Paleo-Marsh Elevation

Components 1 and 2 of the WA-PLS provided reasonable fits to the training data set (R^2 of 0.49 and 0.58, respectively); subsequent components (3–5) provided little gain in terms of R^2 (Table 3.4). Between component 1 and 2, improvement on RMSE was 9.2% and predictive loss on RMSEP was 6.1% (Table 3.4; Fig. 3.7). Subsequent components (e.g. between 2 and 3) saw little gain in RMSE (i.e., less than 9.2%) and additional loss in predictive skill (i.e., RMSEP greater than 6.1%). Using component 2, eighty-three percent of all measured sample elevations were within range of transfer function elevation estimates. In 17% of cases there was no overlap within error, which was predominantly the case for estimated elevations with residuals greater than 0.2 m (Fig. 3.7). The application of the transfer function to the fossil assemblages yielded PME estimates with cross-validated errors for each sample individually.

In GB53R, PME was 0.39 m MHW shortly after first peat was deposited. The PME decreased to 0.03 m MHW at the core top, which was within the elevation range of the dGPS measurement (Fig. 3.4A). In GB60R, PME was first reconstructed at 0.24 m MHW, had a dip in the middle of the core (0–0.1 m MHW), and increased rapidly in the core top section. However, the reconstruction of the core top is significantly higher than the dGPS measured surface elevation. This trend was likely caused by the increasing abundance of *H. wilberti*, which had one of the highest species optima (0.18 m MHW).

Both, DA40R and DA42R had PME values near 0.2 m MHW in the lower core sections and showed a rapid decline to ~0 m MHW between 10 and 20 cm core depth (Fig. 3.5). This coincided with the lithology change to grey silt and the shift from Low Marsh to Middle Marsh indicator species. The core-top reconstructions of both Dauphin Island cores were well aligned with dGPS measurements.

As quality control for the PME reconstructions we used the MinDC parameter calculated by a Weighted Average transfer function. The MinDC measured assemblage dissimilarity between each reconstructed sample and its closest analogue in the training set. In each core one sample exceeded the 10^{th} percentile dissimilarity threshold and was not included in subsequent analysis. These samples contained particularly high abundances of either *H. wilberti* (57%; GB60R 0–1 cm) or *A. mexicana* (>80%; DA40R, 35 cm, DA42R, 25 cm), which was for both cases the highest recorded.

Relative Sea Level

All PME predictions that passed the MinDC quality control were first assigned age estimates with age uncertainties from the Bayesian age-depth models (Fig. 3.8). Next, Relative Sea Level was calculated for each PME point using formula (1).

In the Grand Bay Cores, RSL rose 1.2 m between the base of the cores to the core top with almost constant rate (Figs. 3.8A, B). At GB53R, linear interpolation between RSL points yielded an average RSL rate of 1.17 ±0.88 mm/year pre-1900 and 4.67 ±2.3 mm/year post-1900 CE. At coring site GB60R, RSL was more stable with -1.10 ±0.34 mm/year (pre-1900 CE) and 0.9 ±2.63 mm/year (post-1900 CE). However, GB60R showed an RSL offset of 0.26 m at the top of the reconstruction.

The two Dauphin Island cores both recorded a steady sea-level rise from the bottom of cores to about 1900 CE, and rapid increase after 1900 CE (Figs. 3.8C, D). Average rates pre-1900 for DA40R and DA42R were 0.29± 0.23 mm/year and 0.4 ±0.2 mm/year. Post-1900 they averaged 7.13 ± 2.77 mm/year and 11.24 ±4.62 mm/year respectively.

Discussion

Influences on Transfer-Function Precision

Paleo-environment and sea-level reconstructions target regional trends through the application of a broad, robust transfer function. However, local variance can obscure regional trends, and efforts to

identify and isolate local effects are critical to a quantitative regional interpretation. Such local effects manifest in the uncertainty in transfer-function predictability. Despite being quantitative, the RMSEP for this study represents 33% and 39% of the Mean Range of Tide at Grand Bay and Dauphin Island, respectively (Tables 3.1, 3.4). For comparison, the RMSEP for Mississippi Sound is two to three times that reported in other elevation/sea-level reconstruction studies (e.g., 10–15% reported by Barlow et al., 2013). Factors affecting RMSEP often reflect ambiguity in training data sets, effects of taphonomy, and/or regional coherency.

Distributions of modern salt-marsh foraminifera in the four regions sampled by Haller et al. (in review; Chapter 2) were consistent with distributions observed in other salt marshes of the southeastern U.S.A. as reported from Mississippi (Phleger, 1954), Texas (Phleger, 1965), Florida (Gerlach et al., 2017) and the Gulf of Mexico region in general (Phleger and Bradshaw, 1966; Poag, 2015). Haller et al. (in review; Chapter 2), using cluster analysis, found that nine assemblages were reflected in the 168 samples analyzed. While elevation in the intertidal zone was found to be an important environmental variable, statistical analyses indicated that there was considerable overlap among biofacies and elevation ranges (Fig. 3.3). For example, two biofacies in the Low Marsh (D3, D4) had overlapping elevation ranges; similar results occurred for the Middle Marsh (D5, D6) and High Marsh and Upland Transition (D7–9; see Table 3.2). Such overlap is not uncommon in sufficiently large training sets, encompassing multiple regions (Kemp et al., 2009a; Wright et al., 2011; Gerlach et al., 2017), and is inherently influencing the accuracy in the RMESP obtained for Mississippi Sound transfer function.

All four cores were impacted by lowered foraminiferal test densities in the top 10–20 cm (Figs. 3.4–3.5), which coincided with the depth of the modern *J. roemerianus* root horizon. Lithology was different between the Grand Bay and Dauphin Island cores. At Grand Bay, the decrease in density may be caused by taphonomic breakdown or bioturbation that introduced oxygen and allowed bacterial degradation of inner organic linings of marsh foraminifera (Tobin et al., 2005). Species suggested as the first affected by physical and chemical breakdown is *M. fusca* (Goldstein and Harben, 1993; Hippensteel

et al., 2000). In addition, *A. mexicana* experienced a significant decrease in abundance of 20% (GB53R 8–9 cm and 10–11 cm), leading to a drop of ca. 10 cm in PME values (Fig. 3.4A).

High dissimilarity between fossil samples and the modern surface training set was found in the upper 15 cm of GB60R (Fig. 3.4B). The core samples included higher abundances of *H. wilberti* (57%) than any sample in the modern training set, in which the highest recorded abundance of *H. wilberti* was 44%. The transfer function reconstructed a PME of 0.28 m MHW, whereas the dGPS surface measurement was -0.01 m MHW. This discrepancy indicates that the distribution of *H. wilberti* does not follow the unimodal curve assumed in WA-PLS transfer functions (Barlow et al., 2013). Newer modelling approaches such as Bayesian transfer functions use more flexible statistics, which can incorporate skewed unimodal distributions (Cahill et al., 2016). Another possible explanation is the lack of close assemblage analogues in the surface training set. The species optimum of *H. wilberti* (0.18 m MHW) is located at an elevation with relatively sparse vertical sample density (Fig. 3.2). The complete vertical distribution of *H. wilberti* probably was not sampled and was not adequately represented in the training set, which led to overprediction of elevation. As comparison, we compiled a second hypothetical reconstruction of GB60R without any abundance of *H. wilberti*, which produced a PME within the range of measured elevation (Fig. 3.9). This result corroborates that the surface training set was not sufficient to render a comprehensive abundance range for all species, despite its size.

Mississippi Sound Relative Sea Level Trends

Two recent studies of Relative Sea Level are available from the Gulf of Mexico spanning the time frame of our cores. The study produced by Gerlach et al. (2017) reconstructed RSL for the last 2500 years from Little Manatee River, west-central Florida (Fig. 3.10A). For elevation estimates they employed a foraminiferal transfer function that yielded PME and RSL data. After removal of local glacioisostatic adjustment of 0.3 mm/yr, Gerlach et al.'s results indicated that sea level rose insignificantly between 0 CE to ~1500 CE, and after 1500 CE to modern, climbed to ~2 mm/year. They concluded that the eastern Gulf

of Mexico sea level did not diverge, at least not within error, from globally recognized trends (e.g., Kopp et al., 2016).

West of the study area, González and Törnqvist (2009) provided a Common Era sea-level record from the Mississippi Delta with radiocarbon dates produced from basal peats (i.e., non-compressible substrate). The sea-level index points spanning the time between 600 and 1200 CE were retrieved from cores from three regions, which made the sea level curve more robust (Fig. 3.10A). Clustering and oscillations of sea-level index points between 1000 and 1200 CE suggested a sudden increase in RSL, however errors were large enough that a linear trend cannot be excluded. Gerlach et al. (2017) re-modeled the González and Törnqvist (2009) dataset and corrected for local glacioisostatic adjustment and delta subsidence (0.6 mm/year). During the period between 600 and 1600 CE, Gerlach et al. (2017) found an increase in SLR from 0 to 0.2 mm/year, which was not distinguishable within uncertainty.

The Grand Bay and Dauphin Island core pairs reproduced their local trends (Fig. 3.10). However, there were differences between backbarrier marshes on Dauphin Island and mainland marshes at Grand Bay. Dauphin Island behaved in alignment with most of the González and Törnqvist (2009) and Gerlach et al. (2017) datasets. In comparison, on the mainland, Grand Bay experienced a faster rising RSL than other Gulf of Mexico trends would suggest.

Prior to the publication of the first geographic maps of the area (U.S. Coast Survey, 1848; United States Coast and Geodetic Survey, 1853), the paleo-Grand Bay Pascagoula/Escatawpa fluvial system emptied via Bayou Cumbest into the Mississippi Sound, an active delta headland (Fig. 3.1; Eleuterius and Criss, 1991). At this time, Grand Bay was protected from intense waves by the barrier island belt (Dauphin Island, Petit Bois Island, Horn Island, Ship Island, etc.), which sheltered Mississippi Sound (Buster and Morton, 2011). Lateral barrier island migration led to the opening of a wide passage between Petit Bois and Dauphin Island south of Grand Bay, which exposed Grand Batture Island to northerly-directed waves (Otvos, 1970; Eleuterius and Criss, 1991; Buster and Morton, 2011). Simultaneously, long-term reduction in fluvial sedimentation coupled with erosion initiated a sequence of geomorphic events similar to an abandonment event of a river delta lobe (Meyer-Arendt and Kramer, 1991; Nienhuis

et al., 2013). The combination of sediment starvation and raised wave energies led to the gradual reduction in size of Grand Batture Island beginning pre-1840s (Meyer-Arendt and Kramer, 1991), and culminated in the complete disintegration and erosion to the sub-aqueous shoals seen today. We suggest that the protected position of Grand Bay behind Grand Batture Island and sediment flux from the now diverted Escatawpa River led to sediment accumulation rates about twice as high as on Dauphin Island, thus increasing apparent RSL rise rates at least until the mid-1800s (see Appendix B2). After the Escatawpa River was cut off, enhanced sediment flux from the disintegrating Grand Batture Island and recycled material from more effective storm surges may have been responsible for continued sediment accumulation, which is a typical process observed in modern Gulf of Mexico marshes (Rejmánek et al., 1988; Goodbred et al., 1998; Turner et al., 2007). Estuarine sediment input often possesses sedimentological properties (grain size, bulk density, and organic matter content) that are identical to the underlying marsh deposits (Goodbred and Hine, 1995; Khan et al., 2013) and also may not be distinguished based on foraminifera due to calcium carbonate dissolution (Edwards and Horton, 2000; Tobin et al., 2005).

Regional Trends in the 1900s

Post-demise of Grand Batture Island (Meyer-Arendt and Kramer, 1991), the Grand Bay and Dauphin Island cores recorded similar RSL trends. We compared the post-1900 recorded RSL reconstructions to a regional tide gauge composite containing six of the longest instrumental records of the Gulf of Mexico reaching back to 1913 (Fig. 3.11). Tide-gauge derived average RSL rise over the last 100 years was 2.76 mm/year, which is less than all four reconstructions (Fig. 3.10B).

The comparison of historic shoreline data with modern shoreline positions revealed strong influence of coastal erosion at the coring sites (Fig. 3.12). Published erosion rates indicate rapid shoreline retreat of -1.31 m in Dauphin Island backbarrier marshes (Henderson et al., 2017), and similarly high rates of -0.3 to -1.7 m at Grand Bay (Table 3.5; Terrano et al., 2017). The lithology logs of DA40R and

DA42R showed increasing deposition of minerogenic silt since the 1900s, accompanied by a foraminiferal biofacies shift indicating low marsh environments. Lithological changes were not observed at the Grand Bay sites, however foraminiferal data from GB53R showed a clear shift towards Low Marsh species, which is typically caused by increased flooding frequency (Scott and Medioli, 1980b; Horton et al., 1999). Furthermore, modelling studies of the Grand Bay water body suggest that tidal amplitudes increased and flow became successively more ebb-dominated after change of geomorphic configuration and erosion of its protective headland, Grand Batture Island (Fig. 1B; Passeri et al., 2015). As a result, the Grand Bay estuary is currently in a transgressive state as it has become subject to intensive lateral erosion in some areas (Wu et al., 2017). We suggest that encroachment of subtidal facies and increased flooding both are mechanisms driving relatively rapid environmental change, which renders the tops of the Dauphin Island and Grand Bay cores only of local significance (Figs. 3.8C, D).

Conclusions

We collected four cores from two regions in the Mississippi Sound to address paleo-environmental change and Relative Sea Level from Grand Bay (mainland marsh) and Dauphin Island (backbarrier marsh). The regional surface training set demonstrated vertical variance sufficient to establish a transfer function with an RMSEP of 0.14 m, which is 33% of the Mean Range of Tide at Grand Bay, and 39% at Dauphin Island. This is a relatively imprecise value caused by properties of the dataset and ultimately the geomorphic configuration of the flat and wide marsh systems of the region.

By application of the transfer function to fossil foraminifera from dated sediment cores, we reconstructed Paleo-Marsh Elevation and Relative Sea Level over the last ~1800 years. We compared our Mississippi Sound data with reconstructions of similar age range from the Mississippi Delta and western Florida. By comparison, the Grand Bay region experienced faster sediment accumulation and faster (apparent) RSL increase than Dauphin Island. Such between-region differences cannot be adequately

explained without taking into account regional geomorphologic change. We suggest that pre-1840s the Grand Bay region received sediment influx from the still active Escatawpa River, while subsequent avulsion and decline of sediment supply eroded the protective headland, Grand Batture Island, to a submerged shoal. In this context, smaller scale (e.g., distance to estuarine channels, anthropogenic influence, etc.) should be taken into account during site selection, as well as larger geomorphic processes acting in the past.

Reconstructed Relative Sea Level rise rates in three out of four sediment cores increased sharply after 1900 CE. According to our proxy reconstructions, all four core sites experienced RSL increases greater than indicated by instrumental records over the last 100 years. This trend is accompanied by a change in biofacies from Middle Marsh to Low Marsh likely caused by lateral erosion, and shorelines progressively encroaching towards the coring sites. At Dauphin Island the erosion is lithologically reflected by deposition of grey silt in the top 20 cm of the cores. Relative Sea Level reconstructed for the last ~100 years should thus only be considered of local significance and not in accordance with sea level trends in the Mississippi Sound. For an accurate regional reconstruction we suggest that not only small-scale process have to be taken into account during site selection (e.g. distance to avulsion channels, length of record), but also larger geomorphic processes in the past.

Acknowledgments

Marci Marot provided lead and polonium data, Alisha Ellis and Marci Marot helped sampling the Dauphin Island cores. Terry McCloskey and C. Scott Adams were of great help coring in the field at Grand Bay. The professional societies AAPG and GSA provided student grants for radiocarbon dating at NOSAMS. Thank you to the employees of the Grand Bay NERR for access to their reserve and permit to collect cores. All laboratory work and analyses were conducted at the U.S. Geological Survey St. Petersburg Coastal and Marine Science Center. The foraminiferal census of this study is also available as

USGS Data Release https://doi.org/10.5066/F7445KSG. Any use of trade names is for descriptive purposes only and does not imply endorsement by the U.S. Government.

References

Appleby, P.G., 2001. Chronostratigraphic Techniques in Recent Sediments, in: Last, W.M., Smol, J.P. (Eds.), Tracking Environmental Change Using Lake Sediments - Basin Analysis, Coring, and Chronological Techniques. Springer Netherlands, pp. 171-203.

Appleby, P.G., Oldfield, F., 1978. The calculation of lead-210 dates assuming a constant rate of supply of unsupported 210Pb to the sediment. CATENA 5, 1–8. 10.1016/S0341-8162(78)80002-2

Barlow, N.L.M., Shennan, I., Long, A.J., Gehrels, W.R., Saher, M.H., Woodroffe, S.A., Hillier, C., 2013. Salt marshes as late Holocene tide gauges. Global and Planetary Change 106, 90–110. 10.1016/j.gloplacha.2013.03.003

Binford, M.W., 1990. Calculation and uncertainty analysis of ^{210}Pb dates for PIRLA project lake sediment cores. Journal of Paleolimnology 3, 253–267. 10.1007/bf00219461

Birks, H.J.B., 1995. Quantitative paleoenvironmental reconstruction. Technical guide, in: Maddy, D., Brew, J.S. (Eds.), Statistical modelling of Quaternary science data. Quaternary Research Association, Cambridge, p. 271.

Birks, H.J.B., 2010. Numerical methods for the analysis of diatom assemblage data, in: Stoermer, E.F., Smol, J.P. (Eds.), The Diatoms: Applications for the Environmental and Earth Sciences, 2 ed. Cambridge University Press, Cambridge, pp. 23–54.

Blum, M., Martin, J., Milliken, K., Garvin, M., 2013. Paleovalley systems: Insights from Quaternary analogs and experiments. Earth-Science Reviews 116, 128–169. 10.1016/j.earscirev.2012.09.003

Bregy, J.C., Wallace, D.J., Minzoni, R.T., Cruz, V.J., in press. 2500-year paleotempestological record of intense storms for the northern Gulf of Mexico, United States. Marine Geology. 10.1016/j.margeo.2017.09.009

Buster, N.A., Morton, R.A., 2011. Historical bathymetry and bathymetric change in the Mississippi-Alabama coastal region, 1847–2009. Map and Accompanying pamphlet., p. 13.

Cahill, N., Kemp, A.C., Horton, B.P., Parnell, A.C., 2016. A Bayesian hierarchical model for reconstructing relative sea level: from raw data to rates of change. Climate of the Past 12, 525–542. 10.5194/cp-12-525-2016

Culver, S.J., Horton, B.P., 2005. Infaunal marsh foraminifera from the Outer Banks, North Carolina, U.S.A. Journal of Foraminiferal Research 35, 148–170. 10.2113/35.2.148

Culver, S.J., Woo, H.J., Oertel, G.F., Buzas, M.A., 1996. Foraminifera of coastal depositional environments, Virginia, U.S.A.; distribution and taphonomy. Palaios 11, 459–486. 10.2307/3515213

Cutshall, N.H., Larsen, I.L., Olsen, C.R., 1983. Direct analysis of 210Pb in sediment samples: Self-absorption corrections. Nuclear Instruments & Methods B 206, 309–312.

Edwards, R.J., Horton, B.P., 2000. Reconstructing relative sea-level change using UK salt-marsh foraminifera. Marine Geology 169, 41–56. 10.1016/S0025-3227(00)00078-5

Edwards, R.J., van de Plassche, O., Gehrels, W.R., Wright, A.J., 2004. Assessing sea-level data from Connecticut, USA, using a foraminiferal transfer function for tide level. Marine Micropaleontology 51, 239–255. 10.1016/j.marmicro.2003.11.003

El-Daoushy, F., Olsson, K., Garcia-Tenorio, R., 1991. Accuracies in Po-210 determination for lead-210 dating. Hydrobiologia 214, 43–52. 10.1007/bf00050930

Eleuterius, C.K., Criss, G.A., 1991. Point aux Chenes: Past, Present, and Future perspective of erosion. Physical Oceanography Section Gulf Coast Research Laboratory, Ocean Springs, Mississippi, p. 47.

Engelhart, S.E., Horton, B.P., Vane, C.H., Nelson, A.R., Witter, R.C., Brody, S.R., Hawkes, A.D., 2013. Modern foraminifera, $\delta^{13}C$, and bulk geochemistry of central Oregon tidal marshes and their application in paleoseismology. Palaeogeography, Palaeoclimatology, Palaeoecology 377, 13–27. 10.1016/j.palaeo.2013.02.032

Fagherazzi, S., 2014. Storm-proofing with marshes. Nature Geoscience 7, 701–702. 10.1038/ngeo2262

Feagin, R.A., Williams, A.M., 2008. Sediment spatial patterns in a Hurricane Katrina overwash fan on Dauphin Island, Alabama, U.S.A. Journal of Coastal Research 244, 1063–1070. 10.2112/07-0862.1

Flynn, W.W., 1968. The determination of low levels of polonium-210 in environmental materials. Analytica Chimica Acta 43, 221–227. 10.1016/S0003-2670(00)89210-7

Gehrels, W.R., 2000. Using foraminiferal transfer functions to produce high-resolution sea-level records from salt-marsh deposits, Maine, USA. The Holocene 10, 367–376. 10.1191/095968300670746884

Gehrels, W.R., van de Plassche, O., 1999. The use of *Jadammina macrescens* (Brady) and *Balticammina pseudomacrescens* Brönnimann, Lutze and Whittaker (Protozoa: Foraminiferida) as sea-level indicators. Palaeogeography, Palaeoclimatology, Palaeoecology 149, 89–101. 10.1016/S0031-0182(98)00194-1

Gerlach, M.J., Engelhart, S.E., Kemp, A.C., Moyer, R.P., Smoak, J.M., Bernhardt, C.E., Cahill, N., 2017. Reconstructing Common Era relative sea-level change on the Gulf Coast of Florida. Marine Geology 390, 254–269. 10.1016/j.margeo.2017.07.001

Goldstein, S.T., Harben, E.B., 1993. Taphofacies implications of infaunal foraminiferal assemblages in a Georgia salt marsh, Sapelo Island. Micropaleontology 39, 53–62. 10.2307/1485974

Goldstein, S.T., Watkins, G.T., Kuhn, R.M., 1995. Microhabitats of salt marsh foraminifera: St. Catherines Island, Georgia, USA. Marine Micropaleontology 26, 17–29. 10.1016/0377-8398(95)00006-2

González, J.L., Törnqvist, T.E., 2009. A new Late Holocene sea-level record from the Mississippi Delta: evidence for a climate/sea level connection? Quaternary Science Reviews 28, 1737–1749. 10.1016/j.quascirev.2009.04.003

Goodbred, S.L., Hine, A.C., 1995. Coastal storm deposition: Salt-marsh response to a severe extratropical storm, March 1993, west-central Florida. Geology 23, 679-682. 10.1130/0091-7613(1995)023<0679:csdsmr>2.3.co;2

Goodbred, S.L., Wright, E.E., Hine, A.C., 1998. Sea-level change and storm-surge deposition in a late Holocene Florida salt marsh. Journal of Sedimentary Research 68, 240–252. 10.2110/jsr.68.240

Greene, D.L., Rodriguez, A.B., Anderson, J.B., 2007. Seaward-branching coastal-plain and piedmont incised-valley systems through multiple sea-level cycles: Late Quaternary examples from Mobile Bay and Mississippi Sound, U.S.A. Journal of Sedimentary Research 77, 139–158. 10.2110/jsr.2007.016

Haller, C., Smith, C.G., Hallock, P., Hine, A.C., Osterman, L.E., McCloskey, T.A., in review. Distribution of modern salt-marsh foraminifera from the eastern Mississippi Sound, U.S.A. Journal of Foraminiferal Research.

Haslett, J., Parnell, A.C., 2008. A simple monotone process with application to radiocarbon-dated depth chronologies. Journal of the Royal Statistical Society: Series C (Applied Statistics) 57, 399–418. 10.1111/j.1467-9876.2008.00623.x

Henderson, R.E., Nelson, P.R., Long, J.W., Smith, C.G., 2017. Vector shorelines and associated shoreline change rates derived from lidar and aerial imagery for Dauphin Island, Alabama: 1940-2015. U.S. Geological Survey data release. 10.5066/F7T43RB5

Hippensteel, S.P., Martin, R.E., Nikitina, D., Pizzuto, J.E., 2000. The formation of Holocene marsh foraminiferal assemblages, middle Atlantic coast, U.S.A.: Implications for Holocene sea-level change. Journal of Foraminiferal Research 30, 272–293. 10.2113/0300272

Hippensteel, S.P., Martin, R.E., Nikitina, D., Pizzuto, J.E., 2002. Interannual variation of marsh foraminiferal assemblages (Bombay Hook National Wildlife Refuge, Smyrna, DE): Do foraminiferal assemblages have a memory? Journal of Foraminiferal Research 32, 97–109. 10.2113/0320097

Holgate, S.J., Matthews, A., Woodworth, P.L., Rickards, L.J., Tamisiea, M.E., Bradshaw, E., Foden, P.R., Gordon, K.M., Jevrejeva, S., Pugh, J., 2012. New data systems and products at the Permanent Service for Mean Sea Level. Journal of Coastal Research, 493–504. 10.2112/JCOASTRES-D-12-00175.1

Horton, B.P., Edwards, R.J., 2006. Quantifying Holocene sea level change using intertidal foraminifera: Lessons from the British Isles. Cushman Foundation for Foraminiferal Research, Special Publication 40, p. 97.

Horton, B.P., Edwards, R.J., Lloyd, J.M., 1999. A foraminifera-based transfer function: implications for sea-level studies. Journal of Foraminiferal Research 29, 117–129. 10.2113/gsjfr.29.2.117

Imbrie, J., Kipp, N.G., 1971. A new micropaleontological method for quantitative paleoclimatology: Application to a late Pleistocene Caribbean core, in: Turekian, K.K. (Ed.), The Late Cenozoic Glacial Ages, Yale University Press, New Haven, CT, pp. 71–181.

Jackson, S.T., Williams, J.W., 2004. Modern analogs in Quarternary paleoecology: Here today, gone yesterday, gone tomorrow? Annual Review of Earth and Planetary Sciences 32, 495–537. 10.1146/annurev.earth.32.101802.120435

Juggins, S., 2016. C2 Version 1.7.7. https://www.staff.ncl.ac.uk/stephen.juggins/software/C2Home.htm

Juggins, S., Birks, H.J.B., 2012. Quantitative environmental reconstructions from biological data, in: Birks, H.J.B., Lotter, A.F., Juggins, S., Smol, J.P. (Eds.), Tracking Environmental Change Using Lake Sediments: Data Handling and Numerical Techniques. Springer Netherlands, Dordrecht, pp. 431–494.

Kearney, M.S., Turner, R.E., 2016. Microtidal marshes: Can these widespread and fragile marshes survive increasing climate–sea level variability and human action? Journal of Coastal Research, 686–699. 10.2112/JCOASTRES-D-15-00069.1

Kemp, A.C., Hill, T.D., Vane, C.H., Cahill, N., Orton, P.M., Talke, S.A., Parnell, A.C., Sanborn, K., Hartig, E.K., 2017a. Relative sea-level trends in New York City during the past 1500 years. The Holocene 27, 1169–1186. 10.1177/0959683616683263

Kemp, A.C., Horton, B.P., Culver, S.J., 2009a. Distribution of modern salt-marsh foraminifera in the Albemarle-Pamlico estuarine system of North Carolina, USA: Implications for sea-level research. Marine Micropaleontology 72, 222–238. 10.1016/J.Marmicro.2009.06.002

Kemp, A.C., Horton, B.R., Corbett, D.R., Culver, S.J., Edwards, R.J., van de Plassche, O., 2009b. The relative utility of foraminifera and diatoms for reconstructing late Holocene sea-level change in North Carolina, USA. Quaternary Research 71, 9–21. 10.1016/J.Yqres.2008.08.007

Kemp, A.C., Kegel, J.J., Culver, S.J., Barber, D.C., Mallinson, D.J., Leorri, E., Bernhardt, C.E., Cahill, N., Riggs, S.R., Woodson, A.L., Mulligan, R.P., Horton, B.P., 2017b. Extended late Holocene relative sea-level histories for North Carolina, USA. Quaternary Science Reviews 160, 13–30. 10.1016/j.quascirev.2017.01.012

Kemp, A.C., Nelson, A.R., Horton, B.P., 2013a. 14.31 Radiocarbon dating of plant macrofossils from tidal-marsh sediment, in: Shroder, J.F. (Ed.), Treatise on Geomorphology. Academic Press, San Diego, pp. 370–388.

Kemp, A.C., Telford, R.J., Horton, B.P., Anisfeld, S.C., Sommerfield, C.K., 2013b. Reconstructing Holocene sea level using salt-marsh foraminifera and transfer functions: lessons from New Jersey, USA. Journal of Quaternary Science 28, 617–629. 10.1002/jqs.2657

Khan, N.S., Horton, B.P., McKee, K.L., Jerolmack, D., Falcini, F., Enache, M.D., Vane, C.H., 2013. Tracking sedimentation from the historic A.D. 2011 Mississippi River flood in the deltaic wetlands of Louisiana, USA. Geology 41, 391–394. 10.1130/g33805.1

Kindinger, J.L., Balson, P.S., Flocks, J.G., 1994. Stratigraphy of the Mississippi-Alabama shelf and the Mobile River incised-valley system, in: Dalrymple, R.W., Boyd, R., Zaitlain, B.A. (Eds.), Incised-Valley Systems: Origin and Sedimentary Sequences. SEPM Special Publication No. 51, pp. 83–95.

Kirwan, M.L., Temmerman, S., Skeehan, E.E., Guntenspergen, G.R., Fagherazzi, S., 2016. Overestimation of marsh vulnerability to sea level rise. Nature Climate Change 6, 253–260. 10.1038/nclimate2909

Kopp, R.E., Kemp, A.C., Bittermann, K., Horton, B.P., Donnelly, J.P., Gehrels, W.R., Hay, C.C., Mitrovica, J.X., Morrow, E.D., Rahmstorf, S., 2016. Temperature-driven global sea-level variability in the Common Era. Proceedings of the National Academy of Sciences 113, E1434–E1441. 10.1073/pnas.1517056113

Kramer, K.A., 1990. Late Pleistocene to Holocene geologic evolution of the Grand Batture headland area, Jackson County, Mississippi, Masters thesis at Department of Geology and Geography. Mississippi State University, p. 165.

Lamb, G.M., 1972. Distribution of Holocene foraminifera in Mobile Bay and the effect of salinity changes, in: Scarbrough, W.L. (Ed.), Recent sedimentation along the Alabama coast. Alabama Geological Society, pp. 8–26.

Leorri, E., Cearreta, A., Horton, B.P., 2008a. A foraminifera-based transfer function as a tool for sea-level reconstructions in the southern Bay of Biscay. Geobios 41, 787–797. 10.1016/j.geobios.2008.03.003

Leorri, E., Horton, B.P., Cearreta, A., 2008b. Development of a foraminifera-based transfer function in the Basque marshes, N. Spain: Implications for sea-level studies in the Bay of Biscay. Marine Geology 251, 60–74. 10.1016/j.margeo.2008.02.005

Martin, E.A., Rice, C.A., 1981. Sampling and analizing sediment cores for ^{210}Pb geochronology, U.S. Geological Survey Open File Report 81–983, p. 31.

Meyer-Arendt, K.J., Kramer, K.A., 1991. Deterioration and restoration of the Grande Batture Islands, Mississippi. The Department Of Environmental Quality, Mississippi Geology 11, 1–5.

Müller-Navarra, K., Milker, Y., Schmiedl, G., 2017. Applicability of transfer functions for relative sea-level reconstructions in the southern North Sea coastal region based on salt-marsh foraminifera. Marine Micropaleontology 135, 15–31. 10.1016/j.marmicro.2017.06.003

Murray, J.W., Bowser, S.S., 2000. Mortality, protoplasm decay rate, and reliability of staining techniques to recognize 'living' foraminifera: A review. Journal of Foraminiferal Research 30, 66–70. 10.2113/0300066

Nelson, P.R., Bosse, S.T., Smith, C.G., 2018. A GIS compilation of vector shorelines derived from aerial imagery for the Grand Bay region of Mississippi and Alabama—2010 and 2012. U.S. Geological Survey data release. 10.5066/F7VT1R8Q

Nienhuis, J.H., Ashton, A.D., Roos, P.C., Hulscher, S.J.M.H., Giosan, L., 2013. Wave reworking of abandoned deltas. Geophysical Research Letters 40, 5899–5903. 10.1002/2013GL058231

Osterman, L.E., 2003. Benthic foraminifers from the continental shelf and slope of the Gulf of Mexico: an indicator of shelf hypoxia. Estuarine, Coastal and Shelf Science 58, 17–35. 10.1016/S0272-7714(02)00352-9

Osterman, L.E., Smith, C.G., 2012. Over 100 years of environmental change recorded by foraminifers and sediments in Mobile Bay, Alabama, Gulf of Mexico, USA. Estuarine Coastal and Shelf Science 115, 345–358. 10.1016/J.Ecss.2012.10.001

Otvos, E.G., 1970. Development and migration of barrier islands, northern Gulf of Mexico. Geological Society of America Bulletin 81, 241–246. 10.1130/0016-7606(1970)81[241:damobi]2.0.co;2

Otvos, E.G., 1985a. Barrier platforms: Northern Gulf of Mexico. Marine Geology 63, 285–305. 10.1016/0025-3227(85)90087-8

Otvos, E.G., 1985b. Coastal evolution - Louisiana to northwest Florida. The New Orleans Geological Society, AAPG Annual Meeting Guidebook, March 27-29, 1985, New Orleans, pp.

Parnell, A.C., Buck, C.E., Doan, T.K., 2011. A review of statistical chronology models for high-resolution, proxy-based Holocene palaeoenvironmental reconstruction. Quaternary Science Reviews 30, 2948–2960. 10.1016/j.quascirev.2011.07.024

Parnell, A.C., Haslett, J., Allen, J.R.M., Buck, C.E., Huntley, B., 2008. A flexible approach to assessing synchroneity of past events using Bayesian reconstructions of sedimentation history. Quaternary Science Reviews 27, 1872–1885. 10.1016/j.quascirev.2008.07.009

Passeri, D.L., Hagen, S.C., Medeiros, S.C., Bilskie, M.V., 2015. Impacts of historic morphology and sea level rise on tidal hydrodynamics in a microtidal estuary (Grand Bay, Mississippi). Continental Shelf Research 111, 150–158. 10.1016/j.csr.2015.08.001

Phleger, F.B., 1954. Ecology of foraminifera and associated microorganisms from Mississippi Sound and environs. AAPG Bulletin 38, 584–646.

Phleger, F.B., 1960. Sedimentary patterns of microfaunas in Northern Gulf of Mexico, in: Shepard, F.P., Phleger, F.B., van Andel, T.H. (Eds.), Recent Sediments, Northwest Gulf of Mexico. AAPG Special Publication 21, pp. 267–301.

Phleger, F.B., 1965. Patterns of marsh foraminifera, Galveston Bay, Texas. Limnology and Oceanography 10, R169–R184. 10.4319/lo.1965.10.suppl2.r169

Phleger, F.B., Bradshaw, J.S., 1966. Sedimentary environments in a marine marsh. Science 154, 1551–1553. 10.1126/science.154.3756.1551

Phleger, F.B., Walton, W.R., 1950. Ecology of marsh and bay foraminifera, Barnstable, Massachusetts. American Journal of Science 248, 274–294. 10.2475/ajs.248.4.274

Plant, N.G., Thieler, E.R., Passeri, D.L., 2016. Coupling centennial-scale shoreline change to sea-level rise and coastal morphology in the Gulf of Mexico using a Bayesian network. Earth's Future 4, 143–158. 10.1002/2015EF000331

Poag, C.W., 2015. Benthic foraminifera of the Gulf of Mexico - distribution, ecology, paleoecology. Texas A&M Univesity Press, College Station, 255 pp.

Priddy, R.R., Crisler, R.M., Sebren, C.P., Powell, J.D., Burford, H., 1955. Sediments of Mississippi Sound and inshore waters: a cumulative report of summer investigations, 1952, 1953, 1954, Mississippi State Geological Survey Bulletin 82, University, Mississippi, p. 54.

Redfield, A.C., 1972. Development of a New England salt marsh. Ecological Monographs 42, 201–237. 10.2307/1942263

Reimer, P.J., Bard, E., Bayliss, A., Beck, J.W., Blackwell, P.G., Bronk Ramsey, C., Buck, C.E., Cheng, H., Edwards, R.L., Friedrich, M., Grootes, P.M., Guilderson, T.P., Haflidason, H., Hajdas, I., Hatté, C., Heaton, T.J., Hoffmann, D.L., Hogg, A.G., Hughen, K.A., Kaiser, K.F., Kromer, B., Manning, S.W., Niu, M., Reimer, R.W., Richards, D.A., Scott, E.M., Southon, J.R., Staff, R.A., Turney, C.S.M., van der Plicht, J., 2013. IntCal13 and Marine13 radiocarbon age calibration curves 0–50,000 years cal BP. Radiocarbon 55, 1869–1887. 10.2458/azu_js_rc.55.16947

Rejmánek, M., Sasser, C.E., Peterson, G.W., 1988. Hurricane-induced sediment deposition in a gulf coast marsh. Estuarine, Coastal and Shelf Science 27, 217–222. 10.1016/0272-7714(88)90091-1

Rodriguez, A.B., Greene, D.L., Anderson, J.B., Simms, A.R., 2008. Response of Mobile Bay and eastern Mississippi Sound, Alabama, to changes in sediment accommodation and accumulation. Geological Society of America Special Papers 443, 13–29. 10.1130/2008.2443(02)

Rose, K.V.G., 2010. Configuration of the Pleistocene surface beneath Cat Island, Mississippi and implications for barrier island formation and evolution, Masters thesis at Earth and Environmental Sciences. University of New Orleans, p. 94.

Scott, D.B., Medioli, F.S., 1980a. Living vs. total foraminiferal populations: Their relative usefulness in paleoecology. Journal of Paleontology 54, 814–831. 10.2307/1304312

Scott, D.B., Medioli, F.S., 1980b. Quantitative studies of marsh foraminiferal distributions in Nova Scotia: implications for sea level studies. Cushman Foundation for Foraminiferal Research, Special Publication 17, p. 58.

Scott, D.S., Medioli, F.S., 1978. Vertical zonations of marsh foraminifera as accurate indicators of former sea-levels. Nature 272, 528–531. 10.1038/272528a0

Šmilauer, P., Lepš, J., 2014. Multivariate analysis of ecological data using CANOCO 5, 2nd Edition. Cambridge University Press, Cambridge, 376 pp.

Smith, C.G., Osterman, L.E., Poore, R.Z., 2013. An examination of historical inorganic sedimentation and urganic matter accumulation in several marsh types within the Mobile Bay and Mobile–Tensaw River Delta region. Journal of Coastal Research, 68–83. 10.2112/si63-007.1

ter Braak, C.J.F., Juggins, S., 1993. Weighted averaging partial least squares regression (WA-PLS): An improved method for reconstructing environmental variables from species assemblages. Hydrobiologia 269-270, 485–502. 10.1007/BF00028046

ter Braak, C.J.F., Šmilauer, P., 2012. Canoco reference manual and user's guide: Software for ordination (version 5.0). Microcomputer Power, Ithaca, USA, 496 pp.

Terrano, J.F., Smith, K.E.L., Khan, N., Smith, C., Wang, P., Pitchford, J., 2017. An evaluation of marsh shoreline erosion and deposition in the Grand Bay National Estuarine Research Reserve, Mississippi, USA, The American Association of Geographers Annual Meeting, April 5–9, 2017, Boston, MA.

Tobin, R., Scott, D.B., Collins, E.S., Medioli, F.S., 2005. Infaunal benthic foraminifera in some North American marshes and their influence on fossil assemblages. Journal of Foraminiferal Research 35, 130–147. 10.2113/35.2.130

Turner, R.E., 1991. Tide gauge records, water level rise, and subsidence in the Northern Gulf of Mexico. Estuaries 14, 139–147. 10.2307/1351687

Turner, R.E., Swenson, E.M., Milan, C.S., Lee, J.M., 2007. Hurricane signals in salt marsh sediments: Inorganic sources and soil volume. Limnology and Oceanography 52, 1231–1238.

U.S. Coast Survey, 1848. T-00273, The topography of the north shore of Mississippi Sound from Grand Batture Island to West Pascagoula River. NOAA.

United States Coast and Geodetic Survey, 1853. Coastal Survey of Mississippi Sound, scale 1:20,000.

Walton, W.R., 1952. Techniques for recognition of living foraminifera. Contributions from the Cushman Foundation for Foraminiferal Research 3, 56–60.

Wright, A.J., Edwards, R.J., van de Plassche, O., 2011. Reassessing transfer-function performance in sea-level reconstruction based on benthic salt-marsh foraminifera from the Atlantic coast of NE North America. Marine Micropaleontology 81, 43–62. 10.1016/j.marmicro.2011.07.003

Wu, W., Biber, P., Bethel, M., 2017. Thresholds of sea-level rise rate and sea-level rise acceleration rate in a vulnerable coastal wetland. Ecology and Evolution 7, 10890–10903. 10.1002/ece3.3550

Tables

Table 3.1. Tide gauges in the study area with tidal datums referenced to Mean High Water. Note that in Pascagoula no NAVD88-referenced tide gauge was available. MN = Mean Range of Tide; MHHW = Mean Higher-High Water; MHW = Mean High Water; MTL = Mean Tide Level; MLW = Mean Low Water; MLLW = Mean Lower-Low Water.

Name	NOAA ID	MN (m)	MHHW (m)	MHW (m)	MTL (m)	MLW (m)	MLLW (m)
Grand Bay NERR, MS	8740166	0.417	0.029	0	-0.208	-0.417	-0.456
Dauphin Island, AL	8735180	0.358	0.006	0	-0.179	-0.358	-0.361
West Fowl River Bridge, AL	8738043	0.422	0.047	0	-0.211	-0.421	-0.468

Table 3.2. Elevation ranges of the nine biofacies identified by Cluster Analysis (Haller et al., in review; Chapter 2).

ID	Biofacies	Upper boundary (m MHW)	Lower boundary (m MHW)
D7–9	High Marsh/Upland	0.63	0.30
D5–6	Middle Marsh	0.41	-0.28
D3–4	Low Marsh/ Low Salinity	0.11	-2.27
D2	Restricted Estuary	-0.27	-2.67
D1	Open Estuary	-2.47	-4.17

Table 3.3. Radiocarbon data from *J. roemerianus* rhizomes.

Core	Depth (cm)	NOSAMS#	^{14}C age	^{14}C error	$\delta^{13}C$ (‰VPDB)	Highest density region (%)	Highest density region (cal. years CE)
GB53R	88	130538	725	20	-23.82	88.3	1262–1284
GB60R	60	130541	305	20	-25.33	82.6, 11.2	1516–1594, 1618–1646
GB60R	84	130537	810	20	-25.95	92.7	1208–1264
DA40R	80	134057	1580	20	-21.51	94.4	426–536
DA42R	80	134058	1490	20	-21.75	92.9	546–609

Table 3.4. Transfer function performance.

Component	R^2	RMSE (m)	R^2_{boot}	RMSEP (m)	% Change
1	0.49	0.118	0.39	0.13	-
2	0.58	0.108	0.44	0.14	-6.1
3	0.63	0.101	0.46	0.16	-10.4
4	0.66	0.097	0.46	0.17	-10.0
5	0.67	0.096	0.45	0.20	-12.6

Table 3.5. Published linear regression rates near the reconstruction core sites from transects at Grand Bay (Terrano et al., 2017) and Dauphin Island (Henderson et al., 2017).

Station	Time Period	Linear Regression Rate (m/yr)	R^2
GB53R	1848–2012	-1.31	0.61
GB60R	N/A	N/A	N/A
DA40R	1940-2015	-0.30	0.84
DA40R	1940-2015	-0.78	0.93
DA42R	1940-2015	-1.25	0.89
DA42R	1940-2015	-1.70	0.80

Figures

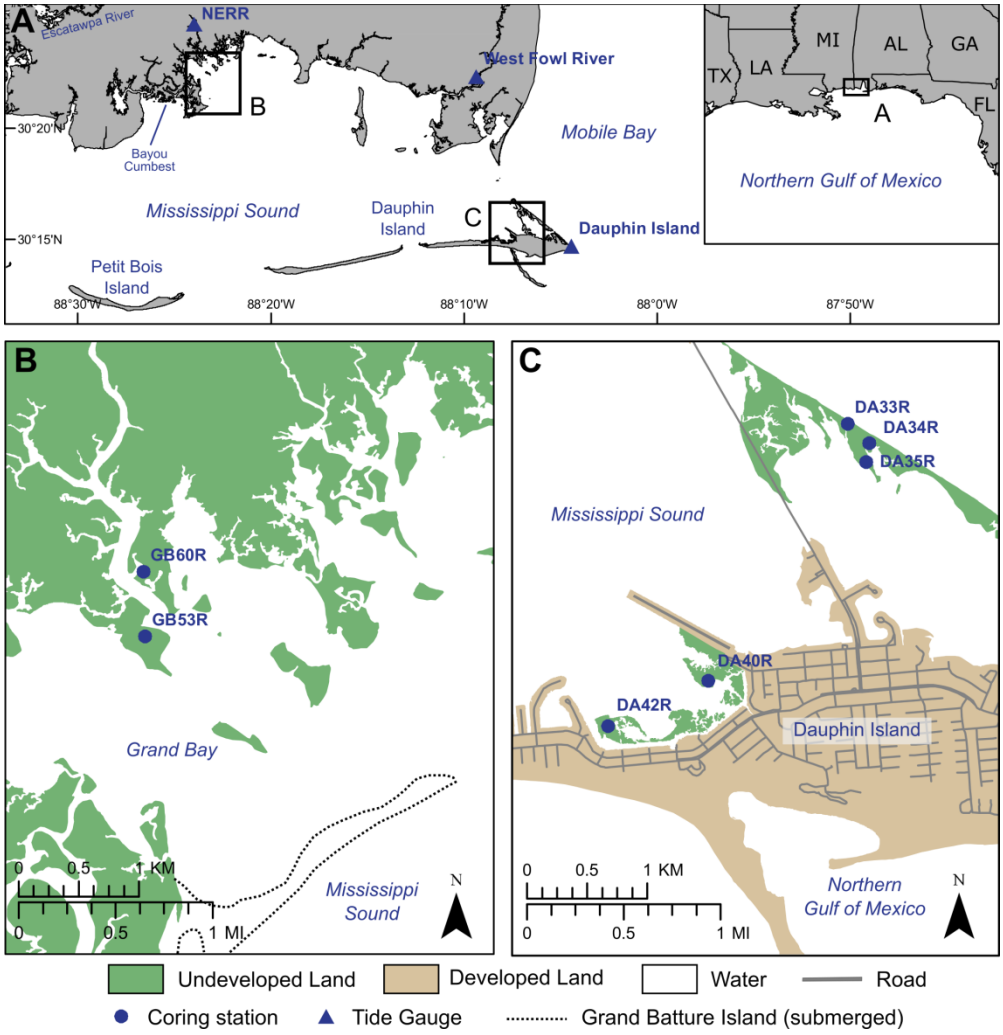

Figure 3.1. Location of study sites in the eastern Mississippi Sound. (A) Tide gauges for regional tidal-frame adjustment. (B) Sediment coring stations in the Grand Bay National Estuarine Research Reserve. Undeveloped land includes marsh wetlands. Dotted line indicates the extent of the now submerged Grand Batture Island in 1853 (United States Coast and Geodetic Survey, 1853; Meyer-Arendt and Kramer, 1991). (C) Sediment coring stations on Dauphin Island. We reconstructed PME from two sites (DA42R and DA40R on the north western side of the island's core. Stained foraminiferal cores for depth distribution of living foraminifera were retrieved from three sites in the north east of Dauphin Island (DA33R, DA34R, and DA35R).

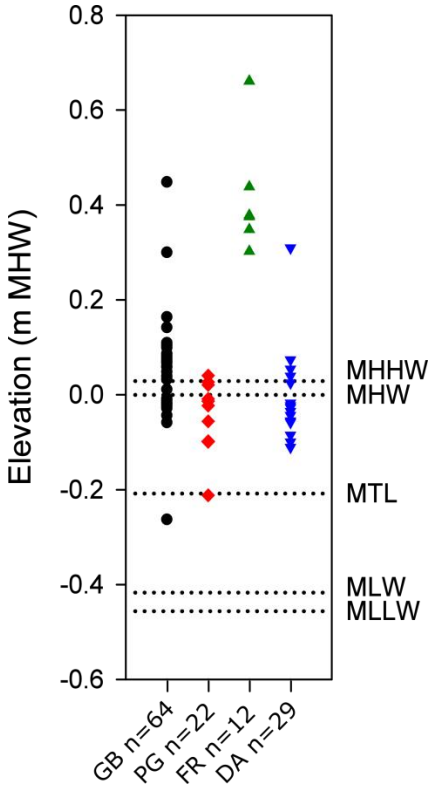

Figure 3.2. Vertical position of the 127 marsh training set samples and distribution across the four regions. GB = Grand Bay, PG = Pascagoula, FR = Fowl River, DA = Dauphin Island.

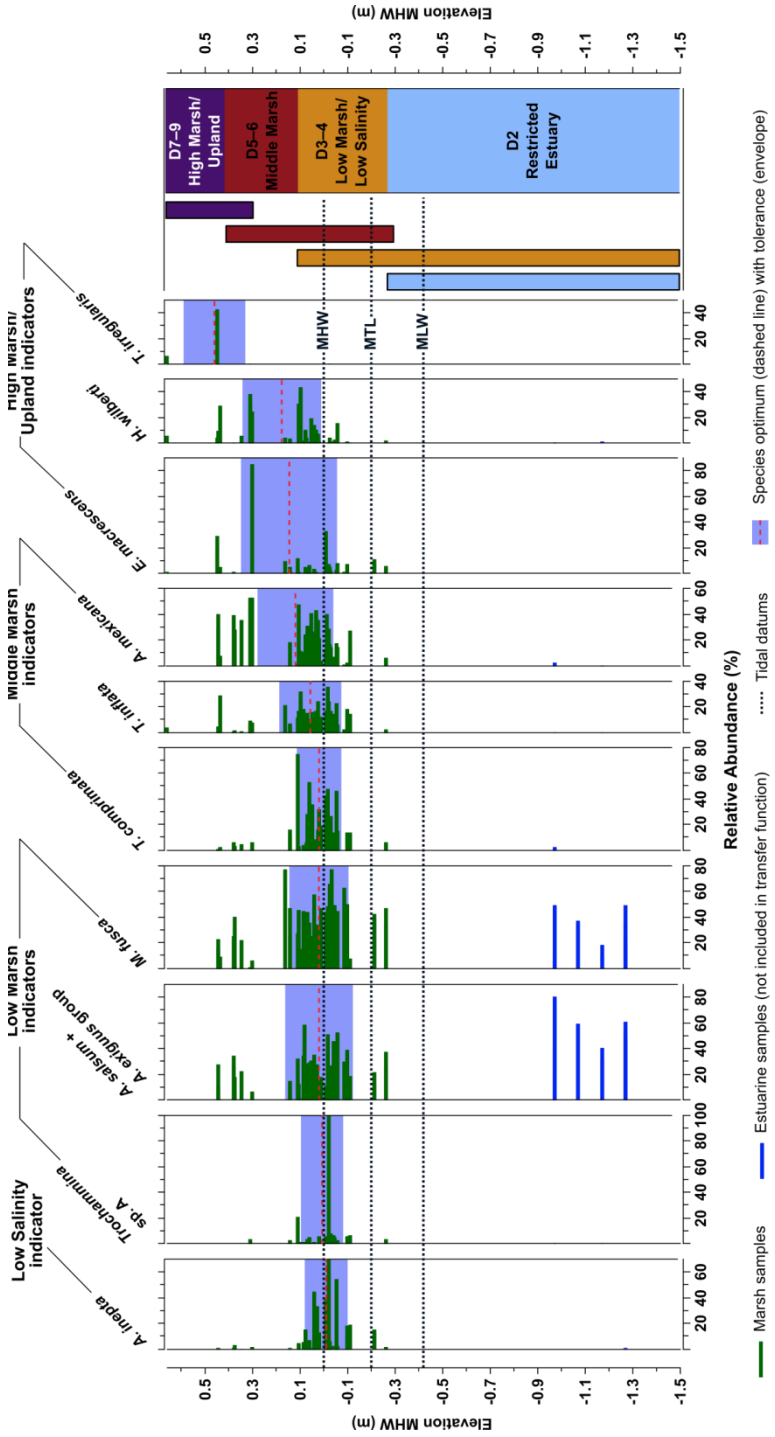

Figure 3.3. Abundances of most common foraminifera relative to m Mean High Water, and Weighted Average regression-derived species optima and tolerances. Biofacies assignments were made by Haller et al. (in review; Chapter 2). Tidal datums MTL and MLW in this plot are specific to the Grand Bay NERR tide gauge (Table 3.1).

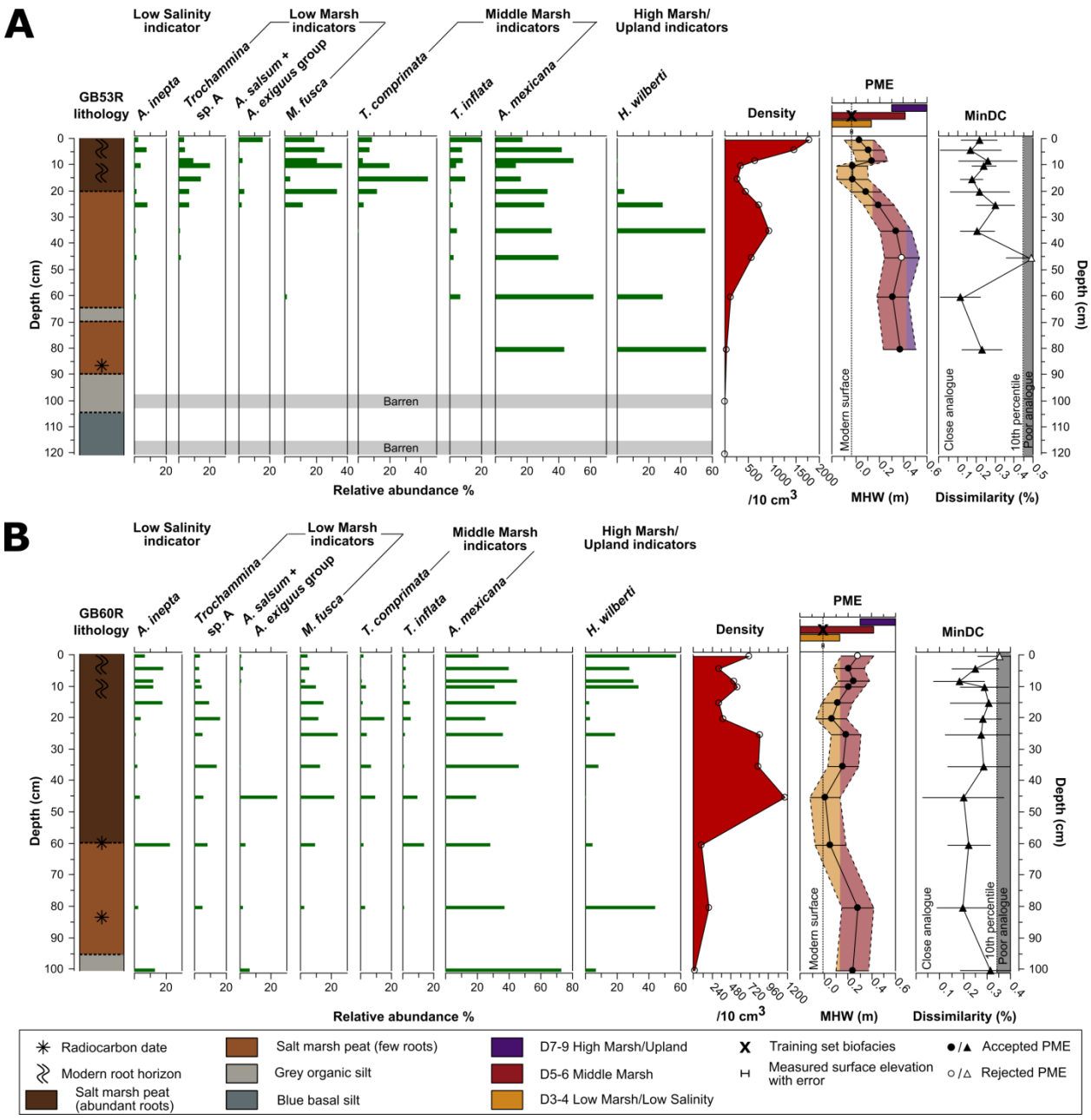

Figure 3.4. Stratigraphy, foraminiferal abundance, foraminiferal density, and Paleo-Marsh Elevation reconstruction with MinDC validation for core GB53R (A) and GB60R (B). Foraminiferal elevation optimum is ascending from left to right.

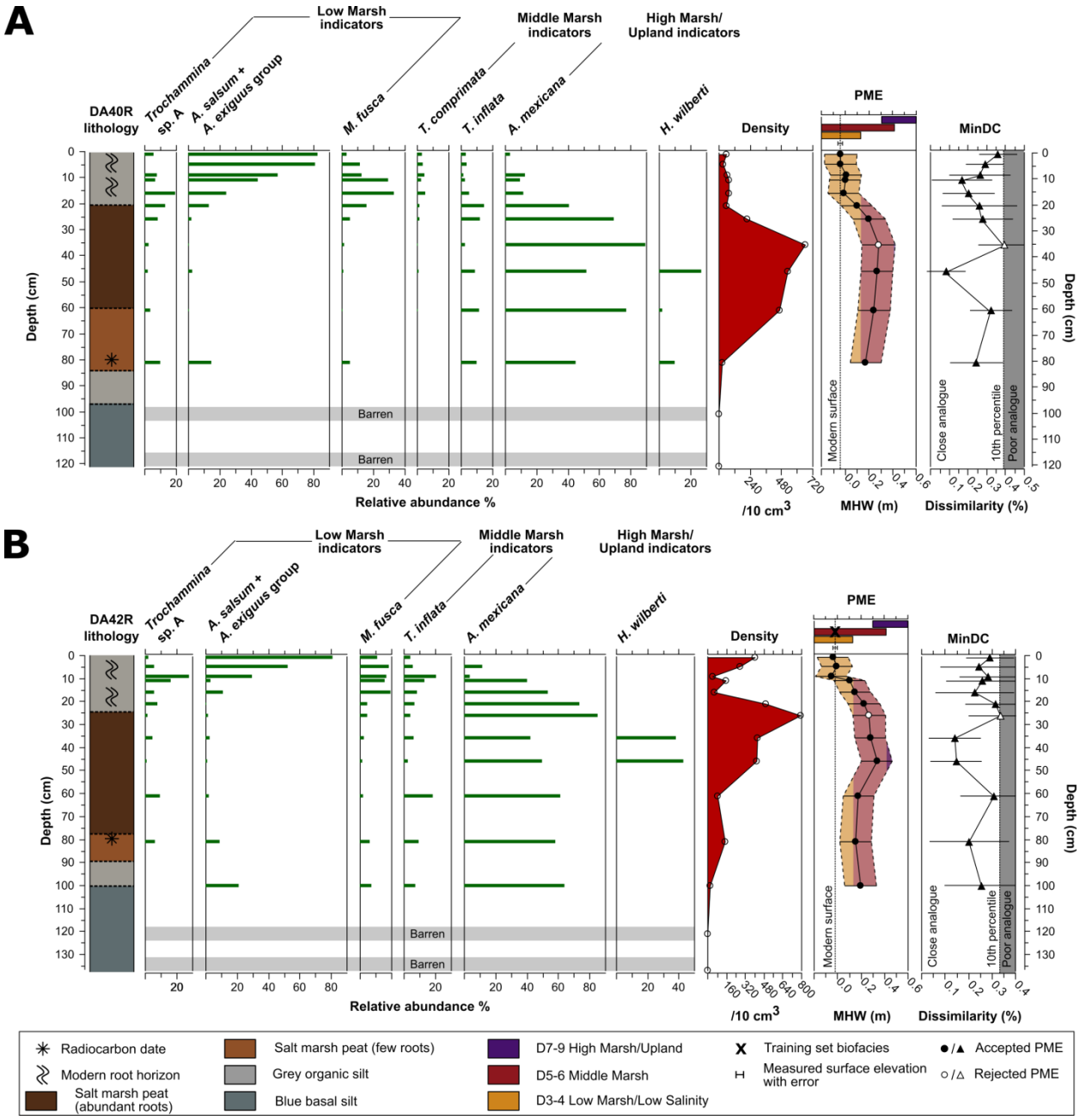

Figure 3.5. Stratigraphy, foraminiferal abundance, foraminiferal density, and Paleo-Marsh Elevation reconstruction with MinDC validation for core DA40R (A) and DA42R (B). Foraminiferal elevation optimum is ascending from left to right. Note that DA40R does not have a training set biofacies assigned due to census counts below the threshold for cluster analysis biofacies classification (Haller et al., in review; Chapter 2).

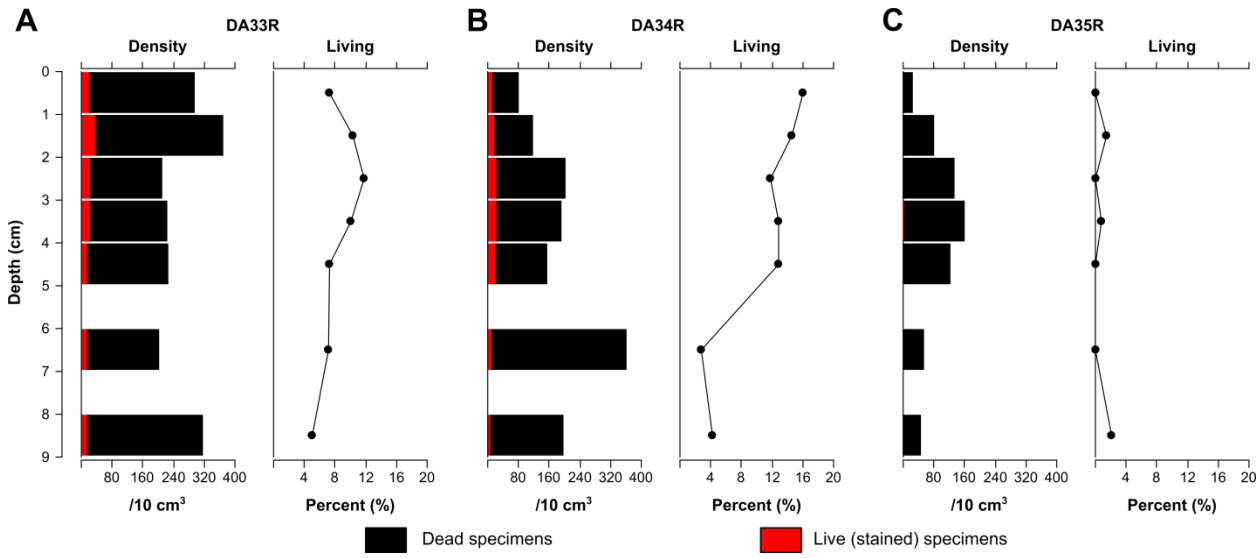

Figure 3.6. Abundances of dead and live foraminifera in stained short cores from Dauphin Island. (A) DA33R; (B) DA34R; (C) DA35R. Cores were collected in August 2015.

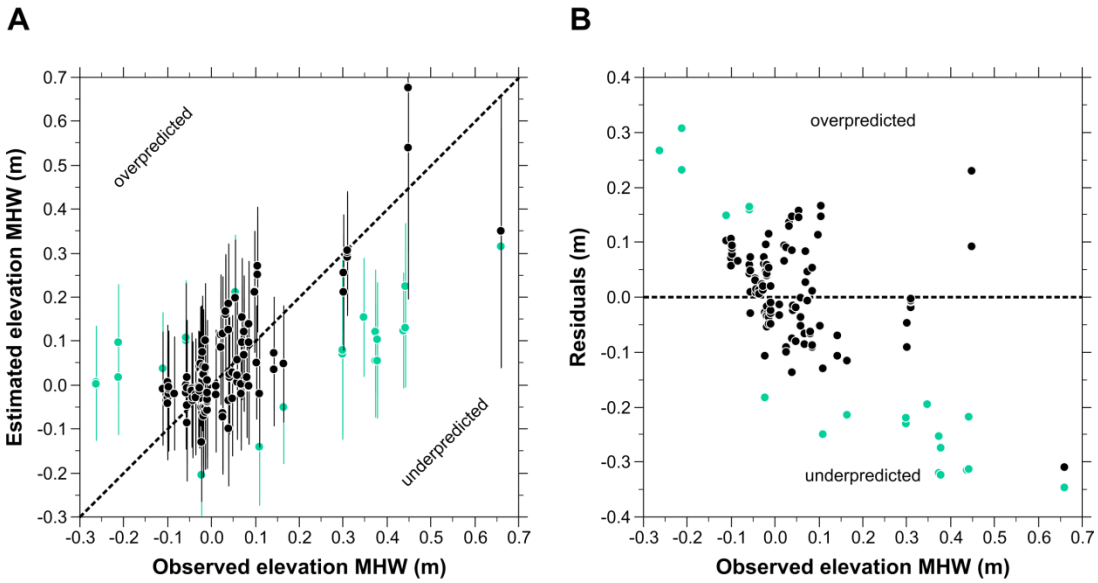

Figure 3.7. Weighted Average-Partial Least Squares (WA-PLS) transfer function (2 components) applied to the surface training set. (A) Comparison of dGPS-measured (observed) elevation versus transfer function (predicted) elevation. (B) Difference (residuals) between dGPS measured (observed) and predicted values. Green points mean no overlap between observed values and predicted value within individual errors.

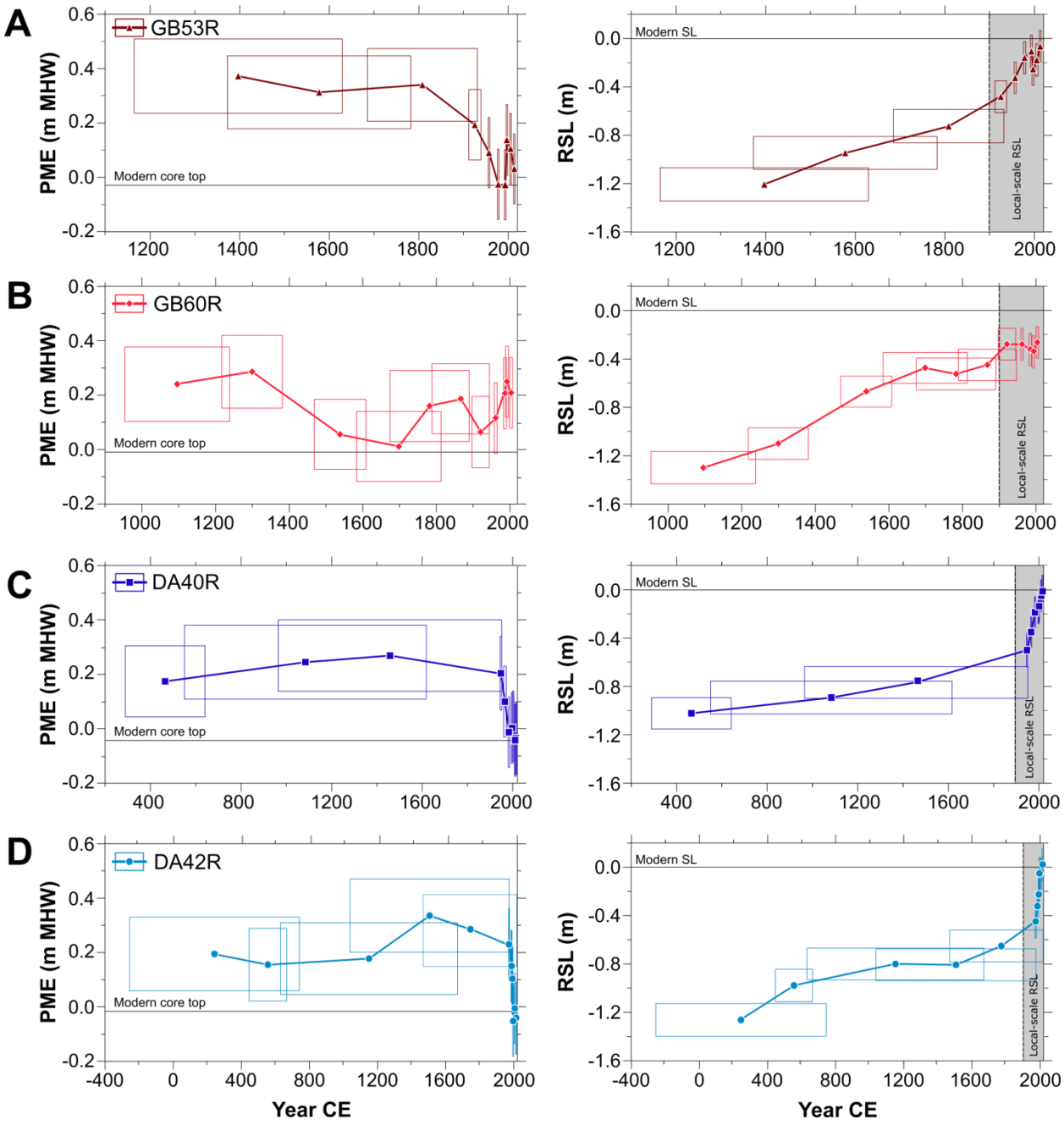

Figure 3.8. Age-calibration of Paleo-Marsh Elevation (PME) and Relative Sea Level (RSL). (A) core GB53R; (B) core GB60R; (C) core DA40R; (D) core DA42R. Paleo-Marsh Elevation points are defined by extracted ages from the Bayesian age models plus the elevation estimated from the WA-PLS transfer function. Relative Sea Level data were calculated using formula (1).

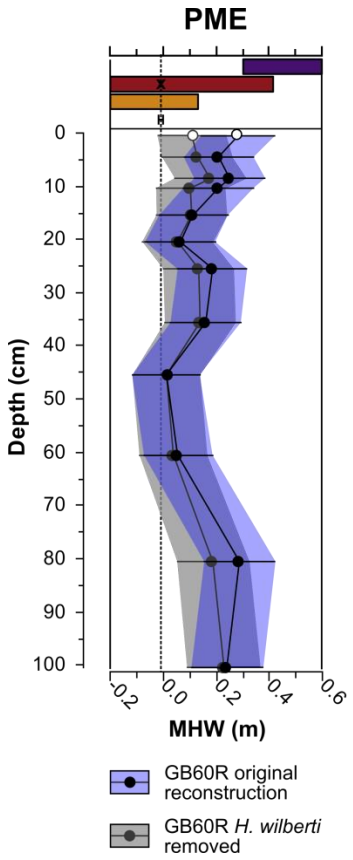

Figure 3.9. Paleo-Marsh Elevation reconstruction for GB60R compared with a hypothetical reconstruction dataset with *H. wilberti* deleted.

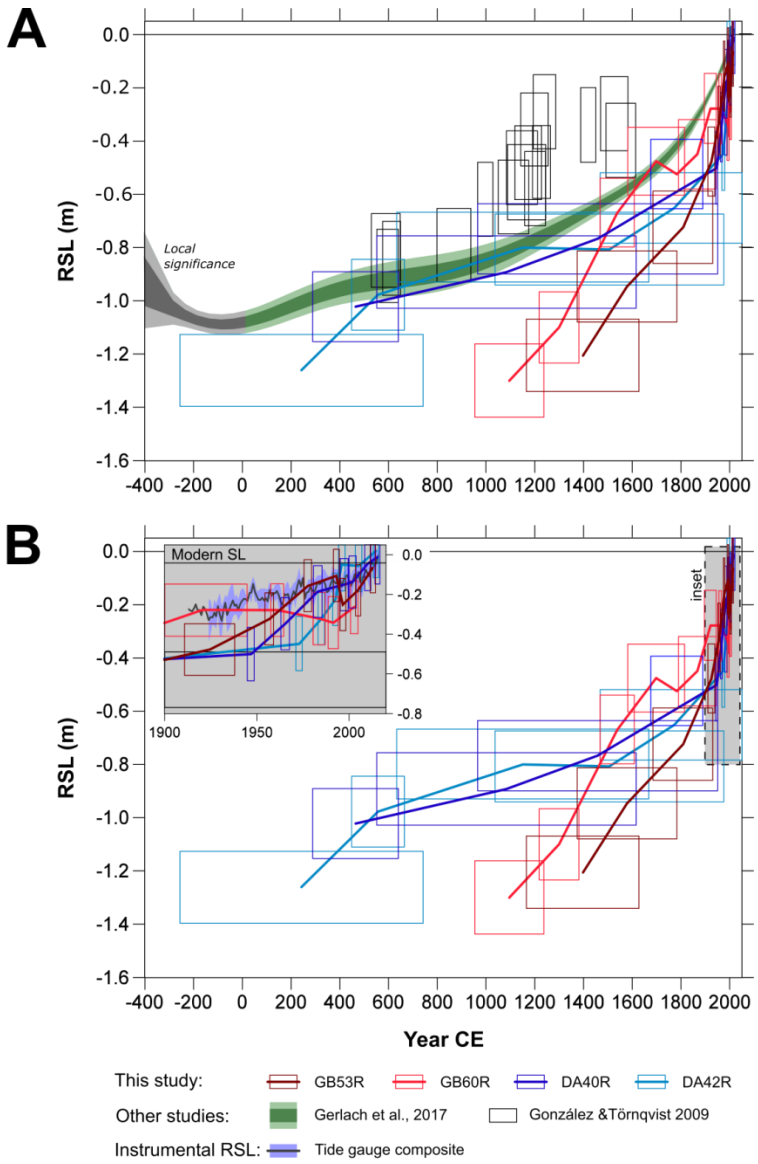

Figure 3.10. (A) Comparison of the Grand Bay and Dauphin Island sea-level reconstructions with similar Gulf of Mexico records from Little Manatee River (west Florida; Gerlach et al., 2017) and Mississippi Delta (González and Törnqvist, 2009). The western Florida reconstruction employed Bayesian modelling of Relative Sea Level using a foraminiferal transfer function (1 and 2σ confidence intervals), while the Mississippi Delta record used radiocarbon dates from basal peats at three different sites (error boxes 2σ confidence intervals). (B) Comparison of the of the RSL reconstructions from Grand Bay and Dauphin Island. Lines are connecting midpoints of each core. Inset contains composite record of the northern Gulf of Mexico tide gauges (2σ confidence intervals; see Fig. 3.11). All data are raw, non-detrended.

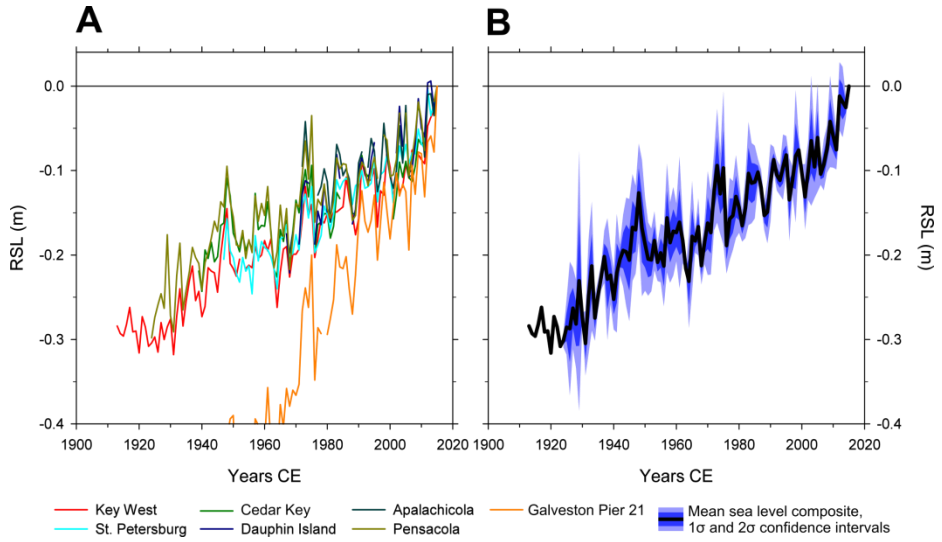

Figure 3.11. (A) Seven of the longest tide-gauge records in the northern Gulf of Mexico including Galveston II, which is a barrier island affected by subsidence. The oldest record from Key West dates back to 1913 CE. (B) Composite record of the six consistent tide gauge records, excluding Galveston II. Data product from the Permanent Service for Mean Sea Level (PSMSL; National Oceanography Centre Liverpool, UK; http://www.psmsl.org)

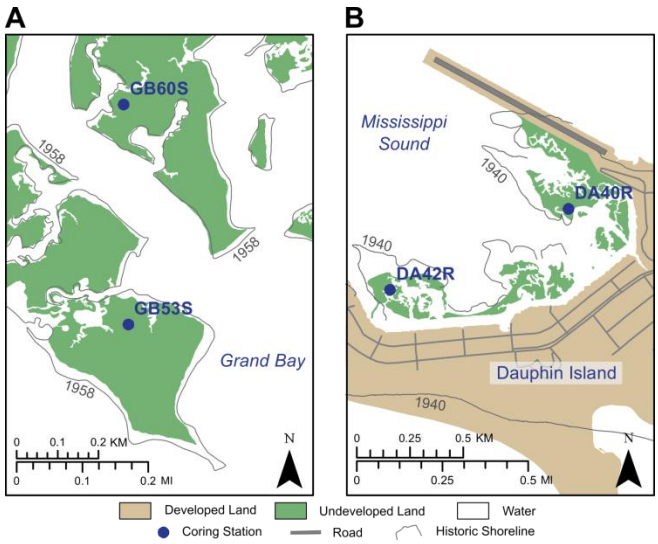

Figure 3.12. Modern salt-marsh extent compared with historic shorelines (grey contours). (A) Grand Bay: modern shoreline (2010) from Nelson et al. (2018), historic shoreline (1958) provided by Terrano et al. (2017). (B) Dauphin Island: modern (2015) shoreline (2015) and historic shoreline (1940) from Henderson et al. (2017).

Chapter 4.

Recent Outer-Shelf Foraminiferal Assemblages on the Carnarvon Ramp and Northwestern Shelf of Western Australia

Abstract

The carbonate sediments of the Western Australian shelf in the Indian Ocean host diverse assemblages of benthic foraminifera. Environments of the shelf are dominated by the southward-flowing Leeuwin Current, which impacts near-surface circulation and influences biogeographic ranges of Indo-Pacific warm-water foraminifera. Analyses of outer ramp to upper slope sediments (127–264 m water depth) at four different sites (some with replicates) revealed 185 benthic species. A shift from benthic to planktonic foraminifera was accompanied by the decrease of "larger" benthic foraminifera below the lowermost euphotic zone. Fisher α and proportions of buliminid and textularid taxa increased with water depth, as miliolids and rotalids decreased in proportion. Cluster analyses on the 125–250 μm and 250–850 μm size fractions revealed distinct assemblages, with the former distinguishing between deeper and shallower sites, and the latter distinguishing between the Carnarvon Ramp-site in the south and the three sites on the Northwestern Shelf (NWS). The assemblage shift with depth was likely caused by rapidly changing physical conditions in the upper thermocline. The assemblage differences between the NWS and the Carnarvon Ramp indicate limited horizontal transport and migration rates on the outer shelf below the influence of the Leeuwin Current. Similarity in bottom-water temperature at the studied sites indicates that water mass characteristics, biogeographic history or possibly diversity in benthic shelf habitats rather than temperature and depth are responsible for differences between the two regions.

Introduction

The Western Australian (WA) continental margin is a carbonate ramp, that extends from 16° S to 35° S and traverses from northerly tropical environments to warm-temperate environments in the south (Collins, 1988; Wilson, 2013). The Leeuwin Current (LC) is a warm, shallow current (~100 m) that transports tropical water southward along the Western Australian margin (Fig. 4.1A; Cresswell and Golding, 1980; Waite et al., 2007). During winter, when flow is strongest, upwelling is largely suppressed and the waters remain oligotrophic (Pearce and Phillips, 1988). Heat transport along the shelf is responsible for the maintenance of a broad biotic transition zone between the tropical northern and warm-temperate southern biotic zones (Betjeman, 1969; Wilson, 2013; Wilson and Gillett, 1980). The warm surface water facilitates reef growth: examples include reefs on the Rowley Shoals (17° S), the Ningaloo fringing reef (22–23° S), and the Houtman-Abrolhos Reef Complex (29° S; Fig. 4.1B).

The Western Australia shelf and shelf-margin is characterized by diverse foraminiferal assemblages that have been studied from geographically distinct regions, mostly from inner- shelf waters. More limited data are available for benthic foraminifera on the middle and outer shelf regions. Benthic foraminifera from the coast of Western Australia have been previously studied by Betjeman (1969), Loeblich and Tappan (1994), Haig (1997), James et al. (1999), Li et al. (1999), Orpin et al. (1999), Semeniuk (2001), Quilty and Hosie (2006), Gallagher et al. (2009), Parker (2009), and Mays (2007). Betjeman (1969) published the first major study, reporting 397 benthic foraminiferal species between 0–300 m water depth from Cape Leeuwin in the south to the Rowley Shelf in the north. Betjeman proposed tropical-subtropical and temperate faunal regions divided alongshore based on a latitudinal temperature gradient. However, Betjeman's species classifications are not consistent with current use and complex statistical analyses of distributions were in their infancy at that time. James et al. (1999) described several facies, including seafloor morphology, benthos and "larger" benthic foraminifera (LBF) along the Rottnest and Carnarvon shelves. In 2004, a similar effort extended the assessment to the northwest shelf (James et al., 2004). Most of the other WA shelf foraminiferal studies focused on inshore assemblages,

including Haig (1997) and Orpin et al. (1999) on Exmouth Gulf, Parker (2009) on the Ningaloo Reef, Semeniuk (2001) on the shallow Rottnest Shelf, Quilty and Hosie (2006) on the Swan River estuary, Mckenzie (1962) and Revets (2000) on estuaries from the Cape Leeuwin region, and Li et al. (1999) sampled the southern shelf.

More pertinent to our study, Gallagher et al. (2009) assessed abundances of LBF from 4.4 Ma to modern from the northwestern shelf as indicators for dynamic Leeuwin Current paleo-flow and connectivity with the Western Pacific Warm Pool. Mays (2007), in his thesis, analyzed benthic and planktonic foraminifera from 6 transects (24–31° S) on the Rottnest Shelf and Carnarvon Ramp, reporting evidence for influence of upwelling and saline downwelling along the shelf. However, only Betjeman (1969) focused on benthic foraminiferal distributions on middle to outer shelf environments in the upper thermocline.

Objectives

Shelf margins are among the most diverse environments for benthic foraminifera requiring, assessments of regional biogeography and habitat preferences of benthic foraminifera (Armstrong and Brasier, 2005). The goal of our study was to document species occurrences, diversity, and assemblages of benthic foraminifera from the Western Australian outer shelf and shelf break, which are influenced by the eastern Indian Ocean. Our data will be useful in the interpretation of regional biogeography and habitat preferences of benthic foraminifera in the eastern Indian Ocean. Furthermore, the resulting data will aid in studies of paleoecology of the Western Australian province (e.g., Chaproniere, 1984; Corliss, 1979b; Gallagher et al., 2009; Moss et al., 2004; Renema, 2007), water-mass circulation (Corliss, 1979a; Murgese and De Deckker, 2005, 2007; Spooner et al., 2011; Wells et al., 1994) and carbonate ramps in general (Parker and Gischler, 2015).

Study Area

The Western Australian shelf is divisible into three regions: a northwest-facing shelf from 16 – 21° S (NWS), the Carnarvon Ramp from 21–28° S, and the southwestern shelf (SWS) from 28–35° S (Fig. 4.1B). Depositional provinces on the NWS are the Northern Carnarvon Basin and the Roebuck Basin, which are surface expressions of 15 km thick sequences of Paleozoic to Cenozoic sediments (Hocking et al., 1987; Stagg and Colwell, 1994). The Mesozoic of the Northern Carnarvon Basin has been of geological interest for hydrocarbon extraction in the recent decades (Bradshaw and Bernecker, 2015). Most of the NWS is a distally steepened ramp that is 600 km in length, up to 250 km across to the 200 m depth mark, and then gradually falling to 1000 m depth. In the Roebuck Basin, the Rowley Shoals are reef-rimmed platforms that extend upward to the surface from ~400 m depth on the continental slope.

The Carnarvon Ramp in the Southern Carnarvon Basin is the sedimentary domain of about 10–100 km width along Cape Range, Shark Bay, and Exmouth Gulf, which is significantly narrower than the shelf in adjacent areas. On the SWS, the Perth Basin forms a 1,500 km-long depocenter for Paleozoic to recent sediments (Stagg et al., 1999), spanning the distance between Shark Bay to the north and Cape Leeuwin to the south. The Rottnest Shelf is the modern surface of the Perth Basin, with very little active benthic carbonate production taking place (James et al., 1999). The Houtman Abrolhos Reef Complex (latitude 28–29.5° S) occurs at the boundary between the Carnarvon Ramp and the Rottnest Shelf (Collins, 1988; James et al., 1999).

Seafloor Sedimentology

The SWS seabed is dominated by modern and palimpsest sediments, reworked coral fragments, ooids, peloids, coralline algae, sponge spicules, and intraclasts (James et al., 1999). Spiculitic muds are interpreted as deposited in areas of temporary upwelling where the LC thins during its flow south and ceases completely. Coralline algae and foraminifera that are classified as stranded and relict are iron-stained yellow to black due to exposure during sea-level lowstands. James et al. (1999) characterized the sediment production on the SWS and Carnarvon Ramp as very slow to inactive ("subtropical starved

ramp"). The slow sedimentation rate is confirmed by authigenic glauconite formation in many facies on the shelf (James et al., 1999; Odin and Morton, 1988).

The NWS sediments are a mixture of skeletal and lithic, relict and Holocene particles similar to the SWS. Terrigenous sediments introduced by rivers occur infrequently beyond the inner shelf (Jones, 1973). Collins et al. (2014) described the Holocene sediment as a skeletal, peloidal, and oolitic carbonate of sand-size or coarser, with active sedimentation on the inner ramp and planktonic foraminifera dominant at mid ramp and deeper. Authigenic phosphate and glauconite minerals are common in sediments near the outer edge of the NWS (Collins et al., 2014; Jones, 1973), which is a common association in low sedimentation/low oxygenation provinces (Miller et al., 2004). James et al. (2004) suggest periodic upwelling or "iron-redox pumping" to trigger such accumulations at >200 m water depth. Widespread limestone pavements (i.e., post-depositional cementation) covered by a veneer of unconsolidated sediment were reported by both Jones (1973) and Collins et al. (2014). Seawater temperatures and water transparency on the SWS and NWS are generally favorable for autotrophic life forms to dominate carbonate production. However, the diminishment of the warm Leeuwin Current by northward-flowing cooler water on the SWS supports warm-temperate biota (coralline algae, bryozoans, and larger benthic foraminifera), while more tropical zooxanthellate corals and calcareous green algae are generally sparse (James et al., 1999). Moreover, intense evaporation in nearshore and hypersaline embayments such as Shark Bay generates saline bottom waters, which flow downslope onto the ramp. James et al. (1999) suggest that these saline bottom waters suppress coral abundance and high carbonate sedimentation rates as observed in comparable climates (e.g., James, 1997; Mutti and Hallock, 2003).

Oceanography

On the WA shelf there is a gradient from warmer to cooler sea-surface temperatures (SST) and oligotrophic to mesotrophic nutrient concentrations (chlorophyll a) as climate ranges from semi-arid to humid from north-to-south (Table 4.1; Tomczak and Godfrey, 2003; Wilson, 2013). The driver for this gradient is the influence of the LC, which is a coherent southward flowing shelf-edge current fed by the

Indonesian Throughflow (ITF) and ultimately by the Western Pacific Warm Pool (Schott et al., 2009). The Leewin Current is the only southward-flowing eastern boundary current in the Southern Hemisphere (Pearce, 2009) and displaces at the surface the cold equatorward flowing Western Australian Current toward the open Indian Ocean. If the LC was removed, an upwelling system would exist on the shelf, initiated by the Western Australian Current as occur with similar conditions as along eastern boundaries such as the coasts of Chile/Peru and Namibia (Reason et al., 1999). The LC can be detected from north of the Exmouth Gulf/Barrow Island area (21° S; Fig. 4.1B) along the shelf break to Cape Leeuwin (34° S) where it travels eastward toward the Great Australian Bight (Cresswell and Golding, 1980). The driver for this current is the steric height difference between the lower density, lower salinity waters in the Timor Sea compared to the cooler, denser waters off the coast of Perth (see Fig. 4.1A). The oligotrophic waters of the LC flow in a shallow (<100 m) and narrow band (<100 km), and are strongest during the winter months (March–November). The current slows or stops in summer (November–March) due to increased northward wind stress (Feng et al., 2003; Smith et al., 1991). Although shelf waters are near the lower latitudinal limits for reef growth, the LC moderates winter temperatures such that modern coral-reef growth is prolific in the lee of natural barriers at Ningaloo Reef and the Houtman Abrolhos Reef Complex to 29° S (Collins et al., 1991; 1993; Fig. 4.1B). The subtropical-temperate nearshore transition extends as far south as Rottnest Island off Perth (33° S; Greenstein and Pandolfi, 2008). The benthic foraminifera reported by Betjeman (1969) reveal two faunal regions. The north-south temperature gradient controls the distribution of a warm-temperate fauna on the Carnarvon Ramp and Rottnest Shelf and a tropical-subtropical fauna on the Rowley Shoals shelf. Similarly as for coral growth, the Houtman Abrolhos Reef Complex is an "oasis" of tropical-subtropical benthic foraminifera within the temperate faunal region served by the Leeuwin Current (Betjeman, 1969).

Materials and Methods

Eight surface samples (0–2 cm) were collected from four International Ocean Discovery Program (IODP) drill sites on a coring transect along the WA shelf (Carnarvon Ramp: U1460; NWS: U1461, U1463 and U1464, Fig. 4.1B) using Advanced Piston Coring in August–September 2015 (Gallagher et al., 2017). Sampling sites were located between 27° S and 18° S in depths from 127–264 m (Table 4.1). Samples were collected from the mudline of the uppermost section of the first core barrel. At each site a maximum of three replicate samples were taken from sites at a maximum distance of 16 m to each other.

Sea-surface satellite data from Moderate-Resolution Imaging Spectroradiometer (MODIS) from 2009–2011 showed that the latitudinal distance between the northern sites and the Carnarvon Ramp site accounted for temperature differences averaging 4.6°C (Table 4.1) and a southerly chlorophyll increase averaging 40%. Bottom-water temperatures were based on data from CTD casts published by James et al. (1999) for the southwestern shelf and James et al. (2004) for the northwestern shelf (Table 4.1). The sediment substrate ranged from light brown to greenish pelagic sediment. James et al. (1999, 2004) described the facies sampled as a thin band of muddy to sandy carbonate with trace amounts of glaucony along the skirts of the outer ramp, becoming progressively muddier with depth (Table 4.1).

For foraminiferal analysis, a wet unit volume of 10 cm^3 was boiled with hydrogen peroxide until the reaction faded. This dissolved carbonate aggregates and helped to remove carbonate coatings. The sediment was washed over 63 μm and 850 μm sieves and the fractions retained on those sieves were dried overnight at 50°C. The >63 μm dry residue was sieved on 125 μm and 250 μm mesh sieves. Rarefraction picking was applied in the 125–250 μm, 250–850 μm, and >850 μm fraction, that is, continuation until no new species were found (Raup, 1975). Foraminifera were mounted onto micropaleontological faunal slides, counted, and identified to species level when possible. All size fractions are reported separately. Most species were imaged with a scanning electron microscope. The assemblages encompassed live and dead specimens, providing a time-averaged mean for defining benthic habitats (Murray, 2006). The

Planktonic/Benthic Ratio (Grimsdale and van Morkhoven, 1955) was determined by counting a minimum of 100 planktonic and benthic tests from each fraction, if available.

The abundance data of the 125–250 μm fraction were converted to relative abundance data (percentages) for each sample, arcsine transformed, and analyzed in the PAST 3.18 software package (Hammer et al., 2001). Fisher α is a measure of assemblage diversity independent of sample size, calculated based on the number of specimens and number of species (Fisher et al., 1943). To determine structure in the foraminiferal data, Q-mode (samples) and R-mode (species) analyses of the 30 most frequent species were performed with Euclidean distances (Kaufman and Rousseeuw, 1990), which grouped samples or species. Clustering for both analyses was repeated 9,999 times in a bootstrapping procedure to test stability of branches.

Results

The analyzed size-fractions included foraminiferal shells, sponge spicules, fecal pellets, pteropods, other mollusk shells, and fragments of all such biota. Sediments at Site U1460 were sandy, with light brown to whitish coloration. Site U1461 sediments were glauconitic silt to sand that was rich in sponge spicules. At Sites U1463 and U1464 we recovered light-green to brownish, coarse-grained sediments with fewer sponge spicules and glauconite.

After picking 8,887 benthic foraminiferal tests from the Western Australian outer shelf to shelf break samples, a total of 185 species from 123 genera were identified (Plates 4.1–4.6; Appendix C1). A systematic taxonomic section for all species with basis of identification can be found in Appendix C2. The assemblage comprised 37 porcelaneous-walled, 126 hyaline-walled, and 19 agglutinated-walled species. The most specimens were picked from the 125–250 μm fraction (60–97% per sample), fewer from the 250-850 μm fraction (3–40%) and the >850 μm fraction, if present, comprised a maximum of 1% per sample. The number of species per sample was highest in the smaller size fraction (67–96 in 125–250 μm, 16–62 in 250–850 μm), which is also reflected in higher Fisher α diversity (Table 4.2). Due to

the inconsistent presence and low numerical strength of the >850 μm fraction, the following results focus on the two smaller size classes.

Amongst the 30 most abundant taxa in the 125–250 μm and 250–850 μm fractions, 16 taxa were common in both fractions, 14 were unique to each fraction. These 16 abundant taxa observed from both fractions were: *Bolivina striatula*, *Textularia* cf. *T. agglutinans*, *Planulina retia*, *Cibicides* cf. *C. refulgens*, *Triloculina tricarinata*, *Textularia cushmani*, *Plotnikovina timorea*, *Operculina ammonoides*, *Textularia catenata*, *Miliolinella* sp. 1 sensu Parker 2009, *Anomalinulla glabrta*, *Spirorutilus carinatus*, *Sprioloculina subimpressa*, *Textularia kerimbaensis*, *Quinqueloculina* sp. 5 sensu Parker 2009, and *Caribeanella elatensis*.

Larger benthic foraminifera (LBF, i.e., those known to host algal endosymbionts), notably *Amphistegina papillosa* and *Operculina ammonoides*, were most abundant in the three samples from the shallowest site (U1461 at 127 m; up to 19% in 125–250 μm, and 13% in 250–850 μm) and were only a minor constituent at deeper locations (0.1–4.2%; see Fig. 4.2A). However, specimens encountered were predominantly smaller juveniles. Occasionally a few specimens of other LBF were found in very low numbers. The symbiont-bearing miliolids were typically fragmented. Smaller, warm-water rotalid taxa that lack algal symbionts included *Neoeponides margaritifer* (all sites), *Planorbulinella larvata* (U1460 and U1461), *Rotalinoides gaimardi* (U1461 and U1463).

Benthic foraminifera decreased in relative abundance with depth (Figs. 4.2B, D), however, in the 250–850 μm fraction this trend was stronger. The rotaliids and miliolids decreased in proportion, whereas the buliminids increased strongly, particularly in the 125–250 μm size-fraction (Figs. 4.2A, C). Textulariids gained in proportion with depth particularly in the 250–850 μm fraction. Lituolids, trochamminids, spirillinids, and robertinids had an accessory abundance (<3% combined) in both size fractions. Planktonic tests increased in deeper samples, with keeled planktonics found more commonly in the fraction 250–850 μm (Fig. 4.2D). Relict or stranded foraminifera with discoloration (blackened or oxidized from subaerial exposure) described from continental shelf terraces (Carrigy and Fairbridge,

1954; James et al., 1999; Jones, 1973) were not found in any sample. No major groups with heavy abrasion patterns were found.

Sample Clusters (Q-mode)

Based on relative abundance data in the 125–250 μm fraction, foraminiferal samples grouped into two clusters (Fig. 4.3A), which are well defined by water depth on the shelf. Cluster A ("Shallow") consisted of samples from the shallowest site U1461 (127 m); Cluster B ("Deep") the Carnarvon Ramp site U1460 (214 m) and the northwestern shelf deeper-water sites (U1463, 145 m and U1464, 264 m).

Sediments from Cluster A samples ("Shallow", 24°C bottom water) contained 66% hyaline foraminifera, 25% porcelaneous, and 9% agglutinated. The most abundant species were (in descending order): *Amphistegina papillosa*, *Operculina ammonoides*, *Miliolinella circularis*, *Miliolinella* sp. 1 sensu Parker 2009 and, *Caribeanella elatensis*. Fisher α in Cluster A ranged between 20 and 24 (84–89 species; see Fig. 4.3A).

Sediments in Cluster B ("Deep", 14–23°C bottom water), were from Sites U1460 from the Carnarvon Ramp and the deeper Sites U1463 and U1464 from the NWS. Hyaline foraminifera dominated at 72%, porcelaneous miliolids constituted 15%, and agglutinated taxa contributed 12%. Dominant taxa were *Globocassidulina subglobosa*, *Bolivina robusta*, *Anomalinulla glabrata*, and *Paracassidulina neocarinata*. Fisher α-index mean was 24 (67–96 species), however the NWS samples were more diverse than the Carnarvon Ramp samples (see bottom Fig. 4.3A)

Abundance data for the size fraction 250–850 μm revealed two groups within the dataset, separating the NWS from the Carnarvon Ramp (Fig. 4.3B). However, within the NWS cluster, site U1464 was the most similar to the Carnarvon Ramp Samples.

The Cluster A samples (NWS) exclusively were from the northwestern shelf from all sampled depths. Most common taxa were *Planulina retia*, *Miliolinella* sp. 1 sensu Parker 2009, *Operculina ammonoides*, *Cancris auriculus*, and *Glandulina symmetrica*. Fisher α-indices had a wide range from 10 to 21 (16–62 species; see Fig. 4.3B).

Cluster B encompassed the two samples from the Carnarvon Ramp. The species most common in descending order were *Bigenerina aspratilis*, *Uvigerina peregrina*, *Anomalinulla glabrata*, *Asanonella tubulifera*, and *Quinqueloculina* sp. 5 sensu Parker 2009. Fisher α in Cluster B ranged from 12–16 (42–53 species).

Species Clusters (R-mode)

The cluster analysis grouping species (R-mode), based on the 30 most abundant species in 125–250 μm, showed two major groups separated at similarity distance=0.9 (Fig. 4.4A). Cluster 1 species were abundant at all sites (33–76%), but increased at the shallowest site (U1461) on the NWS and decreased with depth (Fig. 4.5A). Cluster 2 species were most abundant at the Carnarvon Ramp (Site U1460, 27–36%) and at the deeper NWS sites (U1463, U1464, 17–40%), but gradually diminished to 3% at Site U1461 at 127 m.

Cluster 1 included 20 of the 30 species of which the most abundant were *Cibicides* cf. *C. refulgens*, *Caribeanella elatensis*, *Triloculina tricarinata*, and the LBF *O. ammonoides* and *A. papillosa* (see Fig. 4.4A).

Cluster 2 contained 10 of the 30 species, most abundantly *Bolivina robusta*, *Anomalinulla glabrata*, *Paracassidulina neocarinata,* and *Globocassidulina subglobosa*.

The species clustering based on the 30 most abundant taxa in the 250–850 μm fraction revealed two distinct groups (Fig. 4.4B). Cluster 1 species were more abundant on the Carnarvon Ramp (50–73%), while Cluster 2 foraminifera were most common at the NWS sites (41–75%) (Fig. 4.5B).

Twelve out of the 30 species were assigned to Cluster 1. The four most abundant were *Cibicides* cf. *C. refulgens*, *Textularia* cf. *T. agglutinans*, *Bigenerina aspratilis*, and *Quinqueloculina* sp. 5 sensu Parker.

Cluster 2 comprised 18 of the 30 species including many miliolids. The four most common were *Caribeanella elatensis*, *Spiroloculina subimpressa*, *Triloculina tricarinata*, and *Miliolinella* sp. 1 sensu Parker 2009.

Discussion

The benthic foraminiferal distributions identified in this study indicate the influence of lowermost euphotic to subeuphotic thermocline transition with depth, and the weakening and thinning of the Leeuwin Current as it flows southward. Observed were latitudinal diversity gradients, while the predominance of planktonic taxa at the deeper sites also reflected the increasing oceanic influence. Based on visual inspection, sedimentary substrata did not vary greatly among the collected samples and likely did not strongly influence benthic assemblages.

The tropical/subtropical benthic foraminiferal assemblages are relatively well known in the Indo-Western Pacific region. The shallow waters of carbonate shelves and reefs tend to be dominated by miliolids and rotalids, especially the larger benthic taxa that host algal endosymbionts. The foraminifera of the Sahul Shelf and the Timor Sea were extensively documented by Loeblich and Tappan (1994). Based upon 378 samples from depths from 20 to nearly 3,500 m, they reported 946 species. This seminal work is still a major taxonomic resource. In addition, the benthic assemblages of New Caledonia were sampled by Debenay (2013), who reported 1043 species from depths between 0 and 700 m. New Caledonia is located in the south-western Pacific at similar latitudes as the Western Australian shelf (15–26° S).

We found 185 species of benthic foraminifera from four sites (8 samples) over a depth range of 127–264 m (Fig. 4.1B). While Betjeman (1969) identified 397 species from 50 stations on the WA shelf, his research included shore-perpendicular depth gradients (19–34° S). Per sample data were quite comparable (Table 4.2). However, our study's higher specimen count per sample (we identified 948–1387 specimens; Betjeman 109–460 specimens) yielded a higher minimum diversity, as expected. On the Carnarvon Ramp, Betjeman (1969) reported 31–94 species per sample (we found 74–93), and on the NWS (Rowley Shoals) between 43–102 species per sample (we found 83–106, all size fractions combined).

The increase in planktonic foraminifera on the outer shelf and upper continental slope observed by Betjeman (1969) and James et al. (2004) was corroborated by the samples in this study (Figs. 4.2B, 4.3B). Increasing Fisher α diversity downslope is indicative of diverse faunas found in shelf regions worldwide (Murray, 2006). Betjeman (1969) reported a Fisher α peak between 50 and 150 m (α = 45–50) and then a decline on the outer shelf, which corroborates our observation (Fig. 4.6).

The rather surprising difference in the benthic assemblages between the 127 m and 145 m samples on the NWS is largely a consequence of the greater abundances of tests of symbiont-bearing LBF at the shallower site. We found numerous juvenile specimens of *Operculina ammonoides* and *Amphistegina papillosa* in the 125–250 μm size fraction at Site U1461 (127 m). *Operculina ammonoides* occupies a low light-intensity niche in the West Indian Ocean and its range extends to the base of the photic zone (Hohenegger, 2000). Similarly, *A. papillosa* is the deepest-dwelling amphisteginid (>100 m; Hohenegger, 1994). Sufficient light for recruitment of *O. ammonoides* and *A. papillosa* must reach the benthos at Site U1461 (127 m) at least intermittently. Light reaching Site U1463 (145 m) was not sufficient. As all sample sites were located at uppermost thermocline depths, temperatures declined sharply between 127 m depth (24°C; CTD data from James et al. (1999, 2004) in Table 4.1) and 264 m depth (14°C). Yet, the benthic foraminiferal assemblages differed most between 127 m depth and 145 m depth, where only a 1°C temperature difference was found. Thus, the evidence for light penetration to 127 m appears to be more important than temperature as a factor influencing the benthic foraminiferal assemblages on the NWS.

The presence of few inner shelf LBF associated with coral reefs and adjacent lagoons (>30 m water depth; Parker, 2009; Yassini and Jones, 1995) at Site U1461 indicates that downslope transport cannot be excluded. Many other species have a wide bathymetric range from inner-neritic shallow embayments (<30 m) such as Exmouth Gulf (Haig, 1997) or Ningaloo Reef (Parker, 2009), but also all across the Sahul Shelf (Loeblich and Tappan, 1994) down to depths >1000 m, which makes them less suitable as proxies for allochthonous sediment. Fellowes et al. (2017) assessed abrasion signatures to quantify transport distances, at least in reef and lagoonal settings where wave energy is high, and intense

storms are episodic disturbances (Strotz et al., 2016). Wave energy decreases as a function of water depth (Peters and Loss, 2012) and wave-related transport and abrasion must co-vary. Consequently, foraminiferal test abrasion from transport is minimal on the outer shelf, but we can only assume that all benthic species we counted were in-situ and recent.

The Q- and R-mode analyses of the smaller size fraction (125–250 μm) indicated two distinct assemblages separated by water depth (Fig. 4.5A). The shallower station (U1461) was dominated by taxa common to middle and outer shelf depths, including *Cibicides* cf. *C. refulgens* and several miliolid taxa. The deeper sites (U1460, U1463, and U1464) were characterized by *Bolivina robusta* and many buliminids. Differences between the two clusters indicate increased depth, and influence of thermocline waters and potentially the deep and cold Western Australian Current. Comparison of published depth ranges and temperature preferences revealed that many of the abundant species in the deep-water cluster can occur at inner shelf to shelf-break depths. Amongst these were several cosmopolitan taxa, such as *Paracassidulina neocarinata*, *Bolivina robusta*, *Bolivina striatula*, *Siphouvigerina proboscidea*, *Bulimina marginata*, and *Globocassidulina subglobosa* that have been reported as living down to abyssal plains (Corliss, 1979b; Hayward et al., 2010; van Morkhoven et al., 1986).

In contrast, the analyses on the intermediate size fraction (250–850 μm) sorted foraminifera from the NWS and Carnarvon Ramp into separate clusters (Fig. 4.5B). Many of these specimens are adult forms of species that occur in the finer fraction, but also include different, larger-sized taxa. Both shelf regions host numerous taxa common in the Indo-Pacific region (Abu-Zied et al., 2016; Cherif et al., 1997; Haig, 1997; Loeblich and Tappan, 1994; Panchang and Nigam, 2014; Parker, 2009; Thissen and Langer, 2017), however their distributions vary with latitude on the WA shelf (Betjeman, 1969). For example, *Bigenerina aspratilis*, *Asanonella tubulifera*, *Anomalinulla glabrata*, *Lenticulina domantayi*, *Quinqueloculina* sp. 5 sensu Parker, and *Spirorutilus carinatus* clearly show a preference for the Carnarvon Shelf. Species specifically abundant in the NWS samples were *Caribeanella elatensis*, *Spiroloculina subimpressa*, *Triloculina tricarinata*, *Miliolinella* sp. 1 sensu Parker 2009, *Textularia*

catenata, and *Planulina retia*. This differentiation was accompanied with higher faunal diversity in NWS samples (Fisher α = 12–21) than in Carnarvon Ramp samples (Fisher α = 12–16).

The latitudinal assemblage change between the NWS and Carnarvon Ramp is likely associated with the gradual transition from tropical-subtropical fauna to temperate fauna found by Betjeman (1969). Environmental parameters do not show marked short-range variation, thus the region is not clearly subdivided into faunal zones. Betjeman assessed the foraminifera on the WA shelf from 18° S (Rowley Shelf) to 34° S (Cape Leeuwin) and found a rapid decrease in tropical-subtropical Indo-Pacific species at latitudes higher than 23° S (Exmouth Gulf). The faunal regions overlap in a transition zone at 25 to 30° S. Sites U1461, U1463, and U1464 lie in the region of the tropical-subtropical faunal zone (18–25° S), while U1460 lies in the transitional zone (25–30° S) towards the warm-temperate faunal region. However, given that the bottom temperature at the Carnarvon Ramp site (18°C) is warmer than at the deepest NWS site (14°C), temperature cannot be invoked as a factor to explain latitudinal differences. Rather, water mass characteristics present and past (i.e., glacial-interglacial) and relative influence of the Leeuwin Current are more likely factors associated with those assemblage differences (e.g., Spooner et al., 2011; Wells and Wells, 1994; Wyrwoll et al., 2009).

The detected differences between the assemblages from the NWS and Carnarvon Ramp may indicate that latitudinal foraminiferal migration on the outer shelf assisted by the LC is limited, at least at the depths sampled. The reduced influence of the LC's warm waters at the Carnarvon Ramp site compared to the NWS sites is likely associated with the shallow nature and flow path of the LC (<100 m deep; Thompson, 1984). The LC becomes narrower and more focused as it converges towards the inner- and mid-shelf (Fig. 4.1A), which enhances the influence of cooler, north-flowing, waters of the Western Australian Current at the Carnarvon Ramp site. Furthermore, the Carnarvon Ramp may not provide sufficiently contiguous suitable habitats for colonization by some taxa. The Carnarvon Ramp along Cape Range is a very narrow continental shelf (ca. 10 km), which lacks the diversity of shelf habitats that exist on the NWS and SWS (Fig. 4.1B). This present condition of the Carnarvon Ramp is comparable to the

restriction of benthic shelf habitat the SWS and NWS faced during marine regressions such as the Last Glacial Maximum (Chapter 2 in Wilson, 2013).

The confinement of highly diverse tropical assemblages confirms the presence of a biogeographic province transition from tropical-subtropical to warm-temperate between Shark Bay and the Exmouth Gulf (26–22° S). Future paleoenvironmental and paleobathymetric assessments of carbonate ramps can be guided by indicator species and their characteristic abundances on the WA shelf. Identifying characteristic assemblages will assist in recognizing paleo-temperature gradients and variations in poleward extent of tropical warm water along Western Australia related to glacial-interglacial cycles.

Conclusions

Examination of samples from the outer shelf shows that foraminiferal assemblages and their variability are a viable means to reconstruct paleoecological conditions on the WA shelf. This is underpinned by the following findings:

1. Foraminiferal assemblages (benthic and planktonic) represent prominent components of the carbonate sediments on the WA shelf.

2. As planktonic foraminifera become more abundant offshore, rotaliida, and miliolida decrease in relative abundance, while textulariids and buliminids increase in proportions downslope. Lagenids retain similar proportions.

3. The abundance of benthic species that host algal endosymbionts (*Amphistegina papillosa*, *Operculina ammonoides*) at the shallowest site on the NWS (127 m) indicated the influence of light, compared with the 145 m site, where light-dependent species were relatively rare.

4. Displacement of allochthonous reefal LBF species (e.g., *Peneroplis pertusus*) indicates downslope transport from inner-neritic environments to outer shelf. Future research assessing the live assemblage (e.g., staining with rose Bengal) may help to distinguish in-situ specimens.

5. The assemblages in the 125–250 μm size fraction were more diverse than in the 250–850 μm fraction. As indicated by both species richness and Fisher α, NWS samples were more diverse than samples from the Carnarvon Ramp site. In the NWS samples diversity increased with depth.

6. Based on cluster analyses of the 125–250 μm fraction, assemblages were divided into "lowermost euphotic" and "subeuphotic thermocline": In the shallower assemblage (127 m), mid-shelf species such as *Cibicides* cf. *C. refulgens*, *Caribeanella elatensis*, *Triloculina tricarinata*, and the LBF *Operculina ammonoides* and *Amphistegina papillosa* were common. The deeper water sites (145–264 m) were characterized by higher abundances *Bolivina robusta*, *Anomalinulla glabrata*, *Paracassidulina neocarinata*, and *Globocassidulina subglobosa*, which are common outer shelf and upper slope taxa.

7. The 250–850 μm fraction indicated a latitudinal distinction between NWS and Carnarvon Ramp. Indicative for the Carnarvon Ramp were *Cibicides* cf. *C. refulgens*, *Textularia* cf. *T. agglutinans*, *Bigenerina aspratilis*, and *Quinqueloculina* sp. 5 sensu Parker. In the NWS samples, *Caribeanella elatensis*, and miliolid taxa including *Spiroloculina subimpressa*, *Triloculina tricarinata*, and *Miliolinella* sp. 1 sensu Parker 2009, were particularly abundant.

8. Water-mass characteristics, limited shelf habitats, and possibly biogeographic history, rather than temperature and depth, appear to be responsible for assemblage differences between Northwestern Shelf and Carnarvon Ramp. Water temperature at 216 m depth on the Carnarvon Ramp (~18°C) was comparable to that at the NWS sites (145–264 m and 14–23°C).

Acknowledgments

Sampling assistance was provided by the IODP Expedition 356 technicians on shipboard in 2015 and the IODP Gulf Coast Repository at Texas A&M College Station in 2016. Sample processing was supported by the USGS St. Petersburg Coastal and Marine Science Center, St. Petersburg, Florida, U.S.A. Scanning electron microscopy was conducted at the USF College of Marine Science's Electron Microscopy Laboratory and supported by its manager Tony Greco. C. Haller was supported by USF and

the IODP U.S. Science Support Program, which provided financial and logistical support obtaining the sample material. Brianna Michaud and Jennifer Brizzolara made helpful editorial comments on earlier versions of this manuscript. Furthermore, we are very thankful for the peer-review comments by David Haig and Justin Parker, which improved this manuscript substantially. Any use of trade names is for descriptive purposes only and does not imply endorsement by the U.S. Government.

References

Abu-Zied, R.H., Al-Dubai, T.A.M., Bantan, R.A., 2016. Environmental conditions of shallow waters alongside the Southern Corniche of Jeddah based on benthic foraminifera, physico-chemical parameters and heavy metals. Journal of Foraminiferal Research 46, 149–170. 10.2113/gsjfr.46.2.149

Armstrong, H., Brasier, M., 2005. Microfossils, 2nd Edition. Blackwell Publishing, Oxford, pp. 306.

Betjeman, K.J., 1969. Recent foraminifera from the western continental shelf of Western Australia. Contributions from the Cushman Laboratory for Foraminiferal Research 20, 119–138.

Bradshaw, M., Bernecker, T., 2015. Science capabilities unlock Australia's oil and gas potential. The Leading Edge 35, 15-21. 10.1190/tle35010015.1

Carrigy, M.A., Fairbridge, R.W., 1954. Recent sedimentation, physiography and structure of the continental shelves of Western Australia. Journal of the Royal Society of Western Australia 38, 65–95.

Chaproniere, G.C.H., 1984. Oligocene and Miocene larger foraminiferida from Australia and New Zealand. Bureau of Mineral Resources, Geology and Geophysics, Canberra, pp. 98.

Cherif, O.H., Al-Ghadban, A.-N., Al-Rifaiy, I.A., 1997. Distribution of foraminifera in the Arabian Gulf. Micropaleontology 43, 253–280. 10.2307/1485827

Collins, L.B., 1988. Sediments and history of the Rottnest Shelf, southwest Australia: A swell-dominated, non-tropical carbonate margin. Sedimentary Geology 60, 15–49. 10.1016/0037-0738(88)90109-1

Collins, L.B., James, N.P., Bone, Y., 2014. Chapter 19 Carbonate shelf sediments of the western continental margin of Australia. Geological Society of London Memoirs 41, 255–272. 10.1144/m41.19

Collins, L.B., Wyrwoll, K.H., France, R.E., 1991. The Abrolhos carbonate platforms: geological evolution and Leeuwin Current activity. Journal of the Royal Society of Western Australia 74, 47–57.

Collins, L.B., Zhu, Z.R., Wyrwoll, K.H., Hatcher, B.G., Playford, P.E., Eisenhauer, A., Chen, J.H., Wasserburg, G.J., Bonani, G., 1993. Holocene growth history of a reef complex on a cool-water carbonate margin: Easter Group of the Houtman Abrolhos, Eastern Indian Ocean. Marine Geology 115, 29–46. 10.1016/0025-3227(93)90073-5

Corliss, B.H., 1979a. Quaternary Antarctic Bottom-Water history: Deep-sea benthonic foraminiferal evidence from the southeast Indian Ocean. Quaternary Research 12, 271-289. 10.1016/0033-5894(79)90062-0

Corliss, B.H., 1979b. Taxonomy of Recent Deep-Sea Benthonic Foraminifera from the Southeast Indian Ocean. Micropaleontology 25, 1–19. 10.2307/1485207

Cresswell, G.R., Golding, T.J., 1980. Observations of a south-flowing current in the southeastern Indian Ocean. Deep Sea Research Part A. Oceanographic Research Papers 27, 449–466. 10.1016/0198-0149(80)90055-2

CSIRO Oceans & Atmosphere - Integrated Marine Observing System (IMOS), 2017. Gridded sea level anomaly - Delayed mode, http://oceancurrent.imos.org.au.

Debenay, J.-P., 2013. A guide to 1,000 foraminifera from Southwestern Pacific New Caledonia. IRD Éditions, Publications Scientifiques du Muséum, Marseille, Paris, pp. 378.

Fellowes, T.E., Gacutan, J., Harris, D.L., Vila-Concejo, A., Webster, J.M., Byrne, M., 2017. Patterns of sediment transport using foraminifera tracers across sand aprons on the Great Barrier Reef. Journal of Coastal Research 33, 864–873. 10.2112/JCOASTRES-D-16-00082.1

Feng, M., Meyers, G., Pearce, A., Wijffels, S., 2003. Annual and interannual variations of the Leeuwin Current at 32°S. Journal of Geophysical Research: Oceans 108, 3355. 10.1029/2002JC001763

Fisher, R.A., Corbet, A.S., Williams, C.B., 1943. The relation between the number of species and the number of individuals in a random sample of an animal population. Journal of Animal Ecology 12, 42–58. 10.2307/1411

Gallagher, S.J., Fulthorpe, C.S., Bogus, K., the Expedition 356 Scientists, 2017. Expedition 356 Preliminary Report: Indonesian Throughflow. International Ocean Discovery Program, College Station, Texas, pp. 53.

Gallagher, S.J., Wallace, M.W., Li, C.L., Kinna, B., Bye, J.T., Akimoto, K., Torii, M., 2009. Neogene history of the West Pacific Warm Pool, Kuroshio and Leeuwin currents. Paleoceanography 24, PA1206. 10.1029/2008PA001660

Geoscience Australia, 2017a. MODIS derived Chlorophyll a datasets, in: Australia, G. (Ed.), http://data.gov.au/dataset/62a6b9b2-756b-44f7-aab0-a7fee405b0f9.

Geoscience Australia, 2017b. MODIS derived Sea Surface Temperature (SST) datasets, http://data.gov.au/dataset/53f9de2f-d6e2-4c48-b13a-90ae3fe06f74.

Greenstein, B.J., Pandolfi, J.M., 2008. Escaping the heat: range shifts of reef coral taxa in coastal Western Australia. Global Change Biology 14, 513–528. 10.1111/j.1365-2486.2007.01506.x

Grimsdale, T.F., van Morkhoven, F.P.C.M., 1955. 4. The ratio between pelagic and benthonic foraminifera as a means of estimating depth of deposition of of estimating depth of deposition of sedimentary rocks. 4th World Petroleum Congress, 6-15 June, Rome, Italy

Haig, D.W., 1997. Foraminifera from Exmouth Gulf, Western Australia. Journal of the Royal Society of Western Australia 80, 263–280.

Hammer, Ø., Harper, D.A.T., Ryan, P.D., 2001. PAST: Paleontological statistics software package for education and data analysis. Palaeontologia Electronica 4, 9. http://palaeo-electronica.org/2001_1/past/issue1_01.htm

Hayward, B.W., Grenfell, H.R., Sabaa, A.T., Neil, H.L., Buzas, M.A., 2010. Recent New Zealand deep-water benthic foraminifera: Taxonomy, ecologic distribution, biogeography, and use in paleoenvironmental assessment. Institute of Geological & Nuclear Sciences, Lower Hutt, New Zealand, pp. 363.

Hocking, R.M., Moors, H.T., Van De Graaff, W.J.E., 1987. Geology of the Carnarvon Basin Western Australia. Geological Survey of Western Australia, Perth, pp. 289.

Hohenegger, J., 1994. Distribution of Living Larger Foraminifera NW of Sesoko-Jima, Okinawa, Japan. Marine Ecology 15, 291–334. 10.1111/j.1439-0485.1994.tb00059.x

Hohenegger, J., 2000. Coenoclines of larger foraminifera. Micropaleontology 46, 127–151.

James, N.P., 1997. The cool-water carbonate depositional realm, in: James, N.P., Clarke, J.A.D. (Eds.), Cool-water carbonates. SEPM Society for Sedimentary Geology, pp. 1–20.

James, N.P., Bone, Y., Kyser, T.K., Dix, G.R., Collins, L.B., 2004. The importance of changing oceanography in controlling late Quaternary carbonate sedimentation on a high-energy, tropical, oceanic ramp: North-western Australia. Sedimentology 51, 1179–1205. 10.1111/j.1365-3091.2004.00666.x

James, N.P., Collins, L.B., Bone, Y., Hallock, P., 1999. Subtropical carbonates in a temperate realm: Modern sediments on the southwest Australian shelf. Journal of Sedimentary Research 69, 1297–1321. 10.2110/jsr.69.1297

Jones, H.A., 1973. Marine geology of the northwest Australian continental shelf. Bulletin 136. Bureau of Mineral Resources, Geology and Geophysics, Canberra, pp.

Kaufman, L., Rousseeuw, P.J., 1990. Finding groups in data: An introduction to Cluster Analysis. John Wiley & Sons, Inc., pp. 342.

Li, Q., James, N.P., Bone, Y., McGowran, B., 1999. Palaeoceanographic significance of recent foraminiferal biofacies on the southern shelf of Western Australia: a preliminary study. Palaeogeography, Palaeoclimatology, Palaeoecology 147, 101–120. 10.1016/S0031-0182(98)00150-3

Loeblich, A.R., Tappan, H., 1994. Foraminifera of the Sahul Shelf and Timor Sea. Cushman Foundation for Foraminiferal Research Special Pubublication 31, Cambridge, MA, pp. 661.

Mays, C., 2007. The current distribution of foraminifera on the Western Australian shelf: A modern analogue for Cenozoic palaeoceanography, School of Earth Sciences. University of Melbourne, Australia, p. 74.

Mckenzie, K.G., 1962. A Record of Foraminifera from Oyster Harbour, near Albany, Western Australia. Journal of the Royal Society of Western Australia 45, 117–132.

Miller, K.G., Sugarman, P.J., Browning, J.V., Kominz, M.A., Olsson, R.K., Feigenson, M.D., Hernández, J.C., 2004. Upper Cretaceous sequences and sea-level history, New Jersey Coastal Plain. Geological Society of America Bulletin 116, 368-393. 10.1130/b25279.1

Moss, G.D., Cathro, D.L., Austin, J.A., 2004. Sequence biostratigraphy of prograding clinoforms, Northern Carnarvon Basin, Western Australia: A proxy for variations in Oligocene to Pliocene global sea level? Palaios 19, 206–226. 10.1669/0883-1351(2004)019<0206:sbopcn>2.0.co;2

Murgese, D.S., De Deckker, P., 2005. The distribution of deep-sea benthic foraminifera in core tops from the eastern Indian Ocean. Marine Micropaleontology 56, 25–49. j.marmicro.2005.03.005

Murgese, D.S., De Deckker, P., 2007. The Late Quaternary evolution of water masses in the eastern Indian Ocean between Australia and Indonesia, based on benthic foraminifera faunal and carbon isotopes analyses. Palaeogeography, Palaeoclimatology, Palaeoecology 247, 382–401. 10.1016/j.palaeo.2006.11.002

Murray, J.W., 2006. Ecology and Applications of Benthic Foraminifera. Cambridge University Press, pp. 426.

Mutti, M., Hallock, P., 2003. Carbonate systems along nutrient and temperature gradients: some sedimentological and geochemical constraints. International Journal of Earth Sciences 92, 465-475. 10.1007/s00531-003-0350-y

Odin, G.S., Morton, A.C., 1988. Authigenic green particles from marine environments, in: Chilingarian, G.V., Wolf, K.H. (Eds.), Diagenesis, vol. II. Elsevier, Amsterdam, pp. 219–264.

Orpin, A.R., Haig, D.W., Woolfe, K.J., 1999. Sedimentary and foraminiferal facies in Exmouth Gulf, in arid tropical northwestern Australia. Australian Journal of Earth Sciences 46, 607–621. 10.1046/j.1440-0952.1999.00728.x

Panchang, R., Nigam, R., 2014. Benthic ecological mapping of the Ayeyarwady Delta Shelf off Myanmar, using foraminiferal assemblages. Journal of the Palaeontological Society of India 59, 121–168.

Parker, J.H., 2009. Taxonomy of foraminifera from Ningaloo Reef, Western Australia. Memoir of the Association of Australasian Palaeontologists 36, Canberra, pp. 810.

Parker, J.H., Gischler, E., 2015. Modern and relict foraminiferal biofacies from a carbonate ramp, offshore Kuwait, northwest Persian Gulf. Facies 61. 10.1007/s10347-015-0437-5

Pearce, A., 2009. Introduction: some historical “milestones” in the Leeuwin Current, and the Leeuwin Current Symposium 2007. Journal of the Royal Society of Western Australia 92, 31–36.

Pearce, A.F., Phillips, B.F., 1988. Enso Events, the Leeuwin Current, and Larval Recruitment of the Western Rock Lobster. ICES Journal of Marine Science - Journal Du Conseil 45, 13–21.

Peters, S.E., Loss, D.P., 2012. Storm and fair-weather wave base: A relevant distinction? Geology 40, 511–514. 10.1130/G32791.1

Quilty, P.G., Hosie, G., 2006. Modern foraminifera, Swan River Estuary, Western Australia: Distribution and controlling factors. Journal of Foraminiferal Research 36, 291–314. 10.2113/gsjfr.36.4.291

Raup, D.M., 1975. Taxonomic diversity estimation using rarefaction. Paleobiology 1, 333–342.

Reason, C.J.C., Gamble, D., Pearce, A.F., 1999. The Leeuwin Current in the Parallel Ocean Climate Model and applications to regional meteorology and fisheries. Meteorological Applications 6, 211–225. 10.1017/S1350482799001255

Renema, W., 2007. Fauna development of larger benthic foraminifera in the Cenozoic of Southeast Asia, in: Renema, W. (Ed.), Biogeography, Time, and Place: Distributions, Barriers, and Islands. Springer Netherlands, pp. 179–215.

Revets, S.A., 2000. Foraminifera of Leschenault Inlet. Journal of the Royal Society of Western Australia 83, 365–375.

Schott, F.A., Xie, S.-P., McCreary, J.P., 2009. Indian Ocean circulation and climate variability. Reviews of Geophysics 47, RG1002. 10.1029/2007RG000245

Semeniuk, T.A., 2001. Epiphytic foraminifera along a climatic gradient, Western Australia. Journal of Foraminiferal Research 31, 191–200. 10.2113/31.3.191

Smith, R.L., Huyer, A., Godfrey, J.S., Church, J.A., 1991. The Leeuwin Current off Western Australia, 1986–1987. Journal of Physical Oceanography 21, 323–345. 10.1175/1520-0485(1991)021<0323:TLCOWA>2.0.CO;2

Spooner, M.I., De Deckker, P., Barrows, T.T., Fifield, L.K., 2011. The behaviour of the Leeuwin Current offshore NW Australia during the last five glacial–interglacial cycles. Global and Planetary Change 75, 119–132. 10.1016/j.gloplacha.2010.10.015

Stagg, H.M.J., Colwell, J.B., 1994. The structural foundations of the Northern Carnarvon Basin, in: Purcell, P.G., Purcell, R.R. (Eds.), The sedimentary basins of Western Australia, pp. 349–372.

Strotz, L.C., Mamo, B.L., Dominey-Howes, D., 2016. Effects of cyclone-generated disturbance on a tropical reef foraminifera assemblage. Scientific Reports 6, 24846. 10.1038/srep24846

Thissen, J.M., Langer, M.R., 2017. Spatial patterns and structural composition of foraminiferal assemblages from the Zanzibar Archipelago (Tanzania). Palaeontographica Abteilung A 308, 1–67. 10.1127/pala/308/2017/1

Thompson, R.O.R.Y., 1984. Observations of the Leeuwin Current off Western Australia. Journal of Physical Oceanography 14, 623–628. 10.1175/1520-0485(1984)014<0623:ootlco>2.0.co;2

Tomczak, M., Godfrey, J.S., 2003. Regional Oceanography: An Introduction 2nd edn. Daya Publishing House, Delhi, pp. 390.

van Morkhoven, F.P.C.M., Berggren, W.A., Edwards, A.S., 1986. Cenozoic Cosmopolitan Deep-Water Benthic Foraminifera. Bulletin des Centres de Recherches Exploration-Production Elf-Aquitaine Mem. 11, Pau, pp. 421.

Waite, A.M., Thompson, P.A., Pesant, S., Feng, M., Beckley, L.E., Domingues, C.M., Gaughan, D., Hanson, C.E., Holl, C.M., Koslow, T., Meuleners, M., Montoya, J.P., Moore, T., Muhling, B.A., Paterson, H., Rennie, S., Strzelecki, J., Twomey, L., 2007. The Leeuwin Current and its eddies: An introductory overview. Deep Sea Research Part II: Topical Studies in Oceanography 54, 789–796. 10.1016/j.dsr2.2006.12.008

Wells, P., Wells, G., Cali, J., Chivas, A., 1994. Response of deep-sea benthic foraminifera to Late Quaternary climate changes, southeast Indian Ocean, offshore Western Australia. Marine Micropaleontology 23, 185–229. 10.1016/0377-8398(94)90013-2

Wells, P.E., Wells, G.M., 1994. Large-scale reorganization of ocean currents offshore Western Australia during the Late Quaternary. Marine Micropaleontology 24, 157–186. 10.1016/0377-8398(94)90020-5

Whiteway, T., 2009. Australian Bathymetry and Topography Grid, June 2009, in: Geoscience Australia (Ed.).

Wilson, B., 2013. The Biogeography of the Australian North West Shelf. Elsevier, Boston, pp. 413.

Wilson, B.R., Gillett, K., 1980. Australian Shells. Reed Pty. Ltd, Sydney, pp. 152.

Wyrwoll, K.-H., Greenstein, B.J., Kendrick, G.W., Chen, G.S., 2009. The palaeoceanography of the Leeuwin Current: implications for a future world. Journal of the Royal Society of Western Australia 92, 37-51.

Yassini, I., Jones, B.G., 1995. Recent foraminifera and ostracoda from estuarine and shelf environments on the southestern coast of Australia. The University of Wollongong Press, Wollongong, Australia, pp. 484.

Tables

Table 4.1. Sample site information (see map Fig. 4.1B) with water depth. Sea-surface temperature (SST) and chlorophyll a are three-year averages of monthly data from January 2009 to December 2011 measured by the Moderate-Resolution Imaging Spectroradiometer (MODIS) satellite (Geoscience Australia, 2017a, b). Sea-floor temperature measured by Conductivity, Temperature, and Depth (CTD) instrument cast and sedimentary facies of the seafloor were adopted from the literature: * = James et al. (1999) Figures 11 and Fig. 13, ** = Figures 3 and 7 in James et al. (2004). NWS = Northwestern shelf, CR = Carnarvon Ramp

Location								
Sample	Latitude	Longitude	Region	Depth (m)	SST (°C)	Chlorophyll a (mg/m^3)	Bottom water temp. (°C)	Sedimentary facies
U1460A	27.22495°S	112.55430°E	CR	215	24	0.14	18*	S1 Spiculitic carbonate silt facies*
U1460B	27.22487°S	112.55427°E	CR	214	24	0.14	18*	S1 Spiculitic carbonate silt facies*
U1461A	20.12863°S	115.03950°E	NWS	127	27	0.15	24**	Pelagic sand and mud**
U1461B	20.12852°S	115.03940°E	NWS	128	27	0.15	24**	Pelagic sand and mud**
U1461C	20.12843°S	115.03937°E	NWS	128	27	0.15	24**	Pelagic sand and mud**
U1463C	18.57931°S	117.37434°E	NWS	145	28	0.10	23**	Pelagic sand and mud**
U1463D	18.57929°S	117.37422°E	NWS	145	28	0.10	23**	Pelagic sand and mud**
U1464D	18.03923°S	118.37884°E	NWS	264	28	0.09	14**	Pelagic sand and mud**

Table 4.2. Census data for all three analyzed size fractions (125–250 µm, 250–850 µm, and >850 µm): collected foraminiferal specimens, species richness, and Fisher α index.

Sample	Number of individuals	Number of species	Fisher α index
U1460A	868 / 382 / 8	74 / 42 / 4	19.3 / 12.0 / 3.2
U1460B	658 / 436 / 1	67 / 53 / 1	18.7 / 15.8 / 0
U1461A	1062 / 38 / -	85 / 16 / -	21.8 / 10.4 / -
U1461B	1312 / 75 / -	84 / 32 / -	20.0 / 21.1 / -
U1461C	940 / 130 / 3	89 / 39 / 3	24.1 / 18.9 / 0
U1463C	866 / 82 / -	96 / 25 / -	27.6 / 12.3 / -
U1463D	865 / 99 / 6	92 / 31 / 5	26.0 / 15.5 / 14.1
U1464D	671 / 385 / -	86 / 62 / -	26.2 / 20.9 / -

Figures

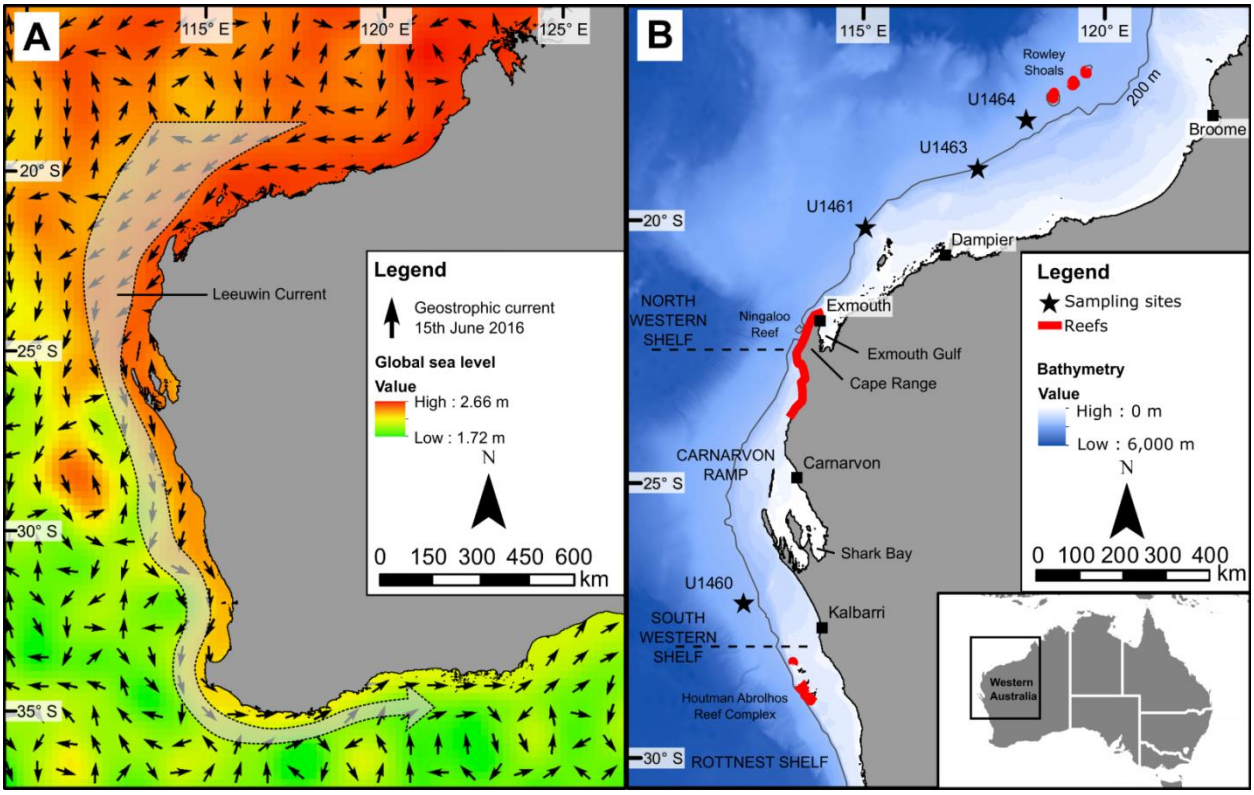

Fig. 4.1. Location map of the study area along the coastline of Western Australia. A) Surface geostrophic flow direction on the southwestern shelf (SWS) and northwestern shelf (NWS) indicated by vector arrows. Flow pattern of the Leeuwin Current and eddies shed are illustrated by gridded total global sea

level measured by a NOAA radar altimetry satellite on 15th June 2016, in the season when the Leeuwin Current flow is the strongest (CSIRO Oceans & Atmosphere - Integrated Marine Observing System (IMOS), 2017). B) Sampling site locations (stars) and site names, location of modern coral reefs, and seafloor bathymetry (Whiteway, 2009).

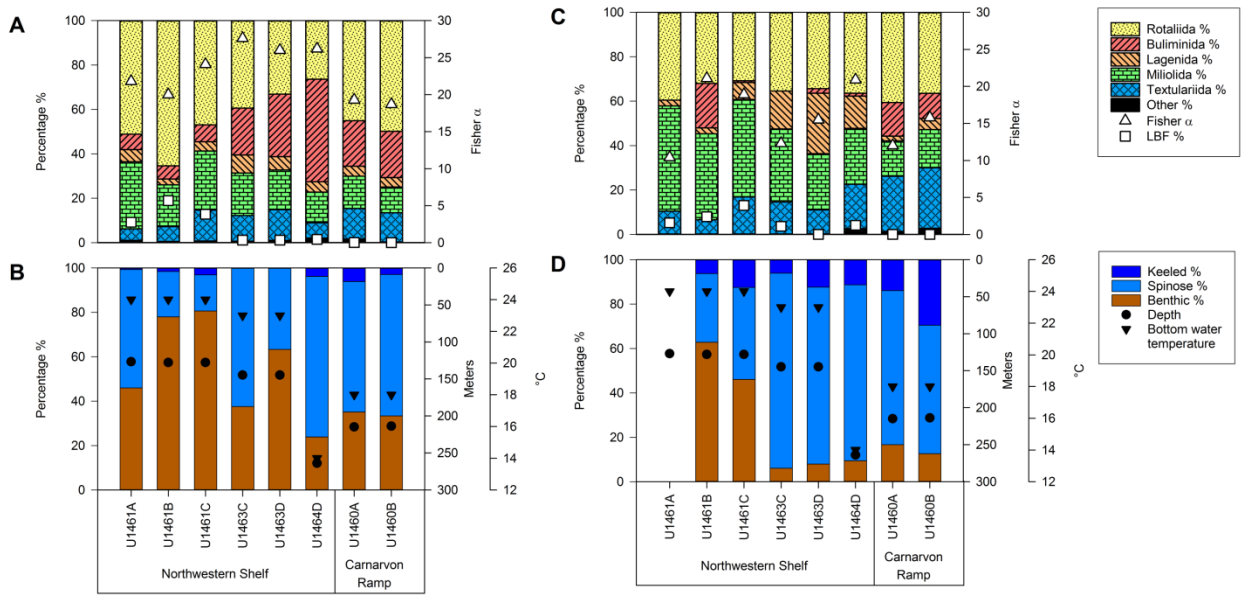

Fig. 4.2. Foraminiferal assemblage data from the 125–250 µm and 250–850 µm fractions by sample. A) 125–250 µm: Percentages of benthic orders, percentage LBF of the total benthic assemblage, and Fisher α (see Table 4.2). B) 125–250 µm: Planktonic (keeled and spinose taxa) and benthic percentages, water depth, and bottom water temperature (see Table 4.1). C) 250–850 µm: Percentages of benthic orders, percentage LBF of the total benthic assemblage, and Fisher α (see Table 4.2). D) 250–850 µm: Planktonic (keeled and spinose taxa) and benthic percentages, water depth, and bottom water temperature (see Table 4.1). LBF = "larger" symbiont-bearing foraminifera. "Other" = Lituolida, Trochamminida, Spirillinida, and Robertinida.

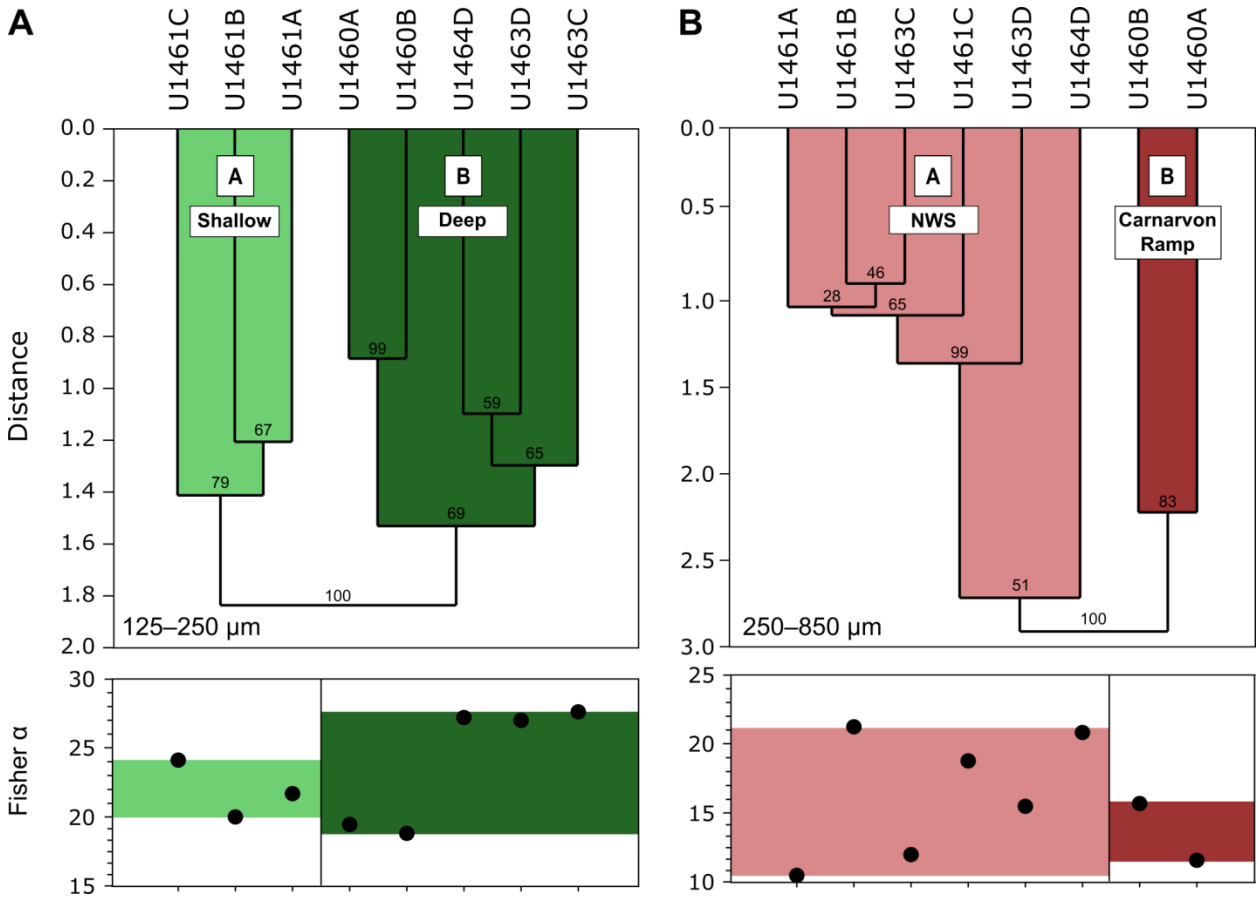

Fig. 4.3. Q-mode (samples) cluster dendrograms with Euclidean distances for the respective 30 most abundant species. Bootstrapping percentages (cycles n=9,999) indicate the stability of the formed branches. A) 125–250 µm fraction exhibiting two major cluster groups (cophenetic correlation coefficient=0.71). B) 250–850 µm fraction exhibiting two major cluster groups (cophenetic correlation coefficient=0.98).

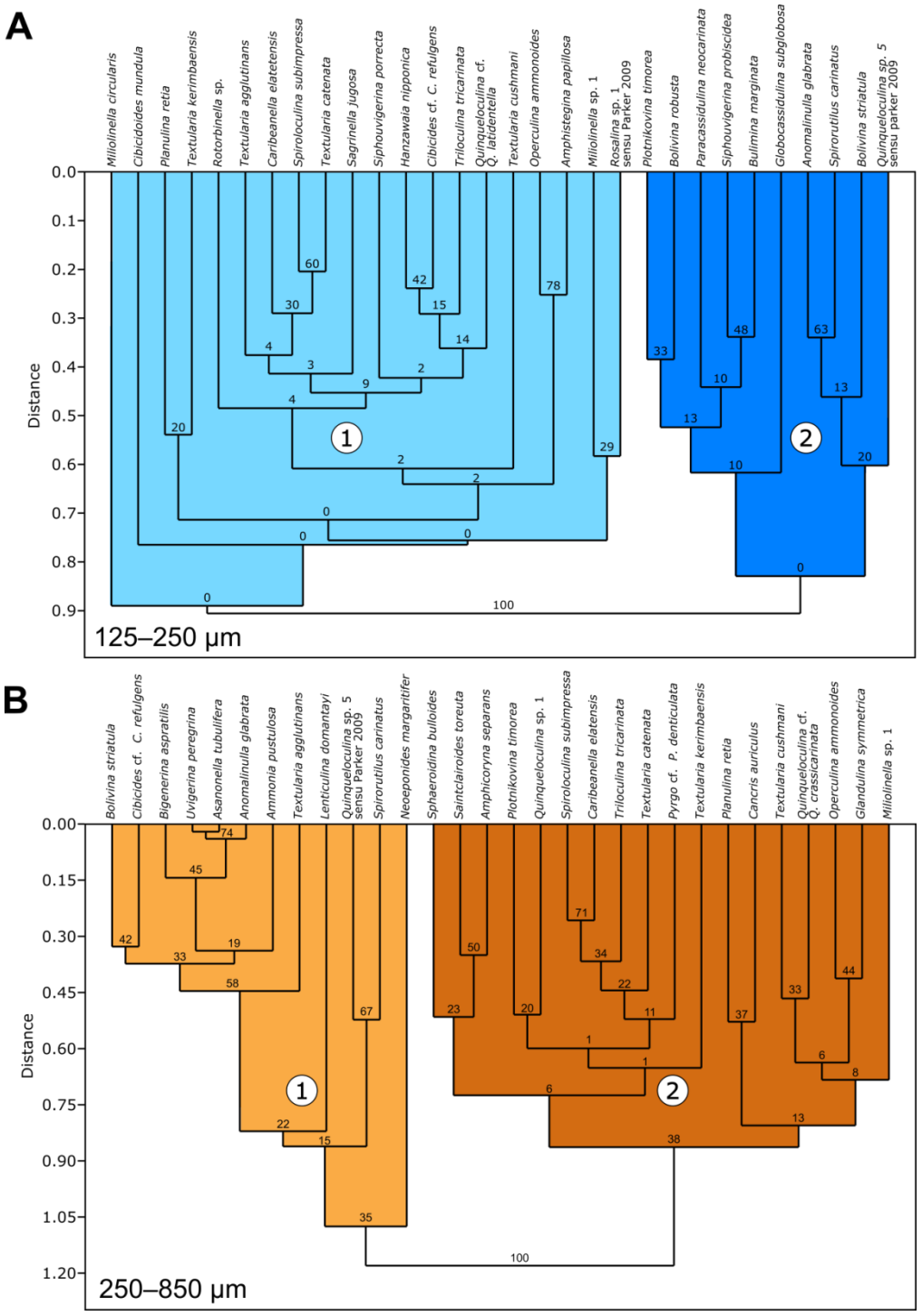

Fig. 4.4. R-mode (species) cluster dendrogram with Euclidean distances from the respective 30 most abundant species. Bootstrapping percentages (cycles n=9,999) indicate the stability of the formed branches. A) 125–250 µm fraction (cophenetic correlation coefficient=0.89). B) 250–850 µm fraction (cophenetic correlation coefficient=0.80).

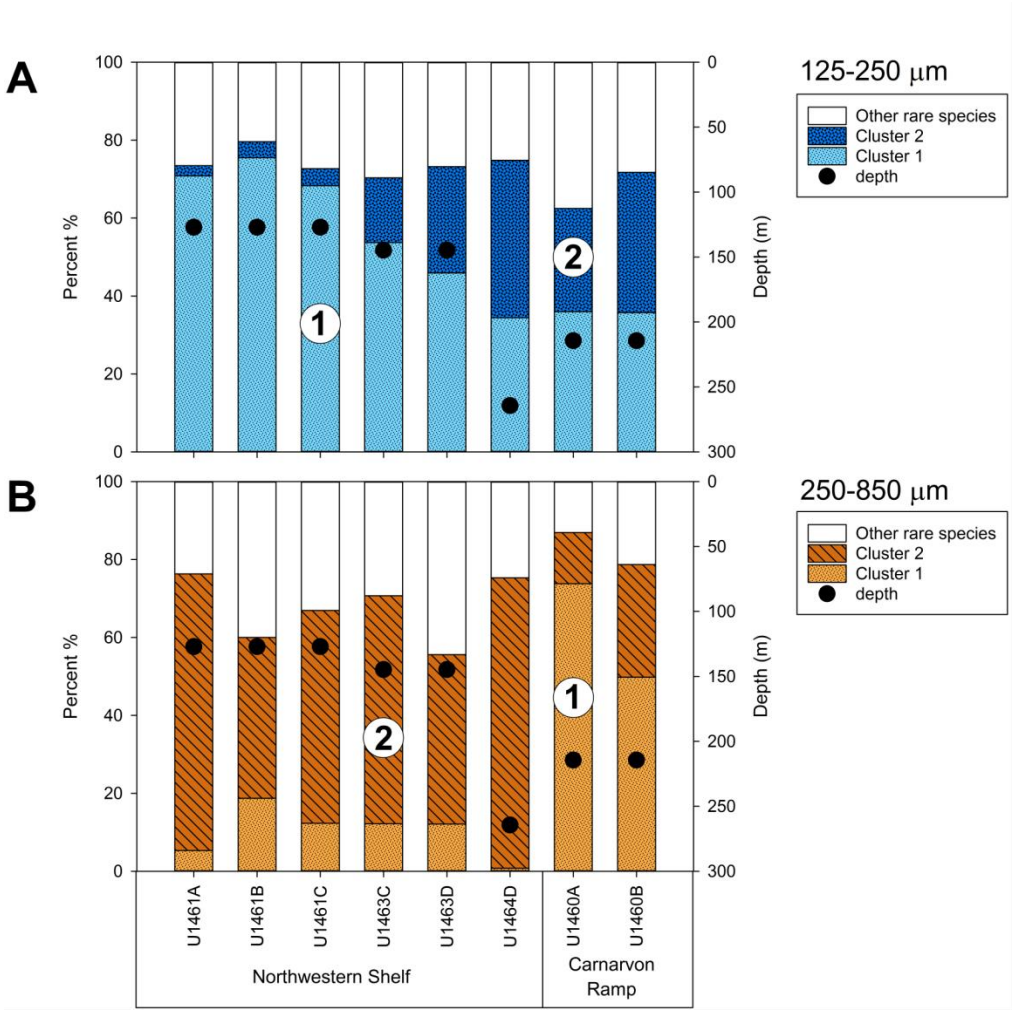

Fig. 4.5. Distribution of species clusters (R-mode) along the Western Australian shelf including "Other rare species", which were excluded from cluster analysis. A) 125–250 µm fraction. B) 250–850 µm fraction.

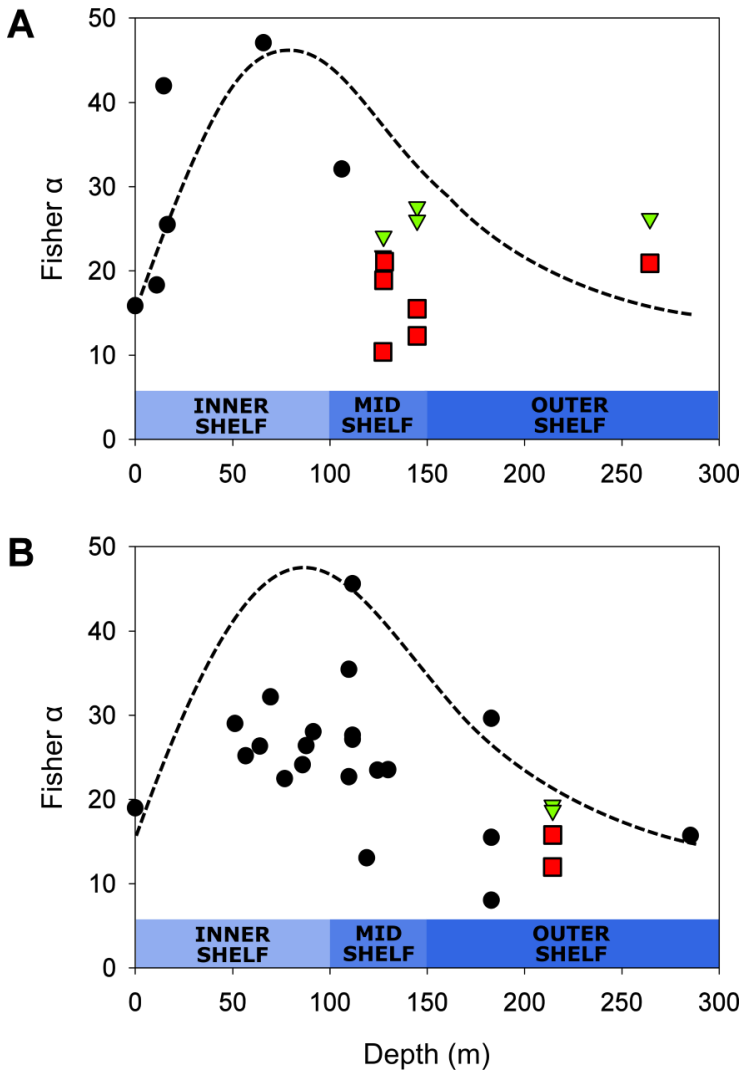

Fig. 4.6. Fisher α on the Western Australian shelf. A) Northwestern Shelf; B) Carnarvon Ramp. Green triangles: 125–250 μm; red squares: 250–850 μm ; black dots: recalculated from Betjeman (1969); stippled line: manual fit.

Plates

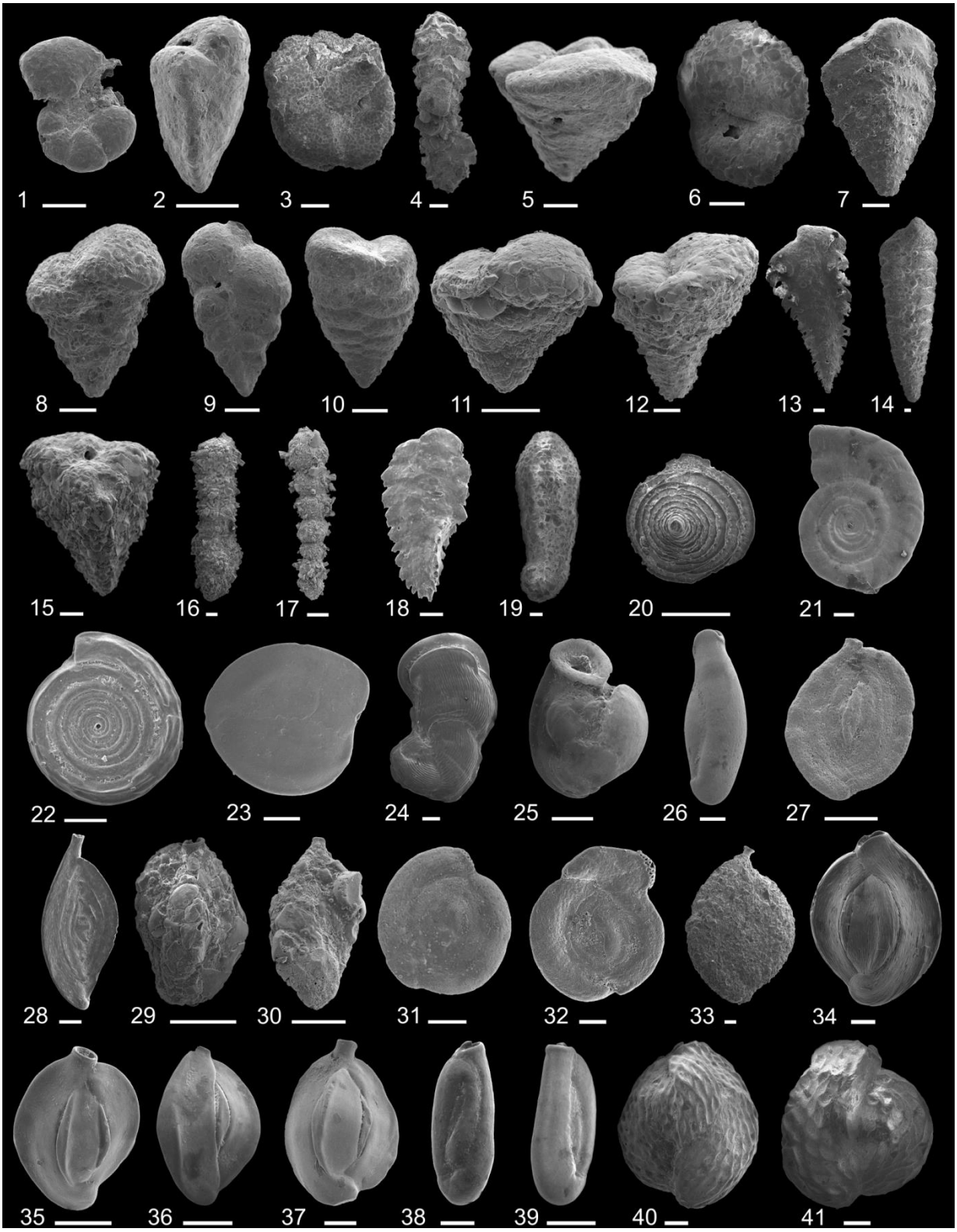
1
2
3
4
5
6
7
8
9
10
11
12
13
14
15
16
17
18
19
20
21
22
23
24
25
26
27
28
29
30
31
32
33
34
35
36
37
38
39
40
41

Plate 4.1. (previous page) Foraminifera from the Western Australian shelf. 1: *Haplophragmoides pusillus* Collins, 1974; 2: *Gaudryina convexa* (Karrer, 1865); 3 *Paratrochammina madeirae* Brönniman, 1979; 4: *Bigenerina aspratilis* Loeblich & Tappan, 1994; 5–6: *Sahulia barkeri* (Hofker, 1978); 7: *Spirorutilus carinatus* (d'Orbigny, 1846); 8: *Textularia* cf. *T. agglutinans* d'Orbigny, 1839; 9: *Textularia catenata* Cushman, 1911; 10: *Textularia cushmani* Said, 1949; 11: *Textularia kerimbaensis* Said, 1949; 12: *Textularia orbica* Lalicker & McCulloch, 1940; 13: *Textularia tubulosa* Zheng, 1980; 14: *Textularia stricta* Cushman, 1911; 15: *Migros flintii* (Cushman, 1911); 16: *Pseudoclavulina robusta* Zheng, 1988; 17: *Pseudoclavulina serventyi* (Chapman & Parr, 1936); 18: *Plotnikovina timorea* Loeblich & Tappan, 1994; 19: *Cylindroclavulina bradyi* (Cushman, 1911); 20: *Patellina* cf. *P. formosa* Heron-Allen & Earland, 1932; 21: *Cornuspira foliacea* (Philippi, 1844); 22: *Cornuspira* sp.; 23: *Planispirinella involuta* Collins, 1958; 24: *Vertebralina striata* d'Orbigny, 1826; 25: *Wiesnerella ujiiei* Hatta in Hatta & Ujiié, 1992; 26: *Edentostomina rupertiana* (Brady, 1881); 27: *Spiroloculina abatholopa* Loeblich & Tappan, 1994; 28: *Spiroloculina subimpressa* Parr, 1950; 29–30: *Agglutinella arenata* (Said, 1949); 31: *Hauerina fragilissima* Brady Em. Ponder, 1975; 32 *Sigmoihauerina bradyi* (Cushman, 1917); 33: *Proemassilina arenaria* (Brady, 1884); 34: *Quinqueloculina barnardi* Rasheed, 1971; 35–36: *Quinqueloculina* cf. *Q. crassicarinata* Collins, 1958; 37: *Quinqueloculina exmouthensis* Parker, 2009; 38–39 *Quinqueloculina* cf. *Q. latidentella*; 40–41: *Quinqueloculina philippinensis* Cushman, 1921. – Scale bar is always 100 μm.

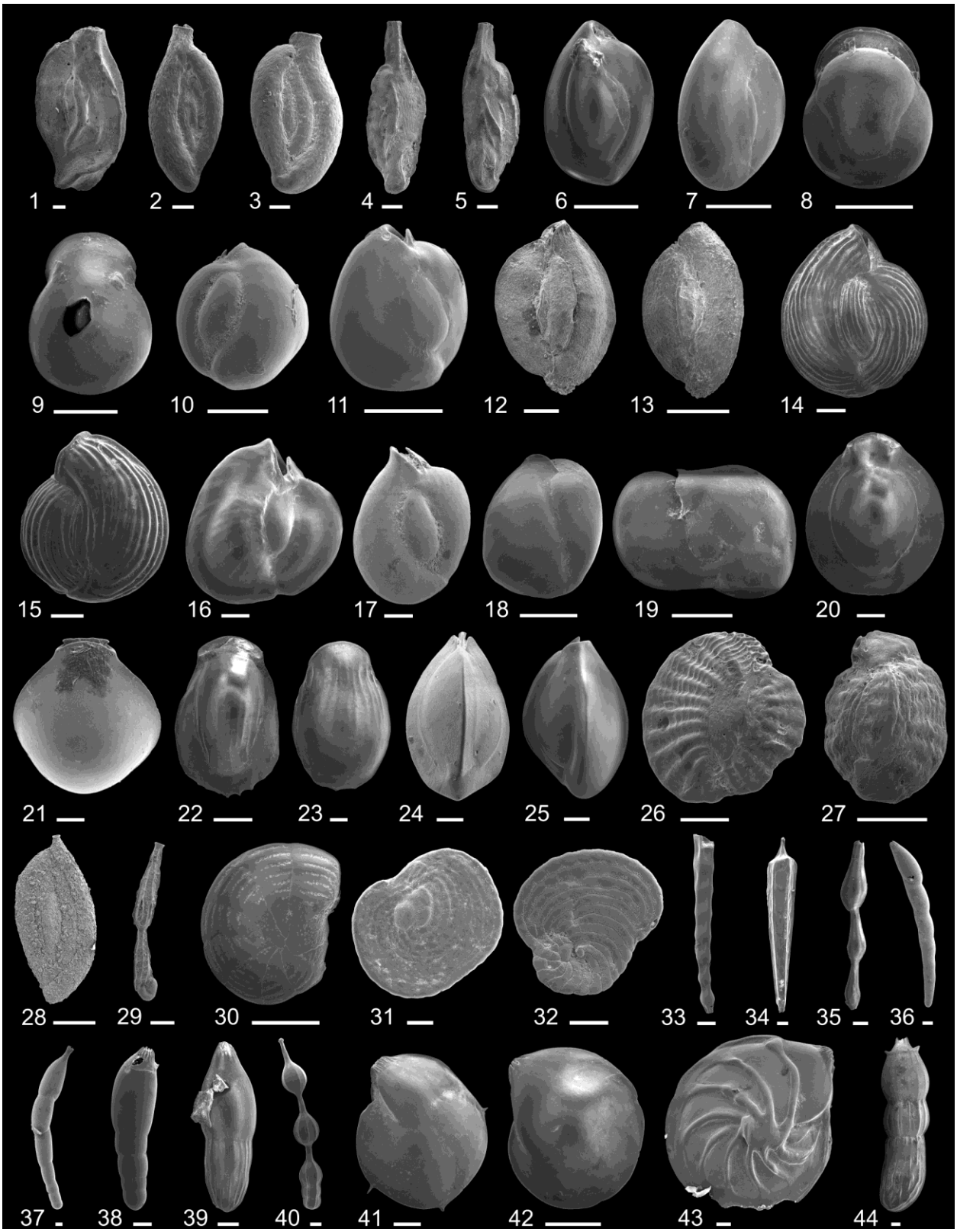
1
2
3
4
5
6
7
8
9
10
11
12
13
14
15
16
17
18
19
20
21
22
23
24
25
26
27
28
29
30
31
32
33
34
35
36
37
38
39
40
41
42
43
44

Plate 4.2. (previous page) Foraminifera from the Western Australian shelf. 1: *Quinqueloculina subpolygona* Parr, 1945; 2–3: *Quinqueloculina timorensis* (Loeblich & Tappan, 1994); 4–5: *Quinqueloculina* sp. 1; 6–7: *Quinqueloculina* sp. 5 sensu Parker; 8-9: *Biloculinella labiata* (Schlumberger, 1891); 10–11: *Miliolinella circularis* (Bornemann, 1855); 12–13: *Miliolinella oceanica* (Cushman, 1932); 14–15: *Miliolinella webbiana* (d'Orbigny, 1839); 16: *Miliolinella pilasensis* McCulloch, 1977; 17–18: *Miliolinella* sp. 1 sensu Parker; 19: *Miliolinella* sp. 2; 20–21: *Pyrgo* cf. *P. denticulata* (Brady, 1884); 22–23: *Pyrgo striolata* (Brady, 1884); 24–25: *Triloculina tricarinata* d'Orbigny, 1826; 26–27: *Sigmoihauerina involuta* (Cushman, 1946), (26) adult, (27) juvenile; 28: *Sigmoilopsis minuta* (Collins, 1958); 29: *Articulina alticostata* Cushman, 1944; 30: *Peneroplis pertusus* (Forskål, 1775); 31–32: *Parasorites orbitolitoides* (Hofker, 1930); 33: *Dentalina catenulata* (Brady, 1884); 34: *Dentalina* cf. *D. mutsui* Hada, 1931; 35: *Grigelis orectus* Loeblich & Tappan, 1994; 36: *Laevidentalina bradyensis* (Dervieux, 1894); 37: *Laevidentalina inflexa* (Reuss, 1866); 38: *Laevidentalina sidebottomi* (Cushman, 1933); 39: *Pyramidulina comatula* (Cushman, 1923); 40: *Pyramidulina luzonensis* (Cushman, 1921); 41: *Lenticulina calcar* (Linnaeus, 1767); 42: *Lenticulina domantayi* (McCulloch, 1977); 43: *Lenticulina submamilligera* (Cushman, 1917); 44: *Marginulinopsis philippinensis* (Cushman, 1921). – Scale bar is always 100 μm.

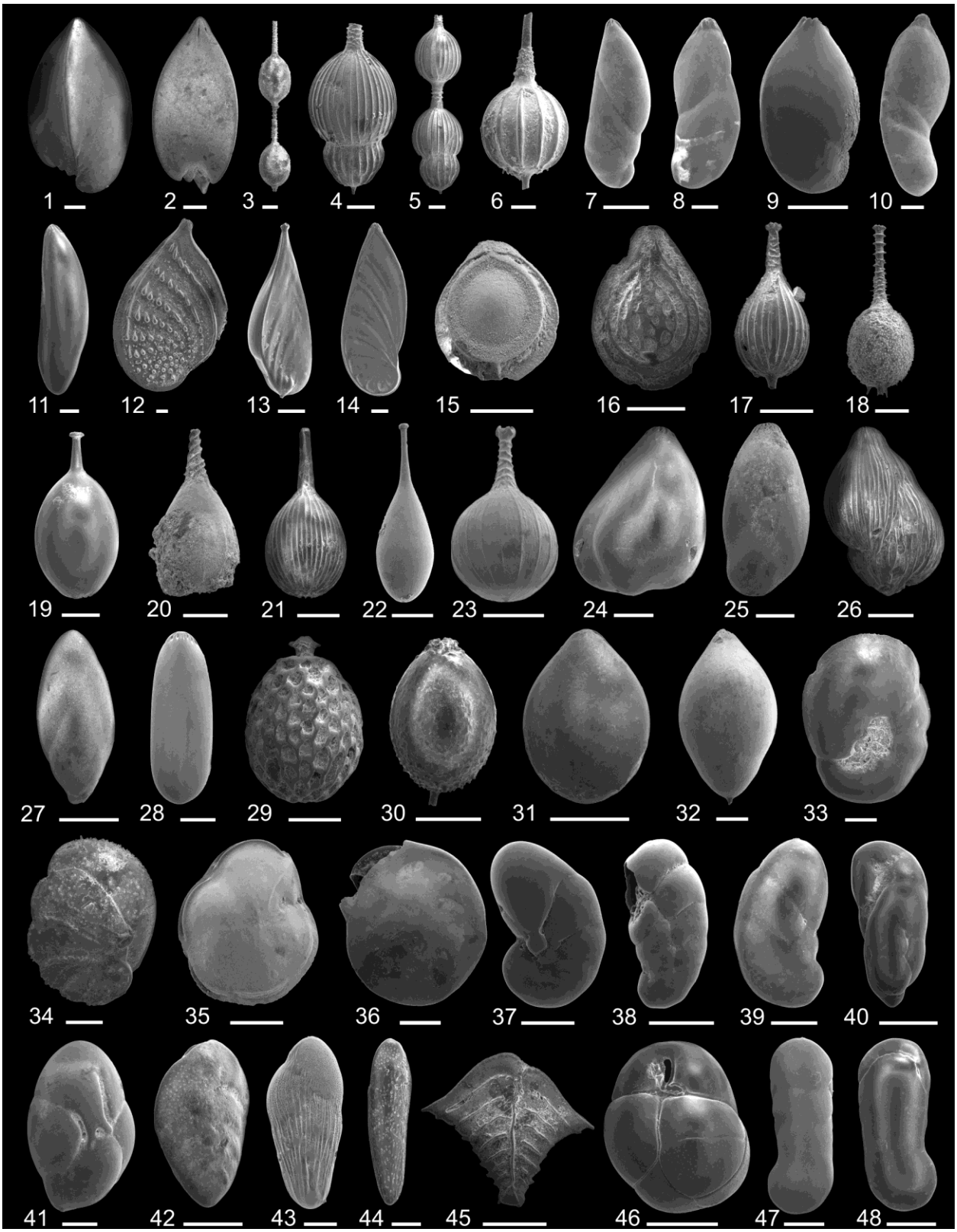
1
2
3
4
5
6
7
8
9
10
11
12
13
14
15
16
17
18
19
20
21
22
23
24
25
26
27
28
29
30
31
32
33
34
35
36
37
38
39
40
41
42
43
44
45
46
47
48

Plate 4.3. (previous page) Foraminifera from the Western Australian shelf. 1–2: *Saracenaria angularis* Natland, 1938; 5: *Amphicoryna* cf. *A. meringella*, Loeblich & Tappan, 1994; 4–5: *Amphicoryna separans* (Brady, 1884); 6: *Amphicoryna sublineata* (Brady, 1884); 7: *Astacolus crepidulus* (Fichtel & Moll, 1798); 8–9: *Marginulina musai* Saidova, 1975; 10: *Vaginulinopsis pseudoplanulata* (Zheng, 1980); 11: *Vaginulinopsis sublegumen* Parr, 1950; 12: *Planularia gemmata* (Brady, 1881); 13: *Planularia patens* (Brady, 1884); 14: *Planularia spinipes* (Cushman, 1913); 15: *Cerebrina* cf. *C. claricerviculata*, (McCulloch, 1977); 16: *Cerebrina lacunata* (Burrows & Holland, 1895); 17: *Lagena annellatrachia* Loeblich & Tappan, 1994; 18: *Lagena annulatacollare* (Loeblich & Tappan, 1994); 19: *Lagena cyrillion* (Loeblich & Tappan, 1994); 20: *Lagena fidicularia* Patterson, 1991; 21: *Lagena substriata* Williamson, 1848; 22: *Procerolagena oceanica* (Albani, 1974); 23: *Reussoolina trachiella* Loeblich & Tappan, 1994; 24: *Guttulina bartschi* Cushman & Ozawa, 1930; 25: *Guttulina yamazaki* Cushman & Ozawa, 1930; 26: *Guttulina regina* (Brady, Parker & Jones, 1870); 27: *Pyrulina angusta* (Egger, 1857); 28: *Laryngosigma afueraensis* McCulloch, 1977; 29: *Favulina hexagoniformis* (McCulloch, 1997); 30: *Oolina caudigera* (Wiesner, 1931); 31: *Fissurina circularis* Todd, 1954; 32: *Glandulina symmetrica* (McCulloch, 1977); 33–34: *Saintclairoides toreuta* Loeblich & Tappan, 1994; 35–36: *Hoeglundina elegans* (d'Orbigny, 1826); 37: *Alliatina variabilis* (Zheng, 1978); 38–39: *Geminospira bradyi* Bermúdez, 1952; 40: *Robertinoides australis* (Collins, 1958); 41: *Robertinoides oceanica* (Cushman & Parker, 1947); 42: *Bolivina robusta* Brady, 1881; 43: *Bolivina striatula* Cushman, 1922; 44: *Bolivinellina translucens* (Phleger & Parker, 1951); 45: *Rugobolivinella elegans* (Parr, 1932); 46: *Globocassidulina subglobosa* (Brady, 1881); 47–48: *Heterocassidulina albida* McCulloch, 1977. – Scale bar is always 100 μm.

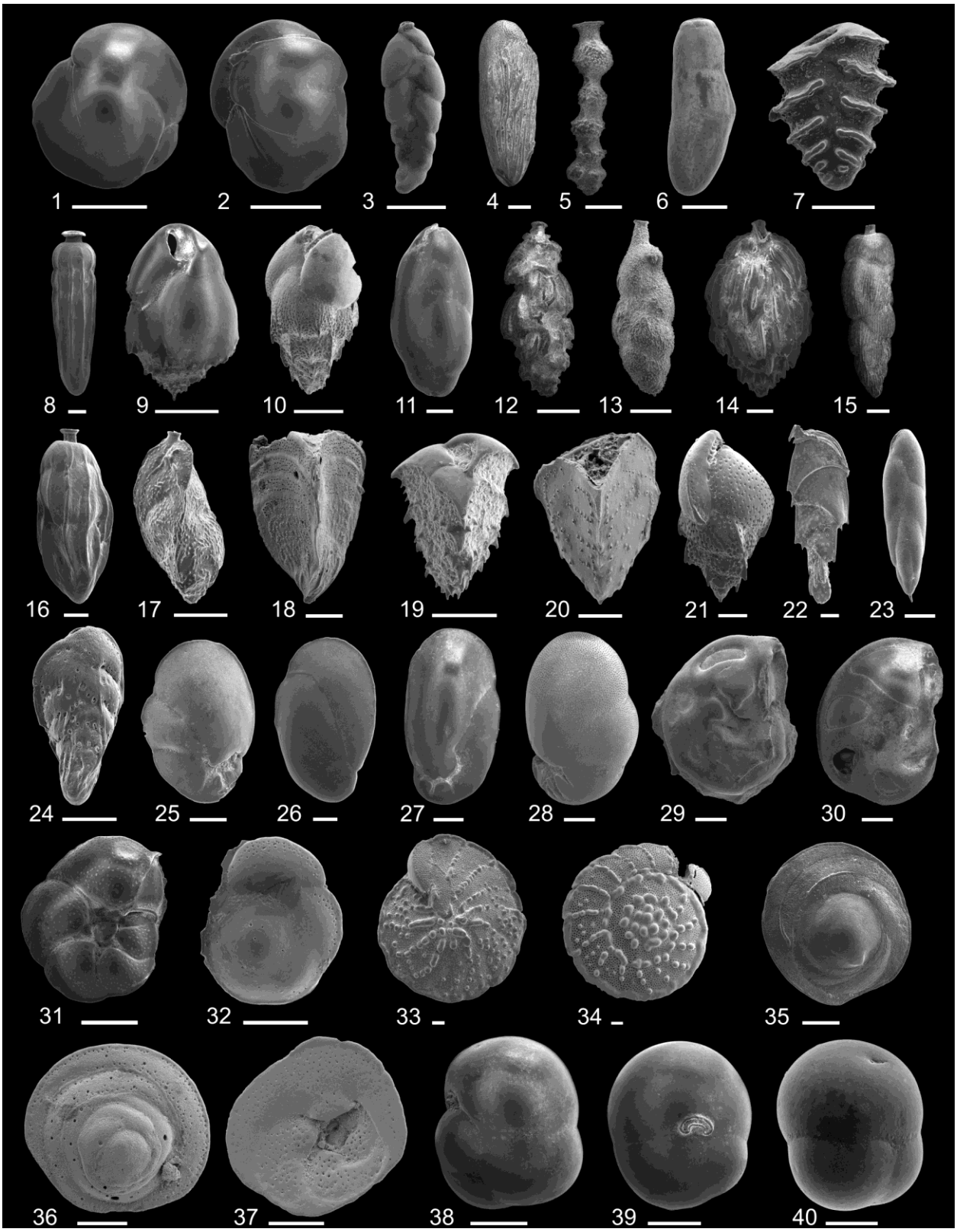
1
2
3
4
5
6
7
8
9
10
11
12
13
14
15
16
17
18
19
20
21
22
23
24
25
26
27
28
29
30
31
32
33
34
35
36
37
38
39
40

Plate 4.4. (previous page) Foraminifera from the Western Australian shelf. 1–2: *Paracassidulina neocarinata* (Thalmann, 1950); 3: *Hopkinsinella glabra* (Millett, 1903); 4: *Loxostomina mayori* (Cushman, 1922); 5: *Stilostomelloides virgula* (Brady, 1879); 6: *Rectobolivina bifrons* (Brady, 1881); 7: *Sagrinella jugosa* (Brady, 1884); 8: *Siphogenerina indica* Leroy, 1941; 9: *Bulimina marginata* d'Orbigny, 1826; 10: *Bulimina subornata* Brady, 1884; 11: *Protoglobobulimina pupoides* (d'Orbigny, 1846); 12: *Siphouvigerina hispida* (Schwager, 1866); 13: *Siphouvigerina porrecta* (Brady, 1879); 14: *Uvigerina peregrina* Cushman, 1923; 15: *Uvigerina reineri* (Belford, 1966); 16: *Uvigerina schwageri* Brady, 1884; 17: *Trifarina bradyi* Cushman, 1923; 18: *Chrysalidinella pacifica* (Uchio, 1952); 19: *Reussella hayasakai* Oki, 1989; 20: *Reussella pulchra* Cushman, 1945; 21: *Mimosina* sp.; 22: *Valvobifarina mackinnonii* (Millett, 1900); 23: *Fursenkoina pauciloculata* (Brady, 1884); 24: *Sigmavirgulina tortuosa* (Brady, 1881); 25–26: *Cancris auriculus* (Fichtel & Moll, 1798); 27: *Cancris oblongus* (Williamson, 1858); 28: *Cancris bubnanensis* (McCulloch, 1977); 29–30: *Stomatorbina concentrica* (Parker & Jones, 1864); 31–31–32: *Rotorbinella* sp.; 33–34: *Neoeponides margaritifer* (Brady, 1881); 35: *Neoconorbina albida* McCulloch, 1977; 36–37: *Neoconorbina neapolitana* Hofker, 1951. 38: *Eusphaeroidina inflata* Ujiié, 1990; 39–40: *Sphaeroidina bulloides* d'Orbigny, 1826 – Scale bar is always 100 μm.

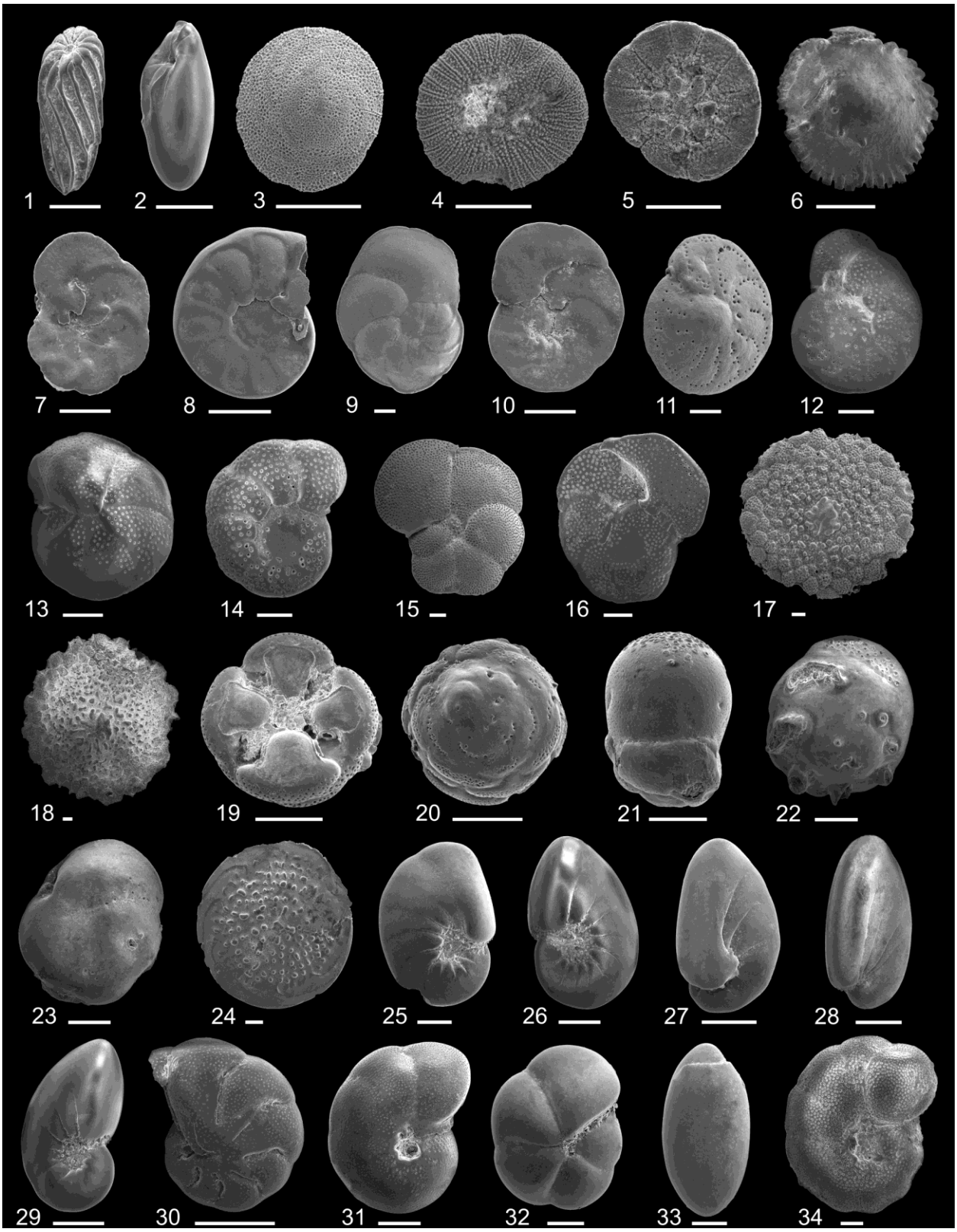
1
2
3
4
5
6
7
8
9
10
11
12
13
14
15
16
17
18
19
20
21
22
23
24
25
26
27
28
29
30
31
32
33
34

Plate 4.5 (previous page). Foraminifera from the Western Australian shelf. 1: *Buliminoides williamsoniana* (Brady, 1881); 2: *Elongobula parallela* (Cushman & Parker, 1931); 3–4: *Pileolina minogasaformis* (Ujiié, 1992); 5: *Pileolina patelliformis* (Brady, 1884); 6: *Siphonina tubulosa* Cushman, 1924; 7: *Planulinoides biconcava* (Parker & Jones, 1862); 8: *Hyalinea florenceae* McCulloch, 1977; 9–10: *Planulina retia* Belford, 1966; 11–12: *Cibicides mabahethi* Said, 1949; 13–14: *Cibicides* cf. *C. refulgens* Montfort, 1808; 15–16: *Caribeanella elatensis* Perelis & Reiss, 1975; 17–18: *Planorbulinella larvata* (Parker & Jones, 1865); 19–21: *Millettiana millettii* (Heron-Allen & Earland, 1915); 22–23: *Asanonella tubulifera* (Heron-Allen & Earland, 1915); 24: *Amphistegina papillosa* Said, 1949; 25–26: *Nonion subturgidum* (Cushman, 1924); 27–28: *Nonionella pulchella* Hada, 1931; 29: *Nonionoides grateloupii* (d'Orbigny, 1839); 30: *Astrononion* sp.; 31: *Melonis barleeanus* (Williamson, 1858); 32: *Pullenia borealis* Saidova, 1975; 33: *Chilostomella ovoidea* Reuss, 1850; 34: *Anomalinoides globulosa* (Chapman & Parr, 1937). – Scale bar is always 100 μm.

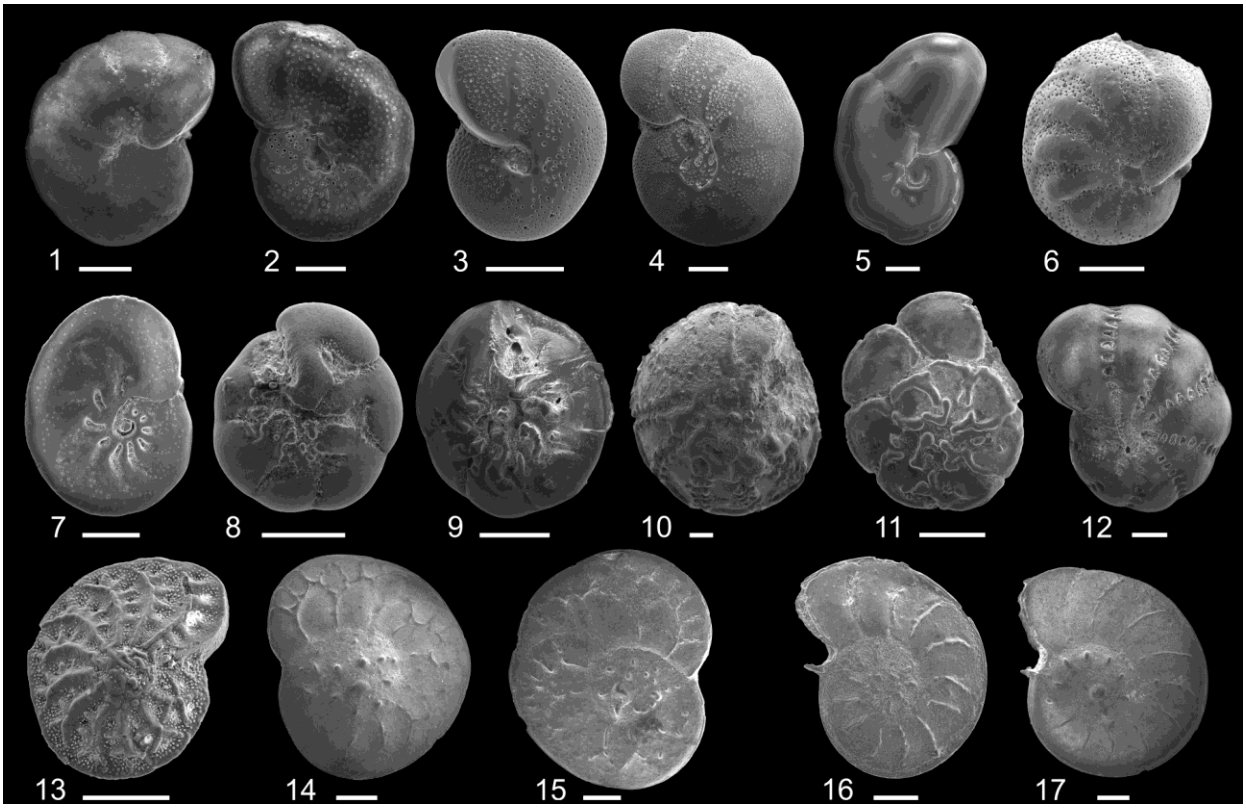

Plate 4.6. Foraminifera from the Western Australian shelf. 1–2: *Anomalinoides colligera* (Chapman & Parr, 1937); 3–4: *Anomalinulla glabrata* (Cushman, 1924); 5: *Mississippina pacifica* Parr, 1950; 6–7: *Hanzawaia nipponica* Asano, 1944; 8: *Ammonia* cf. *A. faceta* He, Hu & Wang, 1965; 9: *Ammonia pustulosa* (Albani & Barbero, 1982); 10–11: *Rotalinoides gaimardi* (d'Orbigny in Fornasini, 1906); 12: *Elphidium lene* Cushman & McCulloch, 1940; 13: *Elphidium macellum* (Fichtel & Moll, 1798), juvenile specimen; 14–15: *Heterostegina depressa* d'Orbigny, 1826; 16–17: *Operculina ammonoides* Sidebottom, 1918. – Scale bar is always 100 µm.

Chapter 5.

Benthic Foraminifera from the Carnarvon Ramp Reveal Variability in Leeuwin Current Activity (Western Australia) since the Pliocene

Abstract

Outer carbonate ramp benthic foraminifera from a ~300 m deep core off Western Australia (International Ocean Discovery Program Core U1460A) were examined to reconstruct the paleoceanographic evolution of the Carnarvon Ramp and the warm surficial Leeuwin Current for the last 3.54 Ma. Of the identified 179 benthic foraminiferal species, the 15 most abundant taxa were studied by means of Q-mode Cluster Analysis and Non-Metric Dimensional Scaling. Diversity, equitability, planktonic/benthic index, microhabitat preference, and sedimentary parameters such as lithology and sponge spicule content were analyzed to gather information about past intermediate- and surface-water circulation. These observations were used to make inferences about past environmental conditions. The co-variance of organic matter supply and oxygen levels affected the distribution of benthic foraminifera. Relative abundances of infaunal species such as *Uvigerina peregrina*, *Lagena annellatrachia*, *Trifarina brady*, and *Bolivina robusta* were applied to indicate episodes of increased organic matter supply to the sea floor. Abundance records of epifaunal species such as *Spirorutilus carinatus*, *Rotorbinella* sp., *Hyalinea florenceae*, and *Hanzawaia nipponica* were used to indicate higher oxygenation and hypoxia at the sediment-seafloor interface.

Below a water depth of 200 m, influence of upwelling was recognized by a high infaunal species ratio, faunal dominance by *U. peregrina* and abundance of *L. annellatrachia* and *T. bradyi*. When the

paleo-Leeuwin Current was established at the sea surface the infaunal ratio was lowered and *U. peregrina*, *T. bradyi*, and *L. annellatrachia* were less abundant. Epifaunal species such as *Hanzawaia nipponica* and *Hyalinea florenceae* gradually became more abundant around 1.14 Ma, which indicates waning of hypoxic conditions. A more substantial change was initiated by 0.91 Ma as marked by key species *Spirorutilus carinatus* and *Rotorbinella* sp. together with faunal diversity and benthic foraminiferal productivity increase. On the outer ramp position (>200 m), the presence of strong bottom currents such as the Leeuwin Undercurrent led to settlement of suspension feeding sponges. Under high-flow conditions of the Leeuwin Current, sponge spicules and skeletal carbonate production reached an optimum at ~0.6 Ma. With the Leeuwin Current flow suppressing upwelling, and an oxygen-rich Leeuwin Undercurrent entering the deep shelf, the environment favored epifaunal agglutinates, rotalids, and miliolids, while buliminids decreased. Supported by this observation we propose the following paleoceanographic evolution of the Carnarvon Ramp:

- Late Pliocene to mid Pleistocene (3.54–0.91 Ma): conditions of deep-water upwelling from the Western Australian Current and Indian Ocean Gyre and absence of the capping Leeuwin Current on the outer carbonate ramp.
- A transitional phase in the mid Pleistocene (1.14–0.61 Ma): waning surface productivity despite falling sea levels during amplified glacio-eustatic cycles. The paleo-Leeuwin Current triggered gradual oxygenation at the sediment-water interface.
- From mid Pleistocene to present (0.91–0 Ma): The Leeuwin Current reached modern intensity and flow rates increased until they peaked at ~0.6 Ma. Benthic foraminiferal productivity reached a high until they decreased again to present-day rates. Temporarily, sea surface productivity was moderately enhanced in this period, likely due to fluctuating Leeuwin Current persistence or landward shift during more intense glacials.

Introduction

Oceanographic currents are influenced by climatic conditions, global temperature gradients, sea-level elevation, tectonics and shelf-slope structure (Tomczak and Godfrey, 2003). Unravelling these interactions requires proxies that can respond independently and collectively to these drivers and their influence on currents (Gooday, 2003; van Sebille et al., 2015; Christensen et al., 2017). Benthic foraminifera are among the most abundant and ubiquitous organisms in marine sediments and are widely used as proxies to help to understand paleoceanographic conditions thanks to their preservation potential (van der Zwaan et al., 1999). Key species and assemblages have the potential to be used as indicators for various environmental parameters in shallow-water and deep-water paleoceanographic studies (Schnitker, 1974; Corliss, 1979; Haig, 1997; Mamo et al., 2013). Microfaunas can be influenced by a variety of parameters such as oxygen, gradients in light, temperature, salinity, organic matter, substrate, water masses, and velocity and turbulence of surface-water currents (Gooday, 2003; Hohenegger, 2005; Fellowes et al., 2017). Assemblage variability reflects habitat shifts (Gallagher et al., 2009; Langer and Mouanga, 2016), extinctions (Mateo et al., 2017), stress factors (Quilty and Hosie, 2006), and inter-species competition (Debenay et al., 2009). Furthermore, previous workers suggest that benthic assemblages can be associated with processes occurring at the surface of the ocean (e.g., surface currents, upwelling) and respond to changes in environmental conditions (Smith, 1992; Gooday, 2003; Murray, 2006; Murgese and De Deckker, 2007).

Benthic foraminifera have recently been investigated from a number of eastern Indian Ocean and Western Australia (WA) locations, from shallow waters to the deep sea. Western Australian bays, reefs, and seagrass meadows have in recent time been studied by Haig (1997), Li et al. (1999), Orpin et al. (1999), Semeniuk (2001), Parker (2009), and May et al. (2016). Deep-sea records from the waters off WA have been subject to examination by a number of workers primarily for taxonomy and to reconstruct sea-surface temperatures and productivity (Corliss, 1979; McCorkle et al., 1994; Wells et al., 1994; Wells and

Wells, 1994; Rai and Singh, 2001; Holbourn et al., 2005; Murgese and De Deckker, 2005, 2007; Spooner et al., 2011). However, middle- to outer-shelf environments have received relatively little attention; studies focusing on such areas came from Betjeman (1969), Mays (2007), Buckley (2016), and Haller et al. (in review) (Chapter 4).

In August and September 2015, six sites (U1458–U1464) were drilled by the International Ocean Discovery Program JOIDES Resolution on Expedition 356 (Perth to Darwin) along the Western Australian shelf edge on a transect from 29°S to 18°S. The expedition aimed at recovering sediment to understand the history of the Australian monsoon and its variability, the development of aridity on the Australian continent, and constraining the vertical motions caused by the northward subduction of the Australian continental plate (Gallagher et al., 2012).

The goal of this study was to contribute to understanding oceanographic circulation on the Carnarvon Ramp and the variability and interaction between the Leeuwin Current (LC) and the Western Australian Current during the late Neogene and Quaternary. To provide data on foraminiferal assemblages, this study examined Core U1460A, a 300.1 m long sediment record obtained from the Carnarvon Ramp, north Perth Basin (Fig. 5.1). The first objective was to taxonomically inventory the benthic foraminiferal species and document the relative abundances across the entire 300.1 m. The second objective was to interpret the depositional environments associated with these abundances. The results provide new insights into the long-term development of the shelf and complement previous deep-water circulation studies that involve paleoenvironmental reconstructions of current activity, nutrient flux, and oxygenation at the sediment-water interface.

Regional Setting

Oceanography

Circulation in the Indian Ocean is complex with interactions among various water masses (Fig. 5.1; Tomczak and Godfrey, 2003). The eastern region is dominated by the effects of the Indonesian Throughflow ITF, which connects the Indo-Pacific Warm Pool (~28°C) with the Indian Ocean and the Western Australian shelf (Wyrtki, 1987; Potemra, 2005). The warm water facilitates the growth of the Ningaloo Reef (Collins et al., 2003), Houtman Abrolhos Reef Complex (Collins et al., 1998), and larger benthic foraminifera (Gallagher et al., 2009). While travelling through the Indonesian Archipelago, water masses of the ITF become less saline and interact with the eastern part of the Indian Ocean gyre to form a frontal system when meeting the South Indian Central Water. Part of the ITF is absorbed in the swiftly flowing South Equatorial Current (SEC), which is driven by southeast trade winds between 5°S and 15°S (Wyrtki, 1973). Another part is incorporated into the LC flowing south.

Leeuwin Current

The Leeuwin Current is a well-studied natural phenomenon of the south-eastern Indian Ocean (Cresswell, 1991; Smith et al., 1991; Waite et al., 2007) essential for poleward heat transport in the Indian Ocean (Karas et al., 2011). Compared to other locations in the southern hemisphere, the LC is an anomalous eastern boundary current displacing the cold Western Australian Current westward towards the open Indian Ocean (Fig. 5.1a). At its starting point, the LC is believed to be fed by the tropical ITF, the South Java Current (SJC), and the subtropical waters of the Eastern Gyral Current (EGC) (Wijffels et al., 2002). The warm-water influence extends along the WA shelf edge from the North West Cape down to Cape Leeuwin at the south-western tip of WA. The LC extends 100–200 m deep and follows a path along the shelf edge, transporting an annual mean ~3.4 Sverdrup (Feng et al., 2003). The LC is seasonally variable, being stronger during the austral winter due to a steepened alongshore pressure gradient and slacking equatorward winds (Feng et al., 2003). In summer, geostrophic dynamics of the LC are offset by

wind-generated countercurrents (the Ningaloo and Capes Currents) that flow equatorward (Hanson et al., 2005). Furthermore, the current is also strongly influenced by ENSO (El Niño Southern Oscillation), gaining intensity during La Niña years and weakening during El Niño years. In winters during La Niña climate phases, coinciding with the relaxation of the westerlies, the LC can extend as far as the west coast of Tasmania (De Deckker et al., 2012). The low-salinity nature of the LC makes it buoyant and prevents the West Australian Current (WAC; sometimes called South Indian Current) from reaching the surface through coastal wind stress and Ekman transport. Without the LC, an upwelling system would exist (Reason et al., 1999), as is common along other eastern boundaries such as the coasts of Chile/Peru (Humboldt Current) and Namibia (Benguela Current). The LC sits on top of the equatorward flowing Leeuwin Undercurrent (LUC; Thompson, 1984), which is part of the broader WAC and delivers South Indian Central Waters high in salinity and oxygen from below the shelf edge (Cresswell, 1991).

Paleoceanographic Evolution

Most paleoceanographic studies along the WA coast have focused on developments since the latest Pleistocene, including the last glaciations and the Last Glacial Maximum (LGM). Various studies (Wells and Wells, 1994; De Deckker, 1997; Martínez et al., 1999) concur that the reduced ITF and lower sea-levels would have re-directed the ITF into the SEC and/or SJC and thus enhancing these systems at the cost of reducing the LC strength. Furthermore, several authors who analyzed sediment facies (James et al., 1999) and microfossil assemblages (Wells and Wells, 1994; Okada and Wells, 1997; Takahashi and Okada, 2000; Barrows and Juggins, 2005) have suggested that the WAC was the dominant water mass on the shelf during glacial periods, thus reducing the influence of the LC. Takahashi and Okada (2000) studied calcareous nannofossils from three cores, finding evidence for the absence of warm LC waters during the LGM at 24°S (near Shark Bay). Using radiolaria as a temperature proxy, Rogers and De Deckker (2007) concluded that the LC was probably not flowing south of 20°S (Barrow Island) during the LGM. Other sea surface temperature reconstructions by Barrows and Juggins (2005), Spooner et al. (2011) and Wells and Wells (1994) came to similar conclusions, however their sea-surface temperature

reconstructions found temperatures common for the LC all the way to 32°S (Perth). These studies suggest, that as the LC thinned and the ITF/SICW front shifted 3–4° equatorward, the cooler waters of the WAC entered the region. Furthermore, Gingele et al. (2001) analyzed clay minerals from cores in the Northwest Shelf region and suggested decreased flow volume of the ITF during the LGM because less kaolinite and chlorite reached the Indonesian Gateway from the Banda Sea.

In the light of a strengthened WAC during glacial periods, there is some evidence for upwelling of nutrient-rich waters along the WA coastline, which requires the LC to be absent (McCorkle et al., 1994; Wells et al., 1994; Okada and Wells, 1997; Sinha et al., 2006). However, other authors don't see enough evidence for intense sea surface productivity. For example, Veeh et al. (2000) found in their cores from the Perth Basin and Exmouth Plateau, based on isotope-derived mass accumulation rates, little evidence for surface productivity resembling Peru/Chile or Namibia during the LGM and argued for the continued presence of the LC. Conversely, during warm interglacial periods, the LC was most likely warmer, deeper, and stronger, especially during the marine isotope stage 11 (~400 ka; Spooner et al., 2011). Expansion of subtropical faunas such as zooxanthellate corals, which require minimum temperatures of 14°C to survive, have been used to indicate enhanced LC reaching the Houtman Abrolhos Reef Complex (James et al., 1999; Collins et al., 2003; Greenstein and Pandolfi, 2008). Gallagher et al. (2009) showed that temperature sensitive shelfal benthic foraminiferal species (*Asterorotalia* spp., *Pseudorotalia* spp., and *Heterolepa margaritiferus*) migrated from the southwest Pacific to the Western Australian shelf during periods of expanded influence of the ITF. Kendrick et al. (1991) found the subtropical estuarine arcoid bivalve *Anadara trapezia* in marine isotope stages 5 (~130 ka) and 7 (~243 ka) in the Perth and Carnarvon basins, where it is now extinct.

In addition to glacial/interglacial cycles, the ITF volume is also moderated by the size of the Indo-Pacific Warm Pool and tectonic configuration, that is, the width of waterways in the Indonesian archipelago (Molnar and Cronin, 2015). Jian et al. (2006) suggested that the abundance of deep-dwelling planktonic foraminifera in the South China Sea provided evidence for a proto-Indo Pacific Warm Pool present in late Miocene (11.5–10.6 Ma), with a modern extension developing around 4.0–3.2 Ma.

Furthermore, Karas et al. (2011) used comparisons between the Mg/Ca and stable isotope data from two drilled cores on the western and eastern sides of the Indian Ocean to suggest ITF restriction from 3.5–3.0 Ma that caused ~3°C cooling in the region.

The onset of the LC was estimated by various workers across a relatively wide range of time. McGowran et al. (1997) compiled a broad suite of organic biomarkers and fossil faunas to suggest that the LC has flowed since the late Eocene (~40 Ma). Kendrick et al. (1991), in contrast, used fossil bivalves to suggest the onset occurred <500 kyrs ago. Sinha et al. (2006) and Karas et al. (2011) proposed onset at 2.5 Ma, whereas Gallagher et al. (2014) related reef growth and expansion on the Northwest Australian Shelf to conclude that the 'modern' LC is younger than 1 Ma.

Material and Methods

Sample Collection and Analysis

The core U1460A was drilled during the International Ocean Discovery Program Expedition 356 'Indonesian Throughflow' by the JOIDES Resolution in August 2015 as one of two replicate cores at Site U1460. The core was obtained from coordinates 27°22.4949′S, 112°55.4296′E at 214.5 m water depth (Fig. 5.1). The coring device was the Half-Length Advanced Piston Corer (4.7 m barrel length; HLAPC) throughout to a total penetration depth of 300.1 m. Utilized depth scale was 'Core depth below Sea Floor-A' (CSF-A), which measures distance from sea floor to target within recovered core and does not take incomplete recovery or core expansion into account (IODP-MI, 2011). The core was split, logged, and sampled during Expedition 356 (Gallagher et al., 2017b). A 10 cm^3 aliquot of every second core catcher (CC), in-section samples, and the two mudline samples (core top) from U1460A and U1460B were obtained for post-expedition analysis. Lithified samples were gently broken by hand and then boiled on a hotplate in 30% H_2O_2 solution until the reaction faded in order to remove carbonate coatings (partial lithification). The loosened samples were subsequently washed through 63 μm and 850 μm mesh sieves and rinsed for mud removal. After drying at 50°C, samples were dry-sieved at 125 μm. Cross

contamination was avoided by ultrasonic-cleaning of sieves between samples. All samples (>125 μm fraction) were picked for benthic foraminifera with >300 specimens per sample (Appendix D1). Taxa were counted and identified using a range of taxonomic atlases (Haig, 1993; Loeblich and Tappan, 1994; Haig, 1997; Hayward et al., 1999; Parker, 2009; Hayward et al., 2010; Debenay, 2012) (Appendix D2). Additionally, the percentages of planktonic and benthic taxa (P/B ratio) were recorded with counts of >300 specimens (Berger and Diester-Haass, 1988; van der Zwaan et al., 1990). Tests were distinguished as planktonic spinose, planktonic keeled (deep-dwelling planktonic species), and benthic specimens.

Cluster Analysis, Non-Metric Multidimensional Scaling, and Diversity Measures

Assemblages were discriminated with cluster analysis (Q-mode, samples) and Non-metric Multidimensional Scaling (NMDS). Relative abundances were transformed with the arcsine of the square root and analyses performed in PAST version 3.15 (Hammer et al., 2001). The Bray-Curtis Similarity Index (Bray and Curtis, 1957), which was designed to assess ecological abundances, was used in both statistical tests. Cluster analysis assumes a minimum of two clusters and produces a dendrogram with branches between samples at discrete similarity levels. Cluster analysis has been applied successfully many times in micropaleontological studies (Murray, 2006). Since it is not clear if the minimum amount of clusters actually occurred in nature, cluster analysis was supplemented with NMDS. The NMDS algorithm places data points in a two-dimensional coordinate system such that ranked differences are preserved and provides additional support for taxonomic results and assemblages recognized.

The Fisher α and Shannon-Wiener indices were calculated to measure species diversity from Site U1460 samples. Fisher α index takes into account the number of taxa (S) and the number of individuals (n) of a sample to give a standardized value (α) of diversity regardless of counted individuals in a given sample (Fisher et al., 1943; Murray, 2006). The Shannon-Wiener index measures diversity by giving less abundant species a proportionally lower influence and more abundant ones more influence, and thus provides a more accurate representation of abundance and composition. Effectively, a sample of equally abundant taxa will score the highest (Shannon, 1948).

Application of Shipboard Data

The lithology of U1460 sediments recovered during IODP Expedition 356 was determined using macroscopic visual core descriptions (Gallagher et al., 2017a). Carbonate naming classification follows the texture classification of Dunham (1962). Disturbances of the regular sedimentation were noted and described in detail. By means of smear-slide microscopy, biogenic fragment abundance such as sponge spicules were recorded. These data can be obtained online from the IODP LIMS Reports portal (http://web.iodp.tamu.edu/LORE).

The shipboard biostratigraphic survey throughout Core U1460A was conducted based on core catcher (CC) samples (Gallagher et al., 2017b). Calcareous nannofossil and planktonic foraminifera assemblages were identified and occurrences calibrated to the ages of bioevents from the Geologic Time Scale 2012 (Gradstein et al., 2012). For calcareous nannofossils, the biozonation scheme of Martini (1971) was used to report on the Neogene (NN code). The planktonic foraminifer zonation schemes of Berggren et al. (1995), as modified by Wade et al. (2011), were used for foraminiferal bioevents (Table 5.1).

Results

Sedimentology

Sediments from Core U1460A yielded a complete stratigraphic succession (recovery = 97.1%) and are composed of greenish silt with bioclasts, varying degrees of dolomitization, authigenic glauconite mineralization, carbonate hardgrounds, and in intervals, abundance sponge-spicule fragments (Gallagher et al., 2017b). The lithology of Core U1460A can be divided into two larger units: the upper Unit I 0–252.7 m CSF-A, and the lower Unit II 252.7–300.1 m CSF-A (Fig. 5.2). Unit I consists of predominantly unlithified to partially lithified skeletal packstone with wackestone and grainstone intervals, and was subdivided in three subunits (Gallagher et al., 2017b). The top interval of Unit I is beige to greenish-gray in colour and dominated by macrofossil content (0.0–44.9 m CSF-A) indicating hemipelagic to neritic

conditions. The middle part shows higher concentrations of sponge spicules (44.9–174.5 m CSF-A), which indicates a hemipelagic setting. The lower part of Unit I is dominated by authigenic glauconite, increased dolomite, and macrofossils (174.5–252.7 m CSF-A; Gallagher et al., 2017c). The three subunits are separated by hardground-lithified grainstone layers similar in composition with high natural gamma radiation values likely caused by subaerial exposure. Planktonic foraminifera and calcareous nannofossils date Unit I to the Holocene (very thin top >2.13 m) and mostly Pleistocene age (Fig. 5.2). Unit II is defined by occurrence of mass-wasting deposits, graded or contorted beds, slumped sediments, debris flows, and turbidity currents (252.7–300.1 m CSF-A). The sharp contact between Unit I and II is inclined, separating unlithified homogeneous cream-colored packstone from greenish glauconite-rich sandy packstone of Unit I. The mass-wasting deposits contain angular grains and recumbent fold structures and were interpreted by Gallagher et al. (2017b) to be hemipelagic to pelagic in origin. Biostratigraphic fossils indicate Unit II to be of early Pleistocene to late Pliocene (~2.5–3.5 Ma; Fig. 5.2). The allochthonous nature of the mass wasting deposits makes origin of fossils, biostratigraphic datums, sedimentation rates, and environmental interpretations uncertain due to mixing and gravitational displacement (Figs. 5.2 and 5.3). According to McCormack and McClay (2013), slope over-steepening and possible distal seismicity from Australia's northern subduction boundary may be potential triggering mechanisms for the mass wasting deposits, of which a similar complex in the Pliocene to Pleistocene was found in seismic studies on the Gorgon Platform (Exmouth Plateau) north of the Carnarvon Ramp.

Overall modelled sedimentation trends from late Pliocene to the present indicate that the core received high sedimentation rates most of the time (Fig. 5.3). In the mass-wasting deposits between total depth and 252.7 m CSF-A, sedimentation rates were calculated separately for calcareous nannofossils and planktonic foraminifers, where the fossil datums are not in concordance and are most likely skewed. The first datum both fossil groups agree upon is 1.6 Ma: Top *Calcidiscus macintyrei* (Table 5.1). The short core length between 1.6 Ma and 1.14 Ma (194.99–176.24 m CSF-A) indicates that this early Pleistocene interval received relatively low sediment input of 4 cm/ky. At 1.14 Ma (176.25–128.88 m CSF-A) there was a relatively large increase to 21 cm/ky and then remained stable at 14 cm/ky between 0.91 and 0.61

Ma (128.88–86.59 m CSF-A). The late Pleistocene was first marked by a large increase in sedimentation rate to 39 cm/ky between 0.61 and 0.44 Ma (86.59–20.65 m CSF-A) and then a decreased to 12 cm/ky between 0.44 and 0.29 Ma (20.65–2.13 m CSF-A).

Foraminiferal Analysis

To produce biodiversity and relative abundance data, a total of 13,992 specimens from 35 samples were picked, identified and counted from mudline, core catcher, and other in-section samples. On average, a sample was analyzed every 8.8 m downcore from present sea floor down to a depth of 300.0 m CSF-A (see Appendix D1). Ages of the faunas can be constrained by eight biostratigraphic datums (planktonic foraminifera and calcareous nannoplankton) established earlier on core catcher material (Table 5.1; Gallagher et al., 2017b).

In the whole dataset, a total of 179 benthic foraminieral taxa were recorded, of which 15 species sufficiently abundant (>200 specimens or >1.5% of all foraminifera throughout Core U1460A samples) to provide enough explanatory power for discussion. Highest diversity was found in the mudline sample U1460B (93 species) where preservation was excellent. The ewest species were found in U1460A 31F CC (143.0 m CSF-A), which had moderate preservation.

Cibicides cf. *C. refulgens* Montfort, 1808 was the most abundant species throughout the core and, in 10 out of 35, samples the most abundant species (Fig. 5.2). However, nine out of these ten samples were above 133.8 m CSF-A and one sample was at 265.3 m CSF-A. *Cibicides* cf. *C. refulgens* was present in every sample of the core and reached its peak abundance at 30.1 m CSF-A, representing 28.5% of specimens counted between 0.44 and 0.61 Ma. In the lower 157 m of the core, *Trifarina bradyi* Cushman, 1923 was the most abundant taxon in most samples and second most abundant species in the census. When *T. bradyi* abruptly decreased at 143.04 m CSF-A, *Cibicides* cf. *C. refulgens* became the dominant taxon in the upper section between 0.91 Ma and present.

There were 13 other taxa of benthic foraminifera that were significantly frequent. These taxa included (in decreasing abundance): *Hyalinea florenceae* McCulloch, 1977, *Hanzawaia nipponica* Asano,

1944, *Uvigerina peregrina* Cushman, 1923, *Anomalinulla glabrata* (Cushman, 1924), *Bolivina robusta* (Brady, 1881), *Globocassidulina subglobosa* (Brady, 1881), *Cibicidoides mundula* (Brady, Parker & Jones, 1888), *Sigmavirgulina tortuosa* (Brady, 1881), *Bolivina striatula* Cushman, 1922, *Paracassidulina neocarinata* (Thalmann, 1950), *Lagena annellatrachia* Loeblich & Tappan, 1994, *Spirorutilus carinatus* (d'Orbigny, 1846), and *Rotorbinella* sp.

Foraminiferal microhabitat preference for infaunal lifestyle ranged between 21% (30.1 m CSF-A) and 73% (190.1 m CSF-A), presenting a steady trend upsection from infaunal to epifaunal. Foraminiferal results show two distinctly different foraminiferal assemblages within U1460A, including fluctuating indicator taxa within the assemblages. The lower half of the core was dominated by rotalids, lagenids, and buliminids (Appendix D3). In the upper half, rotalids, textulariids, miliolids and other minor taxa increased in relative abundance, while buliminids and lagenids decreased.

Taphonomy

Partial loss of specimens can be attributed to post-depositional dolomitization (encrustation) in the lower section (Gallagher et al., 2017b). Except for the mudline samples (core top), varying degrees of abrasion, bioerosion, and glauconite infill were observed. Damage to the tests was interpreted to be caused by current transportation, corrosion, and drilling predation that obscured morphology, making identification problematic in some intervals. Nevertheless, the data overall indicated that the census results represent a reliable fossil record of the benthic foraminiferal variability.

Statistical Analyses and Diversity

Cluster analysis and NMDS (Bray-Curtis similarity) on abundance data both revealed two distinct assemblages (Foraminiferal Assemblage 1 and 2) (Fig. 5.5). The older assemblage from the bottom half core interval (FA1; 300.0–143.0 m CSF-A) was distinct from the assemblage in the overlying younger core samples (FA2, 133.8–0.0 m CSF-A). The NMDS discriminated between FA1 and FA2 mainly on axis 1. However, NMDS axis 2 correlated with a third assemblage spanning the transition from FA1 to

FA2 (171.5–96.3 m CSF-A; Fig. 5.4). This Transitional Assemblage was difficult to delineate in the NMDS graph (Fig. 5.5b) likely because the assemblage composition did not considerably change at this interval, rather the fluctuating abundance of specific key taxa (*Hanzawaia nipponica* and *Hyalinea florenceae*) indicated changes in sea floor conditions.

Fisher α and the Shannon-Wiener H index were calculated for all processed samples (Fig. 5.4; Appendix D1). Fisher α values ranged from 9.1 (143.0 m CSF-A) to 24.7 (U1460B mudline) showing that diversity increased toward the modern sediment surface. Shannon-Wiener values ranged from 2.3 (190.1 m CSF-A) to 3.7 (U1460B mudline), indicating some horizons are more strongly dominated by few species and were characterized by a lower evenness than other horizons, where assemblages were more evenly distributed.

Foraminiferal Assemblage 1 (FA1)

Foraminiferal Assemblage 1 was found in the bottom part of U1460A, from the lowest sample at 300.0 m CSF-A to 143.0 m CSF-A. Most dominant were *Uvigerina peregrina*, *Lagena annellatrachia*, and *Trifarina bradyi*. Low species evenness (Fig. 5.4) seems to be associated with the dominance of *U. peregrina* and *T. bradyi* in several horizons of this assemblage. The section had intervals where these taxa made up more than 50% of the benthic specimens (Fig. 5.6). Planktonic tests dominated the sediment, while the benthic fraction was dominated by taxa preferring infaunal habitats (Figs. 5.4). Diversity in FA1 was low compared to other samples: Fisher α values for FA1 ranged from 9.1 (143.0 m CSF-A) to 14.1 (293.3 and 171.5 m CSF-A) with an average value of 11.6. The Shannon-Wiener index ranged from 2.3 (190.1 m CSF-A) to 3.2 (300.0 m CSF-A) with an average of 2.7.

Transitional Foraminiferal Assemblage

The Transitional Foraminiferal Assemblage (Transitional FA) was first recognized at 171.5 m CSF-A and is a subset of taxa overlapping FA1 and FA2. The overall diversity in the

interval was closely related to fluctuations of epifaunal taxa (see Fig. 5.4). The shift occurs where *Hanzawaia nipponica* and *Hyalinea florenceae* sharply increased in abundance (14–29%, average 22%). *Uvigerina peregrina* and *T. bradyi* were always present, although in successively smaller numbers.

Foraminiferal Assemblage 2 (FA2)

This assemblage occurred within the upper part of U1460A between 133.8 m CSF-A and the core top (mudline) with *Spirorutilus carinatus*, *Rotorbinella* sp., and *Bolivina robusta* as the dominant species group (Figs. 5.2 and 5.4). However, *U. peregrina*, *L. annellatrachia*, and *T. bradyi* were still present, reaching up to 9% (Fig. 5.6a). Despite this assemblage being characterized by fewer infaunal taxa than older assemblages (21–60%, average 33%; Figs. 5.4 and 5.6b), *B. robusta* peaked three times (67.6, 77.0, 11.3 m CSF-A). Agglutinated taxa became abundant from 124.55 m CSF-A and higher, and miliolids first appeared at the horizon at 86.5 m CSF-A (Appendix D3). Fisher α values in FA2 range from 10.3 (2.1 m CSF-A) to 24.7 (U1460B mudline) with an average of 15.5. Species richness increased rapidly upward and peaked in the mudline samples. Shannon-Wiener values ranged from 2.7 (30.1 and 96.3 m CSF-A) to 3.7 (U1460B mudline), with an average of 3.1.

Discussion

Biodiversity, abundance patterns, and morphogroups of benthic foraminiferal assemblages can be utilized as proxies for measuring and interpreting (paleo-)environmental variability (e.g., Mamo et al., 2013). When infaunal taxa such as *Uvigerina* dominated the assemblage (Fig. 5.6), this indicated increased organic matter flux from the surface to the seafloor, and bottom water hypoxia (Schnitker, 1974; Gupta and Srinivasan, 1990, 1992; Wells et al., 1994; Rai and Singh, 2001; Murgese and De Deckker, 2007). Varying oxygen levels at the sea floor and in the upper centimeters of the sediment can

be inferred by the abundance of infaunal and stress tolerant species such as *T. bradyi* and *U. peregrina*. Suboxic to anoxic conditions at the sediment-water interface are caused by elevated respiration of bacteria, which feed on organic matter (Gooday, 2003). *Uvigerina peregrina* and other taxa have been reported to increase in these conditions (e.g., Wells et al., 1994). For this established relationship in the region, benthic foraminiferal assemblages in U1460A can be used to estimate paleoenvironmental conditions over the last ~3.54 million years on the Carnarvon Ramp.

Environmental Conditions Foraminiferal Assemblage 1

FA1 spans roughly late Pliocene to mid Pleistocene (3.54 to 0.91 Ma). This interval was characterized by continuous high relative abundance of infaunal species (average 60%), particularly the key species *U. peregrina*, *T. bradyi*, and *L. annellatrachia* (Fig. 5.4). These three increased in abundance in several pulses and were especially abundant in low-diversity environments (combined up to 53%; Fig. 5.6a). Above 133.8 m CSF-A, the combined species abundance of this group dropped to an average of 4%.

Infaunal morphotypes tend to dominate in high productivity areas (Corliss and Chen, 1988), which reflects abundance of organic matter within the sediment (van der Zwaan et al., 1999). Some deep infaunal species are known to tolerate anoxic conditions, feed on refractory organic matter, and are linked to vertical redox fronts in the sediment (Jorissen, 1999).

Uvigerina peregrina is a shallow infaunal species encountered in food- and bacteria-rich sediments between water depths of 100 m (shelf) and 4,500 m (abyssal; Fontanier et al., 2002; Murray, 2006). This species is also relatively tolerant of dysoxic conditions and a wide variety of eutrophic settings where organic flux exported to the seafloor is at least 2.5g C/m^2/yr (Altenbach et al., 1999; Fontanier et al., 2002).

Trifarina bradyi is like *U. peregrina*; a cosmopolitan, shallow-infaunal taxon found between 100 and 1000 m depth (Hayward et al., 2010), with a facultative anaerobic life-style (Sen Gupta et al., 1997). However, *T. bradyi* maintained a more steady relative abundance than *U. peregrina* across FA1, which

might be related to different tolerances for hypoxia. *Uvigerina peregrina* dominated the benthic fauna at intervals that might reflect a labile organic-matter flux events (Gooday et al., 2010; Gooday and Jorissen, 2012).

Lagena annellatrachia is a shallow-to-deep infaunal species first described by Loeblich and Tappan (1994) from the Sahul Shelf. Maximum observed abundance in FA1 was 9%. Lagenids are found at almost all water depths (inner shelf to lower abyssal). However, Hayward et al. (2010) found that, in New Zealand, relative abundance of the genus seldom ranged above 2% at any water depth. Deep infaunal taxa are typical for mesotrophic to eutrophic environments where insufficient oxygen is present for organic matter to be fully metabolized at the sediment-water interface. Higher abundance of deep infaunal taxa such as *Lagena annellatrachia* is an indicator for effective burial of refractory phytodetritus during prevailing anoxic conditions in bottom waters and sediment (Jorissen, 1999; Kaiho, 1999).

Stress-tolerant taxa such as *U. peregrina*, *T. bradyi*, and *L. annellatrachia* are adapted to increased supply of labile organic matter and therefore provide a useful proxy for areas that receive a strong and relatively continuous input of organic matter, usually derived from intense primary production associated with upwelling, hydrographic fronts, or riverine input (De Rijk et al., 2000; Gooday, 2003). A number of deep-sea benthic foraminiferal studies have concluded that the quantity and quality of organic carbon flux to the seafloor are the most significant factors influencing benthic foraminiferal assemblage composition and distribution (Loubere, 1991; Schmiedl et al., 1997; Gooday and Hughes, 2002). Water depth and planktonic ratio might be subordinate environmental factors, since organic matter is consumed as it sinks and becomes scarcer at greater depths (De Rijk et al., 2000), and benthic foraminiferal accumulation rate might increase as water depth and planktonic foraminiferal test input remain steady (Gooday, 2003).

Wells et al. (1994)'s and Rai and Singh (2001)'s studies of Western Australian bathyal assemblages also documented low-diversity assemblages of uvigerinids with high species dominance similar to that of FA1. The species composition of FA1 may be driven by a combination of environmental variables, comprising sea-surface productivity, hypoxia at the sea bottom, and conditions associated with

glacial/interglacial cycles. The LC, as an upwelling inhibitor, appeared to play a subordinate role at Site U1460 during this interval.

Environmental Conditions Transitional FA

The Transitional Foraminiferal Assemblage between 1.14 and 0.61 Ma (mid Pleistocene) is especially interesting because it preceded the more prominent shift toward epifaunal taxa of FA2. The fluctuation was more subtle and was only revealed by NMDS axis 2 scores. Within this horizon, key infaunal species decreased, while abundances of *Hanzawaia nipponica* and *Hyalinea florenceae* increased. Both of these species are epifaunal calcareous (plano-convex trochospiral), which are relatively intolerant of dysoxic conditions and feed largely on labile particular organic matter (Corliss and Chen, 1988; Gooday, 2003). This change indicates a gradual environmental regime rearrangement with an onset before the relatively rapid end of FA1.

Hanzawaia nipponica was reported by Van Marle (1988) from the middle shelf to upper bathyal (60–400 m) and mainly at intermediate oxygen contents (2.3–2.7 ml/l).

Hyalinea florenceae is a taxon previously documented from the WA shelf (Van Marle, 1988; Gallagher et al., 2009) and Timor/Java shelves (Murgese and De Deckker, 2005). The sister species, *H. balthica*, has been found to prefer well-oxygenated conditions (den Dulk et al., 1998) though temporarily tolerating low levels of oxygen and seasonal stratification (Nordberg et al., 2000) and is a useful indicator for intermittent low oxygenation bottom waters.

Environmental Conditions Foraminiferal Assemblage 2

Foraminiferal Assemblage 2 is represented in the upper core half, spanning roughly mid Pleistocene (0.91 Ma) to recent. This interval is characterized by a lower abundance of infaunal taxa (average 33%), higher Fisher α, and benthic increasing over planktonic foraminifera (Fig. 5.4). Key environmental taxa in FA2 are *Spirorutilus carinatus*, *Rotorbinella* sp., and *Bolivina robusta*. *Spirorutilus carinatus* and *Rotorbinella* sp. are both epifaunal species indicating a change towards more oligotrophic

conditions (e.g., Gooday, 2003; Murgese and De Deckker, 2007). *Bolivina robusta* in contrast is a high organic flux infaunal taxon, becoming more numerous twice in FA2 (67.6 and 11.3 m CSF-A; Fig. 5.2).

Spirorutilus carinatus is an epifaunal agglutinated species especially common in the Indian and Pacific Oceans(Loeblich and Tappan, 1994; Lei and Li, 2016). The keeled biserial morphology of *S. carinatus* belongs to morphogroup M2c of agglutinated foraminifera, which is common in shallow-marine environments on the shelf (Kaminski and Gradstein, 2005). Haller et al. (in review) (Chapter 4) found *S. carinatus* to be more common on the Carnarvon Ramp than the Northwest Shelf of Australia, likely influenced by oxygen-rich water masses bathing the Carnarvon Ramp.

Rotorbinella sp. is a plano-convex trochospiral species that has been found in the Ningaloo Reef (*Rotorbinella* sp.1 in Parker, 2009) and at 73 m depth in the north eastern Timor Sea (*Gavelinopsis praegeri* in Loeblich and Tappan, 1994), which indicates a shallow depth range and preference for warmer shelfal waters.

Bolivina robusta is an infaunal cosmopolitan species often found in temperate (Culver and Buzas, 1980; Hayward et al., 2007; Dorst and Schönfeld, 2013) and subtropical regions (Van Marle, 1988; Loeblich and Tappan, 1994; Murgese and De Deckker, 2005) from middle to upper bathyal depths (150–1400 m; Van Marle, 1988). This taxon is considered stress-tolerant and able to withstand increasing eutrophication. It has previously been found in association with *Uvigerina proboscidea* (Murgese and De Deckker, 2007). Jorissen (1999) suggested that all *Bolivina* species, along with *Bulimina* and *Uvigerina*, are useful indicators or low oxygen conditions at the sea floor. Data from FA2 show that when *B. robusta* increases, buliminids are also more abundant (e.g. 77.0 m CSF-A; Fig. 5.4).

In FA2, sedimentation rate increased sharply from 14 to 39 cm/ky at 0.61 Ma (85.6 m CSF-A) and subsequently dropped to 12 cm/ky at 0.44 Ma, accompanied by a change in lithology from mudstone to packstone (increase in carbonaceous skeletal fragments).

Paleoceanographic Interpretation

Upwelling Phase/High Flux of Organic Matter (3.54–0.91 Ma)

In the late Pliocene/early Pleistocene the global sea level was temporarily higher than today (Miller et al., 2005) and sedimentation rates on the Carnarvon Ramp were relatively low (Fig. 5.3). If a paleo-Leeuwin Current already existed, it would have been shifted towards the mid ramp or inner ramp, east of Site U1460 (Fig. 5.7). Karas et al. (2011) and Karas et al. (2017) reported that tectonic restriction of the Indonesian Gateway by gradual tectonic uplift at ~3.5–3.0 Ma led to a considerably weakened LC since ~3.3 Ma. Hence, the cold, northbound WAC would have had increased influence on the Carnarvon Ramp, leading to upwelling at Site U1460 (Fig. 5.7), which is a different configuration than upwelling during glacial lowstands as suggested by Okada and Wells (1997), Sinha et al. (2006), and Wells et al. (1994). In the regime of upwelling, sea-surface productivity resulted in a relatively high flux of organic matter to the sea floor with suboxic to anoxic conditions at the sediment-water interface as indicated by dominant FA1 species such as *U. peregrina*, *T. bradyi*, and *L. annellatrachia*. This is in agreement with a ~2°C temperature drop in the Western Pacific Warm Pool since the early Pliocene (Zhang et al., 2014) and increased abundance of *U. proboscidea* and other infaunal taxa on the deeper Exmouth Plateau as reported by Rai and Singh (2001). Climatically, WA transitioned between 3.3 and 2.4 Ma from a humid phase into an interval of aridity and monsoon-like seasonality that persists till today (Dodson and Macphail, 2004; Christensen et al., 2017).

Transitional Phase (1.14–0.61 Ma)

The mid Pleistocene was a phase of falling sea level and intensifying polar glaciation. At the sediment, surface species less tolerant of hypoxia such as *Hyalinea florenceae* and *Hanzawaia nipponica* gained in abundance (up to 29% combined) as sedimentation rates increased on the carbonate ramp (14–21 cm/ky; Fig. 5.3). Sponge spicules (sessile suspension-feeding megafauna; Fig. 5.2) indicate relatively strong bottom water flow delivering food, from which suspension feeders would have benefited. Associations between certain epifaunal foraminiferal species and

currents are well established, particularly in upper bathyal settings (Gooday, 2003). As in the modern oceanographic configuration, the lower Carnarvon Ramp was bathed by the LUC (Fig. 5.7), which delivered water with high oxygen concentration and salinity to the deep shelf (Thompson, 1984). Simultaneously the oligotrophic paleo-LC extended south, widened and deepened. This raised the temperatures on the shelf and decreased the upwelling potential gradually. Hence, the change in bottom-water oxygenation can be interpreted as an early signal for the transition into modern LC conditions.

Fully Developed Leeuwin Current: Punctuated Oligotrophic Phase (0.91–0 Ma)

Since the mid Pleistocene, the shelf environment at Site U1460A has experienced modern oceanographic conditions, including the fully developed LC (Fig. 5.7). The relatively sudden change of foraminiferal assemblages around 0.91 Ma indicates that a threshold of environmental parameters was crossed. By 0.91 Ma, the Leeuwin Current reached a magnitude similar to present, which is later than 1.6 Ma as previously proposed by Gallagher et al. (2009), but nearly synchronous with the emerging reef structures at 1 Ma on the WA Northwestern Shelf (Gallagher et al., 2014).

Sea-surface productivity was largely capped by the LC, supressing upwelling from deeper waters of the WAC and LUC, even during glacials (Spooner et al., 2011). The more oxygen-rich bottom waters led the benthic foraminiferal fauna to diversify and to be less dominated by opportunists. This development is recorded by maximum abundance of epifaunal species such as *Cibicides* cf. *C. refulgens* and the sharp increase of *S. carinatus* and *Rotorbinella* sp. Minor groups such as lituolids, trochamminids, spirilinids, miliolids, and robertinids appear for the first time, possibly due to higher alkalinity, temperatures and light penetration to the deep shelf. However, multiple times in this interval infaunal species such as *B. robusta*, and *U. peregrina* increased in abundance, indicating temporary upwelling conditions during some glacials, but never to a level seen in the Pliocene and early Pleistocene (Fig. 5.4).

Benthic foraminifera increased in abundance compared to planktonic forms (P/B ratio; Fig. 5.4), which was likely caused by decrease of paleo-productivity in surface waters and optimal benthic conditions (Berger and Diester-Haass, 1988). This aspect has been confirmed by the study of Buckley (2016), who calculated the BFAR index for Core U1460A and found increased accumulation rates of benthic foraminifera at around 0.6 Ma. Sponge spicule data (Fig. 5.3) suggests that the late Pleistocene (~0.61 Ma) was a time of increased current activity, which coincides with enhancement of the ITF during the Middle Pleistocene Transition period (Karas et al., 2011). The peak of sponge spicule abundance is synchronous with a lithologic shift to packstone, which was due to flourishing reef-builders benefiting from higher water temperatures and increased alkalinity (Gallagher et al., 2014). Intensifying aridity on the Australian continent at the end of the Middle Pleistocene Transition (0.6 Ma) triggered ooid formation and poleward reef expansion associated with the switch to higher amplitude glacio-eustatic cycles (Collins, 2002; Gallagher et al., 2014; Christensen et al., 2017). Fluvial input of detrital material became scarcer, which suggests that the high carbonate sedimentation rates were mainly autochthonous (James et al., 1999; James et al., 2004; Gallagher et al., 2014). When high-flow conditions waned to modern conditions, the sedimentation rate dropped (12 cm/ky) and glauconite, an authigenic slow sedimentation indicator, became more prevalent on the deeper shelf (Fig. 5.2; James et al., 1999; Collins et al., 2014).

Based on planktonic foraminiferal sea-surface temperature reconstructions of the last 500 kyrs, Spooner et al. (2011) and Sinha et al. (2006) suggested that during late Pleistocene glacial periods, the LC was less strong, which shifted waters of the ITF 3-4° equatorward, giving way to cooler waters of the WAC. During such conditions moderate upwelling increased sea surface productivity and flux of organic matter temporarily. This is reflected by dominance of low-oxygen tolerating taxa during sea-level lowstands (Wells et al., 1994; Murgese and De Deckker, 2007). However, our observations do not indicate strong oxygen depletion on the outer shelf.

Conclusions

A total of 179 species of benthic foraminifera were found within U1460A (Appendix D1) with 15 species sufficiently abundant to provide quantitative correlation data for interpretation and paleoenvironmental and paleoceanographic reconstruction of the Carnarvon Ramp over the last ~3 Ma. The events from old to young are summarized:

Late Pliocene to mid Pleistocene (3.54–0.91 Ma): U1460A Pliocene sediments are mass wasting-related and most likely triggered by slope oversteepening or seismic activity. The early Pliocene period was characterized by a low sedimentation rate, high sea surface productivity, and low oxygenation at the sediment-water interface. This increased level of sea surface productivity is inferred to be the result of the landward shift of the LC due to relatively high sea level and restriction of the Indonesian Gateway by uplift. Restricted Indonesian Throughflow volume due to tectonic uplift would have controlled the Leeuwin Current, decreasing its capability of capping deeper water. Upwelled water of the Western Australian Current would have dominated the outer Carnarvon Ramp, facilitating higher sea surface productivity.

The mid Pleistocene (1.14–0.61 Ma): The incursion of the paleo-Leeuwin Current gradually amplified bottom water oxygenation and sponges flourished. Despite falling global sea levels caused by increasing polar glaciation, upwelling on the Carnarvon Ramp decreased.

Late Pleistocene to Holocene (0.91–0 Ma): The second step of environmental transition was the onset of modern-magnitude Leeuwin Current activity, which more effectively prevented upwelling from promoting surface productivity. A foraminiferal assemblage developed under more oligotrophic conditions, which has continued to the present. Temporary intensification of the Leeuwin Current and Indonesian Throughflow created a temperature optimum, which is expressed by a significant increase in sedimentation rates and reef expansion in Western Australia. However, from ~0.44 Ma onwards, Leeuwin Current flow and sedimentation rates decreased to modern magnitude. Occurrences of moderate oxygen

fluctuations may have been related to sporadic upwelling during stronger glacials and successively increasing sea-level variability.

Relative abundance, diversity, and assemblage composition of the 15 most abundant benthic foraminifera revealed three, temporally overlapping foraminiferal assemblages over the last 3.54 Ma on the Carnarvon Ramp. Foraminiferal Assemblage 1 dominated the lower-most 157 m of the core U1460A from Pliocene to mid Pleistocene. With high relative abundances of infaunal species, the dominant taxa were *Uvigerina peregrina, Lagena annellatrachia*, and *Trifarina bradyi*, which are shallow and deep infaunal representatives. The Transitional Foraminiferal Assemblage was characterized by a notable increase in the epifaunal species *Hanzawaia nipponica* and *Hyalinea florenceae*, and the waning of the infaunal species of Foraminiferal Assemblage 1. The upper 134 m of the core are dominated by the epifaunal species of Foraminiferal Assemblage 2. The shift towards higher species richness and benthic proportion clearly reflect the higher oxygenation at the sediment-water interface, with only limited influence of upwelling.

This assessment has revealed that Pliocene to Holocene benthic foraminifera from the Carnarvon Ramp are useful indicators of regional sea-surface currents. Assemblages have been impacted by suite of environmental factors amongst which are glacial sea-level changes, deep-shelf and shallow-water currents, nutrient flux to the sea floor, sedimentation rates, sea surface productivity, and oxygenation levels.

Acknowledgments

The IODP Expedition 356 “Indonesian Throughflow” on board the JOIDES Resolution was led by Dr. Stephen Gallagher and Dr. Craig Fulthorpe, who provided many insights at sea and post-cruise. We are grateful for the work of the shipboard scientists of Expedition 356, especially the sedimentology shifts and the shipboard- and the IODP Gulf Coast Repository technicians. Location of post-cruise sample processing was the U.S. Geological Survey St. Petersburg Coastal and Marine Science Center, whose

help in this study is very much appreciated. Any use of trade names is for descriptive purposes only and does not imply endorsement by the U.S. Government.

References

Altenbach, A.V., Pflaumann, U., Schiebel, R., Thies, A., Timm, S., Trauth, M., 1999. Scaling percentages and distributional patterns of benthic Foraminifera with flux rates of organic carbon. Journal of Foraminiferal Research 29, 173–185.

Barrows, T.T., Juggins, S., 2005. Sea-surface temperatures around the Australian margin and Indian Ocean during the Last Glacial Maximum. Quaternary Science Reviews 24, 1017–1047. 10.1016/j.quascirev.2004.07.020

Berger, W.H., Diester-Haass, L., 1988. Paleoproductivity: The benthic/planktonic ratio in foraminifera as a productivity index. Marine Geology 81, 15–25. 10.1016/0025-3227(88)90014-X

Berggren, W.A., Kent, D.V., Swisher, C.C.I., Aubry, M.-P., 1995. A revised Cenozoic geochronology and chronostratigraphy, in: Berggren, W.A., Kent, D.V., Aubry, M.-P., Hardenbol, J. (Eds.), Geochronology, time scales and global stratigraphic correlation. SEPM Special Publication #54, pp. 129–212.

Betjeman, K.J., 1969. Recent foraminifera from the western continental shelf of Western Australia. Contributions from the Cushman Laboratory for Foraminiferal Research 20, 119–138.

Bray, J.R., Curtis, J.T., 1957. An ordination of the upland forest communities of southern Wisconsin. Ecological Monographs 27, 325–349. 10.2307/1942268

Buckley, T., 2016. Cenozoic stratigraphy of the North Perth Basin and the formation of the Houtman Abrolhos, School of Earth Sciences. University of Melbourne, Melbourne, Australia, p. 190.

Christensen, B.A., Renema, W., Henderiks, J., De Vleeschouwer, D., Groeneveld, J., Castaneda, I.S., Reuning, L., Bogus, K., Auer, G., Ishiwa, T., McHugh, C.M., Gallagher, S.J., Fulthorpe, C.S., Scientists, I.E., 2017. Indonesian Throughflow drove Australian climate from humid Pliocene to arid Pleistocene. Geophysical Research Letters 44, 6914–6925. 10.1002/2017gl072977

Collins, L.B., 2002. Tertiary Foundations and Quaternary Evolution of Coral Reef Systems of Australia's North West Shelf, in: Keep, M., Moss, S.J. (Eds.), PESA Symposium Perth. Petroleum Exploration Society of Australia, Perth, pp. 129–152.

Collins, L.B., James, N.P., Bone, Y., 2014. Chapter 19 Carbonate shelf sediments of the western continental margin of Australia. Geological Society of London Memoirs 41, 255–272. 10.1144/m41.19

Collins, L.B., Zhu, Z.R., Wyrwoll, K.-H., 1998. Late Tertiary-Quaternary Geological Evolution of the Houtman Abrolhos Carbonate Platforms, Northern Perth Basin, in: Purcell, R., Purcell, P. (Eds.), The sedimentary basins of Western Australia 2: Proceedings. Petroleum Exploration Society of Australia Symposium, Perth, Western Australia, pp. 647–663.

Collins, L.B., Zhu, Z.R., Wyrwoll, K.-H., Eisenhauer, A., 2003. Late Quaternary structure and development of the northern Ningaloo Reef, Australia. Sedimentary Geology 159, 81-94. 10.1016/s0037-0738(03)00096-4

Corliss, B.H., 1979. Taxonomy of Recent Deep-Sea Benthonic Foraminifera from the Southeast Indian Ocean. Micropaleontology 25, 1–19. 10.2307/1485207

Corliss, B.H., Chen, C., 1988. Morphotype patterns of Norwegian Sea deep-sea benthic foraminifera and ecological implications. Geology 16, 716–719. 10.1130/0091-7613(1988)016<0716:MPONSD>2.3.CO;2

Cresswell, G.R., 1991. The Leeuwin Current - observations and recent models. Journal of the Royal Society of Western Australia 74, 1–14.

Culver, S.J., Buzas, M.A., 1980. Distribution of Recent Benthic Foraminifera off the North American Atlantic Coast. Smithsonian Institution Press, Washington, 512 pp.

De Deckker, P., 1997. The significance of the oceans in the Australasian region with respect to global palaeoclimates: future directions. Palaeogeography, Palaeoclimatology, Palaeoecology 131, 511–515. 10.1016/S0031-0182(97)00093-X

De Deckker, P., Moros, M., Perner, K., Jansen, E., 2012. Influence of the tropics and southern westerlies on glacial interhemispheric asymmetry. Nature Geoscience 5, 266–269. 10.1038/ngeo1431

De Rijk, S., Jorissen, F.J., Rohling, E.J., Troelstra, S.R., 2000. Organic flux control on bathymetric zonation of Mediterranean benthic foraminifera. Marine Micropaleontology 40, 151–166. 10.1016/S0377-8398(00)00037-2

Debenay, J.-P., 2012. A Guide to 1,000 Foraminifera from southwestern Pacific: New Caledonia. Marseille: IRD Éditions.; Paris: Publications Scientifiques du Museum, 384 pp.

Debenay, J.-P., Patrona, L.D., Goguenheim, H., 2009. Colonization of coastal environments by foraminifera: insight from shrimp ponds in New Caledonia (SW Pacific). Journal of Foraminiferal Research 39, 249–266. 10.2113/gsjfr.39.4.249

den Dulk, M., Reichart, G.J., Memon, G.M., Roelofs, E.M.P., Zachariasse, W.J., van der Zwaan, G.J., 1998. Benthic foraminiferal response to variations in surface water productivity and oxygenation in the northern Arabian Sea. Marine Micropaleontology 35, 43–66. 10.1016/S0377-8398(98)00015-2

Dodson, J.R., Macphail, M.K., 2004. Palynological evidence for aridity events and vegetation change during the Middle Pliocene, a warm period in Southwestern Australia. Global and Planetary Change 41, 285–307. 10.1016/j.gloplacha.2004.01.013

Dorst, S., Schönfeld, J., 2013. Diversity of benthic foraminifera on the shelf and slope of the NE Atlantic: Analyses of datasets. Journal of Foraminiferal Research 43, 238–254. 10.2113/gsjfr.43.3.238

Dunham, R.J., 1962. Classification of carbonate rocks according to depositional textures, in: Ham, W.E. (Ed.), Classification of carbonate rocks. AAPG Memoir, pp. 108–121.

Fellowes, T.E., Gacutan, J., Harris, D.L., Vila-Concejo, A., Webster, J.M., Byrne, M., 2017. Patterns of sediment transport using foraminifera tracers across sand aprons on the Great Barrier Reef. Journal of Coastal Research 33, 864–873. 10.2112/JCOASTRES-D-16-00082.1

Feng, M., Meyers, G., Pearce, A., Wijffels, S., 2003. Annual and interannual variations of the Leeuwin Current at 32°S. Journal of Geophysical Research: Oceans 108, 3355. 10.1029/2002JC001763

Fisher, R.A., Corbet, A.S., Williams, C.B., 1943. The relation between the number of species and the number of individuals in a random sample of an animal population. Journal of Animal Ecology 12, 42–58. 10.2307/1411

Fontanier, C., Jorissen, F.J., Licari, L., Alexandre, A., Anschutz, P., Carbonel, P., 2002. Live benthic foraminiferal faunas from the Bay of Biscay: faunal density, composition, and microhabitats. Deep Sea Research Part I: Oceanographic Research Papers 49, 751–785. 10.1016/S0967-0637(01)00078-4

Gallagher, S., Fulthorpe, C., Heap, A., Heine, C., Czarnota, K., Exon, N., Greenwood, D., Herold, N., Iryu, Y., Renema, W., Rosenthal, Y., Sniderman, K., Talukder, A., Wagstaff, B., Wallace, M., 2012. IODP Proposal Indonesian Throughflow, p. 39.

Gallagher, S.J., Fulthorpe, C.S., Bogus, K., Auer, G., Baranwal, S., Castañeda, I.S., Christensen, B.A., De Vleeschouwer, D., Franco, D.R., Groeneveld, J., Gurnis, M., Haller, C., He, Y., Henderiks, J., Himmler, T., Ishiwa, T., Iwatani, H., Jatiningrum, R.S., Kominz, M.A., Korpanty, C.A., Lee, E.Y., Levin, E., Mamo, B.L., McGregor, H.V., McHugh, C.M., Petrick, B.F., Potts, D.C., Rastegar Lari, A., Renema, W., Reuning, L., Takayanagi, H., Zhang, W., 2017a. Expedition 356 methods, in: Gallagher, S.J., Fulthorpe, C.S., Bogus, K., the Expedition 356 Scientists (Eds.), Proceedings of the International Ocean Discovery Program. International Ocean Discovery Program, College Station, Texas, p. 37.

Gallagher, S.J., Fulthorpe, C.S., Bogus, K., Auer, G., Baranwal, S., Castañeda, I.S., Christensen, B.A., De Vleeschouwer, D., Franco, D.R., Groeneveld, J., Gurnis, M., Haller, C., He, Y., Henderiks, J., Himmler, T., Ishiwa, T., Iwatani, H., Jatiningrum, R.S., Kominz, M.A., Korpanty, C.A., Lee, E.Y., Levin, E., Mamo, B.L., McGregor, H.V., McHugh, C.M., Petrick, B.F., Potts, D.C., Rastegar Lari, A., Renema, W., Reuning, L., Takayanagi, H., Zhang, W., 2017b. Site U1460, in: Gallagher, S.J., Fulthorpe, C.S., Bogus, K., the Expedition 356 Scientists (Eds.), Indonesian Throughflow. Proceedings of the International Ocean Discovery Program. International Ocean Discovery Program, College Station, Texas, p. 31.

Gallagher, S.J., Fulthorpe, C.S., Bogus, K., the Expedition 356 Scientists, 2017c. Expedition 356 Preliminary Report: Indonesian Throughflow. International Ocean Discovery Program, College Station, Texas, 53 pp.

Gallagher, S.J., Wallace, M.W., Hoiles, P.W., Southwood, J.M., 2014. Seismic and stratigraphic evidence for reef expansion and onset of aridity on the Northwest Shelf of Australia during the Pleistocene. Marine and Petroleum Geology 57, 470–481. 10.1016/j.marpetgeo.2014.06.011

Gallagher, S.J., Wallace, M.W., Li, C.L., Kinna, B., Bye, J.T., Akimoto, K., Torii, M., 2009. Neogene history of the West Pacific Warm Pool, Kuroshio and Leeuwin currents. Paleoceanography 24, PA1206. 10.1029/2008PA001660

Gingele, F.X., De Deckker, P., Hillenbrand, C.-D., 2001. Late Quaternary fluctuations of the Leeuwin Current and palaeoclimates on the adjacent landmasses - clay mineral evidence. Australian Journal of Earth Sciences 48, 867–874.

Gooday, A.J., 2003. Benthic foraminifera (Protista) as tools in deep-water palaeoceanography: Environmental influences on faunal characteristics. Advances in Marine Biology 46, 1–90. 10.1016/S0065-2881(03)46002-1

Gooday, A.J., Hughes, J.A., 2002. Foraminifera associated with phytodetritus deposits at a bathyal site in the northern Rockall Trough (NE Atlantic): seasonal contrasts and a comparison of stained and dead assemblages. Marine Micropaleontology 46, 83–110. 10.1016/S0377-8398(02)00050-6

Gooday, A.J., Jorissen, F.J., 2012. Benthic foraminiferal biogeography: Controls on global distribution patterns in deep-water settings. Annual Review of Marine Science 4, 237–262. 10.1146/annurev-marine-120709-142737

Gooday, A.J., Malzone, M.G., Bett, B.J., Lamont, P.A., 2010. Decadal-scale changes in shallow-infaunal foraminiferal assemblages at the Porcupine Abyssal Plain, NE Atlantic. Deep Sea Research Part II: Topical Studies in Oceanography 57, 1362–1382. 10.1016/j.dsr2.2010.01.012

Gradstein, F.M., Ogg, J.G., Schmitz, M.D., Ogg, G.M., 2012. The Geologic Time Scale 2012. Elsevier, 1176 pp.

Greenstein, B.J., Pandolfi, J.M., 2008. Escaping the heat: range shifts of reef coral taxa in coastal Western Australia. Global Change Biology 14, 513–528. 10.1111/j.1365-2486.2007.01506.x

Gupta, A.K., Srinivasan, M.S., 1990. Response of Northern Indian Ocean deep-sea benthic foraminifera to global climates during Pliocene-Pleistocene. Marine Micropaleontology 16, 77–91. 10.1016/0377-8398(90)90030-P

Gupta, A.K., Srinivasan, M.S., 1992. Uvigerina proboscidea abundances and paleoceanography of the northern Indian Ocean DSDP Site 214 during the Late Neogene. Marine Micropaleontology 19, 355–367. 10.1016/0377-8398(92)90038-L

Haig, D.W., 1993. Buliminid foraminifera from inner neritic sand and mud facies of the Papuan Lagoon, New Guinea. Journal of Foraminiferal Research 23, 162–179. 10.2113/gsjfr.23.3.162

Haig, D.W., 1997. Foraminifera from Exmouth Gulf, Western Australia. Journal of the Royal Society of Western Australia 80, 263–280.

Haller, C., Hallock, P., Hine, A.C., Smith, C.G., in review. Recent outer shelf foraminiferal assemblages on the Carnarvon Ramp and Northwestern Shelf of Western Australia, SEPM Special Publication: Proceedings Microfossils IV. NAMS-SEPM.

Hammer, Ø., Harper, D.A.T., Ryan, P.D., 2001. PAST: Paleontological statistics software package for education and data analysis. Palaeontologia Electronica 4, 9. http://palaeo-electronica.org/2001_1/past/issue1_01.htm

Hanson, C.E., Pattiaratchi, C.B., Waite, A.M., 2005. Sporadic upwelling on a downwelling coast: Phytoplankton responses to spatially variable nutrient dynamics off the Gascoyne region of Western Australia. Continental Shelf Research 25, 1561–1582. 10.1016/j.csr.2005.04.003

Hayward, B.W., Grenfell, H.R., Reid, C.M., Hayward, K.A., 1999. Recent New Zealand shallow-water benthic foraminifera: taxonomy, ecologic distribution, biogeography, and use in paleoenvironmental assessment. Institute of Geological and Nuclear Sciences, Lower Hutt, New Zealand, 258 pp.

Hayward, B.W., Grenfell, H.R., Sabaa, A.T., Neil, H.L., 2007. Factors influencing the distribution of Subantarctic deep-sea benthic foraminifera, Campbell and Bounty Plateaux, New Zealand. Marine Micropaleontology 62, 141–166. 10.1016/j.marmicro.2006.08.001

Hayward, B.W., Grenfell, H.R., Sabaa, A.T., Neil, H.L., Buzas, M.A., 2010. Recent New Zealand deep-water benthic foraminifera: Taxonomy, ecologic distribution, biogeography, and use in paleoenvironmental assessment. Institute of Geological & Nuclear Sciences, Lower Hutt, New Zealand, 363 pp.

Hohenegger, J., 2005. Estimation of environmental paleogradient values based on presence/absence data: a case study using benthic foraminifera for paleodepth estimation. Palaeogeography, Palaeoclimatology, Palaeoecology 217, 115–130. 10.1016/j.palaeo.2004.11.020

Holbourn, A., Kuhnt, W., Kawamura, H., Jian, Z., Grootes, P., Erlenkeuser, H., Xu, J., 2005. Orbitally paced paleoproductivity variations in the Timor Sea and Indonesian Throughflow variability during the last 460 kyr. Paleoceanography 20, PA3002. 10.1029/2004PA001094

IODP-MI, 2011. IODP Depth Scales Terminology, p. 20.

James, N.P., Bone, Y., Kyser, T.K., Dix, G.R., Collins, L.B., 2004. The importance of changing oceanography in controlling late Quaternary carbonate sedimentation on a high-energy, tropical, oceanic ramp: North-western Australia. Sedimentology 51, 1179–1205. 10.1111/j.1365-3091.2004.00666.x

James, N.P., Collins, L.B., Bone, Y., Hallock, P., 1999. Subtropical carbonates in a temperate realm: Modern sediments on the southwest Australian shelf. Journal of Sedimentary Research 69, 1297–1321. 10.2110/jsr.69.1297

Jian, Z., Yu, Y., Li, B., Wang, J., Zhang, X., Zhou, Z., 2006. Phased evolution of the south–north hydrographic gradient in the South China Sea since the middle Miocene. Palaeogeography, Palaeoclimatology, Palaeoecology 230, 251–263. 10.1016/j.palaeo.2005.07.018

Jorissen, F.J., 1999. Benthic foraminiferal microhabitats below the sediment–water interface, in: Sen Gupta, B.K. (Ed.), Modern Foraminifera. Kluwer, Dordrecht, pp. 161–179.

Kaiho, K., 1999. Effect of organic carbon flux and dissolved oxygen on the benthic foraminiferal oxygen index (BFOI). Marine Micropaleontology 37, 67–76. 10.1016/S0377-8398(99)00008-0

Kaminski, M.A., Gradstein, F.M., 2005. Atlas of Paleogene cosmopolitan deep-water agglutinated foraminifera. Grzybowski Foundation, 548 pp.

Karas, C., Nürnberg, D., Bahr, A., Groeneveld, J., Herrle, J.O., Tiedemann, R., deMenocal, P.B., 2017. Pliocene oceanic seaways and global climate. Scientific Reports 7, 39842. 10.1038/srep39842

Karas, C., Nürnberg, D., Tiedemann, R., Garbe-Schönberg, D., 2011. Pliocene Indonesian Throughflow and Leeuwin Current dynamics: Implications for Indian Ocean polar heat flux. Paleoceanography 26, PA2217. 10.1029/2010PA001949

Kendrick, G.W., Wyrwoll, K.-H., Szabo, B.J., 1991. Pliocene-Pleistocene coastal events and history along the western margin of Australia. Quaternary Science Reviews 10, 419–439. 10.1016/0277-3791(91)90005-F

Langer, M.R., Mouanga, G.H., 2016. Invasion of amphisteginid foraminifera in the Adriatic Sea. Biological Invasions 18, 1335–1349. 10.1007/s10530-016-1070-0

Lei, Y., Li, T., 2016. Atlas of Benthic Foraminifera from China Seas. The Bohai Sea and the Yellow Sea. Springer, Beiijing, 399 pp.

Li, Q., James, N.P., Bone, Y., McGowran, B., 1999. Palaeoceanographic significance of recent foraminiferal biofacies on the southern shelf of Western Australia: a preliminary study. Palaeogeography, Palaeoclimatology, Palaeoecology 147, 101–120. 10.1016/S0031-0182(98)00150-3

Loeblich, A.R., Tappan, H., 1994. Foraminifera of the Sahul Shelf and Timor Sea. Cushman Foundation for Foraminiferal Research Special Pubublication 31, Cambridge, MA, 661 pp.

Loubere, P., 1991. Deep-Sea Benthic Foraminiferal Assemblage Response to a Surface Ocean Productivity Gradient: A Test. Paleoceanography 6, 193-204. 10.1029/90PA02612

Mamo, B.L., Brock, G.A., Gretton, E.J., 2013. Deep sea benthic foraminifera as proxies for palaeoclimatic fluctuations in the New Caledonia Basin, over the last 140,000 years. Marine Micropaleontology 104, 1–13. 10.1016/j.marmicro.2013.08.002

Martínez, J.I., De Deckker, P., Barrows, T.T., 1999. Palaeoceanography of the last glacial maximum in the eastern Indian Ocean: planktonic foraminiferal evidence. Palaeogeography, Palaeoclimatology, Palaeoecology 147, 73–99. 10.1016/S0031-0182(98)00153-9

Martini, E., 1971. Standard Tertiary and Quaternary calcareous nannoplankton zonation, in: Farinacci, A. (Ed.), Proceedings of the Second Planktonic Conference, Roma 1970 (Edizioni Tecnoscienza), Rome, pp. 739–785.

Mateo, P., Keller, G., Punekar, J., Spangenberg, J.E., 2017. Early to Late Maastrichtian environmental changes in the Indian Ocean compared with Tethys and South Atlantic. Palaeogeography, Palaeoclimatology, Palaeoecology 478, 121–138. 10.1016/j.palaeo.2017.01.027

May, S.M., Falvard, S., Norpoth, M., Pint, A., Brill, D., Engel, M., Scheffers, A., Dierick, M., Paris, R., Squire, P., Brückner, H., 2016. A mid-Holocene candidate tsunami deposit from the NW Cape (Western Australia). Sedimentary Geology 332, 40–50. 10.1016/j.sedgeo.2015.11.010

Mays, C., 2007. The current distribution of foraminifera on the Western Australian shelf: A modern analogue for Cenozoic palaeoceanography, School of Earth Sciences. University of Melbourne, Australia, p. 74.

McCorkle, D.C., Veeh, H.H., Heggie, D.T., 1994. Glacial-Holocene paleoproductivity off Western Australia: a Comparison of proxy records, in: Zahn, R., Pedersen, T.F., Kaminski, M.A., Labeyrie, L. (Eds.), Carbon cycling in the glacial ocean: constraints on the ocean's role in global change: quantitative approaches in paleoceanography. Springer Berlin Heidelberg, Berlin, Heidelberg, pp. 443–479.

McCormack, K.D., McClay, K., 2013. Structural architecture of the Gorgon Platform, North West Shelf, Australia, West Australian Basins Symposium (WABS) 2013. Petroleum Exploration Society of Australia, Perth, Western Australia, p. 23.

McGowran, B., Li, Q., Cann, J., Padley, D., McKirdy, D.M., Shafik, S., 1997. Biogeographic impact of the Leeuwin Current in southern Australia since the late middle Eocene. Palaeogeography, Palaeoclimatology, Palaeoecology 136, 19-40. 10.1016/S0031-0182(97)00073-4

Miller, K.G., Kominz, M.A., Browning, J.V., Wright, J.D., Mountain, G.S., Katz, M.E., Sugarman, P.J., Cramer, B.S., Christie-Blick, N., Pekar, S.F., 2005. The Phanerozoic record of global sea-level change. Science 310, 1293–1298. 10.1126/science.1116412

Molnar, P., Cronin, T.W., 2015. Growth of the Maritime Continent and its possible contribution to recurring Ice Ages. Paleoceanography 30, 196–225. 10.1002/2014PA002752

Murgese, D.S., De Deckker, P., 2005. The distribution of deep-sea benthic foraminifera in core tops from the eastern Indian Ocean. Marine Micropaleontology 56, 25–49. j.marmicro.2005.03.005

Murgese, D.S., De Deckker, P., 2007. The Late Quaternary evolution of water masses in the eastern Indian Ocean between Australia and Indonesia, based on benthic foraminifera faunal and carbon isotopes analyses. Palaeogeography, Palaeoclimatology, Palaeoecology 247, 382–401. 10.1016/j.palaeo.2006.11.002

Murray, J.W., 2006. Ecology and Applications of Benthic Foraminifera. Cambridge University Press, 426 pp.

Nordberg, K., Gustafsson, M., Krantz, A.-L., 2000. Decreasing oxygen concentrations in the Gullmar Fjord, Sweden, as confirmed by benthic foraminifera, and the possible association with NAO. Journal of Marine Systems 23, 303–316. 10.1016/S0924-7963(99)00067-6

Okada, H., Wells, P., 1997. Late Quaternary nannofossil indicators of climate change in two deep-sea cores associated with the Leeuwin Current off Western Australia. Palaeogeography, Palaeoclimatology, Palaeoecology 131, 413–432. 10.1016/S0031-0182(97)00014-X

Orpin, A.R., Haig, D.W., Woolfe, K.J., 1999. Sedimentary and foraminiferal facies in Exmouth Gulf, in arid tropical northwestern Australia. Australian Journal of Earth Sciences 46, 607–621. 10.1046/j.1440-0952.1999.00728.x

Parker, J.H., 2009. Taxonomy of foraminifera from Ningaloo Reef, Western Australia. Memoir of the Association of Australasian Palaeontologists 36, Canberra, 810 pp.

Potemra, J.T., 2005. Indonesian Throughflow transport variability estimated from satellite altimetry. Oceanography 18, 98–107. 10.5670/oceanog.2005.10

Quilty, P.G., Hosie, G., 2006. Modern foraminifera, Swan River Estuary, Western Australia: Distribution and controlling factors. Journal of Foraminiferal Research 36, 291–314. 10.2113/gsjfr.36.4.291

Rai, A.K., Singh, V.B., 2001. Late Neogene deep-sea benthic foraminifera at ODP Site 762B, eastern Indian Ocean: diversity trends and palaeoceanography. Palaeogeography, Palaeoclimatology, Palaeoecology 173, 1–8. 10.1016/S0031-0182(01)00299-1

Reason, C.J.C., Gamble, D., Pearce, A.F., 1999. The Leeuwin Current in the Parallel Ocean Climate Model and applications to regional meteorology and fisheries. Meteorological Applications 6, 211–225. 10.1017/S1350482799001255

Rogers, J., De Deckker, P., 2007. Radiolaria as a reflection of environmental conditions in the eastern and southern sectors of the Indian Ocean: A new statistical approach. Marine Micropaleontology 65, 137–162. 10.1016/j.marmicro.2007.07.001

Schmiedl, G., Mackensen, A., Müller, P.J., 1997. Recent benthic foraminifera from the eastern South Atlantic Ocean: Dependence on food supply and water masses. Marine Micropaleontology 32, 249–287. 10.1016/S0377-8398(97)00023-6

Schnitker, D., 1974. West Atlantic abyssal circulation during the past 120,000 years. Nature 248, 385–387. 10.1038/248385a0

Semeniuk, T.A., 2001. Epiphytic foraminifera along a climatic gradient, Western Australia. Journal of Foraminiferal Research 31, 191–200. 10.2113/31.3.191

Sen Gupta, B.K., Platon, E., Bernhard, J.M., Aharon, P., 1997. Foraminiferal colonization of hydrocarbon-seep bacterial mats and underlying sediment, Gulf of Mexico slope. Journal of Foraminiferal Research 27, 292–300. 10.2113/gsjfr.27.4.292

Shannon, C.E., 1948. A mathematical theory of communication. The Bell System Technical Journal 27, 379–423, 623–656.

Sinha, D.K., Singh, A.K., Tiwari, M., 2006. Palaeoceanographic and palaeoclimatic history of ODP site 763A (Exmouth Plateau), southeast Indian Ocean: 2.2 Ma record of planktic foraminifera. Current Science 90, 1363–1369.

Smith, R.L., 1992. Coastal upwelling in the modern ocean. Geological Society, London, Special Publications 64, 9–28. 10.1144/gsl.sp.1992.064.01.02

Smith, R.L., Huyer, A., Godfrey, J.S., Church, J.A., 1991. The Leeuwin Current off Western Australia, 1986–1987. Journal of Physical Oceanography 21, 323–345. 10.1175/1520-0485(1991)021<0323:TLCOWA>2.0.CO;2

Spooner, M.I., De Deckker, P., Barrows, T.T., Fifield, L.K., 2011. The behaviour of the Leeuwin Current offshore NW Australia during the last five glacial–interglacial cycles. Global and Planetary Change 75, 119–132. 10.1016/j.gloplacha.2010.10.015

Takahashi, K., Okada, H., 2000. The paleoceanography for the last 30,000 years in the southeastern Indian Ocean by means of calcareous nannofossils. Marine Micropaleontology 40, 83–103. 10.1016/S0377-8398(00)00033-5

Thompson, R.O.R.Y., 1984. Observations of the Leeuwin Current off Western Australia. Journal of Physical Oceanography 14, 623–628. 10.1175/1520-0485(1984)014<0623:ootlco>2.0.co;2

Tomczak, M., Godfrey, J.S., 2003. Regional Oceanography: An Introduction 2nd edn. Daya Publishing House, Delhi, 390 pp.

van der Zwaan, G.J., Duijnstee, I.A.P., den Dulk, M., Ernst, S.R., Jannink, N.T., Kouwenhoven, T.J., 1999. Benthic foraminifers: proxies or problems? Earth-Science Reviews 46, 213–236. 10.1016/S0012-8252(99)00011-2

van der Zwaan, G.J., Jorissen, F.J., de Stigter, H.C., 1990. The depth dependency of planktonic/benthic foraminiferal ratios: Constraints and applications. Marine Geology 95, 1–16. 10.1016/0025-3227(90)90016-D

Van Marle, L.J., 1988. Bathymetric distribution of benthic foraminifera on the Australian-Irian Jaya continental margin, eastern Indonesia. Marine Micropaleontology 13, 97–152. 10.1016/0377-8398(88)90001-1

van Sebille, E., Scussolini, P., Durgadoo, J.V., Peeters, F.J.C., Biastoch, A., Weijer, W., Turney, C., Paris, C.B., Zahn, R., 2015. Ocean currents generate large footprints in marine palaeoclimate proxies. Nature Communications 6, 6521. 10.1038/ncomms7521

Veeh, H.H., McCorkle, D.C., Heggie, D.T., 2000. Glacial/interglacial variations of sedimentation on the West Australian continental margin: constraints from excess 230Th. Marine Geology 166, 11–30. 10.1016/S0025-3227(00)00011-6

Wade, B.S., Pearson, P.N., Berggren, W.A., Pälike, H., 2011. Review and revision of Cenozoic tropical planktonic foraminiferal biostratigraphy and calibration to the geomagnetic polarity and astronomical time scale. Earth-Science Reviews 104, 111–142. 10.1016/j.earscirev.2010.09.003

Waite, A.M., Thompson, P.A., Pesant, S., Feng, M., Beckley, L.E., Domingues, C.M., Gaughan, D., Hanson, C.E., Holl, C.M., Koslow, T., Meuleners, M., Montoya, J.P., Moore, T., Muhling, B.A., Paterson, H., Rennie, S., Strzelecki, J., Twomey, L., 2007. The Leeuwin Current and its eddies: An introductory overview. Deep Sea Research Part II: Topical Studies in Oceanography 54, 789–796. 10.1016/j.dsr2.2006.12.008

Wells, P., Wells, G., Cali, J., Chivas, A., 1994. Response of deep-sea benthic foraminifera to Late Quaternary climate changes, southeast Indian Ocean, offshore Western Australia. Marine Micropaleontology 23, 185–229. 10.1016/0377-8398(94)90013-2

Wells, P.E., Wells, G.M., 1994. Large-scale reorganization of ocean currents offshore Western Australia during the Late Quaternary. Marine Micropaleontology 24, 157–186. 10.1016/0377-8398(94)90020-5

Wijffels, S., Sprintall, J., Fieux, M., Bray, N., 2002. The JADE and WOCE I10/IR6 Throughflow sections in the southeast Indian Ocean. Part 1: water mass distribution and variability. Deep Sea Research Part II: Topical Studies in Oceanography 49, 1341–1362. 10.1016/S0967-0645(01)00155-2

Wyrtki, K., 1973. Physical Oceanography of the Indian Ocean, in: Zeitzschel, B., Gerlach, S.A. (Eds.), The Biology of the Indian Ocean. Springer, Berlin, pp. 18–36.

Wyrtki, K., 1987. Indonesian through flow and the associated pressure gradient. Journal of Geophysical Research: Oceans 92, 12941-12946. 10.1029/JC092iC12p12941

Zhang, Y.G., Pagani, M., Liu, Z., 2014. A 12-million-year temperature history of the tropical Pacific Ocean. Science 344, 84–87. 10.1126/science.1246172

Tables

Table 5.1 Biostratigraphic markers (shipboard data) in Core U1460A (Gallagher et al., 2017b). All events are calibrated to bioevents of Geologic Time Scale 2012 (Gradstein et al., 2012). PF = planktonic foraminifera, CN = calcareous nannofossils, asterisks = diverging age-model between planktonic calcareous nannofossils.

Section	Depth CFS-A (m)	Fossil type	Marker species	Zone name	Age (Ma)
1F-CC	2.13	CN	Base *Emiliania huxleyi*	NN21	0.29
5F-CC	20.65	CN	Top *Pseudoemiliania lacunosa*	NN19	0.44
19F-CC	86.59	PF	Top *Globorotalia tosaensis*	PT1a	0.61
28F-CC	128.88	PF	Top *Reticulofenestra asanoi*	NN19	0.91
38F-CC	176.24	CN	Base *Reticulofenestra asanoi*	NN19	1.14
42F-CC	194.99	CN	Top *Calcidiscus macintyrei*	NN19	1.60
45F-CC	208.85	CN	Top *Discoaster brouweri*	NN18	1.93*
57F-CC	265.26	PF	Base *Globorotalia truncatulinoides*	Pt1a	1.93*
60F-CC	279.36	CN	Top *Discoaster surculus*	NN16	2.49*
60F-CC	279.36	PF	Top *Dentoglobigerina altispira*	PL4	3.47*
63F-CC	293.4	CN	Top *Sphaenolithus* spp.	NN16	3.54*

Figures

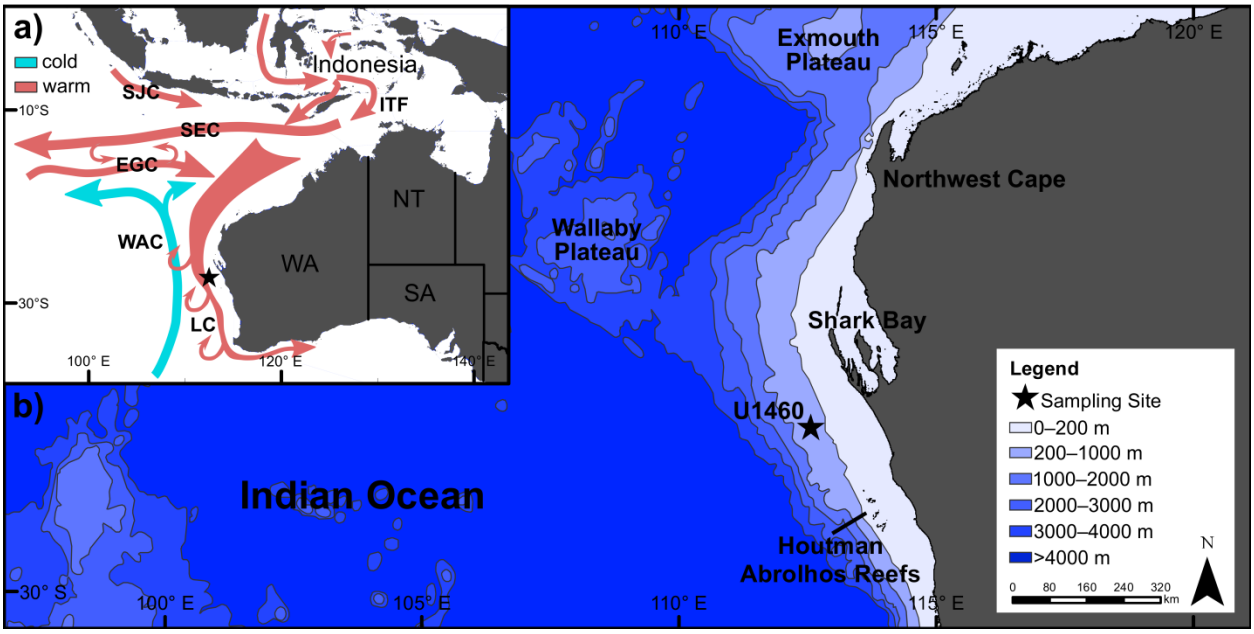

Figure 5.1. (a) Location and significant oceanic currents in the Indian Ocean affecting the Western Australian shelf. Abbreviations stand for the following: ITF – Indonesian Throughflow; SEC – South Equatorial Current; SJC – South Java Current; EGC – Eastern Gyral Current; WAC – West Australian Current; LC – Leeuwin Current. The Leeuwin Undercurrent is not shown. (b) Location map illustrating the drillsite of U1460A by the JOIDES Resolution in 2015 and the Western Australian shelf and significant bathymetric features.

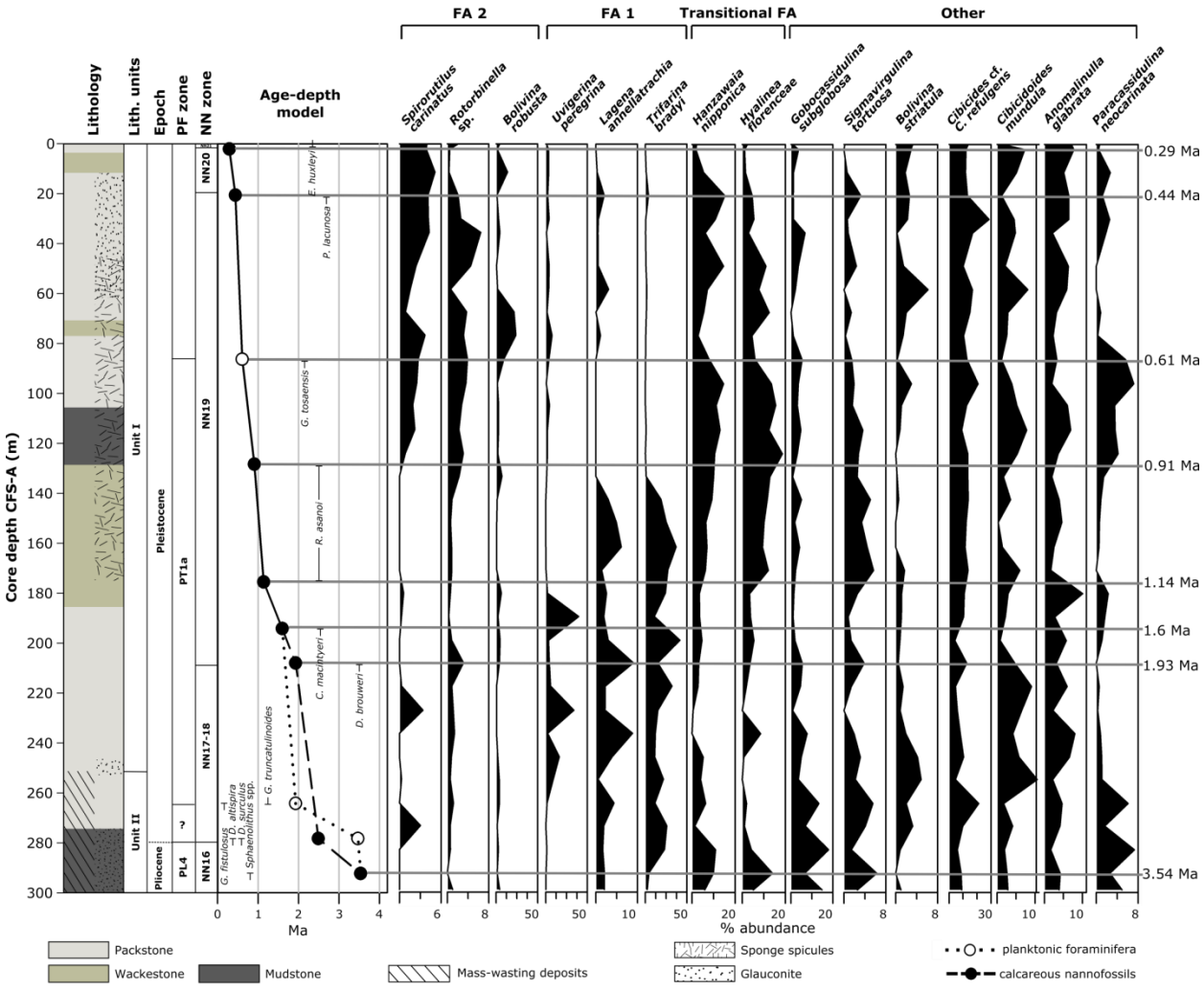

Figure 5.2. Lithology log (redrawn after Gallagher et al., 2017b), mass wasting deposits (MWD), stratigraphic framework from shipboard age-depth model (IODP Expedition 356), and relative abundance of the 15 most abundant taxa. Species are ordered by their association with the two foraminiferal assemblages (FA2, FA1), or 'Other' if direct association is absent. Specified ages mark the biostratigraphic datums (see Table 5.1). The age-depth model for calcareous nannofossils and planktonic foraminifera bifurcates in the lower part of the core probably due to reworking in the mass-wasting deposits. Glauconite mineral abundance is indicated when applicable. Mass wasting deposits were found below 252.7 m CSF-A (Core Section 55F-2) (Gallagher et al., 2017b).

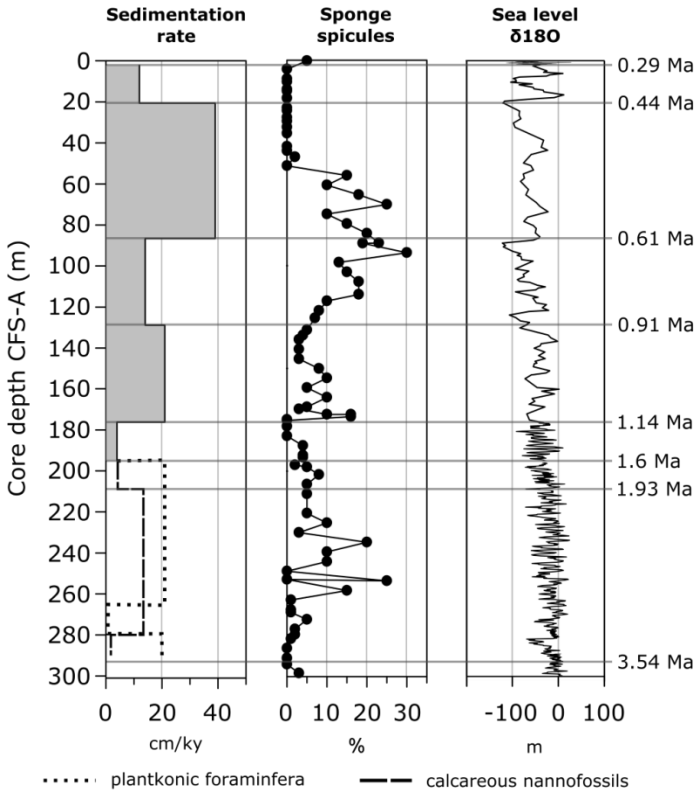

Figure 5.3. Graphs of sedimentation rate (Gallagher et al., 2017b), sponge-spicule abundance (Gallagher et al., 2017b), and sea level based on oxygen isotopes from Miller et al. (2005). Biostratigraphic datums are marked by horizontal grey lines.

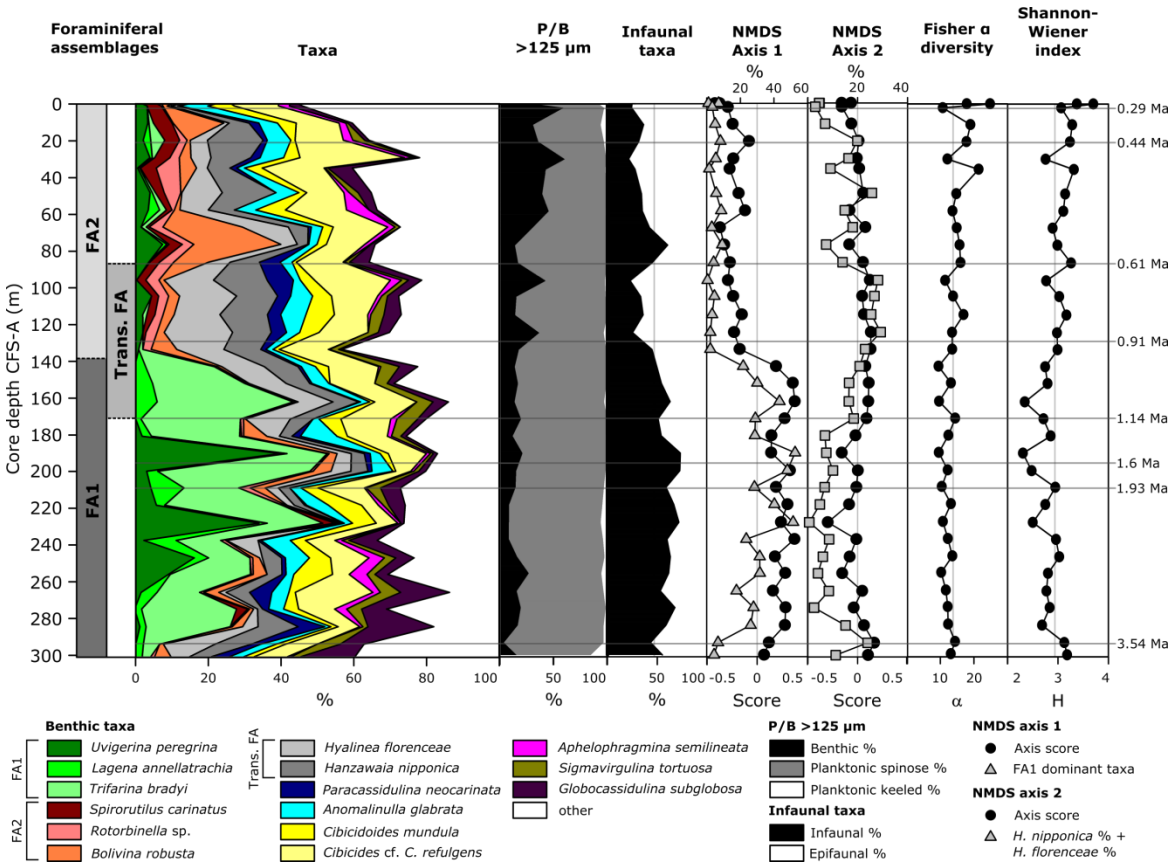

Figure 5.4. Proportions of the 15 most abundant benthic foraminifera ('other' is constituted by all taxa less abundant), planktonic/benthic percentages, Non-metric multidimensional scaling (NMDS) axis scores, Fisher a diversity, and Shannon-Wiener index in all samples studied of U1460A. Abbreviations: FA 1 = Foraminiferal Assemblage 1; FA2 = Foraminiferal Assemblage 2; Trans. FA = Transitional Foraminiferal Assemblage.

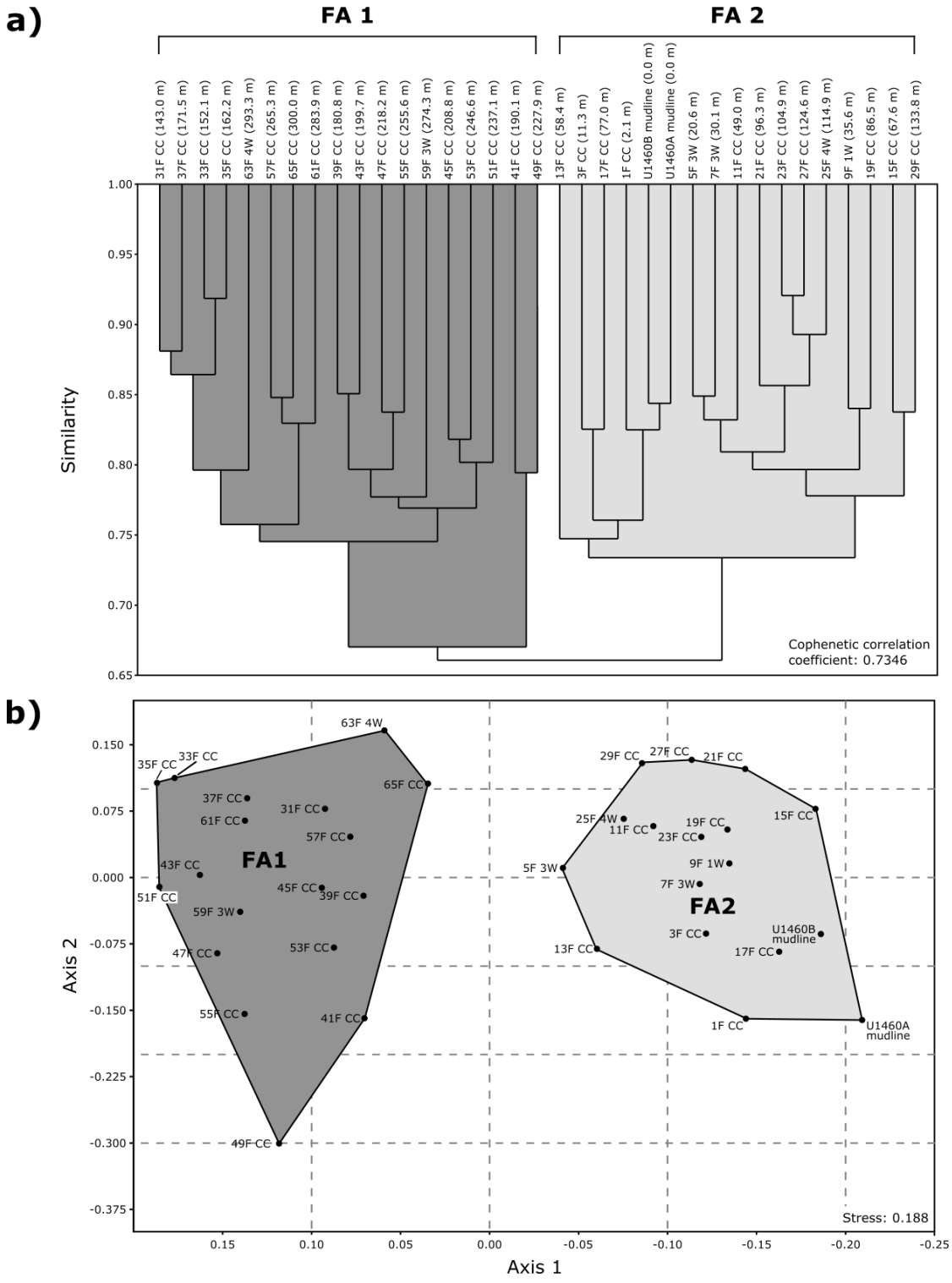

Figure 5.5. Results of Bray-Curtis a) Q-mode cluster analysis and b) Non-metric multidimensional scaling (NMDS). Depths indicated are in CFS-A scale.

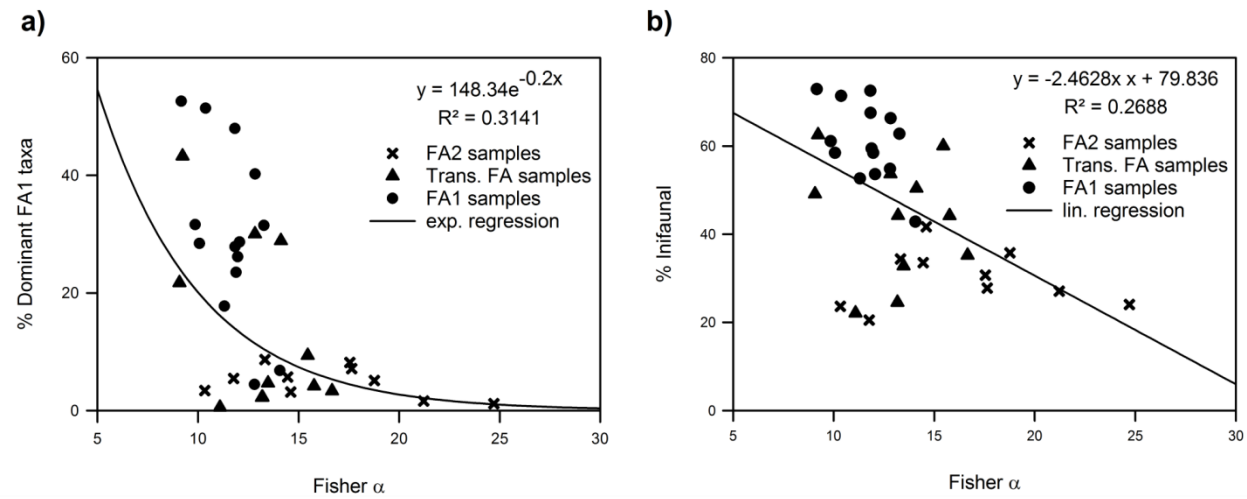

Figure 5.6. Fisher α versus (a) percent of dominant FA1 taxa: *Uvigerina peregrina*, *Lagena annellatrachia*, and *Trifarina bradyi*; exponential regression model; (b) percent of infaunal taxa; linear regression model. Abbreviations: Trans. FA1 = Foraminiferal Assemblage 1; FA2 = Foraminiferal Assemblage 2; Trans. FA = Transitional Foraminiferal Assemblage, subset of FA1 and FA2.

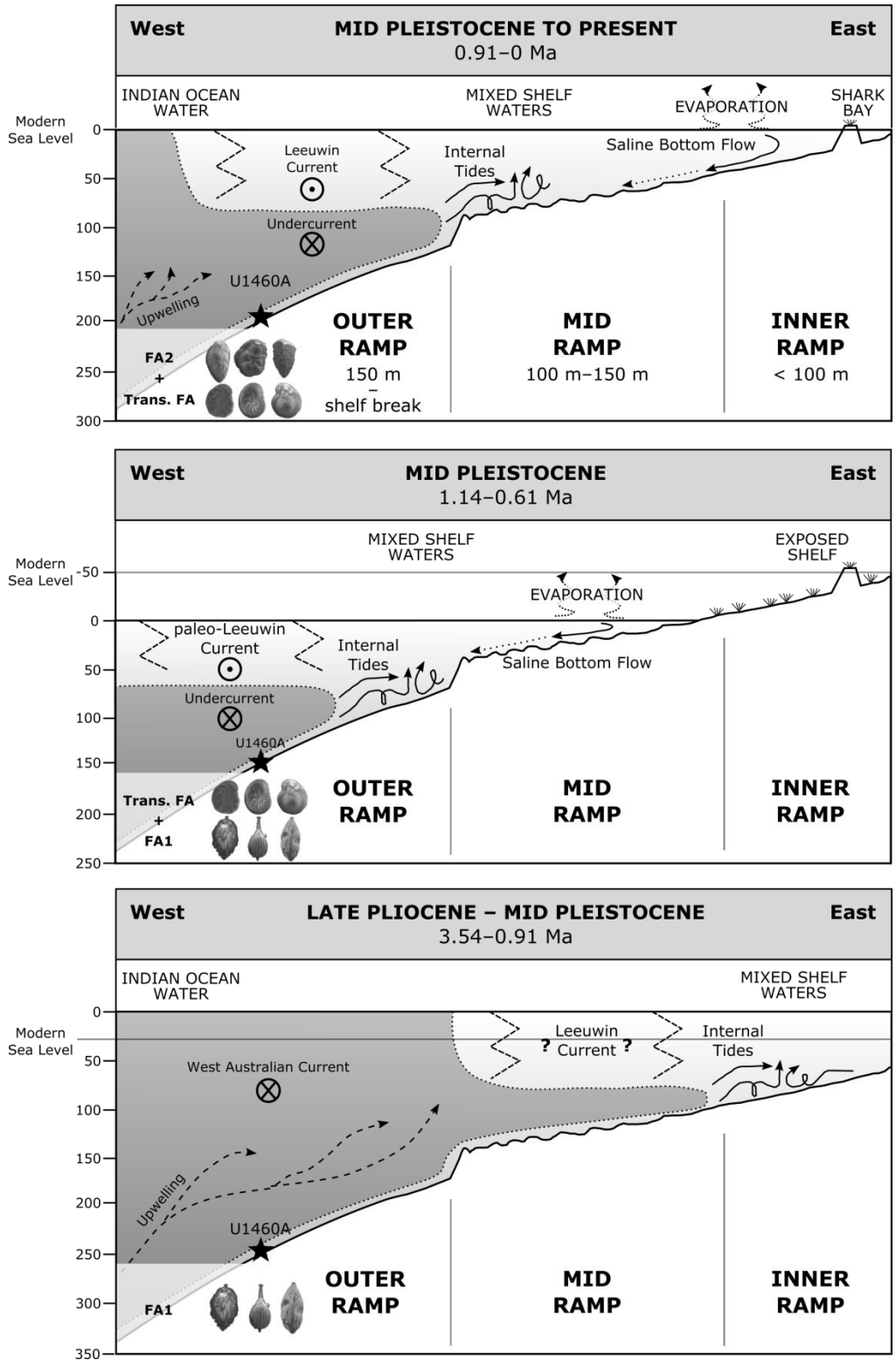

Figure 5.7. Schematic of current systems influencing benthic foraminfera at site U1460A between 3.45 Ma and modern conditions.

Chapter 6.

Conclusions

The goal of this dissertation was to evaluate of the fidelity of using foraminifera as proxies in both qualitative and quantitative paleoenvironmental interpretations. Application of proxies is a training-based inversion problem; whether the inversion is quantitative or qualitative. In both case studies, one in coastal environments and the other outer shelf settings, the same systematic approach was used: 1) foraminifera from surface sediments were surveyed to evaluate the control environmental gradients (e.g., elevation/bathymetry, salinity, etc.) had on assemblages, and 2) applied the knowledge gained from the surface sediment to interpret fossil assemblages obtained from the same region as the modern dataset. Modern foraminiferal assemblages require assessment in conjunction with their environmental parameters, whereas for fossil analyses it is imperative to establish chronological framework in context with lithological analyses to better understand changing environmental conditions.

The Mississippi Sound foraminifera were sampled from a variety of physiographic regions and analyzed for correlation with environmental parameters such as elevation, salinity, organic matter, and grain size. The quantitative transfer function used the surface distribution of dead marsh foraminifera as a training set for the modeled reconstruction of the paleo-marsh elevation.

The Leeuwin Current's influence on benthic foraminifera was evaluated from outer shelf samples. The modern seafloor assemblages were recorded in a study, that focused on taxonomy and distribution patterns. The paleoceanographic evolution and effects of water masses were assessed from a 300 m core.

Summary of Findings

Chapter 2 reported distribution patterns of live and dead foraminifera from the Eastern Mississippi Sound (Grand Bay, Fowl River, Pascagoula, and Dauphin Island). Statistical analyses revealed five live assemblages and nine dead biofacies of mostly agglutinated species across the marshes of the eastern Mississippi Sound covering the Estuarine, Low Marsh, Middle Marsh, High Marsh, and Upland Transition. Despite gradual transitions of species distributions, an analysis of environmental parameters indicated that elevation, a metric to characterize flooding frequency, had the strongest influence on abundances. Salinity was the second strongest environmental parameter driving assemblage variance. This distinguished open estuarine from restricted estuarine, and high freshwater input areas (Pascagoula River) from higher salinities. In addition, replicate sampling indicated a relatively low influence of patchiness on biofacies assignment. However, comparison of live and dead assemblages revealed a strong taphonomic difference, particularly due to dissolution of calcareous specimens in the organic-rich marsh sediments. For paleoenvironmental reconstructions, the nine biofacies of the dead assemblages were used, since they represented the wider spectrum of the fauna and better compared with fossil downcore assemblages.

In Chapter 3, the marsh evolution from two regions in the eastern Mississippi Sound (Grand Bay and Dauphin Island) was addressed using four cores that recovered the whole marsh sequence since emergence from estuarine, reduced, clays in the Late Holocene. Surface abundances of dead the assemblages from subaerial environments of Chapter 2 were used as the training set. A quantitative transfer function relating species abundances to elevation was developed from these data and applied to downcore samples, which yielded paleo-marsh elevations. These paleo-marsh elevations were converted from core depth to age using age-depth models established for each core. Correcting PME for local modern mean sea-level (reconstruction of RSL) indicated that (apparent) sea level was rising faster in Grand Bay than Dauphin Island between 200 and 1900 CE. Different trends between Grand Bay and Dauphin Island from 200 to 1900 CE indicated that local-scale processes drove sediment accumulation at

both Grand Bay sites. The Grand Bay coring sites historically received enhanced sediment influx from the now-cut-off Escatawpa River system, and were sheltered by the now-submerged Grand Batture Island. The effect of marsh-edge erosion was evident in the top core sections representing the 20th century, which were dominated by grey clay. The lithological change from marsh peat to clay was accompanied by an assemblage swing from middle marsh to low marsh, which is direct consequence of a higher inundation frequency. Analyzing multiple cores and regions revealed possible influences on the validity of a transfer function that may have remained undetected if only a single core had been used in favor of increased sample resolution and age-model accuracy.

Chapter 4 focused on the taxonomic inventory and distribution of benthic foraminifera from the Northwestern Shelf and Carnarvon Ramp in Western Australia. The four sampling sites were all on the outer shelf (127–264 m water depth) in a carbonate depositional environment. The results revealed that the small size fraction (125–250 μm) distinguished between deeper and shallower sites, which was likely caused by rapidly changing physical conditions in the upper thermocline and decreasing light intensity to support benthic foraminifera with algal symbionts. The intermediate size fraction (250–850 μm), which distinguished between the Carnarvon Ramp-site in the south and the three sites on the Northwestern Shelf (NWS), indicated limited horizontal transport and migration rates on the outer shelf below the influence of the Leeuwin Current. Similar bottom-water temperatures at the studied sites indicated that water-mass characteristics, biogeographic history or possibly diversity in benthic shelf habitats rather than temperature and depth were responsible for differences between the two shelf regions. Test abundance in the large size fraction (>850 μm) was insufficient to incorporate the fraction into the analysis.

In Chapter 5 the fossil abundances of foraminifera on the Carnarvon Ramp were analyzed from a ~300 m core (35 samples). Relative abundances of infaunal species such as *Uvigerina peregrina*, *Lagena annellatrachia*, *Trifarina brady*, and *Bolivina robusta* were applied to indicate episodes of increased supply of organic matter to the sea floor. Abundance records of epifaunal species such as *Spirorutilus carinatus*, *Rotorbinella* sp., *Hyalinea florenceae*, and *Hanzawaia nipponica* were used to indicate higher oxygenation at the sediment-seafloor interface. A high infaunal ratio was interpreted as absence of the

paleo-Leeuwin Current at the sea surface above the sampling site and likely unhindered upwelling of the cold waters of the Western Australian Current between 3.54 and 0.91 Ma. After a transitional phase, the regime shifted into epifaunal dominance. Flourishing sponges and carbonate sedimentation rate peaked around 0.6 Ma, which was interpreted as an indicator for optimal flow conditions of the Leeuwin Current and Leeuwin Undercurrent on the deep shelf. The epifaunal dominance was punctuated by short increases of infaunal taxa, which likely reflected glacial cycles when sea level was ~100 m lower and the Leeuwin Current was weakened or absent on the outer shelf.

Implications and Future Work

Coastal Reconstructions

Quantitative sea-level studies using transfer functions have improved substantially with the advent of new statistical methods for parameter reconstruction (Barlow et al., 2013; Kemp and Telford, 2015; Cahill et al., 2016). Age-dating was improved by Bayesian modeling, which mainly improved the assessment of uncertainties of age-depth models (Trachsel and Telford, 2017). This, however, does not absolve providing enough input dates for the age model. A common hindrance for an optimal radiocarbon date resolution is cost of analysis. For example Telford et al. (2004) came to the conclusion that 24 radiocarbon dates over an 8 m lake-sediment core was optimal, which was more than most studies use and also more than were available in Chapter 3. The downcore density of fossil assemblage samples in Chapter 3 was also lower than in comparable studies (e.g., Edwards and Horton, 2006; Kemp et al., 2009; Wright et al., 2011; Gerlach et al., 2017). The presented surface training set encompassed a similar or even larger set of samples and physiographical regions than in the literature (Horton et al., 1999). Nevertheless, after analyzing the reconstruction it was evident that large training sets are still prone to under-sampling, depending on the morphology of the sampling region, and may not contain sufficiently close analogues for all fossil samples encountered.

In the present study of paleo-marsh elevation, trends were discernable and differences in trends between cores were clearly observable. Most studies have focused efforts on one core, while making assumptions about the representativeness of the record (e.g., Horton et al., 1999; Edwards and Horton, 2000; Leorri et al., 2008). Having multiple reconstructions available improved recognition of outliers and showed which regions developed in agreement with published records. Thus, low-resolution reconstructions can be a useful tool to indicate environmental change when interpreted in the proper context. With continuing projects and sampling programs in the Gulf of Mexico and Mississippi Sound, the USGS St. Petersburg Coastal and Marine Science Center will collect more surface training set samples and be able to generate new transfer functions, which will decrease the uncertainties on new and existing reconstructions.

Outer Shelf Reconstructions

Chapters 4 and 5 inventoried the Western Australia outer shelf benthic foraminifera and provided a record of foraminiferal faunas over the last 3.54 Ma. Foraminiferal functional groups were used as a tool to interpret evolution of water masses on the Carnarvon Ramp from Pliocene to modern. Scientists are interested in the inception and intensity of the climatic monsoon, which brings heavy summer rains to Northern Australia while overall making the continent dryer (Spooner et al., 2005; Herold et al., 2011; Kuhnt et al., 2015; Christensen et al., 2017). Dust cycles discovered in sediment records (radioactive potassium isotopes) provide a continuous drought indicator, which could be a benchmark for benthic foraminiferal assemblages reacting to monsoonal intensities (Christensen et al., 2017). A closer sample spacing from the presented Core U1460A could easily be accommodated for additional analysis. Furthermore, IODP Expedition 356 provided expanded Pliocene and Pleistocene sequences, which are the geological ages of onset and deepening of northern the hemisphere glaciation. Following the findings of Chapter 5, timing and intensity of the Leeuwin Current moderates the influence of upwelling on the Carnarvon Ramp, which the literature showed also had some variability during the last glacials (Wells et al., 1994; Spooner et al., 2011). An analysis of Pleistocene sedimentary strata from the Northwestern

Shelf and Carnarvon Ramp offers the possibility to assess changes in Leeuwin Current intensity and may provide proof of reduced and expanded warm water-influence during glacial-interglacial cycles. A similar benthic foraminiferal reconstruction was presented by Murgese and De Deckker (2007), who used three piston cores spanning ca. 60 kyr. However, the IODP core material bears potential to extend this time frame greatly. An extension of this work could test benthic assemblages for concordance with Spooner et al. (2011)'s results, who reconstructed sea surface temperatures and Leeuwin Current intensity from planktonic foraminifera using various cores along Western Australia for the last 500 kyrs.

References

Barlow, N.L.M., Shennan, I., Long, A.J., Gehrels, W.R., Saher, M.H., Woodroffe, S.A., Hillier, C., 2013. Salt marshes as late Holocene tide gauges. Global and Planetary Change 106, 90–110. 10.1016/j.gloplacha.2013.03.003

Cahill, N., Kemp, A.C., Horton, B.P., Parnell, A.C., 2016. A Bayesian hierarchical model for reconstructing relative sea level: from raw data to rates of change. Climate of the Past 12, 525–542. 10.5194/cp-12-525-2016

Christensen, B.A., Renema, W., Henderiks, J., De Vleeschouwer, D., Groeneveld, J., Castaneda, I.S., Reuning, L., Bogus, K., Auer, G., Ishiwa, T., McHugh, C.M., Gallagher, S.J., Fulthorpe, C.S., Scientists, I.E., 2017. Indonesian Throughflow drove Australian climate from humid Pliocene to arid Pleistocene. Geophysical Research Letters 44, 6914–6925. 10.1002/2017gl072977

Edwards, R.J., Horton, B.P., 2000. Reconstructing relative sea-level change using UK salt-marsh foraminifera. Marine Geology 169, 41–56. 10.1016/S0025-3227(00)00078-5

Edwards, R.J., Horton, B.P., 2006. Developing detailed records of relative sea-level change using a foraminiferal transfer function: an example from North Norfolk, UK. Philosophical Transactions of the Royal Society A: Mathematical, Physical and Engineering Sciences 364, 973-991. 10.1098/rsta.2006.1749

Gerlach, M.J., Engelhart, S.E., Kemp, A.C., Moyer, R.P., Smoak, J.M., Bernhardt, C.E., Cahill, N., 2017. Reconstructing Common Era relative sea-level change on the Gulf Coast of Florida. Marine Geology 390, 254–269. 10.1016/j.margeo.2017.07.001

Herold, N., Huber, M., Greenwood, D.R., Müller, R.D., Seton, M., 2011. Early to Middle Miocene monsoon climate in Australia. Geology 39, 3–6. 10.1130/g31208.1

Horton, B.P., Edwards, R.J., Lloyd, J.M., 1999. A foraminifera-based transfer function: implications for sea-level studies. Journal of Foraminiferal Research 29, 117–129. 10.2113/gsjfr.29.2.117

Kemp, A.C., Horton, B.P., Culver, S.J., Corbett, D.R., van de Plassche, O., Gehrels, W.R., Douglas, B.C., Parnell, A.C., 2009. Timing and magnitude of recent accelerated sea-level rise (North Carolina, United States). Geology 37, 1035–1038. 10.1130/g30352a.1

Kemp, A.C., Telford, R.J., 2015. Transfer functions, Handbook of Sea-Level Research. John Wiley & Sons, Ltd, pp. 470–499.

Kuhnt, W., Holbourn, A., Xu, J., Opdyke, B., De Deckker, P., Röhl, U., Mudelsee, M., 2015. Southern Hemisphere control on Australian monsoon variability during the late deglaciation and Holocene. Nature Communications 6, 5916. 10.1038/ncomms6916

Leorri, E., Horton, B.P., Cearreta, A., 2008. Development of a foraminifera-based transfer function in the Basque marshes, N. Spain: Implications for sea-level studies in the Bay of Biscay. Marine Geology 251, 60–74. 10.1016/j.margeo.2008.02.005

Murgese, D.S., De Deckker, P., 2007. The Late Quaternary evolution of water masses in the eastern Indian Ocean between Australia and Indonesia, based on benthic foraminifera faunal and carbon isotopes analyses. Palaeogeography, Palaeoclimatology, Palaeoecology 247, 382–401. 10.1016/j.palaeo.2006.11.002

Spooner, M.I., Barrows, T.T., De Deckker, P., Paterne, M., 2005. Palaeoceanography of the Banda Sea, and Late Pleistocene initiation of the Northwest Monsoon. Global and Planetary Change 49, 28–46. 10.1016/j.gloplacha.2005.05.002

Spooner, M.I., De Deckker, P., Barrows, T.T., Fifield, L.K., 2011. The behaviour of the Leeuwin Current offshore NW Australia during the last five glacial–interglacial cycles. Global and Planetary Change 75, 119–132. 10.1016/j.gloplacha.2010.10.015

Telford, R.J., Heegaard, E., Birks, H.J.B., 2004. All age–depth models are wrong: but how badly? Quaternary Science Reviews 23, 1–5. 10.1016/j.quascirev.2003.11.003

Trachsel, M., Telford, R.J., 2017. All age–depth models are wrong, but are getting better. The Holocene 27, 860–869. 10.1177/0959683616675939

Wells, P., Wells, G., Cali, J., Chivas, A., 1994. Response of deep-sea benthic foraminifera to Late Quaternary climate changes, southeast Indian Ocean, offshore Western Australia. Marine Micropaleontology 23, 185–229. 10.1016/0377-8398(94)90013-2

Wright, A.J., Edwards, R.J., van de Plassche, O., 2011. Reassessing transfer-function performance in sea-level reconstruction based on benthic salt-marsh foraminifera from the Atlantic coast of NE North America. Marine Micropaleontology 81, 43–62. 10.1016/j.marmicro.2011.07.003

Appendix A

Appendix A1. Sampling Stations.

Table A1.1 GPS coordinates, elevation, and observed vegetation zone.

Study Area	Station	USGS field activity + project	Sampling dates	Latitude	Longitude	Horizontal error (m)	Elevation (m NAVD88)	Elevation error (m)	National Geodetic Survey benchmark (PID)	Vegetation zone
Grand Bay	GB18-1S	13BIM01	13–20 April 2013	30.382393°	-88.430972°	0.001	0.378	0.047	DO5986, Grand Bay NEER[1]	*J. roemerianus*
Grand Bay	GB18-2S	13BIM01	13–20 April 2013	30.382330°	-88.430962°	0.001	0.305	0.047	DO5986, Grand Bay NEER[1]	*J. roemerianus*
Grand Bay	GB18-3S	13BIM01	13–20 April 2013	30.382138°	-88.431037°	0.001	0.312	0.047	DO5986, Grand Bay NEER[1]	*J. roemerianus*
Grand Bay	GB18-4S	13BIM01	13–20 April 2013	30.381859°	-88.430960°	0.001	0.359	0.047	DO5986, Grand Bay NEER[1]	*J. roemerianus*
Grand Bay	GB18-5S	13BIM01	13–20 April 2013	30.381610°	-88.430690°	0.001	0.321	0.047	DO5986, Grand Bay NEER[1]	*J. roemerianus*
Grand Bay	GB19-1S	13BIM01	13–20 April 2013	30.397490°	-88.398020°	0.001	0.284	0.045	DO5986, Grand Bay NEER[1]	*J. roemerianus*
Grand Bay	GB30S	2014-323-FA (14CCT01)	15–19 Sept 2014	30.382830°	-88.432160°	0.007	0.252	0.014	DO5986, Grand Bay NEER[1]	*J. roemerianus*
Grand Bay	GB34S	2016-331-FA (16CCT03)	14–18 May 2016	30.360670°	-88.415550°	0.001	0.26	0.016	DO5986, Grand Bay NEER[1]	*J. roemerianus*
Grand Bay	GB36S	2014-323-FA (14CCT01)	15–19 Sept 2014	30.379530°	-88.412770°	N/A	0.2552	0.014	DO5986, Grand Bay NEER[1]	*J. roemerianus*
Grand Bay	GB38S	2014-323-FA (14CCT01)	15–19 Sept 2014	30.369340°	-88.419330°	0.005	0.372	0.015	DO5986, Grand Bay NEER[1]	salt panne
Grand Bay	GB39S	2014-323-FA (14CCT01)	15–19 Sept 2014	30.354840°	-88.405690°	N/A	0.255	0.016	DO5986, Grand Bay NEER[1]	*J. roemerianus*
Grand Bay	GB42S	2014-323-FA (14CCT01)	15–19 Sept 2014	30.350440°	-88.396320°	0.002	0.3533	0.017	DO5986, Grand Bay NEER[1]	*S. alterniflora*
Grand Bay	GB49S	2014-323-FA (14CCT01)	15–19 Sept 2014	30.406500°	-88.398670°	0.02	0.3825	0.012	DO5986, Grand Bay NEER[1]	*J. roemerianus*
Grand Bay	GB50S	2014-323-FA (14CCT01)	15–19 Sept 2014	30.398510°	-88.401860°	0.025	0.3317	0.012	DO5986, Grand Bay NEER[1]	*J. roemerianus*

Table A1 (Continued)

Study Area	Station	USGS field activity + project	Sampling dates	Latitude	Longitude	Horizontal error (m)	Elevation (m NAVD88)	Elevation error (m)	National Geodetic Survey benchmark (PID)	Vegetation zone
Grand Bay	GB53S	2014-323-FA (14CCT01)	15–19 Sept 2014	30.384520°	-88.397870°	N/A	0.2445	0.013	DO5986, Grand Bay NEER[1]	*J. roemerianus*
Grand Bay	GB54S	2014-323-FA (14CCT01)	15–19 Sept 2014	30.401820°	-88.379480°	0.017	0.3433	0.011	DO5986, Grand Bay NEER[1]	*J. roemerianus*
Grand Bay	GB55S	2014-323-FA (14CCT01)	15–19 Sept 2014	30.392690°	-88.396640°	0.021	0.2645	0.012	DO5986, Grand Bay NEER[1]	*J. roemerianus*
Grand Bay	GB56S	2014-323-FA (14CCT01)	15–19 Sept 2014	30.389360°	-88.397540°	N/A	0.2645	0.013	DO5986, Grand Bay NEER[1]	*J. roemerianus*
Grand Bay	GB57S	2014-323-FA (14CCT01)	15–19 Sept 2014	30.350600°	-88.396400°	0.003	0.3767	0.017	DO5986, Grand Bay NEER[1]	*J. roemerianus*
Grand Bay	GB60S	2014-323-FA (14CCT01)	15–19 Sept 2014	30.389360°	-88.397540°	N/A	0.2645	0.013	DO5986, Grand Bay NEER[1]	*J. roemerianus*
Grand Bay	GB64S	2014-323-FA (14CCT01)	15–19 Sept 2014	30.387170°	-88.382070°	N/A	0.2293	0.014	DO5986, Grand Bay NEER[1]	*J. roemerianus*
Grand Bay	GB68S	2014-323-FA (14CCT01)	15–19 Sept 2014	30.398480°	-88.401200°	0.017	0.2145	0.012	DO5986, Grand Bay NEER[1]	*S. alterniflora*
Grand Bay	GB280S	2016-331-FA (16CCT03)	14–18 May 2016	30.409870°	-88.398230°	0.006	0.721	0.011	DO5986, Grand Bay NEER[1]	*Pinus elliottii*
Grand Bay	GB281S	2016-331-FA (16CCT03)	14–18 May 2016	30.409460°	-88.398170°	0.001	0.437	0.011	DO5986, Grand Bay NEER[1]	salt panne
Grand Bay	GB282S	2016-331-FA (16CCT03)	14–18 May 2016	30.409580°	-88.397220°	0.001	0.573	0.011	DO5986, Grand Bay NEER[1]	*J. roemerianus*
Grand Bay	GB283S	2016-331-FA (16CCT03)	14–18 May 2016	30.409140°	-88.398960°	0.002	0.415	0.011	DO5986, Grand Bay NEER[1]	*J. roemerianus*
Grand Bay	GB284S	2016-331-FA (16CCT03)	14–18 May 2016	30.408980°	-88.399540°	0.001	0.348	0.011	DO5986, Grand Bay NEER[1]	*J. roemerianus*
Grand Bay	GB285S	2016-331-FA (16CCT03)	14–18 May 2016	30.408690°	-88.399770°	0.002	-0.01	0.011	DO5986, Grand Bay NEER[1]	*S. alterniflora*
Grand Bay	GB286S	2016-331-FA (16CCT03)	14–18 May 2016	30.383400°	-88.432580°	0.001	0.249	0.014	DO5986, Grand Bay NEER[1]	*S. alterniflora*

Table A1 (Continued)

Study Area	Station	USGS field activity + project	Sampling dates	Latitude	Longitude	Horizontal error (m)	Elevation (m NAVD88)	Elevation error (m)	National Geodetic Survey benchmark (PID)	Vegetation zone
Grand Bay	GB287S	2016-331-FA (16CCT03)	14–18 May 2016	30.383540°	-88.432640°	0.001	0.332	0.014	DO5986, Grand Bay NEER[1]	*J. roemerianus*
Grand Bay	GB288S	2016-331-FA (16CCT03)	14–18 May 2016	30.383820°	-88.432820°	0.003	0.34	0.014	DO5986, Grand Bay NEER[1]	*J. roemerianus*
Grand Bay	GB289S	2016-331-FA (16CCT03)	14–18 May 2016	30.384280°	-88.432980°	0.002	0.359	0.014	DO5986, Grand Bay NEER[1]	*D. spicata*
Grand Bay	GB35G	2014-323-FA (14CCT01)	15–19 Sept 2014	30.353030°	-88.414310°	N/A	NR	0.43	-	estuarine
Grand Bay	GB37G	2014-323-FA (14CCT01)	15–19 Sept 2014	30.348330°	-88.411040°	N/A	-0.7	0.43	-	estuarine
Grand Bay	GB40G	2014-323-FA (14CCT01)	15–19 Sept 2014	30.398260°	-88.406070°	N/A	-0.7	0.43	-	estuarine
Grand Bay	GB43G	2014-323-FA (14CCT01)	15–19 Sept 2014	30.340100°	-88.402800°	N/A	-2.3	0.43	-	estuarine
Grand Bay	GB44G	2014-323-FA (14CCT01)	15–19 Sept 2014	30.409780°	-88.402460°	N/A	-2	0.43	-	estuarine
Grand Bay	GB45G	2014-323-FA (14CCT01)	15–19 Sept 2014	30.396250°	-88.401470°	N/A	-1	0.43	-	estuarine
Grand Bay	GB58G	2014-323-FA (14CCT01)	15–19 Sept 2014	30.385680°	-88.396240°	N/A	-2.4	0.43	-	estuarine
Grand Bay	GB59G	2014-323-FA (14CCT01)	15–19 Sept 2014	30.378890°	-88.395870°	N/A	-0.9	0.43	-	estuarine
Grand Bay	GB61G	2014-323-FA (14CCT01)	15–19 Sept 2014	30.374390°	-88.392230°	N/A	-1.7	0.43	-	estuarine
Grand Bay	GB62G	2014-323-FA (14CCT01)	15–19 Sept 2014	30.369950°	-88.388020°	N/A	-1.6	0.43	-	estuarine
Grand Bay	GB63G	2014-323-FA (14CCT01)	15–19 Sept 2014	30.368250°	-88.382160°	N/A	-1.6	0.43	-	estuarine
Grand Bay	GB67G	2014-323-FA (14CCT01)	15–19 Sept 2014	30.348330°	-88.411040°	N/A	-0.7	0.43	-	estuarine

Table A1 (Continued)

Study Area	Station	USGS field activity + project	Sampling dates	Latitude	Longitude	Horizontal error (m)	Elevation (m NAVD88)	Elevation error (m)	National Geodetic Survey benchmark (PID)	Vegetation zone
Grand Bay	GB70G	2014-323-FA (14CCT01)	15–19 Sept 2014	30.369950°	-88.388020°	N/A	-1.6	0.43	-	estuarine
Pascagoula	PG71S	2014-323-FA (14CCT01)	15–19 Sept 2014	30.430420°	-88.602240°	0.016	0.2594	0.016	DL8822, Pascagoula HWY90[2]	*J. roemerianus/ S. alterniflora*
Pascagoula	PG72S	2014-323-FA (14CCT01)	15–19 Sept 2014	30.414790°	-88.600780°	N/A	0.175	0.015	DL8822, Pascagoula HWY90[2]	*J. roemerianus/ S. alterniflora*
Pascagoula	PG73S	2014-323-FA (14CCT01)	15–19 Sept 2014	30.441640°	-88.598450°	N/A	0.2502	0.018	DL8822, Pascagoula HWY90[2]	*J. roemerianus/ S. alterniflora*
Pascagoula	PG74S	2014-323-FA (14CCT01)	15–19 Sept 2014	30.357990°	-88.600340°	0.021	0.3136	0.013	DL8822, Pascagoula HWY90[2]	*J. roemerianus*
Pascagoula	PG75S	2014-323-FA (14CCT01)	15–19 Sept 2014	30.404600°	-88.597300°	0.037	0.2172	0.013	DL8822, Pascagoula HWY90[2]	*J. roemerianus/ S. alterniflora*
Pascagoula	PG76S	2014-323-FA (14CCT01)	15–19 Sept 2014	30.377950°	-88.604310°	0.017	0.2999	0.012	DL8822, Pascagoula HWY90[2]	*J. roemerianus/ S. alterniflora*
Pascagoula	PG77S	2014-323-FA (14CCT01)	15–19 Sept 2014	30.369140°	-88.597110°	N/A	0.2938	0.010	DL8822, Pascagoula HWY90[2]	*J. roemerianus*
Pascagoula	PG80S	2014-323-FA (14CCT01)	15–19 Sept 2014	30.387670°	-88.601770°	0.018	0.1741	0.012	DL8822, Pascagoula HWY90[2]	*J. roemerianus/ S. alterniflora*
Pascagoula	PG81S	2014-323-FA (14CCT01)	15–19 Sept 2014	30.398930°	-88.597250°	N/A	0.2642	0.013	DL8822, Pascagoula HWY90[2]	*J. roemerianus*

Table A1 (Continued)

Study Area	Station	USGS field activity + project	Sampling dates	Latitude	Longitude	Horizontal error (m)	Elevation (m NAVD88)	Elevation error (m)	National Geodetic Survey benchmark (PID)	Vegetation zone
Pascagoula	PG92S	2014-323-FA (14CCT01)	15–19 Sept 2014	30.414790°	-88.600780°	0.017	0.175	0.015	DL8822, Pascagoula HWY90[2]	*J. roemerianus/ S. alterniflora*
Pascagoula	PG100S	2014-323-FA (14CCT01)	15–19 Sept 2014	30.414490°	-88.600880°	N/A	0.0612	0.015	DL8822, Pascagoula HWY90[2]	*J. roemerianus/ S. alterniflora*
Pascagoula	PG82G	2014-323-FA (14CCT01)	15–19 Sept 2014	30.366130°	-88.595180°	0	-1	0.43	-	estuarine
Pascagoula	PG84G	2014-323-FA (14CCT01)	15–19 Sept 2014	30.371110°	-88.593370°	0	-0.8	0.43	-	estuarine
Pascagoula	PG85G	2014-323-FA (14CCT01)	15–19 Sept 2014	30.349960°	-88.593450°	0	-1.4	0.43	-	estuarine
Pascagoula	PG87G	2014-323-FA (14CCT01)	15–19 Sept 2014	30.340010°	-88.591520°	0	-1.6	0.43	-	estuarine
Pascagoula	PG89G	2014-323-FA (14CCT01)	15–19 Sept 2014	30.322970°	-88.587360°	0	-2.4	0.43	-	estuarine
Pascagoula	PG91G	2014-323-FA (14CCT01)	15–19 Sept 2014	30.386305°	-88.582532°	0	-0.7	0.43	-	estuarine
Fowl River	FR17-1S	13BIM01	13–20 April 2013	30.361244°	-88.168578°	0.002	0.539	0.025	BH1755, East Dauphin Island[3]	tidal flat
Fowl River	FR17-2S	13BIM01	13–20 April 2013	30.361502°	-88.168185°	0.002	0.612	0.025	BH1755, East Dauphin Island[3]	*J. roemerianus*
Fowl River	FR17-3S	13BIM01	13–20 April 2013	30.361637°	-88.168117°	0.002	0.585	0.025	BH1755, East Dauphin Island[3]	*J. roemerianus*
Fowl River	FR17-4S	13BIM01	13–20 April 2013	30.361950°	-88.168073°	0.002	0.615	0.025	BH1755, East Dauphin Island[3]	*J. roemerianus*
Fowl River	FR17-5S	13BIM01	13–20 April 2013	30.361965°	-88.167558°	0.002	0.675	0.025	BH1755, East Dauphin Island[3]	*S. patens*
Fowl River	FR17-6S	13BIM01	13–20 April 2013	30.362205°	-88.167097°	0.002	0.898	0.025	BH1755, East Dauphin Island[3]	*S. patens/S. alterniflora*

Table A1 (Continued)

Study Area	Station	USGS field activity + project	Sampling dates	Latitude	Longitude	Horizontal error (m)	Elevation (m NAVD88)	Elevation error (m)	National Geodetic Survey benchmark (PID)	Vegetation zone
Fowl River	FR26S	13BIM01	13–20 April 2013	30.362197°	-88.186485°	0.002	0.68	0.026	BH1755, East Dauphin Island[3]	*J. roemerianus*
Dauphin Island	DA05S	13BIM01	13–20 April 2013	30.254527°	-88.100605°	0.001	0.281	0.012	BH1755, East Dauphin Island[3]	*J. roemerianus*
Dauphin Island	DA04S	13BIM01	13–20 April 2013	30.275522°	-88.116970°	0.001	0.152	0.015	BH1755, East Dauphin Island[3]	*J. roemerianus/S. alterniflora*
Dauphin Island	DA13S	13BIM01	13–20 April 2013	30.253574°	-88.134217°	0.003	0.122	0.012	BH1755, East Dauphin Island[3]	*J. roemerianus/S. alterniflora*
Dauphin Island	DA27S	13BIM01	13–20 April 2013	30.275682°	-88.116585°	0.002	0.232	0.015	BH1755, East Dauphin Island[3]	*J. roemerianus*
Dauphin Island	DA30S	2015-322-FA (15BIM09)	11–21 Aug. 2015	30.276740°	-88.117270°	0.001	0.1799	0.016	BH1755, East Dauphin Island[3]	*J. roemerianus*
Dauphin Island	DA31S	2015-322-FA (15BIM09)	11–21 Aug. 2015	30.273790°	-88.117090°	0.001	0.1721	0.016	BH1755, East Dauphin Island[3]	*J. roemerianus/S. alterniflora*
Dauphin Island	DA32S	2015-322-FA (15BIM09)	11–21 Aug. 2015	30.273720°	-88.117310°	0.002	0.184	0.016	BH1755, East Dauphin Island[3]	*J. roemerianus*
Dauphin Island	DA34S	2015-322-FA (15BIM09)	11–21 Aug. 2015	30.272670°	-88.110000°	0.002	0.0963	0.015	BH1755, East Dauphin Island[3]	*S. alterniflora*
Dauphin Island	DA35S	2015-322-FA (15BIM09)	11–21 Aug. 2015	30.271291°	-88.110370°	0.001	0.2465	0.015	BH1755, East Dauphin Island[3]	*S. alterniflora*
Dauphin Island	DA36S	2015-322-FA (15BIM09)	11–21 Aug. 2015	30.268440°	-88.102710°	0.056	0.5166	0.014	BH1755, East Dauphin Island[3]	*J. roemerianus*
Dauphin Island	DA37S	2015-322-FA (15BIM09)	11–21 Aug. 2015	30.2683681°	-88.1027075°	0.056	0.5166	0.014	BH1755, East Dauphin Island[3]	*J. roemerianus*
Dauphin Island	DA38S	2015-322-FA (15BIM09)	11–21 Aug. 2015	30.267980°	-88.102580°	0.002	0.2613	0.014	BH1755, East Dauphin Island[3]	*J. roemerianus*
Dauphin Island	DA39S	2015-322-FA (15BIM09)	11–21 Aug. 2015	30.267670°	-88.102910°	0.002	0.149	0.014	BH1755, East Dauphin Island[3]	*S. alterniflora*
Dauphin Island	DA40S	2015-322-FA (15BIM09)	11–21 Aug. 2015	30.2559909°	-88.125549°	0.001	0.1638	0.016	BH1755, East Dauphin Island[3]	*S. alterniflora*

Table A1 (Continued)

Study Area	Station	USGS field activity + project	Sampling dates	Latitude	Longitude	Horizontal error (m)	Elevation (m NAVD88)	Elevation error (m)	National Geodetic Survey benchmark (PID)	Vegetation zone
Dauphin Island	DA42S	2015-322-FA (15BIM09)	11–21 Aug. 2015	30.253210°	-88.134560°	0.002	0.1898	0.016	BH1755, East Dauphin Island[3]	*S. alterniflora*
Dauphin Island	DA46S	2015-322-FA (15BIM09)	11–21 Aug. 2015	30.252740°	-88.134390°	0.001	0.1075	0.017	WDAU, parking lot end of Bienville Blvd[4]	*S. alterniflora*
Dauphin Island	DA138G	2015-322-FA (15BIM09)	11–21 Aug. 2015	30.283960°	-88.094783°	N/A	-3.9	0.100	-	estuarine
Dauphin Island	DA189G	2015-322-FA (15BIM09)	11–21 Aug. 2015	30.265424°	-88.121304°	N/A	-2.2	0.100	-	estuarine

[1]https://www.ngs.noaa.gov/cgi-bin/ds_mark.prl?PidBox=DO5986
[2]https://www.ngs.noaa.gov/cgi-bin/ds_mark.prl?PidBox=DL8822
[3]https://www.ngs.noaa.gov/cgi-bin/ds_mark.prl?PidBox=BH1755
[4]unpublished

Appendix A2. Sediment Data.

Table A2.1 Grain-size data, organic matter, and pore water salinity for each sampling station. NR= Not recorded.

Study Area	Station	Mean (μm)	SAND (%)	SILT (%)	CLAY (%)	LOI OC (%)	Salinity
Grand Bay	GB18-1S		NR			16.69	NR
Grand Bay	GB18-2S		NR			NR	NR
Grand Bay	GB18-3S		NR			NR	NR
Grand Bay	GB18-4S		NR			NR	NR
Grand Bay	GB18-5S		NR			16.69	NR
Grand Bay	GB19-1S		NR			NR	NR
Grand Bay	GB30S	18.796	23.452	67.376	9.172	13.18	72.910
Grand Bay	GB34S	18.771	25.043	63.811	11.146	10.48	18.760
Grand Bay	GB36S	23.359	32.105	58.618	9.277	5.97	26.260
Grand Bay	GB38S	41.880	36.029	60.116	3.855	0.65	45.000
Grand Bay	GB39S	8.440	10.267	70.626	19.107	9.29	26.760
Grand Bay	GB42S	35.111	42.318	51.576	6.106	3.20	18.870
Grand Bay	GB49S	24.786	30.036	61.662	8.302	18.58	14.100
Grand Bay	GB50S	15.480	17.138	72.345	10.517	10.62	19.420
Grand Bay	GB53S	27.512	29.460	63.984	6.556	6.33	24.360
Grand Bay	GB54S	13.028	12.992	74.622	12.386	8.13	22.210
Grand Bay	GB55S	15.369	19.222	68.782	11.996	11.12	24.940
Grand Bay	GB56S	38.630	50.049	44.344	5.608	6.50	26.250
Grand Bay	GB57S	34.531	43.374	50.221	6.404	2.85	19.890
Grand Bay	GB60S	17.648	22.074	68.013	9.914	10.66	26.250
Grand Bay	GB64S	10.943	17.533	66.429	16.039	8.66	23.510
Grand Bay	GB68S	19.340	24.285	65.738	9.978	6.46	23.780
Grand Bay	GB280S	28.313	31.572	62.153	6.275	9.46	NR
Grand Bay	GB281S	35.377	34.941	59.479	5.580	2.01	NR
Grand Bay	GB282S	42.237	44.652	50.424	4.925	5.18	NR
Grand Bay	GB283S	7.301	6.014	75.759	18.227	13.61	15.360
Grand Bay	GB284S	24.846	23.949	69.115	6.936	2.89	14.340
Grand Bay	GB285S	19.857	23.198	67.463	9.339	5.36	15.890
Grand Bay	GB286S	9.415	9.706	73.967	16.327	9.50	16.080
Grand Bay	GB287S	64.776	64.831	31.002	4.166	3.49	15.090
Grand Bay	GB288S	20.223	26.308	64.430	9.262	17.41	15.830

Table A2.1 (Continued)

Study Area	Station	Mean (μm)	SAND (%)	SILT (%)	CLAY (%)	LOI OC (%)	Salinity
Grand Bay	GB289S	39.464	43.307	51.365	5.328	5.26	15.050
Grand Bay	GB35G	18.796	23.452	67.376	9.172	13.18	26.950
Grand Bay	GB37G	43.924	45.800	49.213	4.988	0.69	26.620
Grand Bay	GB40G	58.651	58.074	37.934	3.992	1.82	28.230
Grand Bay	GB43G	80.996	66.487	30.189	3.324	0.78	26.030
Grand Bay	GB44G	17.294	19.583	69.509	10.908	2.09	28.480
Grand Bay	GB45G	40.599	47.167	44.370	8.463	1.45	27.820
Grand Bay	GB58G	29.202	34.166	58.527	7.308	2.01	27.160
Grand Bay	GB59G	73.404	67.578	30.160	2.262	0.69	26.830
Grand Bay	GB61G	25.315	24.766	67.936	7.298	1.64	26.930
Grand Bay	GB62G	84.799	72.620	24.831	2.549	0.79	26.970
Grand Bay	GB63G	70.014	67.078	29.344	3.577	0.85	26.990
Grand Bay	GB67G	68.991	65.239	32.094	2.667	0.64	26.620
Grand Bay	GB70G	84.595	72.711	24.233	3.056	0.67	26.970
Pascagoula	PG71S	19.054	27.797	62.730	9.473	13.02	0.930
Pascagoula	PG72S	17.795	24.758	65.834	9.408	8.24	6.600
Pascagoula	PG73S	15.156	18.202	71.348	10.450	11.95	2.540
Pascagoula	PG74S	25.671	33.829	57.839	8.332	6.50	20.090
Pascagoula	PG75S	22.346	30.290	60.964	8.746	12.31	7.800
Pascagoula	PG76S	29.058	37.243	55.461	7.296	6.79	18.000
Pascagoula	PG77S	20.671	26.770	64.026	9.204	11.92	18.290
Pascagoula	PG80S	20.815	27.442	63.926	8.632	8.57	8.940
Pascagoula	PG81S	30.671	36.996	55.386	7.618	NR	7.620
Pascagoula	PG92S	17.693	22.521	68.093	9.386	10.80	6.600
Pascagoula	PG100S	14.074	20.548	67.435	12.017	15.35	5.690
Pascagoula	PG82G	15.006	20.127	67.978	11.895	2.56	15.920
Pascagoula	PG84G	14.873	22.372	64.882	12.746	2.54	16.870
Pascagoula	PG85G	91.171	74.167	22.292	3.541	1.11	21.120
Pascagoula	PG87G	31.586	45.540	45.190	9.271	1.71	21.020
Pascagoula	PG89G	11.209	11.369	74.018	14.613	2.92	23.600
Pascagoula	PG91G	9.072	8.239	74.309	17.452	3.73	18.110

Table A2.1 (Continued)

Study Area	Station	Mean (μm)	SAND (%)	SILT (%)	CLAY (%)	LOI OC (%)	Salinity
Fowl River	FR17-1S		NR			NR	NR
Fowl River	FR17-2S		NR			NR	NR
Fowl River	FR17-3S		NR			NR	NR
Fowl River	FR17-4S		NR			NR	NR
Fowl River	FR17-5S		NR			NR	NR
Fowl River	FR17-6S		NR			NR	NR
Fowl River	FR26S	105.116	84.560	13.477	1.963	0.72	NR
Dauphin Island	DA04S		NR			8.85	NR
Dauphin Island	DA05S		NR			1.19	NR
Dauphin Island	DA13S	7.828	7.022	74.903	18.075	7.22	NR
Dauphin Island	DA27S	5.690	3.524	74.035	22.441	7.22	NR
Dauphin Island	DA30S	102.735	60.059	31.881	8.060	4.83	22.980
Dauphin Island	DA31S	7.988	9.156	67.256	23.588	12.09	24.800
Dauphin Island	DA32S	10.230	13.028	69.473	17.499	11.92	30.960
Dauphin Island	DA34S	27.123	37.519	43.685	18.796	8.45	NR
Dauphin Island	DA35S	10.098	13.597	68.169	18.234	10.48	25.340
Dauphin Island	DA36S	14.904	22.288	58.194	19.519	6.18	NR
Dauphin Island	DA37S	15.824	22.364	58.154	19.482	5.68	NR
Dauphin Island	DA38S	13.278	23.070	59.896	17.034	12.61	NR
Dauphin Island	DA39S	261.644	80.504	14.832	4.663	3.60	25.590
Dauphin Island	DA40S	7.504	9.973	68.419	21.608	NR	25.220
Dauphin Island	DA42S	133.310	77.211	16.352	6.437	5.52	25.210
Dauphin Island	DA46S	306.069	94.472	4.259	1.268	1.48	27.040
Dauphin Island	DA138G	8.628	12.821	65.579	21.600	4.15	28.490
Dauphin Island	DA189G	10.101	17.770	61.688	20.542	4.51	26.550

Appendix A3. Foraminiferal Data.

Table A3.1 Census data of live foraminifera

	14CCT01 GB30S A	14CCT01 GB30S B	14CCT01 GB35G A	14CCT01 GB35G B	14CCT01 GB36S A	14CCT01 GB36S B	14CCT01 GB37G A	14CCT01 GB37G B	14CCT01 GB38S A	14CCT01 GB38S B	14CCT01 GB39S A	14CCT01 GB39S B	14CCT01 GB40G A
Live (rB stained)/Dead	Live	Live	Live	Live	Live	Live	Live	Live	Live	Live	Live	Live	Live
Percent examined	50	25	25	25	50	25	50	50	100	100	100	100	6.25
Vol (cm^3)	37	50	33	31	47	52	34	27	34	40	43	46	38
Pseudothurammina limnetis													
Ammoastuta inepta	21	29			7								
Ammotium salsum/ Ammobaculites exiguus group	43	14	5	3	2	2	16	10					5
Ammobaculites cf. A. *foliaceus*													
Ammotium cassis	2				4								
Arenoparrella mexicana	24	33			7	4					7	2	
Entzia macrescens													
Haplophragmoides bonplandi													
Haplophragmoides manilaensis													
Haplophragmoides wilberti									1				
Leptohalysis scotti			1										
Paratrochammina simplissima			2	4			3	1					
Siphotrochammina lobata													
Trochammina sp. A		3				5					1	1	
Tiphotrocha comprimata		2									1	2	
Trochammina inflata	4	3			8	2			2	5	1	3	
Trochamminita irregularis													
Textularia earlandi													
Ammodiscus sp.													
Ammodiscus tenuis													
Affinetrina alcidi													
Miliammina fusca		9	17	8	9	50	9	8		2	4		3
Miliolinella subrotunda													
Ammonia parkinsoniana							5						
Ammonia tepida			2	1			12	4					
Cribroelphidium excavatum							2						2
Cribroelphidium poeyanum													
Elphidium mexicanum													
Haynesina germanica									23				
Helenina anderseni													
Other Aggltutinated													
Other Calcareous													

Table A3.1 (continued)

	14CCT01 GB40G B	14CCT01 GB42S A	14CCT01 GB42S B	14CCT01 GB43G A	14CCT01 GB43G B	14CCT01 GB44G A	14CCT01 GB44G B	14CCT01 GB45G A	14CCT01 GB45G B	14CCT01 GB49S A	14CCT01 GB49S B	14CCT01 GB50S A	14CCT01 GB50S B
Live (rB stained)/Dead	Live	Live	Live	Live	Live	Live	Live	Live	Live	Live	Live	Live	Live
Percent examined	6.25	25	25	12.5	12.5	25	12.5	12.5	12.5	100	100	100	100
Vol (cm^3)	43	50	43	33	33	41	42	45	43	44	45	43	43
Pseudothurammina limnetis				1									
Ammoastuta inepta				2								7	6
Ammotium salsum/ Ammobaculites exiguus group	10	2		62	84	23	22	33	43		1		
Ammobaculites cf. A. *foliaceus*													
Ammotium cassis													
Arenoparrella mexicana										2	4	6	3
Entzia macrescens													
Haplophragmoides bonplandi													
Haplophragmoides manilaensis													
Haplophragmoides wilberti													
Leptohalysis scotti		3	1				1						
Paratrochammina simplissima				2	2			1					
Siphotrochammina lobata													
Trochammina sp. A		1										5	
Tiphotrocha comprimata										6		4	7
Trochammina inflata										1		1	2
Trochamminita irregularis													
Textularia earlandi													
Ammodiscus sp.													
Ammodiscus tenuis													
Affinetrina alcidi													
Miliammina fusca				1	3	21	14	6	17	4	3	4	
Miliolinella subrotunda													
Ammonia parkinsoniana													
Ammonia tepida				20	22		1	8	8			2	
Cribroelphidium excavatum					7								
Cribroelphidium poeyanum									1				
Elphidium mexicanum													
Haynesina germanica				1	1	2		1					
Helenina anderseni												5	
Other Aggltutinated													
Other Calcareous													

Table A3.1 (continued)

	14CCT01 GB53S A	14CCT01 GB53S B	14CCT01 GB54S A	14CCT01 GB54S B	14CCT01 GB55S A	14CCT01 GB55S B	14CCT01 GB56S A	14CCT01 GB56S B	14CCT01 GB57S A	14CCT01 GB57S B	14CCT01 GB58G A	14CCT01 GB58G B	14CCT01 GB59G A
Live (rB stained)/Dead	Live	Live	Live	Live	Live	Live	Live	Live	Live	Live	Live	Live	Live
Percent examined	50	50	25	100	100	100	50	25	25	25	25	100	12.5
Vol (cm^3)	40	47	46	41	50	35	52	53	41	34	37	50	38
Pseudothurammina limnetis													
Ammoastuta inepta	7	7	17	25	14	5	3	4	11	8			
Ammotium salsum/													
Ammobaculites exiguus group	22	22					6	1	6		7		5
Ammobaculites cf. A. *foliaceus*													
Ammotium cassis			1	1					4	3			
Arenoparrella mexicana	14	24	24	15	10	9	9	11	32	18			
Entzia macrescens													
Haplophragmoides bonplandi													
Haplophragmoides manilaensis													
Haplophragmoides wilberti			10	2									
Leptohalysis scotti									1				
Paratrochammina simplissima											5	4	25
Siphotrochammina lobata									1				
Trochammina sp. A	1	6		3	3	6	10	7	2	4			
Tiphotrocha comprimata	7	13	5	9	2	1	6	3		1			
Trochammina inflata	6	7	18	38	15	7	8	4	6				
Trochamminita irregularis													
Textularia earlandi													
Ammodiscus sp.													
Ammodiscus tenuis													
Affinetrina alcidi													
Miliammina fusca	14	7		2			22	11	19	40		2	15
Miliolinella subrotunda													
Ammonia parkinsoniana											1		
Ammonia tepida												4	6
Cribroelphidium excavatum													1
Cribroelphidium poeyanum													2
Elphidium mexicanum													
Haynesina germanica	3										3	24	
Helenina anderseni													
Other Aggltutinated													
Other Calcareous													

Table A3.1 (continued)

	14CCT01 GB59G B	14CCT01 GB60S A	14CCT01 GB60S B	14CCT01 GB61G A	14CCT01 GB61G B	14CCT01 GB62G A	14CCT01 GB62G B	14CCT01 GB63G A	14CCT01 GB63G B	14CCT01 GB64S A	14CCT01 GB64S B	14CCT01 GB67G A	14CCT01 GB67G B
Live (rB stained)/Dead	Live	Live	Live	Live	Live	Live	Live	Live	Live	Live	Live	Live	Live
Percent examined	25	100	50	25	25	12.5	12.5	12.5	12.5	50	100	100	50
Vol (cm^3)	36	45	45	48	46	37	34	37	34	50	50	31	25
Pseudothurammina limnetis													
Ammoastuta inepta		11	8							2			
Ammotium salsum/ Ammobaculites exiguus group	4	1	1	5	16		3	43	51	5	5	46	28
Ammobaculites cf. A. *foliaceus*													
Ammotium cassis										4			
Arenoparrella mexicana		19	14							1			
Entzia macrescens													
Haplophragmoides bonplandi													
Haplophragmoides manilaensis													
Haplophragmoides wilberti													
Leptohalysis scotti													
Paratrochammina simplissima	16			13	5	29	16	43	27			8	5
Siphotrochammina lobata											1		
Trochammina sp. A		5	6							2	7		
Tiphotrocha comprimata		7	7							6	4		
Trochammina inflata		7	4							1	4		
Trochamminita irregularis													
Textularia earlandi													
Ammodiscus sp.													
Ammodiscus tenuis													
Affinetrina alcidi													
Miliammina fusca	22	21	17	9			4			26	16	15	
Miliolinella subrotunda									1				
Ammonia parkinsoniana	2			5	2	2	1					19	12
Ammonia tepida	2			31	16	44	18	77	88	1	2	26	53
Cribroelphidium excavatum	3			13	6	8	2	12	2	3		3	12
Cribroelphidium poeyanum					2	1		5	2			2	2
Elphidium mexicanum													
Haynesina germanica	3			16	42	1	3		1				
Helenina anderseni													
Other Aggltutinated													
Other Calcareous													

Table A3.1 (continued)

	14CCT01 GB68S A	14CCT01 GB68S B	14CCT01 GB70G A	14CCT01 GB70G B	14CCT01 PG71S A	14CCT01 PG71S B	14CCT01 PG72S A	14CCT01 PG72S B	14CCT01 PG73S A	14CCT01 PG73S B	14CCT01 PG74S A	14CCT01 PG74S B	14CCT01 PG75S A
Live (rB stained)/Dead	Live	Live	Live	Live	Live	Live	Live	Live	Live	Live	Live	Live	Live
Percent examined	25	50	12.5	12.5	100	100	100	100	100	100	100	100	100
Vol (cm^3)	48	50	41	33	37	41	45	37	45	43	35	34	50
Pseudothurammina limnetis													
Ammoastuta inepta	2	6			7	38	11		19	7	57	64	77
Ammotium salsum/ Ammobaculites exiguus group	16	8	10	2		4	56	29				8	1
Ammobaculites cf. A. *foliaceus*													
Ammotium cassis	1												
Arenoparrella mexicana											74	26	
Entzia macrescens		3											
Haplophragmoides bonplandi					2	5	6						
Haplophragmoides manilaensis					1								
Haplophragmoides wilberti													
Leptohalysis scotti				1									
Paratrochammina simplissima			53	47									
Siphotrochammina lobata													
Trochammina sp. A	1	1											
Tiphotrocha comprimata	2	1										2	
Trochammina inflata											19	5	
Trochamminita irregularis													
Textularia earlandi													
Ammodiscus sp.													
Ammodiscus tenuis													
Affinetrina alcidi													
Miliammina fusca	14	11	8	7	3	5	12	4	1		7	7	1
Miliolinella subrotunda			1										
Ammonia parkinsoniana			2										
Ammonia tepida			55	49		1	6						
Cribroelphidium excavatum			7	1									
Cribroelphidium poeyanum				3									
Elphidium mexicanum													
Haynesina germanica	1		5										
Helenina anderseni													
Other Aggltutinated													
Other Calcareous													

Table A3.1 (continued)

	14CCT01 PG75S B	14CCT01 PG76S A	14CCT01 PG76S B	14CCT01 PG77S A	14CCT01 PG77S B	14CCT01 PG80S A	14CCT01 PG80S B	14CCT01 PG81S A	14CCT01 PG81S B	14CCT01 PG82G A	14CCT01 PG82G B	14CCT01 PG84G A	14CCT01 PG84G B
Live (rB stained)/Dead	Live	Live	Live	Live	Live	Live	Live	Live	Live	Live	Live	Live	Live
Percent examined	100	100	100	100	100	100	100	100	100	100	100	50	100
Vol (cm^3)	50	35	40	43	47	45	40	37	33	37	35	35	35
Pseudothurammina limnetis													
Ammoastuta inepta	130	191	88	47	177	8	8						
Ammotium salsum/ Ammobaculites exiguus group	6	3	6			4	1			55	26	68	175
Ammobaculites cf. A. *foliaceus*													
Ammotium cassis												1	
Arenoparrella mexicana	8		1	1	33								
Entzia macrescens													
Haplophragmoides bonplandi			4			1	4						
Haplophragmoides manilaensis					1								
Haplophragmoides wilberti													
Leptohalysis scotti													
Paratrochammina simplissima										1			
Siphotrochammina lobata													
Trochammina sp. A				2	1								
Tiphotrocha comprimata					3		1						
Trochammina inflata					1								
Trochamminita irregularis													
Textularia earlandi													
Ammodiscus sp.													
Ammodiscus tenuis													
Affinetrina alcidi													
Miliammina fusca	2	3				1				83	35	37	50
Miliolinella subrotunda													
Ammonia parkinsoniana													
Ammonia tepida										5			10
Cribroelphidium excavatum										2			31
Cribroelphidium poeyanum													
Elphidium mexicanum													
Haynesina germanica										16	4	4	21
Helenina anderseni													
Other Aggltutinated													
Other Calcareous													

Table A3.1 (continued)

	14CCT01 PG85G A	14CCT01 PG85G B	14CCT01 PG87G A	14CCT01 PG87G B	14CCT01 PG89G A	14CCT01 PG89G B	14CCT01 PG91G	14CCT01 PG92S A	14CCT01 PG92S B	14CCT01 PG100S A	14CCT01 PG100S B	13BIM01 GB18-1S A	13BIM01 GB18-1S B
Live (rB stained)/Dead	Live	Live	Live	Live	Live	Live	Live	Live	Live	Live	Live	Live	Live
Percent examined	6.25	3.125	6.25	3.125	12.5	12.5	100	100	100	100	100	100	100
Vol (cm^3)	33	39	30	35	35	33	40	44	38	39	46	28	21
Pseudothurammina limnetis													1
Ammoastuta inepta								1	1		2		1
Ammotium salsum/ Ammobaculites exiguus group	27	19	44	25		1	25	18	21	3	2	3	3
Ammobaculites cf. A. *foliaceus*													
Ammotium cassis	1	2										1	1
Arenoparrella mexicana												44	26
Entzia macrescens									1			1	1
Haplophragmoides bonplandi													
Haplophragmoides manilaensis													
Haplophragmoides wilberti												14	23
Leptohalysis scotti													
Paratrochammina simplissima	3	4	1		11	14							
Siphotrochammina lobata												1	
Trochammina sp. A													
Tiphotrocha comprimata												3	
Trochammina inflata												61	27
Trochamminita irregularis													
Textularia earlandi													
Ammodiscus sp.													
Ammodiscus tenuis													
Affinetrina alcidi													
Miliammina fusca	5	4	2				23	4	3			22	27
Miliolinella subrotunda		2											
Ammonia parkinsoniana			1	1			2						
Ammonia tepida	86	58	62	30	76	58	79					3	3
Cribroelphidium excavatum	3	2	4	3			10		4				1
Cribroelphidium poeyanum	1			1			7						
Elphidium mexicanum													
Haynesina germanica	1		3	2	1	1	45						
Helenina anderseni													
Other Aggltutinated													
Other Calcareous													

Table A3.1 (continued)

	13BIM01 GB18-2S A	13BIM01 GB18-2S B	13BIM01 GB18-3S A	13BIM01 GB18-3S B	13BIM01 GB18-4S A	13BIM01 GB18-4S B	13BIM01 GB18-5S A	13BIM01 GB18-5S B	13BIM01 GB19-1S A	13BIM01 GB19-1S B	13BIM01 FR17-1S A	13BIM01 FR17-1S B	13BIM01 FR17-2S A
Live (rB stained)/Dead	Live	Live	Live	Live	Live	Live	Live	Live	Live	Live	Live	Live	Live
Percent examined	50	100	15.625	30.5	100	100	100	100	100	100	75	37.5	50
Vol (cm^3)	20	21	18	16	7	16	9	7	8	17	16	23	25
Pseudothurammina limnetis					8		1						
Ammoastuta inepta	2	2		1		1			1	2	5	6	1
Ammotium salsum/ Ammobaculites exiguus group	5	8	7	13	24	20	25	7	48	110	35	51	14
Ammobaculites cf. A. *foliaceus*													
Ammotium cassis	3	6		4	7	14			15	2	1	8	3
Arenoparrella mexicana	25	40	9	6	50	64	53	71	5	13	154	115	61
Entzia macrescens						6		1	1				
Haplophragmoides bonplandi													
Haplophragmoides manilaensis													
Haplophragmoides wilberti		1			3	4			4	1	9	21	
Leptohalysis scotti													
Paratrochammina simplissima			1										
Siphotrochammina lobata	3	1					2	7	7	1	2	1	
Trochammina sp. A													
Tiphotrocha comprimata	1	5	1		25	40	58	56	26	14	10	3	7
Trochammina inflata	7	18	13	13	75	167	44	37	21	13	31	20	19
Trochamminita irregularis													
Textularia earlandi						1							
Ammodiscus sp.													
Ammodiscus tenuis					2	2				1			
Affinetrina alcidi			1								2		
Miliammina fusca	70	162	30	17	26	23	9	10	113	149	14	20	204
Miliolinella subrotunda													
Ammonia parkinsoniana													
Ammonia tepida	23	15	66	49	49	58	4	10	60	2	3	1	185
Cribroelphidium excavatum	2								21		3	13	7
Cribroelphidium poeyanum													
Elphidium mexicanum													
Haynesina germanica									1				
Helenina anderseni				2	3				11		1		
Other Aggltutinated	1				3								
Other Calcareous		1	4		4								

Table A3.1 (continued)

	13BIM01 FR17-2S B	13BIM01 FR17-3S	13BIM01 FR17-4S A	13BIM01 FR17-4S B	13BIM01 FR17-5S	13BIM01 FR17-6S A	13BIM01 FR17-6S B	13BIM01 FR26S A	13BIM01 FR26S B	13BIM01 DA04S A	13BIM01 DA04S B	13BIM01 DA05S	13BIM01 DA13S
Live (rB stained)/Dead	Live	Live	Live	Live	Live	Live	Live	Live	Live	Live	Live	Live	Live
Percent examined	100	50	75	50	100	100	100	25	12.5	50	50	37.5	37.5
Vol (cm^3)	15	14	7	10	26	13	7	20	23	37.5	38	7	23
Pseudothurammina limnetis						25	15						
Ammoastuta inepta	5	5	3	1				2	3		5	6	
Ammotium salsum/ Ammobaculites exiguus group	21	26	151	84				18	48			41	23
Ammobaculites cf. A. *foliaceus*													
Ammotium cassis	4												
Arenoparrella mexicana	167	132	105	103	1			34	4		1	46	
Entzia macrescens							3						
Haplophragmoides bonplandi							1						
Haplophragmoides manilaensis													
Haplophragmoides wilberti	1		1	3	2	84	2	4			1	6	1
Leptohalysis scotti													
Paratrochammina simplissima								47	28				
Siphotrochammina lobata						4						2	3
Trochammina sp. A													
Tiphotrocha comprimata	8	7	12	31	2				2		1	82	
Trochammina inflata	23	8	5	6	6		7	17	1			11	8
Trochamminita irregularis						2							
Textularia earlandi												1	
Ammodiscus sp.													
Ammodiscus tenuis													
Affinetrina alcidi				1									
Miliammina fusca	237	80	206	156	21		1	113	143	2	10	78	183
Miliolinella subrotunda													
Ammonia parkinsoniana								5	3				
Ammonia tepida	101	27	18	47				8	1		1	5	1
Cribroelphidium excavatum	33	10	3	2				25	17		1	16	
Cribroelphidium poeyanum													
Elphidium mexicanum													
Haynesina germanica												44	
Helenina anderseni				3									
Other Aggltutinated													
Other Calcareous								1					

Table A3.1 (continued)

	13BIM01 DA27S	15BIM09 DA30S A	15BIM09 DA30S B	15BIM09 DA31S A	15BIM09 DA31S B	15BIM09 DA32S A	15BIM09 DA32S B	15BIM09 DA34S A	15BIM09 DA34S B	15BIM09 DA35S A	15BIM09 DA35S B	15BIM09 DA36S A	15BIM09 DA36S B
Live (rB stained)/Dead	Live	Live	Live	Live	Live	Live	Live	Live	Live	Live	Live	Live	Live
Percent examined	18.8	25	25	50	50	50	50	50	25	50	50	50	50
Vol (cm^3)	32	29.5	35	29	24	27.5	26	36	35	35	38	25	27
Pseudothurammina limnetis													
Ammoastuta inepta								13	7	15			
Ammotium salsum/ Ammobaculites exiguus group	3	14	9	3	6			15	4		5	1	
Ammobaculites cf. A. *foliaceus*													
Ammotium cassis			1										
Arenoparrella mexicana	9		3					19	35			36	25
Entzia macrescens													
Haplophragmoides bonplandi													
Haplophragmoides manilaensis												2	1
Haplophragmoides wilberti	3											18	42
Leptohalysis scotti												1	
Paratrochammina simplissima													
Siphotrochammina lobata	1												
Trochammina sp. A								4				1	
Tiphotrocha comprimata									2				
Trochammina inflata								10	8			7	4
Trochamminita irregularis													
Textularia earlandi													
Ammodiscus sp.		1						4	2				
Ammodiscus tenuis	1	1						4	2				
Affinetrina alcidi													
Miliammina fusca	2	15	19	1						2		2	
Miliolinella subrotunda													
Ammonia parkinsoniana													
Ammonia tepida			2										
Cribroelphidium excavatum													
Cribroelphidium poeyanum													
Elphidium mexicanum													
Haynesina germanica													
Helenina anderseni													
Other Aggltutinated													
Other Calcareous													

Table A3.1 (continued)

	15BIM09 DA37S A	15BIM09 DA37S B	15BIM09 DA38S A	15BIM09 DA38S B	15BIM09 DA39S A	15BIM09 DA39S B	15BIM09 DA40S A	15BIM09 DA40S B	15BIM09 DA42S A	15BIM09 DA42S B	15BIM09 DA46S A	15BIM09 DA46S B	15BIM09 DA138G A
Live (rB stained)/Dead	Live	Live	Live	Live	Live	Live	Live	Live	Live	Live	Live	Live	Live
Percent examined	25	25	25	25	25	12.5	50	50	50	50	25	50	12.5
Vol (cm^3)	31	21	29	32	30	27	25	19	20	20	26	26	30
Pseudothurammina limnetis													
Ammoastuta inepta													
Ammotium salsum/													
Ammobaculites exiguus group				2		5			6	13	7	7	
Ammobaculites cf. A. *foliaceus*									3	2			
Ammotium cassis												1	
Arenoparrella mexicana	34	9	9	7							2	2	
Entzia macrescens													
Haplophragmoides bonplandi													
Haplophragmoides manilaensis	1	2											
Haplophragmoides wilberti	1	10											
Leptohalysis scotti												1	
Paratrochammina simplissima													
Siphotrochammina lobata													
Trochammina sp. A													
Tiphotrocha comprimata											2	12	
Trochammina inflata	18	6									3	12	
Trochamminita irregularis													
Textularia earlandi													
Ammodiscus sp.													
Ammodiscus tenuis													
Affinetrina alcidi													
Miliammina fusca	2								1	5	5	10	
Miliolinella subrotunda													
Ammonia parkinsoniana													1
Ammonia tepida													6
Cribroelphidium excavatum													1
Cribroelphidium poeyanum													
Elphidium mexicanum													
Haynesina germanica													1
Helenina anderseni													
Other Aggltutinated													
Other Calcareous													

Table A3.1 (continued)

	15BIM09 DA138G B	15BIM09 DA189G A	15BIM09 DA189G B	16CCT03 GB34S A	16CCT03 GB34S B	16CCT03 GB280S A	16CCT03 GB280S B	16CCT03 GB281S A	16CCT03 GB281S B	16CCT03 GB282S A	16CCT03 GB282S B	16CCT03 GB283S A	16CCT03 GB283S B
Live (rB stained)/Dead	Live	Live	Live	Live	Live	Live	Live	Live	Live	Live	Live	Live	Live
Percent examined	12.5	1.5625	1.5625	100	100	25	25	100	100	25	25	12.5	12.5
Vol (cm^3)	31	71	67.5	50	45	40	35	25	28	35	32	50	42
Pseudothurammina limnetis													
Ammoastuta inepta				1								2	2
Ammotium salsum/													
Ammobaculites exiguus group	1	1	1	1								83	219
Ammobaculites cf. A. *foliaceus*													
Ammotium cassis													
Arenoparrella mexicana				104	245							7	23
Entzia macrescens				3						25	17	5	1
Haplophragmoides bonplandi													
Haplophragmoides manilaensis													
Haplophragmoides wilberti												3	10
Leptohalysis scotti													
Paratrochammina simplissima													
Siphotrochammina lobata										4	5		
Trochammina sp. A				7	4							6	11
Tiphotrocha comprimata				7	1			1				21	25
Trochammina inflata				12	4							8	11
Trochamminita irregularis						5	4						
Textularia earlandi													
Ammodiscus sp.													
Ammodiscus tenuis				4	1								
Affinetrina alcidi													
Miliammina fusca		1		20	22			1		1	5	13	22
Miliolinella subrotunda		1											
Ammonia parkinsoniana	1	15	11										
Ammonia tepida	13	12	3	6									
Cribroelphidium excavatum	5	11	6										1
Cribroelphidium poeyanum		1	1										
Elphidium mexicanum	2												
Haynesina germanica	1	2	1										
Helenina anderseni					5							6	27
Other Aggltutinated													
Other Calcareous													

Table A3.1 (continued)

	16CCT03 GB284S A	16CCT03 GB284S B	16CCT03 GB285S A	16CCT03 GB285S B	16CCT03 GB286S A	16CCT03 GB286S B	16CCT03 GB287S A	16CCT03 GB287S B	16CCT03 GB288S A	16CCT03 GB288S B	16CCT03 GB289S A
Live (rB stained)/Dead	Live	Live	Live	Live	Live	Live	Live	Live	Live	Live	Live
Percent examined	12.5	12.5	12.5	12.5	50	50	6.25	6.25	12.5	12.5	6.25
Vol (cm^3)	33	39	35	35	39	45	35	30	40	50	35
Pseudothurammina limnetis											
Ammoastuta inepta	18	9			9	4	5	11			19
Ammotium salsum/											
Ammobaculites exiguus group	12	9	10	9	3	3	21	20	4	7	62
Ammobaculites cf. A. *foliaceus*											
Ammotium cassis		2									3
Arenoparrella mexicana	21	18	1		14	11	14	21	12	11	14
Entzia macrescens	4	1			5	2					
Haplophragmoides bonplandi											
Haplophragmoides manilaensis		2									
Haplophragmoides wilberti	5	4				1	1				1
Leptohalysis scotti											
Paratrochammina simplissima											
Siphotrochammina lobata						1	2				
Trochammina sp. A			1		1		14	5	3	1	12
Tiphotrocha comprimata	2						2		1	7	1
Trochammina inflata	4	5						1	1		8
Trochamminita irregularis											
Textularia earlandi											
Ammodiscus sp.											
Ammodiscus tenuis											
Affinetrina alcidi											
Miliammina fusca	6	5	3		9	10	4	3		3	27
Miliolinella subrotunda											
Ammonia parkinsoniana											
Ammonia tepida	52	19									
Cribroelphidium excavatum	9	3									
Cribroelphidium poeyanum											
Elphidium mexicanum											
Haynesina germanica	11	4									
Helenina anderseni	28	1								2	3
Other Aggltutinated											
Other Calcareous											

Table A3.2 Census data of dead foraminifera

	14CCT01 GB30S A	14CCT01 GB30S B	14CCT01 GB35G A	14CCT01 GB35G B	14CCT01 GB36S A	14CCT01 GB36S B	14CCT01 GB37G A	14CCT01 GB37G B	14CCT01 GB38S A	14CCT01 GB38S B	14CCT01 GB39S A
Live (rB stained)/Dead	Dead	Dead	Dead	Dead	Dead	Dead	Dead	Dead	Dead	Dead	Dead
Percent examined	50	25	25	25	50	25	50	50	100	100	100
Vol (cm^3)	37	50	33	31	47	52	34	27	34	40	43
Pseudothurammina limnetis	3	10			7	5				2	
Ammoastuta inepta	26	27			8	1					
Ammotium salsum/ Ammobaculites exiguus group	36	12	142	197	45	31	228	276	2		
Ammobaculites cf. A. *foliaceus*											
Ammobaculites crassus											
Ammotium cassis	1			1	22	5		1			
Arenoparrella mexicana	46	74	2	3	36	14	6	9	21	32	26
Entzia macrescens	9	20			3						
Haplophragmoides bonplandi											
Haplophragmoides manilaensis											
Haplophragmoides wilberti		1			3	1	2		73	159	
Leptohalysis scotti				2							
Paratrochammina simplissima			23	30	2	3	32	24			
Siphotrochammina lobata					10	7			6	12	
Trochammina sp. A	2	11	2		14	6			3	6	
Tiphotrocha comprimata	31	31			67	15					75
Trochammina inflata	13	27	1		53	20	1		56	95	54
Trochamminita irregularis											
Textularia earlandi											
Ammodiscus sp.		1		1	8						
Ammodiscus tenuis		1		1	8						
Affinetrina alcidi											
Miliammina fusca	58	39	43	27	152	104	21	22	12	58	29
Miliammina petila											
Miliolinella subrotunda			2								
Pyrgo nasutua			1								
Quinqueloculina jugosa											
Ammonia parkinsoniana			55	45			5	9			
Ammonia tepida			6	3			19				
Cribroelphidium excavatum			1	10	6		8				
Cribroelphidium poeyanum			8	11			6	1			
Elphidium gunteri			4	5							
Elphidium mexicanum											
Haynesina germanica			13								

Table A3.2 (continued)

	14CCT01 GB30S A	14CCT01 GB30S B	14CCT01 GB35G A	14CCT01 GB35G B	14CCT01 GB36S A	14CCT01 GB36S B	14CCT01 GB37G A	14CCT01 GB37G B	14CCT01 GB38S A	14CCT01 GB38S B	14CCT01 GB39S A
Helenina anderseni											
Other Aggltutinated											
Other Calcareous											
Indeterminate Planktonic		1									

Table A3.2 (continued)

	14CCT01 GB39S B	14CCT01 GB40G A	14CCT01 GB40G B	14CCT01 GB42S A	14CCT01 GB42S B	14CCT01 GB43G A	14CCT01 GB43G B	14CCT01 GB44G A	14CCT01 GB44G B	14CCT01 GB45G A	14CCT01 GB45G B
Live (rB stained)/Dead	Dead	Dead	Dead	Dead	Dead	Dead	Dead	Dead	Dead	Dead	Dead
Percent examined	100	6.25	6.25	25	25	12.5	12.5	25	12.5	12.5	12.5
Vol (cm^3)	46	38	43	50	43	33	33	41	42	45	43
Pseudothurammina limnetis	2								1		
Ammoastuta inepta		1	2								7
Ammotium salsum/ Ammobaculites exiguus group		205	211	304	318	157	155	172	172	286	317
Ammobaculites cf. A. *foliaceus*											
Ammobaculites crassus											
Ammotium cassis		6	31					8			
Arenoparrella mexicana	10	4	8	6	9	2		2	3		1
Entzia macrescens		1									
Haplophragmoides bonplandi											
Haplophragmoides manilaensis											
Haplophragmoides wilberti		3	5	1	5			3			
Leptohalysis scotti			1		3						
Paratrochammina simplissima		6	1	23	22	47	37	5	1	14	13
Siphotrochammina lobata	1		5		1						
Trochammina sp. A	4		2					1			
Tiphotrocha comprimata	57	13	1	4	1						
Trochammina inflata	39	5	1	1	2						
Trochamminita irregularis											
Textularia earlandi											
Ammodiscus sp.											
Ammodiscus tenuis											
Affinetrina alcidi											
Miliammina fusca	4	239	265	203	180	1		118	102	100	148
Miliammina petila											
Miliolinella subrotunda						11					
Pyrgo nasutua											
Quinqueloculina jugosa						3	2				
Ammonia parkinsoniana	1		2				1			32	27
Ammonia tepida				1		110	58	4		108	28
Cribroelphidium excavatum						34	16	1		12	17
Cribroelphidium poeyanum						1	1				7
Elphidium gunteri										4	
Elphidium mexicanum											
Haynesina germanica						1	1			10	6

Table A3.2 (continued)

	14CCT01 GB39S B	14CCT01 GB40G A	14CCT01 GB40G B	14CCT01 GB42S A	14CCT01 GB42S B	14CCT01 GB43G A	14CCT01 GB43G B	14CCT01 GB44G A	14CCT01 GB44G B	14CCT01 GB45G A	14CCT01 GB45G B
Helenina anderseni											
Other Aggltutinated											
Other Calcareous											
Indeterminate Planktonic											

Table A3.2 (continued)

	14CCT01 GB49S A	14CCT01 GB49S B	14CCT01 GB50S A	14CCT01 GB50S B	14CCT01 GB53S A	14CCT01 GB53S B	14CCT01 GB54S A	14CCT01 GB54S B	14CCT01 GB55S A	14CCT01 GB55S B	14CCT01 GB56S A
Live (rB stained)/Dead	Dead	Dead	Dead	Dead	Dead	Dead	Dead	Dead	Dead	Dead	Dead
Percent examined	100	100	100	100	50	50	25	100	100	100	50
Vol (cm^3)	44	45	43	43	40	47	46	41	50	35	52
Pseudothurammina limnetis	2		18	10	8	4	26	57	18	17	1
Ammoastuta inepta			1	2	2	4	7	1	6	1	2
Ammotium salsum/ Ammobaculites exiguus group		90	1		15	11	9		1		8
Ammobaculites cf. A. *foliaceus*											
Ammobaculites crassus											
Ammotium cassis					2		6	1			7
Arenoparrella mexicana	2	7	32	13	22	26	73	105	70	33	20
Entzia macrescens	16	33	11	6	3	4	4	15	11	2	4
Haplophragmoides bonplandi											
Haplophragmoides manilaensis									3		1
Haplophragmoides wilberti		2			2	2				1	
Leptohalysis scotti											
Paratrochammina simplissima		3									1
Siphotrochammina lobata							7		3		
Trochammina sp. A	7	59	9		7	15	7	13	19	6	5
Tiphotrocha comprimata	223	6	66	57	54	47	62	95	98	53	101
Trochammina inflata	35		18	10	34	24	42	40	85	72	27
Trochamminita irregularis											
Textularia earlandi											
Ammodiscus sp.			1		4	3	1	1		2	1
Ammodiscus tenuis			1		4	3	1	1		2	1
Affinetrina alcidi											
Miliammina fusca	11	79	4	8	43	30	24	1	25	10	145
Miliammina petila											
Miliolinella subrotunda											
Pyrgo nasutua											
Quinqueloculina jugosa											
Ammonia parkinsoniana		1									
Ammonia tepida			3								
Cribroelphidium excavatum											
Cribroelphidium poeyanum											
Elphidium gunteri											
Elphidium mexicanum											
Haynesina germanica			1								1

Table A3.2 (continued)

	14CCT01 GB49S A	14CCT01 GB49S B	14CCT01 GB50S A	14CCT01 GB50S B	14CCT01 GB53S A	14CCT01 GB53S B	14CCT01 GB54S A	14CCT01 GB54S B	14CCT01 GB55S A	14CCT01 GB55S B	14CCT01 GB56S A
Helenina anderseni											
Other Aggltutinated											
Other Calcareous											
Indeterminate Planktonic											

Table A3.2 (continued)

	14CCT01 GB56S B	14CCT01 GB57S A	14CCT01 GB57S B	14CCT01 GB58G A	14CCT01 GB58G B	14CCT01 GB59G A	14CCT01 GB59G B	14CCT01 GB60S A	14CCT01 GB60S B	14CCT01 GB61G A	14CCT01 GB61G B
Live (rB stained)/Dead	Dead	Dead	Dead	Dead	Dead	Dead	Dead	Dead	Dead	Dead	Dead
Percent examined	25	25	25	25	100	12.5	25	100	50	25	25
Vol (cm^3)	53	41	34	37	50	38	36	45	45	48	46
Pseudothurammina limnetis								10	6		
Ammoastuta inepta	3	16	7		3			2	8		
Ammotium salsum/ Ammobaculites exiguus group	1	40	26	318	657	116	120	7		253	193
Ammobaculites cf. A. *foliaceus*											
Ammobaculites crassus											
Ammotium cassis		18	24		5	10		2			
Arenoparrella mexicana	28	53	50	1	11	3	4	42	34		2
Entzia macrescens	1	6	3					23	12		
Haplophragmoides bonplandi											
Haplophragmoides manilaensis											
Haplophragmoides wilberti	1	1			3	1	5	1			
Leptohalysis scotti		1		3	1						
Paratrochammina simplissima		7	1	42	133	80	133		1	77	71
Siphotrochammina lobata		3					2	4			1
Trochammina sp. A	17	3	4	1			2	23	17		
Tiphotrocha comprimata	85	11	4		2		1	192	102		
Trochammina inflata	49	11	7	1		1	2	76	35		
Trochamminita irregularis											
Textularia earlandi											
Ammodiscus sp.		1	1	1	1			1	1		
Ammodiscus tenuis		1	1	1	1			1	1		
Affinetrina alcidi											
Miliammina fusca	139	148	99	54	125	30	71	61	69	163	63
Miliammina petila											
Miliolinella subrotunda						4	1			46	28
Pyrgo nasutua											
Quinqueloculina jugosa											
Ammonia parkinsoniana				8	35	2	5			4	
Ammonia tepida				20	59	14	8		2	153	60
Cribroelphidium excavatum				4		7	12			8	26
Cribroelphidium poeyanum				3	18	16	14			37	13
Elphidium gunteri				2			1			1	
Elphidium mexicanum											
Haynesina germanica					9	2				7	6

Table A3.2 (continued)

	14CCT01 GB56S B	14CCT01 GB57S A	14CCT01 GB57S B	14CCT01 GB58G A	14CCT01 GB58G B	14CCT01 GB59G A	14CCT01 GB59G B	14CCT01 GB60S A	14CCT01 GB60S B	14CCT01 GB61G A	14CCT01 GB61G B
Helenina anderseni											
Other Aggltutinated											
Other Calcareous											
Indeterminate Planktonic											

Table A3.2 (continued)

	14CCT01 GB62G A	14CCT01 GB62G B	14CCT01 GB63G A	14CCT01 GB63G B	14CCT01 GB64S A	14CCT01 GB64S B	14CCT01 GB67G A	14CCT01 GB67G B	14CCT01 GB68S A	14CCT01 GB68S B	14CCT01 GB70G A
Live (rB stained)/Dead	Dead	Dead	Dead	Dead	Dead	Dead	Dead	Dead	Dead	Dead	Dead
Percent examined	12.5	12.5	12.5	12.5	50	100	100	50	25	50	12.5
Vol (cm^3)	37	34	37	34	50	50	31	25	48	50	41
Pseudothurammina limnetis					3	17					
Ammoastuta inepta					1				2	1	
Ammotium salsum/ Ammobaculites exiguus group	368	249	165	134	36	35	419	175	124	42	434
Ammobaculites cf. A. *foliaceus*											
Ammobaculites crassus											
Ammotium cassis					4	4				3	
Arenoparrella mexicana					12	20	12	1	14	24	
Entzia macrescens									29	13	1
Haplophragmoides bonplandi											
Haplophragmoides manilaensis											
Haplophragmoides wilberti					8	9			5	4	
Leptohalysis scotti											2
Paratrochammina simplissima	59	52	31	41			43	13			84
Siphotrochammina lobata					5	14			2		
Trochammina sp. A					3	34	4		14	6	
Tiphotrocha comprimata					35	81			41	38	
Trochammina inflata					41	85			17	17	
Trochamminita irregularis											
Textularia earlandi						1					
Ammodiscus sp.					2	7					
Ammodiscus tenuis					2	7					
Affinetrina alcidi											
Miliammina fusca	18	15	5	7	120	311	37	16	206	94	33
Miliammina petila											
Miliolinella subrotunda	24	5	39	26				4			23
Pyrgo nasutua											
Quinqueloculina jugosa	5		7	14							5
Ammonia parkinsoniana	2						14	9			
Ammonia tepida	75	57	175	212	1			45			120
Cribroelphidium excavatum	12	8	22	21			3	15			27
Cribroelphidium poeyanum	5	3	27	18			3	7			15
Elphidium gunteri											1
Elphidium mexicanum											
Haynesina germanica	1			1							

Table A3.2 (continued)

	14CCT01 GB62G A	14CCT01 GB62G B	14CCT01 GB63G A	14CCT01 GB63G B	14CCT01 GB64S A	14CCT01 GB64S B	14CCT01 GB67G A	14CCT01 GB67G B	14CCT01 GB68S A	14CCT01 GB68S B	14CCT01 GB70G A
Helenina anderseni											
Other Aggltutinated											
Other Calcareous											
Indeterminate Planktonic											

Table A3.2 (continued)

	14CCT01 GB70G B	14CCT01 PG71S A	14CCT01 PG71S B	14CCT01 PG72S A	14CCT01 PG72S B	14CCT01 PG73S A	14CCT01 PG73S B	14CCT01 PG74S A	14CCT01 PG74S B	14CCT01 PG75S A	14CCT01 PG75S B
Live (rB stained)/Dead	Dead	Dead	Dead	Dead	Dead	Dead	Dead	Dead	Dead	Dead	Dead
Percent examined	12.5	100	100	100	100	100	100	100	100	100	100
Vol (cm^3)	33	37	41	45	37	45	43	35	34	50	50
Pseudothurammina limnetis		10	9	10	12		6	1			4
Ammoastuta inepta		38	116	42	74	28	41	14	29	61	92
Ammotium salsum/ Ammobaculites exiguus group	220	6	22	251	291		2	16	103	9	
Ammobaculites cf. A. *foliaceus*											
Ammobaculites crassus		2	3						2		
Ammotium cassis											
Arenoparrella mexicana	1			2				34	85	5	17
Entzia macrescens											
Haplophragmoides bonplandi		24	52	49	48	7	13	11	11	8	11
Haplophragmoides manilaensis				1							1
Haplophragmoides wilberti									16		
Leptohalysis scotti											
Paratrochammina simplissima	49			2	7				1		
Siphotrochammina lobata											
Trochammina sp. A								1		1	
Tiphotrocha comprimata					8			7	6	5	15
Trochammina inflata								28	23		
Trochamminita irregularis											
Textularia earlandi									1		
Ammodiscus sp.											
Ammodiscus tenuis											
Affinetrina alcidi											
Miliammina fusca	15	22	113	376	297	5	7	93	316	22	40
Miliammina petila											
Miliolinella subrotunda	9										
Pyrgo nasutua											
Quinqueloculina jugosa	2							1			
Ammonia parkinsoniana	2			1							
Ammonia tepida	48		3	8				1			
Cribroelphidium excavatum	20			4							
Cribroelphidium poeyanum	9										
Elphidium gunteri											
Elphidium mexicanum											
Haynesina germanica											

Table A3.2 (continued)

	14CCT01 GB70G B	14CCT01 PG71S A	14CCT01 PG71S B	14CCT01 PG72S A	14CCT01 PG72S B	14CCT01 PG73S A	14CCT01 PG73S B	14CCT01 PG74S A	14CCT01 PG74S B	14CCT01 PG75S A	14CCT01 PG75S B
Helenina anderseni											
Other Aggltutinated											
Other Calcareous		1									
Indeterminate Planktonic		1									

Table A3.2 (continued)

	14CCT01 PG76S A	14CCT01 PG76S B	14CCT01 PG77S A	14CCT01 PG77S B	14CCT01 PG80S A	14CCT01 PG80S B	14CCT01 PG81S A	14CCT01 PG81S B	14CCT01 PG82G A	14CCT01 PG82G B	14CCT01 PG84G A
Live (rB stained)/Dead	Dead	Dead	Dead	Dead	Dead	Dead	Dead	Dead	Dead	Dead	Dead
Percent examined	100	100	100	100	100	100	100	100	100	100	50
Vol (cm^3)	35	40	43	47	45	40	37	33	37	35	35
Pseudothurammina limnetis	2		14	31	2	4					
Ammoastuta inepta	101	75	7	30		18	1	14			
Ammotium salsum/ Ammobaculites exiguus group	82	63			22	23	1	3	173	120	232
Ammobaculites cf. A. *foliaceus*											
Ammobaculites crassus											
Ammotium cassis											5
Arenoparrella mexicana	5	1	11	47	2						1
Entzia macrescens							3	5			
Haplophragmoides bonplandi	12	10	1	13	10	9					
Haplophragmoides manilaensis	1		1	2							
Haplophragmoides wilberti				4	1						
Leptohalysis scotti											
Paratrochammina simplissima											
Siphotrochammina lobata											
Trochammina sp. A			4	11	2	6		1			
Tiphotrocha comprimata	1		21	71	6	10					
Trochammina inflata				2			1				
Trochamminita irregularis											
Textularia earlandi											
Ammodiscus sp.											
Ammodiscus tenuis											
Affinetrina alcidi											
Miliammina fusca	93	79	6	8	16	27	3	13	179	72	148
Miliammina petila											
Miliolinella subrotunda										1	
Pyrgo nasutua											
Quinqueloculina jugosa											
Ammonia parkinsoniana									1		1
Ammonia tepida					2				5	2	3
Cribroelphidium excavatum									1	1	
Cribroelphidium poeyanum											
Elphidium gunteri											
Elphidium mexicanum											
Haynesina germanica									3	1	3

Table A3.2 (continued)

	14CCT01 PG76S A	14CCT01 PG76S B	14CCT01 PG77S A	14CCT01 PG77S B	14CCT01 PG80S A	14CCT01 PG80S B	14CCT01 PG81S A	14CCT01 PG81S B	14CCT01 PG82G A	14CCT01 PG82G B	14CCT01 PG84G A
Helenina anderseni											
Other Aggltutinated											
Other Calcareous											
Indeterminate Planktonic											

Table A3.2 (continued)

	14CCT01 PG84G B	14CCT01 PG85G A	14CCT01 PG85G B	14CCT01 PG87G A	14CCT01 PG87G B	14CCT01 PG89G A	14CCT01 PG89G B	14CCT01 PG91G	14CCT01 PG92S A	14CCT01 PG92S B	14CCT01 PG100S A
Live (rB stained)/Dead	Dead	Dead	Dead	Dead	Dead	Dead	Dead	Dead	Dead	Dead	Dead
Percent examined	100	6.25	3.125	6.25	3.125	12.5	12.5	100	100	100	100
Vol (cm^3)	35	33	39	30	35	35	33	40	44	38	39
Pseudothurammina limnetis									6	7	8
Ammoastuta inepta					1	1			20	15	6
Ammotium salsum/ Ammobaculites exiguus group	461	344	294	177	250	2	27	88	112	102	6
Ammobaculites cf. A. *foliaceus*											
Ammobaculites crassus											
Ammotium cassis			10								
Arenoparrella mexicana						1					
Entzia macrescens									24	19	5
Haplophragmoides bonplandi											
Haplophragmoides manilaensis											
Haplophragmoides wilberti				1							
Leptohalysis scotti											
Paratrochammina simplissima		5	8	19	17	20	39			1	
Siphotrochammina lobata											
Trochammina sp. A									1	2	
Tiphotrocha comprimata											
Trochammina inflata											
Trochamminita irregularis											
Textularia earlandi											
Ammodiscus sp.											
Ammodiscus tenuis											
Affinetrina alcidi											
Miliammina fusca	266	85	52	20	32	2	3	40	142	138	19
Miliammina petila											
Miliolinella subrotunda			6	90	38						
Pyrgo nasutua											
Quinqueloculina jugosa				5							
Ammonia parkinsoniana	4	6	2	2	3	1		8			
Ammonia tepida	7	150	79	354	232	353	522	158	6	3	
Cribroelphidium excavatum	29	10	8	25	15	2	9	9			
Cribroelphidium poeyanum		6	3	7	4	2		26			
Elphidium gunteri											
Elphidium mexicanum											
Haynesina germanica	2	8	15	10	14	6	1	53			

Table A3.2 (continued)

	14CCT01 PG84G B	14CCT01 PG85G A	14CCT01 PG85G B	14CCT01 PG87G A	14CCT01 PG87G B	14CCT01 PG89G A	14CCT01 PG89G B	14CCT01 PG91G	14CCT01 PG92S A	14CCT01 PG92S B	14CCT01 PG100S A
Helenina anderseni											
Other Aggltutinated											
Other Calcareous											
Indeterminate Planktonic											

Table A3.2 (continued)

	14CCT01 PG100S B	13BIM01 GB18-1S A	13BIM01 GB18-1S B	13BIM01 GB18-2S A	13BIM01 GB18-2S B	13BIM01 GB18-3S A	13BIM01 GB18-3S B	13BIM01 GB18-4S A	13BIM01 GB18-4S B	13BIM01 GB18-5S A	13BIM01 GB18-5S B
Live (rB stained)/Dead	Dead	Dead	Dead	Dead	Dead	Dead	Dead	Dead	Dead	Dead	Dead
Percent examined	100	100	100	50	100	15.625	30.5	100	100	100	100
Vol (cm^3)	46	28	21	20	21	18	16	7	16	9	7
Pseudothurammina limnetis	5				6			41	83	2	1
Ammoastuta inepta	8	2		16	14	3	1	1	3		
Ammotium salsum/ Ammobaculites exiguus group	11	1	2	12	45	1	11	23	77	12	46
Ammobaculites cf. A. *foliaceus*											
Ammobaculites crassus											
Ammotium cassis		2	1	5	19		3	6	50		1
Arenoparrella mexicana		146	69	162	395	21	43	14	66	70	52
Entzia macrescens	5	1	3	1	14	3		1			2
Haplophragmoides bonplandi		1		1		1					
Haplophragmoides manilaensis											
Haplophragmoides wilberti		77	61	44	55	12	19	1	5		3
Leptohalysis scotti											
Paratrochammina simplissima			1	2	2	2			1		
Siphotrochammina lobata			18	21	35	3	4		11	4	11
Trochammina sp. A											
Tiphotrocha comprimata		8	4	33	80	1	9	7	27	89	180
Trochammina inflata		52	33	54	154	10	13	12	110	42	73
Trochamminita irregularis											
Textularia earlandi									2		
Ammodiscus sp.											
Ammodiscus tenuis						1		3	9		
Affinetrina alcidi						1					
Miliammina fusca	19	14	4	61	81	14	51	57	132	37	129
Miliammina petila											
Miliolinella subrotunda											
Pyrgo nasutua											
Quinqueloculina jugosa											
Ammonia parkinsoniana											
Ammonia tepida				1		11	7	6			
Cribroelphidium excavatum				1				1			
Cribroelphidium poeyanum		1									
Elphidium gunteri											
Elphidium mexicanum											

Table A3.2 (continued)

	14CCT01 PG100S B	13BIM01 GB18-1S A	13BIM01 GB18-1S B	13BIM01 GB18-2S A	13BIM01 GB18-2S B	13BIM01 GB18-3S A	13BIM01 GB18-3S B	13BIM01 GB18-4S A	13BIM01 GB18-4S B	13BIM01 GB18-5S A	13BIM01 GB18-5S B
Haynesina germanica											
Helenina anderseni											
Other Aggltutinated				4	2			3	3		1
Other Calcareous	1							1			
Indeterminate Planktonic	1										

Table A3.2 (continued)

	13BIM01 GB19-1S A	13BIM01 GB19-1S B	13BIM01 FR17-1S A	13BIM01 FR17-1S B	13BIM01 FR17-2S A	13BIM01 FR17-2S B	13BIM01 FR17-3S	13BIM01 FR17-4S A	13BIM01 FR17-4S B	13BIM01 FR17-5S	13BIM01 FR17-6S A
Live (rB stained)/Dead	Dead	Dead	Dead	Dead	Dead	Dead	Dead	Dead	Dead	Dead	Dead
Percent examined	100	100	75	37.5	50	100	50	75	50	100	100
Vol (cm^3)	8	17	16	23	25	15	14	7	10	26	13
Pseudothurammina limnetis	4	1				2			1	9	259
Ammoastuta inepta			14	7	10	12	3	3	6		1
Ammotium salsum/ Ammobaculites exiguus group	31	30	31	29	49	56	80	80	120	2	
Ammobaculites cf. A. *foliaceus*											
Ammobaculites crassus											
Ammotium cassis	15	3	3	9	3	5				1	
Arenoparrella mexicana	7	9	297	219	96	85	126	120	101	25	2
Entzia macrescens	1		3	4			3	5		15	3
Haplophragmoides bonplandi										17	
Haplophragmoides manilaensis											
Haplophragmoides wilberti			143	62	1		21		3	87	19
Leptohalysis scotti											
Paratrochammina simplissima											
Siphotrochammina lobata	3	12	7				1			14	4
Trochammina sp. A											
Tiphotrocha comprimata	10	39	21	17	11	12	18	21	21	10	
Trochammina inflata	6	25	32	35	1	8	4	1	4	86	8
Trochamminita irregularis			1								4
Textularia earlandi											
Ammodiscus sp.											
Ammodiscus tenuis	6	2									
Affinetrina alcidi											
Miliammina fusca	80	79	15	29	107	124	80	67	90	29	
Miliammina petila											
Miliolinella subrotunda											
Pyrgo nasutua											
Quinqueloculina jugosa											
Ammonia parkinsoniana											
Ammonia tepida	4				33						
Cribroelphidium excavatum					25		12	3			
Cribroelphidium poeyanum											
Elphidium gunteri											
Elphidium mexicanum											

Table A3.2 (continued)

	13BIM01 GB19-1S A	13BIM01 GB19-1S B	13BIM01 FR17-1S A	13BIM01 FR17-1S B	13BIM01 FR17-2S A	13BIM01 FR17-2S B	13BIM01 FR17-3S	13BIM01 FR17-4S A	13BIM01 FR17-4S B	13BIM01 FR17-5S	13BIM01 FR17-6S A
Haynesina germanica											
Helenina anderseni											
Other Aggltutinated	1		6								
Other Calcareous											
Indeterminate Planktonic											

Table A3.2 (continued)

	13BIM01 FR17-6S B	13BIM01 FR26S A	13BIM01 FR26S B	13BIM01 DA04S A	13BIM01 DA04S B	13BIM01 DA05S	13BIM01 DA13S	13BIM01 DA27S	15BIM09 DA30S A	15BIM09 DA30S B	15BIM09 DA31S A
Live (rB stained)/Dead	Dead	Dead	Dead	Dead	Dead	Dead	Dead	Dead	Dead	Dead	Dead
Percent examined	100	25	12.5	50	50	37.5	37.5	18.8	25	25	50
Vol (cm^3)	7	20	23	37.5	38	7	23	32	29.5	35	29
Pseudothurammina limnetis	318								3	2	
Ammoastuta inepta		4	5		2	3		9	6	6	
Ammotium salsum/ Ammobaculites exiguus group		93	29		26	13	18	7	64	71	27
Ammobaculites cf. A. *foliaceus*											
Ammobaculites crassus											
Ammotium cassis									1	9	
Arenoparrella mexicana		100	111	3	11	19	1	69	13	26	2
Entzia macrescens	6		2		2		1				
Haplophragmoides bonplandi	34		1							2	
Haplophragmoides manilaensis											
Haplophragmoides wilberti	12	17	27		2	4		15		1	
Leptohalysis scotti									3	4	
Paratrochammina simplissima		19	32			1					
Siphotrochammina lobata	15	1		1	1			7			
Trochammina sp. A										7	
Tiphotrocha comprimata	1	6	3	8	11	6		31	11	9	
Trochammina inflata	21	14	15	4	11	2	2	47	11	12	1
Trochamminita irregularis	29										
Textularia earlandi											
Ammodiscus sp.											
Ammodiscus tenuis											
Affinetrina alcidi											
Miliammina fusca	1	78	45	1	8	37	38	4	194	291	106
Miliammina petila											
Miliolinella subrotunda											
Pyrgo nasutua											
Quinqueloculina jugosa											
Ammonia parkinsoniana			1								
Ammonia tepida		4	1								
Cribroelphidium excavatum											
Cribroelphidium poeyanum											
Elphidium gunteri											
Elphidium mexicanum											
Haynesina germanica											

Table A3.2 (continued)

	13BIM01 FR17-6S B	13BIM01 FR26S A	13BIM01 FR26S B	13BIM01 DA04S A	13BIM01 DA04S B	13BIM01 DA05S	13BIM01 DA13S	13BIM01 DA27S	15BIM09 DA30S A	15BIM09 DA30S B	15BIM09 DA31S A
Helenina anderseni											
Other Aggltutinated	4							2			
Other Calcareous											
Indeterminate Planktonic											

Table A3.2 (continued)

	15BIM09 DA31S B	15BIM09 DA32S A	15BIM09 DA32S B	15BIM09 DA34S A	15BIM09 DA34S B	15BIM09 DA35S A	15BIM09 DA35S B	15BIM09 DA36S A	15BIM09 DA36S B	15BIM09 DA37S A	15BIM09 DA31S A
Live (rB stained)/Dead	Dead	Dead	Dead	Dead	Dead	Dead	Dead	Dead	Dead	Dead	Dead
Percent examined	50	50	50	50	25	50	50	50	50	25	50
Vol (cm^3)	24	27.5	26	36	35	35	38	25	27	31	29
Pseudothurammina limnetis				1	4			6	2	3	
Ammoastuta inepta				99	50	52	1			1	
Ammotium salsum/ Ammobaculites exiguus group	67	1		94	27		29	1			27
Ammobaculites cf. A. *foliaceus*											
Ammobaculites crassus											
Ammotium cassis				9	2						
Arenoparrella mexicana	1			91	92			277	237	179	2
Entzia macrescens											
Haplophragmoides bonplandi				5	4		2	6	9	5	
Haplophragmoides manilaensis								28	14	25	
Haplophragmoides wilberti				2	1			124	143	128	
Leptohalysis scotti				6	6			14	8	12	
Paratrochammina simplissima											
Siphotrochammina lobata											
Trochammina sp. A			1	23	23		1	5	5	15	
Tiphotrocha comprimata	4			53	48	1			3	1	
Trochammina inflata		1		41	50		1	49	32	21	1
Trochamminita irregularis											
Textularia earlandi											
Ammodiscus sp.				18	4	1					
Ammodiscus tenuis				18	4	1					
Affinetrina alcidi											
Miliammina fusca	174	1		40	15	61	47	8	6	2	106
Miliammina petila											
Miliolinella subrotunda											
Pyrgo nasutua											
Quinqueloculina jugosa											
Ammonia parkinsoniana											
Ammonia tepida		1									
Cribroelphidium excavatum											
Cribroelphidium poeyanum											
Elphidium gunteri											
Elphidium mexicanum											
Haynesina germanica											

Table A3.2 (continued)

	15BIM09 DA31S B	15BIM09 DA32S A	15BIM09 DA32S B	15BIM09 DA34S A	15BIM09 DA34S B	15BIM09 DA35S A	15BIM09 DA35S B	15BIM09 DA36S A	15BIM09 DA36S B	15BIM09 DA37S A	15BIM09 DA31S A
Helenina anderseni											
Other Aggltutinated											
Other Calcareous											
Indeterminate Planktonic											

Table A3.2 (continued)

	15BIM09 DA138G B	15BIM09 DA189G A	15BIM09 DA189G B	16CCT03 GB34S A	16CCT03 GB34S B	16CCT03 GB280S A	16CCT03 GB280S B	16CCT03 GB281S A	16CCT03 GB281S B	16CCT03 GB282S A	16CCT03 GB282S B
Live (rB stained)/Dead	Dead	Dead	Dead	Dead	Dead	Dead	Dead	Dead	Dead	Dead	Dead
Percent examined	12.5	1.5625	1.5625	100	100	25	25	100	100	25	25
Vol (cm^3)	31	71	67.5	50	45	40	35	25	28	35	32
Pseudothurammina limnetis						52	55			10	6
Ammoastuta inepta				1	3						
Ammotium salsum/ Ammobaculites exiguus group	3	23	21	50	52						
Ammobaculites cf. A. *foliaceus*											
Ammobaculites crassus											
Ammotium cassis				2	21						
Arenoparrella mexicana				112	290						
Entzia macrescens				3		107	64	2		323	289
Haplophragmoides bonplandi											
Haplophragmoides manilaensis						51	46			4	6
Haplophragmoides wilberti				1		4	14	1		8	3
Leptohalysis scotti											
Paratrochammina simplissima		3		2	2						
Siphotrochammina lobata				2	1			5		37	20
Trochammina sp. A				8	20						
Tiphotrocha comprimata				109	74	2	1			28	3
Trochammina inflata				42	27				2		1
Trochamminita irregularis						128	135				
Textularia earlandi											
Ammodiscus sp.											
Ammodiscus tenuis				5	23						
Affinetrina alcidi											
Miliammina fusca		5	1	109	194			13	7	7	
Miliammina petila						2				10	10
Miliolinella subrotunda	5	23	20								
Pyrgo nasutua											
Quinqueloculina jugosa	1	4	1								
Ammonia parkinsoniana	32	66	75								
Ammonia tepida	280	218	268	4		1					
Cribroelphidium excavatum	278	102	82			1					
Cribroelphidium poeyanum		3	5								
Elphidium gunteri											
Elphidium mexicanum		6	15								
Haynesina germanica	5	7	5								

Table A3.2 (continued)

	15BIM09 DA138G B	15BIM09 DA189G A	15BIM09 DA189G B	16CCT03 GB34S A	16CCT03 GB34S B	16CCT03 GB280S A	16CCT03 GB280S B	16CCT03 GB281S A	16CCT03 GB281S B	16CCT03 GB282S A	16CCT03 GB282S B
Helenina anderseni											
Other Aggltutinated				18	15	11					
Other Calcareous	1										
Indeterminate Planktonic											

Table A3.2 (continued)

	16CCT03 GB283S A	16CCT03 GB283S B	16CCT03 GB284S A	16CCT03 GB284S B	16CCT03 GB285S A	16CCT03 GB285S B	16CCT03 GB286S A	16CCT03 GB286S B	16CCT03 GB287S A	16CCT03 GB287S B	16CCT03 GB288S A
Live (rB stained)/Dead	Dead	Dead	Dead	Dead	Dead	Dead	Dead	Dead	Dead	Dead	Dead
Percent examined	12.5	12.5	12.5	12.5	12.5	12.5	50	50	6.25	6.25	12.5
Vol (cm^3)	50	42	33	39	35	35	39	45	35	30	40
Pseudothurammina limnetis	24	24	8	9						3	1
Ammoastuta inepta	4	2	40	44	8	5	18	20	40	29	
Ammotium salsum/ Ammobaculites exiguus group	46	45	24	26	81	128	13	15	139	129	90
Ammobaculites cf. A. *foliaceus*											
Ammobaculites crassus						3					
Ammotium cassis			3	7		1	1	4		2	
Arenoparrella mexicana	56	19	45	74	21	18	37	62	86	71	39
Entzia macrescens		21	13	11	18	13	15	11	12	1	1
Haplophragmoides bonplandi											
Haplophragmoides manilaensis		3	2	4					3	3	
Haplophragmoides wilberti	11	10	13	32	8	7	12	9	7	5	
Leptohalysis scotti			1	3	1						1
Paratrochammina simplissima											
Siphotrochammina lobata		3	3	5		5		1	8	1	1
Trochammina sp. A	10	10	4	1	3	12	2	5	13	20	6
Tiphotrocha comprimata	50	45	6	1	21	17	8	2	26	15	32
Trochammina inflata	22	25	13	23	3	11	15	12	10	10	4
Trochamminita irregularis								2			
Textularia earlandi											
Ammodiscus sp.											
Ammodiscus tenuis											
Affinetrina alcidi											
Miliammina fusca	78	191	75	63	149	119	154	212	196	154	141
Miliammina petila											
Miliolinella subrotunda											
Pyrgo nasutua											
Quinqueloculina jugosa											
Ammonia parkinsoniana											
Ammonia tepida			4								
Cribroelphidium excavatum											
Cribroelphidium poeyanum											
Elphidium gunteri											
Elphidium mexicanum											
Haynesina germanica											

Table A3.2 (continued)

	16CCT03 GB283S A	16CCT03 GB283S B	16CCT03 GB284S A	16CCT03 GB284S B	16CCT03 GB285S A	16CCT03 GB285S B	16CCT03 GB286S A	16CCT03 GB286S B	16CCT03 GB287S A	16CCT03 GB287S B	16CCT03 GB288S A
Helenina anderseni	1	5									
Other Aggltutinated											
Other Calcareous											
Indeterminate Planktonic					1						

Table A3.2 (continued)

	16CCT03 GB288S B	16CCT03 GB289S A	16CCT03 GB289S B
Live (rB stained)/Dead	Dead	Dead	Dead
Percent examined	12.5	6.25	6.25
Vol (cm^3)	50	35	37
Pseudothurammina limnetis		2	
Ammoastuta inepta	1	24	38
Ammotium salsum/ Ammobaculites exiguus group	109	183	206
Ammobaculites cf. A. *foliaceus*			
Ammobaculites crassus			
Ammotium cassis		4	4
Arenoparrella mexicana	36	31	49
Entzia macrescens	7	4	2
Haplophragmoides bonplandi			
Haplophragmoides manilaensis			
Haplophragmoides wilberti	1	10	11
Leptohalysis scotti			
Paratrochammina simplissima			
Siphotrochammina lobata	1	7	12
Trochammina sp. A	5	8	7
Tiphotrocha comprimata	71	14	13
Trochammina inflata	6	7	6
Trochamminita irregularis			
Textularia earlandi			
Ammodiscus sp.			
Ammodiscus tenuis			
Affinetrina alcidi			
Miliammina fusca	158	226	287
Miliammina petila			
Miliolinella subrotunda			
Pyrgo nasutua			
Quinqueloculina jugosa			
Ammonia parkinsoniana			
Ammonia tepida			
Cribroelphidium excavatum			
Cribroelphidium poeyanum			
Elphidium gunteri			
Elphidium mexicanum			
Haynesina germanica			

Table A3.2 (continued)

	16CCT03 GB288S B	16CCT03 GB289S A	16CCT03 GB289S B
Helenina anderseni		1	
Other Aggltutinated			
Other Calcareous			
Indeterminate Planktonic			

Appendix A4. Species Abbreviations.

Order Astrorhizida	
Pseudothurammina limnetis (Scott & Medioli, 1980)	*– Pst. limnetis*
Order Lituolida	
Ammoastuta inepta (Cushman & McCulloch, 1939)	*– Ams. inepta*
Ammotium cassis (Parker, 1870)	*– Amm. cassis*
Ammotium salsum (Cushman & Brönnimann, 1948)	*– Amt. salsum*
Ammobaculites exiguus Cushman & Brönnimann, 1948	*– Amb. exiguus*
Ammobaculites crassus Warren, 1957	*– Amb. crassus*
Ammobaculites cf. *A. foliaceus* (Brady)	
Arenoparrella mexicana (Kornfeld, 1931)	*– Are. mexicana*
Entzia macrescens (Brady, 1870)	*– Ent. macrescens*
Haplophragmoides bonplandi Todd & Brönniman, 1957	*– Hap. bonplandi*
Haplophragmoides manilaensis Andersen, 1953	*– Hap. manilaensis*
Haplophragmoides wilberti Andersen, 1953	*– Hap. wilberti*
Leptohalysis scotti (Chaster, 1892)	*– Lep. scotti*
Paratrochammina simplissima (Cushman & McCulloch, 1939)	*– Par. simplissima*
Siphotrochammina lobata Saunders, 1957	*– Sph. lobata*
Tiphotrocha comprimata (Cushman & Brönnimann, 1948)	*– Tph. comprimata*
Trochammina inflata (Montagu, 1808)	*– Tro. inflata*
Trochammina sp. A	
Trochamminita irregularis Cushman & Brönnimann, 1948	*– Tta. irregularis*
Order Textulariida	
Textularia earlandi Parker, 1952	*– Tex. earlandi*
Order Spirillinida	
Ammodiscus sp.	
Ammodiscus tenuis Brady, 1884	*– Amd. tenuis*
Order Miliolida	
Affinetrina alcidi Levy, Mathieu, Poignant, Rosset-Moulinier, 1992	*– Aff. alcidi*
Miliammina fusca (Brady, 1870)	*– Mlm. fusca*
Miliammina petila Saunders, 1958	*– Mlm. petila*
Miliolinella subrotunda (Montagu, 1803)	*– Mil. subrotunda*
Pyrgo nasuta Cushman, 1935	*– Pyr. nasuta*
Quinqueloculina jugosa Cushman, 1944	*– Qui. jugosa*
Order Rotaliida	
Ammonia parkinsoniana (d'Orbigny, 1839)	*– Amn. parkinsoniana*
Ammonia tepida (Cushman, 1926)	*– Amn. tepida*
Cribroelphidium excavatum (Terquem, 1875)	*– Cel. excavatum*
Cribroelphidium poeyanum (d'Orbigny, 1839)	*– Cel. poeyanum*
Elphidium gunteri Cole, 1931	*– Elp. gunteri*
Elphidium mexicanum Kornfeld, 1931	*– Elp. mexicanum*
Haynesina germanica (Ehrenberg, 1840)	*– Hay. germanica*
Helenina anderseni (Warren, 1957)	*– Hel. anderseni*

Appendix A5. NMDS and Cluster Analyses.

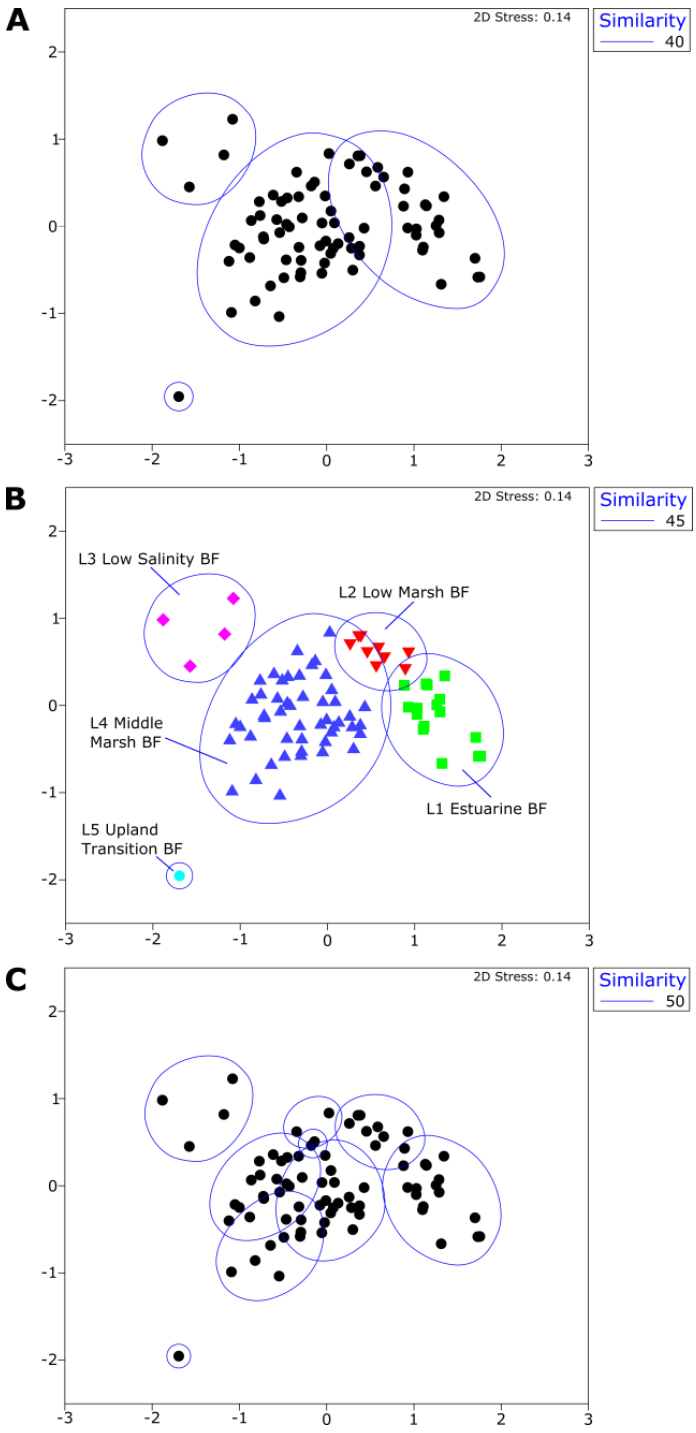

Figure A5.1. Non-metric multidimensional scaling of live assemblage with Bray-Curtis Similarity limits (A): 40%, 4 clusters; (B): 45%, 5 clusters; (C): 50%, 9 clusters.

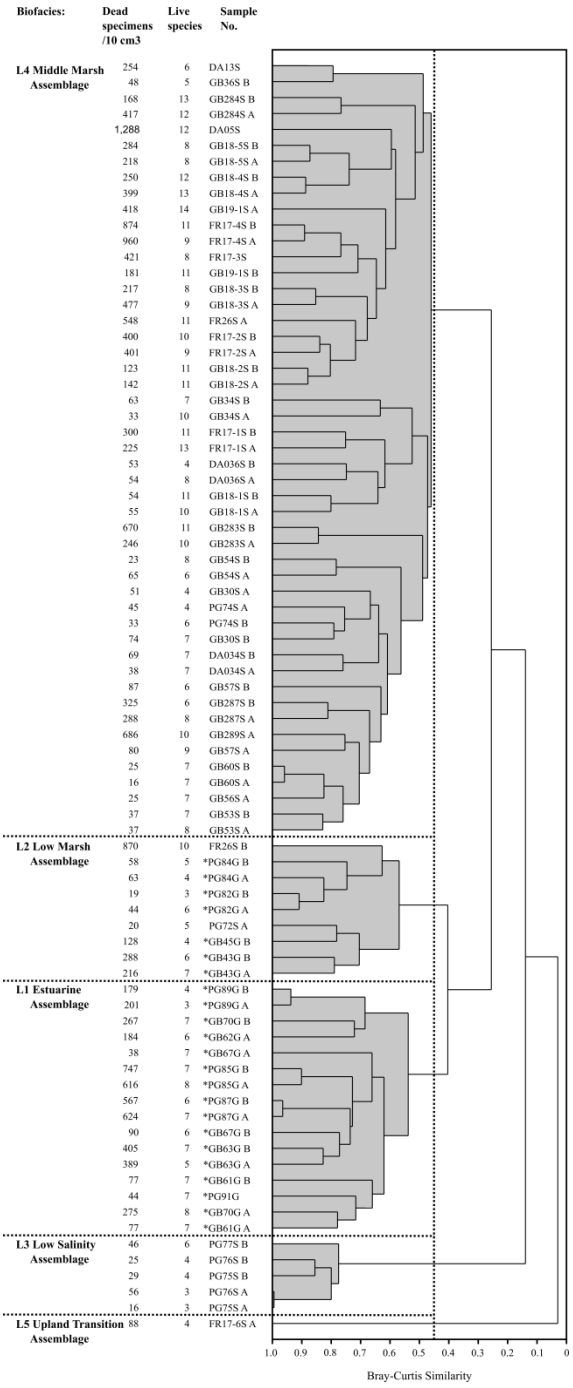

Figure A5.2. Cluster analysis of live foraminiferal data from all marsh and estuarine samples containing >57 specimens. Dendrogram from cluster analysis of transformed percentage data of species comprising 2% or more of the assemblage in any one sample. At a similarity level of 0.45, five clusters can be recognized.

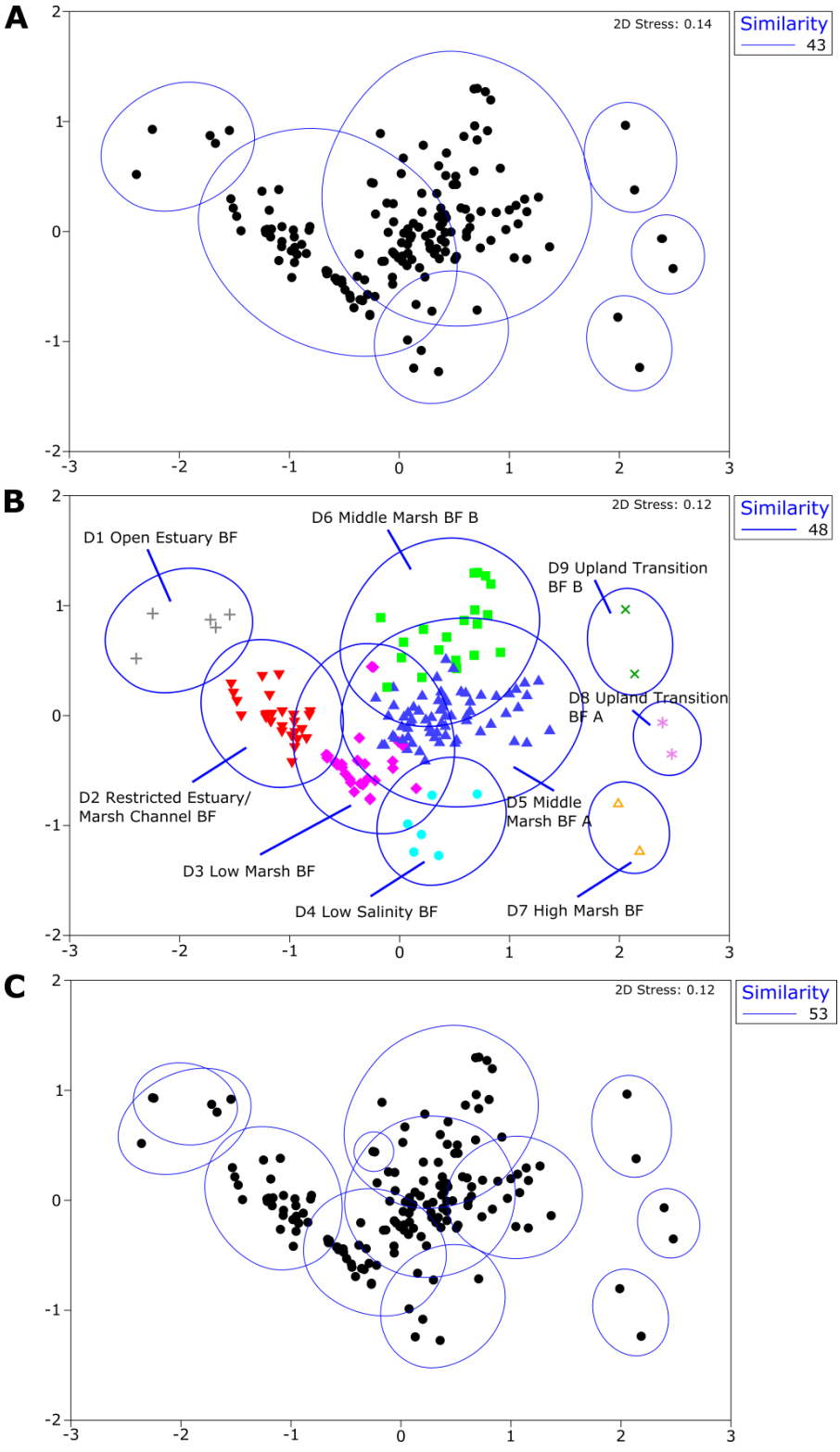

Figure 5.3. Non-metric multidimensional scaling of dead assemblage with Bray-Curtis Similarity limits (A): 43%, 7 clusters; (B): 48%, 9 clusters; (C): 53%, 12 clusters.

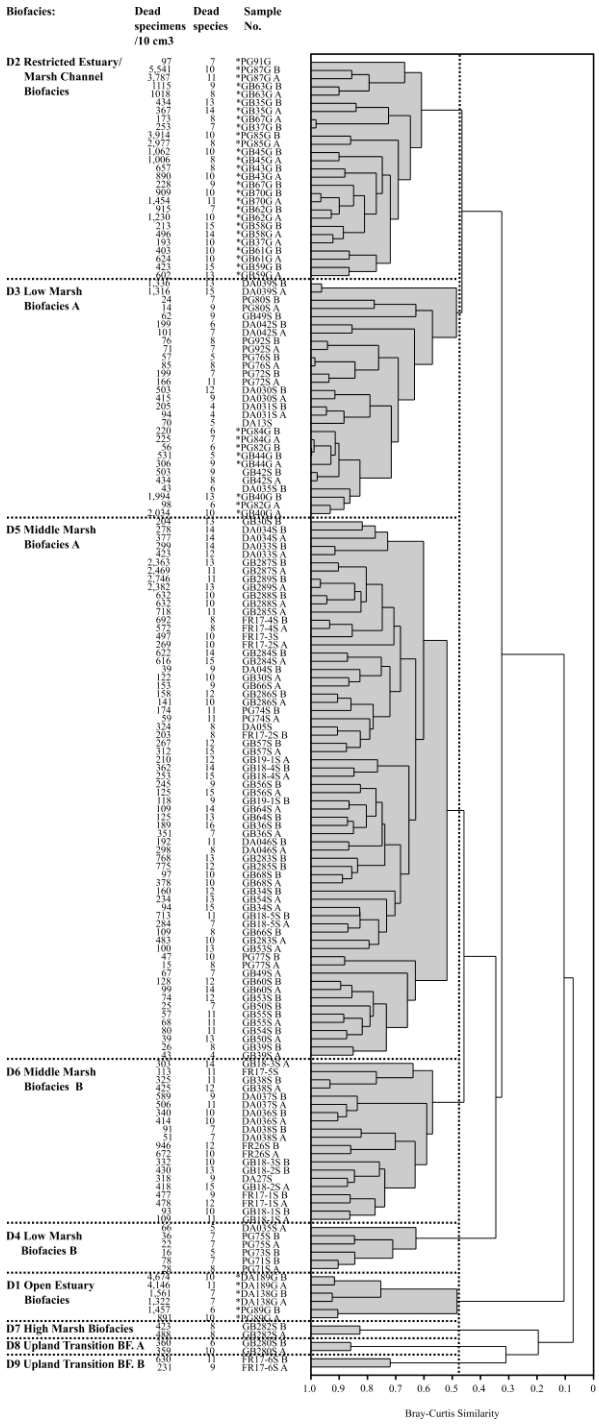

Figure A5.4. Cluster analysis of dead foraminiferal data from all marsh and estuarine samples >57 specimens. Dendrogram from cluster analysis of transformed percentage data of species comprising 2% or more of the assemblage in any one sample. At a similarity level of 0.48, nine clusters are distinguished.

Appendix A6. Biofacies, Constancy, Occurrence Analysis Data

Table A6.1 Live assemblage BFCO data. Bold values meet minimum criteria.

		L1 Estuarine Assemblage			L2 Low Marsh Assemblage			L3 Low Salinity Assemblage			L4 Middle Marsh Assemblage			L5 Upland Transition Assemblage		
	Species	O	C	BF	O	C	BF	O	C	BF	O	C	BF	O	C	BF
calcareous	*Ammonia parkinsoniana*	8	**5**	**8**	1	1	2	0	0	0	1	0	0	0	0	0
	Ammonia tepida	16	**10**	**5**	6	7	3	0	0	0	22	4	2	0	0	0
	Cribroelphidium excavatum	13	**8**	**5**	4	4	3	0	0	0	11	2	2	0	0	0
	Cribroelphidium poeyanum	9	**6**	**8**	1	1	2	0	0	0	0	0	0	0	0	0
	Haynesina germanica	9	**6**	**5**	5	**6**	**5**	0	0	0	4	1	1	0	0	0
	Helenina andersoni	0	0	0	0	0	0	0	0	0	9	2	10	0	0	0
	Other calcareous	0	0	0	0	0	0	0	0	0	2	0	10	0	0	0
agglutinated	*Miliolinella subrotunda*	1	1	10	0	0	0	0	0	0	0	0	0	0	0	0
	Ammodiscus tenuis	0	0	0	0	0	0	0	0	0	3	1	10	0	0	0
	Ammoastuta inepta	0	0	0	3	3	2	5	**10**	**5**	26	5	3	0	0	0
	A. salsum + A. exiguus group	14	9	2	9	10	3	4	8	2	42	9	2	0	0	0
	Ammotium cassis	1	1	2	0	0	0	0	0	0	14	3	8	0	0	0
	Arenoparella mexicana	0	0	0	1	1	1	3	6	4	48	**10**	**6**	0	0	0
	Entzia macrescens	0	0	0	0	0	0	0	0	0	5	1	10	0	0	0
	Cornuspira spp.	0	0	0	0	0	0	0	0	0	2	0	10	0	0	0
	Haplophragmoides bonplandi	0	0	0	1	1	4	1	2	6	0	0	0	0	0	0
	Haplophragmoides wilberti	0	0	0	0	0	0	0	0	0	17	3	3	1	10	7
	Haplophragmoides manilaensis	0	0	0	0	0	0	0	0	0	3	1	10	0	0	0
	Miliammina fusca	8	5	2	9	10	3	3	6	2	44	9	3	0	0	0
	Paratrochammina simplissima	13	**8**	**7**	3	3	3	0	0	0	1	0	0	0	0	0
	Pseudothurammina limnetis	0	0	0	1	1	1	0	0	0	1	0	0	1	10	9
	Siphotrochammina lobata	0	0	0	0	0	0	0	0	0	7	1	1	1	10	9
	Tiphotrocha compirmata	0	0	0	0	0	0	1	2	2	32	**7**	**8**	0	0	0
	Trochammina inflata	0	0	0	0	0	0	0	0	0	46	**9**	**10**	0	0	0
	Trochammina sp. A	0	0	0	0	0	0	0	0	0	19	4	10	0	0	0

Table A6.2 Dead assemblage BFCO data. Bold values meet minimum criteria.

		D1 Open Estuary Biofacies			D2 Restricted Estuary/Marsh Channel Biofacies			D3 Low Marsh Biofacies			D4 Low Salinity Biofacies			D5 Middle Marsh Biofacies A		
	Species	O	C	BF	O	C	BF	O	C	BF	O	C	BF	O	C	BF
calcareous	*Affinitrina alcidi*	0	0	0	0	0	0	0	0	0	0	0	0	0	0	0
	Ammonia parkinsoniana	4	**7**	**6**	12	4	4	0	0	0	0	0	0	0	0	0
	Ammonia tepida	6	10	4	24	9	4	7	2	1	0	0	0	6	1	0
	Cribroelphidium excavatum	5	**8**	**5**	22	**8**	**5**	1	0	0	0	0	0	3	0	0
	Cribroelphidium poeyanum	1	2	2	15	**6**	**8**	0	0	0	0	0	0	0	0	0
	Elphidium gunteri	0	0	0	2	1	10	0	0	0	0	0	0	0	0	0
	Elphidium mexicanum	2	3	10	0	0	0	0	0	0	0	0	0	0	0	0
	Haynesina germanica	3	**5**	**6**	9	3	4	0	0	0	0	0	0	0	0	0
	Helenina anderseni	0	0	0	0	0	0	0	0	0	0	0	0	1	0	10
	Miliolinella subrotunda	2	3	4	14	**5**	**6**	0	0	0	0	0	0	0	0	0
	Quinqueloculina jugosa	0	0	0	2	1	10	0	0	0	0	0	0	0	0	0
agglutinated	*Ammodiscus tenuis*	0	0	0	0	0	0	0	0	0	0	0	0	12	2	8
	Ammoastuta inepta	0	0	0	1	0	0	12	4	2	6	**10**	**5**	34	5	2
	A. salsum + *A. exiguus* group	3	5	1	27	10	2	29	10	2	4	7	1	52	8	2
	Ammobaculites cf. *A. foliaceus*	0	0	0	0	0	0	2	1	10	0	0	0	0	0	0
	Ammobaculites crassus	0	0	0	0	0	0	0	0	0	1	2	10	0	0	0
	Ammobaculites minutissimus	0	0	0	0	0	0	0	0	0	0	0	0	7	1	10
	Ammotium cassis	0	0	0	2	1	1	5	2	2	0	0	0	20	3	4
	Arenoparella mexicana	0	0	0	6	2	1	15	5	2	2	3	1	63	10	3
	Entzia macrescens	0	0	0	0	0	0	6	2	1	0	0	0	29	5	1
	Haplophragmodes bonplandi	0	0	0	0	0	0	8	3	1	5	8	4	8	1	1
	Haplophragmoides manilaensis	0	0	0	0	0	0	0	0	0	0	0	0	2	0	0
	Haplophragmoides wilberti	0	0	0	1	0	0	3	1	0	0	0	0	24	4	1
	Leptohalysis scotti	0	0	0	0	0	0	1	0	1	0	0	0	4	1	2
	Miliammina fusca	1	2	0	25	9	2	29	10	2	6	10	2	63	10	2
	Miliammina petila	0	0	0	0	0	0	1	0	0	0	0	0	0	0	0
	Other agglutinated	0	0	0	0	0	0	0	0	0	0	0	0	3	0	1
	Paratrochammina simplissima	2	3	2	25	**9**	**6**	5	2	1	0	0	0	4	1	0
	Pseudothurammina limnetis	0	0	0	0	0	0	6	2	0	4	7	2	30	5	1
	Siphotrochammina lobata	0	0	0	0	0	0	0	0	0	0	0	0	17	3	1
	Tiphotrocha comprimata	0	0	0	0	0	0	11	4	1	2	3	1	62	10	3
	Trochammina inflata	0	0	0	0	0	0	5	2	1	0	0	0	58	9	3
	Trochammina sp. A	0	0	0	0	0	0	6	2	2	0	0	0	42	**7**	**6**
	Trochamminita irregularis	0	0	0	0	0	0	0	0	0	0	0	0	0	0	0

Table A6.2 (Continued)

		D6 Middle Marsh Biofacies B			D7 High Marsh Biofacies			D8 Upland Transition Biofacies A			D9 Upland Transition Biofacies B		
	Species	O	C	BF	O	C	BF	O	C	BF	O	C	BF
calcareous	*Affinitrina alcidi*	1	1	10	0	0	0	0	0	0	0	0	0
	Ammonia parkinsoniana	0	0	0	0	0	0	0	0	0	0	0	0
	Ammonia tepida	3	2	1	0	0	0	0	0	0	0	0	0
	Cribroelphidium excavatum	0	0	0	0	0	0	0	0	0	0	0	0
	Cribroelphidium poeyanum	0	0	0	0	0	0	0	0	0	0	0	0
	Elphidium gunteri	0	0	0	0	0	0	0	0	0	0	0	0
	Elphidium mexicanum	0	0	0	0	0	0	0	0	0	0	0	0
	Haynesina germanica	0	0	0	0	0	0	0	0	0	0	0	0
	Helenina anderseni	0	0	0	0	0	0	0	0	0	0	0	0
	Miliolinella subrotunda	0	0	0	0	0	0	0	0	0	0	0	0
	Quinqueloculina jugosa	0	0	0	0	0	0	0	0	0	0	0	0
agglutinated	*Ammodiscus tenuis*	1	1	2	0	0	0	0	0	0	0	0	0
	Ammoastuta inepta	10	5	2	0	0	0	0	0	0	0	0	0
	A. salsum + A. exiguus group	13	7	1	0	0	0	0	0	0	0	0	0
	Ammobaculites cf. *A. foliaceus*	0	0	0	0	0	0	0	0	0	0	0	0
	Ammobaculites crassus	0	0	0	0	0	0	0	0	0	0	0	0
	Ammobaculites minutissimus	0	0	0	0	0	0	0	0	0	0	0	0
	Ammotium cassis	4	2	3	0	0	0	0	0	0	0	0	0
	Arenoparella mexicana	20	10	3	0	0	0	0	0	0	0	0	0
	Entzia macrescens	4	2	1	2	10	3	2	10	3	1	5	1
	Haplophragmodes bonplandi	8	4	2	0	0	0	0	0	0	1	5	2
	Haplophragmoides manilaensis	5	3	1	1	5	3	2	**10**	**6**	0	0	0
	Haplophragmoides wilberti	20	10	2	1	5	1	2	10	2	2	10	2
	Leptohalysis scotti	6	3	8	0	0	0	0	0	0	0	0	0
	Miliammina fusca	18	9	2	1	5	1	0	0	0	0	0	0
	Miliammina petila	0	0	0	2	**10**	**10**	0	0	0	0	0	0
	Other agglutinated	2	1	2	0	0	0	1	**5**	**8**	0	0	0
	Paratrochammina simplissima	3	2	1	0	0	0	0	0	0	0	0	0
	Pseudothurammina limnetis	2	1	0	2	10	2	2	10	2	2	10	2
	Siphotrochammina lobata	10	5	2	2	10	4	0	0	0	2	10	4
	Tiphotrocha comprimata	13	7	2	1	5	2	0	0	0	0	0	0
	Trochammina inflata	19	10	3	0	0	0	0	0	0	2	10	3
	Trochammina sp. A	5	3	2	0	0	0	0	0	0	0	0	0
	Trochamminita irregularis	0	0	0	0	0	0	2	**10**	**5**	2	**10**	**5**

Appendix A7. Patchiness and Diversity Raw Data.

Table A7.1 Wilcoxon two-sample comparison between replicates and Fisher's α data.

Study Area	Station	Wilcoxon live p(exact)	Wilcoxon dead p(exact)	Fisher's α live Sample A	Fisher's α live Sample B	Fisher's α dead Sample A	Fisher's α dead Sample B
Grand Bay	GB42S	1.00	0.51	2.39	0.00	1.33	1.53
Grand Bay	GB57S	0.49	0.25	2.58	1.54	3.26	2.70
Grand Bay	GB39S	1.00	0.62	2.78	3.18	0.72	1.94
Grand Bay	GB34S	0.10	0.81	2.34	1.30	2.96	2.04
Grand Bay	GB38S	1.00	0.84	0.88	0.94	1.46	1.23
Grand Bay	GB30S	0.38	0.66	1.13	1.76	2.15	2.90
Grand Bay	GB53S	0.95	0.72	2.28	1.80	3.11	2.93
Grand Bay	GB56S	0.81	0.52	2.00	2.43	3.25	1.72
Grand Bay	GB60S	0.94	0.85	1.93	2.10	2.75	2.53
Grand Bay	GB55S	1.00	0.42	1.45	1.77	2.18	2.51
Grand Bay	GB50S	0.81	0.26	3.30	1.59	3.30	1.68
Grand Bay	GB68S	0.91	0.90	2.56	2.26	1.81	2.10
Grand Bay	GB49S	1.00	0.28	1.97	1.74	1.29	1.78
Grand Bay	GB18-1S	0.49	0.99	2.40	3.00	2.23	2.23
Grand Bay	GB18-2S	0.53	0.98	2.78	2.33	3.04	2.15
Grand Bay	GB18-3S	1.00	0.64	2.19	2.01	4.80	2.36
Grand Bay	GB18-4S	0.23	0.97	2.82	2.33	3.91	2.59
Grand Bay	GB18-5S	1.00	0.40	1.68	1.67	1.33	1.99
Grand Bay	GB280S	N/A	N/A	0.38	0.43	1.91	1.05
Grand Bay	GB281S	0.50	1.00	0.00	N/A	1.47	0.80
Grand Bay	GB282S	1.00	0.57	0.83	0.86	1.40	1.47
Grand Bay	GB283S	0.83	0.33	2.39	2.16	1.99	2.57
Grand Bay	GB284S	0.45	0.76	2.94	4.35	3.49	3.03
Grand Bay	GB285S	0.75	0.89	1.79	0.29	2.22	2.43
Grand Bay	GB286S	0.92	0.83	1.94	2.77	2.04	2.40
Grand Bay	GB287S	0.71	0.89	2.43	1.65	1.96	2.51
Grand Bay	GB288S	1.00	0.50	2.08	2.22	1.97	1.87
Grand Bay	GB289S	0.99	0.79	2.41	2.37	2.42	1.89
Grand Bay	GB19-1S	0.35	0.61	2.96	2.23	2.96	1.94
Grand Bay	GB36S	0.47	0.37	2.03	1.28	3.03	2.76
Grand Bay	GB54S	0.74	0.88	1.54	2.08	2.85	2.19
Grand Bay	GB64S	0.97	1.00	3.72	2.49	3.12	2.32
Grand Bay	GB35G	0.81	0.73	1.81	1.71	3.03	2.69
Grand Bay	GB37G	1.00	0.62	1.88	1.40	1.99	1.25
Grand Bay	GB40G	1.00	0.89	1.45	0.28	1.78	2.40
Grand Bay	GB43G	0.84	0.68	1.78	1.33	1.90	1.55
Grand Bay	GB44G	1.00	0.31	0.72	1.13	1.73	0.87
Grand Bay	GB45G	0.50	0.56	1.39	0.92	1.32	1.72
Grand Bay	GB58G	1.00	0.30	1.71	1.18	2.73	2.47
Grand Bay	GB59G	0.95	0.93	1.73	2.18	2.81	3.12
Grand Bay	GB61G	0.74	0.97	1.76	1.78	1.63	1.80
Grand Bay	GB62G	1.00	0.77	1.47	2.28	1.72	1.21
Grand Bay	GB63G	0.91	1.00	0.95	1.47	1.37	1.58

Table A7.1 (Continued)

Study Area	Station	Wilcoxon live p(exact)	Wilcoxon dead p(exact)	Fisher's α live Sample A	Fisher's α live Sample B	Fisher's α dead Sample A	Fisher's α dead Sample B
Grand Bay	GB67G	0.81	1.00	1.63	1.36	1.33	1.77
Grand Bay	GB70G	1.00	0.80	1.84	1.66	1.83	1.89
Pascagoula	PG74S	0.94	0.38	0.75	1.36	2.48	1.92
Pascagoula	PG77S	0.81	0.85	0.70	1.14	2.40	2.16
Pascagoula	PG76S	1.00	0.52	0.50	0.13	1.51	0.90
Pascagoula	PG80S	1.00	0.61	1.87	1.87	2.87	1.73
Pascagoula	PG81S	-	-	-	-	4.63	1.58
Pascagoula	PG75S	0.88	0.91	0.62	0.76	1.66	1.45
Pascagoula	PG100S	1.00	0.78	0.53	1.59	1.45	2.22
Pascagoula	PG72S	0.63	0.83	1.14	0.47	1.83	1.07
Pascagoula	PG92S	1.00	0.74	0.92	1.71	1.27	1.53
Pascagoula	PG71S	1.00	0.55	1.97	1.35	2.02	1.27
Pascagoula	PG73S	1.00	1.00	0.55	0.32	0.75	1.24
Pascagoula	PG82G	0.84	0.94	1.23	0.65	1.02	1.17
Pascagoula	PG84G	0.69	0.84	0.81	0.93	1.21	0.96
Pascagoula	PG85G	0.88	0.70	1.90	1.77	1.30	1.79
Pascagoula	PG87G	0.95	0.85	1.63	1.64	1.85	1.70
Pascagoula	PG89G	0.88	0.69	0.60	0.91	1.87	0.93
Pascagoula	PG91G	0.58	1.00	1.46	0.84	1.27	1.67
Fowl River	FR17-1S	0.79	0.42	2.85	2.33	2.15	1.63
Fowl River	FR17-2S	0.43	0.41	1.56	1.71	1.94	1.51
Fowl River	FR17-3S	-	1.52	-	1.92	-	-
Fowl River	FR17-4S	0.46	1.00	1.56	2.05	1.51	1.46
Fowl River	FR17-5S	-	1.66	-	2.25	-	-
Fowl River	FR17-6S	0.52	0.46	0.81	2.30	1.51	1.82
Fowl River	FR26S	0.47	0.58	2.30	2.09	1.94	2.57
Dauphin Isl.	DA04S	0.28	0.91	0.80	3.83	2.39	2.69
Dauphin Isl	DA05S	-	2.43	-	2.17	-	-
Dauphin Isl	DA13S	-	1.14	-	1.30	-	-
Dauphin Isl	DA27S	-	3.02	-	1.96	-	-
Dauphin Isl	DA30S	0.78	0.79	1.22	1.62	1.74	2.28
Dauphin Isl	DA31S	1.00	1.00	1.59	0.34	0.77	0.68
Dauphin Isl	DA32S	N/A	0.75	N/A	N/A	0.00	0.00
Dauphin Isl	DA34S	0.45	0.89	1.95	2.05	2.67	2.97
Dauphin Isl	DA35S	1.00	0.41	0.59	0.38	1.06	1.50
Dauphin Isl	DA36S	0.20	0.37	2.36	0.91	1.76	1.80
Dauphin Isl	DA37S	1.00	0.89	1.33	1.30	2.10	1.74
Dauphin Isl	DA38S	1.00	0.52	0.29	0.80	2.49	2.33
Dauphin Isl	DA39S	1.00	0.94	N/A	0.38	2.51	2.50
Dauphin Isl	DA40S	N/A	0.71	N/A	N/A	2.03	3.98
Dauphin Isl	DA42S	1.00	0.94	1.45	0.98	1.71	1.17
Dauphin Isl	DA46S	1.00	0.37	2.21	2.32	1.68	2.36
Dauphin Isl	DA138G	0.94	1.00	3.18	2.81	1.17	1.12
Dauphin Isl	DA189G	0.77	0.76	2.86	2.72	2.06	1.78

Appendix A8. Patchiness Statistics.

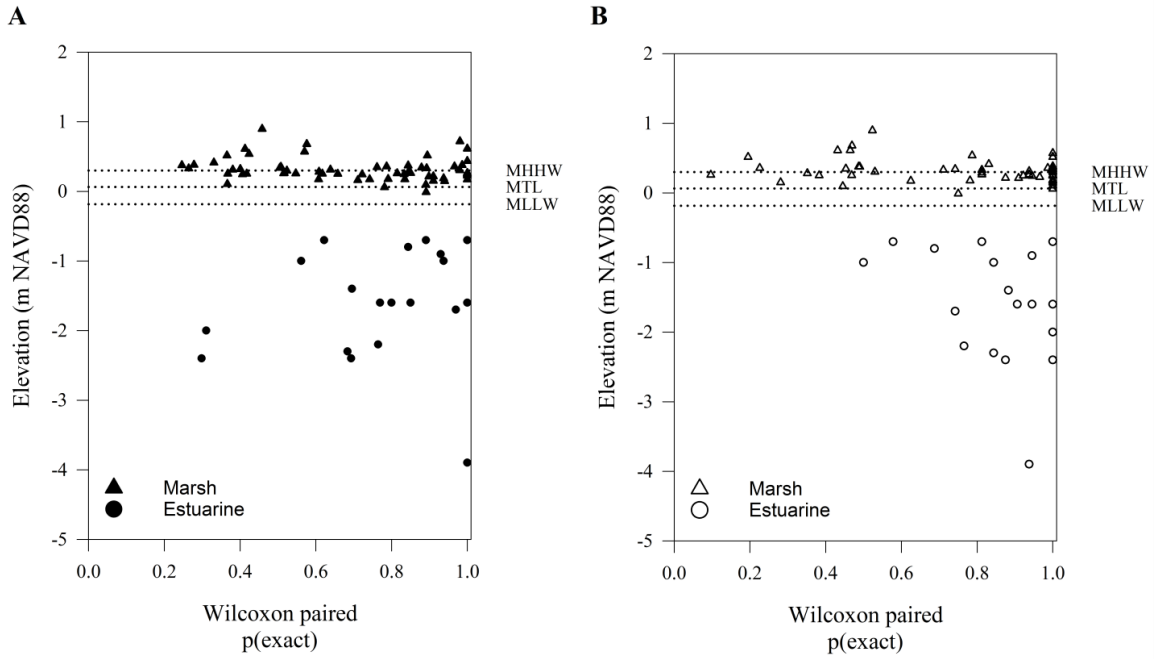

Figure A8.1. Patchiness versus elevation. (A): dead assemblage. (B): live (rB stained) assemblage.

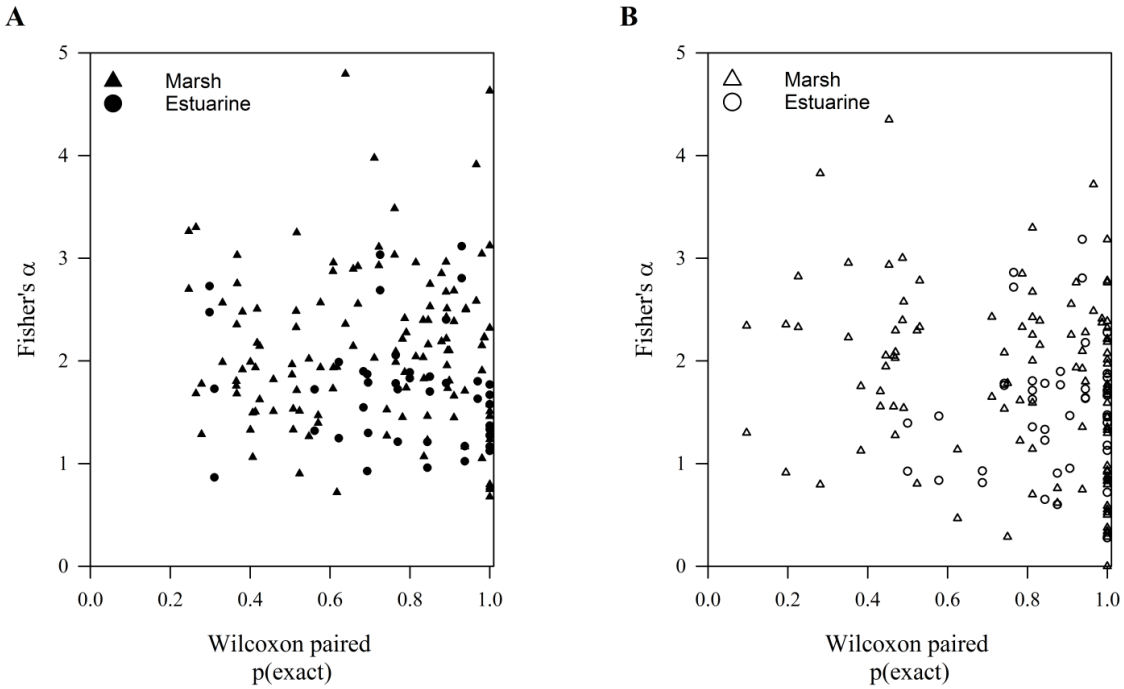

Figure A8.2. Patchiness versus diversity. (A): dead assemblage. (B): live (rB stained) assemblage)

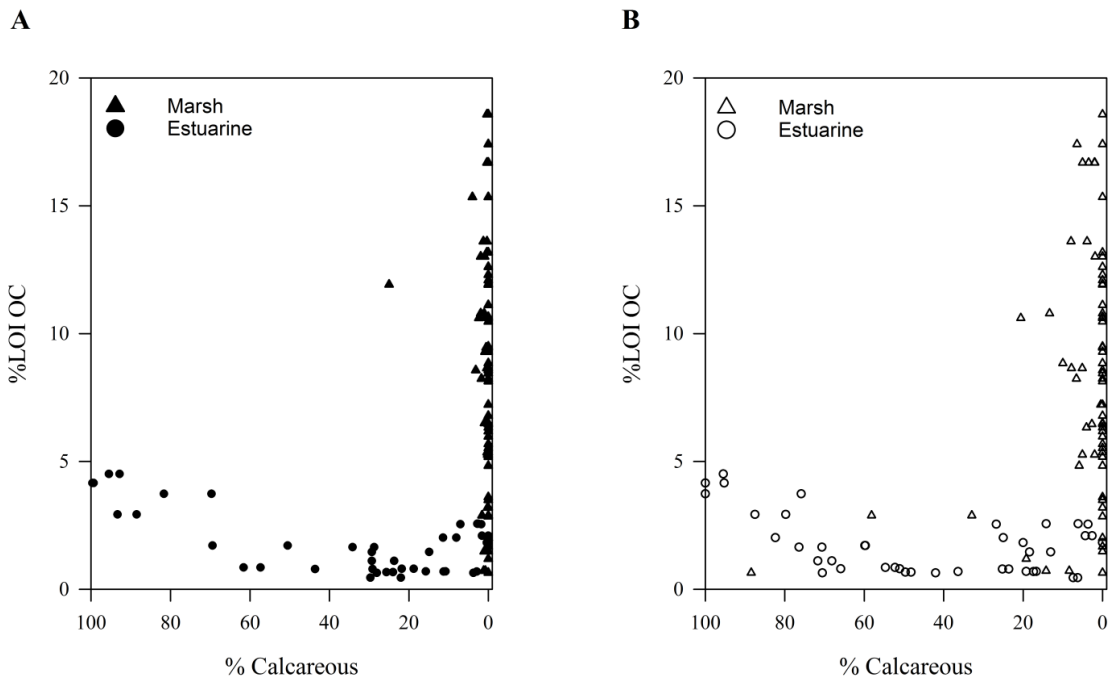

Figure A8.3. Calcareous percentage versus organics. (A): dead assemblage. (B): live (rB stained) assemblage.

Appendix B

Appendix B1. Foraminiferal Data.

Table B1.1 Reconstruction cores relative abundance (total assemblage). Raw counts will be made available in a USGS Data Release.

Project							14CCT01						
Core							GB53R						
Depth (cm)	0-1	4-5	8-9	10-11	15-16	20-21	25-26	35-36	45-46	60-61	80-81	100-101	120-121
Volume (cm^3)	5	6	6	6	6	10	11	10	10	10	10	10	10
Examined (%)	50	50	100	100	100	100	50	50	50	100	100	BARREN	BARREN
Density ($10cm^{-3}$)	1792	1470	632	330	270	439	720	940	574	124	32	0	0
Pseudothurammina limnetis (Scott & Medioli, 1980)	5.6	0.0	0.0	0.0	0.0	0.0	0.0	0.0	0.0	0.0	0.0	0.0	0.0
Ammoastuta inepta (Cushman & McCulloch, 1939)	2.7	7.7	0.3	4.2	0.6	1.7	8.7	1.1	1.4	0.8	0.0	0.0	0.0
Ammotium salsum + Ammobaculites exiguus group	15.9	0.7	2.7	0.0	0.6	3.8	2.3	0.0	0.0	0.0	0.0	0.0	0.0
Ammobaculites cf. *A. foliaceus* (Brady, 1881)	0.0	0.0	0.0	0.0	0.0	0.0	0.0	0.0	0.0	0.0	0.0	0.0	0.0
Ammobaculites crassus Warren, 1957	0.0	0.0	0.0	0.0	0.0	0.0	0.0	0.0	0.0	0.0	0.0	0.0	0.0
Ammotium cassis (Parker, 1870)	2.0	0.0	0.0	0.0	0.0	0.0	0.0	0.0	0.0	0.0	0.0	0.0	0.0
Arenoparrella mexicana (Kornfeld, 1931)	17.5	41.9	49.3	13.1	16.5	33.1	31.0	35.8	40.2	62.0	43.8	0.0	0.0
Entzia macrescens (Brady, 1870)	0.2	0.7	4.5	0.0	8.2	2.8	3.3	0.9	1.7	0.0	0.0	0.0	0.0
Haplophragmoides bonplandi Todd & Brönniman, 1957	0.0	0.0	0.0	0.0	0.0	0.0	0.0	0.0	0.0	0.0	0.0	0.0	0.0
Haplophragmoides manilaensis Andersen, 1953	0.0	0.0	0.0	0.0	0.0	0.2	0.5	0.0	51.4	0.0	0.0	0.0	0.0
Haplophragmoides wilberti Andersen, 1953	0.0	0.2	0.3	0.0	0.6	4.5	29.0	55.7	0.0	28.9	56.3	0.0	0.0
Leptohalysis scotti (Chaster, 1892)	0.0	0.0	0.3	0.0	0.0	0.0	0.0	0.0	0.0	0.0	0.0	0.0	0.0
Paratrochammina simplissima (Cushman & McCulloch, 1939)	0.2	0.5	0.0	0.0	0.0	0.0	0.0	0.0	0.0	0.0	0.0	0.0	0.0
Siphotrochammina lobata Saunders, 1957	0.0	0.5	0.0	1.0	0.0	0.0	0.0	0.6	0.0	0.0	0.0	0.0	0.0
Tiphotrocha comprimata (Cushman & Brönnimann, 1948)	9.2	7.3	3.2	20.4	44.9	12.1	3.8	0.6	0.0	0.0	0.0	0.0	0.0
Trochammina inflata (Montagu, 1808)	20.0	7.7	8.2	4.2	10.1	0.9	2.3	4.5	2.8	6.6	0.0	0.0	0.0
Trochammina sp. A	3.6	4.1	9.8	20.4	14.6	7.1	7.1	0.9	1.4	0.0	0.0	0.0	0.0

Table B1.1 (Continued)

Project							14CCT01						
Core							GB53R						
Depth (cm)	0-1	4-5	8-9	10-11	15-16	20-21	25-26	35-36	45-46	60-61	80-81	100-101	120-121
Trochamminita irregularis Cushman & Brönnimann, 1948	0.0	0.0	0.0	0.0	0.0	0.0	0.0	0.0	0.0	0.0	0.0	0.0	0.0
Textularia earlandi Parker, 1952	0.0	0.0	0.0	0.0	0.0	0.0	0.0	0.0	0.0	0.0	0.0	0.0	0.0
Ammodiscus sp.	0.0	0.0	0.0	0.0	0.0	0.0	0.0	0.0	0.0	0.0	0.0	0.0	0.0
Ammodiscus tenuis Brady, 1884	4.0	0.9	0.3	0.0	0.0	0.0	0.0	0.0	0.0	0.0	0.0	0.0	0.0
Affinetrina alcidi Levy, Mathieu, Poignant, Rosset-Moulinier, 1992	0.0	0.0	0.0	0.0	0.0	0.0	0.0	0.0	0.0	0.0	0.0	0.0	0.0
Miliammina fusca (Brady, 1870)	19.1	25.5	21.0	36.6	3.8	33.8	12.0	0.0	0.0	1.7	0.0	0.0	0.0
Miliammina petila Saunders, 1958	0.0	1.1	0.3	0.0	0.0	0.0	0.0	0.0	1.0	0.0	0.0	0.0	0.0
Miliolinella subrotunda (Montagu, 1803)	0.0	0.0	0.0	0.0	0.0	0.0	0.0	0.0	0.0	0.0	0.0	0.0	0.0
Pyrgo nasuta Cushman, 1935	0.0	0.0	0.0	0.0	0.0	0.0	0.0	0.0	0.0	0.0	0.0	0.0	0.0
Quinqueloculina jugosa Cushman, 1944	0.0	0.0	0.0	0.0	0.0	0.0	0.0	0.0	0.0	0.0	0.0	0.0	0.0
Ammonia parkinsoniana (d'Orbigny, 1839)	0.0	0.0	0.0	0.0	0.0	0.0	0.0	0.0	0.0	0.0	0.0	0.0	0.0
Ammonia tepida (Cushman, 1926)	0.0	0.0	0.0	0.0	0.0	0.0	0.0	0.0	0.0	0.0	0.0	0.0	0.0
Cribroelphidium excavatum (Terquem, 1875)	0.0	0.0	0.0	0.0	0.0	0.0	0.0	0.0	0.0	0.0	0.0	0.0	0.0
Cribroelphidium poeyanum (d'Orbigny, 1839)	0.0	0.0	0.0	0.0	0.0	0.0	0.0	0.0	0.0	0.0	0.0	0.0	0.0
Elphidium gunteri Cole, 1931	0.0	0.0	0.0	0.0	0.0	0.0	0.0	0.0	0.0	0.0	0.0	0.0	0.0
Elphidium mexicanum Kornfeld, 1931	0.0	0.0	0.0	0.0	0.0	0.0	0.0	0.0	0.0	0.0	0.0	0.0	0.0
Haynesina germanica (Ehrenberg, 1840)	0.0	0.0	0.0	0.0	0.0	0.0	0.0	0.0	0.0	0.0	0.0	0.0	0.0
Helenina anderseni (Warren, 1957)	0.0	0.0	0.0	0.0	0.0	0.0	0.0	0.0	0.0	0.0	0.0	0.0	0.0
Other agglutinated	0.0	1.1	0.0	0.0	0.0	0.0	0.0	0.0	0.0	0.0	0.0	0.0	0.0
Other calcareous	0.0	0.0	0.0	0.0	0.0	0.0	0.0	0.0	0.0	0.0	0.0	0.0	0.0
Indeterminate planktonic	0.0	0.0	0.0	0.0	0.0	0.0	0.0	0.0	0.0	0.0	0.0	0.0	0.0

Table B1.1 (Continued)

Project	14CCT01											
Core	GB60R											
Depth (cm)	0-1	4-5	8-9	10-11	15-16	20-21	25-26	35-36	45-46	60-61	80-81	100-101
Volume (cm^3)	11	8	9	10	11	11	11	11	10	10	12	10
Examined (%)	50	100	100	100	100	100	50	50	25	100	100	100
Density ($10cm^{-3}$)	707	330	522	563	327	385	845	829	1168	105	204	16
Pseudothurammina limnetis (Scott & Medioli, 1980)	0.0	0.0	0.0	0.0	0.0	0.0	0.0	0.0	0.0	0.0	0.0	0.0
Ammoastuta inepta (Cushman & McCulloch, 1939)	7.0	18.3	12.3	12.3	17.9	4.3	1.3	2.2	3.9	22.6	2.9	13.3
Ammotium salsum + Ammobaculites exiguus group	1.3	2.3	0.9	0.4	0.0	0.0	0.0	0.4	23.9	3.6	2.0	6.7
Ammobaculites cf. *A. foliaceus* (Brady, 1881)	0.0	0.0	0.0	0.0	0.0	0.0	0.0	0.0	0.0	0.0	0.0	0.0
Ammobaculites crassus Warren, 1957	0.0	0.0	0.0	0.0	0.0	0.0	0.0	0.0	0.0	0.0	0.0	0.0
Ammotium cassis (Parker, 1870)	0.3	0.0	0.0	0.0	0.0	0.0	0.0	0.0	1.4	1.2	0.0	0.0
Arenoparrella mexicana (Kornfeld, 1931)	20.9	39.9	45.0	31.2	44.8	25.2	36.3	46.2	19.6	28.6	37.3	73.3
Entzia macrescens (Brady, 1870)	0.3	0.0	2.2	1.8	3.1	16.7	7.8	4.4	1.4	2.4	0.0	0.0
Haplophragmoides bonplandi Todd & Brönniman, 1957	0.0	0.0	0.0	0.0	0.0	0.0	0.0	0.0	0.0	0.0	0.0	0.0
Haplophragmoides manilaensis Andersen, 1953	0.0	0.0	0.2	0.0	0.0	0.0	0.4	1.8	0.0	0.0	0.0	0.0
Haplophragmoides wilberti Andersen, 1953	57.4	28.1	30.5	33.7	2.5	3.1	18.9	8.6	0.4	4.8	44.3	6.7
Leptohalysis scotti (Chaster, 1892)	0.0	0.0	0.0	0.0	0.0	0.0	0.0	0.0	0.0	0.0	0.0	0.0
Paratrochammina simplissima (Cushman & McCulloch, 1939)	0.0	0.0	0.0	0.0	0.0	0.0	0.0	0.0	0.0	0.0	0.0	0.0
Siphotrochammina lobata Saunders, 1957	0.0	0.0	0.0	0.0	0.3	1.7	0.0	0.0	0.0	1.2	0.8	0.0
Tiphotrocha comprimata (Cushman & Brönnimann, 1948)	2.1	0.4	0.9	3.6	1.4	15.5	4.1	7.1	9.8	2.4	3.3	0.0
Trochammina inflata (Montagu, 1808)	2.1	2.3	1.3	2.2	5.0	5.5	1.5	1.1	9.5	14.3	1.2	0.0
Trochammina sp. A	3.9	3.0	3.7	4.9	9.2	16.2	5.2	14.4	6.0	8.3	5.3	0.0

Table B1.1 (Continued)

Project	14CCT01											
Core	GB60R											
Depth (cm)	0-1	4-5	8-9	10-11	15-16	20-21	25-26	35-36	45-46	60-61	80-81	100-101
Trochamminita irregularis Cushman & Brönnimann, 1948	0.0	0.0	0.0	0.0	0.0	0.0	0.0	0.0	0.0	0.0	0.0	0.0
Textularia earlandi Parker, 1952	0.0	0.0	0.0	0.0	0.0	0.0	0.0	0.0	0.0	0.0	0.0	0.0
Ammodiscus sp.	0.0	0.0	0.0	0.0	0.0	0.0	0.0	0.0	0.0	0.0	0.0	0.0
Ammodiscus tenuis Brady, 1884	0.0	0.0	0.0	0.0	0.0	0.0	0.0	0.9	2.1	1.2	0.0	0.0
Affinetrina alcidi Levy, Mathieu, Poignant, Rosset-Moulinier, 1992	0.0	0.0	0.0	0.0	0.0	0.0	0.0	0.0	0.0	0.0	0.0	0.0
Miliammina fusca (Brady, 1870)	4.7	5.7	3.0	10.0	15.1	11.9	24.3	12.8	22.1	9.5	2.9	0.0
Miliammina petila Saunders, 1958	0.0	0.0	0.0	0.0	0.6	0.0	0.0	0.0	0.0	0.0	0.0	0.0
Miliolinella subrotunda (Montagu, 1803)	0.0	0.0	0.0	0.0	0.0	0.0	0.0	0.0	0.0	0.0	0.0	0.0
Pyrgo nasuta Cushman, 1935	0.0	0.0	0.0	0.0	0.0	0.0	0.0	0.0	0.0	0.0	0.0	0.0
Quinqueloculina jugosa Cushman, 1944	0.0	0.0	0.0	0.0	0.0	0.0	0.0	0.0	0.0	0.0	0.0	0.0
Ammonia parkinsoniana (d'Orbigny, 1839)	0.0	0.0	0.0	0.0	0.0	0.0	0.0	0.0	0.0	0.0	0.0	0.0
Ammonia tepida (Cushman, 1926)	0.0	0.0	0.0	0.0	0.0	0.0	0.0	0.0	0.0	0.0	0.0	0.0
Cribroelphidium excavatum (Terquem, 1875)	0.0	0.0	0.0	0.0	0.0	0.0	0.0	0.0	0.0	0.0	0.0	0.0
Cribroelphidium poeyanum (d'Orbigny, 1839)	0.0	0.0	0.0	0.0	0.0	0.0	0.0	0.0	0.0	0.0	0.0	0.0
Elphidium gunteri Cole, 1931	0.0	0.0	0.0	0.0	0.0	0.0	0.0	0.0	0.0	0.0	0.0	0.0
Elphidium mexicanum Kornfeld, 1931	0.0	0.0	0.0	0.0	0.0	0.0	0.0	0.0	0.0	0.0	0.0	0.0
Haynesina germanica (Ehrenberg, 1840)	0.0	0.0	0.0	0.0	0.0	0.0	0.0	0.0	0.0	0.0	0.0	0.0
Helenina anderseni (Warren, 1957)	0.0	0.0	0.0	0.0	0.0	0.0	0.0	0.0	0.0	0.0	0.0	0.0
Other agglutinated	0.0	0.0	0.0	0.0	0.0	0.0	0.0	0.0	0.0	0.0	0.0	0.0
Other calcareous	0.0	0.0	0.0	0.0	0.0	0.0	0.0	0.0	0.0	0.0	0.0	0.0
Indeterminate planktonic	0.0	0.0	0.0	0.0	0.0	0.0	0.0	0.0	0.0	0.0	0.0	0.0

Table B1.1 (Continued)

Project	15BIM09											
Core	DA40R											
Depth (cm)	0-1	4-5	8-9	10-11	15-16	20-21	25-26	35-36	45-46	60-61	80-81	100-101
Volume (cm^3)	6	8	10	10	10	12	10	14	13	11	14	12
Examined (%)	100	100	100	100	100	100	100	50	50	50	50	BARREN
Density ($10cm^{-3}$)	57	33	63	74	78	58	217	661	528	467	29	0
Pseudothurammina limnetis (Scott & Medioli, 1980)	0.0	0.0	0.0	0.0	0.0	0.0	0.0	0.0	0.0	0.0	0.0	0.0
Ammoastuta inepta (Cushman & McCulloch, 1939)	0.0	0.0	0.0	0.0	0.0	0.0	0.9	1.1	2.0	1.6	0.0	0.0
Ammotium salsum + Ammobaculites exiguus group	82.4	80.8	57.1	44.6	24.4	13.0	2.3	0.6	2.6	0.8	15.0	0.0
Ammobaculites cf. *A. foliaceus* (Brady, 1881)	0.0	0.0	0.0	0.0	0.0	0.0	0.0	0.0	0.0	0.0	0.0	0.0
Ammobaculites crassus Warren, 1957	0.0	0.0	0.0	0.0	0.0	0.0	0.0	0.0	0.0	0.0	0.0	0.0
Ammotium cassis (Parker, 1870)	0.0	0.0	0.0	0.0	0.0	0.0	0.0	0.0	0.9	0.0	0.0	0.0
Arenoparrella mexicana (Kornfeld, 1931)	2.9	0.0	12.7	9.5	11.5	40.6	69.6	89.6	51.9	77.0	45.0	0.0
Entzia macrescens (Brady, 1870)	0.0	0.0	1.6	0.0	1.3	0.0	0.5	1.3	0.6	0.0	0.0	0.0
Haplophragmoides bonplandi Todd & Brönniman, 1957	0.0	0.0	0.0	0.0	0.0	0.0	0.0	0.0	0.0	0.0	0.0	0.0
Haplophragmoides manilaensis Andersen, 1953	0.0	0.0	1.6	0.0	0.0	0.0	0.0	0.0	0.0	0.0	0.0	0.0
Haplophragmoides wilberti Andersen, 1953	0.0	0.0	0.0	0.0	0.0	0.0	0.0	0.2	26.8	1.9	10.0	0.0
Leptohalysis scotti (Chaster, 1892)	0.0	0.0	0.0	0.0	0.0	0.0	0.0	0.0	0.0	0.8	0.0	0.0
Paratrochammina simplissima (Cushman & McCulloch, 1939)	0.0	0.0	0.0	0.0	0.0	0.0	0.0	0.0	0.0	0.0	0.0	0.0
Siphotrochammina lobata Saunders, 1957	0.0	0.0	0.0	4.1	0.0	0.0	0.0	0.0	1.7	1.2	5.0	0.0
Tiphotrocha comprimata (Cushman & Brönnimann, 1948)	2.9	3.8	4.8	2.7	5.1	1.4	1.4	0.6	1.2	0.8	0.0	0.0
Trochammina inflata (Montagu, 1808)	2.9	3.8	1.6	2.7	5.1	14.5	12.0	2.4	8.7	11.7	10.0	0.0
Trochammina sp. A	5.9	0.0	7.9	6.8	19.2	13.0	8.3	2.4	2.0	3.5	10.0	0.0

Table B1.1 (Continued)

Project	15BIM09											
Core	DA40R											
Depth (cm)	0-1	4-5	8-9	10-11	15-16	20-21	25-26	35-36	45-46	60-61	80-81	100-101
Trochamminita irregularis Cushman & Brönnimann, 1948	0.0	0.0	0.0	0.0	0.0	0.0	0.0	0.0	0.0	0.0	0.0	0.0
Textularia earlandi Parker, 1952	0.0	0.0	0.0	0.0	0.0	0.0	0.0	0.0	0.0	0.0	0.0	0.0
Ammodiscus sp.	0.0	0.0	0.0	0.0	0.0	0.0	0.0	0.0	0.0	0.0	0.0	0.0
Ammodiscus tenuis Brady, 1884	0.0	0.0	0.0	0.0	0.0	0.0	0.0	0.2	0.3	0.0	0.0	0.0
Affinetrina alcidi Levy, Mathieu, Poignant, Rosset-Moulinier, 1992	0.0	0.0	0.0	0.0	0.0	0.0	0.0	0.0	0.0	0.0	0.0	0.0
Miliammina fusca (Brady, 1870)	2.9	11.5	12.7	29.7	33.3	15.9	5.1	1.5	1.2	0.8	5.0	0.0
Miliammina petila Saunders, 1958	0.0	0.0	0.0	0.0	0.0	1.4	0.0	0.0	0.0	0.0	0.0	0.0
Miliolinella subrotunda (Montagu, 1803)	0.0	0.0	0.0	0.0	0.0	0.0	0.0	0.0	0.0	0.0	0.0	0.0
Pyrgo nasuta Cushman, 1935	0.0	0.0	0.0	0.0	0.0	0.0	0.0	0.0	0.0	0.0	0.0	0.0
Quinqueloculina jugosa Cushman, 1944	0.0	0.0	0.0	0.0	0.0	0.0	0.0	0.0	0.0	0.0	0.0	0.0
Ammonia parkinsoniana (d'Orbigny, 1839)	0.0	0.0	0.0	0.0	0.0	0.0	0.0	0.0	0.0	0.0	0.0	0.0
Ammonia tepida (Cushman, 1926)	0.0	0.0	0.0	0.0	0.0	0.0	0.0	0.0	0.0	0.0	0.0	0.0
Cribroelphidium excavatum (Terquem, 1875)	0.0	0.0	0.0	0.0	0.0	0.0	0.0	0.0	0.0	0.0	0.0	0.0
Cribroelphidium poeyanum (d'Orbigny, 1839)	0.0	0.0	0.0	0.0	0.0	0.0	0.0	0.0	0.0	0.0	0.0	0.0
Elphidium gunteri Cole, 1931	0.0	0.0	0.0	0.0	0.0	0.0	0.0	0.0	0.0	0.0	0.0	0.0
Elphidium mexicanum Kornfeld, 1931	0.0	0.0	0.0	0.0	0.0	0.0	0.0	0.0	0.0	0.0	0.0	0.0
Haynesina germanica (Ehrenberg, 1840)	0.0	0.0	0.0	0.0	0.0	0.0	0.0	0.0	0.0	0.0	0.0	0.0
Helenina anderseni (Warren, 1957)	0.0	0.0	0.0	0.0	0.0	0.0	0.0	0.0	0.0	0.0	0.0	0.0
Other agglutinated	0.0	0.0	0.0	0.0	0.0	0.0	0.0	0.0	0.0	0.0	0.0	0.0
Other calcareous	0.0	0.0	0.0	0.0	0.0	0.0	0.0	0.0	0.0	0.0	0.0	0.0
Indeterminate planktonic	0.0	0.0	0.0	0.0	0.0	0.0	0.0	0.0	0.0	0.0	0.0	0.0

Table B1.1 (Continued)

Project	15BIM09													
Core	DA42R													
Depth (cm)	0-1	4-5	8-9	10-11	15-16	20-21	25-26	35-36	45-46	60-61	80-81	99-100	120-121	136-137
Volume (cm^3)	10	12	12	13	12	12	14	13	12	12	12	12	12	12
Examined (%)	100	100	100	100	100	50	25	50	50	100	100	50	BARREN	BARREN
Density ($10cm^{-3}$)	401	278	45	152	59	495	794	428	417	87	146	23	0	0
Pseudothurammina limnetis (Scott & Medioli, 1980)	0.0	0.0	0.0	0.0	0.0	0.0	0.0	0.0	0.0	0.0	0.0	0.0	0.0	0.0
Ammoastuta inepta (Cushman & McCulloch, 1939)	0.0	0.3	0.0	0.5	0.0	0.3	0.4	2.2	0.8	3.8	7.4	0.0	0.0	0.0
Ammotium salsum + Ammobaculites exiguus group	81.0	52.3	29.6	3.0	11.3	0.3	1.4	2.5	1.2	1.9	9.1	21.4	0.0	0.0
Ammobaculites cf. *A. foliaceus* (Brady, 1881)	0.0	0.0	0.0	0.0	0.0	0.0	0.0	0.0	0.0	0.0	0.0	0.0	0.0	0.0
Ammobaculites crassus Warren, 1957	0.0	0.0	0.0	0.0	0.0	0.0	0.0	0.0	0.0	0.0	0.0	0.0	0.0	0.0
Ammotium cassis (Parker, 1870)	0.0	0.0	0.0	0.0	0.0	0.0	0.0	0.4	0.0	0.0	0.0	0.0	0.0	0.0
Arenoparrella mexicana (Kornfeld, 1931)	0.2	11.4	3.7	40.4	53.5	73.7	85.3	42.4	49.6	61.5	58.3	64.3	0.0	0.0
Entzia macrescens (Brady, 1870)	0.0	0.0	0.0	7.6	0.0	4.0	0.7	0.0	0.0	0.0	0.0	0.0	0.0	0.0
Haplophragmoides bonplandi Todd & Brönniman, 1957	0.0	0.0	0.0	0.0	0.0	0.0	0.0	0.0	0.0	0.0	0.0	0.0	0.0	0.0
Haplophragmoides manilaensis Andersen, 1953	0.0	0.3	0.0	0.0	0.0	0.0	0.0	0.0	0.0	0.0	0.0	0.0	0.0	0.0
Haplophragmoides wilberti Andersen, 1953	0.0	0.0	0.0	0.0	0.0	0.0	0.0	38.1	43.2	0.0	0.0	0.0	0.0	0.0
Leptohalysis scotti (Chaster, 1892)	0.0	0.0	0.0	0.0	0.0	0.0	0.0	0.0	0.0	0.0	0.0	0.0	0.0	0.0
Paratrochammina simplissima (Cushman & McCulloch, 1939)	0.0	0.0	0.0	0.0	0.0	0.0	0.0	0.0	0.0	0.0	0.0	0.0	0.0	0.0
Siphotrochammina lobata Saunders, 1957	0.0	0.0	0.0	0.0	0.0	0.0	0.4	0.0	0.4	2.9	0.0	0.0	0.0	0.0
Tiphotrocha comprimata (Cushman & Brönnimann, 1948)	1.2	5.4	1.9	3.5	1.4	1.7	1.8	1.1	0.0	0.0	2.9	0.0	0.0	0.0
Trochammina inflata (Montagu, 1808)	4.0	6.0	20.4	13.1	8.5	7.1	4.0	6.1	2.4	18.3	9.7	7.1	0.0	0.0
Trochammina sp. A	2.2	6.0	27.8	16.2	5.6	7.7	1.4	4.7	0.8	9.6	6.3	0.0	0.0	0.0

Table B1.1 (Continued)

Project	15BIM09													
Core	DA42R													
Depth (cm)	0-1	4-5	8-9	10-11	15-16	20-21	25-26	35-36	45-46	60-61	80-81	99-100	120-121	136-137
Trochamminita irregularis Cushman & Brönnimann, 1948	0.0	0.0	0.0	0.0	0.0	0.0	0.0	0.0	0.0	0.0	0.0	0.0	0.0	0.0
Textularia earlandi Parker, 1952	0.0	0.0	0.0	0.0	0.0	0.0	0.0	0.0	0.0	0.0	0.0	0.0	0.0	0.0
Ammodiscus sp.	0.0	0.0	0.0	0.0	0.0	0.0	0.0	0.0	0.0	0.0	0.0	0.0	0.0	0.0
Ammodiscus tenuis Brady, 1884	0.0	0.0	0.0	0.0	0.0	0.0	0.0	0.0	0.0	0.0	0.0	0.0	0.0	0.0
Affinetrina alcidi Levy, Mathieu, Poignant, Rosset-Moulinier, 1992	0.0	0.0	0.0	0.0	0.0	0.0	0.0	0.0	0.0	0.0	0.0	0.0	0.0	0.0
Miliammina fusca (Brady, 1870)	11.2	18.3	16.7	15.7	19.7	4.7	4.7	2.5	1.6	1.9	6.3	7.1	0.0	0.0
Miliammina petila Saunders, 1958	0.0	0.0	0.0	0.0	0.0	0.0	0.0	0.0	0.0	0.0	0.0	0.0	0.0	0.0
Miliolinella subrotunda (Montagu, 1803)	0.0	0.0	0.0	0.0	0.0	0.0	0.0	0.0	0.0	0.0	0.0	0.0	0.0	0.0
Pyrgo nasuta Cushman, 1935	0.0	0.0	0.0	0.0	0.0	0.0	0.0	0.0	0.0	0.0	0.0	0.0	0.0	0.0
Quinqueloculina jugosa Cushman, 1944	0.0	0.0	0.0	0.0	0.0	0.0	0.0	0.0	0.0	0.0	0.0	0.0	0.0	0.0
Ammonia parkinsoniana (d'Orbigny, 1839)	0.0	0.0	0.0	0.0	0.0	0.0	0.0	0.0	0.0	0.0	0.0	0.0	0.0	0.0
Ammonia tepida (Cushman, 1926)	0.0	0.0	0.0	0.0	0.0	0.3	0.0	0.0	0.0	0.0	0.0	0.0	0.0	0.0
Cribroelphidium excavatum (Terquem, 1875)	0.0	0.0	0.0	0.0	0.0	0.0	0.0	0.0	0.0	0.0	0.0	0.0	0.0	0.0
Cribroelphidium poeyanum (d'Orbigny, 1839)	0.0	0.0	0.0	0.0	0.0	0.0	0.0	0.0	0.0	0.0	0.0	0.0	0.0	0.0
Elphidium gunteri Cole, 1931	0.0	0.0	0.0	0.0	0.0	0.0	0.0	0.0	0.0	0.0	0.0	0.0	0.0	0.0
Elphidium mexicanum Kornfeld, 1931	0.0	0.0	0.0	0.0	0.0	0.0	0.0	0.0	0.0	0.0	0.0	0.0	0.0	0.0
Haynesina germanica (Ehrenberg, 1840)	0.0	0.0	0.0	0.0	0.0	0.0	0.0	0.0	0.0	0.0	0.0	0.0	0.0	0.0
Helenina anderseni (Warren, 1957)	0.0	0.0	0.0	0.0	0.0	0.0	0.0	0.0	0.0	0.0	0.0	0.0	0.0	0.0
Other agglutinated	0.0	0.0	0.0	0.0	0.0	0.0	0.0	0.0	0.0	0.0	0.0	0.0	0.0	0.0
Other calcareous	0.0	0.0	0.0	0.0	0.0	0.0	0.0	0.0	0.0	0.0	0.0	0.0	0.0	0.0
Indeterminate planktonic	0.0	0.0	0.0	0.0	0.0	0.0	0.0	0.0	0.0	0.0	0.0	0.0	0.0	0.0

Table B1.2 Stained cores (live and dead assemblages separate). Raw counts will be made available in a USGS Data Release.

Project				15BIM09							15BIM09			
Core				DA33R FA							DA33R FA			
Live/dead abundance				live (stained)							dead			
Depth (cm)	0-1	1-2	2-3	3-4	4-5	6-7	8-9	0-1	1-2	2-3	3-4	4-5	6-7	8-9
Volume (cm^3)	7	5	12	15	15	15	12	7	5	12	15	15	15	12
Examined (%)	100	100	100	100	100	100	100	100	100	100	100	100	100	100
Density ($10cm^{-3}$)	21	38	25	23	17	15	16	274	332	188	201	212	190	301
Pseudothurammina limnetis (Scott & Medioli, 1980)	33.3	21.1	50.0	61.8	52.0	45.5	42.1	15.6	19.3	12.0	16.2	11.3	8.4	6.6
Ammoastuta inepta (Cushman & McCulloch, 1939)	6.7	0.0	3.3	8.8	0.0	0.0	0.0	10.4	9.0	10.2	14.6	15.7	0.0	14.1
Ammotium salsum + Ammobaculites exiguus group	0.0	0.0	0.0	0.0	0.0	0.0	0.0	0.0	0.0	0.0	0.0	0.0	0.0	0.0
Ammobaculites cf. *A. foliaceus* (Brady, 1881)	0.0	0.0	0.0	0.0	0.0	0.0	0.0	0.0	0.0	0.0	0.3	0.0	0.0	0.0
Ammobaculites crassus Warren, 1957	6.7	0.0	0.0	2.9	0.0	0.0	0.0	0.5	3.6	0.9	2.6	0.6	1.1	0.8
Ammotium cassis (Parker, 1870)	13.3	10.5	23.3	11.8	16.0	9.1	15.8	18.2	19.9	19.1	15.2	20.4	30.2	21.3
Arenoparrella mexicana (Kornfeld, 1931)	0.0	0.0	0.0	0.0	0.0	0.0	0.0	0.0	3.0	0.0	0.0	2.5	0.0	3.0
Entzia macrescens (Brady, 1870)	0.0	0.0	0.0	0.0	0.0	0.0	0.0	0.0	0.0	0.0	0.0	0.0	0.0	0.0
Haplophragmoides bonplandi Todd & Brönniman, 1957	0.0	0.0	0.0	0.0	0.0	0.0	0.0	1.0	0.0	0.0	0.0	0.3	0.4	0.3
Haplophragmoides manilaensis Andersen, 1953	26.7	26.3	6.7	2.9	16.0	27.3	21.1	20.8	17.5	16.9	15.6	13.5	23.2	26.0
Haplophragmoides wilberti Andersen, 1953	0.0	0.0	0.0	2.9	0.0	4.5	0.0	0.0	0.0	0.4	0.7	0.3	1.4	1.4
Leptohalysis scotti (Chaster, 1892)	0.0	0.0	0.0	0.0	0.0	0.0	0.0	0.0	0.0	0.0	0.0	0.0	0.0	0.0
Paratrochammina simplissima (Cushman & McCulloch, 1939)	13.3	0.0	0.0	0.0	0.0	0.0	0.0	3.1	3.6	1.8	0.0	2.2	7.4	1.4
Siphotrochammina lobata Saunders, 1957	0.0	0.0	0.0	0.0	0.0	0.0	0.0	3.1	3.0	2.2	2.3	1.6	2.1	2.5
Tiphotrocha comprimata (Cushman & Brönnimann, 1948)	0.0	31.6	16.7	0.0	16.0	13.6	21.1	18.2	11.4	27.6	23.2	18.9	17.5	15.8
Trochammina inflata (Montagu, 1808)	0.0	0.0	0.0	0.0	0.0	0.0	0.0	1.0	2.4	3.1	4.0	4.1	3.5	1.7
Trochammina sp. A	0.0	0.0	0.0	0.0	0.0	0.0	0.0	0.0	0.0	0.0	0.7	0.6	0.0	1.4
Trochamminita irregularis Cushman & Brönnimann, 1948	0.0	0.0	0.0	0.0	0.0	0.0	0.0	0.0	0.0	0.0	0.0	0.0	0.0	0.0

Table B1.2 (Continued)

Project				15BIM09							15BIM09			
Core				DA33R FA							DA33R FA			
Live/dead abundance				live (stained)							dead			
Depth (cm)	0-1	1-2	2-3	3-4	4-5	6-7	8-9	0-1	1-2	2-3	3-4	4-5	6-7	8-9
Textularia earlandi Parker, 1952	0.0	0.0	0.0	0.0	0.0	0.0	0.0	0.0	0.0	0.0	0.0	0.0	0.0	0.0
Ammodiscus sp.	0.0	0.0	0.0	0.0	0.0	0.0	0.0	0.0	0.0	0.0	0.0	0.0	0.0	0.0
Ammodiscus tenuis Brady, 1884	0.0	0.0	0.0	0.0	0.0	0.0	0.0	0.0	0.0	0.0	0.0	0.0	0.0	0.0
Affinetrina alcidi Levy, Mathieu, Poignant, Rosset-Moulinier, 1992	0.0	0.0	0.0	0.0	0.0	0.0	0.0	4.2	3.6	4.4	2.0	1.3	0.7	1.4
Miliammina fusca (Brady, 1870)	0.0	0.0	0.0	2.9	0.0	0.0	0.0	3.1	3.6	1.3	2.6	6.3	3.9	2.2
Miliammina petila Saunders, 1958	0.0	0.0	0.0	0.0	0.0	0.0	0.0	0.0	0.0	0.0	0.0	0.0	0.0	0.0
Miliolinella subrotunda (Montagu, 1803)	0.0	0.0	0.0	0.0	0.0	0.0	0.0	0.0	0.0	0.0	0.0	0.0	0.0	0.0
Pyrgo nasuta Cushman, 1935	0.0	0.0	0.0	0.0	0.0	0.0	0.0	0.0	0.0	0.0	0.0	0.0	0.0	0.0
Quinqueloculina jugosa Cushman, 1944	0.0	0.0	0.0	0.0	0.0	0.0	0.0	0.0	0.0	0.0	0.0	0.0	0.0	0.0
Ammonia parkinsoniana (d'Orbigny, 1839)	0.0	0.0	0.0	5.9	0.0	0.0	0.0	0.0	0.0	0.0	0.0	0.0	0.0	0.0
Ammonia tepida (Cushman, 1926)	0.0	0.0	0.0	0.0	0.0	0.0	0.0	0.0	0.0	0.0	0.0	0.0	0.0	0.0
Cribroelphidium excavatum (Terquem, 1875)	0.0	0.0	0.0	0.0	0.0	0.0	0.0	0.0	0.0	0.0	0.0	0.0	0.0	0.0
Cribroelphidium poeyanum (d'Orbigny, 1839)	0.0	0.0	0.0	0.0	0.0	0.0	0.0	0.0	0.0	0.0	0.0	0.0	0.0	0.0
Elphidium gunteri Cole, 1931	0.0	0.0	0.0	0.0	0.0	0.0	0.0	0.0	0.0	0.0	0.0	0.0	0.0	0.0
Elphidium mexicanum Kornfeld, 1931	0.0	0.0	0.0	0.0	0.0	0.0	0.0	0.0	0.0	0.0	0.0	0.0	0.0	0.0
Haynesina germanica (Ehrenberg, 1840)	0.0	10.5	0.0	0.0	0.0	0.0	0.0	0.0	0.0	0.0	0.0	0.0	0.0	0.0
Helenina anderseni (Warren, 1957)	0.0	0.0	0.0	0.0	0.0	0.0	0.0	0.5	0.0	0.0	0.0	0.3	0.4	0.0
Other agglutinated	0.0	0.0	0.0	0.0	0.0	0.0	0.0	0.0	0.0	0.0	0.0	0.0	0.0	0.0
Other calcareous	0.0	0.0	0.0	0.0	0.0	0.0	0.0	0.0	0.0	0.0	0.0	0.0	0.0	0.0
Indeterminate planktonic	0.0	0.0	0.0	0.0	0.0	0.0	0.0	0.0	0.0	0.0	0.0	0.0	0.0	0.0

Table B1.2 (Continued)

Project	15BIM09							15BIM09						
Core	DA34R FA							DA34R FA						
Live/dead abundance	live (stained)							dead						
Depth (cm)	0-1	1-2	2-3	3-4	4-5	6-7	8-9	0-1	1-2	2-3	3-4	4-5	6-7	8-9
Volume (cm^3)	10	12	12	20	20	15	20	10	12	12	20	20	15	20
Examined (%)	100	100	100	100	100	100	100	100	100	100	100	100	100	100
Density ($10cm^{-3}$)	13	18	24	25	20	10	9	68	103	180	170	136	352	191
Pseudothurammina limnetis (Scott & Medioli, 1980)	46.2	33.3	20.7	18.0	0.0	33.3	29.4	13.2	21.1	18.5	20.1	22.4	19.1	22.8
Ammoastuta inepta (Cushman & McCulloch, 1939)	7.7	4.8	0.0	0.0	25.0	0.0	0.0	17.6	20.3	11.1	8.8	14.0	18.6	9.7
Ammotium salsum + Ammobaculites exiguus group	0.0	0.0	0.0	0.0	0.0	0.0	0.0	0.0	0.0	0.0	0.0	0.0	0.0	0.0
Ammobaculites cf. *A. foliaceus* (Brady, 1881)	0.0	0.0	0.0	0.0	0.0	0.0	0.0	0.0	0.0	0.0	0.0	0.0	0.0	0.0
Ammobaculites crassus Warren, 1957	0.0	0.0	0.0	0.0	0.0	0.0	0.0	0.0	0.0	0.5	0.3	0.0	0.0	0.8
Ammotium cassis (Parker, 1870)	23.1	47.6	65.5	72.0	67.5	33.3	47.1	13.2	20.3	25.5	29.5	26.1	19.3	30.9
Arenoparrella mexicana (Kornfeld, 1931)	0.0	0.0	0.0	0.0	0.0	0.0	11.8	0.0	1.6	0.5	5.3	2.9	3.8	5.0
Entzia macrescens (Brady, 1870)	0.0	0.0	0.0	0.0	0.0	0.0	0.0	0.0	0.0	0.0	0.0	0.0	0.0	0.0
Haplophragmoides bonplandi Todd & Brönniman, 1957	0.0	0.0	0.0	0.0	0.0	0.0	0.0	0.0	0.0	0.0	0.3	1.5	0.9	0.5
Haplophragmoides manilaensis Andersen, 1953	0.0	0.0	0.0	0.0	0.0	0.0	0.0	0.0	0.0	0.0	0.0	0.0	0.8	0.0
Haplophragmoides wilberti Andersen, 1953	0.0	0.0	0.0	0.0	0.0	0.0	0.0	0.0	0.0	0.0	0.0	0.0	0.0	0.0
Leptohalysis scotti (Chaster, 1892)	0.0	0.0	0.0	0.0	0.0	0.0	0.0	0.0	0.8	0.0	0.0	0.0	0.0	0.0
Paratrochammina simplissima (Cushman & McCulloch, 1939)	0.0	0.0	0.0	0.0	0.0	0.0	0.0	0.0	0.8	2.8	0.0	0.0	0.0	0.0
Siphotrochammina lobata Saunders, 1957	0.0	4.8	6.9	0.0	0.0	6.7	0.0	27.9	10.6	8.3	6.8	4.4	2.7	1.6
Tiphotrocha comprimata (Cushman & Brönnimann, 1948)	7.7	9.5	3.4	6.0	0.0	13.3	0.0	16.2	12.2	18.1	12.7	7.7	13.4	13.6
Trochammina inflata (Montagu, 1808)	7.7	0.0	0.0	2.0	2.5	0.0	5.9	5.9	2.4	2.8	3.5	5.9	4.4	5.8
Trochammina sp. A	0.0	0.0	0.0	0.0	0.0	0.0	0.0	0.0	0.0	0.0	0.0	0.0	0.0	0.0
Trochamminita irregularis Cushman & Brönnimann, 1948	0.0	0.0	0.0	0.0	0.0	0.0	0.0	0.0	0.0	0.0	0.0	0.0	0.0	0.0

Table B1.2 (Continued)

Project				15BIM09							15BIM09			
Core				DA34R FA							DA34R FA			
Live/dead abundance				live (stained)							dead			
Depth (cm)	0-1	1-2	2-3	3-4	4-5	6-7	8-9	0-1	1-2	2-3	3-4	4-5	6-7	8-9
Textularia earlandi Parker, 1952	0.0	0.0	0.0	0.0	0.0	0.0	0.0	0.0	0.0	0.0	0.0	0.0	0.0	0.0
Ammodiscus sp.	0.0	0.0	0.0	0.0	0.0	0.0	0.0	0.0	0.8	0.0	0.3	0.0	0.0	0.0
Ammodiscus tenuis Brady, 1884	0.0	0.0	0.0	0.0	0.0	0.0	0.0	0.0	0.0	0.0	0.0	0.0	0.0	0.0
Affinetrina alcidi Levy, Mathieu, Poignant, Rosset-Moulinier, 1992	7.7	0.0	0.0	2.0	5.0	13.3	5.9	5.9	8.9	12.0	12.4	15.1	17.0	8.9
Miliammina fusca (Brady, 1870)	0.0	0.0	0.0	0.0	0.0	0.0	0.0	0.0	0.0	0.0	0.0	0.0	0.0	0.0
Miliammina petila Saunders, 1958	0.0	0.0	0.0	0.0	0.0	0.0	0.0	0.0	0.0	0.0	0.0	0.0	0.0	0.0
Miliolinella subrotunda (Montagu, 1803)	0.0	0.0	0.0	0.0	0.0	0.0	0.0	0.0	0.0	0.0	0.0	0.0	0.0	0.0
Pyrgo nasuta Cushman, 1935	0.0	0.0	0.0	0.0	0.0	0.0	0.0	0.0	0.0	0.0	0.0	0.0	0.0	0.0
Quinqueloculina jugosa Cushman, 1944	0.0	0.0	0.0	0.0	0.0	0.0	0.0	0.0	0.0	0.0	0.0	0.0	0.0	0.0
Ammonia parkinsoniana (d'Orbigny, 1839)	0.0	0.0	3.4	0.0	0.0	0.0	0.0	0.0	0.0	0.0	0.0	0.0	0.0	0.0
Ammonia tepida (Cushman, 1926)	0.0	0.0	0.0	0.0	0.0	0.0	0.0	0.0	0.0	0.0	0.0	0.0	0.0	0.0
Cribroelphidium excavatum (Terquem, 1875)	0.0	0.0	0.0	0.0	0.0	0.0	0.0	0.0	0.0	0.0	0.0	0.0	0.0	0.0
Cribroelphidium poeyanum (d'Orbigny, 1839)	0.0	0.0	0.0	0.0	0.0	0.0	0.0	0.0	0.0	0.0	0.0	0.0	0.0	0.0
Elphidium gunteri Cole, 1931	0.0	0.0	0.0	0.0	0.0	0.0	0.0	0.0	0.0	0.0	0.0	0.0	0.0	0.0
Elphidium mexicanum Kornfeld, 1931	0.0	0.0	0.0	0.0	0.0	0.0	0.0	0.0	0.0	0.0	0.0	0.0	0.0	0.0
Haynesina germanica (Ehrenberg, 1840)	0.0	0.0	0.0	0.0	0.0	0.0	0.0	0.0	0.0	0.0	0.0	0.0	0.0	0.0
Helenina anderseni (Warren, 1957)	0.0	0.0	0.0	0.0	0.0	0.0	0.0	0.0	0.0	0.0	0.0	0.0	0.0	0.5
Other agglutinated	0.0	0.0	0.0	0.0	0.0	0.0	0.0	0.0	0.0	0.0	0.0	0.0	0.0	0.0
Other calcareous	0.0	0.0	0.0	0.0	0.0	0.0	0.0	0.0	0.0	0.0	0.0	0.0	0.0	0.0
Indeterminate planktonic	0.0	0.0	0.0	0.0	0.0	0.0	0.0	0.0	0.0	0.0	0.0	0.0	0.0	0.0

Table B1.2 (Continued)

Project				15BIM09							15BIM09			
Core				DA35R FA							DA35R FA			
Live/dead abundance				live (stained)							dead			
Depth (cm)	0-1	1-2	2-3	3-4	4-5	6-7	8-9	0-1	1-2	2-3	3-4	4-5	6-7	8-9
Volume (cm^3)	10	17	20	15	7	15	10	10	17	20	15	7	15	10
Examined (%)	100	100	100	100	100	100	100	100	100	100	100	100	100	100
Density ($10cm^{-3}$)	0	1	0	1	0	0	1	27	82	135	161	124	55	46
Pseudothurammina limnetis (Scott & Medioli, 1980)	0.0	0.0	0.0	0.0	0.0	0.0	0.0	0.0	0.0	0.0	0.4	0.0	4.9	2.2
Ammoastuta inepta (Cushman & McCulloch, 1939)	0.0	0.0	0.0	0.0	0.0	0.0	0.0	59.3	59.7	78.1	60.2	62.1	23.2	56.5
Ammotium salsum + Ammobaculites exiguus group	0.0	0.0	0.0	0.0	0.0	0.0	0.0	0.0	0.0	0.0	0.0	0.0	0.0	0.0
Ammobaculites cf. *A. foliaceus* (Brady, 1881)	0.0	0.0	0.0	0.0	0.0	0.0	0.0	0.0	0.0	0.0	0.0	0.0	0.0	0.0
Ammobaculites crassus Warren, 1957	0.0	0.0	0.0	0.0	0.0	0.0	0.0	0.0	0.0	0.0	0.0	0.0	0.0	0.0
Ammotium cassis (Parker, 1870)	0.0	0.0	0.0	0.0	0.0	0.0	100.0	0.0	0.7	1.1	5.4	3.4	14.6	6.5
Arenoparrella mexicana (Kornfeld, 1931)	0.0	0.0	0.0	0.0	0.0	0.0	0.0	0.0	0.0	0.0	1.7	1.1	0.0	2.2
Entzia macrescens (Brady, 1870)	0.0	0.0	0.0	0.0	0.0	0.0	0.0	0.0	0.0	0.0	0.0	0.0	0.0	0.0
Haplophragmoides bonplandi Todd & Brönniman, 1957	0.0	0.0	0.0	0.0	0.0	0.0	0.0	0.0	0.0	0.0	0.0	0.0	0.0	0.0
Haplophragmoides manilaensis Andersen, 1953	0.0	0.0	0.0	0.0	0.0	0.0	0.0	0.0	0.0	0.0	0.0	2.3	7.3	2.2
Haplophragmoides wilberti Andersen, 1953	0.0	0.0	0.0	0.0	0.0	0.0	0.0	0.0	0.0	0.0	0.0	0.0	0.0	0.0
Leptohalysis scotti (Chaster, 1892)	0.0	0.0	0.0	0.0	0.0	0.0	0.0	0.0	0.0	0.0	0.0	0.0	0.0	0.0
Paratrochammina simplissima (Cushman & McCulloch, 1939)	0.0	0.0	0.0	0.0	0.0	0.0	0.0	0.0	0.0	0.0	0.0	0.0	1.2	2.2
Siphotrochammina lobata Saunders, 1957	0.0	0.0	0.0	0.0	0.0	0.0	0.0	0.0	1.4	2.6	6.2	0.0	6.1	2.2
Tiphotrocha comprimata (Cushman & Brönnimann, 1948)	0.0	0.0	0.0	0.0	0.0	0.0	0.0	0.0	0.0	3.0	1.7	4.6	25.6	6.5
Trochammina inflata (Montagu, 1808)	0.0	0.0	0.0	100.0	0.0	0.0	0.0	0.0	0.0	0.4	0.0	3.4	2.4	0.0
Trochammina sp. A	0.0	0.0	0.0	0.0	0.0	0.0	0.0	0.0	0.0	0.0	0.0	0.0	0.0	0.0
Trochamminita irregularis Cushman & Brönnimann, 1948	0.0	0.0	0.0	0.0	0.0	0.0	0.0	0.0	0.0	0.0	0.0	0.0	0.0	0.0

Table B1.2 (Continued)

Project				15BIM09							15BIM09			
Core				DA35R FA							DA35R FA			
Live/dead abundance				live (stained)							dead			
Depth (cm)	0-1	1-2	2-3	3-4	4-5	6-7	8-9	0-1	1-2	2-3	3-4	4-5	6-7	8-9
Textularia earlandi Parker, 1952	0.0	0.0	0.0	0.0	0.0	0.0	0.0	0.0	0.0	0.0	0.0	0.0	0.0	0.0
Ammodiscus sp.	0.0	0.0	0.0	0.0	0.0	0.0	0.0	0.0	0.0	0.0	0.0	0.0	0.0	0.0
Ammodiscus tenuis Brady, 1884	0.0	0.0	0.0	0.0	0.0	0.0	0.0	0.0	0.0	0.0	0.0	0.0	0.0	0.0
Affinetrina alcidi Levy, Mathieu, Poignant, Rosset-Moulinier, 1992	0.0	0.0	0.0	0.0	0.0	0.0	0.0	37.0	38.1	14.5	23.7	21.8	14.6	19.6
Miliammina fusca (Brady, 1870)	0.0	0.0	0.0	0.0	0.0	0.0	0.0	0.0	0.0	0.0	0.0	0.0	0.0	0.0
Miliammina petila Saunders, 1958	0.0	0.0	0.0	0.0	0.0	0.0	0.0	0.0	0.0	0.0	0.0	0.0	0.0	0.0
Miliolinella subrotunda (Montagu, 1803)	0.0	0.0	0.0	0.0	0.0	0.0	0.0	0.0	0.0	0.0	0.0	0.0	0.0	0.0
Pyrgo nasuta Cushman, 1935	0.0	0.0	0.0	0.0	0.0	0.0	0.0	0.0	0.0	0.0	0.0	0.0	0.0	0.0
Quinqueloculina jugosa Cushman, 1944	0.0	0.0	0.0	0.0	0.0	0.0	0.0	0.0	0.0	0.0	0.0	0.0	0.0	0.0
Ammonia parkinsoniana (d'Orbigny, 1839)	0.0	100.0	0.0	0.0	0.0	0.0	0.0	0.0	0.0	0.0	0.0	0.0	0.0	0.0
Ammonia tepida (Cushman, 1926)	0.0	0.0	0.0	0.0	0.0	0.0	0.0	3.7	0.0	0.0	0.8	1.1	0.0	0.0
Cribroelphidium excavatum (Terquem, 1875)	0.0	0.0	0.0	0.0	0.0	0.0	0.0	0.0	0.0	0.0	0.0	0.0	0.0	0.0
Cribroelphidium poeyanum (d'Orbigny, 1839)	0.0	0.0	0.0	0.0	0.0	0.0	0.0	0.0	0.0	0.0	0.0	0.0	0.0	0.0
Elphidium gunteri Cole, 1931	0.0	0.0	0.0	0.0	0.0	0.0	0.0	0.0	0.0	0.0	0.0	0.0	0.0	0.0
Elphidium mexicanum Kornfeld, 1931	0.0	0.0	0.0	0.0	0.0	0.0	0.0	0.0	0.0	0.0	0.0	0.0	0.0	0.0
Haynesina germanica (Ehrenberg, 1840)	0.0	0.0	0.0	0.0	0.0	0.0	0.0	0.0	0.0	0.0	0.0	0.0	0.0	0.0
Helenina anderseni (Warren, 1957)	0.0	0.0	0.0	0.0	0.0	0.0	0.0	0.0	0.0	0.4	0.0	0.0	0.0	0.0
Other agglutinated	0.0	0.0	0.0	0.0	0.0	0.0	0.0	0.0	0.0	0.0	0.0	0.0	0.0	0.0
Other calcareous	0.0	0.0	0.0	0.0	0.0	0.0	0.0	0.0	0.0	0.0	0.0	0.0	0.0	0.0
Indeterminate planktonic	0.0	0.0	0.0	0.0	0.0	0.0	0.0	0.0	0.0	0.0	0.0	0.0	0.0	0.0

Appendix B2. Radiometric Dating (^{210}Pb, ^{226}Ra, ^{137}Cs).

Table B2.1. GB53M radiometric data and age model. ND = Not Detected.

Core	Depth (cm)	Total ^{210}Pb activity (dpm/g)	SD Total ^{210}Pb activity (dpm/g)	^{226}Ra activity (dpm/g)	SD ^{226}Ra activity (dpm/g)	^{137}Cs activity (dpm/g)	SD ^{137}Cs activity (dpm/g)	CRS modeled depth (cm)	Modeled year (CE)	SD modeled year
14CCT01 GB53M	0-1	10.601	0.746	1.489	0.199	ND	-	0.0	2014	0.0
14CCT01 GB53M	1-2	7.840	0.372	1.294	0.098	ND	-	0.5	2013	1.2
14CCT01 GB53M	2-3	6.540	0.316	1.398	0.088	ND	-	1.6	2010	1.2
14CCT01 GB53M	3-4	5.623	0.324	1.329	0.091	0.089	0.052	2.7	2008	1.2
14CCT01 GB53M	4-5	5.409	0.320	1.435	0.102	0.087	0.053	3.8	2006	1.2
14CCT01 GB53M	5-6	7.041	0.320	1.268	0.090	0.155	0.055	4.9	2004	1.2
14CCT01 GB53M	6-7	5.802	0.347	1.216	0.107	0.208	0.071	6.0	2001	1.3
14CCT01 GB53M	7-8	6.293	0.297	1.278	0.086	0.127	0.049	7.1	1999	1.3
14CCT01 GB53M	8-9	6.184	0.330	1.312	0.099	0.237	0.069	8.2	1997	1.3
14CCT01 GB53M	9-10	4.639	0.324	1.379	0.110	0.170	0.064	9.3	1995	1.3
14CCT01 GB53M	10-11	6.558	0.417	1.249	0.133	0.347	0.091	10.4	1993	1.3
14CCT01 GB53M	11-12	7.483	0.438	1.266	0.133	0.392	0.105	11.5	1991	1.3
14CCT01 GB53M	12-13	7.601	0.495	1.566	0.155	0.142	0.088	12.6	1989	1.3
14CCT01 GB53M	13-14	6.521	0.392	1.368	0.116	0.243	0.076	13.7	1985	1.3
14CCT01 GB53M	14-15	5.986	0.398	1.346	0.113	0.674	0.090	14.8	1980	1.3
14CCT01 GB53M	15-16	5.525	0.551	1.391	0.159	0.728	0.123	15.9	1976	1.4
14CCT01 GB53M	16-17	5.505	0.566	1.518	0.183	0.966	0.150	17.0	1972	1.3
14CCT01 GB53M	17-18	3.616	0.315	1.369	0.107	0.503	0.081	18.1	1967	1.3
14CCT01 GB53M	18-19	5.115	0.342	1.418	0.111	0.303	0.077	19.2	1963	1.3
14CCT01 GB53M	19-20	4.419	0.509	1.546	0.170	0.293	0.117	20.3	1958	1.3
14CCT01 GB53M	21-22	2.786	0.300	1.377	0.105	0.099	0.056	21.4	1952	1.2
14CCT01 GB53M	23-24	2.629	0.278	1.472	0.095	0.102	0.053	23.6	1941	1.2
14CCT01 GB53M	25-26	1.713	0.207	1.269	0.076	ND	-	25.8	1917	1.4
14CCT01 GB53M	29-30	1.702	0.244	1.491	0.097	ND	-	-	-	-
14CCT01 GB53M	33-34	1.560	0.193	1.546	0.073	ND	-	-	-	-
14CCT01 GB53M	37-38	1.840	0.144	1.482	0.053	ND	-	-	-	-
14CCT01 GB53M	41-42	1.630	0.245	1.608	0.091	ND	-	-	-	-

Table B2.1. (Continued)

Core	Depth (cm)	Total ^{210}Pb activity (dpm/g)	SD Total ^{210}Pb activity (dpm/g)	^{226}Ra activity (dpm/g)	SD ^{226}Ra activity (dpm/g)	^{137}Cs activity (dpm/g)	SD ^{137}Cs activity (dpm/g)	CRS modeled depth (cm)	Modeled year (CE)	SD modeled year
14CCT01 GB53M	45-46	1.452	0.238	1.525	0.092	ND	-	-	-	-
14CCT01 GB53M	49-50	1.657	0.207	1.597	0.079	ND	-	-	-	-
14CCT01 GB53M	53-54	1.746	0.226	1.581	0.084	ND	-	-	-	-
14CCT01 GB53M	57-58	1.496	0.267	1.580	0.107	ND	-	-	-	-
14CCT01 GB53M	61-62	1.714	0.291	1.593	0.103	ND	-	-	-	-
14CCT01 GB53M	65-66	1.603	0.161	1.447	0.059	ND	-	-	-	-
14CCT01 GB53M	66-67	1.679	0.184	1.508	0.065	ND	-	-	-	-

Table B2.2. GB60M radiometric data and age model. ND = Not Detected.

Core	Depth (cm)	Total ^{210}Pb activity (dpm/g)	SD Total ^{210}Pb activity (dpm/g)	^{226}Ra activity (dpm/g)	SD ^{226}Ra activity (dpm/g)	^{137}Cs activity (dpm/g)	SD ^{137}Cs activity (dpm/g)	CRS modeled depth (cm)	Modeled year (CE)	SD modeled year
14CCT01 GB60M	0-1	12.489	0.515	1.402	0.093	0.252	0.065	0.0	2014	0.0
14CCT01 GB60M	1-2	6.425	0.351	1.564	0.072	0.154	0.045	0.7	2013	1.3
14CCT01 GB60M	2-3	6.379	0.300	1.595	0.062	0.164	0.038	2.0	2010	1.4
14CCT01 GB60M	3-4	6.270	0.295	1.500	0.058	0.162	0.041	3.3	2007	1.4
14CCT01 GB60M	4-5	5.348	0.294	1.402	0.063	0.208	0.046	4.6	2002	1.4
14CCT01 GB60M	5-6	6.346	0.315	1.233	0.064	0.364	0.051	5.9	1999	1.5
14CCT01 GB60M	6-7	6.025	0.383	1.242	0.076	0.263	0.052	7.2	1995	1.5
14CCT01 GB60M	7-8	5.018	0.342	1.410	0.074	0.333	0.055	8.5	1992	1.5
14CCT01 GB60M	8-9	5.332	0.345	1.395	0.074	0.455	0.055	9.8	1987	1.6
14CCT01 GB60M	9-10	5.663	0.342	1.199	0.069	0.466	0.056	11.1	1981	1.6
14CCT01 GB60M	10-11	5.423	0.378	0.992	0.072	0.850	0.073	12.4	1975	1.7
14CCT01 GB60M	11-12	4.682	0.259	1.126	0.053	1.028	0.053	13.7	1970	1.8
14CCT01 GB60M	12-13	2.952	0.296	1.418	0.067	1.257	0.069	15.0	1963	1.9
14CCT01 GB60M	13-14	4.066	0.292	1.201	0.061	3.212	0.088	16.3	1958	2.0
14CCT01 GB60M	14-15	5.934	0.268	1.100	0.053	3.798	0.083	17.7	1952	2.0
14CCT01 GB60M	15-16	3.327	0.327	1.358	0.072	1.250	0.073	19.0	1941	2.4
14CCT01 GB60M	16-17	3.023	0.297	1.317	0.067	0.491	0.051	20.3	1927	3.0

Table B2.2. (Continued)

Core	Depth (cm)	Total ^{210}Pb activity (dpm/g)	SD Total ^{210}Pb activity (dpm/g)	^{226}Ra activity (dpm/g)	SD ^{226}Ra activity (dpm/g)	^{137}Cs activity (dpm/g)	SD ^{137}Cs activity (dpm/g)	CRS modeled depth (cm)	Modeled year (CE)	SD modeled year
14CCT01GB60M	17-18	2.915	0.362	1.254	0.084	0.243	0.063	-	-	-
14CCT01GB60M	18-19	1.425	0.271	1.372	0.071	0.071	0.045	-	-	-
14CCT01GB60M	19-20	1.382	0.279	1.349	0.072	0.084	0.048	-	-	-
14CCT01GB60M	20-21	1.723	0.323	1.557	0.078	0.149	0.045	-	-	-
14CCT01GB60M	21-22	1.605	0.294	1.465	0.076	0.070	0.041	-	-	-
14CCT01GB60M	22-23	1.636	0.263	1.490	0.067	0.108	0.041	-	-	-
14CCT01GB60M	23-24	1.626	0.237	1.435	0.060	0.076	0.038	-	-	-
14CCT01GB60M	24-25	1.600	0.325	1.550	0.082	0.108	0.052	-	-	-
14CCT01GB60M	27-28	1.611	0.327	1.564	0.083	ND	-	-	-	-
14CCT01GB60M	31-32	1.095	0.236	1.393	0.061	ND	-	-	-	-
14CCT01GB60M	35-36	1.367	0.292	1.555	0.072	ND	-	-	-	-
14CCT01GB60M	39-40	1.307	0.261	1.380	0.065	ND	-	-	-	-
14CCT01GB60M	45-46	1.436	0.269	1.566	0.062	ND	-	-	-	-
14CCT01GB60M	49-50	1.100	0.270	1.389	0.068	ND	-	-	-	-

Table B2.3. DA40M radiometric data and age model. ND = Not Detected.

Core	Depth (cm)	Total ^{210}Pb activity (dpm/g)	SD Total ^{210}Pb activity (dpm/g)	CRS modeled depth (cm)	Modeled year (CE)	SD modeled year
15BIM09DA40M	0-1	5.244	0.350	0.0	2015	0.0
15BIM09DA40M	1-2	6.508	0.099	0.6	2015	1.4
15BIM09DA40M	2-3	6.934	0.012	1.9	2012	1.4
15BIM09DA40M	3-4	6.586	0.270	3.2	2009	1.4
15BIM09DA40M	4-5	5.624	0.095	4.4	2005	1.4
15BIM09DA40M	5-6	5.359	0.091	5.7	2002	1.5
15BIM09DA40M	6-7	5.091	0.141	7.0	1999	1.4
15BIM09DA40M	7-8	5.076	0.031	8.2	1996	1.4
15BIM09DA40M	8-9	4.790	0.252	9.5	1993	1.4
15BIM09DA40M	9-10	4.433	0.151	10.8	1992	1.4
15BIM09DA40M	10-11	4.524	0.032	12.0	1991	1.4

Table B2.3. (Continued)

Core	Depth (cm)	Total ^{210}Pb activity (dpm/g)	SD Total ^{210}Pb activity (dpm/g)	CRS modeled depth (cm)	Modeled year (CE)	SD modeled year
15BIM09DA40M	11-12	4.213	0.080	13.3	1989	1.4
15BIM09DA40M	12-13	3.651	0.034	14.6	1987	1.4
15BIM09DA40M	13-14	2.823	0.113	15.8	1984	1.4
15BIM09DA40M	14-15	2.334	0.008	17.1	1981	1.4
15BIM09DA40M	15-16	2.428	0.088	18.4	1978	1.5
15BIM09DA40M	16-17	2.239	0.045	19.6	1975	1.5
15BIM09DA40M	17-18	2.181	0.019	20.9	1972	1.5
15BIM09DA40M	18-19	1.996	0.006	22.2	1968	1.5
15BIM09DA40M	19-20	1.500	0.006	23.4	1963	1.6
15BIM09DA40M	20-21	1.385	0.009	24.7	1958	1.6
15BIM09DA40M	21-22	1.234	0.123	26.0	1953	1.6
15BIM09DA40M	22-23	1.121	0.029	27.2	1947	1.7
15BIM09DA40M	23-24	0.968	0.013	28.5	1942	1.8
15BIM09DA40M	24-25	1.193	0.007	29.8	1936	1.8
15BIM09DA40M	25-26	1.023	0.016	31.0	1930	1.8
15BIM09DA40M	26-27	0.959	0.060	32.3	1923	1.8
15BIM09DA40M	27-28	0.790	0.019	-	-	-
15BIM09DA40M	28-29	0.658	0.010	-	-	-
15BIM09DA40M	29-30	0.582	0.032	-	-	-
15BIM09DA40M	30-31	0.519	0.071	-	-	-
15BIM09DA40M	31-32	0.515	0.041	-	-	-
15BIM09DA40M	32-33	0.501	0.068	-	-	-
15BIM09DA40M	33-34	0.494	0.014	-	-	-
15BIM09DA40M	34-35	0.503	0.022	-	-	-
15BIM09DA40M	35-36	0.472	0.017	-	-	-
15BIM09DA40M	36-37	0.418	0.033	-	-	-
15BIM09DA40M	37-38	0.394	0.002	-	-	-
15BIM09DA40M	38-39	0.274	0.035	-	-	-

Table B2.3. (Continued)

Core	Depth (cm)	Total ^{210}Pb activity (dpm/g)	SD Total ^{210}Pb activity (dpm/g)	CRS modeled depth (cm)	Modeled year (CE)	SD modeled year
15BIM09 DA40M	39-40	0.309	0.010	-	-	-

Table B2.4. DA42M radiometric data and age model. ND = Not Detected.

Core	Depth (cm)	Total ^{210}Pb activity (dpm/g)	SD Total ^{210}Pb activity (dpm/g)	CRS modeled depth (cm)	Modeled year (CE)	SD modeled year
15BIM09 DA42M	0-1	3.074	0.008	0.0	2015	0.0
15BIM09 DA42M	1-2	2.752	0.150	0.6	2015	1.4
15BIM09 DA42M	2-3	2.266	0.021	1.9	2012	1.4
15BIM09 DA42M	3-4	2.215	0.070	3.2	2009	1.4
15BIM09 DA42M	4-5	1.951	0.115	4.4	2005	1.4
15BIM09 DA42M	5-6	1.716	0.076	5.7	2002	1.5
15BIM09 DA42M	6-7	0.984	0.031	7.0	1999	1.4
15BIM09 DA42M	7-8	0.865	0.020	8.2	1996	1.4
15BIM09 DA42M	8-9	1.398	0.043	9.5	1993	1.4
15BIM09 DA42M	9-10	1.528	0.026	10.8	1992	1.4
15BIM09 DA42M	10-11	1.918	0.011	12.0	1991	1.4
15BIM09 DA42M	11-12	2.511	0.062	13.3	1989	1.4
15BIM09 DA42M	12-13	2.538	0.126	14.6	1987	1.4
15BIM09 DA42M	13-14	2.434	0.108	15.8	1984	1.4
15BIM09 DA42M	14-15	2.034	0.019	17.1	1981	1.4
15BIM09 DA42M	15-16	1.572	0.087	18.4	1978	1.5
15BIM09 DA42M	16-17	1.770	0.022	19.6	1975	1.5
15BIM09 DA42M	17-18	1.862	0.053	20.9	1972	1.5
15BIM09 DA42M	18-19	1.511	0.001	22.2	1968	1.5
15BIM09 DA42M	19-20	1.765	0.061	23.4	1963	1.6
15BIM09 DA42M	20-21	1.763	0.062	24.7	1958	1.6
15BIM09 DA42M	22-23	1.466	0.069	27.2	1947	1.7
15BIM09 DA42M	23-24	1.163	0.065	28.5	1942	1.8
15BIM09 DA42M	24-25	1.333	0.013	29.8	1936	1.8

Table B2.4. (Continued)

Core	Depth (cm)	Total ^{210}Pb activity (dpm/g)	SD Total ^{210}Pb activity (dpm/g)	CRS modeled depth (cm)	Modeled year (CE)	SD modeled year
15BIM09 DA42M	26-27	1.385	0.115	32.3	1923	1.8
15BIM09 DA42M	27-28	1.165	0.047	-	-	-
15BIM09 DA42M	28-29	0.853	0.005	-	-	-
15BIM09 DA42M	29-30	0.957	0.022	-	-	-
15BIM09 DA42M	30-31	0.587	0.017	-	-	-
15BIM09 DA42M	31-32	0.466	0.066	-	-	-
15BIM09 DA42M	32-33	0.427	0.024	-	-	-
15BIM09 DA42M	33-34	0.431	0.008	-	-	-
15BIM09 DA42M	34-35	0.464	0.032	-	-	-
15BIM09 DA42M	35-36	0.485	0.048	-	-	-
15BIM09 DA42M	36-37	0.558	0.029	-	-	-
15BIM09 DA42M	37-38	0.382	0.007	-	-	-
15BIM09 DA42M	38-39	0.490	0.040	-	-	-
15BIM09 DA42M	39-40	0.419	0.016	-	-	-

Appendix B3. Age-Depth Models and Accumulation Rates.

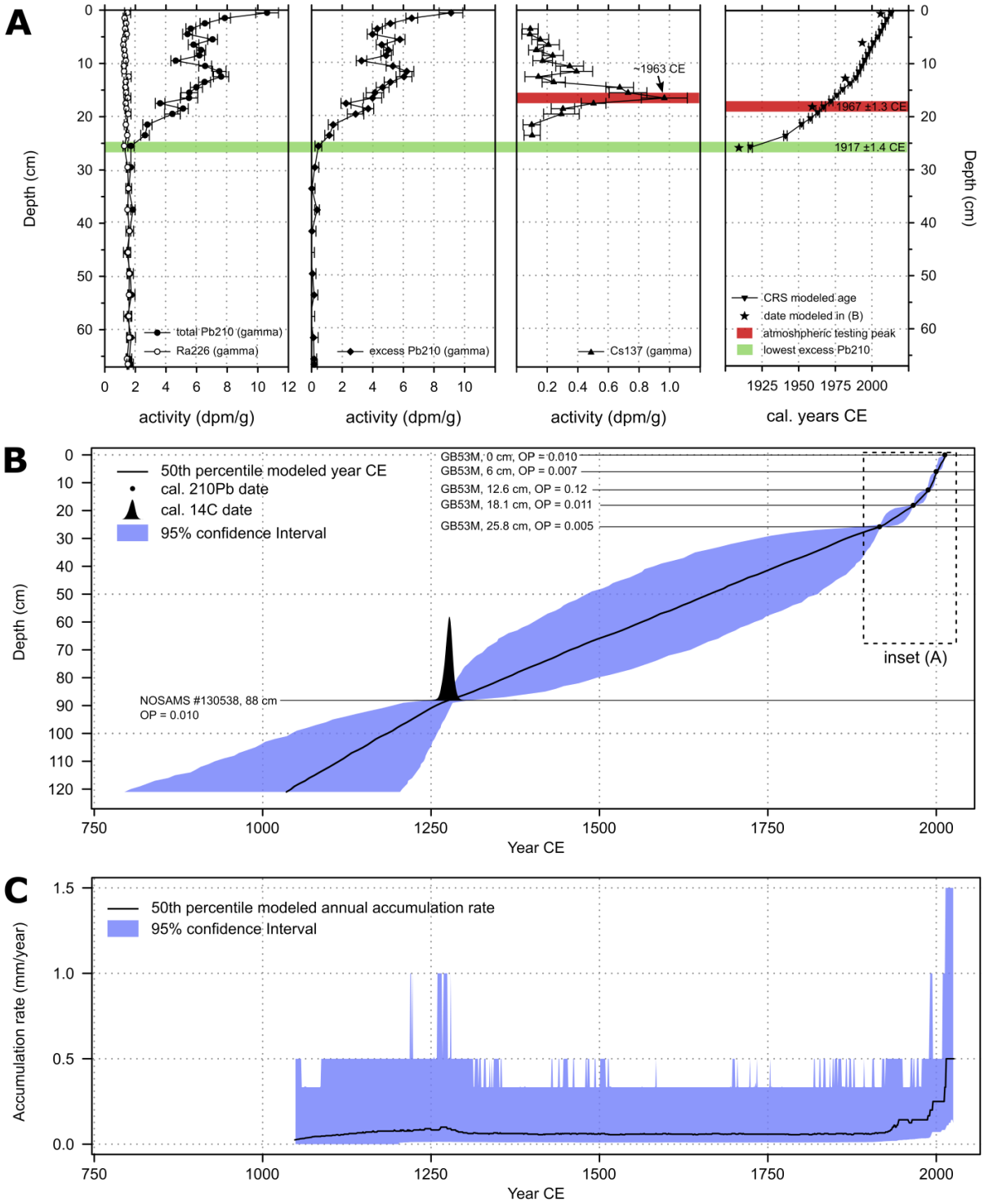

Figure B3.1. Age estimates for GB53R and GB53M. (A) Radiometric dates for push core GB53M; (B) Integrated Bchron age-depth model with Bayesian confidence intervals; (C) Modeled accumulation rate.

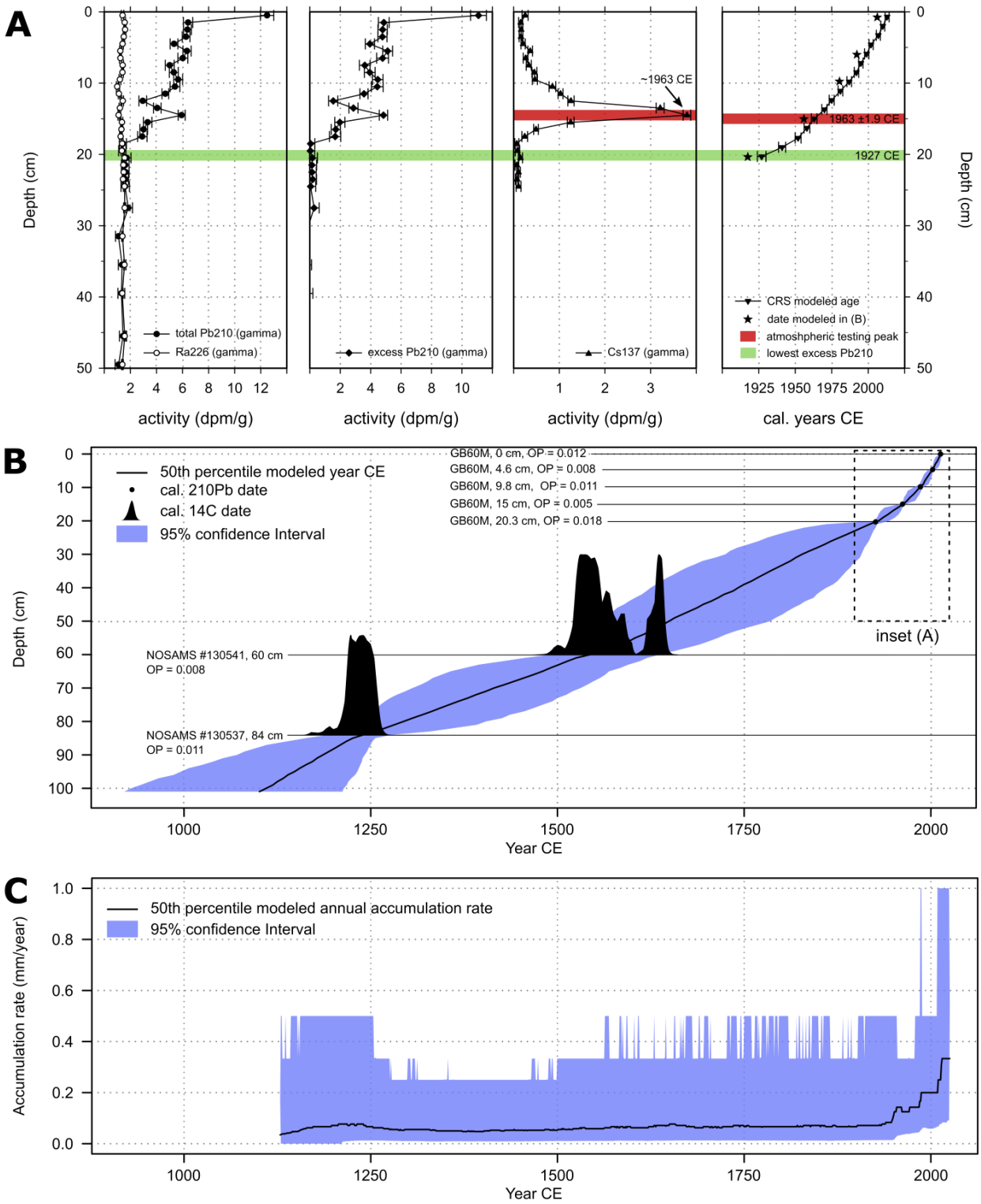

Figure B3.2. Age estimates for GB60R and GB60M. (A) Radiometric dates for push core GB60M; (B) Integrated Bchron age-depth model with Bayesian confidence intervals; (C) Modeled accumulation rate.

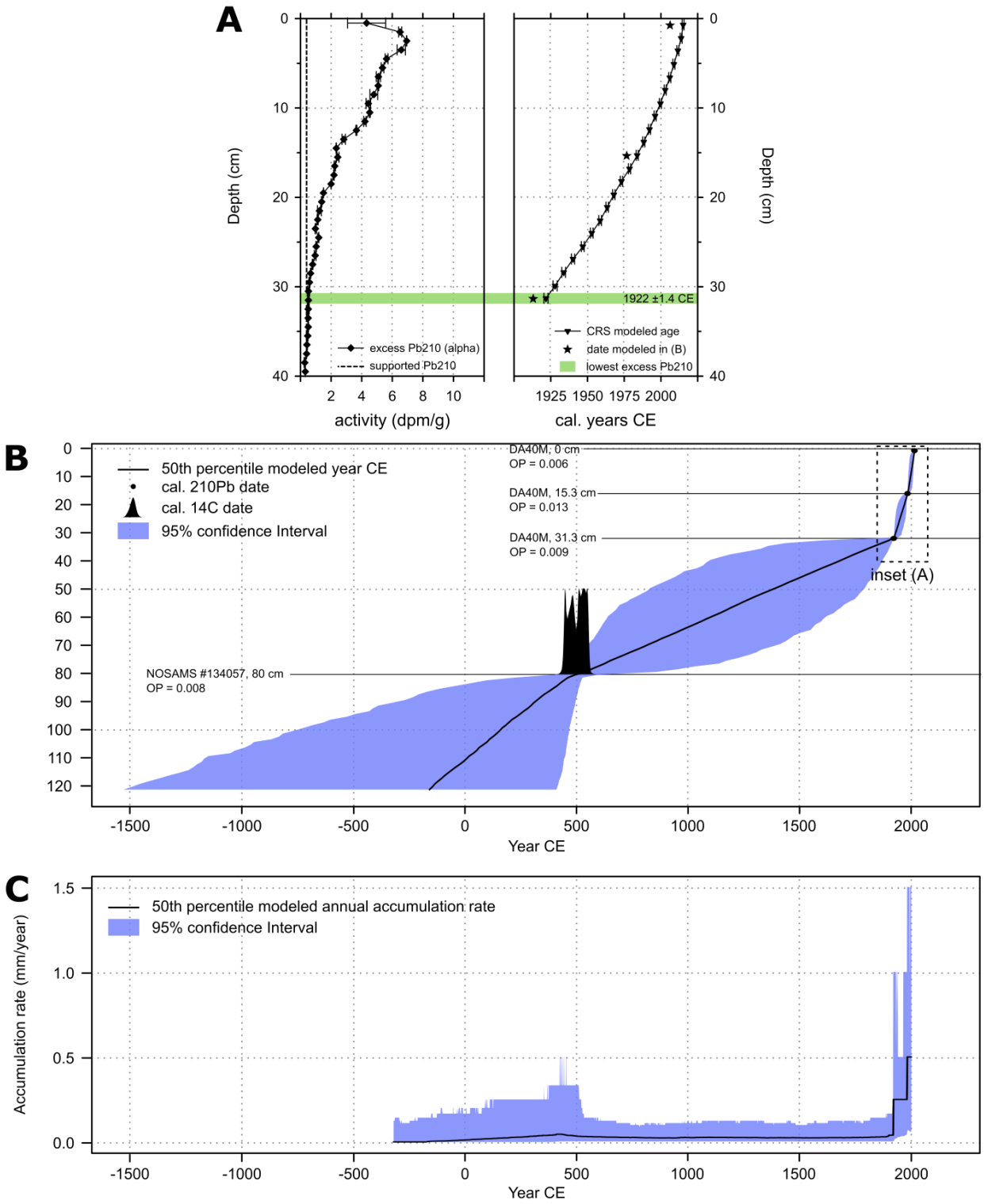

Figure B3.3. Age estimates for DA40R and DA40M. (A) Radiometric dates for push core DA40M; (B) Integrated Bchron age-depth model with Bayesian confidence intervals; (C) Modeled accumulation rate.

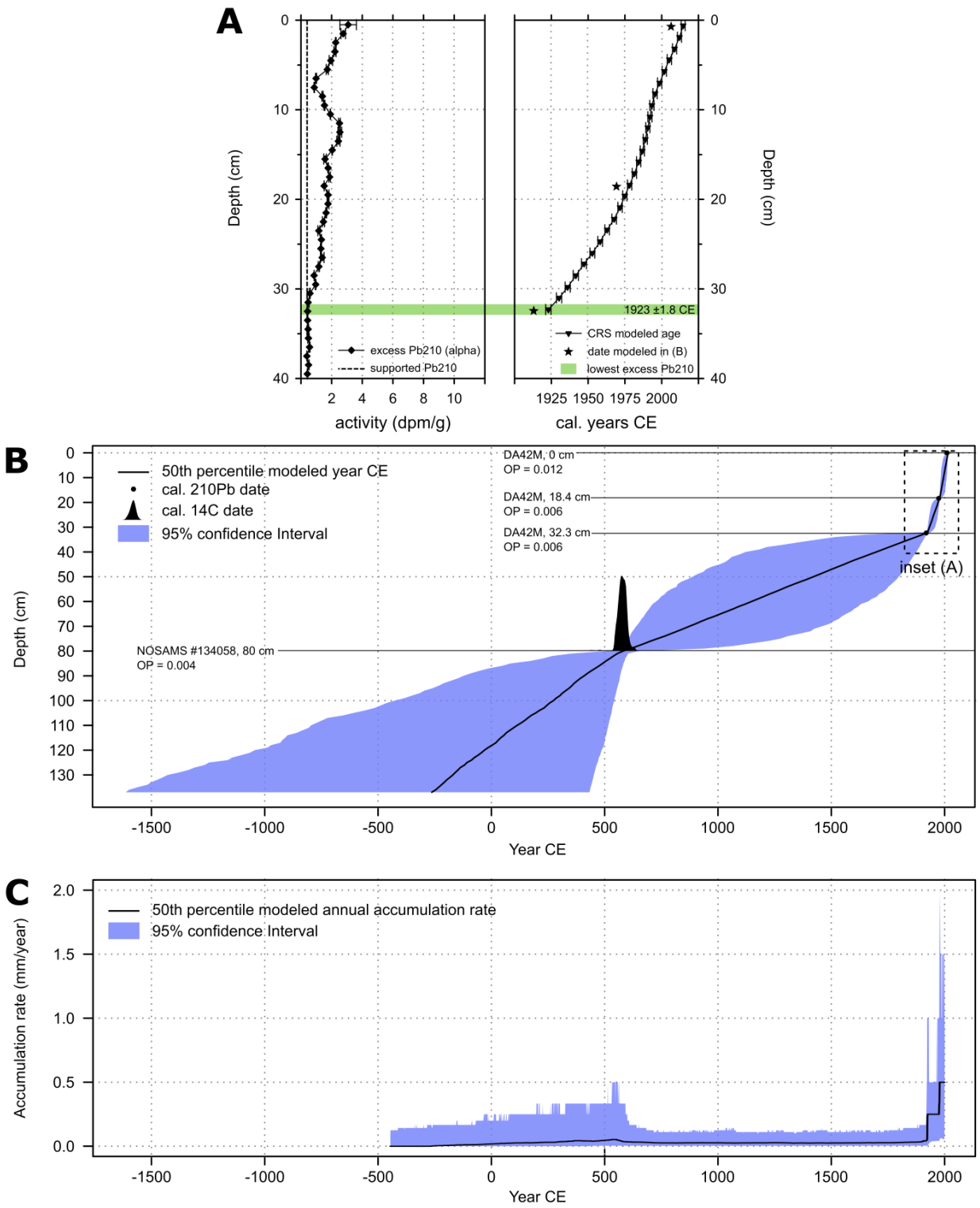

Figure B3.4. Age estimates for DA42R and DA42M. (A) Radiometric dates for push core DA42M; (B) Integrated Bchron age-depth model with Bayesian confidence intervals; (C) Modeled accumulation rate.

Appendix C

Appendix C1. Foraminiferal data.

Table C1.1. Foraminiferal counts, P/B index, and diversity data. Unfilled cells = 0, N/A = Not available.

Sample name	U1460A			U1460B			U1461A			U1461B		
Water depth (m)	215			214			127			128		
Size fraction (μm)	125–250	250–850	>850	125–250	250–850	>850	125–250	250–850	>850	125–250	250–850	>850
Total no. of species	74	42	4	67	53	1	85	16	N/A	84	32	N/A
Total no. of individuals	868	382	8	658	436	1	1062	38	N/A	1312	75	N/A
Fisher α Index	19.3	12.0	3.2	18.7	15.8	0	21.8	10.4	N/A	20.0	21.1	N/A
P/B index: Benthic	40	18	N/A	34	12	N/A	67	N/A	N/A	99	71	N/A
P/B index: Planktonic spinose	67	75	N/A	65	55	N/A	78	N/A	N/A	26	35	N/A
P/B index: Planktonic keeled	7	15	N/A	3	28	N/A	1	N/A	N/A	2	7	N/A
Haplophragmoides pusillus							1					
Gaudryina convexa	3						2			2		
Paratrochammina madeirae												
Bigenerina aspratilis	24	34			45							
Sahulia barkeri					1		1			6		
Textularia agglutinans	16	21	1		30		23			18		
Textularia catenata	4			6	6		14	3		14	2	
Textularia cushmani	28	10		2	1		8			20	2	
Textularia kerimbaensis	1				9		4	1		19		
Textularia orbica	1	6			2							
Textularia stricta												
Textularia tubulosa	5			10	7		2			1		
Textularia sp. 3 sensu Parker 2009					1							
Spirorutilus carinatus	26	13		41						7		
Migros flintii	3	8			1							
Pseudoclavulina robusta		1			3							
Pseudoclavulina serventyi												
Plotnikovina timorea	12			28	8		3			3	1	
Cylindroclavulina bradyi		2			5							
Patellina cf. *P. formosa*	1											
Cornuspira foliacea												
Cornuspira sp.				2	1		17			17		
Planispirinella involuta				1			3	1		8		
Vertebralina striata							1	2		4		
Wiesnerella ujiiei				1			5			3		
Edentostomina rupertiana												
Spiroloculina abatholopa							3			7		
Spiroloculina subimpressa	5	3	1	7	25		53	3		35	9	

Table C1.1. (Continued)

Sample name	U1460A			U1460B			U1461A			U1461B		
Size fraction (μm)	125–250	250–850	>850	125–250	250–850	>850	125–250	250–850	>850	125–250	250–850	>850
Agglutinella arenata	1	1			1					3		
Hauerina fragilissima							7	1		11		
Sigmoihauerina bradyi												
Sigmoihauerina involuta										1	1	
Proemassilina arenaria		1									1	
Quinqueloculina barnadi	1				11							
Quinqueloculina cf. *Q. crassicarinata*	7	2								11	1	
Quinqueloculina exmouthensis												
Quinqueloculina cf. *Q. latidentella*	11			24			16			11	2	
Quinqueloculina patagonica	12											
Quinqueloculina philippinensis		2								1		
Quinqueloculina subpolygona					7							
Quinqueloculina timorensis												
Quinqueloculina sp. 1	11	1			8		9			7	2	
Quinqueloculina sp. 5 sensu Parker 2009	31	40		19	3		7			31	3	
Biloculinella labiata							3					
Miliolinella circularis				4	2		46			24	2	
Miliolinella oceanica	2			1			7					
Miliolinella webbiana								1				
Miliolinella pilasensis							5			1		
Miliolinella sp. 1 sensu Parker 2009				5			61	3		9	2	
Miliolinella sp. 2					4		3			1		
Pyrgo cf. *P. denticulata*	1	2			5		3	3		2		
Pyrgo striolata	3						2			2		
Triloculina tricarinata	39	9		9	6		62	3		53	5	
Sigmoilopsis minuta	2			3	2		1					
Articulina alticostata							3	1		1		
Peneroplis pertusus							2			1		
Parasorites orbitolitoides							2			3	1	
Dentalina catenulata					1							
Dentalina cf. *D. mutsui*	2											
Grigelis orectus							1					
Laevidentalina bradyensis					3							
Laevidentalina inflexa				1			4			1		
Laevidentalina sidebottomi												

Table C1.1. (Continued)

Sample name	U1460A			U1460B			U1461A			U1461B		
Size fraction (μm)	125–250	250–850	>850	125–250	250–850	>850	125–250	250–850	>850	125–250	250–850	>850
Pseudonodosaria brevis												
Pyramidulina comatula												
Pyramidulina luzonensis				1								
Lenticulina calcar				1	3							
Lenticulina domantayi	13	4		4	3		1			10	2	
Lenticulina submamilligera										1		
Marginulinopsis philippinensis					3							
Saracenaria angularis												
Amphicoryna cf. *A. meringella*												
Amphicoryna separans	4	3		3	8		1					
Amphicoryna sublineata							1			1		
Astacolus crepidulus												
Marginulina musai							2					
Vaginulinopsis pseudoplanulata												
Vaginuliopsis sublegumen												
Planularia gemmata												
Planularia patens												
Planularia spinipes												
Cerebrina cf. *C. claricerviculata*							1			1		
Cerebrina lacunata	1			1			3			2		
Lagena annellatrachia				8			8	1		6		
Lagena annulatacollare							1					
Lagena cyrillion												
Lagena fidicularia												
Lagena substriata							9			2		
Procerolagena oceanica							1			1		
Reussoolina trachiella				2								
Globulina rotundata				1								
Guttulina bartschi	4			1								
Guttulina yamazaki												
Guttulina regina	1	1										
Pyrulina angusta												
Favulina hexagoniformis				2						1		
Oolina caudigera	1						1					
Fissurina circularis	6			2			13			4		
Laryngosigma afueraensis												
Glandulina symmetrica	7			1	1		11			4		
Saintclairoides toreuta	9	4		1	11					1		

Table C1.1. (Continued)

Sample name	U1460A			U1460B			U1461A			U1461B		
Size fraction (μm)	125–250	250–850	>850	125–250	250–850	>850	125–250	250–850	>850	125–250	250–850	>850
Hoeglundina elegans	1	1			1		1					
Alliatina variabilis										1		
Geminospira bradyi				1			7			3		
Robertinoides australis												
Robertinoides oceanica												
Bolivina robusta	48			47			2			1		
Bolivina striatula	28	9		23	11					6	2	
Bolivinellina translucens											1	
Rugobolivinella elegans							2			2		
Globocassidulina subglobosa	29	4		10								
Heterocassidulina albida												
Paracassidulina neocarinata				7						2		
Hopkinsinella glabra												
Loxostomina mayori	1				1					2	1	
Stilostomelloides virgula							3					
Rectobolivina bifrons	1											
Sagrinella jugosa							16			32		
Siphogenerina indica	10	5		19	5							
Bulimina marginata	4			9			9			2		
Bulimina subornata												
Protoglobobulimina pupoides							2					
Siphouvigerina porrecta	3			3			17			11		
Siphouvigerina proboscidea	1			6			7			2		
Uvigerina peregrina	46	36		9	32							
Uvigerina reineri												
Uvigerina schwageri		1									1	
Trifarina bradyi				1			1					
Chrysalidinella pacifica	1						3			1	1	
Reussella hayasakai		2		1			6			7	3	
Reussella pulchra	1	1					6			7	6	
Mimosina sp.												
Valvobifarina mackinnonii												
Fursenkoina pauciloculata												
Sigmavirgulina tortuosa	5			2						3		
Cancris auriculus		1		4			15			5	2	
Cancris oblongus												
Cancris bubnanensis	1	2			1							
Stomatorbina concentrica	1	2			8							

Table C1.1. (Continued)

Sample name	U1460A			U1460B			U1461A			U1461B		
Size fraction (μm)	125–250	250–850	>850	125–250	250–850	>850	125–250	250–850	>850	125–250	250–850	>850
Mississippina pacifica												
Rotorbinella sp.	3			22			44			81		
Neoeponides margaritifer		9	3									
Neoconorbina albida	13			6			2					
Neoconorbina neapolitana							11	2		13		
Rosalina sp. 1 sensu Parker 2009	1			1			11					
Eusphaeroidina inflata							3					
Sphaeroidina bulloides	2	5		3	8		1					
Buliminoides williamsoniana												
Elongobula parallela	7			4						2		
Pileolina minogasaformis				2								
Pileolina patelliformis	13			18			2					
Siphonina tubulosa	4			17	1							
Planulinoides biconcava	2			3								
Hyalinea florenceae	28	3		25								
Planulina retia	1			9			43			11	1	
Cibicides mabahethi	8			2	1					13	1	
Cibicides cf. *C. refulgens*	165	56		101	42		117	2		216	7	
Cibicidoides mundula	4			12	7		8			13	1	
Cibicidoides sp.					1							
Lobatula lobatula	2			2	2							
Caribeanella elatensis	9	10		5	30		95	9		80	4	
Planorbulinella larvata		6	3		5	1					1	
Millettiana millettii							33			9		
Asanonella tubulifera	29	17		10	16					9		
Monspeliensina sp.	1											
Amphistegina papillosa	1						35			116	3	
Nonion subturgidum							5			7		
Nonionella pulchella							1					
Nonionoides grateloupii							9			9		

Table C1.1. (Continued)

Sample name	U1460A			U1460B			U1461A			U1461B		
Size fraction (μm)	125–250	250–850	>850	125–250	250–850	>850	125–250	250–850	>850	125–250	250–850	>850
Astrononion sp. 1 sensu Parker 2009				1			1					
Melonis barleeanus												
Pullenia borealis				1			2			1		
Chilostomella ovoidea												
Anomalinoides colligera												
Anomalinoides globulosa												
Anomalinulla glabrata	51	33		47	27							
Hanzawaia nipponica	23			22			30			110	2	
Ammonia cf. *A. faceta*							1					
Ammonia pustulosa	14	10		1	8		4			5		
Rotalinoides gaimardii										3		
Elphidium lene	1						11			1		
Elphidium limbatum										23		
Elphidium macellum	7	1		10	2					2		
Heterostegina depressa										3	2	
Operculina ammonoides							59	2		126		

Table C1.1. (Continued)

Sample name	U1461C			U1463C			U1463D			U1464D		
Water depth (m)	128			145			145			264		
Size fraction (μm)	125–250	250–850	>850	125–250	250–850	>850	125–250	250–850	>850	125–250	250–850	>850
Total no. of species	89	39	3	96	25	N/A	92	31	5	86	62	N/A
Total no. of individuals	940	130	3	866	82	N/A	865	99	6	671	385	N/A
Fisher α Index	24.1	18.9	0	27.6	12.3	N/A	26.0	15.5	14.1	26.2	20.9	N/A
P/B index: Benthic	79	81	N/A	42	7	N/A	76	9	N/A	31	10	N/A
P/B index: Planktonic spinose	16	73	N/A	70	102	N/A	44	90	N/A	94	84	N/A
P/B index: Planktonic keeled	3	22	N/A	0	7	N/A	0	14	N/A	5	12	N/A
Haplophragmoides pusillus												
Gaudryina convexa	3						1			9		
Paratrochammina madeirae							1					
Bigenerina aspratilis				5			7					
Sahulia barkeri	10	2		2						3	1	
Textularia agglutinans	50	5		21	5		23			10		
Textularia catenata	10	3		20	3		10	1		3	21	
Textularia cushmani	49	6		15						12	35	
Textularia kerimbaensis		3		19			25			5	8	
Textularia orbica												
Textularia stricta	1						1					
Textularia tubulosa	8	1		5			5	3			3	
Textularia sp. 3 sensu Parker 2009												
Spirorutilus carinatus	1	2		2			5			5		
Migros flintii												
Pseudoclavulina robusta												
Pseudoclavulina serventyi					1		9	2			1	
Plotnikovina timorea	2			11	3		35	5	1	8	8	
Cylindroclavulina bradyi												
Patellina cf. *P. formosa*												
Cornuspira foliacea				1			1				1	
Cornuspira sp.	2			8			1			2	1	
Planispirinella involuta	3			1			2				1	
Vertebralina striata	4	2								2		
Wiesnerella ujiiei	5									6		
Edentostomina rupertiana		1										
Spiroloculina abatholopa				1								
Spiroloculina subimpressa	53	19		53	8		37	6		6	36	

Table C1.1. (Continued)

Sample name	U1461C			U1463C			U1463D			U1464D		
Size fraction (μm)	125–250	250–850	>850	125–250	250–850	>850	125–250	250–850	>850	125–250	250–850	>850
Agglutinella arenata	1							2		1		
Hauerina fragilissima	6	5		1			2	2		2	5	
Sigmoihauerina bradyi	1											
Sigmoihauerina involuta	1											
Proemassilina arenaria		1					1					
Quinqueloculina barnadi	10			1			2	1				
Quinqueloculina cf. *Q. crassicarinata*	3	3		2	2						7	
Quinqueloculina exmouthensis	13	1		1								
Quinqueloculina cf. *Q. latidentella*	17	3		10			12			6		
Quinqueloculina patagonica												
Quinqueloculina philippinensis	1			1						1		
Quinqueloculina subpolygona												
Quinqueloculina timorensis	1	1					2			3		
Quinqueloculina sp. 1	13	2		4	2		3	3		7	2	
Quinqueloculina sp. 5 sensu Parker 2009	10						5			12		
Biloculinella labiata										2		
Miliolinella circularis										6		
Miliolinella oceanica	1			3	1		8	3				
Miliolinella webbiana	2											
Miliolinella pilasensis				5			3			2		
Miliolinella sp. 1 sensu Parker 2009	57	9		24	3		2			1	7	
Miliolinella sp. 2				3			2					
Pyrgo cf. *P. denticulata*	4	1	1	6			5	2		2	8	
Pyrgo striolata	9	3					7					
Triloculina tricarinata	24	5	1	29	11		41	6		21	25	
Sigmoilopsis minuta	1			12			18			9	2	
Articulina alticostata	1									2	2	
Peneroplis pertusus	1											
Parasorites orbitolitoides	6	1										
Dentalina catenulata							2			1		
Dentalina cf. *D. mutsui*												
Grigelis orectus												
Laevidentalina bradyensis				1			6	7		4	2	
Laevidentalina inflexa					3		1	1		1	5	
Laevidentalina sidebottomi				1				3			2	

Table C1.1. (Continued)

Sample name	U1461C			U1463C			U1463D			U1464D		
Size fraction (μm)	125–250	250–850	>850	125–250	250–850	>850	125–250	250–850	>850	125–250	250–850	>850
Pseudonodosaria brevis							2				2	
Pyramidulina comatula	1											
Pyramidulina luzonensis	2	1		4	2		8	8				
Lenticulina calcar											1	
Lenticulina domantayi	4	3		6	3		6	2		7		
Lenticulina submamilligera								1				
Marginulinopsis philippinensis												
Saracenaria angularis				1							9	
Amphicoryna cf. *A. meringella*				5			2				11	
Amphicoryna separans	4			6			1	2		1	5	
Amphicoryna sublineata		1		1						2	5	
Astacolus crepidulus					1		2	1		1	3	
Marginulina musai				1			3	1		2		
Vaginulinopsis pseudoplanulata				1						1		
Vaginuliopsis sublegumen							1					
Planularia gemmata					1		1					
Planularia patens	1											
Planularia spinipes		1		1	1		5	1				
Cerebrina cf. *C. claricerviculata*				2			1			1		
Cerebrina lacunata	2			1								
Lagena annellatrachia	6	1		3			3			5	1	
Lagena annulatacollare				7			1					
Lagena cyrillion										1		
Lagena fidicularia	1											
Lagena substriata	1											
Procerolagena oceanica												
Reussoolina trachiella												
Globulina rotundata												
Guttulina bartschi	1			1						1		
Guttulina yamazaki	1	1										
Guttulina regina												
Pyrulina angusta							2					
Favulina hexagoniformis												
Oolina caudigera												
Fissurina circularis	5			3			2			2		
Laryngosigma afueraensis	1											
Glandulina symmetrica	9	2		25	3		3			1	10	
Saintclairoides toreuta	1			2						2	8	

Table C1.1. (Continued)

Sample name	U1461C			U1463C			U1463D			U1464D		
Size fraction (μm)	125–250	250–850	>850	125–250	250–850	>850	125–250	250–850	>850	125–250	250–850	>850
Hoeglundina elegans				1			7					
Alliatina variabilis	3			1								
Geminospira bradyi										1		
Robertinoides australis				2								
Robertinoides oceanica										2	2	
Bolivina robusta				73			114		2	89	1	
Bolivina striatula	16			6			3			1		
Bolivinellina translucens	4			2			7			7		
Rugobolivinella elegans												
Globocassidulina subglobosa				8			8		1	42		
Heterocassidulina albida										11		
Paracassidulina neocarinata	2			14			23		1	50	1	
Hopkinsinella glabra										1		
Loxostomina mayori		1		5				1		1		
Stilostomelloides virgula	2						1					
Rectobolivina bifrons												
Sagrinella jugosa	15			15			16			10	1	
Siphogenerina indica							2					
Bulimina marginata				10			17			23		
Bulimina subornata				1								
Protoglobobulimina pupoides							1					
Siphouvigerina porrecta	15			5			9			20		
Siphouvigerina proboscidea	6			18			16			31	1	
Uvigerina peregrina				2								
Uvigerina reineri											1	
Uvigerina schwageri				5			7	1				
Trifarina bradyi				6			13			6		
Chrysalidinella pacifica	1						1					
Reussella hayasakai	8			6			5			15		
Reussella pulchra												
Mimosina sp.				1								
Valvobifarina mackinnonii				1								
Fursenkoina pauciloculata				5			1			2		
Sigmavirgulina tortuosa	3									1		
Cancris auriculus	11			15			11	1		5	21	
Cancris oblongus				1						2		
Cancris bubnanensis												
Stomatorbina concentrica												

Table C1.1. (Continued)

Sample name	U1461C			U1463C			U1463D			U1464D		
Size fraction (μm)	125–250	250–850	>850	125–250	250–850	>850	125–250	250–850	>850	125–250	250–850	>850
Mississippina pacifica										1		
Rotorbinella sp.	15			16			5			7	3	
Neoeponides margaritifer		1		1			5	10			1	
Neoconorbina albida		1										
Neoconorbina neapolitana	3											
Rosalina sp. 1 sensu Parker 2009	17			37	4		1			2		
Eusphaeroidina inflata	2			5	1		1	3			3	
Sphaeroidina bulloides	2			2			1			4	26	
Buliminoides williamsoniana				1								
Elongobula parallela	1						1					
Pileolina minogasaformis												
Pileolina patelliformis	1											
Siphonina tubulosa	2			2			3			6		
Planulinoides biconcava				5			4			1	1	
Hyalinea florenceae				4			6				1	
Planulina retia				24	2		32	9		14	22	
Cibicides mabahethi	3						2			2		
Cibicides cf. *C. refulgens*	110	4		49	2		110		1	46	1	
Cibicidoides mundula	2			49				2		18	4	
Cibicidoides sp.										1	4	
Lobatula lobatula												
Caribeanella elatensis	75	16		41	8		27	8		2	24	
Planorbulinella larvata											1	
Millettiana millettii	17			1						2	1	
Asanonella tubulifera												
Monspeliensina sp.												
Amphistegina papillosa	52	9					2			3	1	
Nonion subturgidum	7			3			1				2	
Nonionella pulchella												
Nonionoides grateloupii	1			8			5			3		

Table C1.1. (Continued)

Sample name	U1461C			U1463C			U1463D			U1464D		
Size fraction (μm)	125–250	250–850	>850	125–250	250–850	>850	125–250	250–850	>850	125–250	250–850	>850
Astrononion sp. 1 sensu Parker 2009	1			1			2					
Melonis barleeanus					1						1	
Pullenia borealis	1			2			1			4	2	
Chilostomella ovoidea				36	8		6				2	
Anomalinoides colligera										2		
Anomalinoides globulosa	2	1										
Anomalinulla glabrata	4			2			10			10		
Hanzawaia nipponica	33			15			30			21	1	
Ammonia cf. *A. faceta*				1								
Ammonia pustulosa	3	1		8			7			6	1	
Rotalinoides gaimardii							5	1			2	
Elphidium lene	5			1						5		
Elphidium limbatum	9			1						3		
Elphidium macellum			1									
Heterostegina depressa	5	5									1	
Operculina ammonoides	57	2		10	3		8			7	14	

Appendix C2. Systematic Taxonomy with Base of Identification.

Class FORAMINIFERIDA Eichwald, 1830
Order LITUOLIDA Lankester, 1885
Superfamily LITUOLOIDEA Blainville, 1827
Family HAPLOPHRAGMOIDEA
Haplophragmoides pusillus Collins, 1974 (Pl. 1, Fig. 1)
1994 *Haplopbragmoides pusillus* Collins; Loeblich & Tappan, Timor Sea, p. 16, Pl. 7, Figs. 1–7.
2013 *Haplophragmoides pusillus* Collins, 1974; Debenay, New Caledonia, p. 83, 256.
Superfamily VERNEUILINOIDEA Cushman, 1911
Family VERNEUILINIDAE Cushman, 1911
Subfamily VERNEUILININAE Cushman, 1911
Gaudryina convexa **(**Karrer, 1864) (Pl. 1, Fig. 2)
1997 *Gaudryina convexa* (Karrer); Haig, Exmouth Gulf, p. 264, Fig. 3:3.
2009 *Gaudryina convexa* (Karrer, 1965); Parker, Ningaloo Reef, p. 31, Fig. 23a–h.
2013 *Gaudryina convexa* (Karrer, 1865); Debenay, New Caledonia, p. 81, 260.
Order TROCHAMMINIDA Saidova, 1981
Superfamily TROCHAMMINACEA Schwager, 1877
Family TROCHAMMINIDAE Schwager, 1877
Subfamily TROCHAMMININAE Schwager, 1877
Paratrochammina madeirae Brönniman, 1979 (Pl. 1, Fig. 3)
1993 *Paratrochammina madeirae* Brönniman; Hottinger et al., Gulf of Aquaba, Pl. 7, Figs. 11–15.
Order TEXTULARIIDA Lankester. 1885
Superfamily TEXTULARIACEA Ehrenberg, 1838
Family TEXTULARIIDAE Ehrenberg, 1838
Subfamily TEXTULARIINAE Ehrenberg, 1838
Bigenerina aspratilis Loeblich & Tappan, 1994 (Pl. 1, Fig. 4)
1994 *Bigenerina aspratilis* n.sp.; Loeblich and Tappan, Timor Sea, p. 26, Pl. 31, Figs. 13–22.
Sahulia barkeri (Hofker, 1978) (Pl. 1, Figs. 5–6)
1994 *Sahulia barkeri* (Hofker); Loeblich and Tappan, Timor Sea, p. 27, Pl. 32, Figs. 1–8.
2009 *Sahulia barkeri* (Hofker 1978); Parker, Ningaloo Reef, p. 35, Fig. 28a–d.
2013 *Sahulia barkeri* (Hofker, 1978); Debenay, New Caledonia, p. 92, 263.
Textularia **cf.** ***T. agglutinans*** d'Orbigny, 1839 (Pl. 1, Fig. 8)
1994 *Textularia agglutinans* d'Orbigny; Loeblich and Tappan, Timor Sea, p. 27, Pl. 33, Figs. 8–12.
Textularia catenata Cushman, 1911 (Pl. 1, Fig. 9)
1969 *Siphotextularia* sp. A, Betjeman, Western Australian shelf, Pl. 19, Fig. 14
1979 *Siphotextularia catenata* (Cushman); Corliss, south east Indian Ocean, p. 5, Pl. 1, Figs. 1–2.

Textularia cushmani Said, 1949 (Pl. 1, Fig. 10)

1994 *Textularia cushmani* Said, Loeblich and Tappan, Timor Sea, p. 28, Pl. 35, Figs. 1–4.

1993 *Textularia cushmani* Said; Hottinger et al., Gulf of Aquaba, p. 36, Pl. 13, Figs. 10–14.

2009 *Textularia cushmani* Said 1949; Parker, Ningaloo Reef, p. 44, Fig. 35a–i.

2013 *Textularia cushmani* Said, 1949; Debenay, New Caledonia, p. 96, 264.

Textularia kerimbaensis Said, 1949 (Pl. 1, Fig. 11)

2009 *Textularia kerimbaensis* Said 1949; Parker, Ningaloo Reef, p. 51, Figs. 38a–o, 39a–i.

2013 *Textularia kerimbaensis* (Said, 1949); Debenay, New Caledonia, p. 97, 264.

Textularia orbica Lalicker & McCulloch, 1940 (Pl. 1, Fig. 12)

1994 *Textularia orbica* Lalicker and McCulloch; Loeblich and Tappan, Timor Sea, p. 29, Pl. 36, Figs. 1–2.

Textularia stricta Cushman, 1911 (Pl. 1, Fig. 14)

1994 *Textularia stricta* Cushman; Loeblich and Tappan, Timor Sea, p. 30, Pl. 38, Figs. 1–9.

2013 *Textularia stricta* Cushman, 1911; Debenay, New Caledonia, 98.

Textularia tubulosa Zheng, 1980 (Pl. 1, Fig. 13)

1994 *Textularia tubulosa* Zheng; Loeblich and Tappan, Timor Sea, p. 30, Pl. 36, Figs. 7–12.

2013 *Textularia tubulosa* Zheng 1980; Debenay, New Caledonia, p. 99, 265

***Textularia* sp. 3** sensu Parker 2009 (not pictured)

2009 *Textularia* sp. 3; Parker, Ningaloo Reef, p. 61, Fig. 45, Fig. 45a–h.

Family KAMINSKIIDAE Neagu, 1999

Spirorutilus carinatus (d'Orbigny, 1846) (Pl. 1, Fig. 7)

1994 *Spiroplectinella pseudocarinata* (Cushman); Loeblich and Tappan, Timor Sea, p. 19, Pl. 15, Figs. 1–14.

Family PSEUDOGAUDRYINIDAE Loeblich and Tappan 1985

Subfamily PSEUDOGAUDRYININAE

Migros flintii (Cushman, 1911) (Pl. 1, Fig. 15)

1994 *Migros flintii* (Cushman); Loeblich and Tappan, Timor Sea, p. 32, Pl. 19, Figs. 10–13, Pl. 44, Figs. 10–13.

Pseudoclavulina robusta Zheng, 1988 (Pl. 1, Fig. 16)

1994 *Pseudoclavulina robusta* Zheng; Loeblich and Tappan, Timor Sea, p. 32, Pl. 45, Figs. 8–11.

Pseudoclavulina serventyi (Chapman & Parr, 1936) (Pl. 1, Fig. 17)

1994 *Pseudoclavulina serventyi* (Chapman and Parr); Loeblich and Tappan, Timor Sea, p. 32, Pl. 45, Figs. 12–19.

1994 *Pseudoclavulina serventyi* Chapman and Parr 1945; Jones, Brady's specimens, p. 53, Pl. 48, Figs. 1–16.

2013 *Pseudoclavulina serventyi* (Chapman & Parr, 1935); Debenay, New Caledonia, p. 88, 262.

Subfamily SIPHONIFEROIDINAE Loeblich and Tappan, 1985

Plotnikovina timorea Loeblich & Tappan, 1994 (Pl. 1, Fig. 18)

1994 *Plotnikovina timorea* n.sp.; Loeblich and Tappan; Timor Sea, p. 33, Pl. 17, Figs. 17–21, Pl. 47, Figs. 1–10.

2013 *Plotnikovina timorea* Loeblich & Tappan, 1994; Debenay, New Caledonia, p. 87, 262.

Family VALVULINIDAE Berthelin. 1880

Subfamily VALVULININAE Berthelin. 1880

Cylindroclavulina bradyi (Cushman, 1911) (Pl. 1, Fig. 19)

1994 *Cylindroclavulina bradyi* (Cushman); Loeblich and Tappan; Timor Sea, Pl. 48, Figs. 7–19.

1994 *Cylindroclavulina bradyi* (Cushman 1911), Jones, Brady's specimens, Pl. 49, Figs. 32–38.

2013 *Cylindroclavulina bradyi* (Cushman, 1911); Debenay, New Caledonia, p. 79, 263.

Order SPIRILLINIDA Hohenegger & Piller, 1975

Family PATELLINIDAE Rhumbler, 1906

Subfamily PATELLININAE Rhumbler, 1906

Patellina* cf. *P. formosa Heron-Allen & Earland, 1932 (Pl. 1, Fig. 20)

1994 *Patellina corrugata* Williamson; Loeblich and Tappan, Timor Sea, p. 36, Pl. 55, Figs. 1–9.

2009 *Patellina* cf. *P. formosa* Heron-Allen & Earland, 1932; Parker, Ningaloo Reef, p. 70, Fig. 52a–h.

2013 *Patellina* cf. *P. formosa* Heron-Allen & Earland, 1932; Debenay, New Caledonia, p. 207, 284.

Order MILIOLIDA Lankester, 1885

Superfamily CORNUSPIRACEA Schultze, 1854

Family CORNUSPIRIDAE Schultze, 1854

Subfamily CORNUSPIRINAE Schultze, 1854

Cornuspira foliacea (Philippi, 1844) (Pl. 1, Fig. 21)

1994 *Cornuspira foliacea* (Philippi); Loeblich and Tappan, Timor Sea, p. 36, Pl. 55, Figs. 10–11.

1994 *Cornuspira foliacea* (Philippi); Jones, Brady's specimens, Pl. 11, Figs. 5–6.

2013 *Cornuspira foliacea* (Philippi); Debenay, New Caledonia, p. 105, 266.

***Cornuspira* sp.** (Pl. 1, Fig. 22)

2013 *Cornuspira involvens* (Reuss); Debenay, New Caledonia, p. 105, p. 266.

Superfamily NUBECULARIACEA T. R. Jones in Griffith and Henfrey, 1875

Family FISCHERINIDAE Millett, 1898

Subfamily FISCHERININAE Millett, 1898b

Planispirinella involuta Collins, 1958 (Pl. 1, Fig. 23)

2009 *Planispirinella involuta* Collins 1958; Parker, Ningaloo Reef, p. 158, Fig. 111a–f.

2013 *Planispirinella involuta* Collins; Debenay, New Caledonia, p. 114, 266.

Subfamily NODOBACULARIELLINAE Bogdanovich in Subbotina, Voloshinova, and Azbel, 1981

Vertebralina striata d'Orbigny, 1826 (Pl. 1, Fig. 24)

1993 *Vertebralina striata* d'Orbigny; Hottinger et al., Gulf of Aquaba, p. 43, Pl. 23, Figs. 8–15.

1994 *Vertebralina striata* d'Orbigny; Loeblich and Tappan; Timor Sea, p. 39, Pl. 60, Figs. 1–7.

1994 *Vertebralina striata* d'Orbigny 1826, Jones, Brady's specimens, p. 28, Pl. 12, Figs. 14–16.

2009 *Vertebralina striata* d'Orbigny; Parker, Ningaloo Reef, p. 379, Fig. 274a–h.

2013 *Vertebralina striata* d'Orbigny; Debenay, New Caledonia, p. 139, 267.

Wiesnerella ujiiei Hatta in Hatta and Ujiie, 1992 (Pl. 1, Fig. 25)

1994 *Wiesnerella ujiiei* Hatta in Halta and Ujiie; Loeblich and Tappan, Timor Sea, p. 39, Figs. 4–6.

Family OPHTALMIDIIDAE Wiesner, 1920

Edentostomina rupertiana (Brady, 1881) (Pl. 1, Fig. 26)

1993 *Rupertianella rupertiana* (Brady); Hottinger et al., Gulf of Aquaba, p. 67, Pl. 73, Figs. 1–10.

1994 *Rupertianella rupertiana* (Brady); Loeblich and Tappan, Sahul Shelf, p. 60, Pl. 106, Figs. 1–14.

1994 *Edentostomina rupertiana* (Brady 1881); Jones, Brady's specimens, p. 23, Pl. 7, Figs. 7–12.

2009 *Edentostomina rupertiana* (Brady 1881); Parker, Ningaloo Reef, p. 97, Fig. 69a–k.

Superfamily MILIOLACEA Ehrenberg. 1839

Family SPIROLOCULINIDAE Wiesner. 1920

Subfamily SPIROLOCULININAE Wiesner, 1920

Spiroloculina abatholopa Loeblich and Tappan, 1994 (Pl. 1, Fig. 27)

1994 *Spiroloculina abatholopa* n.sp.; Loeblich and Tappan, Timor Sea, p. 43, Pl. 68, Figs. 3–4.

Spiroloculina subimpressa Parr, 1950 (Pl. 1, Fig. 28)

1988 *Spiroloculina depressa* d'Orbigny, Van Marle, Eastern Indonesia, p. 149, Pl. IV, Fig. 25.

1994 *Spiroloculina subimpressa* Parr; Loeblich and Tappan, Timor Sea, p. 44, Figs. 9–15.

2009 *Spiroloculina subimpressa* Parr 1950; Parker, Ningaloo Reef, p. 350, Fig. 254a–k.

2013 *Spiroloculina subimpressa* Parr; Debenay, New Caledonia, p. 135, 269.

Family HAUERINIDAE Schwager, 1876

Subfamily SIPHONAPERTINAE Saidova, 1975

Agglutinella arenata (Said, 1949) (Pl. 1, Figs. 29–30)

1994 *Agglutinella arenata* (Said); Loeblich and Tappan, Timor Sea, p. 45, Pl. 69, Figs. 9–11, Pl. 70, Figs. 10–15, Pl. 74, Figs. 10–13.

2009 *Quinqueloculina arenata* Said 1949; Parker, Ningaloo Reef, p. 179, Figs. 126a–j, 127a–h, 128a–i.

2013 *Quinqueloculina arenata* Said; Debenay, New Caledonia, p. 119, 270.

Subfamily HAUERININAE Schwager, 1876

Hauerina fragilissima (Brady 1884) emend. Ponder 1975 (Pl. 1, Fig. 31)

1993 *Sigmoihauerina fragilissima* (Brady); Hottinger et al., Gulf of Aquaba, p. 62, Figs. 1–3.

1994 *Hauerina fragilissima* (Brady 1884); Jones, Brady's specimens, p. 25, Pl. 9, Figs. 12–14.

1994 *Parahauerinoides fragilissimus* (Brady); Loeblich and Tappan, Timor Sea, p. 51, Pl. 87, Figs. 1–6.

2009 *Hauerina fragilissima* (Brady 1884) emend. Ponder 1975; Parker, Ningaloo Reef, p. 107, Fig. 75a–g.

2013 *Hauerina fragilissima* (Brady); Debenay, New Caledonia, p. 108, 270.

Subfamily SIGMOILINITINAE

Sigmoihauerina bradyi (Cushman, 1917) (Pl.1, Fig. 32)

1993 *Sigmoihauerina bradyi* (Cushman); Hottinger et al., Gulf of Aquaba, p. 62, Pl. 60, Figs. 1–12.

1994 *Sigmoihauerina bradyi* (Cushman 1917); Jones, Brady's specimens, p. 27, Pl. 11, Figs. 12–13.

Sigmoihauerina involuta (Cushman, 1946) (Pl. 2, Figs. 26–27)

1994 *Sigmoihauerina involuta* (Cushman); Loeblich and Tappan, Timor Sea, p. 58, Pl. 100, Figs. 8–12..

1994 *Pseudohauerina occidentalis involuta* (Cushman 1946); Jones, Brady's specimens, p. 23, Pl. 7, Figs. 15–17.

2009 *Pseudohauerina involuta* (Cushman 1946); Parker, Ningaloo Reef, p. 158, Fig. 112a–i.

2013 *Pseudohauerina involuta* (Cushman); Debenay, New Caledonia, p. 114, 280.

Proemassilina arenaria (Brady, 1884) (Pl. 1, Fig. 33)

1994 *Proemassilina arenaria* (Brady); Loeblich and Tappan, Timor Sea, p. 47, Pl. 72, Figs. 1–4.

1994 *Proemassilina arenaria* (Brady 1884); Jones, Brady's specimens, p. 24, Pl. 8, Fig. 12

Quinqueloculina barnardi Rasheed, 1971 (Pl. 1, Fig. 34)

1997 *Quinqueloculina barnardi* Rasheed; Haig, Exmouth Gulf, Pl. 3, Figs. 23–24.

2009 *Quinqueloculina barnardi* Rasheed 1971; Parker, Ningaloo Reef, p. 184, Figs. 129a–f, 130a–k.

2013 *Quinqueloculina barnadi* Rasheed; Debenay, New Caledonia, p. 119, 270.

Quinqueloculina* cf. *Q. crassicarinata Collins, 1958 (Pl. 1, Figs. 35–36)

1994 *Quinqueloculina crassicarinata* Collins; Loeblich and Tappan, Timor Sea, p. 48, Pl. 77, Figs. 4–12.

2009 *Quinqueloculina crassicarinata* Collins 1958; Parker, Ningaloo Reef, p. 189, Fig. 135a–j.

2013 *Quinqueloculina crassicarinata* Collins; Debenay, New Caledonia, p. 121, 271.

Quinqueloculina exmouthensis Parker, 2009 (Pl. 1, Fig. 37)

1993 *Cycloforina collumnosa* Cushman 1922; Hottinger et al., Gulf of Aquaba, p. 49, Pl. 32, Figs. 10–15.

2009 *Quinqueloculina exmouthensis* n. sp.; Parker, Ningaloo Reef, p. 207, Figs. 146a–h, 147a–i, 148a–i.

2013 *Quinqueloculina exmouthensis*, Parker; Debenay, New Caledonia, p. 122, 272.

Quinqueloculina* cf. *Q. latidentella Loeblich & Tappan, 1994 (Pl. 1, Figs. 38–39)

1994 *Quinqueloculina latidentella* Loeblich and Tappan, n.sp.; Loeblich and Tappan, Timor Sea, p. 49, Pl. 80, Figs. 10–12.

2009 *Quinqueloculina latidentella* Loeblich and Tappan 1994; Parker, Ningaloo Reef, p. 217, Figs. 154a–f, 155a–g.

2013 *Quinqueloculina latidentella* Loeblich & Tappan; Debenay, New Caledonia, p. 123, 272.

Quinqueloculina patagonica d'Orbigny, 1839 (not figured)

1993 *Quinqueloculina patagonica* d'Orbigny; Hottinger et al., p. 60, Pl. 55, Figs. 11–17.

1994 *Pseudotriloculina patagonica* (d'Orbigny); Loeblich and Tappan, p. 53, Pl. 80, Figs. 16–18, Pl. 83, Figs. 10–12.

Quinqueloculina philippinensis Cushman, 1921 (Pl. 1, Figs. 40–41)

1994 *Quinqueloculina philippinensis* Cushman; Loeblich and Tappan, Timor Sea, Pl. 81, Figs. 1–10.

2009 *Quinqueloculina* gr. *Q. pseudoreticulata* Parr 1941; Parker, Ningaloo Reef, p. 243, Figs. 174a–j, 175a–h.

Quinqueloculina subpolygona Parr, 1945 (Pl. 2, Fig. 1)

1993 *Lachlanella subpolygona*, Parr; Hottinger et al., Gulf of Aquaba, p. 51, Pl. 37, Figs. 4–10.

2009 *Quinqueloculina subpolygona* Parr, 1945; Parker, Ningaloo Reef, p. 262, Figs. 191a–j, 192a–l.

Quinqueloculina timorensis (Loeblich & Tappan, 1994) (Pl. 2, Figs. 2–3)

1994 *Massilina timorensis*, n.sp.; Loeblich and Tappan, Timor Sea, p. 47, Pl. 83, Figs. 13–15.

2009 *Quinqueloculina timorensis* (Loeblich & Tappan 1994); Parker, Ningaloo Reef, p. 275, Fig. 197a–e.

***Quinqueloculina* sp. 1** (Pl. 2, Figs. 4–5)

2009 *Quinqueloculina zhengi* n.sp.; Parker, Ningaloo Reef, p. 285, Figs. 206a–l, 207a–g.

***Quinqueloculina* sp. 5** sensu Parker 2009 (Pl. 2, Figs. 6–7)

1993 *Quinqueloculina* sp. E; Hottinger, Gulf of Aquaba, p. 61, Pl. 58, Figs. 50–10.

2009 *Quinqueloculina* sp. 5; Parker, Ningaloo Reef, p. 299, Fig. 215a–g)

Subfamily MILIOLINELLINAE Vella, 1957

Biloculinella labiata (Schlumberger, 1891) (Pl. 2, Figs. 8–9)

1994 *Biloculinella labiata* (Schlumberger); Loeblich and Tappan, Timor Sea, Pl. 86, Figs. 5–11.

Miliolinella circularis (Bornemann, 1855) (Pl. 2, Figs. 10–11)

1993 *Miliolinella* sp. A; Hottinger et al., Gulf of Aquaba, p. 52, Pl. 38, 7–13.

2009 *Miliolinella circularis* (Bornemann 1855); Parker, Ningaloo Reef, p. 120, Fig. 85a–c.
2013 *Miliolinella circularis* (Bornemann); Debenay, New Caledonia, p. 109, 275.

Miliolinella oceanica (Cushman, 1932) (Pl. 2, Fig. 12–13)
1994 *Miliolinella quinquangula* n.sp.; Loeblich and Tappan, Timor Sea, p. 52, Pl. 82, Figs. 14–16, Pl. 87, Figs. 7–9.
1997 *Miliolinella* cf. *M. baragwanathi* (Parr); Haig, Exmouth Gulf, p.271, Pl. 3, Fig. 21.
2009 *Miliolinella oceanica* (Cushman 1932); Parker, Ningaloo Reef, p. 120, Fig. 86a–h.

Miliolinella webbiana (d'Orbigny, 1839) (Pl. 2, Figs. 14–15)
1994 *Miliolinella suborbicularis* (d'Orbigny); Loeblich & Tappan, Timor Sea, p. 52, Pl. 89, Figs. 1–9, Pl. 96, Figs. 11–16.
2009 *Miliolinella webbiana* (d'Orbigny 1839), Parker, Ningaloo Reef, p. 124, Fig. 90a–e.
2013 *Miliolinella webbiana* (d'Orbigny); Debenay, New Caledonia, p.110, 275.

Miliolinella pilasensis McCulloch, 1977 (Pl. 2, Fig. 16)
1994 *Triloculinella pilasensis* (McCulloch); Loeblich and Tappan, Timor Sea, p. 57, Pl. 99, Figs. 1–9.
2009 *Miliolinella* sp. 2; Parker, Ningaloo Reef, p. 128, Figs. 92a–i, 93a–j, 94a–k.
2013 *Miliolinella pilasensis* McCulloch; Debenay, New Caledonia, p. 110, 275.

***Miliolinella* sp. 1** sensu Parker 2009 (Pl. 2, Figs. 17–18)
1994 *Triloculinella pseudooblonga* (Zheng); Loeblich and Tappan, Timor Sea, p. 57, Pl. 88, Figs. 7–18, Pl. 97, Figs. 10–12, Pl. 98, Figs. 1–3, 7–9.
2009 *Miliolinella* sp. 1; Parker, Ningaloo Reef, p. 127, Fig. 91a–l.

***Miliolinella* sp. 2**; (Pl. 2, Fig. 19)
1994 *Miliolinella labiosa* (d'Orbigny); Loeblich and Tappan, Timor Sea, p. 52, Pl. 87, Figs. 10–12.
2013 *Miliolinella labiosa* (d'Orbigny); Debenay, New Caledonia, p. 109, 275.

Pyrgo* cf. *P. denticulata (Brady, 1884) (Pl. 2, Figs. 20–21)
1993 *Pyrgo denticulata* (Brady); Hottinger et al., Gulf of Aquaba, p. 56, Pl. 49, Figs. 8–12.
1994 *Pyrgo denticulata* (Brady); Loeblich and Tappan, Timor Sea, p. 54, Pl. 92, Figs. 1–2.
1994 *Pyrgo denticulata* (Brady 1844); Jones, Brady's specimens, p. 19, Pl. 3, Fig. 4–5.
2009 *Pyrgo denticulata* (Brady 1844); Parker, Ningaloo Reef, p. 168, Fig. 119a–h.
2013 *Pyrgo denticulata* (Brady); Debenay, New Caledonia, p. 117, 276.

Pyrgo striolata (Brady, 1884) (Pl. 2, Figs. 22–23)
1993 *Pyrgo striolata* (Brady) (s.l.); Hottinger et al.; Gulf of Aquaba, p. 57, Pl. 51, Figs. 5–11.

1994 *Pyrgo striolata* (Brady); Loeblich and Tappan, Timor Sea, p. 54, Pl. 92, Figs. 9–15.
2009 *Pyrgo striolata* (Brady 1884); Parker, Ningaloo Reef, p. 172, Fig. 122a–k.
2013 *Pyrgo striolata* (Brady); Debenay, New Caledonia, p. 118, 277.
Triloculina tricarinata d'Orbigny in Deshayes, 1832 (Pl. 2, Figs. 24–25.
1988 *Triloculina tricarinata* d'Orbigny; Van Marle, East Indonesia, p. 149, Pl. IV, Fig. 24.
1993 *Triloculina tricarinata* d'Orbigny; Hottinger et al., Gulf of Aquaba, p. 65, Pl. 68, Figs. 7–12.
1994 *Triloculina tricarinata* d'Orbigny; Loeblich and Tappan, Timor Sea, p. 56, Pl. 96, Figs. 1–7.
1994 *Triloculina tricarinata* sensu Parker, Jones and Brady 1865; Jones, Brady's specimens, p. 20, Pl. 3, Fig. 17.
2009 *Triloculina* cf. *T. tricarinata* d'Orbigny 1826; Parker, Ningaloo Reef, p. 364, Fig. 265a–k.
2013 *Triloculina tricarinata*; Debenay, New Caledonia, p. 138, 278.

Subfamily SIGMOILOPSINAE Vella, 1957

Sigmoilopsis minuta (Collins, 1958) (Pl. 2, Fig. 28)
1993 *Sigmoilopsis minuta* (Collins); Hottinger et al., Gulf of Aquaba, p. 62, Pl. 61, Figs. 4–9.
1994 *Massilina minuta* Collins, 1958; Loeblich and Tappan, Timor Sea, p. 47, Pl. 75, Figs. 7–12.

Subfamily TUBINELLINAE Rhumbler, 1906

Articulina alticostata Cushman, 1944 (Pl. 2, Fig. 29)
1994 *Articulina alticostata* Cushman; Loeblich and Tappan, Timor Sea, p. 59, Pl. 104, Figs. 5–10.
2009 *Articulina alticostata* Cushman 1944; Parker, Ningaloo Reef, p. 88, Fig. 63a–g.
2013 *Articulina alticostata* Cushman; Debenay, New Caledonia, p. 103, 280.

Superfamily SORITOIDEA Ehrenberg, 1839

Family PENEROPLIDAE Schultze, 1854

Peneroplis pertusus (Forskål, 1775) (Pl. 2, Fig. 30)
1994 *Peneroplis pertusus* (Forskål); Loeblich and Tappan, Timor Sea, p. 62, Pl. 110, Figs. 1–5.
1994 *Peneroplis pertusus* (Forskål 1775); Jones, Brady's specimens, p. 29, Figs. 16–17, 23.
2009 *Peneroplis pertusus* (Forskål 1775); Parker, Ningaloo Reef, p. 152, Figs. 108a–l, 109a–l.
2013 *Peneroplis pertusus* (Forskål) ; Debenay, New Caledonia, p. 113, 281.

Family SORITIDAE Ehrenberg, 1839

Subfamily ARCHAIASINAE Cushman 1927

Parasorites orbitoloides (Hofker, 1930) (Pl. 2, Fig. 31–32)
1994 *Parasorites orbitolitoides* (Hofker 1930); Jones, Brady's specimens, p. 30, Pl. 15, Fig. 4.
2013 *Parasorites orbitolitoides* (Hofker); Debenay, New Caledonia, p. 113, 282.

Order LAGENIDA Lankester, 1885

Superfamily NODOSARIACEA Ehrenberg, 1838

Family NODOSARIIDAE Ehrenberg, 1838

Subfamily NODOSARIINAE Ehrenberg. 1838

Dentalina catenulata (Brady, 1884) (Pl. 2, Fig. 33)

1994 *Dentalina catenulata* (Brady), Loeblich and Tappan, Timor Sea, p. 63, Pl. 113, Figs. 1–4.

1994 *Dentalina catenulata* (Brady 1884); Jones, Brady's specimens, p. 75, Pl.63, Figs. 32–34.

Dentalina* cf. *D. mutsui Hada, 1931 (Pl. 2, Fig. 34)

1994 *Dentalina mutsui* Hada; Loeblich and Tappan, Timor Sea, p. 63, Pl. 113, Figs. 5–9.

Grigelis orectus Loeblich & Tappan, 1994 (Pl. 2, Fig. 35)

1994 *Grigelis orectus*, n.sp.; Loeblich and Tappan, Timor Sea, p. 64, Pl. 115, Fig. 22.

1999 *Grigelis orectus* Loeblich and Tappan; Hayward et al., New Zealand, p. 64, Pl. 115, Fig. 22.

2013 *Grigelis orectus* Loeblich and Tappan 1994; Debenay, New Caledonia, p. 165, 284.

Laevidentalina bradyensis (Dervieux, 1894) (Pl. 2, Fig. 36)

1994 *Laevidentalina bradyensis* (Deriveux); Loeblich and Tappan, Timor Sea, p. 64, Pl. 114, Figs. 1–9, Pl. 115, Fig. 5.

2010 *Laevidentalina haueri* (Neugeboren, 1856); Hayward et al., New Zealand, p. 171, Pl. 43–47.

Laevidentalina inflexa (Reuss, 1866) (Pl. 2, Fig. 37)

1994 *Laevidentalina inflexa* (Reuss); Loeblich and Tappan, Timor Sea, p. 65, Pl. 114, Figs. 10–16, Pl. 115, Fig. 6.

2013 *Laevidentalina inflexa* (Reuss, 1866); Debenay, New Caledonia, p. 166, 284.

Laevidentalina sidebottomi (Cushman, 1933) (Pl. 2, Fig. 38)

1994 *Laevidentalina sidebottomi* (Cushman); Loeblich and Tappan, Timor Sea, p. 65, Pl. 113, Figs. 13–19.

2013 *Laevidentalina sidebottomi* (Cushman, 1933); Debenay, New Caledonia, p. 166, p. 285.

Pseudonodosaria brevis (d'Orbigny, 1846) (not figured)

1994 *Pseudonodosaria discreta* (Reuss); Loeblich and Tappan, Timor Sea, p. 66, Pl. 117, Fig. 1–6.

2010 *Pseudonodosaria brevis* (d'Orbigny 1846); Hayward et al., New Zealand, p. 172, Pl. 12, Figs. 62–63.

2013 *Pseudonodosaria discreta* (Reuss, 1850); Debenay, New Caledonia, p. 168, p. 285.

Pyramidulina catesbyi (d'Orbigny, 1839) (not figured)

1994 *Pyramidulina catesbyi* (d'Orbigny), Loeblich and Tappan, Timor Sea, p. 66, Pl. 116, Figs. 10–12.

Pyramidulina comatula (Cushman, 1923) (Pl. 2, Fig. 39)

1994 *Pseudonodosaria comatula* (Cushman); Loeblich and Tappan, Timor Sea, p. 66, Figs. 13–16.

1994 *Pseudoglandulina comatula* (Cushman 1923); Jones, Brady's specimens, p. 76, Pl. 64, Figs. 1–5.

Pyramidulina luzonensis (Cushman, 1921); (Pl. 2, Fig. 40)

1994 *Pyramidulina luzonensis* (Cushman), Loeblich and Tappan, Timor Sea, p. 66, Pl. 117, Figs. 9–11.

Family VAGINULINIDAE Reuss, 1862

Subfamily LENTICULININAE Chapman, Parr, and Collins, 1934

Lenticulina calcar (Linnaeus, 1758) (Pl. 2, Fig. 41)

1994 *Lenticulina calcar* (Linné); Loeblich and Tappan, Timor Sea, p. 68, Pl. 120, Figs. 1–8.

2010 *Lenticulina calcar* (Linnaeus 1758); Hayward et al.; New Zealand, p. 177, Pl. 14, Figs. 9–10, Pl. 15, Figs. 1–2.

2013 *Lenticulina calcar* (Linné, 1758); Debenay, New Caledonia, p. 223, 286.

Lenticulina domantayi (McCulloch, 1977) (Pl. 2, Fig. 42)

1994 *Lenticulina domantayi* (McCulloch); Loeblich and Tappan, Timor Sea, p. 68, Pl. 121, Figs. 1–8.

Lenticulina submamilligera (Cushman, 1917) (Pl. 2, Fig. 43)

1994 *Lenticulina submamilligera* (Cushman); Loeblich and Tappan, Timor Sea, p. 68, Pl. 120, Figs. 9–14.

1994 *Lenticulina submamilligera* (Cushman 1917); Jones, Brady's specimens, p. 82, Pl. 70, Figs. 17–18.

Marginulinopsis philippinensis (Cushman, 1921) (Pl. 2, Fig. 44)

1994 *Marginulinopsis philippinensis* (Cushman); Loeblich and Tappan, Timor Sea, p. 69, Pl. 123, Figs. 10–13.

Saracenaria angularis Natland, 1938 (Pl. 3, Figs. 1–2)

1994 *Saracenaria angularis* Natland; Loeblich and Tappan, Timor Sea, p. 69, Pl. 125, Figs. 1–8.

2010 *Saracenaria latifrons* (Brady, 1884); Hayward et al., New Zealand, p. 181, Pl. 15, Figs. 28–34.

Subfamily MARGINULININAE Wedekind, 1937

Amphicoryna* cf. *A. meringella Loeblich & Tappan, 1994 (Pl. 3, Fig. 3)

1994 *Amphicoryna meringella*, n.sp.; Loeblich and Tappan, Timor Sea, p. 71, Pl. 128, Figs. 1–7.

Amphicoryna separans (Brady, 1884) (Pl. 3, Fig. 4–5)

1988 Amphicoryna scalaris

1994 *Amphicoryna separans* (Brady); Loeblich and Tappan, Timor Sea, p. 71, Pl. 127, Figs. 1–18.

1994 *Amphicoryna separans* (Brady 1884); Jones, Brady's specimens, p. 76, Pl. 64, Figs. 16–19.

2010 *Amphicoryna separans* (Brady 1884); Hayward et al., New Zealand, p. 175, Pl. 13, Figs. 21–22.

2013 *Amphicoryna separans* (Brady, 1884); Debenay, New Caledonia, p. 162, 287.

Amphicoryna sublineata (Brady, 1884) (Pl. 3, Fig. 6)

1994 *Amphicoryna sublineata* (Brady); Loeblich and Tappan, Timor Sea, p. 72, Pl. 128, Fig. 8–14.

1994 *Amphicoryna sublineata* (Brady 1884); Jones, Brady's specimens, p. 75, Pl. 63, Figs. 19–22.

2010 *Amphicoryna hirsuta* f. *sublineata* (Brady, 1884); Hayward et al., New Zealand, p. 174, Pl. 13, Fig. 20.

Astacolus crepidulus (Fichtel & Moll, 1798) (Pl. 3, Fig. 7)

1994 *Astacolus crepidulus* (Fichtel and Moll); Loeblich and Tappan, Timor Sea, p. 72, Pl. 130, Figs. 1–10.

1994 *Astacolus crepidulus* (Fichtel and Moll 1798); Jones, Brady's specimens, p. 79, Pl. 67, Fig. 20.

2010 *Astacolus crepidulus* (Fichtel & Moll 1798); Hayward et al., New Zealand, p. 175, Pl. 13, Figs. 23–24, Pl. 14, Figs. 1–2.

2013 *Astacolus crepidulus* (Fichtel & Moll, 1798); Debenay, New Caledonia, p. 217, 288.

Marginulina musai Saidova, 1975 (Pl. 3, Figs. 8–9)

1994 *Marginulina musai* Saidova; Loeblich and Tappan, Timor Sea, p. 73, Pl. 131, Figs. 6–11.

Vaginulinopsis pseudoplanulata (Zheng, 1980) (Pl. 3, Fig. 10)

1994 *Vaginulinopsis pseudoplanulata* (Zheng); Loeblich and Tappan, Timor Sea, p. 74, Pl. 132, Figs. 1–6.

Vaginulinopsis sublegumen Parr, 1950 (Pl. 3, Fig. 11)

1994 *Vaginulinopsis sublegumen* Parr; Loeblich and Tappan, Timor Sea, p. 74, Pl. 131, Figs. 12–13, Pl. 133, Figs. 10–19.

1994 *Vaginulinopsis sublegumen* Parr 1950; Jones, Brady's specimens, p. 78, Pl. 66, Fig. 13.

2013 *Vaginulinopsis sublegumen* Parr; Debenay, New Caledonia, p. 170, 288.

Subfamily VAGINULININAE Reuss, 1860

Planularia gemmata (Brady, 1881) (Pl. 3. Fig. 12)

1994 *Planularia gemmata* (Brady); Loeblich and Tappan, Timor Sea, p. 75, Pl. 134, Figs. 1–5.

1994 *Planularia gemmata* (Brady 1881); Jones, Brady's specimens, p. 82, Pl. 71, Figs. 6–7.

Planularia patens (Brady, 1884) (Pl. 3, Fig. 13)

1994 *Astacolus patens* (Brady); Loeblich and Tappan, Timor Sea, p. 72, Pl. 129, Figs. 1–6.

1994 *Planularia patens* (Brady 1884); Jones, Brady's specimens, p. 79, 67, Figs. 15–16.

Planularia spinipes (Cushman, 1913)

1994 *Planularia australis* Chapman, 1941; Jones, Brady's specimens, p. 80, Pl. 68, Figs. 3–4

2010 *Planularia spinipes* (Cushman 1913); Hayward et al., New Zealand, p. 180, Pl. 15, Figs. 17–19.

Family LAGENIDAE Reuss, 1862

Cerebrina* cf. *C. claricerviculata (McCulloch, 1977) (Pl. 3, Fig. 15)

2009 *Cerebrina* cf. *C. claricerviculata* (McCulloch, 1977); Parker, Ningaloo Reef, p. 390, Figs. 292a–c, 283a–j.

2013 *Cerebrina claricerviculata* (McCulloch, 1977); Debenay, New Caledonia, p. 141, 288.

Cerebrina lacunata (Burrows & Holland, 1895) (Pl. 3, Fig. 16)

1994 *Cerebrina lacunata* (Burrows and Holland); Loeblich and Tappan, Timor Sea, p. 76, Pl. 135, Figs. 8–15.

2009 *Cerebrina lacunata* (Burrows & Holland in Jones 1865); Parker, Ningaloo Reef, p. 395, Fig. 284a–l, 285a–i.

2013 *Cerebrina lacunata* (Burrows & Holland in Jones 1895); Debenay, New Caledonia, p. 142, 289.

Lagena annellatrachia Loeblich & Tappan, 1994 (Pl. 3, Fig. 17)

1994 *Lagena annellatrachia* n.sp.; Loeblich and Tappan, Timor Sea, p. 77, Fig. Pl. 142, Figs. 1–8, 11–12.

Lagena annulatacollare (Loeblich & Tappan, 1994) (Pl. 3, Fig. 18)

1994 *Pygmaeoseistron annulatacollare* n.sp., 1994; Loeblich and Tappan, Timor Sea, p. 80, Pl. 141, Figs. 7–9.

Lagena cyrillion (Loeblich & Tappan, 1994); (Pl. 3, Fig. 19)

1994 *Pygmaeoseistron cyrillion* n.sp., 1994; Loeblich and Tappan, Timor Sea, p. 80, Pl. 143, Figs. 1–5.

Lagena fidicularia Patterson, 1991 (Pl. 3, Fig. 20)

1994 *Lagena fidicularia* Patterson; Loeblich and Tappan, Timor Sea, p. 78, Pl. 138, Figs. 12–15.

Lagena substriata Williamson, 1848 (Pl. 3, Fig. 21)

1994 *Lagena substriata* Williamson, Loeblich and Tappan, Timor Sea, p. 79, Fig. 138, Figs. 1–5.

Procerolagena oceanica (Albani, 1974) (Pl. 3, Fig. 22)

1994 *Pygmaeoseistron oceanicum* (Albani); Loeblich and Tappan, Timor Sea, p. 80, Pl. 144, Figs. 4–7.

2013 *Procerolagena oceanica* (Albani, 1974); Debenay, New Caledonia, p. 160 290.

Reussoolina trachiella Loeblich & Tappan, 1994, (Pl. 3, Fig. 23)

1994 *Reussoolioa trachiella* n.sp., Loeblich and Tappan, Timor Sea, p. 81, Pl. 139, Figs. 17–18.

Superfamily POLYMORPHINACEA d'Orbigny, 1839

Family POLYMORPHINIDAE d'Orbigny, 1839

Subfamily POLYMORPHININAE d'Orbigny, 1839a

Globulina rotundata (Bornemann, 1855) (not figuered)

1994 *Globulina rotundata* (Bornemann 1855); Jones, Brady's specimens, p. 85, Pl. 73, Figs. 7–8.

Guttulina bartschi Cushman & Ozawa, 1930 (Pl. 3, Fig. 24)

1994 *Guttulina bartschi* Cushman and Ozawa; Loeblich and Tappan, Timor Sea, p. 82, Fig. 145, Fig. 5–15.

2009 *Guttulina bartschi* Cushman & Ozawa 1930; Parker, Ningaloo Reef, p. 405, Fig. 291, Fig. 291a–c.

2013 *Guttulina bartschi* Cushman & Ozawa, 1930; Debenay, New Caledonia, p. 240, 290.

Guttulina yamazaki Cushman & Ozawa, 1930 (Pl. 3, Fig. 25)

1994 *Guttulina yamazaki* Cushman and Ozawa; Loeblich and Tappan, p. 82, Pl. 146, Figs. 4–7, Pl. 148, Figs. 1–3.

2013 *Guttulina yamazakii* Cushman & Ozawa, 1930; Debenay, New Caledonia, p. 240 291.

Guttulina regina (Brady, Parker & Jones, 1870), (Pl. 3, Fig. 26)

1994 *Guttulina regina* (Brady, Parker, and Jones); Loeblich and Tappan, p. 82, Pl. 146, Figs. 1–3.

2009 *Guttulina regina* (Brady, Parker & Jones 1870); Parker, Ningaloo Reef, p. 405, Fig. 292a–k.

2013 *Guttulina regina* (Brady, Parker & Jones, 1871); Debenay, New Caledonia, p. 240, p. 290.

Pyrulina angusta (Egger, 1857) (Pl. 3, Fig. 27)

2013 *Pyrulina angusta* (Egger, 1857); Debenay, New Caledonia, p. 247, 291.

Family ELLIPSOLAGENIDAE Silvestri, 1923

Subfamily OOLININAE Loeblich and Tappan, 1961

Favulina hexagoniformis (McCulloch, 1997) (Pl. 3, Fig. 29)

2013 *Favulina hexagoniformis* (McCulloch, 1977); Debenay, New Caledonia, p. 145, 294.

Oolina caudigera (Wiesner, 1931) (Pl. 3, Fig. 30)

1994 *Oolina caudigera* (Wiesner); Loeblich and Tappan, Timor Sea, p. 87, Pl. 152, Figs. 9–11.

2013 *Oolina caudigera* (Wiesner, 1931); Debenay, New Caledonia, p. 156, 295.

Subfamily ELLIPSOLAGENINAE Silvestri, 1923

Fissurina circularis Todd, 1954 (Pl. 3, Fig. 31)

1994 *Fissurina circularis* Todd; Loeblich and Tappan, Timor Sea, p. 88, Pl. 154, Figs. 13–18.

2009 *Fissurina circularis* Todd 1954; Parker, Ningaloo Reef, p. 400, Fig. 287a–c.

2013 *Fissurina circularis* Todd, 1954; Debenay, New Caledonia, p. 146, 292.

Family GLANDULINIDAE Reuss, 1860

Subfamily GLANDULININAE Reuss, 1860

Laryngosigma afueraensis McCulloch, 1977 (Pl. 3, Fig. 28)

2013 *Laryngosigma afueraensis* McCulloch, 1977, Debenay, New Caledonia, p. 242, 296.

Glandulina symmetrica (McCulloch, 1977) (Pl. 3, Fig. 32)

1994 *Glandulina symmetrica* (McCulloch); Loeblich and Tappan, Timor Sea, p. 97, Pl. 168, Figs. 6–8.

Order ROBERTINIDA Mikhalevich, 1980

Superfamily CERATOBULIMINACEA Cushman, 1927

Family CERATOBULIMINIDAE Cushman, 1927

Subfamily CERATOBULIMININAE Cushman, 1927

Saintclairoides toreuta Loeblich & Tappan, 1994 (Pl.3, Fig. 33–34)

1994 *Saintclairoides toreutus* n.sp.; Loeblich and Tappan, Timor Sea, p. 98, Pl. 173, Figs. 1–14.

2009 *Saintclairoides toretus* Loeblich & Tappan 1994; Parker, Ningaloo Reef, p. 388, Fig. 311e–i.

2013 *Saintclairoides toreutus* Loeblich & Tappan, 1994, Debenay, New Caledonia, p. 213, 297.

Family EPISTOMINIDAE Wedekind, 1937

Subfamily EPISTOMININAE Wedekind, 1937

Hoeglundina elegans (d'Orbigny, 1826) (Pl. 3, Fig. 35–36)

1979 *Hoeglundina elegans* (d'Orbigny); Corliss, south east Indian Ocean, p. 12, Pl. 5, Figs. 11–13.

1988 *Hoeglundina elegans* (d'Orbigny); Van Marle, East Indonesia, p. 145, Pl. V, Figs. 18–19.

1993 *Hoeglundina* sp. A; Hottinger et al., Gulf of Aquaba, p.84, Pl. 98, Figs. 1–2.

1994 *Hoeglundina elegans* (d'Orbigny); Loeblich and Tappan, Timor Sea, p. 98, Pl. 174, Figs. 1–6.
1994 *Hoeglundina elegans* (d'Orbigny 1826); Jones, Brady's specimens, p. 104, Pl. 105, Figs.3–6, Text-figure 21.
2010 *Hoeglundina elegans* (d'Orbigny 1826); p. 183, Pl. 16, Figs. 16–21.
2013 *Hoeglundina elegans* (d'Orbigny, 1826); Debenay, New Caledonia, p. 199, 297.

Superfamily ROBERTINACEA Reuss, 1850

Family ROBERTINIDAE Reuss, 1850

Subfamily ALLIATININAE McGowran, 1966

Alliatina variabilis (Zheng, 1978) (Pl. 3, Fig. 37)

1994 *Alliatina variabilis* (Zheng); Loeblich and Tappan, Timor Sea, p. 99, Pl. 174, Figs. 7–12.
2013 *Alliatina variabilis* (Zheng, 1978); Debenay, New Caledonia, p. 215, 297.

Geminospira bradyi Bermúdez, 1952 (Pl. 3, Figs. 38–39)

1969 *Geminospira* sp. A aff. *G. simaensis* Makiyama and Nakagawa; Betjeman, Western Australian shelf, Pl. 18, Figs. 14–15.
1994 *Geminospira bradyi* Bermúdez; Loeblich and Tappan, Timor Sea, p. 99, Pl. 177, Figs. 1–14, Pl. 178, Figs. 1–9.
1994 *Geminospira bradyi* Bermúdez 1952; Jones, Brady's specimens, p. 111, Pl. 113, Fig. 6.
2009 *Geminospira bradyi* Bermúdez 1952; Parker, Ningaloo Reef, p. 385, Fig. 310a–i.
2013 *Geminospira bradyi* Bermudez, 1952; Debenay, New Caledonia, p. 196, 297.

Subfamily ROBERTININAE Reuss, 1850

Robertinoides australis (Collins, 1958) (Pl. 3, Fig. 40)

1994 *Robertinoides cf. australis* (Collins); Loeblich and Tappan, Timor Sea, p. 99, Pl. 176, Figs. 9–14.
2013 *Robertinoides australis* Collins, Debenay, New Caledonia, p. 211, 298.

Robertinoides oceanica (Cushman & Parker, 1947) (Pl. 3, Fig. 41)

1993 *Robertinoides bradyi* Cushman and Parker; Hottinger et al., Gulf of Aquaba, p. 84, Figs. 1–13.
1994 *Robertinoides occanicus* (Cushman and Parker); Loeblich and Tappan, p, 99, Pl. 176, Figs. 4–8.
1994 *Robertinoides oceanicus* (Cushman and Parker 1947); Jones, Brady's material, p. 55, Pl. 50, Fig. 19.
2013 *Robertinoides oceanicus* (Cushman & Parker, 1947); Debenay, New Caledonia, p. 211, 298.

Order BULIMINIDA Fursenko, 1958

Superfamily BOLIVINACEA Glaessner, 1937

Family BOLIVINIDAE Glaessner, 1937

Subfamily BOLIVINITINAE Cushman, 1927

Bolivina robusta (Brady, 1881) (Pl. 3, Fig. 42)

1988 *Bolivina robusta* Brady; Van Marle, East Indoneasea, p. 139, Pl. 1, Figs. 25–26.

1994 *Bolivina robusta* Brady; Loeblich and Tappan, Timor Sea, p. 111, Pl. 215, Figs. 17–18.
2010 *Bolivina robusta* Brady, 1881; Hayward et al., New Zealand, p. 186, Pl. 16, p. 41–42.
2013 *Bolivina robusta* Brady, 1881; Debenay, New Caledonia, p. 171, 298.

Bolivina striatula Cushman, 1922 (Pl. 3, Fig. 43)
1997 *Bolivina striatula* Cushman; Haig, Exmouth Gulf, p.274, Fig. 5:13.
2009 *Bolivina striatula* Cushman 1922; Parker, Ningaloo Reef, p. 433, Fig. 313a–h.
2013 *Bolivina striatula* Cushman, 1922; Debenay, New Caledonia, p. 171, 298.

Bolivinellina translucens (Phleger & Parker, 1951) (Pl. 3, Fig. 44)
1994 *Bolivinellina translucens* (Phleger and F. L. Parker); Loeblich and Tappan, p. 111, Pl. 213, Figs. 9–14.
2013 *Bolivinellina translucens* (Phleger & Parker, 1951); Debenay, New Caledonia, p. 172, 299.

Superfamily LOXOSTOMATACEA Loeblich and Tappan, 1962

Family BOLIVINELLIDAE Hayward in Hayward and Brazier, 1980

Rugobolivinella elegans (Parr, 1932) (Pl. 3, Fig. 45)
1993 *Bolivinella elegans* Parr; Hottinger et al., Gulf of Aquaba, p. 93, Pl. 113, Figs. 1–6.
1994 *Rugobolivinella elegans* (Parr); Loeblich and Tappan, Timor Sea, p. 113, Pl. 220, Figs. 1–6.
2009 *Bolivinella elegans* Parr 1932; Parker, Ningaloo Reef, p. 436, Fig. 316a–f.
2013 *Rugobolivinella elegans* Parr, 1932; Debenay, New Caledonia, p. 177, 299.

Superfamily CASSIDULINACEA d'Orbigny, 1839

Family CASSIDULINIDAE d'Orbigny, 1839

Subfamily CASSIDULININAE d'Orbigny, 1839

Globocassidulina subglobosa (Brady, 1881) (Pl.3, Fig. 46)
1979 *Globocassidulina subglobosa* (Brady); Corliss, south east Indian Ocean; p. 8, Pl. 3, Figs. 12–13.
1988 *Globocassidulina subglobosa* (Brady); Van Marle, East Indonesia, p. 143, Pl. V, Fig. 22.
1994 *Globocassidulina subglobosa* (Brady 1881); Jones, Brady's specimens, p. 60, Pl. 54, Fig. 17.
2010 *Globocassidulina subglobosa* (Brady 1881); Hayward et al., p. 198, Pl. 20, Figs. 4–6.
2013 *Globocassidulina subglobosa* (Brady, 1881); Debenay, New Zealand, p. 239, 300.

Heterocassidulina albida McCulloch, 1977 (Pl. 3, Fig. 47–48)
1994 *Heterocassidulina albida* McCulloch; Loeblich and Tappan, Timor Sea, p. 115, Pl. 224, Figs. 10–15.

Paracassidulina neocarinata (Thalmann, 1950) (Pl. 4, Figs. 1–2)
1993 *Paracassidulina neocarinata* (Thalmann); Hottinger et al., Gulf of Aquaba, p. 94, Pl. 116, Figs. 1–7.

1994 *Paracassidulina neocarinata* (Thalmann); Loeblich and Tappan, Timor Sea, p. 116, Pl. 227, Figs. 1–15.
1994 *Cassidulina laevigata* var. *carinata* Silvestri 1896; Jones, Brady's specimens, p. 60, Pl. 55, Fig. 2–3.
2013 *Paracassidulina neocarinata* (Thalman, 1950); Debenay, New Caledonia, p. 245, 300.

Superfamily BULIMINACEA Jones in Griffith and Henfrey, 1875

Family SIPHOGENERINOIDIDAE Saidova, 1981

Subfamily SIPHOGENERINOIDINAE Saidova, 1981

Hopkinsinella glabra (Millett, 1903) (Pl. 4, Fig. 3)

1993 *Hopkinsinella glabra* (Millett); Hottinger et al., Gulf of Aquaba, p. 96, Pl. 119, Figs. 6–9.
1994 *Hopkinsinella glabra* (Millett); Loeblich and Tappan, Timor Sea, p. 118, Pl. 232, Figs. 1–11.
2013 *Hopkinsinella glabra* (Millett, 1903); Debenay, New Caledonia, p. 174, 301.

Loxostomina mayori (Cushman, 1922) (Pl. 4, Fig. 4)

1994 *Loxostomina mayori* (Cushman); Loeblich and Tappan, Timor Sea, p. 119, Pl. 233, Figs. 9–14.
1994 *Loxostomina mayori* (Cushman 1922), Jones, Brady's specimens, p. 58, Pl. 53, Figs. 14–15.
2013 *Loxostomina barkeri* (Margerel, 1981), Debenay, New Caledonia, p. 174, 301.

Stilostomelloides virgula (Brady, 1879) (Pl. 4, Fig. 5)

1993 *Siphouvigerina virgula* (Brady); Hottinger et al., Gulf of Aquaba, p. 102, Pl. 129, Figs. 1–5.
1994 *Allassoida virgula* (Brady); Loeblich and Tappan, Timor Sea, p. 121, Pl. 238, Figs. 1–11.
2013 *Allassoida virgula* (Brady, 1879), Debenay, New Caledonia, p. 162, 302.

Rectobolivina bifrons (Brady, 1881) (Pl. 4, Fig. 6)

1994 *Rectobolivina bifrons* (Brady); Loeblich and Tappan, Timor Sea, p. 120, Pl. 234, Figs. 13–16.
1994 *Rectobolivina bifrons* (Brady 1881); Jones, Brady's specimens, p. 87, Pl 75, Figs. 18–20.

Sagrinella jugosa (Brady, 1884) (Pl. 4, Fig. 7)

1988 Patellinella jugosa (Brady); Van Marle, East Indonesia, p. 148, Pl. IV, Figs. 14–15.
1994 *Sagrinella jugosa* (Brady 1884), Jones, Brady's specimens, p. 47, Pl. 42, Fig. 7.
2009 *Sagrinella jugosa* (Brady 1884); Parker, Ningaloo Reef, p. 464, Fig. 334a–e.

Subfamily TUBULOGENERININAE Saidova, 1981

Siphogenerina indica LeRoy, 1941 (Pl. 4, Fig. 8)

1994 *Siphogenerina indica* LeRoy; Loeblich and Tappan, Timor Sea, p. 122, Pl. 241, Figs. 12–20.
1994 *Siphogenerina indica* Leroy 1941; Jones, Brady's specimens, p. 87, Pl. 76, Figs. 23–24.

Family BULIMINIDAE Jones, 1875

Bulimina marginata d'Orbigny, 1826 (Pl. 4, Fig. 9)

1988 *Bulimina marginata* d'Orbigny; Van Marle, East Indonesia, Pl. II, Fig. 8.

1993 *Bulimina marginata marginata* d'Orbigny; Hottinger et al., p. 100, Pl. 125, Figs. 1–6.

1994 *Bulimina marginata* d'Orbigny; Loeblich and Tappan, Timor Sea, p. 124, Pl. 242, Figs. 1–4.

Bulimina subornata Brady, 1884 (Pl. 4, Fig. 10)

1994 *Bulimina subornata* Brady; Loeblich and Tappan, Timor Sea, p. 125, Pl. 243, Figs. 7–10.

1994 *Bulimina subornata* Brady 1884; Jones, Brady's specimens, p. 55, Pl. 51, Fig. 6.

Protoglobobulimina pupoides (d'Orbigny, 1846) (Pl. 4, Fig. 11)

1994 *Protoglobobulimina pupoides* (d'Orbigny); p. 125, Pl. 244, Figs. 8–10.

1994 *Praeglobobulimina pupoides* (d'Orbigny 1846); Jones, Brady's specimens, p. 55, Pl. 50, Figs. 14–15.

Family UVIGERINIDAE Haeckel, 1894

Subfamily UVIGERININAE Haeckel, 1894

Siphouvigerina porrecta (Brady, 1879) (Pl. 4, Fig. 13)

1993 *Neouvigerina porrecta* (Brady) *porrecta* (Brady); Hottinger et al., p. 101, Pl. 127, Figs. 9–12.

1994 *Siphouvigerina porrecta* (Brady); Loeblich and Tappan, Timor Sea, p. 127, Pl. 247, Figs. 6–11.

2009 *Neouvigerina porrecta* (Brady 1979); Parker, Ningaloo Reef, p. 462, Fig. 331a–e.

Siphouvigerina proboscidea (Schwager, 1866)

1988 *Uvigerina proboscidea* Schwager; Van Marle, Eastern Indonesia, p. 149, Pl. III, Figs. 12–13.

2013 *Neouvigerina proboscidea* (Schwager, 1866); Debenay, New Caledonia, p. 181, 303.

Uvigerina peregrina Cushman, 1923 (Pl. 4, Fig. 14)

2001 *Uvigerina peregrina* Cushman; Szareck, p. 130, Pl. 18, Fig. 13.

2013 *Uvigerina* cf. *U. peregrina* Cushman, 1923; Debenay, New Caledonia, p. 183, 304.

Uvigerina reineri (Belford, 1966) (Pl. 4, Fig. 15)

1994 *Euuvigerina reineri* Belford; Loeblich and Tappan, Timor Sea, p. 127, Pl. 249, Figs. 1–6.

Uvigerina schwageri Brady, 1884 (Pl. 4, Fig. 16)

1994 *Euuvigerina schwageri* (Brady); Loeblich and Tappan, Timor Sea, p. 128, Pl. 249, Figs. 10–20.

1994 *Uvigerina schwageri* Brady 1884; Jones, Brady's specimens, p. 85, Pl. 74, Figs. 8–10.

Subfamily ANGULOGERININAE Galloway, 1933

Trifarina bradyi Cushman, 1923 (Pl. 4, Fig. 17)

1988 *Trifarina bradyi* Cushman, 1923; Van Marle, Eastern Indonesia, p. 149, Pl. V, Fig. 10.

1994 *Trifarina bradyi* Cushman; Loeblich and Tappan, Timor Sea, p. 128, Pl. 251, Figs. 6–16.

1994 *Trifarina brady* Cushman 1923, Jones, Brady's specimens, p. 78, Pl. 67, Figs. 1–3.
2013 *Trifarina bradyi* Cushman 1923; Debenay, New Caledonia, p. 183, 304.

Family REUSSELLIDAE Cushman, 1933

Chrysalidinella pacifica (Uchio, 1952) (Pl. 4, Fig. 18)
1994 *Chrysalidinella dimorpha* (Brady); Loeblich and Tappan, Timor Sea, p. 129, Pl. 252, Figs. 7–10, not Figs. 11–13.
2009 *Chrysalidinella pacifica* (Uchio, 1952); Parker, Ningaloo Reef, p. 444, Fig. 320a–g.

Reussella hayasakai Oki, 1989 (Pl. 4, Fig. 19)
1994 *Reussella hayasakai* Öki; Loeblich and Tappan, Timor Sea, p. 129, Pl. 252, Figs. 1–4.
2013 *Reussella* cf. *R. hayasakai* Öki, 1989; Debenay, Timor Sea, p. 182, 304.

Reussella pulchra Cushman, 1945 (Pl. 4, Fig. 20)
1994 *Reussella pulchra* Cushman; Loeblich and Tappan, Timor Sea, p. 129, Pl. 253, Figs. 5–7.
2013 *Reussella pulchra* Cushman, 1945; Debenay, New Caledonia, p. 182, 305.

Family TRIMOSINIDAE Saidova, 1981

***Mimosina* sp.** (Pl. 4, Fig. 21)
1993 *Mimosina affinis* Millett; Hottinger et al., Gulf of Aquaba, p. 104, Pl. 133, Figs. 9–12, Pl. 134, Figs. 1–3.
1994 *Mimosona echinata* Heron-Allen and Earland, 1915; Loeblich and Tappan, Timor Sea, p. 129, Pl. 255, Figs. 1–2.

Family PAVONINIDAE Eimer and Fickert, 1899

Valvobifarina mackinnonii (Millett, 1900) (Pl. 4, Fig. 22)
1993 *Valvobifarina mackinnonii* (Millett); Hottinger et al., Gulf of Aquaba, p. 104, Pl. 133, Figs. 4–8.
1994 *Valvobifarina mackinnoni* (Millett); Loeblich and Tappan, Timor Sea, p. 130, Pl. 254, Figs. 9–12.

Superfamily FURSENKOINACEA Loeblich and Tappan, 1961

Family FURSENKOINIDAE Loeblich and Tappan, 1961

Fursenkoina pauciloculata (Brady, 1884) (Pl. 4, Fig. 23)
1993 *Fursenkoina* sp. A; Hottinger et al., Gulf of Aquaba, p. 105, Pl. 135, Figs. 1–10.
1994 *Fursenkoina pauciloculata* (Brady); Loeblich and Tappan, p. 131, Pl. 256, Figs. 1–5.
1994 *Fursenkoina pauciloculata* (Brady 1884); Jones, Brady's specimens, p. 56, Pl. 53, Figs. 4–5.
2013 *Fursenkoina pauciloculata* (Brady, 1884); Debenay, New Caledonia, p. 174, 306.

Sigmavirgulina tortuosa (Brady, 1881) (Pl. 4, Fig. 24)
1988 *Sigmavirgulina tortuosa* (Brady); Van Marle, Eastern Indonesia, p. 149, Plate V, Fig. 9.
1994 *Sigmavirgulina tortuosa* (Brady); Loeblich and Tappan, Timor Sea, p. 132, Pl. 261, Figs. 1–10.
1994 *Sigmavirgulina tortuosa* (Brady 1881); Jones, Brady's specimens, p. 58, Pl. 53, Figs. 31–34.

2009 *Sigmavirgulina tortuosa* (Brady 1881); Parker, Ningaloo Reef, p. 466, Fig. 337a–f.

Order ROTALIIDA Lankester, 1885

Superfamily DISCORBACEA Ehrenberg, 1838

Family BAGGINIDAE Cushman, 1927

Subfamily BAGGININAE Cushman, 1927

Cancris auriculus (Fichtel & Moll, 1798) (Pl. 4, Figs. 25–26)

1993 *Cancris auriculus*; Hottinger et al., Gulf of Aquaba, p. 106, Pl. 136, Figs. 6–12.

1994 *Cancris auriculus* (Fichtel and Moll); Loeblich and Tappan, Timor Sea, p. 134, Pl. 265, Figs. 7–10.

2009 *Cancris* cf. *C. auriculus* (Fichtel & Moll 1798); Parker, Ningaloo Reef, p. 522, Fig. 371a–i.

2013 *Cancris auriculus* (Fichtel & Moll, 1798); Debenay, New Caledonia, p. 189, 307.

Cancris oblongus (Williamson, 1858) (Pl. 4, Fig. 27)

1988 *Cancris oblongus* (d'Orbigny); Van Marle, East Indonesia, p. 141, Pl. IV, Fig. 13.

1994 *Cancris oblongus* (Williamson 1858); Jones, Brady's specimens, p. 105, Pl. 106, Fig. 4.

2013 *Cancris oblongus* (d'Orbigny, 1839); Debenay, New Caledonia, p. 189, 307.

Cancris bubnanensis (McCulloch, 1977) (Pl. 4, Fig. 28)

1994 *Baggina bubnanensis* McCulloch; Loeblich and Tappan, Timor Sea, p. 164, Pl. 264, Figs. 5–10.

2009 *Cancris bubnanensis* (McCulloch 1977); Parker, Ningaloo Reef, p. 525, Fig. 372a–d.

2013 *Baggina bubnaensis* McCulloch, 1977; Debenay, New Caledonia, p. 187, 306.

Family MISSISSIPPINIDAE Saidova, 1981

Subfamily STOMATORBININAE Saidova, 1981

Stomatorbina concentrica (Parker & Jones, 1864) (Pl. 4, 29–30)

1994 *Stomatorbina concentrica* (Parker and Jones); Loeblich and Tappan, Timor Sea, p. 136, Pl. 273, Figs. 1–7.

1994 *Mississippina concentrica* (Parker and Jones in Brady 1864); Jones, Brady's specimens, p. 104, Pl. 105, Fig. 1.

2009 *Stomatorbina concentrica* (Parker & Jones 1864); Parker, Ningaloo Reef, p. 742, p. 521a–i.

2013 *Stomatorbina concentrica* (Parker & Jones, 1864); Debenay, New Caledonia, p. 213, 308.

Subfamily MISSISSIPPIANA Howe, 1930

Mississippina pacifica Parr, 1950 (Pl. 6, Fig. 5)

1994 *Mississippina pacifica* Parr. 1950; Loeblich and Tappan, Timor Sea, p. 137, Pl. 273, Figs. 8–10.

2013 *Mississippina pacifica* Parr, 1950; Debenay, New Caledonia, p. 201, 308.

Family DISCORBIDAE Ehrenberg, 1838

***Rotorbinella* sp.** (Pl. 4, Fig. 31–32)

1993 *Rotorbinella* cf. *R. lepida* McCulloch; Hottinger et al., Gulf of Aquaba, p. 108, Pl. 141, Figs. 1–7.

2009 *Rotorbinella* sp. 1, Parker, Ningaloo Reef, p. 727, Figs 511a–h, 512a–j.

2013 *Rotorbinella lepida* McCulloch, 1977; Debenay, New Caledonia, p. 212, 309.

Family NEOEPONIDIDAE Loeblich and Tappan, 1994

Neoeponides margaritifer (Brady, 1881) (Pl. 4, Figs. 33–34)

1994 *Heterolepa margeritifera* (Brady); Loeblich and Tappan, Timor Sea, p. 162, Pl. 358, Figs. 1–7.

1994 *Neoeponides margaritifer* (Brady 1881); Jones, Brady's specimens, p. 100, Pl. 96, Fig. 2.

2013 *Heterolepa margaritifera* (Brady, 1881); Debenay, New Caledonia, p. 199, 321.

Family ROSALINIDAE Reiss, 1963

Neoconorbina albida McCulloch, 1977 (Pl. 4, Fig. 35)

1994 *Neoconorbina albida* McCulloch; Loeblich and Tappan, Timor Sea, p. 139, Pl. 280, Figs. 5–9.

2013 *Neoconorbina albida* McCulloch, 1977; Debenay, New Caledonia, p. 203, 309.

Neoconorbina neapolitana Hofker, 1951 (Pl. 4, Fig. 36–37)

2009 *Neoconorbina neapolitana* Hofker 1951; Parker, Ningaloo Reef, p. 660, Fig. 466a–e.

***Rosalina* sp. 1** sensu Parker 2009

2009 *Rosalina* sp. 1; Parker, Ningaloo Reef, p. 722, Fig. 507a–h.

Family SPHAEROIDINIDAE Cushman, 1927

Eusphaeroidina inflata Ujiié, 1990 (Pl. 4, Fig. 38)

1994 *Eusphaeroidina inflata* Ujiié; Loeblich and Tappan, Timor Sea, p. 141, Pl. 289, Figs. 4–13.

2013 *Eusphaeroidina inflata* Ujiie, 1990; Debenay, New Caledonia, p. 238, 311

Sphaeroidina bulloides d'Orbigny in Deshayes, 1828 (Pl. 4, Fig. 39–40)

1988 *Sphaeroidina bulloides* d'Orbigny, 1826; Van Marle, East Indonesia, p. 149, Pl. II, Fig. 11.

1993 *Sphaeroidina bulloides* d'Orbigny; Hottinger et al., Gulf of Aquaba, p. 113, Pl. 147, Figs. 4–11.

1994 *Sphaeroidina bulloides* d'Orbigny; Loeblich and Tappan, Timor Sea, p. 141, Pl. 289, Figs. 1–3.

1994 *Sphaeroidina bulloides* Deshayes 1832; Jones, Brady's specimens, p. 91, Pl, 84, Figs. 1–7.

2013 *Sphaeroidina bulloides* d'Orbigny, 1826; Debenay, New Caledonia, p. 249, 311.

Superfamily GLABRATELLACEA Loeblich and Tappan, 1964

Family BULIMINOIDIDAE Seiglie, 1970

Buliminoides williamsoniana (Brady, 1881) (Pl. 5, Fig. 1)

1994 *Buliminoides williamsonianus* (Brady); Loeblich and Tappan, Timor Sea, p. 143, Pl. 297, Figs. 1–9.

1994 *Buliminoides williamsonianus* (Brady 18 81); Jones, Brady's specimens, p. 56, Pl. 51, Figs. 16–17.

2009 *Buliminoides williamsonianus* (Brady 1881); Parker, Ningaloo Reef, p. 440, Fig. 317a–c.

2013 *Buliminoides williamsonianus* (Brady, 1881); Debenay, New Caledonia, p. 188, 312.

Elongobula parallela (Cushman & Parker, 1931) (Pl. 5, Fig. 2)

2009 *Elongobula parallela* (Cushman & Parker 1931); Parker, Ningaloo Reef, p. 446, Fig. 322a–l.

2013 *Elongobula parallela* (Cushman & Parker, 1931); Debenay, New Caledonia, p. 194, 313.

Family GLABRATELLIDAE Loeblich & Tappan, 1964

Pileolina minogasaformis (Ujiié, 1992) (Pl. 5, Figs. 3–4)

1994 *Discorbinoides minogasiformis* Ujiié; Loeblich and Tappan, Timor Sea, p. 141, Pl. 291, Figs. 1–10.

1994 *Glabratella patelliformis* (Brady 1884); Jones, Brady's specimens, p. 95, Pl. 89, Fig. 1.

2009 *Discorbinoides*? *minogasiformis* (Ujiié 1992); Parker, Ningaloo Reef, p. 562, Fig. 398a–k.

2013 *Pileolina minogasiformis* Ujiié, 1992; Debenay, New Caledonia, p. 207, 312.

Pileolina patelliformis (Brady, 1884) (Pl. 5, Fig. 5)

1993 *Discorbinoides* sp. A; Hottinger et al., Gulf of Aquaba, p. 113, Pl. 148, Figs. 1–6.

2009 *Pileolina patelliformis* (Brady 1884); Parker, Ningaloo Reef, p.694, Fig. 489a–i.

2013 *Pileolina patelliformis* (Brady, 1884); Debenay, New Caledonia, p. 208, 312.

Superfamily SIPHONINACEA Cushman, 1927

Family SIPHONINIDAE Cushman, 1927

Subfamily SIPHONININAE Cushman. 1927

Siphonina tubulosa Cushman, 1924 (Pl. 5, Fig. 6)

1993 *Siphonina tubulosa* Cushman; Hottinger et al., p. 114, Pl. 149, Figs. 1–4.

1994 *Siphonina tubulosa* Cushman; Loeblich and Tappan, Timor Sea, p. 144, Pl. 299, Figs. 1–10.

1994 *Siphonina tubulosa* Cushman 1924; Jones, Brady's specimens, p. 100, Pl. 96, Figs. 5–7.

2009 *Siphonina tubulosa* Cushman 1924; Parker, Ningaloo Reef, p. 731, Fig. 515a–i.

2013 *Siphonina tubulosa* Cushman, 1924; Debenay, New Caledonia, p. 213, 313.

Family PLANULINOIDIDAE Saidova, 1981

Planulinoides biconcava (Parker & Jones, 1862) (Pl. 5, Fig. 7)

1994 *Planulinoides biconcavus* (Jones and Parker); Loeblich and Tappan, Timor Sea, p. 147, Pl. 308, Figs. 4–11, Pl. 309, Figs. 1–9.

1994 *Planulinoides biconcavus* (Parker and Jones in Carpenter 1862); Jones, Brady's specimens, p. 96, Pl. 91, Fig. 2.

Superfamily PLANORBULINACEA Schwager, 1877

Family PLANULINIDAE Bermudez, 1952

Hyalinea florenceae McCulloch, 1977

1994 *Hyalinea florenceae* McCulloch; Loeblich and Tappan, Timor Sea, p. 148, Pl. 313, Figs. 1–10.

Planulina retia Belford, 1966

1994 *Planulina retia* Belford; Loeblich and Tappan, Timor Sea, p. 149, Pl. 315, Figs. 1–11, Pl. 316, Figs. 4–7.

2013 *Planulina retia* Belford, 1966; Debenay, New Caledonia, p. 209, 315.

Family CIBICIDIDAE Cushman, 1927

Subfamily CIBICIDINAE Cushman, 1927

Cibicides mabahethi Said, 1949 (Pl. 5, Figs. 11–12)

1993 *Cibicides mabahethi* Said; Hottinger et al., Gulf of Aquaba, p. 114, Pl. 151, Figs. 6–12.

2009 *Cibicidoides* cf. *C. mabahethi* (Said 1949); Parker, Ningaloo Reef, p. 539, Fig. 383a–e.

2013 *Cibicides mabahethi* Said, 1949; Debenay, New Caledonia, p. 190, 315.

Cibicides* cf. *C. refulgens Montfort, 1808 (Pl. 5, Figs. 13–14)

1994 *Cibicides refulgens* Montfort; Loeblich and Tappan, Timor Sea, p. 149, Pl. 318, 7–9.

1994 *Cibicides refulgens* de Montfort 1808; Jones, Brady's specimens, p. 97, Pl. 92, Figs. 7–9.

2009 *Cibicides* cf. *C. refulgens* Montfort 1808; Parker, Ningaloo Reef, p. 532, Figs. 378a–k, 379a–e.

2013 *Cibicides refulgens* Montfort, 1808; Debenay, New Caledonia, p. 191, 315.

Cibicidoides mundula (Brady, Parker & Jones, 1888) (not figured)

1986 *Cibicidoides mundulus* (Brady. Parker and Jones); Van Morkhoven, Abrolhos Bank Brazil, p. 65, Chart No. 21.

***Cibicidoides* sp.** (not figured)

1986 *Cibicidoides alazanensis* (Nuttall); Van Morkhoven et al., Texas, p. 201, Chart No. 68.

Lobatula lobatula (Walker & Jacob, 1798) (not figured)

1994 *Lobatula lobatula* (Walker and Jacob); Loeblich and Tappan, Timor Sea, p. 150, Pl. 316, Figs. 8–11, Pl. 319, Figs. 1–7.

2013 *Lobatula lobatula* Walker & Jacob in Kanmacher, 1798; Debenay, New Caledonia, p. 201, 315.

Family PLANORBULINIDAE Schwager, 1877

Subfamily CARIBEANELLINAE Saidova, 1981

Caribeanella elatensis Perelis & Reiss, 1975 (Pl. 5, Figs. 15–16)

1993 *Caribeanella elatensis* Perelis and Reiss; Hottinger et al., Gulf of Aquaba, p. 118, Pl. 156, Figs. 1–8.

2013 *Caribeanella elatensis* Perelis & Reiss, 1975; Debenay, New Caledonia, p. 190, 316.

Subfamily PLANORBULININAE Schwager, 1877

Planorbulinella larvata (Parker & Jones, 1865) (Pl. 5, Figs. 17–18)

1993 *Planorbulinella larvata* (Parker and Jones); Hottinger et al., Gulf of Aquaba, p. 118, Pl. 158, Figs. 1–12.

1994 *Planorbulinella larvata* (Parker and Jones); Loeblich and Tappan, p. 152, Pl. 327, Figs. 1–7.

1994 *Planorbulinella larvata* (Parker and Jones 1865); Jones, Brady's specimens, p. 97, Pl. 92, Figs. 5–6.

2009 *Planorbulinella larvata* (Parker & Jones 1865); Parker, Ningaloo Reef, p. 709, Fig. 498a–j.

2013 *Planorbulinella larvata* (Parker & Jones, 1865); Debenay, New Caledonia, p. 246, 316.

Family CYMBALOPORIDAE Cushman, 1927

Subfamily CYMBALOPORINAE Cushman 1927

Millettiana millettii (Heron-Allen & Earland, 1915) (Pl. 5, Figs. 19–21)

1994 *Millettiana millettii* (Heron-Allen and Earland); Loeblich and Tappan, Timor Sea, p. 153, Pl. 329, Figs. 1–12.

Superfamily ASTERIGERINACEA d'Orbigny, 1839

Family EPISTOMARIIDAE Hofker, 1954

Subfamily EPISTOMARIINAE Hofker, 1954

Asanonella tubulifera (Heron-Allen & Earland, 1915) (Pl. 5, Figs. 22–23)

1994 *Asanonella tubulifera* (Heron-Allen and Earland); Loeblich and Tappan, p. 155, Pl. 337, Figs. 1–10.

2009 *Asanonella tubulifera* (Heron-Allen & Earland 1915); Parker, Ningaloo Reef, p. 514, Figs. 365a–k, 366a–f.

2013 *Asanonella tubulifera* (Heron-Allen & Earland, 1915); Debenay, New Caledonia, p. 187, 318.

***Monspeliensina* sp.** (not figured)

1994 *Monspeliensina* sp. 1; Parker, Ningaloo Reef, p. 649, Figs. 459a–e, 460a–i.

2013 *Monspeliensina vulpesi* Glaçon & Lys, 1968; Debenay, New Caledonia, p. 202, 318.

Family AMPHISTEGINIDAE Cushman, 1927

Amphistegina papillosa Said, 1949 (Pl. 5, Fig. 24)

1993 *Amphistegina papillosa* Said; Hottinger et al., Gulf of Aquaba, p. 134, Pl. 189, Figs. 1–10, Pl. 190, Figs. 1–7.

1994 *Amphistegina papillosa* Said; Loeblich and Tappan, Timor Sea, p. 157, Pl. 339, Figs. 4–7, Pl. 341, Figs. 1–7.

2013 *Amphistegina papillosa* Said, 1949; Debenay, New Caledonia, p 216, 319.

Superfamily NONIONACEA Schultze, 1854

Family NONIONIDAE Schultze, 1854

Subfamily NONIONINAE Schultze, 1854

Nonion subturgidum (Cushman, 1924) (Pl. 5, Figs. 25–26)

1994 *Nonion subturgidum* (Cushman); Loeblich and Tappan, Timor Sea, p. 158, Pl. 343, Figs. 1–9.

2009 *Nonion* cf. *N. subturgidum* Cushman 1924; Parker, Ningaloo Reef, p. 671, Fig. 474a–j.

2013 *Nonion subturgidum* (Cushman, 1924); Debenay, New Caledonia, p. 227, 319.

Nonionella pulchella Hada, 1931 (Pl. 5, Figs. 27–28)

1994 *Nonionella pulchella* Hada; Loeblich and Tappan, Timor Sea, p. 158, Pl. 345, Figs. 1–4.

Nonionoides grateloupii (d'Orbigny, 1826) (Pl. 5, Fig. 29)

1993 *Nonionoides grateloupi* (d'Orbigny); Hottinger et al., Gulf of Aquaba, p. 138, Pl. 195, Figs. 4–83.

1994 *Nonionoides grateloupi* (d'Orbigny); Loeblich and Tappan, Timor Sea, p. 158, Pl. 342, Figs. 1–5.

2009 *Nonionoides grateloupi* (d'Orbigny 1839); Parker, Ningaloo Reef, p. 675, Fig. 475a–h.

Pseudononion granuloumbilicatum Zheng, 1979

Subfamily ASTRONONIONINAE Saidova, 1981

***Astrononion* sp. 1** sensu Parker 2009 (Pl. 5, Fig. 30)

1997 *Astrononion* sp.; Haig, Exmouth Gulf, p. 276, Fig. 6:5–6.

2009 *Astronionion* sp. 1; Parker, Ningaloo Reef, p. 529, Fig. 369a–e.

Subfamily PULLENIINAE Schwager. 1877

Melonis barleeanus (Williamson, 1858) (Pl. 5, Fig. 31)

1994 *Melonis barleeanus* (Williamson); Loeblich and Tappan, Timor Sea, p. 159, Pl. 347, Figs. 1–5.

2009 *Melonis* sp. 1; Parker, Ningaloo Reef, p. 638, Fig. 451a–e.

Pullenia borealis Saidova, 1975 (Pl. 5, Fig. 32)

1994 *Pullenia borealis* Saidova; Loeblich and Tappan, Timor Sea, p. 160, Pl. 348, Figs. 1–6.

Superfamily CHILOSTOMELLACEA Brady, 188I

Family CHILOSTOMELLIDAE Brady, 1881

Subfamily CHILOSTOMELLINAE Brady, 1881

Chilostomella ovoidea Reuss, 1850 (Pl. 5, Fig. 33)

1994 *Chilostomella ovoidea* Reuss; Loeblich and Tappan, Timor Sea, p. 160, Pl. 350, Figs. 1–3.

1994 *Chilostomella ovoidea* Reuss 1850; Jones, Brady's specimens, p. 61, Pl. 55, Figs. 15–16, 19–23.

Family HETEROLEPIDAE Gonzáles-Donoso, 1969

Anomalinoides colligera (Chapman & Parr, 1937) (Pl. 6, Figs. 1–2)

1994 *Anomalinoides coIligerus* (Chapman and Parr); Loeblich and Tappan, Timor Sea, p. 162, Pl. 355, Figs. 1–3.

1994 *Anomalinoides colligerus* (Chapman and Parr 1937); Jones, Brady's specimens, p. 98, Pl. 94, Figs. 2–3.

2013 *Anomalinoides colligerus* (Chapman & Parr, 1937); Debenay, New Caledonia, p. 186, 321.

Anomalinoides globulosa (Chapman & Parr, 1937) (Pl. 5, Fig. 34)

1994 *Anomalinoides globulosus* (Chapman and Parr); Loeblich and Tappan, Timor Sea, p. 162, Pl. 354, Figs. 11–13, Pl. 355, Figs. 4–13.

2013 *Anomalinoides globulosus* (Chapman & Parr, 1937); Debenay, New Caledonia, p. 186, 321.

Family GAVELINELLIDAE Hofker, 1956

Subfamily GAVELINELLINAE Hofker, 1956

Anomalinulla glabrata (Cushman, 1924) (Pl. 6, Figs. 3–4)

1993 *Anomalinulla glabrata* (Cushman); Hottinger et al., Gulf of Aquaba, p. 139, Pl. 197, Figs. 5–11.

1994 *Gyroidina lamarckiana* (d'Orbigny); Loeblich and Tappan, Timor Sea, p. 163, Pl. 361, Figs. 10–12, not Figs. 7–9.

1997 *Anomalinulla glabrata* (Cushman); Haig, Exmouth Gulf, p. 276, Fig. 6:2–3.

2009 *Anomalinulla glabrata* (Cushman 1924) ; Parker, Ningaloo Reef, p. 508, Fig. 361a–l.

2013 *Anomalinulla glabrata* (Cushman, 1924); Debenay, New Caledonia, p. 187, 321.

Hanzawaia nipponica Asano, 1944 (Pl. 6, Figs. 6–7)

1994 *Hanzawaia nipponica* Asano; Loeblich and Tappan, Timor Sea, p. 164, Pl. 363, Figs. 8–13.

2009 *Hanzawaia* cf. *H. nipponica* Asano 1944; Parker, Ningaloo Reef, p. 623, Fig. 442a–h.

Superfamily ROTALIACEA Ehrenberg, 1839

Family ROTALIIDAE Ehrenberg. 1839

Subfamily AMMONIINAE Saidova, 1981

Ammonia* cf. *A. faceta He, Hu & Wang, 1965 (Pl. 6, Fig. 8)

1994 *Pseudohelenina collinsi* (Parr); Loeblich and Tappan, Timor Sea, p. 136, Pl. 272, Figs. 1–4.

2009 *Ammonia faceta* He, Hu & Wang 1965; Parker, Ningaloo Reef, p. 481, Fig. 446a–m.

2013 *Ammonia* sp. 1; Debenay, New Caledonia, p. 186, 324.

Ammonia pustulosa (Albani & Barbero, 1982) (Pl. 6, Fig. 9)

1994 *Ammonia supera* Belford; Loeblich and Tappan, Timor Sea, p. 165, Pl. 370, Figs. 7–9.

2009 *Ammonia pustulosa* (Albani & Barbero 1982); Parker, Ningaloo Reef, p. 484, Fig. 347a–i.

Rotalinoides gaimardi (d'Orbigny in Fornasini, 1906) (Pl. 6, Figs.10–11)

1993 *Asterorotalia gaimardi* (d'Orbigny); Hottinger et al., Gulf of Aquaba, p. 143, Pl. 202, Figs. 8–9, Pl. 203, Figs. 1–13.

1994 *Asterorotalia gaimardi* (d'Orbigny); Loeblich and Tappan, Timor Sea, p. 166, Pl. 372, Figs. 1–7.

1994 *Rotalinoides gaimardii* (Fornasini 1906); Jones, Brady's specimens, p. 106, Pl. 106, Fig. 9.

Family ELPHIDIIDAE Galloway, 1933

Subfamily ELPHIDIINAE Galloway, 1933

Elphidium lene Cushman & McCulloch, 1940 (Pl.6, Fig. 12)

2009 *Elphidium lene* Cushman & McCulloch 1940; Parker, Ningaloo Reef, p. 579, Fig. 408a–h, Fig. 409a–i.

2013 *Elphidium lene* (Cushman & McCulloch, 1940); Debenay, New Caledonia, p. 220, 324.

Elphidium limbatum (Chapman, 1907) (not figured)

1993 *Elphidium* cf. *E. limbatum* (Chapman); Hottinger et al., p. 149, Pl. 212, Figs. 1–9.

2013 *Elphidium limbatum* (Chapman, 1907); Debenay, New Caledonia, p. 220, 324.

Elphidium macellum (Fichtel & Moll, 1798) (Pl. 6, Fig. 13)

1994 *Elphidium macellum* (Fichtel and Moll 1798); Jones, Brady's specimens, p. 109, Pl. 110, Figs. 8, 11.

2009 *Elphidium* cf. *E. macellum* (Fichtel & Moll 1789), Parker, Ningaloo Reef, p. 582, Fig. 410a–e.

2013 *Elphidium macellum* (Fichtel & Moll, 1798); Debenay, New Caledonia, p. 220, 324.

Superfamily NUMMULITACEA de Blainvillc, 1827
Family NUMMULITIDAE de Blainville, 1827

Heterostegina depressa d'Orbigny, 1826 (Pl. 6, Figs. 14–15)

1993 *Heterostegina depressa* d'Orbigny; Hottinger et al., Gulf of Aquaba, p. 157, Pl. 228, Figs. 1–11, Pl. 229, Figs. 1–8, Pl. 230, Fig. 9.

1994 *Heterostegina depressa* d'Orbigny; Loeblich and Tappan, Timor Sea, p. 171, Pl. 389, Figs. 1–6, Pl. 390, Figs. 1–3.

1994 *Heterostegina depressa* d'Orbigny 1826; Jones, Brady's specimens, p. 111, Pl. 112, Figs. 14–16, 17–18.

2009 *Heterostegina depressa* d'Orbigny 1826; Parker, Ningaloo Reef, p. 625, Fig. 443a–j.

2013 *Heterostegina depressa* d'Orbigny 1826; Debenay, New Caledonia, p. 222, 325.

Operculina ammonoides (Gronovius, 1781) (Pl. 6, Figs. 16–17)

1993 *Assilina ammonoides* (Gronovius); Hottinger et al., Gulf of Aquaba, p. 154, Pl. 222, Figs. 1–8, Pl. 223, Figs. 1–14, Pl. 224, Figs. 1–8, Pl. 225, Figs. 1–9.

1994 *Assilina ammonoides* (Gronovius); Loeblich and Tappan, Timor Sea, p. 170, Pl. 387, Figs. 7–9, Pl. 388, Figs. 1–4.

2009 *Assilina ammonoides* (Schröter 1783); Parker, Ningaloo Reef, p. 515, Fig. 367a–j.

References

Betjeman, K.J., 1969. Recent foraminifera from the western continental shelf of Western Australia. Contributions from the Cushman Laboratory for Foraminiferal Research 20, 119–138.

Corliss, B.H., 1979. Taxonomy of Recent Deep-Sea Benthonic Foraminifera from the Southeast Indian Ocean. Micropaleontology 25, 1–19. 10.2307/1485207

Debenay, J.-P., 2013. A guide to 1,000 foraminifera from Southwestern Pacific New Caledonia. IRD Éditions, Publications Scientifiques du Muséum, Marseille, Paris, pp. 378.

Haig, D.W., 1997. Foraminifera from Exmouth Gulf, Western Australia. Journal of the Royal Society of Western Australia 80, 263–280.

Hayward, B.W., Grenfell, H.R., Sabaa, A.T., Neil, H.L., Buzas, M.A., 2010. Recent New Zealand deep-water benthic foraminifera: Taxonomy, ecologic distribution, biogeography, and use in paleoenvironmental assessment. Institute of Geological & Nuclear Sciences, Lower Hutt, New Zealand, pp. 363.

Hottinger, L., Halicz, E., Reiss, Z., 1993. Recent foraminiferida from the Gulf of Aquaba, Red Sea, Ljubljana, pp. 179.

Jones, R.W., 1994. The Challenger Foraminifera. Oxford University Press, Oxford, pp. 149.

Loeblich, A.R., Tappan, H., 1994. Foraminifera of the Sahul Shelf and Timor Sea. Cushman Foundation for Foraminiferal Research Special Pubublication 31, Cambridge, MA, pp. 661.

Parker, J.H., 2009. Taxonomy of foraminifera from Ningaloo Reef, Western Australia. Memoir of the Association of Australasian Palaeontologists 36, Canberra, pp. 810.

Van Marle, L.J., 1988. Bathymetric distribution of benthic foraminifera on the Australian-Irian Jaya continental margin, eastern Indonesia. Marine Micropaleontology 13, 97–152. 10.1016/0377-8398(88)90001-1

van Morkhoven, F.P.C.M., Berggren, W.A., Edwards, A.S., 1986. Cenozoic Cosmopolitan Deep-Water Benthic Foraminifera. Bulletin des Centres de Recherches Exploration-Production Elf-Aquitaine Mem. 11, Pau, pp. 421.

Appendix D

Appendix D1. Foraminiferal Data.

Table D1.1. Foraminiferal counts, P/B index, and diversity data. Unfilled cells = 0.

Sample name	U1460A mudline	U1460B mudline	U1460A 1F CC	U1460A 3F CC	U1460A 5F 3W	U1460A 7F 3W	U1460A 9F 1W	U1460A 11F CC	U1460A 13F CC	U1460A 15F CC	U1460A 17F CC
Depth CSF-A (m)	0	0	2.0	11.3	20.6	30.1	35.6	49.0	58.4	67.6	77.0
Total no. of species	74	93	39	55	53	39	62	46	43	47	49
Total no. of individuals	1153	1040	440	333	342	312	373	334	323	350	353
Fisher α Index	17.64	24.71	10.33	18.77	17.55	11.77	21.22	14.45	13.32	14.61	15.45
Shannon-Wiener Index	3.361	3.695	3.044	3.267	3.22	2.727	3.3	3.125	3.087	2.869	2.967
P/B index: Benthic	84	103	188	97	113	203	144	128	155	93	45
P/B index: Planktonic spinose	184	195	120	199	193	129	185	197	180	217	278
P/B index: Planktonic keeled	47	26	9	19	10	3	6	1	5	2	2
Spiroplectinella wrightii											
Gaudryina convexa			1								
Paratrochammina globorotaliformis											
Bigenerina aspratilis	58	45	27	3	1		1		1		
Sahulia barkeri		1									
Spirorutilus carinatus	39	41	17	17	14	13	16	8	5	3	13
Textularia agglutinans	20	30	6	2		2	2		8	4	6
Textularia catenata	4	12		1	1				5		1
Textularia cushmani	39	3	3	1	2	1	1				1
Textularia lateralis	1	9									
Textularia orbica	5	1									
Textularia stricta											
Textularia tubulosa	5	17		3							
Textularia sp. 3 sensu Parker 2009		1									
Septotextularia rugosa											
Migros flintii	11	1							8	4	3
Pseudoclavulina robusta	1	4	1	1						3	
Plotnikovina timorea	12	36									
Clavulina subangularis											
Cylindroclavulina bradyi	2	4		2							
Patellina cf. *P. formosa*		1						5		2	
Cornuspira sp.		2									
Planispirinella involuta		1									
Wiesnerella ujiiei		1									
Spiroloculina subimpressa	8	27									
Agglutinella arenata	2	3		1	1					1	
Proemassilina arenaria	1										
Quinqueloculina barnadi	1	11	26	17		10	1				

Table D1.1. (Continued)

Sample name	U1460A mudline	U1460B mudline	U1460A 1F CC	U1460A 3F CC	U1460A 5F 3W	U1460A 7F 3W	U1460A 9F 1W	U1460A 11F CC	U1460A 13F CC	U1460A 15F CC	U1460A 17F CC
Depth CSF-A (m)	0	0	2.0	11.3	20.6	30.1	35.6	49.0	58.4	67.6	77.0
Quinqueloculina cf. *Q. crassicarinata*							28				
Quinqueloculina patagonica	12	24	1	1			2				
Quinqueloculina philippinensis	2			1							
Quinqueloculina subpolygona		4					1				
Quinqueloculina sp. 1	12	4									
Quinqueloculina sp. 5 sensu Parker 2009	55	26	47	4	5	11	19				
Miliolinella circularis		6								4	
Miliolinella oceanica	2	1									
Miliolinella webbiana			2				1				
Miliolinella pilasensis		1									
Miliolinella sp. 1 sensu Parker 2009		2	8	1			1				
Pyrgo denticulata		1	2			1	1				
Pyrgo striolata	3	4									
Triloculina tricarinata	48	15					3				
Sigmoilopsis minuta	2	3		3	2		1	3	4	1	2
Dentalina catenulata		1									
Dentalina cf. *D. mutsui*	2						1			1	
Grigelis orectus											
Laevidentalina bradyensis		3									
Laevidentalina inflexa		1									4
Laevidentalina sidebottomi										1	2
Pseudonodosaria brevis											
Pyramidulina comatula											
Pyramidulina catesbyi		1									
Pyramidulina glanduliniformis											
Lenticulina calcar		4									
Lenticulina domantayi	17	7	2	12		2	10			3	
Marginulinopsis philippinensis		3									
Marginulinopsis tenuis											
Saracenaria angularis		1		1							
Amphicoryna cf. *A. meringella*										1	
Amphicoryna scalaris											1
Amphicoryna separans	7	11	3	9	1		1	3	3	1	1
Astacolus crepidulus											
Marginulina musai											
Vaginulinopsis bradyi							1				

Table D1.1. (Continued)

Sample name	U1460A mudline	U1460B mudline	U1460A 1F CC	U1460A 3F CC	U1460A 5F 3W	U1460A 7F 3W	U1460A 9F 1W	U1460A 11F CC	U1460A 13F CC	U1460A 15F CC	U1460A 17F CC
Depth CSF-A (m)	0	0	2.0	11.3	20.6	30.1	35.6	49.0	58.4	67.6	77.0
Vaginulinopsis gnamptina				1				1			
Vaginulinopsis pseudoplanulata					1						
Vaginulinopsis sublegumen					1						
Planularia gemmata					1						
Planularia spinipes											
Cerebrina cf. *C. claricerviculata*			1		6		1	9	1	5	
Cerebrina lacunata	1	1			2				2	1	6
Cerebrina perforata									2		7
Lagena annellatrachia				1	7	2	2	2	10		4
Lagena annulatacollare		6			1					1	
Lagena meridionalis										1	
Lagena substriata										2	
Procerolagena oceanica											
Reussoolina trachiella		2						4			8
Globulina rotundata		1									
Guttulina bartschi	4	1	1			1	1		2		2
Guttulina regina	2						1				
Pseudopolymorphina sp.											
Sigmoidella elegantissima			5				3	1		1	1
Buchnerina radiatomarginata											
Exsculptina glaphyraheda									2	1	
Favulina favosopunctata		2			1			1			1
Oolina baukalionilla											
Oolina caudigera											1
Oolina globosa					1		1	2	1		
Vasicostella inflatiperforata											8
Fissurina circularis	1	1						6			2
Fissurina subrevertens											
Lagenosolenia levata											
Pseudofissurina marginoradiata											
Glandulina symmetrica	7	2									
Entomorphinoides intricata											
Seabrookia pellucida											
Saintclairoides toreuta	10	12	4	4	3	1					
Hoeglundina elegans	2	1	2			2					
Geminospira bradyi		1									
Bolivina britannica											

Table D1.1. (Continued)

Sample name	U1460A mudline	U1460B mudline	U1460A 1F CC	U1460A 3F CC	U1460A 5F 3W	U1460A 7F 3W	U1460A 9F 1W	U1460A 11F CC	U1460A 13F CC	U1460A 15F CC	U1460A 17F CC
Depth CSF-A (m)	0	0	2.0	11.3	20.6	30.1	35.6	49.0	58.4	67.6	77.0
Bolivina robusta	48	47	5	46	3	10	17	1	5	76	84
Bolivina striatula	37	34	13	6	9	7	1	5	20	7	5
Bolivinellina translucens				1	5		4	1	1	3	3
Rugobolivinella elegans	2							1			
Globocassidulina subglobosa	31	10	16	4	4	4	25	12	7		4
Globocassidulina bisecta								6			
Heterocassidulina albida											
Paracassidulina neocarinata		7	2	9	4	8	7			3	1
Loxostomina mayori	1	1		6	5	12	2	3	2		
Rectobolivina bifrons	1			1					1		3
Sagrinella jugosa						1					
Siphogenerina indica	15	24	14	12	5	2	3	2	13	7	16
Bulimina marginata	4	9			1	1					
Siphouvigerina hispida	1	6		1	2		2	17	5	5	8
Siphouvigerina porrecta	3	3		2	12		1				1
Uvigerina peregrina	82	11	15	12	8	13	3	14	12	6	27
Uvigerina reineri				3		2	8				2
Uvigerina schwageri	1										
Trifarina bradyi		1		4	13	2	1	3	6	5	2
Chrysalidinella pacifica	1										
Reussella hayasakai	2	1									1
Fursenkoina pauciloculata											
Sigmavirgulina tortuosa	5	2		2	11	2	3	8		5	1
Cancris auriculus	1	4					1	5	2	1	1
Cancris oblongus				1	2			1			
Cancris bubnanensis	3	1									
Stomatorbina concentrica	3	8	9		2						
Rotorbinella sp.	3	22	2	1	7	8	24	15	2	13	11
Neoeponides margaritifer	12										
Neoeponides procerus				1			1				
Neoconorbina albida					1		1				
Neoconorbina cavalliensis					4		3		6		
Rosalina sp. 1	1	1						7			1
Sphaeroidina bulloides	7	11			1		3		2	3	
Pileolina minogasaformis		2					1		2	4	
Pileolina patelliformis	13	23	6		1		1	1			
Elongobula parallela	7	4	4	1	2	1	4	1			

Table D1.1. (Continued)

Sample name	U1460A mudline	U1460B mudline	U1460A 1F CC	U1460A 3F CC	U1460A 5F 3W	U1460A 7F 3W	U1460A 9F 1W	U1460A 11F CC	U1460A 13F CC	U1460A 15F CC	U1460A 17F CC
Depth CSF-A (m)	0	0	2.0	11.3	20.6	30.1	35.6	49.0	58.4	67.6	77.0
Siphonina tubulosa	4	9		2	2	1	1	1	1	1	1
Facetocochlea pulchra							3			1	
Epistominella exigua							3	2	13	7	
Planulinoides biconcava	2	3				2	1	4			
Discorbinella montereyensis	1	9		1	7		1	2		4	22
Hyalinea florenceae	31	25	5	5	16	17	11	37	25	44	16
Planulina retia				7	23	6	1	3	5	13	1
Cibicides mabahethi	22	6									
Cibicides cf. *C. refulgens*	193	143	53	39	45	89	63	34	54	52	37
Cibicidoides alazanensis						1					
Cibicidoides mundula		16	32	17	4	14	18	7	26	10	9
Cibicidoides subhaidingerii				1							1
Cibicidoides wuellerstorfi											
Cibicidoides sp.											
Lobatula lobatula	2	4	3	2	2		2				
Caribeanella elatensis	19	35	10	12	6	2	4	2	3		1
Planorbulinella larvata	9	6		1				1		2	
Asanonella tubulifera	46	26	27	8	1	2	8	3	2		
Amphistegina papillosa	1								1		
Nonion subturgidum					3			7	2	3	
Nonionella auris											
Nonionoides grateloupii											
Pseudononion granuloumbilicatum											
Astrononion sp. 1		1									1
Pullenia borealis		1									
Pullenia bulloides											
Chilostomella ovoidea											
Anomalinoides colligera		3									
Anomalinoides globulosa											1
Heterolepa bradyi											
Heterolepa ornata					2	1					
Heterolepa praecincta											
Anomalinulla glabrata	84	74	34	17	22	20	8	21	19	11	8
Discanomalina coronata											
Gyroidina orbicularis											
Hanzawaia nipponica	23	22	8	18	52	34	23	49	23	19	10
Ammonia sp.	25	9	20	1		2	7	2	4	2	

Table D1.1. (Continued)

Sample name	U1460A mudline	U1460B mudline	U1460A 1F CC	U1460A 3F CC	U1460A 5F 3W	U1460A 7F 3W	U1460A 9F 1W	U1460A 11F CC	U1460A 13F CC	U1460A 15F CC	U1460A 17F CC
Depth CSF-A (m)	0	0	2.0	11.3	20.6	30.1	35.6	49.0	58.4	67.6	77.0
Rotalinoides gaimardi				1							
Elphidium depressulum			3								
Elphidium lene	1										
Elphidium macellum	8	12		2	4	2	3	11	5	2	

Table D1.1. (Continued)

Sample name	U1460A 19F CC	U1460A 21F CC	U1460A 23F CC	U1460A 25F 4W	U1460A 27F CC	U1460A 29F CC	U1460A 31F CC	U1460A 33F CC	U1460A 35F CC	U1460A 37F CC	U1460A 39F CC
Depth CSF-A (m)	86.5	96.3	104.9	114.9	124.6	133.8	143.0	152.1	162.2	171.5	180.8
Total no. of species	49	39	45	52	44	44	33	42	34	46	41
Total no. of individuals	337	362	366	361	359	357	336	326	358	353	349
Fisher α Index	15.77	11.09	13.48	16.66	13.17	13.2	9.069	12.83	9.23	14.12	12.06
Shannon-Wiener Index	3.243	2.739	3.005	3.149	2.959	2.97	2.719	2.767	2.305	2.685	2.831
P/B index: Benthic	58	140	50	45	121	56	45	53	43	63	37
P/B index: Planktonic spinose	285	181	273	275	200	261	279	264	267	261	274
P/B index: Planktonic keeled	1	7	5	0	11	3	3	2	9	0	5
Spiroplectinella wrightii			2								
Gaudryina convexa											
Paratrochammina globorotaliformis											
Bigenerina aspratilis											
Sahulia barkeri											
Spirorutilus carinatus	9	9	7	8	3						2
Textularia agglutinans	4	1			1						
Textularia catenata											
Textularia cushmani											
Textularia lateralis											
Textularia orbica											
Textularia stricta											1
Textularia tubulosa											
Textularia sp. 3 sensu Parker 2009											
Septotextularia rugosa											
Migros flintii	1										
Pseudoclavulina robusta											
Plotnikovina timorea											
Clavulina subangularis											
Cylindroclavulina bradyi	1										
Patellina cf. *P. formosa*	3		2	2							
Cornuspira sp.											
Planispirinella involuta											
Wiesnerella ujiiei											
Spiroloculina subimpressa											
Agglutinella arenata											
Proemassilina arenaria											
Quinqueloculina barnadi											

Table D1.1. (Continued)

Sample name	U1460A 19F CC	U1460A 21F CC	U1460A 23F CC	U1460A 25F 4W	U1460A 27F CC	U1460A 29F CC	U1460A 31F CC	U1460A 33F CC	U1460A 35F CC	U1460A 37F CC	U1460A 39F CC
Depth CSF-A (m)	86.5	96.3	104.9	114.9	124.6	133.8	143.0	152.1	162.2	171.5	180.8
Quinqueloculina cf. *Q. crassicarinata*											
Quinqueloculina patagonica											
Quinqueloculina philippinensis											
Quinqueloculina subpolygona											
Quinqueloculina sp. 1											
Quinqueloculina sp. 5 sensu Parker 2009											
Miliolinella circularis											
Miliolinella oceanica											
Miliolinella webbiana											
Miliolinella pilasensis											
Miliolinella sp. 1 sensu Parker 2009											
Pyrgo denticulata											
Pyrgo striolata											
Triloculina tricarinata											
Sigmoilopsis minuta	1										
Dentalina catenulata											
Dentalina cf. *D. mutsui*	4			1		1					1
Grigelis orectus								1			
Laevidentalina bradyensis							1	3		1	
Laevidentalina inflexa				1							
Laevidentalina sidebottomi											2
Pseudonodosaria brevis											
Pyramidulina comatula											
Pyramidulina catesbyi		1		1		4		3	2	5	
Pyramidulina glanduliniformis											
Lenticulina calcar											
Lenticulina domantayi	4	1	1	3		1		1	1	2	2
Marginulinopsis philippinensis											
Marginulinopsis tenuis											
Saracenaria angularis		1			1			1			2
Amphicoryna cf. *A. meringella*				1							
Amphicoryna scalaris						3					
Amphicoryna separans			1	2	1	7	1	5	1	2	
Astacolus crepidulus											
Marginulina musai											
Vaginulinopsis bradyi	1										

Table D1.1. (Continued)

Sample name	U1460A 19F CC	U1460A 21F CC	U1460A 23F CC	U1460A 25F 4W	U1460A 27F CC	U1460A 29F CC	U1460A 31F CC	U1460A 33F CC	U1460A 35F CC	U1460A 37F CC	U1460A 39F CC
Depth CSF-A (m)	86.5	96.3	104.9	114.9	124.6	133.8	143.0	152.1	162.2	171.5	180.8
Vaginulinopsis gnamptina											
Vaginulinopsis pseudoplanulata											
Vaginulinopsis sublegumen				1							
Planularia gemmata					1						
Planularia spinipes									1		
Cerebrina cf. *C. claricerviculata*		5	10	12	5	3	6	8	4		
Cerebrina lacunata	4		1						1		2
Cerebrina perforata	2	1		1		2					
Lagena annellatrachia							10	16	22	5	9
Lagena annulatacollare			1							1	
Lagena meridionalis											
Lagena substriata			12	6	4	4				6	
Procerolagena oceanica									1		
Reussoolina trachiella	8		12	12	7	11	13	6	7	2	3
Globulina rotundata											
Guttulina bartschi		5		1	2	2	3	1		3	5
Guttulina regina											
Pseudopolymorphina sp.		2			1						
Sigmoidella elegantissima			1			2				1	
Buchnerina radiatomarginata											
Exsculptina glaphyraheda			1								1
Favulina favosopunctata	2		1			1					
Oolina baukalionilla											
Oolina caudigera											
Oolina globosa		2					4	2	3	1	4
Vasicostella inflatiperforata			1	1							
Fissurina circularis	8	3	2	4	5	1		3	3		3
Fissurina subrevertens					1					3	2
Lagenosolenia levata											
Pseudofissurina marginoradiata											
Glandulina symmetrica			1								
Entomorphinoides intricata					1						
Seabrookia pellucida											
Saintclairoides toreuta											
Hoeglundina elegans											
Geminospira bradyi											
Bolivina britannica						27	7	8		2	

Table D1.1. (Continued)

Sample name	U1460A 19F CC	U1460A 21F CC	U1460A 23F CC	U1460A 25F 4W	U1460A 27F CC	U1460A 29F CC	U1460A 31F CC	U1460A 33F CC	U1460A 35F CC	U1460A 37F CC	U1460A 39F CC
Depth CSF-A (m)	86.5	96.3	104.9	114.9	124.6	133.8	143.0	152.1	162.2	171.5	180.8
Bolivina robusta	32	5	11	11	7	25	4	2	2	2	22
Bolivina striatula	1	11	4	3		1	2			6	4
Bolivinellina translucens	3		3	4	5	1	6	8	5	5	2
Rugobolivinella elegans		1		1	1	1					
Globocassidulina subglobosa	18	13	11	17	11	3	17	6	15	8	5
Globocassidulina bisecta											
Heterocassidulina albida											
Paracassidulina neocarinata	19	26	13	13	15	5	3	2	2		8
Loxostomina mayori						1				1	
Rectobolivina bifrons	1	1	2	2	1						
Sagrinella jugosa											
Siphogenerina indica	6	8	4	1							
Bulimina marginata											
Siphouvigerina hispida	10	4		2	3	11		1	3	1	8
Siphouvigerina porrecta	2		3	6		23	2			1	5
Uvigerina peregrina	13	2	17	8	8	4				1	7
Uvigerina reineri	12	2	4	3	2	1		1			
Uvigerina schwageri											
Trifarina bradyi	1			4		4	63	82	133	96	84
Chrysalidinella pacifica											
Reussella hayasakai	1	1	3							1	1
Fursenkoina pauciloculata								1			
Sigmavirgulina tortuosa	5	7	6	13	10	9	17	11	16	20	9
Cancris auriculus	1	1	2	4	5		4	2	1	3	5
Cancris oblongus						2					
Cancris bubnanensis	1									1	
Stomatorbina concentrica											
Rotorbinella sp.	13	13	10	8	11	8	3	2	3	3	2
Neoeponides margaritifer											
Neoeponides procerus										1	
Neoconorbina albida			2	1	3					1	
Neoconorbina cavalliensis					9	2					
Rosalina sp. 1		1	1	1					1		1
Sphaeroidina bulloides					3					2	2
Pileolina minogasaformis	2	1			7	1	2	4	2	1	
Pileolina patelliformis	1	13		1	2						
Elongobula parallela				1							1

Table D1.1. (Continued)

Sample name	U1460A 19F CC	U1460A 21F CC	U1460A 23F CC	U1460A 25F 4W	U1460A 27F CC	U1460A 29F CC	U1460A 31F CC	U1460A 33F CC	U1460A 35F CC	U1460A 37F CC	U1460A 39F CC
Depth CSF-A (m)	86.5	96.3	104.9	114.9	124.6	133.8	143.0	152.1	162.2	171.5	180.8
Siphonina tubulosa										1	
Facetocochlea pulchra	1										
Epistominella exigua	2				2		1	2		4	
Planulinoides biconcava	3	1	2	3	1	3	5	4		1	1
Discorbinella montereyensis	8		16	1	2	29	6	12	4	1	18
Hyalinea florenceae	20	49	57	45	67	46	39	33	34	43	12
Planulina retia	9	10						4	2		
Cibicides mabahethi											
Cibicides cf. *C. refulgens*	43	75	46	33	48	48	46	40	41	48	38
Cibicidoides alazanensis						1				2	1
Cibicidoides mundula	4	14	19	28	19	6	12	1	5	21	10
Cibicidoides subhaidingerii										2	
Cibicidoides wuellerstorfi				7	3			1			10
Cibicidoides sp.											
Lobatula lobatula							1	1			
Caribeanella elatensis			1		2			1			
Planorbulinella larvata	1					1					
Asanonella tubulifera	1			1							
Amphistegina papillosa											
Nonion subturgidum	6	3	4	2	7		1	2	3		
Nonionella auris											
Nonionoides grateloupii											
Pseudononion granuloumbilicatum						1					
Astrononion sp. 1			2	1		4	6	3		2	3
Pullenia borealis				1		1	1	1	1		
Pullenia bulloides											
Chilostomella ovoidea	1										
Anomalinoides colligera											
Anomalinoides globulosa		2	1	1						2	
Heterolepa bradyi					1						
Heterolepa ornata											
Heterolepa praecincta									1	7	
Anomalinulla glabrata	11	7	22	25	13	7	13	15	9	6	35
Discanomalina coronata											
Gyroidina orbicularis											
Hanzawaia nipponica	27	53	41	47	38	36	31	21	25	22	12
Ammonia sp.	2	1	2	3	1		1		2		

Table D1.1. (Continued)

Sample name	U1460A 19F CC	U1460A 21F CC	U1460A 23F CC	U1460A 25F 4W	U1460A 27F CC	U1460A 29F CC	U1460A 31F CC	U1460A 33F CC	U1460A 35F CC	U1460A 37F CC	U1460A 39F CC
Depth CSF-A (m)	86.5	96.3	104.9	114.9	124.6	133.8	143.0	152.1	162.2	171.5	180.8
Rotalinoides gaimardi											
Elphidium depressulum											
Elphidium lene				1				1			
Elphidium macellum	4	6	1	1	19	3	5	4	2	3	4

Table D1.1. (Continued)

Sample name	U1460A 41F CC	U1460A 43F CC	U1460A 45F CC	U1460A 47F CC	U1460A 49F CC	U1460A 51F CC	U1460A 53F CC	U1460A 55F CC	U1460A 57F CC	U1460A 59F 3W	U1460A 61F CC
Depth CSF-A (m)	190.1	199.7	208.8	218.2	227.9	237.1	246.6	255.6	265.3	274.3	283.9
Total no. of species	34	41	37	43	37	41	45	36	39	41	41
Total no. of individuals	365	367	387	353	356	362	381	370	344	366	356
Fisher α Index	9.167	11.83	10.07	12.84	10.38	11.89	13.27	9.859	11.31	11.84	11.97
Shannon-Wiener Index	2.268	2.444	2.923	2.722	2.468	2.938	3.004	2.777	2.744	2.81	2.655
P/B index: Benthic	68	49	46	27	26	26	53	87	50	61	54
P/B index: Planktonic spinose	256	272	260	275	270	275	271	222	261	250	263
P/B index: Planktonic keeled	2	5	10	14	19	12	8	18	11	5	11
Spiroplectinella wrightii											
Gaudryina convexa											
Paratrochammina globorotaliformis											
Bigenerina aspratilis											
Sahulia barkeri											
Spirorutilus carinatus	1			1	12			1		11	
Textularia agglutinans					1						
Textularia catenata											
Textularia cushmani											
Textularia lateralis											
Textularia orbica											
Textularia stricta					3		3		1		
Textularia tubulosa											
Textularia sp. 3 sensu Parker 2009											
Septotextularia rugosa					1						
Migros flintii					1						
Pseudoclavulina robusta											
Plotnikovina timorea											
Clavulina subangularis										1	
Cylindroclavulina bradyi					1						
Patellina cf. *P. formosa*											
Cornuspira sp.											
Planispirinella involuta											
Wiesnerella ujiiei											
Spiroloculina subimpressa											
Agglutinella arenata											
Proemassilina arenaria											
Quinqueloculina barnadi											

Table D1.1. (Continued)

Sample name	U1460A 41F CC	U1460A 43F CC	U1460A 45F CC	U1460A 47F CC	U1460A 49F CC	U1460A 51F CC	U1460A 53F CC	U1460A 55F CC	U1460A 57F CC	U1460A 59F 3W	U1460A 61F CC
Depth CSF-A (m)	190.1	199.7	208.8	218.2	227.9	237.1	246.6	255.6	265.3	274.3	283.9
Quinqueloculina cf. *Q. crassicarinata*											
Quinqueloculina patagonica											
Quinqueloculina philippinensis											
Quinqueloculina subpolygona											
Quinqueloculina sp. 1											
Quinqueloculina sp. 5 sensu Parker 2009						1					1
Miliolinella circularis	2										
Miliolinella oceanica											
Miliolinella webbiana											
Miliolinella pilasensis											
Miliolinella sp. 1 sensu Parker 2009											
Pyrgo denticulata											
Pyrgo striolata											
Triloculina tricarinata											
Sigmoilopsis minuta											
Dentalina catenulata				1		1					
Dentalina cf. *D. mutsui*	1				1						
Grigelis orectus											
Laevidentalina bradyensis	6	5		2	14	1	10	9	1	15	3
Laevidentalina inflexa	1										
Laevidentalina sidebottomi	1		1	4			1				
Pseudonodosaria brevis	2						2				
Pyramidulina comatula										1	
Pyramidulina catesbyi											
Pyramidulina glanduliniformis								1		1	
Lenticulina calcar											
Lenticulina domantayi		2	2	5	4	3	4	4		5	2
Marginulinopsis philippinensis											
Marginulinopsis tenuis								2		2	
Saracenaria angularis											
Amphicoryna cf. *A. meringella*		1									
Amphicoryna scalaris											
Amphicoryna separans			7	3					1	1	2
Astacolus crepidulus				1	1	1		1	1	1	
Marginulina musai				1							
Vaginulinopsis bradyi											

Table D1.1. (Continued)

Sample name	U1460A 41F CC	U1460A 43F CC	U1460A 45F CC	U1460A 47F CC	U1460A 49F CC	U1460A 51F CC	U1460A 53F CC	U1460A 55F CC	U1460A 57F CC	U1460A 59F 3W	U1460A 61F CC
Depth CSF-A (m)	190.1	199.7	208.8	218.2	227.9	237.1	246.6	255.6	265.3	274.3	283.9
Vaginulinopsis gnamptina											
Vaginulinopsis pseudoplanulata					1						
Vaginulinopsis sublegumen											
Planularia gemmata											
Planularia spinipes				1				1			
Cerebrina cf. *C. claricerviculata*		2		3	3	3	3		1	1	
Cerebrina lacunata	1	1				1	6		4		
Cerebrina perforata											
Lagena annellatrachia	7	11	35	8	8	32	15	2	15	7	6
Lagena annulatacollare											
Lagena meridionalis											
Lagena substriata											
Procerolagena oceanica											
Reussoolina trachiella	4	2	7	1	8	6	8		1	1	1
Globulina rotundata											
Guttulina bartschi	1	5	1	1				2	2	3	2
Guttulina regina				2			1		1		
Pseudopolymorphina sp.											
Sigmoidella elegantissima		1	1		8		1				
Buchnerina radiatomarginata							1		1		
Exsculptina glaphyraheda						1					
Favulina favosopunctata	1	2	4			3	1			1	
Oolina baukalionilla		9									
Oolina caudigera											
Oolina globosa	1	6	1	11		9	7		4	4	
Vasicostella inflatiperforata											
Fissurina circularis		5		1	1	1	2	1	8	3	2
Fissurina subrevertens											
Lagenosolenia levata											
Pseudofissurina marginoradiata				5		1	1		1		2
Glandulina symmetrica											1
Entomorphinoides intricata											
Seabrookia pellucida											
Saintclairoides toreuta											
Hoeglundina elegans											
Geminospira bradyi											
Bolivina britannica	1	7	22								

Table D1.1. (Continued)

Sample name	U1460A 41F CC	U1460A 43F CC	U1460A 45F CC	U1460A 47F CC	U1460A 49F CC	U1460A 51F CC	U1460A 53F CC	U1460A 55F CC	U1460A 57F CC	U1460A 59F 3W	U1460A 61F CC
Depth CSF-A (m)	190.1	199.7	208.8	218.2	227.9	237.1	246.6	255.6	265.3	274.3	283.9
Bolivina robusta	8	18	16	1	2	1	7	14	14	4	10
Bolivina striatula	4	3	2	5	3	7	16	18	7	12	3
Bolivinellina translucens	1	2	2	4	1	2	5		1	1	2
Rugobolivinella elegans											
Globocassidulina subglobosa	4	7	21	16	3	28	19	13	46	25	64
Globocassidulina bisecta											
Heterocassidulina albida							1				
Paracassidulina neocarinata	6	4		2	1	3	4	4	21	6	26
Loxostomina mayori											
Rectobolivina bifrons											
Sagrinella jugosa							1	1			
Siphogenerina indica								3			1
Bulimina marginata			2	2		1	1	2	1	3	5
Siphouvigerina hispida		1	5	7	9	44	4	2	2	8	
Siphouvigerina porrecta	22	2	2	2		2		9	1	29	8
Uvigerina peregrina	145	12	17	21	121	9	62	34	6		5
Uvigerina reineri	11	1	1					2	2		
Uvigerina schwageri									1	8	
Trifarina bradyi	40	153	58	113	54	44	43	81	40	95	82
Chrysalidinella pacifica											
Reussella hayasakai		1			1			6			
Fursenkoina pauciloculata					6		1				
Sigmavirgulina tortuosa	3	5	15	5		7	12	8	19	15	5
Cancris auriculus	2	1	2				1				
Cancris oblongus											
Cancris bubnanensis											
Stomatorbina concentrica											
Rotorbinella sp.	1	3	12	3	4	5	3	2	4	2	2
Neoeponides margaritifer											
Neoeponides procerus											2
Neoconorbina albida											
Neoconorbina cavalliensis		1									
Rosalina sp. 1											
Sphaeroidina bulloides		2	3	3	5	1		15		3	2
Pileolina minogasaformis											
Pileolina patelliformis											1
Elongobula parallela			1								

Table D1.1. (Continued)

Sample name	U1460A 41F CC	U1460A 43F CC	U1460A 45F CC	U1460A 47F CC	U1460A 49F CC	U1460A 51F CC	U1460A 53F CC	U1460A 55F CC	U1460A 57F CC	U1460A 59F 3W	U1460A 61F CC
Depth CSF-A (m)	190.1	199.7	208.8	218.2	227.9	237.1	246.6	255.6	265.3	274.3	283.9
Siphonina tubulosa						1		2		3	1
Facetocochlea pulchra											
Epistominella exigua			11								
Planulinoides biconcava		3		1		1		2	2	3	1
Discorbinella montereyensis	2	5	22	6	10	8					
Hyalinea florenceae	14	20	14	7		31	3		7	4	15
Planulina retia											
Cibicides mabahethi											4
Cibicides cf. *C. refulgens*	38	15	49	16	21	29	40	17	73	36	21
Cibicidoides alazanensis				1				1		2	2
Cibicidoides mundula	8	3	18	32	23	15	22	39	6	15	7
Cibicidoides subhaidingerii					1	1	1			7	1
Cibicidoides wuellerstorfi				5		9	1		1		2
Cibicidoides sp.		1		7	10	2	2	1	2		3
Lobatula lobatula											
Caribeanella elatensis			2				2		2		
Planorbulinella larvata											
Asanonella tubulifera			1								
Amphistegina papillosa											
Nonion subturgidum			2		2						
Nonionella auris							2				
Nonionoides grateloupii				2		5					1
Pseudononion granuloumbilicatum											
Astrononion sp. 1				9		3	6			1	
Pullenia borealis	1	1				1	1			1	1
Pullenia bulloides		1									
Chilostomella ovoidea											
Anomalinoides colligera											
Anomalinoides globulosa					1						
Heterolepa bradyi											
Heterolepa ornata											
Heterolepa praecincta			1								
Anomalinulla glabrata	10	21	12	21	8	29	25	8	16	15	6
Discanomalina coronata								30			
Gyroidina orbicularis		5		1		9	7	17	2	5	11
Hanzawaia nipponica	13	17	12	10	2		20	15	22	5	39
Ammonia sp.											

Table D1.1. (Continued)

Sample name	U1460A 41F CC	U1460A 43F CC	U1460A 45F CC	U1460A 47F CC	U1460A 49F CC	U1460A 51F CC	U1460A 53F CC	U1460A 55F CC	U1460A 57F CC	U1460A 59F 3W	U1460A 61F CC
Depth CSF-A (m)	190.1	199.7	208.8	218.2	227.9	237.1	246.6	255.6	265.3	274.3	283.9
Rotalinoides gaimardi											
Elphidium depressulum											
Elphidium lene											
Elphidium macellum	2		3				3		4		1

Table D1.1. (Continued)

Sample name	U1460A 65F CC	U1460A 65F CC	TOTAL
Depth CSF-A (m)	293.3	300.0	
Total no. of species	47	44	
Total no. of individuals	383	385	
Fisher α Index	14.07	12.81	
Shannon-Wiener Index	3.108	3.164	
P/B index: Benthic	11	57	
P/B index: Planktonic spinose	289	260	
P/B index: Planktonic keeled	11	57	
Spiroplectinella wrightii			2
Gaudryina convexa			1
Paratrochammina globorotaliformis		1	1
Bigenerina aspratilis			136
Sahulia barkeri			1
Spirorutilus carinatus			250
Textularia agglutinans			87
Textularia catenata			24
Textularia cushmani			51
Textularia lateralis			10
Textularia orbica			6
Textularia stricta			8
Textularia tubulosa			25
Textularia sp. 3 sensu Parker 2009			1
Septotextularia rugosa			1
Migros flintii			29
Pseudoclavulina robusta			10
Plotnikovina timorea			48
Clavulina subangularis			1
Cylindroclavulina bradyi			10
Patellina cf. *P. formosa*			15
Cornuspira sp.			2
Planispirinella involuta			1
Wiesnerella ujiiei			1
Spiroloculina subimpressa			35
Agglutinella arenata			8
Proemassilina arenaria			1
Quinqueloculina barnadi			66

Table D1.1. (Continued)

Sample name	U1460A 63F CC	U1460A 65F CC	TOTAL
Depth CSF-A (m)	293.3	300.0	
Quinqueloculina cf. *Q. crassicarinata*			28
Quinqueloculina patagonica			40
Quinqueloculina philippinensis			3
Quinqueloculina subpolygona			5
Quinqueloculina sp. 1			16
Quinqueloculina sp. 5 sensu Parker 2009			169
Miliolinella circularis			12
Miliolinella oceanica			3
Miliolinella webbiana			3
Miliolinella pilasensis			1
Miliolinella sp. 1 sensu Parker 2009			12
Pyrgo denticulata			5
Pyrgo striolata			7
Triloculina tricarinata			66
Sigmoilopsis minuta			22
Dentalina catenulata			3
Dentalina cf. *D. mutsui*			13
Grigelis orectus			1
Laevidentalina bradyensis	9	4	87
Laevidentalina inflexa			7
Laevidentalina sidebottomi	1		13
Pseudonodosaria brevis			4
Pyramidulina comatula			1
Pyramidulina catesbyi			17
Pyramidulina glanduliniformis			2
Lenticulina calcar			4
Lenticulina domantayi	1	6	107
Marginulinopsis philippinensis			3
Marginulinopsis tenuis			4
Saracenaria angularis			7
Amphicoryna cf. *A. meringella*		2	5
Amphicoryna scalaris	1		5
Amphicoryna separans	1	14	89
Astacolus crepidulus		4	10
Marginulina musai			1
Vaginulinopsis bradyi			2

Table D1.1. (Continued)

Sample name	U1460A 63F CC	U1460A 65F CC	TOTAL
Depth CSF-A (m)	293.3	300.0	
Vaginulinopsis gnamptina			2
Vaginulinopsis pseudoplanulata			2
Vaginulinopsis sublegumen			2
Planularia gemmata			2
Planularia spinipes			3
Cerebrina cf. *C. claricerviculata*	2	4	98
Cerebrina lacunata			34
Cerebrina perforata			15
Lagena annellatrachia	8	8	252
Lagena annulatacollare			10
Lagena meridionalis			1
Lagena substriata			34
Procerolagena oceanica			1
Reussoolina trachiella	2	5	141
Globulina rotundata			1
Guttulina bartschi	5	10	66
Guttulina regina			7
Pseudopolymorphina sp.			3
Sigmoidella elegantissima		1	27
Buchnerina radiatomarginata			2
Exsculptina glaphyraheda			6
Favulina favosopunctata	1	2	24
Oolina baukalionilla			9
Oolina caudigera			1
Oolina globosa	6	21	91
Vasicostella inflatiperforata			10
Fissurina circularis	4		70
Fissurina subrevertens		1	7
Lagenosolenia levata	2		2
Pseudofissurina marginoradiata		2	12
Glandulina symmetrica		2	13
Entomorphinoides intricata			1
Seabrookia pellucida	1		1
Saintclairoides toreuta			34
Hoeglundina elegans			7
Geminospira bradyi			1
Bolivina britannica	1		75

Table D1.1. (Continued)

Sample name	U1460A 63F CC	U1460A 65F CC	TOTAL
Depth CSF-A (m)	293.3	300.0	
Bolivina robusta	4	17	581
Bolivina striatula		4	260
Bolivinellina translucens	18	16	115
Rugobolivinella elegans			7
Globocassidulina subglobosa	25	57	569
Globocassidulina bisecta			6
Heterocassidulina albida		1	2
Paracassidulina neocarinata	10	19	253
Loxostomina mayori			34
Rectobolivina bifrons			13
Sagrinella jugosa			3
Siphogenerina indica	8		144
Bulimina marginata	3	3	38
Siphouvigerina hispida	9	6	187
Siphouvigerina porrecta			141
Uvigerina peregrina	1		696
Uvigerina reineri			57
Uvigerina schwageri	1		11
Trifarina bradyi	17	9	1333
Chrysalidinella pacifica			1
Reussella hayasakai	2	1	22
Fursenkoina pauciloculata	5	5	18
Sigmavirgulina tortuosa	24	10	290
Cancris auriculus	3		52
Cancris oblongus			6
Cancris bubnanensis			6
Stomatorbina concentrica			22
Rotorbinella sp.		4	229
Neoeponides margaritifer			12
Neoeponides procerus			5
Neoconorbina albida			9
Neoconorbina cavalliensis	2	2	29
Rosalina sp. 1			15
Sphaeroidina bulloides			68
Pileolina minogasaformis	3		32
Pileolina patelliformis			63
Elongobula parallela			27

Table D1.1. (Continued)

Sample name	U1460A 63F CC	U1460A 65F CC	TOTAL
Depth CSF-A (m)	293.3	300.0	
Siphonina tubulosa		1	32
Facetocochlea pulchra	1		6
Epistominella exigua		3	50
Planulinoides biconcava	4	1	54
Discorbinella montereyensis			197
Hyalinea florenceae	54	20	866
Planulina retia			84
Cibicides mabahethi			32
Cibicides cf. *C. refulgens*	33	35	1731
Cibicidoides alazanensis		5	16
Cibicidoides mundula	10	11	501
Cibicidoides subhaidingerii			15
Cibicidoides wuellerstorfi	6	5	50
Cibicidoides sp.	6	5	39
Lobatula lobatula			17
Caribeanella elatensis			104
Planorbulinella larvata			21
Asanonella tubulifera			126
Amphistegina papillosa			2
Nonion subturgidum		2	49
Nonionella auris			2
Nonionoides grateloupii	1		9
Pseudononion granuloumbilicatum			1
Astrononion sp. 1	1	1	44
Pullenia borealis	1		13
Pullenia bulloides			1
Chilostomella ovoidea			1
Anomalinoides colligera			3
Anomalinoides globulosa	2		10
Heterolepa bradyi			1
Heterolepa ornata			3
Heterolepa praecincta			9
Anomalinulla glabrata	16	15	683
Discanomalina coronata			30
Gyroidina orbicularis	27	17	101
Hanzawaia nipponica	38	23	850
Ammonia sp.			84

Table D1.1. (Continued)

Sample name	U1460A 63F CC	U1460A 65F CC	TOTAL
Depth CSF-A (m)	293.3	300.0	
Rotalinoides gaimardi			1
Elphidium depressulum	1		4
Elphidium lene			3
Elphidium macellum	2		116

Appendix D2. Systematic Taxonomy.

Class FORAMINIFERIDA Eichwald, 1830
Order LITUOLIDA Lankester, 1885
Superfamily SPIROPLECTAMMINACEA Cushman, 1927
Family SPIROPLECTAMMINIDAE Cushman, 1927
Subfamily SPIROPLECTAMMININAE Cushman, 1927
Spiroplectinella wrightii (Silvestri, 1903)
Superfamily SPIROTEXTULARIINAE Saidova. 1975
Spirotextularia fistulosa (Brady, 1884)
Superfamily VERNEUILINOIDEA Cushman, 1911
Family VERNEUILINIDAE Cushman, 1911
Subfamily VERNEUILININAE Cushman, 1911
Gaudryina convexa (Karrer, 1864)
Order TROCHAMMINIDA Saidova, 1981
Superfamily TROCHAMMINACEA Schwager, 1877
Family TROCHAMMINIDAE Schwager, 1877
Subfamily TROCHAMMININAE Schwager, 1877
Paratrochammina globorotaliformis (Zheng, 1988)
Order TEXTULARIIDA Lankester. 1885
Superfamily TEXTULARIACEA Ehrenberg, 1838
Family TEXTULARIIDAE Ehrenberg, 1838
Subfamily TEXTULARIINAE Ehrenberg, 1838
Bigenerina aspratilis Loeblich & Tappan, 1994
Sahulia barkeri (Hofker, 1978)
Textularia agglutinans d'Orbigny, 1839
Textularia catenata Cushman, 1911
Textularia cushmani Said, 1949
Textularia lateralis Lalicker, 1935
Textularia orbica Lalicker & McCulloch, 1940
Textularia stricta Cushman, 1911
Textularia sp. 3 sensu Parker 2009
Family KAMINSKIIDAE Neagu, 1999
Subfamily SEPTOTEXTULARIINAE Loeblich and Tappan, 1985
Septotextularia rugosa Cheng & Zheng, 1978
Family PSEUDOGAUDRYINIDAE Loeblich and Tappan 1985
Subfamily PSEUDOGAUDRYININAE
Migros flintii (Cushman, 1911)
Pseudoclavulina robusta Zheng, 1988
Subfamily SIPHONIFEROIDINAE Loeblich and Tappan, 1985
Plotnikovina timorea Loeblich & Tappan, 1994
Family VALVULINIDAE Berthelin. 1880
Subfamily VALVULININAE Berthelin. 1880
Clavulina subangularis Ishizaki, 1939
Cylindroclavulina bradyi (Cushman, 1911)
Family PATELLINIDAE Rhumbler, 1906
Subfamily PATELLININAE Rhumbler, 1906
Patellina cf. *P. formosa* Heron-Allen & Earland, 1932

Order MILIOLIDA Lankester, 1885
Superfamily CORNUSPIRACEA Schultze, 1854
Family CORNUSPIRIDAE Schultze, 1854
Subfamily CORNUSPIRINAE Schultze, 1854
Cornuspira sp.
Superfamily NUBECULARIACEA T. R. Jones in Griffith and Henfrey, 1875
Family FISCHERINIDAE Millett, 1898
Subfamily FISCHERININAE Millett, 1898b
Planispirinella involuta Collins, 1958
Subfamily NODOBACULARIELLINAE Bogdanovich in Subbotina, Voloshinova, and Azbel, 1981
Wiesnerella ujiiei Hatta in Halta and Ujiie, 1992
Superfamily MILIOLACEA Ehrenberg. 1839
Family SPIROLOCULINIDAE Wiesner. 1920
Subfamily SPIROLOCULININAE Wiesner, 1920
Spiroloculina subimpressa Parr, 1950
Family HAUERINIDAE Schwager, 1876
Subfamily SIPHONAPERTINAE Saidova, 1975
Agglutinella arenata (Said, 1949)
Subfamily HAUERININAE Schwager, 1876
Proemassilina arenaria (Brady, 1884)
Quinqueloculina barnardi Rasheed, 1971
Quinqueloculina cf. *Q. crassicarinata* Collins, 1958
Quinqueloculina patagonica d'Orbigny, 1839
Quinqueloculina philippinensis Cushman, 1921
Quinqueloculina quinquecarinata Collins, 1958
Quinqueloculina subpolygona Parr, 1945
Quinqueloculina sp. 1
Quinqueloculina sp. 5 sensu Parker 2009
Subfamily MILIOLINELLINAE Vella, 1957
Miliolinella circularis (Bornemann, 1855)
Miliolinella oceanica (Cushman, 1932)
Miliolinella webbiana (d'Orbigny, 1839)
Miliolinella pilasensis McCulloch, 1977
Miliolinella sp. 1 sensu Parker 2009
Pyrgo denticulata (Brady, 1884)
Pyrgo striolata (Brady, 1884)
Triloculina tricarinata d'Orbigny in Deshayes, 1832
Subfamily SIGMOILOPSINAE Vella, 1957
Sigmoilopsis minuta (Collins, 1958)
Order LAGENIDA Lankester, 1885
Superfamily NODOSARIACEA Ehrenberg, 1838
Family NODOSARIIDAE Ehrenberg, 1838
Subfamily NODOSARIINAE Ehrenberg. 1838
Dentalina catenulata (Brady, 1884)
Dentalina cf. *D. mutsui* Hada, 1931
Grigelis orectus Loeblich & Tappan, 1994
Laevidentalina bradyensis (Dervieux, 1894)
Laevidentalina inflexa (Reuss, 1866)
Laevidentalina sidebottomi (Cushman, 1933)
Pseudonodosaria brevis (d'Orbigny, 1846)

Pyramidulina comatula (Cushman, 1923)
Pyramidulina catesbyi (d'Orbigny, 1839)
Pyramidulina glanduliniformis (Dervieux, 1894)
Family VAGINULINIDAE Reuss, 1862
Subfamily LENTICULININAE Chapman, Parr, and Collins, 1934
Lenticulina calcar (Linnaeus, 1758)
Lenticulina domantayi (McCulloch, 1977)
Marginulinopsis philippinensis (Cushman, 1921)
Marginulinopsis tenuis (Bornemann, 1855)
Saracenaria angularis Natland, 1938
Subfamily MARGINULININAE Wedekind, 1937
Amphicoryna cf. *A. meringella* Loeblich & Tappan, 1994
Amphicoryna scalaris (Batsch, 1791)
Amphicoryna separans (Brady, 1884)
Astacolus crepidulus (Fichtel & Moll, 1798)
Marginulina musai Saidova, 1975
Vaginulinopsis bradyi (Goës, 1894)
Vaginulinopsis gnamptina Loeblich & Tappan, 1994
Vaginulinopsis pseudoplanulata (Zheng, 1980)
Vaginulinopsis sublegumen Parr, 1950
Subfamily VAGINULININAE Reuss, 1860
Planularia gemmata (Brady, 1881)
Planularia spinipes (Cushman, 1913)
Family LAGENIDAE Reuss, 1862
Cerebrina cf. *C. claricerviculata* (McCulloch, 1977)
Cerebrina lacunata (Burrows & Holland, 1895)
Cerebrina perforata (LeRoy, 1964)
Lagena annellatrachia Loeblich & Tappan, 1994
Lagena annulatacollare (Loeblich & Tappan, 1994)
Lagena meridionalis Wiesner, 1931
Lagena substriata Williamson, 1848
Procerolagena oceanica (Albani, 1974)
Reussoolina trachiella Loeblich & Tappan, 1994
Superfamily POLYMORPHINACEA d'Orbigny, 1839
Family POLYMORPHINIDAE d'Orbigny, 1839
Subfamily POLYMORPHININAE d'Orbigny, 1839a
Globulina rotundata (Bornemann, 1855)
Guttulina bartschi Cushman & Ozawa, 1930
Guttulina regina (Brady, Parker & Jones, 1870)
Pseudopolymorphina sp.
Sigmoidella elegantissima (Parker & Jones, 1865)
Family ELLIPSOLAGENIDAE Silvestri, 1923
Subfamily OOLININAE Loeblich and Tappan, 1961
Buchnerina radiatomarginata (Parker & Jones, 1865)
Exsculptina glaphyraheda Loeblich & Tappan, 1994
Favulina favosopunctata (Brady, 1881)
Oolina baukalionilla Loeblich & Tappan, 1994
Oolina caudigera (Wiesner, 1931)
Oolina globosa (Montagu, 1803)
Vasicostella inflatiperforata (McCulloch, 1977)

- Subfamily ELLIPSOLAGENINAE Silvestri, 1923
  - *Fissurina circularis* Todd, 1954
  - *Fissurina subrevertens* Parr, 1950
  - *Lagenosolenia levata* McCulloch, 1977
- Subfamily PARAFISSURININAE Jones, 1984
  - *Pseudofissurina marginoradiata* (McCulloch, 1977)
- Family GLANDULINIDAE Reuss, 1860
- Subfamily GLANDULININAE Reuss, 1860
  - *Glandulina symmetrica* (McCulloch, 1977)
- Subfamily ENTOLINGULININAE Saidova, 1981
  - *Entomorphinoides intricata* McCulloch, 1977
- Subfamily SEABROOKIINAE Cushman, 1927
  - *Seabrookia pellucida* Brady, 1890

Order ROBERTINIDA Mikhalevich, 1980

- Superfamily CERATOBULIMINACEA Cushman, 1927
- Family CERATOBULIMINIDAE Cushman, 1927
- Subfamily CERATOBULIMININAE Cushman, 1927
  - *Saintclairoides toreuta* Loeblich & Tappan, 1994
- Family EPISTOMINIDAE Wedekind, 1937
- Subfamily EPISTOMININAE Wedekind, 1937
  - *Hoeglundina elegans* (d'Orbigny, 1826)
- Superfamily ROBERTINACEA Reuss, 1850
- Family ROBERTINIDAE Reuss, 1850
- Subfamily ALLIATININAE McGowran, 1966
  - *Geminospira bradyi* Bermúdez, 1952

Order BULIMINIDA Fursenko, 1958

- Superfamily BOLIVINACEA Glaessner, 1937
- Family BOLIVINIDAE Glaessner, 1937
  - *Bolivina britannica* MacFadyen, 1942
  - *Bolivina robusta* (Brady, 1881)
  - *Bolivina striatula* Cushman, 1922
  - *Bolivinellina translucens* (Phleger & Parker, 1951)
- Superfamily LOXOSTOMATACEA Loeblich and Tappan, 1962
- Family BOLIVINELLIDAE Hayward in Hayward and Brazier, 1980
  - *Rugobolivinella elegans* (Parr, 1932)
- Superfamily CASSIDULINACEA d'Orbigny, 1839
- Family CASSIDULINIDAE d'Orbigny, 1839
- Subfamily CASSIDULININAE d'Orbigny, 1839
  - *Globocassidulina bisecta* Nomura, 1983
  - *Globocassidulina subglobosa* (Brady, 1881)
  - *Heterocassidulina albida* McCulloch, 1977
  - *Paracassidulina neocarinata* (Thalmann, 1950)
- Superfamily BULIMINACEA Jones in Griffith and Henfrey, 1875
- Family SIPHOGENERINOIDIDAE Saidova, 1981
- Subfamily SIPHOGENERINOIDINAE Saidova, 1981
  - *Loxostomina mayori* (Cushman, 1922)
  - *Rectobolivina bifrons* (Brady, 1881)
  - *Sagrinella jugosa* (Brady, 1884)
- Subfamily TUBULOGENERININAE Saidova, 1981
  - *Siphogenerina indica* LeRoy, 1941

Family BULIMINIDAE Jones, 1875
Bulimina marginata d'Orbigny, 1826
Family UVIGERINIDAE Haeckel, 1894
Subfamily UVIGERININAE Haeckel, 1894
Siphouvigerina hispida (Schwager, 1866)
Siphouvigerina porrecta (Brady, 1879)
Uvigerina peregrina Cushman, 1923
Uvigerina reineri (Belford, 1966)
Uvigerina schwageri Brady, 1884
Subfamily ANGULOGERININAE Galloway, 1933
Trifarina bradyi Cushman, 1923
Family REUSSELLIDAE Cushman, 1933
Chrysalidinella pacifica (Uchio, 1952)
Reussella hayasakai Oki, 1989
Superfamily FURSENKOINACEA Loeblich and Tappan, 1961
Family FURSENKOINIDAE Loeblich and Tappan, 1961
Fursenkoina pauciloculata (Brady, 1884)
Sigmavirgulina tortuosa (Brady, 1881)
Order ROTALIIDA Lankester, 1885
Superfamily DISCORBACEA Ehrenberg, 1838
Family BAGGINIDAE Cushman, 1927
Subfamily BAGGININAE Cushman, 1927
Cancris auriculus (Fichtel & Moll, 1798)
Cancris oblongus (Williamson, 1858)
Cancris bubnanensis (McCulloch, 1977)
Family MISSISSIPPINIDAE Saidova, 1981
Subfamily STOMATORBININAE Saidova, 1981
Stomatorbina concentrica (Parker & Jones, 1864)
Family DISCORBIDAE Ehrenberg, 1838
Rotorbinella sp.
Neoeponides margaritifer (Brady, 1881)
Neoeponides procerus (Brady, 1881)
Family ROSALINIDAE Reiss, 1963
Neoconorbina albida McCulloch, 1977
Neoconorbina cavalliensis Hayward, Grenfell, Reid & Hayward, 1999
Rosalina sp. 1
Family SPHAEROIDINIDAE Cushman, 1927
Sphaeroidina bulloides d'Orbigny in Deshayes, 1828
Superfamily GLABRATELLACEA Loeblich and Tappan, 1964
Family GLABRATELLIDAE Loeblich & Tappan, 1964
Pileolina minogasaformis (Ujiié, 1992)
Pileolina patelliformis (Brady, 1884)
Family BULIMINOIDIDAE Seiglie, 1970
Elongobula parallela (Cushman & Parker, 1931)
Superfamily SIPHONINACEA Cushman, 1927
Family SIPHONINIDAE Cushman, 1927
Subfamily SIPHONININAE Cushman. 1927
Siphonina tubulosa Cushman, 1924

Family PSEUDOPARRELLIDAE Voloshinova in Voloshinova and Dain, 1952
Subfamily PSEUDOPARRELLINAE Voloshinova in Voloshinova and Dain, 1952
Facetocochlea pulchra (Cushman, 1933)
Epistominella exigua (Brady, 1884)
Family PLANULINOIDIDAE Saidova, 1981
Planulinoides biconcava (Parker & Jones, 1862)
Family DISCORBINELLIDAE Sigal in Piveteau, 1952
Subfamily DISCORBINELLINAE Sigal in Piveteau, 1952
Discorbinella montereyensis Cushman & Martin, 1935
Superfamily PLANORBULINACEA Schwager, 1877
Family PLANULINIDAE Bermudez, 1952
Hyalinea florenceae McCulloch, 1977
Planulina retia Belford, 1966
Family CIBICIDIDAE Cushman, 1927
Subfamily CIBICIDINAE Cushman, 1927
Cibicides mabahethi Said, 1949
Cibicides cf. *C. refulgens* Montfort, 1808
Cibicidoides alazanensis (Nuttall, 1932)
Cibicidoides mundula (Brady, Parker & Jones, 1888)
Cibicidoides subhaidingerii (Parr, 1950)
Cibicidoides wuellerstorfi (Schwager, 1866)
Cibicidoides sp.
Lobatula lobatula (Walker & Jacob, 1798)
Family PLANORBULINIDAE Schwager, 1877
Subfamily CARIBEANELLINAE Saidova, 1981
Caribeanella elatensis Perelis & Reiss, 1975
Subfamily PLANORBULININAE Schwager, 1877
Planorbulinella larvata (Parker & Jones, 1865)
Superfamily ASTERIGERINACEA d'Orbigny, 1839
Family EPISTOMARIIDAE Hofker, 1954
Subfamily EPISTOMARIINAE Hofker, 1954
Asanonella tubulifera (Heron-Allen & Earland, 1915)
Family AMPHISTEGINIDAE Cushman, 1927
Amphistegina papillosa Said, 1949
Superfamily NONIONACEA Schultze, 1854
Family NONIONIDAE Schultze, 1854
Subfamily NONIONINAE Schultze, 1854
Nonion subturgidum (Cushman, 1924)
Nonionella auris (d'Orbigny, 1839)
Nonionoides grateloupii (d'Orbigny, 1826)
Pseudononion granuloumbilicatum Zheng, 1979
Subfamily ASTRONONIONINAE Saidova, 1981
Astrononion sp. 1
Subfamily PULLENIINAE Schwager. 1877
Pullenia borealis Saidova, 1975
Pullenia bulloides (d'Orbigny, 1846)
Superfamily CHILOSTOMELLACEA Brady, 188I
Family CHILOSTOMELLIDAE Brady, 1881
Subfamily CHILOSTOMELLINAE Brady, 1881
Chilostomella ovoidea Reuss, 1850

Family HETEROLEPIDAE Gonzales-Donoso, 1969
Anomalinoides colligera (Chapman & Parr, 1937)
Anomalinoides globulosa (Chapman & Parr, 1937)
Heterolepa bradyi (Trauth, 1918)
Heterolepa ornata (Cushman, 1921)
Heterolepa praecincta (Karrer, 1868)
Family GAVELINELLIDAE Hofker, 1956
Subfamily GAVELINELLINAE Hofker, 1956
Anomalinulla glabrata (Cushman, 1924)
Discanomalina coronata (Parker & Jones, 1865)
Gyroidina orbicularis d'Orbigny in Parker, Jones & Brady, 1865
Hanzawaia nipponica Asano, 1944
Superfamily ROTALIACEA Ehrenberg, 1839
Family ROTALIIDAE Ehrenberg. 1839
Subfamily AMMONIINAE Saidova, 1981
Ammonia sp.
Rotalinoides gaimardi (d'Orbigny in Fornasini, 1906)
Family ELPHIDIIDAE Galloway, 1933
Subfamily ELPHIDIINAE Galloway, 1933
Elphidium depressulum Cushman, 1933
Elphidium lene Cushman & McCulloch, 1940
Elphidium macellum (Fichtel & Moll, 1798)

Appendix D3. Supplemental Figures.

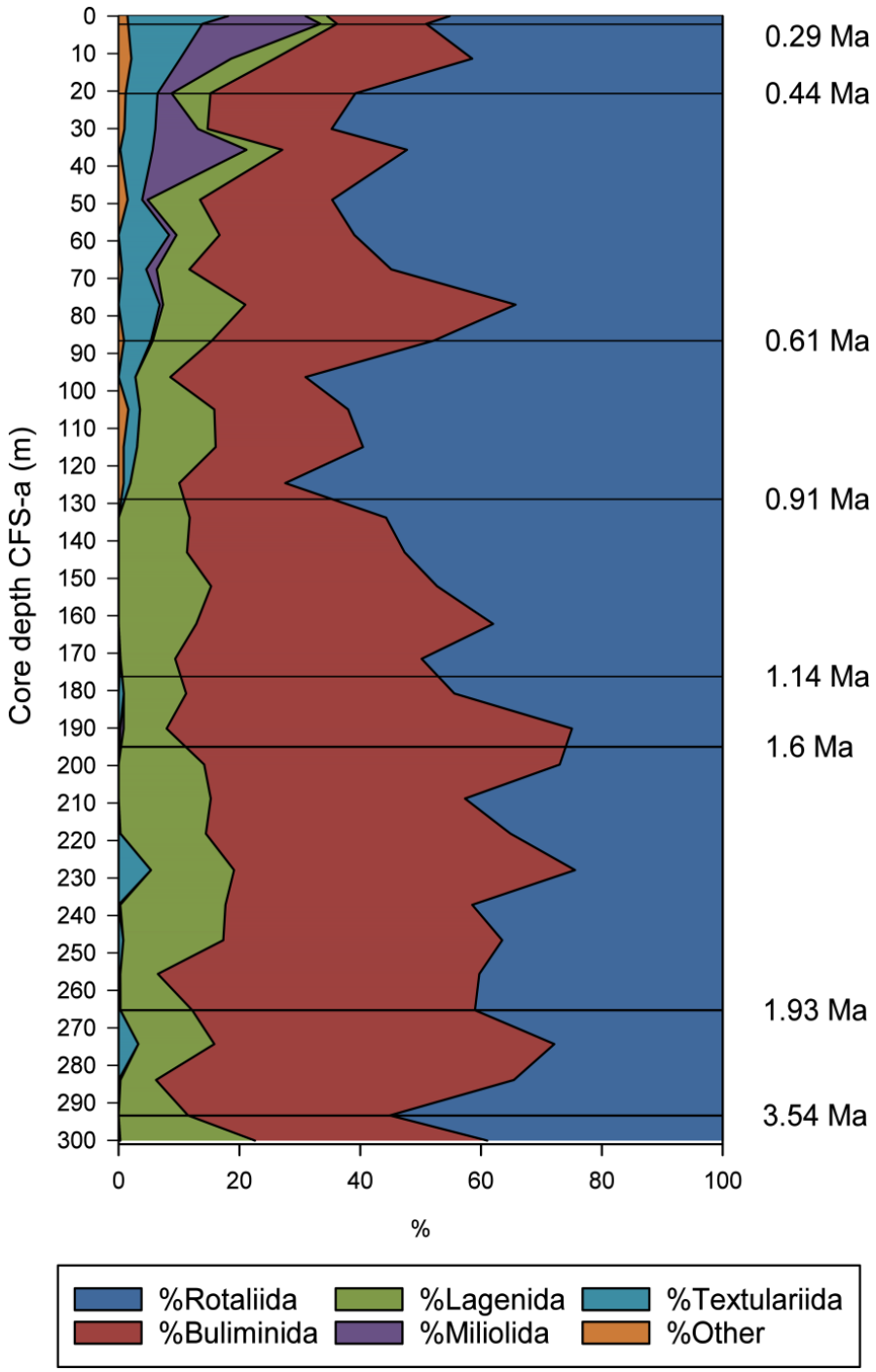

Figure D3.1. Benthic foraminiferal orders in relative abundance. Black lines mark biostratigraphic datums. '%Other' = lituolids, trochamminids, spirilinids, and robertinids.